frontiers | Research Topics

# Antimicrobial resistance: Agriculture, environment and public health within one health framework

**Edited by**
Tao Li and Haihong Hao

**Published in**
Frontiers in Microbiology

ISSN 1664-8714
ISBN 978-2-8325-4052-7
DOI 10.3389/978-2-8325-4052-7

## About Frontiers

Frontiers is more than just an open access publisher of scholarly articles: it is a pioneering approach to the world of academia, radically improving the way scholarly research is managed. The grand vision of Frontiers is a world where all people have an equal opportunity to seek, share and generate knowledge. Frontiers provides immediate and permanent online open access to all its publications, but this alone is not enough to realize our grand goals.

## Frontiers journal series

The Frontiers journal series is a multi-tier and interdisciplinary set of open-access, online journals, promising a paradigm shift from the current review, selection and dissemination processes in academic publishing. All Frontiers journals are driven by researchers for researchers; therefore, they constitute a service to the scholarly community. At the same time, the *Frontiers journal series* operates on a revolutionary invention, the tiered publishing system, initially addressing specific communities of scholars, and gradually climbing up to broader public understanding, thus serving the interests of the lay society, too.

## Dedication to quality

Each Frontiers article is a landmark of the highest quality, thanks to genuinely collaborative interactions between authors and review editors, who include some of the world's best academicians. Research must be certified by peers before entering a stream of knowledge that may eventually reach the public - and shape society; therefore, Frontiers only applies the most rigorous and unbiased reviews. Frontiers revolutionizes research publishing by freely delivering the most outstanding research, evaluated with no bias from both the academic and social point of view. By applying the most advanced information technologies, Frontiers is catapulting scholarly publishing into a new generation.

## What are Frontiers Research Topics?

Frontiers Research Topics are very popular trademarks of the *Frontiers journals series*: they are collections of at least ten articles, all centered on a particular subject. With their unique mix of varied contributions from Original Research to Review Articles, Frontiers Research Topics unify the most influential researchers, the latest key findings and historical advances in a hot research area.

Find out more on how to host your own Frontiers Research Topic or contribute to one as an author by contacting the Frontiers editorial office: frontiersin.org/about/contact

# Antimicrobial resistance: Agriculture, environment and public health within one health framework

**Topic editors**

Tao Li — Shanghai Veterinary Research Institute, Chinese Academy of Agricultural Sciences, China

Haihong Hao — Huazhong Agricultural University, China

**Citation**

Li, T., Hao, H., eds. (2023). *Antimicrobial resistance: Agriculture, environment and public health within one health framework*. Lausanne: Frontiers Media SA. doi: 10.3389/978-2-8325-4052-7

# Table of contents

05 Editorial: Antimicrobial resistance: agriculture, environment and public health within One Health framework
Tao Li, Haihong Hao, Xiaolin Hou and Jiang Xia

08 Associations between antimicrobial resistance in fecal *Escherichia coli* isolates and antimicrobial use in Canadian turkey flocks
Rima D. Shrestha, Agnes Agunos, Sheryl P. Gow, Anne E. Deckert and Csaba Varga

24 World Health Organization critical priority *Escherichia coli* clone ST648 in magnificent frigatebird (*Fregata magnificens*) of an uninhabited insular environment
Ana Carolina Ewbank, Danny Fuentes-Castillo, Carlos Sacristán, Fernanda Esposito, Bruna Fuga, Brenda Cardoso, Silvia Neri Godoy, Roberta Ramblas Zamana, Marco Aurélio Gattamorta, José Luiz Catão-Dias and Nilton Lincopan

34 Effects of salinomycin and ethanamizuril on the three microbial communities *in vivo* and *in vitro*
Xiaolei Cheng, Haihong Zheng, Chunmei Wang, Xiaoyang Wang, Chenzhong Fei, Wen Zhou and Keyu Zhang

55 Geraniol inhibits biofilm formation of methicillin-resistant *Staphylococcus aureus* and increase the therapeutic effect of vancomycin *in vivo*
Kexin Gu, Ping Ouyang, Yuxin Hong, Yuyun Dai, Ting Tang, Changliang He, Gang Shu, Xiaoxia Liang, Huaqiao Tang, Ling Zhu, Zhiwen Xu and Lizi Yin

67 Impacts of soybean agriculture on the resistome of the Amazonian soil
Oscar Cardenas Alegria, Marielle Pires Quaresma, Carlos Willian Dias Dantas, Elaine Maria Silva Guedes Lobato, Andressa de Oliveira Aragão, Sandro Patroca da Silva, Amanda Costa Barros da Silva, Ana Cecília Ribeiro Cruz, Rommel Thiago Jucá Ramos and Adriana Ribeiro Carneiro

83 The source, fate and prospect of antibiotic resistance genes in soil: A review
Binghua Han, Li Ma, Qiaoling Yu, Jiawei Yang, Wanghong Su, Mian Gul Hilal, Xiaoshan Li, Shiheng Zhang and Huan Li

97 Antimicrobial resistance and genomic characterization of *Escherichia coli* from pigs and chickens in Zhejiang, China
Wei Zhou, Rumeng Lin, Zhijin Zhou, Jiangang Ma, Hui Lin, Xue Zheng, Jingge Wang, Jing Wu, Yuzhi Dong, Han Jiang, Hua Yang, Zhangnv Yang, Biao Tang and Min Yue

110 Corrigendum: Antimicrobial resistance and genomic characterization of *Escherichia coli* from pigs and chickens in Zhejiang, China
Wei Zhou, Rumeng Lin, Zhijin Zhou, Jiangang Ma, Hui Lin, Xue Zheng, Jingge Wang, Jing Wu, Yuzhi Dong, Han Jiang, Hua Yang, Zhangnv Yang, Biao Tang and Min Yue

111 Characterization and comparative genomics analysis of RepA_N multi-resistance plasmids carrying *optrA* from *Enterococcus faecalis*
Enbao Zhang, Shuaizhou Zong, Wei Zhou, Jinzhi Zhou, Jianzhong Han and Daofeng Qu

124 Field ponding water exacerbates the dissemination of manure-derived antibiotic resistance genes from paddy soil to surrounding waterbodies
Ming-Sha Zhang, Si-Zhou Liang, Wei-Guo Zhang, Ya-Jun Chang, Zhongfang Lei, Wen Li, Guo-Liang Zhang and Yan Gao

131 IncHI1 plasmids mediated the *tet*(X4) gene spread in *Enterobacteriaceae* in porcine
Jiangang Ma, Juan Wang, Hua Yang, Mengru Su, Ruichao Li, Li Bai, Jie Feng, Yuting Huang, Zengqi Yang and Biao Tang

139 Transcriptome profile of halofuginone resistant and sensitive strains of *Eimeria tenella*
Pei Sun, Chaoyue Wang, Yuanyuan Zhang, Xinming Tang, Dandan Hu, Fujie Xie, Zhenkai Hao, Jingxia Suo, Yonglan Yu, Xun Suo and Xianyong Liu

149 Chitosan can improve antimicrobial treatment independently of bacterial lifestyle, biofilm biomass intensity and antibiotic resistance pattern in non-aureus staphylococci (NAS) isolated from bovine clinical mastitis
Maria Laura Breser, Lucia Tisera, Maria Soledad Orellano, Luciana Paola Bohl, Paula Isaac, Ismael Bianco and Carina Porporatto

161 Antibiotic resistance gene sequencing is necessary to reveal the complex dynamics of immigration from sewers to activated sludge
Claire Gibson, Susanne A. Kraemer, Natalia Klimova, Bing Guo and Dominic Frigon

174 Characterization of two multidrug-resistant *Klebsiella pneumoniae* harboring tigecycline-resistant gene *tet*(X4) in China
Yanxian Yang, Ruowen He, Yiping Wu, Mingyang Qin, Jieyun Chen, Yu Feng, Runping Zhao, Lei Xu, Xilong Guo, Guo-Bao Tian, Min Dai, Bin Yan and Li-Na Qin

182 Predicting antimicrobial resistance of bacterial pathogens using time series analysis
Jeonghoon Kim, Ruwini Rupasinghe, Avishai Halev, Chao Huang, Shahbaz Rezaei, Maria J. Clavijo, Rebecca C. Robbins, Beatriz Martínez-López and Xin Liu

frontiers | Frontiers in Microbiology

TYPE Editorial
PUBLISHED 01 November 2023
DOI 10.3389/fmicb.2023.1252134



OPEN ACCESS

EDITED BY
Rustam Aminov,
University of Aberdeen, United Kingdom

REVIEWED BY
Ziad Daoud,
Central Michigan University, United States
Indranil Samanta,
West Bengal University of Animal and Fishery Sciences, India

*CORRESPONDENCE
Tao Li
litao@shvri.ac.cn

RECEIVED 04 July 2023
ACCEPTED 18 October 2023
PUBLISHED 01 November 2023

CITATION
Li T, Hao H, Hou X and Xia J (2023) Editorial: Antimicrobial resistance: agriculture, environment and public health within One Health framework.
*Front. Microbiol.* 14:1252134.
doi: 10.3389/fmicb.2023.1252134



# Editorial: Antimicrobial resistance: agriculture, environment and public health within One Health framework

Tao Li[1]*, Haihong Hao[2], Xiaolin Hou[3] and Jiang Xia[4]

[1]Shanghai Veterinary Research Institute, Chinese Academy of Agricultural Sciences (CAAS), Shanghai, China, [2]China MOA Laboratory for Risk Assessment of Quality and Safety of Livestock and Poultry Products, Huazhong Agricultural University, Wuhan, China, [3]Beijing Key Laboratory of Chinese Veterinary Medicine, Department of Veterinary Medicine, National Demonstration Center for Experimental Animal Education, Beijing University of Agriculture, Beijing, China, [4]Department of Chemistry, School of Life Sciences, The Chinese University of Hong Kong, Shatin, Hong Kong SAR, China

KEYWORDS

**antimicrobial resistance, agriculture, public health, One Health, ecosystem, drug resistance**

Editorial on the Research Topic
Antimicrobial resistance: agriculture, environment and public health within One Health framework

Recently, due to the increasing spread of antimicrobial resistance (AMR), AMR has received great attention from researchers and governments. It is expected that AMR will be the most important public health issue and challenge in this century (Nahrgang et al., 2018). Infections caused by AMR bacteria are arguably more serious and less responsive to treatment than infections caused by sensitive bacteria. Infections caused by AMR bacteria lead to consequences ranging from treatment failure and the need for more complex treatments to increased morbidity and mortality rates, hospitalization, and healthcare costs (Chinemerem Nwobodo et al., 2022). Therefore, AMR requires urgent multisectoral action in order to achieve the Sustainable Development Goals (SDGs).

Many studies have demonstrated that AMR is an ecological problem, as most bacteria and their antibiotic resistance genes (ARGs) can quickly move between humans, agriculture, and the environment (Bottery et al., 2021; Wang et al., 2023), creating a serious problem. Along with humans and the environment, the One Health framework also encompasses agriculture/plant sciences due to the importance and interdependence of AMR in relation to public health, the environment, and animals.

This Research Topic focuses on recent studies on the impact of AMR on human and/or animal health and innovative technologies and strategies to combat AMR.

## AMR in the ecosystem

As mentioned above, ARGs circulate among the environment, agriculture, and humans, which represent the different components of the One Health framework. In ecological processes, soil bacteria play an important role and are highly influenced by various agricultural activities, which impact the chemical, macroscopic, and microbiological composition. Cardenas Alegria et al. analyzed organic soil from various forests, pastures,

and transgenic soybean monocultures in Brazil. They found diverse ARGs in forest soils, and especially in soybean crop soils. The most common ARGs were those related to aminoglycosides, macrolides, tetracyclines, and fluoroquinolones. Zhang et al. found that certain feces-derived ARGs (such as *aadA1* and *bla1*) could be easily transferred from paddy soil to field water. Similarly, Han et al. reviewed recent studies on the associations of ARGs with microbiomes and the mechanisms of ARG dissemination in soil. They found that the presence of ARGs in soil is inherent and ancient, and plants and animals can absorb ARGs from the soil and then transmit them to humans. Also, Gibson et al. were the first to analyze the impact on AMR in wastewater treatment plants of the effect of microbial immigration on the indigenous resident microbial communities.

Wild birds, which are an integral part of the ecological system, have been assessed as possible reservoirs and disseminators of ARGs to insular biomes in experimental studies, but their potential role as dispersers under real-world conditions remains unknown. Island settings provide a unique opportunity for scientists to evaluate and debate the spread of ARGs by wild birds in the ecological system. Ewbank et al. evaluated cloacal swabs from wild *Fregata magnificens* in the Alcatrazes Archipelago, which is a nature reserve without any human occupation before. They found a highly virulent multidrug-resistant (MDR) ST648 (O153:H9) pandemic *Escherichia coli* clone, which is one of the most commonly reported international sequence types (STs) in the global human–animal–environmental interface. Alcatrazes *Fregata magnificens* most likely have extremely limited to no direct contact with humans, due to their site fidelity and limited roosting and nesting area on the island. The authors speculated that a route of infection of Alcatrazes *Fregata magnificens* by the abovementioned *E. coli* strain may involve their continuous close contact and body fluid exchange with other frigatebirds and birds of other genera [especially (*Sula leucogaster* and *Coragyps atratus*)] using the area.

Shrestha et al. evaluated the association between antimicrobial use in turkey flocks and the development of AMR in North America. Using the indicator bacterium *E. coli*, they reported the effect of the antimicrobial treatment for certain diseases (such as enteric diseases, advanced sepsis, and Colibacillosis) on the development of resistance to certain antimicrobials. they concluded that from an antimicrobial management perspective, interventions at the producer level may have the greatest impact on reducing AMR establishment in *E. coli* isolates.

In recent years, there has been increasing attention on the association between gut dysbiosis and AMR. Gut dysbiosis contributes to the loss of colonization resistance, which can be followed by increased AMR. However, research has mainly focused on the effect of antibiotics on the gut microbiota, while ignoring the effect of other drugs such as antiparasitic drugs. The effects of salinomycin and ethanamizuril (which represent two different classes of coccidiostat, and are widely used in China) on the microbiota of cecal contents, manure compost, and soil were unknown. Cheng et al. compared the effects of these two treatments on the microbiota of coccidia-infected broilers' cecal contents, manure compost, and loam soil. They found that both treatments suppressed certain opportunistic pathogens, but they failed to repair the large changes in the cecal microbiota caused by coccidia infection. The *in vitro* effect of ethanamizuril on compost and soil microbiota seemed to be slight, while salinomycin had a large impact on these microbial communities.

## AMR prevention and control

This Research Topic also focuses on how to prevent and control AMR. Natural product extracts are increasingly being recognized as alternative antimicrobials for the treatment of infectious diseases in animals. Gu et al. reported that geraniol, the main component of various essential oils, not only effectively inhibits the formation of methicillin-resistant *Staphylococcus aureus* biofilms, but also relieves inflammatory symptoms and potentiates vancomycin by destroying biofilm structures. There is evidence that the activity of conventional antibiotics can be enhanced when used synergistically with natural product extracts. Breser et al. studied the effect of cloxacillin and chitosan alone or in combination on non-*S. aureus* isolates with various lifestyles and biofilm-forming abilities. They found that the addition of chitosan to the cloxacillin treatment significantly reduced the bactericidal concentration of the antibiotic, irrespective of the biomass density of the biofilm or the AMR pattern of the non-*S. aureus* isolates.

## AMR diagnostics

Rapid detection of AMR and prediction of future AMR burden and trends are crucial for implementing appropriate interventions to mitigate AMR. Several studies have used various machine learning algorithms to predict AMR rates using data on phenotypes and genotypes. Kim et al. collected 2010–2021 pathogen and AMR data from >600 farms in the United States to conduct AMR time series analyses using machine learning. They established three machine learning-based time series analyses to predict the future AMR rate. They found that the seasonal auto-regressive integrated moving average (SARIMA) approach had low root mean square error compared to other approaches, and it worked even for highly dynamic time series.

Whole-genome sequencing plays an extremely important role in AMR research, and it has provided insights into AMR mechanisms, pathogen evolution, and population dynamics in global pathogen surveillance. Zhou et al. found that 87.85% of *E. coli* isolates from chicken and pigs had MDR (the main MDR pattern was AMP-SPT-TET-FFC-SF-SXT) and there were 65 sequence types (STs) among the *E. coli* isolates. Yang et al. screened a total 921 samples from pigs and humans in China for the plasmid-encoded *tet(X4)* ARG (which mediates tigecycline resistance and has been widely identified in *E. coli* isolates from food-producing animals). They isolated two *tet(X4)*-positive strains, and conjugation experiments showed that the two *tet(X4)*-encoding plasmids could be transferred from *K. pneumoniae* to *E. coli*.

In conclusion, we believe that the data collected in the aforementioned studies and reviews can provide physicians, veterinarians, environmental scientists, public health professionals, wildlife experts, and many others with a toolkit for use within the One Health framework.

## Author contributions

All authors listed have made a substantial, direct, and intellectual contribution to the work and approved it for publication.

## Acknowledgments

TL acknowledge the support of Shanghai Agriculture Applied Technology Development Program, China (Grant No. T20200104), The Agricultural Science and Technology Innovation Program (ASTIP) (Grant No. CAAS-ZDRW202203), and the National Key Research and Development Program of China (2018YFE0192600).

## Conflict of interest

The authors declare that the research was conducted in the absence of any commercial or financial relationships that could be construed as a potential conflict of interest.

## Publisher's note

All claims expressed in this article are solely those of the authors and do not necessarily represent those of their affiliated organizations, or those of the publisher, the editors and the reviewers. Any product that may be evaluated in this article, or claim that may be made by its manufacturer, is not guaranteed or endorsed by the publisher.

## References

Bottery, M. J., Pitchford, J. W., and Friman, V. P. (2021). Ecology and evolution of antimicrobial resistance in bacterial communities. *ISME J.* 15, 939–948. doi: 10.1038/s41396-020-00832-7

Chinemerem Nwobodo, D., Ugwu, M. C., Oliseloke Anie, C., Al-Ouqaili, M. T. S., Chinedu Ikem, J., Victor Chigozie, U., et al. (2022). Antibiotic resistance: The challenges and some emerging strategies for tackling a global menace. *J. Clin. Lab. Anal.* 36, e24655. doi: 10.1093/eurpub/cky212.497

Nahrgang, S., Nolte, E., and Rechel, B. (2018). "Antimicrobial resistance," in *The Role of Public Health Organizations in Addressing Public Health Problems in Europe: The Case of Obesity, Alcohol and Antimicrobial Resistance [Internet]*, eds Rechel, B., Maresso, A., Sagan, A., et al. (eds) (Copenhagen (Denmark): European Observatory on Health Systems and Policies), 51.

Wang, W. J., Wang, Y. F., Jin, Y. J., Song, W. Q., Lin, J. M., Zhang, Y., et al. (2023). Characterization of a blaCTX-M-3, blaKPC-2 and blaTEM-1B co-producing IncN plasmid in Escherichia coli of chicken origin. *J. Integr. Agr.* 22, 320–324. doi: 10.1016/j.jia.2022.08.075

frontiers | Frontiers in Microbiology

TYPE Original Research
PUBLISHED 29 July 2022
DOI 10.3389/fmicb.2022.954123



OPEN ACCESS

EDITED BY
Tao Li,
Shanghai Veterinary Research Institute (CAAS), China

REVIEWED BY
Maria José Saavedra,
Universidade de Trás-os-Montes e Alto Douro, Portugal
Xiaoliang Ba,
University of Cambridge, United Kingdom

*CORRESPONDENCE
Csaba Varga
cvarga@illinois.edu

SPECIALTY SECTION
This article was submitted to Antimicrobials, Resistance and Chemotherapy, a section of the journal Frontiers in Microbiology

RECEIVED 27 May 2022
ACCEPTED 11 July 2022
PUBLISHED 29 July 2022

CITATION
Shrestha RD, Agunos A, Gow SP, Deckert AE and Varga C (2022) Associations between antimicrobial resistance in fecal *Escherichia coli* isolates and antimicrobial use in Canadian turkey flocks. *Front. Microbiol.* 13:954123. doi: 10.3389/fmicb.2022.954123



# Associations between antimicrobial resistance in fecal *Escherichia coli* isolates and antimicrobial use in Canadian turkey flocks

Rima D. Shrestha[1], Agnes Agunos[2], Sheryl P. Gow[3], Anne E. Deckert[2] and Csaba Varga[1,4]*

[1]Department of Pathobiology, College of Veterinary Medicine, University of Illinois Urbana-Champaign, Urbana, IL, United States, [2]Center for Foodborne, Environmental and Zoonotic Infectious Diseases, Public Health Agency of Canada, Guelph, ON, Canada, [3]Center for Foodborne, Environmental and Zoonotic Infectious Diseases, Public Health Agency of Canada, Saskatoon, SK, Canada, [4]Carl R. Woese Institute for Genomic Biology, University of Illinois Urbana-Champaign, Urbana, IL, United States

Antimicrobial resistance (AMR) in enteric bacteria continues to be detected in turkey flocks and retail products worldwide, including in Canada. However, studies assessing linkages between on-farm antimicrobial use (AMU) and the development of AMR are lacking. This study aims to identify AMU characteristics that impact the development of AMR in the indicator bacteria *Escherichia coli* in turkey flocks, building on the Canadian Integrated Program for Antimicrobial Resistance Surveillance methodology for farm-level AMU and AMR data integration. Two analytic approaches were used: (1) multivariable mixed-effects logistic regression models examined associations between AMU (any route, route-specific, and route-disease-specific indication) summarized as the number of defined daily doses in animals using Canadian standards ([nDDDvetCA]/1,000 kg-animal-days at risk) and AMR and (2) multivariable mixed-effects Poisson regression models studied the linkages between AMU and the number of classes to which an *E. coli* isolate was resistant ($nCR_{E.\ coli}$). A total of 1,317 *E. coli* isolates from a network of 16 veterinarians and 334 turkey producers across the five major turkey-producing provinces in Canada between 2016 and 2019 were used. Analysis indicated that AMR emerged with the use of related antimicrobials (e.g., tetracycline use-tetracycline resistance), however, the use of unrelated antimicrobial classes was also impacting AMR (e.g., aminoglycosides/streptogramins use-tetracycline resistance). As for studying AMU-$nCR_{E.\ coli}$ linkages, the most robust association was between the parenteral aminoglycosides use and $nCR_{E.\ coli}$, though in-feed uses of four unrelated classes (bacitracin, folate pathway inhibitors, streptogramins, and tetracyclines) appear to be important, indicating that ongoing uses of these classes may slow down the succession from multidrug-resistant to a more susceptible *E. coli* populations. The analysis of AMU (route and

disease-specific)-AMR linkages complemented the above findings, suggesting that treatment of certain diseases (enteric, late-stage septicemic conditions, and colibacillosis) are influential in the development of resistance to certain antimicrobial classes. The highest variances were at the flock level indicating that stewardship actions should focus on flock-level infection prevention practices. This study added new insights to our understanding of AMU-AMR linkages in turkeys and is useful in informing AMU stewardship in the turkey sector. Enhanced surveillance using sequencing technologies are warranted to explain molecular-level determinants of AMR.

KEYWORDS

**antimicrobial resistance, antimicrobial use, turkey, *E. coli*, farm surveillance, Canada**

## Introduction

Antimicrobial resistance (AMR) is a global health threat that has limited the options for the treatment of bacterial infections in animals and humans (McEwen and Collignon, 2018; Murray et al., 2022). A recent comprehensive study estimated that 1.27 of 4.95 million human deaths in 2019 were attributed to infection with antimicrobial-resistant bacteria (ARB) (Murray et al., 2022). In addition, infections with ARB can have long-term health effects by increasing hospital admissions, treatment failures, morbidity, mortality, and economic burden (World Health Organization [WHO], 2015, 2021; Dadgostar, 2019). Since antimicrobial use (AMU) is a driver for the emergence of AMR, local, national, and global public health stakeholders have expressed concerns about the extent of AMU in humans and food animals (Aidara-Kane et al., 2018; Agunos et al., 2020; Ceccarelli et al., 2020; World Health Organization [WHO], 2021).

Antimicrobials have been used effectively to treat, control, and prevent bacterial infections in poultry for decades; however, AMU (Dorado-García et al., 2016; Callens et al., 2018; Luiken et al., 2019; Van Gompel et al., 2019; Varga et al., 2019a; Ceccarelli et al., 2020) enhances the selection pressure on commensal and pathogenic enteric bacteria that favors the development of AMR (Kolář et al., 2001; Landers et al., 2012; Callens et al., 2018; Mughini-Gras et al., 2021). The zoonotic transmission of ARB through consumption of contaminated poultry products and contact with infected birds and their contaminated environment (Brown et al., 2017; Varga et al., 2018; Agunos et al., 2020) has also been demonstrated.

Globally, Canada is among the top 10 turkey producing countries in terms of value in agricultural production (FAO, 2022). Canadian turkey production is an important commodity to include in surveillance since approximately 157.8 million kilograms of turkey meat is produced each year in Canada, making this commodity the 4th most consumed animal protein with a yearly per capita consumption of 3.8 kg per person (Canadian Turkey Marketing Agency, 2020; Government of Canada, 2021). In response to national and global mandates, the poultry sector in North America is proactively implementing AMU reduction strategies and gradually eliminating the preventive use of medically important antimicrobials to contain the emergence and dissemination of AMR (Prescott, 2019; Turkey farmers of Canada, 2022). However, this policy might limit the antimicrobial therapy options available to treat bacterial infections in poultry, which could impact the sustainability of the poultry industry (Agunos et al., 2021a,b).

Commensal *Escherichia coli* are part of the intestinal flora of humans and animals and are broadly used in many surveillance systems as indicator bacteria to study the emergence, transmission, and spread of AMR determinants in the ecosystem as they can be isolated efficiently and cost-effectively from fecal and environmental samples (McEwen and Fedorka-Cray, 2002). Commensal *E. coli* is also considered a good indicator of the selection pressure of AMU due to their ability to preserve, acquire and transmit AMR genes in the intestinal flora of humans and animals (Kolář et al., 2001; Lambrecht et al., 2019; Mughini-Gras et al., 2021).

Research studies have previously evaluated AMR in *E. coli* isolated from turkey flocks and turkey meat worldwide (**Supplementary Table 1**), including in Canada (Gosling et al., 2012; Sheikh et al., 2012; Giovanardi et al., 2013; Boulianne et al., 2016; Davis et al., 2018; Varga et al., 2019b; Agunos et al., 2020; Tawyabur et al., 2020; Chrétien et al., 2021; Gholami-Ahangaran et al., 2021; Mughini-Gras et al., 2021; Talavera-González et al., 2021). However, surveillance information and research studies in turkeys on the associations between the development of AMR in enteric pathogens and flock-level AMU have been relatively scarce during the last decade. The lower turkey production volume compared to chicken and pork could be one reason for the limited data available. Recently, however, a European study found a high level of multidrug-resistant *E. coli* isolates from turkeys and resistance to third and fourth-generation cephalosporins (Ceccarelli et al., 2020). In another

study involving turkeys in three European countries, resistance to beta-lactams and colistin (by metagenomic sequencing) and ampicillin and ciprofloxacin (by minimum inhibitory concentration) were found to be positively associated with AMU (Horie et al., 2021).

The Canadian Integrated Program for Antimicrobial Resistance Surveillance (CIPARS) has recently reported a decrease in total AMU that corresponded with a decrease in multidrug-resistant (MDR) bacteria (Agunos et al., 2021a,b) in turkeys. However, it is unclear how AMU practices, in broad terms (i.e., shifts in AMU quantity, changes in the route of administration, and the change in the proportion of certain classes of antimicrobials for the prevention and treatment of the most frequently occurring diseases of turkeys), as it relates to the turkey sector's AMU reduction strategy are influencing the maintenance of MDR *E. coli* populations in Canadian turkey flocks. In the context previously described, this study aimed to (1) investigate associations between AMR outcomes [the homologous resistances in indicator *E. coli* isolated from Canadian turkey flocks, and a composite AMR outcome, the number of classes to which an *E. coli* isolate was resistant ($nCR_{E.\ coli}$)] and the corresponding flock-level AMU (class-specific total administered and administration route-specific, measured in the number of defined daily doses using Canadian standards [nDDDvetCA]/1,000 kg-animal days at risk), (2) investigate associations between the two AMR outcomes previously described, and any AMU via a specific-administration route (feed, water, injection) to treat or prevent a specific disease (i.e., enteric, colibacillosis).

# Materials and methods

A schematic diagram with the detail of the study methodology is shown in **Figure 1**.

## Farm and sample collection

At each farm sampling visit, veterinarians administered a questionnaire to producers to collect data regarding on-farm AMU practices throughout the turkeys' grow-out period. The selection criteria of participating turkey farms and flocks, protocols for on-farm fecal sampling, and laboratory procedures are described elsewhere (Government of Canada, 2018; Agunos et al., 2019). Briefly, poultry veterinarians from each province were recruited and asked to select turkey farms from their client list to obtain a representative sample based on the inclusion and exclusion criteria of flocks as outlined by CIPARS (Government of Canada, 2018). Before starting the survey, each veterinarian obtained a signature on the standard informed consent document from each participating turkey producer. The veterinarian visited each turkey farm once a year during the last week of the turkeys' grow-out period, considering their marketing weight (i.e., broiler turkeys, light hens, heavy hens, light toms, heavy toms) as defined by Turkey Farmers of Canada. During each visit, one flock (described as a group of turkeys placed on the same day in the specific production unit) was randomly selected per farm. Four pooled fecal samples (10 fecal droppings per pool) per flock, one from each of the four quadrants of the selected barn were collected and submitted to the CIPARS laboratory for bacterial culture and antimicrobial susceptibility testing.

## Laboratory methods

A 25 g sample from each pooled fecal sample was mixed with 225 mL of buffered peptone water and incubated at 35 ± 1°C for 24 h. One drop from this incubated mixture was streaked onto a MacConkey agar plate and was incubated at 35°C for 18–24 h. Suspect colonies that fermented lactose were transferred onto Luria-Bertani agar. Presumptive *E. coli* colonies were assessed using Simmons citrate and indole tests. Colonies that were negative on the indole test were further confirmed using API® 20E bacterial identification kit.

One *E. coli* isolate per positive fecal sample was tested for antimicrobial susceptibility using a broth microdilution method with the Sensititre Antimicrobial Susceptibility Testing System (Trek$^{TM}$ Diagnostic Systems Ltd., West Sussex, United Kingdom) and the CMV4AGNF National Antimicrobial Resistance Monitoring System (NARMS) plate comprised of 14 antimicrobials. Isolates were classified as susceptible, intermediate, or resistant to a specific antimicrobial by evaluating breakpoints of their minimum inhibitory concentration (MIC) values following the Clinical and Laboratory Standards Institute (CLSI) M7-A8 guidelines where possible. No CLSI interpretive criteria for *Enterobacteriaceae* were available for azithromycin or streptomycin therefore breakpoints were based on the distribution of MIC values and were harmonized with those of the NARMS. For quality control, *Escherichia coli* ATCC 25922 strain was used.

## Antimicrobial use data collection and management

The data analyzed in this study (2016–2019 surveillance years) were extracted from the CIPARS sentinel-farm surveillance AMU database. The CIPARS farm AMU questionnaire (Supplement in Reference #7) generates high-resolution AMU data comprised of flock-level demographics to derive various input parameters for the count-, weight- and dose-based AMU indicators, AMU by route of administration, and syndromic/animal health information. For our study, the AMU measurement chosen was the exploratory indicator,

the number of defined daily doses using Canadian standards (nDDDvetCA)/1,000 kg-animal days at risk (Agunos et al., 2021a), which was calculated using the following formula

$$\text{nDDDvetCA/1000 kg animal days at risk} = \left(\frac{\textit{total antimicrobials (mg)}/DDD_{mg/kg/day}}{\text{total no. of turkeys x kg animal biomass x } \textit{days at risk}}\right) \times 1000 \ldots\ldots (i)$$

The defined daily dose for an antimicrobial class was determined by combining the average of all approved unique doses (for prevention and treatment purposes), based on the Canadian Compendium of Veterinary Products (Canadian Animal Health Institute, 2009) and Compendium of Medicating Ingredients Brochure (Government of Canada, 2019). The days at risk were defined as the average grow-out period, which varied from year to year from 84 to 89 days, and the average kg animal biomass, which varied depending on the year, from 9.44 to 10.26 kg. The kg biomass pertained to the pre-slaughter live weight of the turkey flock at the end of the grow-out period. This is an exploratory AMU indicator being examined by CIPARS and is similar to nDDDvet/kg animal biomass previously used in the integration of AMU-AMR; however, the time at-risk component of the exploratory indicator better reflects the long-term impact of AMU exposure on the emergence of AMR (Agunos et al., 2021a,b).

Three AMU predictor variables, summarized at the antimicrobial class level, were defined (1) the quantity of AMU aggregated across all routes of administration measured in nDDDvetCA/1,000 kg-animal days at risk ($AMU_{any-routes}$), (2) route-specific AMU, also in nDDDvetCA/1,000 kg-animal days at risk ($AMU_{route-specific}$), and (3) route and disease-specific AMU (binomial variable-yes/no), defined as the use of any antimicrobial by a specific administration route to treat or prevent a specific disease ($AMU_{route-disease-specific}$).

## Antimicrobial resistance data management

As per CIPARS routine methodology, susceptible isolates included those that exhibited intermediate susceptibility to a given antimicrobial. AMR outcomes (susceptible as "0" and resistant as "1") by individual antimicrobial agents and by class were extracted from the CIPARS AMR dataset. The following were the AMR outcomes used for this study: (1) seven antimicrobial classes that were included in the NARMS Gram-negative panel including aminoglycosides (gentamicin, streptomycin), beta-lactams (amoxicillin-clavulanic acid, ampicillin, ceftriaxone, cefoxitin), folate pathway inhibitors (trimethoprim-sulfamethoxazole, sulfisoxazole), macrolides (azithromycin), quinolones/fluoroquinolones/ (nalidixic acid/ciprofloxacin), phenicols (chloramphenicol), and tetracyclines (tetracycline); (2) composite AMR outcome variable $nCR_{E.coli}$ that signified the number of antimicrobial classes to which an *E. coli* isolate was resistant. The AMR and the AMU variables were descriptively examined and validated before integrating the data using the common fields of sampling year and flock identifier.

## Statistical analysis

All statistical analyses and data visualization were performed using the R (R Core Team, 2020) software in R-studio (Version 1.4.1106© 2009–2021 RStudio, PBC) platform. **Figure 1** provides an overview of the analytic approach.

## Descriptive statistics

The proportion of *E. coli* isolates resistant to each of the seven antimicrobial classes described above was calculated, by dividing the number of isolates resistant to the antimicrobial class by the total number of isolates tested. The proportion of antimicrobial classes used on farms was calculated by dividing the number of farms that used the antimicrobial class by the total number of farms. Antimicrobial resistance and antimicrobial use variables with proportions $< 5\%$ or $> 95\%$ were excluded from further analysis to keep enough variability in the models. Tetracyclines, aminoglycosides, folate pathway inhibitors, and beta-lactams were the only classes with resistance in $> 5\%$ of the isolates and therefore included as homologous outcome variables of interest. The six antimicrobial classes: tetracyclines, aminoglycosides, folate pathway inhibitors, beta-lactams, bacitracin, and streptogramins were used in a minimum of 5% of the turkey flocks and were used in the AMU predictor variables created.

## Regression analyses

As described in **Figure 1**, the following regression analyses were conducted:

AMR-$AMU_{any-routes}$. The outcome variable was the class-specific resistance for the logistic mixed-effect analysis and the $nCR_{E.\ coli}$, a composite AMR indicator for the Poisson mixed-effect regression analysis. The AMU was summarized by the nDDDvetCA/1,000 kg-animal days at risk for each antimicrobial class across all routes of administration. The purpose of this analysis was to explore if AMU regardless of route of administration (feed, water, or injection) had an impact on AMR.

AMR-$AMU_{route-specific}$. This approach is similar to the above exercise, but the AMU component was disaggregated by the route of administration. The purpose of this analysis was

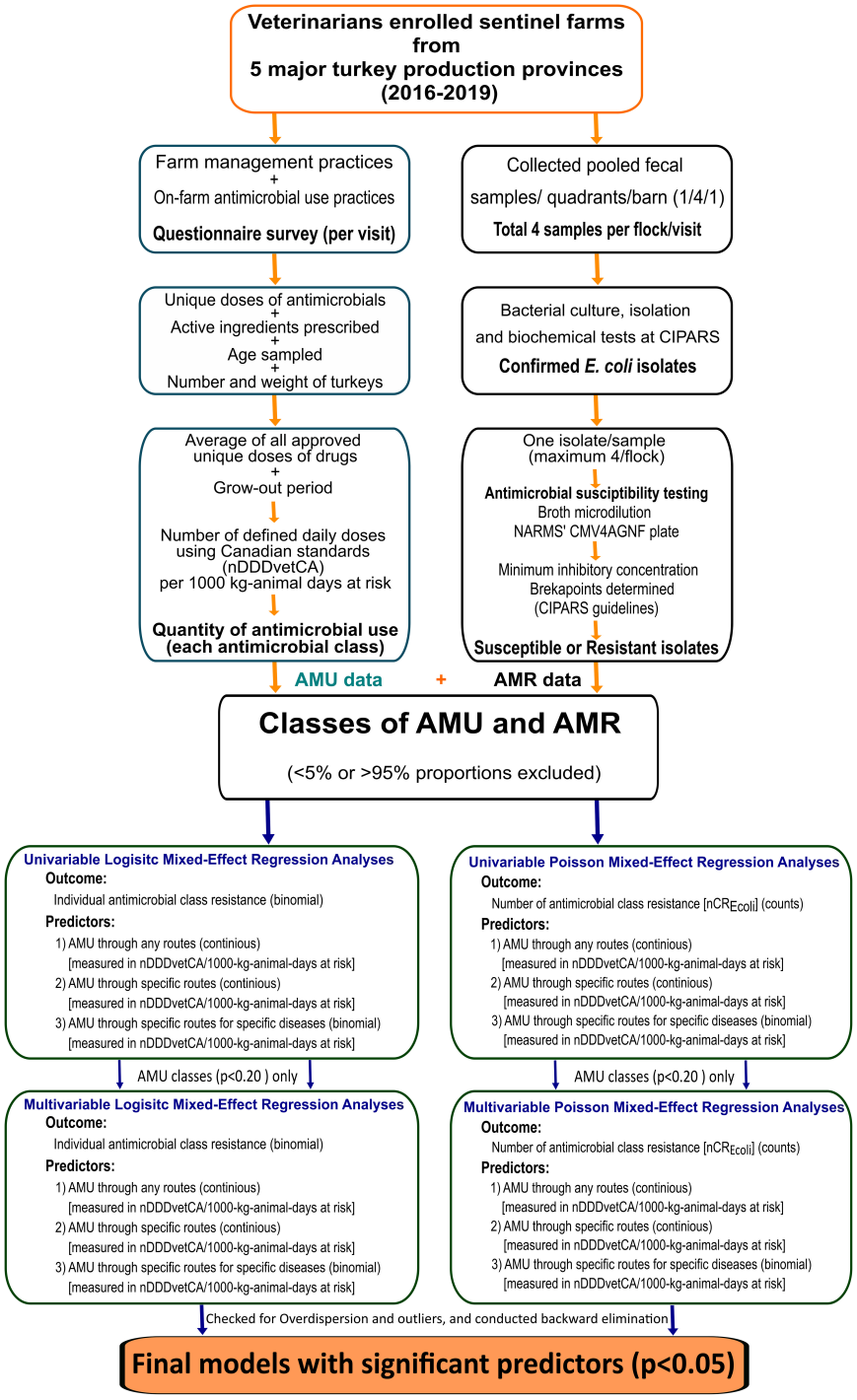


FIGURE 1
Summary of surveillance design, laboratory, and statistical analysis methods. AMU, antimicrobial use; AMR, antimicrobial resistance; $nCR_{E.\ coli}$, number of antimicrobial classes to which an *E. coli* isolate was resistant; nDDDvetCA, number of defined daily doses in animals using Canadian standards.

to characterize if an exposure to an antimicrobial class via a given route could impact AMR differently. This analysis was important for providing context on potential shifts in AMU practices (e.g., feed to water, elimination of parenteral uses) as it relates to the turkey sector's AMU strategy (The turkey farmers of Canada).

AMR- $AMU_{route-disease-specific}$. In addition to the route of administration, disease indication of use was an additional

attribute of the AMU component in this analysis. The purpose of this exercise was to assess if certain routes of administration for treating a given disease condition could also alter AMR differently. As above, the AMR indicator was individual class level resistance for the logistic models and $nCR_{E.\ coli}$ for the Poisson models.

To account for the time-at-risk in the Poisson models, the natural log-transformed age of the birds at the time of sampling was used as an offset. To evaluate the overdispersion of any of the models, a goodness-of-fit chi-squared test was performed.

Each 4-level mixed-effect regression model accounted for clustering and included the contact network of the veterinarians ("sampling network" variable which represents the participating sentinel farms within the veterinary practice), year, and flock as random intercepts. The hierarchical structure of the 4-level nested models included isolates at the lowest, flocks at the second, sampling year at the third, and sampling network at the highest level.

The model building consisted of two steps. First, univariable 4-level regression models were built, and variables with a liberal $p$-value ($p < 0.20$) were offered to a multivariable model. To assess collinearity between AMU variables, a Pearson correlation analysis was performed and examined the coefficients. When highly correlated (rho = 0.8) variables were identified, the variable with the smaller $p$-value was included in the multivariable model.

In the second step, a multivariable 4-level regression model was built using a manual stepwise backward elimination method. All significant ($p$-value $\leq 0.05$) predictor variables were retained in the final multivariable models. When eliminating non-significant variables, the whole and reduced models were compared by assessing the AIC and BIC values, and models with smaller values were considered a better fit. Each final multivariable model was checked for influential observations, normality of residuals, homogeneity of variance, and collinearity among predictor variables using the sjplot package in R software. The normality of random effects was also evaluated using the same package. The Poisson models were checked for overdispersion and inflated zeros. Interaction terms between predictor variables significant in the final multivariable models have been evaluated.

For all model outcomes (odds ratio (OR) for the logistic regression models and incidence rate ratio (IRR) for the Poisson models), 95% confidence intervals and $p$-values were presented. To interpret the findings, when the $p$-value was significant ($p$-value $\leq 0.05$), an OR of $< 1$ indicated that the probability of resistance decreased with decreased AMU, and if $> 1$ then the probability of resistance increased with increased AMU. An IRR of $< 1$ indicated a decrease and $> 1$ indicated an increase in the $nCR_{E.\ coli}$ with each additional unit increase in AMU (nDDDvetCA/1,000 kg-animal days at risk).

Unexplained variance components were also examined at each level (sampling network, year, flock, isolate) of the model, assuming that level 1 (isolate) variance on the logit scale was: $\pi^2 \div 3 = 3.29$; where $\pi = 3.14$ (Snijders and Bosker, 2011). The random effects' impact was shown as none, negligible, moderate, or high based on the variances of 0, 0.01–0.15, 0.16–0.69, >0.69, respectively.

# Results

## Summary of antimicrobial use and antimicrobial resistance outcomes in turkey flocks

### Isolate-level antimicrobial resistance

There were 1,317 *E. coli* isolates recovered from pooled fecal samples collected between 2016 and 2019 from 334 turkey flocks by 16 veterinarians across the five major turkey-producing Canadian provinces. Of the 334 flocks, two *E. coli* isolates were recovered from one flock, three isolates each from 17 flocks, and four isolates each from the remaining 316 flocks. Four antimicrobial classes with at least a 5% prevalence of resistance, including tetracyclines (61.7%), aminoglycosides (45.0%), folate pathway inhibitors (30.4%), and beta-lactams (31.2%) were included in the analysis. Out of 1,317 *E. coli* isolates, 363 were susceptible to all the 7 tested antimicrobial classes, whereas 237 isolates were resistant to one, 301 isolates to two, and 416 (31.6%) isolates resistant to at least 3 or more antimicrobial classes. Resistance to antimicrobial classes in *E. coli* isolated from flocks with no antimicrobial use during the study was detected. In these flocks, a total of 46.73% of isolates were resistant to tetracyclines, 31.55% to aminoglycosides, 21.43% to folate pathway inhibitors, and 17.86% to beta-lactams, respectively (**Supplementary Table 2**).

### Flock-level antimicrobial use

Flock-level nDDDvetCA/1,000 kg-animal days at risk by antimicrobial class are summarized in **Table 1**. There were eight antimicrobial classes used in turkey flocks during the study period. The AMU in these flocks were reported for treatment or prevention of colibacillosis (yolk sac infections, omphalitis, and neonatal septicemia) via injection, for late-stage septicemia via feed or water, and for enteric diseases (necrotic enteritis and non-specific enteric syndromes) via feed or water.

The number of individual antimicrobial classes used on farms varied ($n$ = 42 unique patterns of use), and the three most frequently occurring patterns were the use of bacitracin ($n$ = 55), aminoglycosides-streptogramins ($n$ = 36), and bacitracin-aminoglycosides ($n$ = 32) (**Supplementary Table 3**).

The six antimicrobial classes: tetracyclines, aminoglycosides, folate pathway inhibitors, beta-lactams, bacitracin, and streptogramins were used in a minimum of five percent of the turkey flocks and therefore were included in the regression analysis as predictor variables.

TABLE 1 Quantity, administration route, and disease indication of antimicrobial use (AMU)[1] in Canadian turkey flocks ($n$ = 334) between 2016 and 2019.

| Antimicrobial class (antimicrobial active ingredients)[2] | Administration route (reasons for use) | Number of flocks (%) | AMU mean | AMU range | Included in regression models |
|---|---|---|---|---|---|
| Aminoglycosides (gentamicin; neomycin and streptomycin[3]) | Injection/water *(yolk sac infection or any colibacillosis[4])* | 121 (36.2) | 0.12 | 0.0–15.5 | Yes |
| Bacitracin (*bacitracin methylene disalicylate [BMD]*) | Feed/ *(necrotic enteritis)* | 137 (41.0) | 30.65 | 0.0–180.9 | Yes |
| Beta-lactams (*amoxicillin; penicillin G procaine; penicillin G potassium*) | Feed/water *(yolk sac infection or any colibacillosis and enteric)* | 39 (11.7) | 1.13 | 0.0–119.5 | Yes |
| Fluoroquinolones (*enrofloxacin*) | Water *(any colibacillosis)* | 4 (1.2) | 0.002 | 0.0–0.454 | No |
| Folate pathway inhibitors *(trimethoprim and sulfadiazine; sulfa quinoxaline; sulfa quinoxaline-pyrimethamine combination)* | Feed/water *(late-stage septicemia, respiratory)* | 21 (6.3) | 7.60 | 0.0–312.1 | Yes |
| Macrolides *(tylosin)* | Feed *(enteric)* | 7 (2.1) | 0.18 | 0.0–15.8 | No |
| Orthosomycins *(avilamycin)* | Feed *(enteric)* | 10 (3.0) | 1.53 | 0.0–74.7 | No |
| Streptogramins *(virginiamycin)* | Feed *(enteric)* | 93 (27.8) | 28.35 | 0.0–265.8 | Yes |
| Tetracyclines *(chlortetracycline; oxytetracycline and tetracycline)* | Water/feed *(enteric, early and late septicemia and respiratory)* | 20 (6.0) | 1.34 | 0.0–107.1 | Yes |

[1]Measured as the number of Canadian-defined daily doses using Canadian standards [nDDDvetCA]/1,000 kg-animal days at risk. The median for each class is 0.
[2]Other AMU exposure characteristics including dose or inclusion rates (range), weight at treatment, and duration of exposures have been described elsewhere (Agunos et al., 2019).
[3]Neomycin and streptomycin are in combination products oxy-/tetracycline and penicillin-streptomycin, respectively.
[4]Colibacillosis – pertains to any disease syndrome caused by avian pathogenic *E. coli* such as neonatal diseases (yolk sac infection and early septicemia) and their chronic sequelae including complex bacterial infections/late-stage septicemia and respiratory diseases.

## Associations between antimicrobial resistance and antimicrobial use

Tetracyclines, aminoglycosides, folate pathway inhibitors, and beta-lactams were the only classes with resistance in > 5% of the isolates and were therefore included as outcome variables of interest in the regression analysis. The transformations of the continuous variables did not improve the model estimates; therefore we used the untransformed continuous AMU variables in all of our models. The best-fitting model for the $nCR_{E.\ coli}$ outcome was the Poisson model.

Results of the univariable mixed-effects logistic regression models are presented in **Supplementary Tables 4–6**, and the results of the univariable mixed-effects Poisson models are presented in **Supplementary Table 7**, respectively.

The final multivariable mixed effect models are presented below. No interaction terms among the variables included in the multivariable models were significant.

## $AMR\text{-}AMU_{anyroute}$ associations

The results of the multivariable mixed-effects logistic regression models evaluating associations among the homologous AMR outcome and the $AMU_{anyroute}$ predictors are shown in **Table 2a**, while the results of the multivariable mixed-effects Poisson regression model for the associations among the alternate AMR outcome, $nCR_{E.\ coli}$, and $AMU_{anyroute}$ are shown in **Table 2b**.

## $AMR\text{-}AMU_{anyroute}$ – logistic regression models

Significant associations were observed between aminoglycosides resistance and the use of two unrelated classes of antimicrobials (folate pathway inhibitors and bacitracin), however, effect estimates (ORs and 95% CI's) were very small. Similar effect estimates were noted in other AMR-AMU pairs examined (**Tables 2a,b**), Two homologous AMU-AMR pairs (folate pathway inhibitors resistance-folate pathway inhibitors use; tetracycline resistance-tetracycline use) showed significant association. However, it is important to note that in all the models examined, OR estimates were comparable (minimal difference in ORs) and approached an OR of 1 in the vast majority of the AMU-AMR pairs assessed. For example, if the use of folate pathway inhibitors was reduced by 25%, from the current mean of 7.6 to 5.7 nDDDvetCA/1,000 kg-animal days at risk, in the absence of changes to any other factors in the model, the odds of an *E. coli* isolate being resistant: to aminoglycosides would decrease by 0.017, to beta-lactams would decrease by 0.015, and to folate pathway inhibitors would decrease by 0.024.

## $nCR_{E.\ coli}$ – $AMU_{anyroute}$ – Poisson regression model

The use of four classes (tetracyclines, bacitracin, streptogramins, and folate pathway inhibitors) significantly increased $nCR_{E.\ coli}$. As with the above analysis, the IRR

TABLE 2a Multivariable mixed-effects logistic regression models showing associations between antimicrobial use via any route of administration in turkey flocks ($n$ = 334) and homologous and multiclass resistance in *E. coli* isolates ($n$ = 1,317), 2016–2019.

| Antimicrobial resistance models | $AMU_{anyroute}$[1] | Coefficient | Odds ratio (95% CI) | $p$-value | Random intercepts[2] | Variances (Std. dev) |
|---|---|---|---|---|---|---|
| 1. Aminoglycosides | Bacitracins | 0.004 | 1.004 (1.000–1.008) | 0.042 | Sampling network | 0.035 (0.186) |
| | Folate pathway inhibitors | 0.009 | 1.009 (1.004–1.014) | <0.000 | Year: Sampling network | 0.118 (0.343) |
| | Intercept | 0.474 | 0.622 (0.473–0.819) | 0.001 | Flock: Year: Sampling network | 0.890 (0.943) |
| 2. Beta-lactams | Folate pathway inhibitors | 0.007 | 1.008 (1.002–1.013) | 0.003 | Sampling network | 0.144 (0.379) |
| | Streptogramins | 0.004 | 1.004 (1.000–1.007) | 0.027 | Year: Sampling network | 0.001 (0.033) |
| | Tetracyclines | 0.021 | 1.021 (1.001–1.042) | 0.039 | Flock: Year: Sampling network | 1.149 (1.072) |
| | Intercept | 1.261 | 0.283 (0.209–0.384) | 0.000 | | |
| 3. Folate pathway inhibitors | Folate pathway inhibitors | 0.015 | 1.013 (1.008–1.018) | <0.000 | Sampling network | 0.000 (0.000) |
| | Intercept | 1.029 | 0.344 (0.289–0.41) | <0.000 | Year: Sampling network<br>Flock: Year: Sampling network | $1.355e^{-09}$<br>($3.681e^{-05}$)<br>0.682 (0.826) |
| 4. Tetracyclines | Bacitracins | 0.006 | 1.006 (1.002–1.01) | 0.002 | Sampling network | 0.000 (0.000) |
| | Streptogramins | 0.003 | 1.004 (1.001–1.007) | 0.014 | Year: Sampling network | 0.176 (0.420) |
| | Tetracyclines | 0.076 | 1.087 (1.031–1.145) | 0.002 | Flock: Year: Sampling network | 0.388 (0.623) |
| | Intercept | 0.159 | 1.223 (0.965–1.551) | 0.106 | | |

[1] $AMU_{anyroute}$ – Antimicrobial use across all routes, in the number of defined daily doses using Canadian standards/1,000 kg-animal days at risk.
[2] Four levels: isolates at the lowest, flocks at the second, years at the third, and sampling network at the highest level. Level 1 variance was assumed to be 3.29 (Snijders and Bosker, 2011).
CI, confidence interval. Only significant associations were shown in the Table. Sampling network – pertains to the sentinel veterinary practice-producer contact networks within their province/region of practice.

TABLE 2b Multivariable mixed-effects Poisson regression models show associations between antimicrobial use via any route of administration ($AMU_{anyroute}$[1]) in turkey flocks ($n$ = 334) and resistance to the number of antimicrobial classes in *E. coli* isolates ($nCR_{E.\ coli}$) ($n$ = 1,317), 2016–2019.

| AMU classes | Coefficient | IRR (95% CI) | $p$-value | Random Intercepts | Variances[2] (std. dev) |
|---|---|---|---|---|---|
| Bacitracin | 0.003 | 1.003 (1.002–1.005) | <0.000 | Sampling network | $2.56e^{-35}$<br>($1.27e^{-19}$) |
| Folate pathway inhibitors | 0.003 | 1.003 (1.002–1.005) | <0.000 | Year: Sampling network | 0.015 (0.121) |
| Streptogramins | 0.003 | 1.003 (1.002–1.004) | <0.000 | Flock: Year: Sampling network | 0.134 (0.366) |
| Tetracyclines | 0.010 | 1.010 (1.003–1.016) | 0.003 | | |
| Intercept | −4.229 | 0.015 (0.013–0.016) | <0.000 | | |

[1] $AMU_{anyroute}$ – Antimicrobial use across all administration routes, in number of defined daily doses using Canadian standards/1,000 kg-animal days at risk.
IRR, incidence rate ratio; CI, confidence interval.
[2] Four levels: isolates at the lowest, flocks at the second, years at the third, and veterinarians at the highest level. Level 1 variance was assumed to be 3.29 (Snijders and Bosker, 2011).

estimates were relatively similar across the 4 AMU-AMR pairs modeled and approached an IRR of 1. The predicted marginal effects of antimicrobial use on $nCR_{E.\ coli}$ of turkeys showed an increasing trend with the increase in the quantity of AMU (Figure 2). Again, using folate pathway inhibitors as an example, if the quantity of folate pathway inhibitors were to increase from 90 to 220 nDDDvetCA/1000 kg-animal days at risk, without changes to any other predictors in the model, the incidence of antimicrobial classes that are resistant would increase from 2 to 3.

The model diagnostics for the Poisson model, including normality of residuals, influential observations, collinearity among predictor variables, and homogeneity of variance are presented in Supplementary Figure 1. All residuals were normally distributed and no influential observations were detected. No collinearity among predictor variables and no major issues with homogeneity of variance were detected. The diagnostic plots that assessed the normality of the random effects (sampling network, year, flocks) of the models are presented in Supplementary Figure 2. The residuals of the random effects were normally distributed.

Analysis of the unexplained variance components residing at each level of the mixed-effects regression models indicated that the sampling network have a negligible effect in all of the models, except for the model of resistance to aminoglycosides (Table 2a); whereas year had no effect or

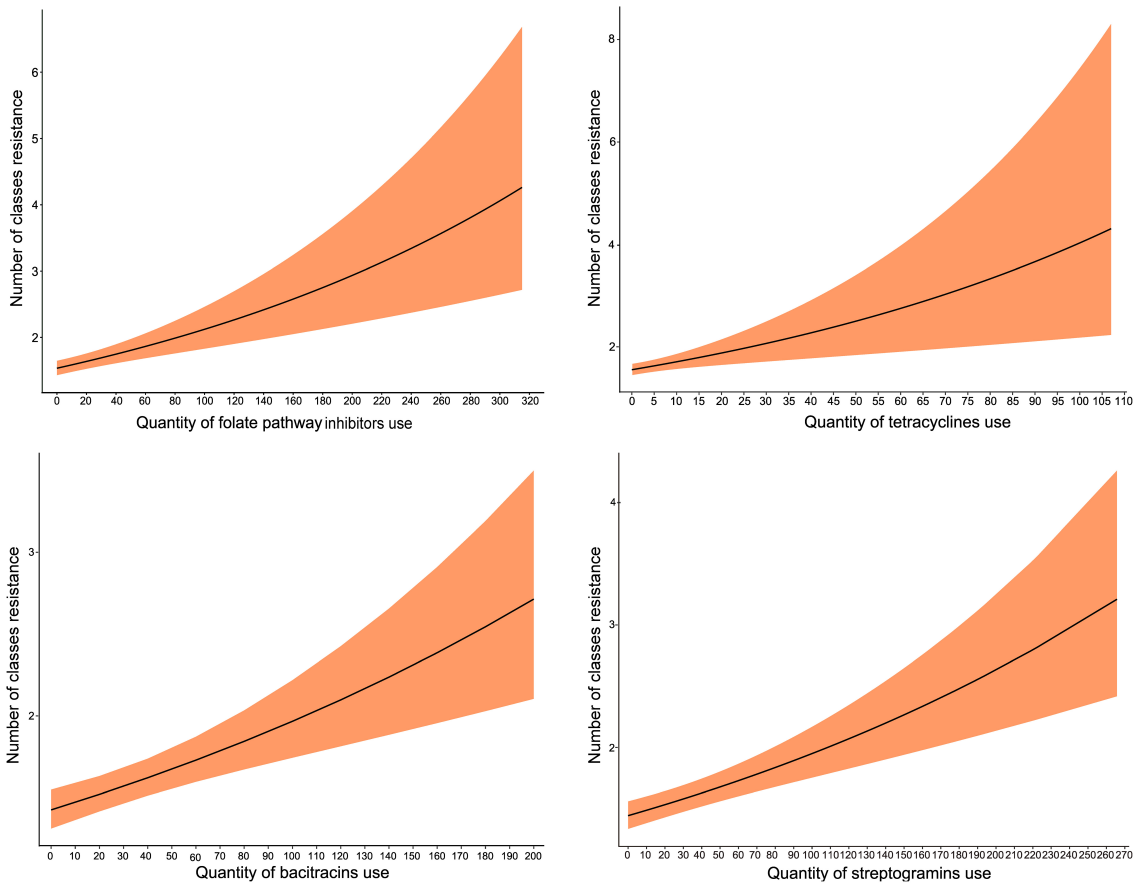


FIGURE 2
Predicted marginal effects of antimicrobial use on the incidence of resistance to the number of antimicrobial classes in *E. coli* isolates ($nCR_{E.\ coli}$) of turkeys. The antimicrobial used was represented by the number of defined daily doses per 1,000 kg-animal days at risk.

had a moderate effect depending on the models. The largest unexplained variances resided at the flock and the isolate levels across all models.

## AMR and $AMU_{route-specific}$ associations

The results of the multivariable mixed-effects logistic regression models assessing the linkages between AMU via specific administration routes and AMR are presented in **Table 3a**. **Table 3b** shows the results of the mixed-effects Poisson regression model using the alternate AMR outcome, $nCR_{E.\ coli}$.

## AMR- $AMU_{route-specific}$ – logistic regression models

The odds of resistance to tetracyclines were increased by using injectable aminoglycosides, in-feed use of folate-pathway inhibitors, and tetracyclines. The highest magnitude of OR estimates was observed for aminoglycoside use (aminoglycosides > folate pathway inhibitors > tetracyclines). A significant association was noted between the unrelated AMR-AMU pairs (beta-lactams resistance-streptogramins use in feed; aminoglycosides resistance and in feed use of two unrelated classes), however, OR is slightly more than 1 (by three decimals) in these models. It also indicates that if there is a 25% decrease in the mean use of injectable aminoglycosides (from 0.12 to 0.09 nDDDvetCA/1,000 kg animal days at risk), the odds of resistance to tetracyclines will decrease by 0.06 given other variables remain constant. A significant association was observed for the homologous pair (folate pathway inhibitors resistance-folate pathway inhibitor use via feed) but OR estimate similarly approached 1.

## $nCR_{E.\ coli}$-$AMU_{route-specific}$ – Poisson regression model

The $nCR_{E.\ coli}$ significantly increased by the injectable use of aminoglycosides (IRR = 2.585), and in-feed use of four

TABLE 3a Multivariable mixed-effects logistic regression models showing associations between antimicrobial use via specific administration routes in turkey flocks ($n$ = 334) and homologous and multidrug-resistant *E. coli* isolates ($n$ = 1,317), 2016–2019.

| Antimicrobial resistance models | $AMU_{route-specific}$[1] | | Coefficient | Odds ratio (95% CI) | $p$-value | Random intercepts | Variances[2] (Std. dev) |
|---|---|---|---|---|---|---|---|
| 1. Aminoglycoside | Feed | Bacitracin | 0.004082 | 1.004 (1.000–1.008) | 0.040 | Sampling network | 0.118 (0.343) |
| | Feed | Folate pathway inhibitors | 0.009117 | 1.009 (1.004–1.014) | <0.000 | Year: Sampling network | 0.035 (0.186) |
| | Intercept | | 0.474326 | 0.622 (0.473–0.819) | 0.001 | Flock: Year: Sampling network | 0.890 (0.943) |
| 2. Beta-lactams | Feed | Streptogramins | 0.003616 | 1.004 (1.000–1.007) | 0.040 | Sampling network | 0.126 (0.355) |
| | Intercept | | −1.161782 | 0.313 (0.234–0.419) | <0.000 | Year: Sampling network<br>Flock: Year: Sampling network | 0.019 (0.140)<br>1.242 (1.115) |
| 3. Folate pathway inhibitors | Feed | Folate pathway inhibitors | 0.013239 | 1.013 (1.008–1.018) | <0.000 | Sampling network | 0.000 (0.000) |
| | Intercept | | −1.066113 | 0.344 (0.289–0.410) | <0.000 | Year: Sampling network<br>Flock: Year: Sampling network | $1.356e^{-09}$ ($3.681e^{-05}$)<br>0.686 (0.826) |
| 4. Tetracyclines | Injectable | Aminoglycosides | 2.05768 | 7.66 (1.46–40.18) | 0.016 | Sampling network | 0.007 (0.082) |
| | Feed | Folate pathway inhibitors | 0.14802 | 1.160 (1.029–1.306) | 0.015 | Year: Sampling network | 0.185 (0.430) |
| | Feed | Tetracyclines | 0.07489 | 1.078 (1.024–1.134) | 0.004 | Flock: Year: Sampling network | 0.389 (0.624) |
| | Intercept | | 0.34121 | 1.407 (1.144–1.730) | 0.001 | | |

[1]$AMU_{route-specific}$ – antimicrobial use disaggregated by routes of administration in the number of defined daily doses using Canadian standards/1,000 kg-animal days at risk.
[2]Four levels: isolates at the lowest, flocks at the second, years at the third, and veterinarians at the highest level. Level 1 variance was assumed to be 3.29 (41).
CI, confidence interval. Only significant associations were shown in the Table. Sampling network – pertains to the sentinel veterinary practice-producer contact networks where each of the practices sampled amongst their turkey client contacts within their province.

TABLE 3b Multivariable mixed-effects Poisson regression models showing associations between antimicrobial use via specific routes of administration in turkey flocks ($n$ = 334) and resistance to the number of antimicrobial classes in *E. coli* isolates ($nCR_{E.\ coli}$; $n$ = 1,317) of turkeys, 2016–2019.

| $AMU_{route-specific}$[1] | | Coefficient | IRR (95% CI) | $p$-value | Random Intercepts | Variances[2] (std. dev) |
|---|---|---|---|---|---|---|
| **Route** | **AMU classes** | | | | | |
| Feed | Bacitracin | 0.003 | 1.003 (1.001–1.004) | <0.000 | Sampling network | $7.525e^{-16}$ ($2.743e^{-08}$) |
| Feed | Folate pathway inhibitors | 0.003 | 1.003 (1.002–1.004) | <0.000 | Year: Sampling network | 0.013 (0.116) |
| Feed | Streptogramins | 0.002 | 1.002 (1.001–1.004) | 0.001 | Flock: Year: Sampling network | 0.129 (0.360) |
| Feed | Tetracyclines | 0.009 | 1.009 (1.003–1.016) | 0.004 | | |
| Injection | Aminoglycosides | 0.950 | 2.585 (1.313–5.091) | 0.006 | | |
| Intercept | | −4.239 | 0.014 (0.013–0.016) | <0.000 | | |

[1]$AMU_{route-specific}$ – antimicrobial use disaggregated by routes of administration in the number of defined daily doses using Canadian standards/1,000 kg-animal days at risk. IRR, incidence rate ratio; CI, confidence interval.
[2]Four levels: isolates at the lowest, flocks at the second, years at the third, and sampling network at the highest level. Level 1 variance was assumed to be 3.29 (Snijders and Bosker, 2011).
Sampling network – pertains to the sentinel veterinary practice-producer contact networks where each of the practices sampled amongst their turkey client contacts within their province.

antimicrobial classes (tetracyclines, folate pathway inhibitors, bacitracin, and streptogramins) but their effect estimates approached 1 (Table 3b). As in previous models, the highest unexplained variance component resided at the isolate and flock levels, whereas there was moderate unexplained variance at the year level and low variance at the sampling network level (Table 3b).

## AMR and $AMU_{route-disease-specific}$ associations

The results of multivariable mixed-effects logistic regression models that evaluated associations of individual class resistances and $nCR_{E.\ coli}$ with the use of any antimicrobial by a specific administration route (feed, water, or injection) to treat or

prevent a specific disease are presented in Figure 3. Table 4 illustrates the results of the multivariable mixed-effects Poisson regression model using the alternate AMR outcome, $nCR_{E.\ coli}$.

### AMR-$AMU_{route-disease-specific}$ – logistic regression models

As shown in Figure 3, the administration of antimicrobials via water for treating enteric diseases had the greatest impact (ORs and 95% CI) on the development of resistance to aminoglycosides and tetracyclines. On the other hand, the use of antimicrobials via feed for treating enteric diseases has the greatest impact on resistance to folate pathway inhibitors and beta-lactam antimicrobials.

The highest variances were observed at the isolate and flock levels. The flock-level variances were 0.78 (standard deviation: 0.88) for aminoglycosides, 1.15 (1.07) for beta-lactams, 0.65 (8.06) for folate pathway inhibitors, and 0.34 (0.58) for tetracyclines models.

### $nCR_{E.\ coli}$-$AMU_{route-disease-specific}$ – Poisson regression model

The $nCR_{E.\ coli}$ significantly increased in turkey flocks treated with antimicrobials via water for enteric diseases and via feed for late septicemia and enteric diseases. Similar to the previous models, there were small variances at the sampling network and year levels (Table 4).

## Discussion

This study builds on previous CIPARS experiences in AMU-AMR data integration and analysis to further explore the relationships between AMU and AMR in indicator *E. coli* from turkey flocks. Accounting for the time the turkeys spent in the barn, and the clustering at the sampling networks (veterinary practices' producer contact network/client list), year, and flock levels, the $nCR_{E.\ coli}$ increased gradually with the increase in the antimicrobial quantity used in turkey flocks. This study identified specific classes of antimicrobials and certain exposure characteristics (disease indications and route of administration) that potentially contribute to AMR emergence. It further highlights the importance of high-resolution AMU data collected from the end-user (reasons for use, route of administration) and the complementarity of different AMR indicators (class-specific and $nCR_{E.\ coli}$) for understanding AMU-AMR linkages.

Comparing our study results to previous studies is difficult because one needs to consider differences in study design (longitudinal or cross-sectional), analytical approaches (isolate-level or flock-level analysis), sample size (large or small number of isolates), AMU indicator used ( dose-, weight- or count-based; class-specific vs. total quantity), health status (disease present in a flock or not), husbandry (conventional vs. reduced antibiotic use program), sampling procedures (on-farm, at slaughter, or diagnostic laboratories), and antimicrobial susceptibility testing (disk diffusion or broth microdilution; clinical breakpoints used).

We identified significant associations between the use of specific antimicrobial classes and the development of AMR in *E. coli* isolates to the same or unrelated antimicrobial classes. However, the odds ratios were positive and slightly more than one in most models, indicating that substantial changes in antimicrobial use may still result in small changes in resistance. The diversity of AMU patterns signifies various AMU practices in turkey flocks ranging from zero or no use (i.e., in raised without antibiotic or organic production), single antimicrobial class to multiple classes that might entail simultaneous or concurrent AMU exposures in turkey flocks. Exposures to $> 1$ antimicrobial class could be a routine practice or could occur in an outbreak situation (i.e., complex bacterial infections with chronic sequelae); it could also be associated with the use of combination products. In our previous analysis, the odds of being a high user of antimicrobials in turkeys were significantly higher for those that used any antimicrobial via water and those that used folate pathway inhibitors, bacitracin, and tetracyclines. These findings highlight the potential role of co-selection for resistance or selection for fitness of specific AMR strains and could be explained by the co-location and transmission of antimicrobial resistance genes on mobile genetic elements (e.g., plasmids or integrons) (Johnson et al., 2012; Sheikh et al., 2012; Ahmed et al., 2013; Cazer et al., 2019; Ramadan et al., 2021). Another potential explanation is that the long-term use of antimicrobials (e.g., bacitracin for prevention of necrotic enteritis) may alter the population of antimicrobial-resistant strains in the gut flora (Agunos et al., 2020) interfering with the succession of the microbial population from resistant toward a more susceptible population. This might also explain why changes in AMU practices do not always follow the development of AMR (Sheikh et al., 2012; Cheng et al., 2019).

As previously demonstrated, once resistance to individual and multiple antimicrobial classes is developed, MDR *E. coli* isolates can persist in the environment (Maal-Bared et al., 2013; Aslam et al., 2021; Bell et al., 2021) and can transmit their AMR determinants to other enteric bacteria (Allocati et al., 2013; Bakkeren et al., 2019; Cheng et al., 2019). In the EU following the ban on the use of glycopeptide antimicrobials for growth promotion, sustained levels of glycopeptide-resistant *Enterococcus faecium* (GRE) in pigs were detected and observance of an abrupt decline only occurred upon the phasing out of other antimicrobials such as macrolides (Aarestrup et al., 2001). It is also important to reassess the

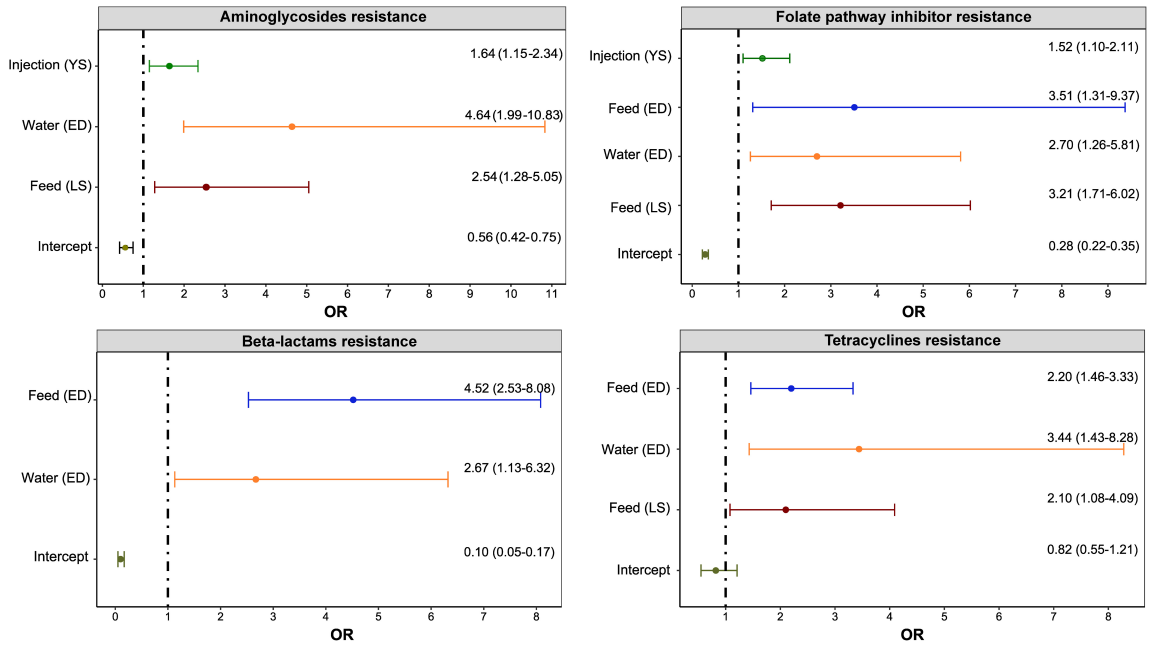


FIGURE 3
Significant associations between antimicrobial use via a specific route for a specific disease and resistance to antimicrobial classes in *E. coli* isolates ($n$ = 1,317) of turkeys. Any antimicrobial class used on the Canadian turkey flocks was included in the multivariable mixed-effects logistic regression model with flocks, years, and sampling networks included as random intercepts. The figure included only significant associations determined. The $x$-axes show an odds ratio (OR) that is represented as a point and the line represents the 95% Confidence Intervals. The $y$-axes with "(YS)" represent yolk saculitis, "(ED)" – enteric diseases, and "(LS)" – late-stage septicemia.

**TABLE 4** Multivariable mixed-effects Poisson regression models showing associations between route and disease-specific antimicrobial use in turkey flocks ($n$ = 334) and resistance to the number of antimicrobial classes in *E. coli* isolates ($n$ = 1,317), 2016–2019.

| $AMU_{route-\ and\ disease-specific}$[1] | | Estimate | IRR (95% CI) | p-value | Random intercepts | Variances[2] (std. dev) |
|---|---|---|---|---|---|---|
| **Route** | **Disease** | | | | | |
| Feed | Late septicemia | 0.336 | 1.398 (1.109–1.763) | 0.004 | Sampling network | (0.000) |
| Feed | Enteric diseases | 0.400 | 1.492 (1.244–1.788) | <0.000 | Year: Sampling network | 0.033 (0.181) |
| Water | Enteric diseases | 0.538 | 1.712 (1.300–2.254) | <0.000 | Flock: Year: Sampling network | 0.129 (0.360) |
| Intercept | | −4.396 | 0.012 (0.010–0.015) | <0.000 | | |

[1] $AMU_{route-disease-specific}$ – Antimicrobial use in the model above is a binomial indicator of whether the flock used the antimicrobial via a given route for a specific disease syndrome. IRR, incidence rate ratio; CI, confidence interval.
[2] Four levels: isolates at the lowest, flocks at the second, years at the third, and veterinarians at the highest level. Level 1 variance was assumed to be 3.29 (Snijders and Bosker, 2011).

impact of the intervention with aggravating health challenges in the field as a result of the elimination of certain classes that may prompt producers to shift from prophylactic/metaphylactic to therapeutic uses (thus, higher tetracyclines, folate pathway inhibitors, beta-lactam penicillins, and aminoglycosides). For example, in the EU, the ban on antimicrobial growth promoters necessitated the use of antimicrobials belonging to aminopenicillins to control necrotic and non-specific enteritis (dysbacteriosis), contributing to the maintenance of beta-lactam resistance (Casewell et al., 2003). Additional surveillance data (beyond the timeframe included in this study) are necessary to understand how the progressive elimination of antimicrobials, are shifting the turkey gut/environment flora and the factors that might delay the succession of susceptible *E. coli* strains.

The administration of antimicrobials via various routes did affect the emergence of AMR in the *E. coli* isolates differently. Given multiple mechanisms underlying the development of AMR (Cheng et al., 2019), it is important to characterize the effects of each administration route to inform the enhancements of stewardship in the poultry sector. For example, reduction targets could include antimicrobials used for treatment or the promotion of enhanced integrated health management

(biosecurity and vaccination). In this regard, the AMU indicator to be used should be able to detect the changes in AMU practices. Dose and duration of exposures vary by route of administration, for example, injection is administered only once in the life of the flock, whereas a treatment course via water could be from 2 to 5 days and medicated feed rations could be administered in a single to multiple rations (one full growing cycle) (Agunos et al., 2020). As previously described, CIPARS developed route-specific DDDvetCA standards to account for dosing variations by route of administration (Bosman et al., 2019) to better capture the shifts in AMU practices. As noted by previous researchers (Collineau et al., 2017), the exact exposure characteristics that are most influential on the selection pressure of AMR are yet to be determined.

A robust association was noted between aminoglycosides use (mainly gentamicin) through injections and tetracycline-resistant *E. coli*. Historically, the widespread use of aminoglycosides at the hatchery was intended to prevent neonatal diseases (i.e., colibacillosis and its sequelae). Previous use of injectable gentamicin may have exerted co-selection of AMR in *E. coli* resulting in tetracycline resistance. The treatment uses of combination products via water (neomycin-oxy-/tetracycline combination products), in part, could also play a role. In response to the Turkey Farmers of Canada's AMU reduction policy, the preventive use of gentamicin was no longer allowed by 2019. Having only 1 year of post-AMU intervention data in the study timeframe, the long-term impact of gentamicin use on the gut and environmental flora of turkeys warrants ongoing monitoring of AMU and AMR. With the elimination of injectable gentamicin use, the potential for a compensatory increase in aminoglycosides administered via other routes will need to be monitored through surveillance.

It is important to identify the most common turkey infectious diseases that initiated the use of different antimicrobial classes and consequently affect the development of AMR. Our previous analysis indicated an increase in enteric and neonatal diseases (colibacillosis and its sequelae) consistent with the timing of the removal of the preventive use of certain antimicrobial classes intended for these syndromes (Burow et al., 2014). This present study indicated that in-feed use of antimicrobials for the prevention and treatment of enteric diseases were most influential in the development of resistance to folate pathway inhibitors, beta-lactams, and tetracyclines. Thus, non-antimicrobial and flock health interventions directed toward the prevention of these diseases are essential.

A recent study has shown the impact of short-term AMU on the development of AMR (Luiken et al., 2019). In our study, the use of antimicrobials via injections to prevent colibacillosis increased the odds of resistance to aminoglycosides and folate pathway inhibitors. As injectable antimicrobials were historically used at the hatchery level (upon hatch), this finding could be explained by the effect of the short-term use of aminoglycosides such as gentamicin.

Our study used a novel approach by building multivariable mixed-effects Poisson regression models, which are ideal for assessing the influence of exposure to antimicrobials on the development of resistance to multiple antimicrobial classes. Compared to the logistic regression model's binary outcome (resistant or susceptible), the Poisson model allowed us to use an outcome variable $nCR_{E.coli}$ that signified the number of antimicrobial classes to which an *E. coli* isolate was resistant. Moreover, we accounted for the time of exposure by including the natural log-transformed age of turkeys at the time of sampling as an offset. Previous studies also demonstrated the effect of simultaneous use of more than one antimicrobial on the development of MDR bacteria (Johnson et al., 2012; Simoneit et al., 2015).

To identify intervention targets, we evaluated the unexplained variance components residing at each level (sample, flock, year, and sampling network) of our mixed-effects regression models. Flocks had the highest variances in all of the models, suggesting flock-level AMU interventions might have the highest impact on reducing the emergence of AMR in *E. coli* isolates. Besides, the odds ratios of AMU predictor variables were close to 1 indicating that an overall reduction in AMU across multiple antimicrobial classes might be needed to decrease AMR. There were negligible to moderate variance components residing at the year level, suggesting that AMU practices did not differ substantially over time. However, the data used include only one-year post-AMU reduction intervention (2019) and thus requires the reevaluation of farm data in subsequent years to fully assess the impact of the turkey sector's AMU strategy. Despite our study showing a negligible to low effect of sampling network on the emergence of AMR in *E. coli* isolates of turkey flocks, veterinarians have an important role in implementing antimicrobial stewardship programs to mitigate the emergence of antimicrobial-resistant bacteria.

The scope of this study was to evaluate associations among the flock-level AMU in turkeys and the development of phenotypic antimicrobial resistance in *E. coli* isolates. Future studies should evaluate the genetic determinants of AMR and identify genetic elements associated with the co-selection of AMR. Our study also identified AMR in *E. coli* isolated from flocks with no previous antimicrobial use history (e.g., tetracyclines and aminoglycosides resistance), stressing the importance of future studies to identify additional risk factors besides AMU (aspects of biosecurity including downtime/rest period, cleaning and disinfection and use of premise disinfectants) that impact the development of AMR. In addition, future studies should evaluate the effectiveness of antimicrobial alternatives (e.g., prebiotics, probiotics) (Brown et al., 2017; Fuhrmann et al., 2022; Reddy et al., 2022) to reduce the emergence of resistance to individual and multiple antimicrobial classes. This study methodology could be used to evaluate the AMU-AMR linkages in other animals as well as in humans.

## Conclusion

This study showed that the flock-level use of antimicrobial classes impacted the emergence of AMR to the same or unrelated antimicrobial classes, highlighting that mechanisms independent of AMU are playing a role (e.g., co-selection or alteration in the gut flora responsible for the perpetuation of resistant strains). This study further highlights the utility of a dose-based AMU indicator in AMU-AMR association studies; the indicator accounted for the average daily doses specific to the antimicrobial, the exposure period, and the weight of birds, which is an ideal method to evaluate the impact of AMU on the prevalence of AMR over the lifetime of turkeys. The use of aminoglycosides administered via injections had the highest impact on homologous resistances. In-feed use of bacitracin, streptogramins, folate pathway inhibitors, and tetracyclines appear to be playing a role in the perpetuation of resistance in turkey flocks. Given that these antimicrobial classes are indicated for specific disease syndromes (enteric disease and late septicemia), infection prevention control measures for the reduction of these diseases are necessary to offset the need for AMU. Flocks had the highest variances in all of the models; from an AMU stewardship perspective, interventions at the producer level might have the highest impact on reducing the emergence of AMR in *E. coli* isolates. At the turkey industry level, reassessment of the AMU reduction strategy on flock health, particularly, trends in the diagnosis of diseases and shifts from preventive to therapeutic AMU would inform additional stewardship measures in addition to an ongoing AMU/AMR surveillance.

## Data availability statement

The datasets presented in this article are not readily available because data requests should be sent to the Public Health Agency of Canada. Requests to access the datasets should be directed to AA, agnes.agunos@phac-aspc.gc.ca.

## Ethics statement

Ethical review and approval was not required for the animal study because there were no animal experiments conducted for this research. An informed consent form was administered by the veterinarian to their producers before the flock visit.

## Author contributions

RS: study design, data analysis, writing – prepared initial draft, review, editing, and visualization. AA: writing – review, editing, resources, and project administration. SG and AD: writing – review and editing, and resources. CV: study design, data analysis, writing – prepared initial draft, review, editing, project administration, and supervision. All authors contributed to the article and approved the submitted version.

## Funding

The Public Health Agency of Canada funded and administered the CIPARS Farm Surveillance. Partial funding was also received from Saskatchewan Agriculture, the Ontario Ministry of Agriculture, Food and Rural Affairs, the Canadian Poultry Research Council, and Alberta Agriculture and Forestry. RS and CV were supported by a start-up fund of the Department of Pathobiology, College of Veterinary Medicine, the University of Illinois at Urbana-Champaign. The funders had no role in the study design, data analyses, and interpretation, in the writing of the manuscript, and in the decision of publishing the results.

## Acknowledgments

We would like to thank the producers for their consent and participation in the CIPARS Farm Surveillance and acknowledge the veterinarians for enabling sample and data collection.

## Conflict of interest

The authors declare that the research was conducted in the absence of any commercial or financial relationships that could be construed as a potential conflict of interest.

## Publisher's note



## Supplementary material

The Supplementary Material for this article can be found online at: https://www.frontiersin.org/articles/10.3389/fmicb.2022.954123/full#supplementary-material

# References


Aarestrup, F. M., Seyfarth, A. M., Emborg, H. D., Pedersen, K., Hendriksen, R. S., and Bager, F. (2001). Effect of abolishment of the use of antimicrobial agents for growth promotion on occurrence of antimicrobial resistance in fecal enterococci from food animals in Denmark. *Antimicrob. Agents Chemother.* 45, 2054–2059. doi: 10.1128/AAC.45.7.2054-2059.2001

Agunos, A., Gow, S. P., Deckert, A. E., Kuiper, G., and Léger, D. F. (2021a). Informing Stewardship Measures in Canadian Food Animal Species through Integrated Reporting of Antimicrobial Use and Antimicrobial Resistance Surveillance Data—Part I. Methodology Development. *Pathogens* 10:1492. doi: 10.3390/pathogens10111492

Agunos, A., Gow, S. P., Deckert, A. E., and Léger, D. F. (2021b). Informing Stewardship Measures in Canadian Food Animal Species through Integrated Reporting of Antimicrobial Use and Antimicrobial Resistance Surveillance Data—*Part II.* Application. *Pathogens* 10:1491. doi: 10.3390/pathogens10111491

Agunos, A., Gow, S. P., Léger, D. F., Carson, C. A., Deckert, A. E., Bosman, A. L., et al. (2019). Antimicrobial Use and Antimicrobial Resistance Indicators—Integration of Farm-Level Surveillance Data From Broiler Chickens and Turkeys in British Columbia, Canada. *Front. Vet. Sci.* 6:131. doi: 10.3389/fvets.2019.00131

Agunos, A., Gow, S. P., Léger, D. F., Deckert, A. E., Carson, C. A., Bosman, A. L., et al. (2020). Antimicrobial Use Indices—The Value of Reporting Antimicrobial Use in Multiple Ways Using Data From Canadian Broiler Chicken and Turkey Farms. *Front. Vet. Sci.* 7:567872. doi: 10.3389/fvets.2020.567872

Ahmed, A. M., Shimamoto, T., and Shimamoto, T. (2013). Molecular characterization of multidrug-resistant avian pathogenic *Escherichia coli* isolated from septicemic broilers. *Int. J. Med. Microbiol.* 303, 475–483. doi: 10.1016/j.ijmm.2013.06.009

Aidara-Kane, A., Angulo, F. J., Conly, J. M., Minato, Y., Silbergeld, E. K., McEwen, S. A., et al. (2018). World Health Organization (WHO) guidelines on use of medically important antimicrobials in food-producing animals. *Antimicrob. Resist. Infect. Control* 7:7.

Allocati, N., Masulli, M., Alexeyev, M. F., and Di Ilio, C. (2013). *Escherichia coli* in Europe: an overview. *Int. J. Environ. Res. Public Health* 10, 6235–6254.

Aslam, B., Khurshid, M., Arshad, M. I., Muzammil, S., Rasool, M., Yasmeen, N., et al. (2021). Antibiotic Resistance: one Health One World Outlook. *Front. Cell. Infect. Microbiol.* 11:771510. doi: 10.3389/fcimb.2021.771510

Bakkeren, E., Huisman, J. S., Fattinger, S. A., Hausmann, A., Furter, M., Egli, A., et al. (2019). *Salmonella* persisters promote the spread of antibiotic resistance plasmids in the gut. *Nature* 573, 276–280. doi: 10.1038/s41586-019-1521-8

Bell, R. L., Kase, J. A., Harrison, L. M., Balan, K. V., Babu, U., Chen, Y., et al. (2021). The Persistence of Bacterial Pathogens in Surface Water and Its Impact on Global Food Safety. *Pathogens* 10:1391. doi: 10.3390/pathogens10111391

Bosman, A. L., Loest, D., Carson, C. A., Agunos, A., Collineau, L., and Léger, D. F. (2019). Developing Canadian defined daily doses for animals: a metric to quantify antimicrobial use. *Front. Vet. Sci.* 6:220. doi: 10.3389/fvets.2019.00220

Boulianne, M., Arsenault, J., Daignault, D., Archambault, M., Letellier, A., and Dutil, L. (2016). Drug use and antimicrobial resistance among *Escherichia coli* and *Enterococcus* spp. isolates from chicken and turkey flocks slaughtered in Quebec, Canada. *Can. J. Vet. Res.* 80, 49–59.

Brown, K., Uwiera, R. R. E., Kalmokoff, M. L., Brooks, S. P. J., and Inglis, G. D. (2017). Antimicrobial growth promoter use in livestock: a requirement to understand their modes of action to develop effective alternatives. *Int. J. Antimicrob. Agents* 49, 12–24. doi: 10.1016/j.ijantimicag.2016.08.006

Burow, E., Simoneit, C., Tenhagen, B.-A., and Käsbohrer, A. (2014). Oral antimicrobials increase antimicrobial resistance in porcine *E. coli*–A systematic review. *Prev. Vet. Med.* 113, 364–375. doi: 10.1016/j.prevetmed.2013.12.007

Callens, B., Cargnel, M., Sarrazin, S., Dewulf, J., Hoet, B., Vermeersch, K., et al. (2018). Associations between a decreased veterinary antimicrobial use and resistance in commensal *Escherichia coli* from Belgian livestock species (2011–2015). *Pre. Vet. Med.* 157, 50–58. doi: 10.1016/j.prevetmed.2017.10.013

Canadian Animal Health Institute (2009). *Compendium of Veterinary Products*. 11th Edn. Waterloo, ON: North American Compendiums Ltd, 928.

Canadian Turkey Marketing Agency (2020). *1944-2020 Canadian Turkey Stats*. Available online at: https://www.turkeyfarmersofcanada.ca/wp-content/uploads/2021/08/TURKEY-FACTBOOK-1974-to-2020-1.pdf (accessed on Feb 11, 2022).

Casewell, M., Friis, C., Marco, E., McMullin, P., and Phillips, I. (2003). The European ban on growth-promoting antibiotics and emerging consequences for human and animal health. *J. Antimicrob. Chemother.* 52, 159–161. doi: 10.1093/jac/dkg313

Cazer, C. L., Al-Mamun, M. A., Kaniyamattam, K., Love, W. J., Booth, J. G., Lanzas, C., et al. (2019). Shared Multidrug Resistance Patterns in Chicken-Associated *Escherichia coli* Identified by Association Rule Mining. *Front. Microbiol.* 10:687. doi: 10.3389/fmicb.2019.00687

Ceccarelli, D., Hesp, A., Van Der Goot, J., Joosten, P., Sarrazin, S., Wagenaar, J. A., et al. (2020). Antimicrobial resistance prevalence in commensal *Escherichia coli* from broilers, fattening turkeys, fattening pigs and veal calves in European countries and association with antimicrobial usage at country level. *J. Med. Microbiol.* 69, 537–547. doi: 10.1099/jmm.0.001176

Cheng, G., Ning, J., Ahmed, S., Huang, J., Ullah, R., An, B., et al. (2019). Selection and dissemination of antimicrobial resistance in Agri-food production. *Antimicrob. Resist. Infect. Control* 8:158.

Chrétien, L., Boutant, J., Lyazrhi, F., and Galliard, N. (2021). Retrospective Assessment of *Escherichia coli* Vaccination in Broiler Turkeys Under Field Conditions in 37 Farms from Brittany (France). *Avian Dis.* 65, 659–662.

Collineau, L., Belloc, C., Stärk, K. D., Hémonic, A., Postma, M., Dewulf, J., et al. (2017). Guidance on the selection of appropriate indicators for quantification of antimicrobial usage in humans and animals. *Zoonoses Public Health* 64, 165–184. doi: 10.1111/zph.12298

Dadgostar, P. (2019). Antimicrobial resistance: implications and costs. *Infect. Drug Resist.* 12:3903.

Davis, G. S., Waits, K., Nordstrom, L., Grande, H., Weaver, B., Papp, K., et al. (2018). Antibiotic-resistant *Escherichia coli* from retail poultry meat with different antibiotic use claims. *BMC Microbiol.* 18:174. doi: 10.1186/s12866-018-1322-5

Dorado-García, A., Mevius, D. J., Jacobs, J. J. H., Van Geijlswijk, I. M., Mouton, J. W., Wagenaar, J. A., et al. (2016). Quantitative assessment of antimicrobial resistance in livestock during the course of a nationwide antimicrobial use reduction in the Netherlands. *J. Antimicrob. Chemother.* 71, 3607–3619. doi: 10.1093/jac/dkw308

FAO (2022). *FAOSTAT. Value of Agricultural Production*. Available online at: https://www.fao.org/faostat/en/#data/QV (accessed on Jul 09, 2022).

Fuhrmann, L., Vahjen, W., Zentek, J., Günther, R., and Saliu, E.-M. (2022). The Impact of Pre- and Probiotic Product Combinations on Ex vivo Growth of Avian Pathogenic *Escherichia coli* and *Salmonella* Enteritidis. *Microorganisms* 10:121. doi: 10.3390/microorganisms10010121

Gholami-Ahangaran, M., Moravvej, A., Safizadeh, Z., Nogoorani, V. S., Zokaei, M., and Ghasemian, S. (2021). The evaluation of ESBL genes and antibiotic resistance rate in *Escherichia coli* strains isolated from meat and intestinal contents of turkey in Isfahan, Iran. *Iran. J. Vet. Res.* 22:318. doi: 10.22099/ijvr.2021.39493.5737

Giovanardi, D., Lupini, C., Pesente, P., Rossi, G., Ortali, G., and Catelli, E. (2013). Characterization and antimicrobial resistance analysis of avian pathogenic *Escherichia coli* isolated from Italian turkey flocks. *Poult. Sci.* 92, 2661–2667. doi: 10.3382/ps.2013-03194

Gosling, R., Clouting, C., Randall, L., Horton, R., and Davies, R. (2012). Ciprofloxacin resistance in *E. coli* isolated from turkeys in Great Britain. *Avian Pathol.* 41, 83–89.

Government of Canada (2018). *Canadian Integrated Program for Antimicrobial Resistance Surveillance (CIPARS) 2018 Annual Report*. Ottawa: Government of Canada.

Government of Canada (2019). *Compendium of Medicating Ingredients Brochure*. Available online at: https://inspection.canada.ca/animal-health/livestock-feeds/medicating-ingredients/eng/1300212600464/1320602461227 (accessed on Apr 15, 2022).

Government of Canada (2021). *Poultry and egg marker information/Turkey*. Available online at: https://agriculture.canada.ca/en/canadas-agriculture-sectors/animal-industry/poultry-and-egg-market-information/turkey (accessed on Feb 11, 2022).

Horie, M., Yang, D., Joosten, P., Munk, P., Wadepohl, K., Chauvin, C., et al. (2021). Risk Factors for Antimicrobial Resistance in Turkey Farms: a Cross-Sectional Study in Three European Countries. *Antibiotics* 10:820. doi: 10.3390/antibiotics10070820

Johnson, T. J., Logue, C. M., Johnson, J. R., Kuskowski, M. A., Sherwood, J. S., Barnes, H. J., et al. (2012). Associations between multidrug resistance, plasmid content, and virulence potential among extraintestinal pathogenic and commensal *Escherichia coli* from humans and poultry. *Foodborne Pathog. Dis.* 9, 37–46. doi: 10.1089/fpd.2011.0961

Kolář, M., Urbanek, K., and Látal, T. (2001). Antibiotic selective pressure and development of bacterial resistance. *Int. J. Antimicrob. Agents* 17, 357–363.

Lambrecht, E., Van Coillie, E., Van Meervenne, E., Boon, N., Heyndrickx, M., and Van de Wiele, T. (2019). Commensal E. coli rapidly transfer antibiotic resistance genes to human intestinal microbiota in the Mucosal Simulator of the Human Intestinal Microbial Ecosystem (M-SHIME). *Int. J. Food Microbiol.* 311:108357. doi: 10.1016/j.ijfoodmicro.2019.108357

Landers, T. F., Cohen, B., Wittum, T. E., and Larson, E. L. (2012). A Review of Antibiotic Use in Food Animals: perspective. Policy, and Potential. *Public Health Rep.* 127, 4–22. doi: 10.1177/003335491212700103

Luiken, R. E., Van Gompel, L., Munk, P., Sarrazin, S., Joosten, P., Dorado-García, A., et al. (2019). Associations between antimicrobial use and the faecal resistome on broiler farms from nine European countries. *J. Antimicrob. Chemother.* 74, 2596–2604.

Maal-Bared, R., Bartlett, K. H., Bowie, W. R., and Hall, E. R. (2013). Phenotypic antibiotic resistance of *Escherichia coli* and *E. coli* O157 isolated from water, sediment and biofilms in an agricultural watershed in British Columbia. *Sci. Total Environ.* 443, 315–323. doi: 10.1016/j.scitotenv.2012.10.106

McEwen, S. A., and Collignon, P. J. (2018). Antimicrobial resistance: a one health perspective. *Microbiol. Spect.* 6. doi: 10.1128/microbiolspec.ARBA-0009-2017

McEwen, S. A., and Fedorka-Cray, P. J. (2002). Antimicrobial use and resistance in animals. *Clin. Infect. Dis.* 34, S93–S106.

Mughini-Gras, L., Pasqualin, D., Tarakdjian, J., Santini, A., Cunial, G., Tonellato, F., et al. (2021). Short-term and long-term effects of antimicrobial use on antimicrobial resistance in broiler and turkey farms. *Avian Pathol.* 51, 120–128. doi: 10.1080/03079457.2021.2007850

Murray, C. J., Ikuta, K. S., Sharara, F., Swetschinski, L., Aguilar, G. R., Gray, A., et al. (2022). Global burden of bacterial antimicrobial resistance in 2019: a systematic analysis. *Lancet* 399, 629–655. doi: 10.1016/S0140-6736(21)02724-0

Prescott, J. (2019). Veterinary antimicrobial stewardship in North America. *Aust. Vet. J.* 97, 243–248.

R Core Team (2020). *R: A Language and Environment for Statistical Computing*. Vienna: R Foundation for Statistical Computing.

Ramadan, H., Soliman, A. M., Hiott, L. M., Elbediwi, M., Woodley, T. A., Chattaway, M. A., et al. (2021). Emergence of Multidrug-Resistant *Escherichia coli* Producing CTX-M, MCR-1, and FosA in Retail Food From Egypt. *Front. Cell. Infect. Microbiol.* 11:681588. doi: 10.3389/fcimb.2021.681588

Reddy, S., Barathe, P., Kaur, K., Anand, U., Shriram, V., and Kumar, V. (2022). "Antimicrobial Resistance and Medicinal Plant Products as Potential Alternatives to Antibiotics in Animal Husbandry," in *Antimicrobial Resistance: Underlying Mechanisms and Therapeutic Approaches*, eds V. Kumar, V. Shriram, A. Paul, and M. Thakur (Singapore: Springer Singapore), 357–384. doi: 10.1007/978-981-16-3120-7_13

Sheikh, A. A., Checkley, S., Avery, B., Chalmers, G., Bohaychuk, V., Boerlin, P., et al. (2012). Antimicrobial Resistance and Resistance Genes in *Escherichia coli* Isolated from Retail Meat Purchased in Alberta. Canada. *Foodborne Pathog. Dis.* 9, 625–631. doi: 10.1089/fpd.2011.1078

Simoneit, C., Burow, E., Tenhagen, B.-A., and Käsbohrer, A. (2015). Oral administration of antimicrobials increase antimicrobial resistance in E. coli from chicken–a systematic review. *Prev. Vet. Med.* 118, 1–7. doi: 10.1016/j.prevetmed.2014.11.010

Snijders, T. A., and Bosker, R. J. (2011). *Multilevel Analysis. An Introduction to Basic and Advanced Multilevel Modelling. 2nd Ed*. London: Sage.

Talavera-González, J. M., Talavera-Rojas, M., Soriano-Vargas, E., Vázquez-Navarrete, J., and Salgado-Miranda, C. (2021). In vitro transduction of antimicrobial resistance genes into *Escherichia coli* isolates from backyard poultry in Mexico. *Can. J. Microbiol.* 67, 415–425. doi: 10.1139/cjm-2020-0280

Tawyabur, M., Islam, M. S., Sobur, M. A., Hossain, M. J., Mahmud, M. M., Paul, S., et al. (2020). Isolation and Characterization of Multidrug-Resistant *Escherichia coli* and *Salmonella* spp. from Healthy and Diseased Turkeys. *Antibiotics* 9:770. doi: 10.3390/antibiotics9110770

Turkey farmers of Canada (2022). *The turkey farmers of Canada Guidelines for Antimicrobial Use in the Turkey Industry*. Available online at: https://www.amstewardship.ca/guidelines-for-antimicrobial-use-in-the-turkey-industry-published-by-the-turkey-farmers-of-canada/ (accessed on Apr 15, 2022).

Van Gompel, L., Luiken, R. E., Sarrazin, S., Munk, P., Knudsen, B. E., Hansen, R. B., et al. (2019). The antimicrobial resistome in relation to antimicrobial use and biosecurity in pig farming, a metagenome-wide association study in nine European countries. *J. Antimicrob. Chemother.* 74, 865–876. doi: 10.1093/jac/dky518

Varga, C., Brash, M. L., Slavic, D., Boerlin, P., Ouckama, R., Weis, A., et al. (2018). Evaluating virulence-associated genes and antimicrobial resistance of avian pathogenic *Escherichia coli* isolates from broiler and broiler breeder chickens in Ontario. Canada. *Avian Dis.* 62, 291–299. doi: 10.1637/11834-032818-Reg.1

Varga, C., Guerin, M. T., Brash, M. L., Slavic, D., Boerlin, P., and Susta, L. (2019a). Antimicrobial resistance in Campylobacter jejuni and Campylobacter coli isolated from small poultry flocks in Ontario. Canada: a two-year surveillance study. *PLoS One* 14:e0221429. doi: 10.1371/journal.pone.0221429

Varga, C., Guerin, M. T., Brash, M. L., Slavic, D., Boerlin, P., and Susta, L. (2019b). Antimicrobial resistance in fecal *Escherichia coli* and *Salmonella enterica* isolates: a two-year prospective study of small poultry flocks in Ontario. Canada. *BMC Vet. Res.* 15:464. doi: 10.1186/s12917-019-2187-z

World Health Organization [WHO] (2015). *Global Action Plan on Antimicrobial Resistance*. Geneva: World Health Organization.

World Health Organization [WHO] (2021). *Antimicrobial Resistance*. Available online at: http://www.who.int/mediacentre/factsheets/fs194/en/ (accessed on Dec 31, 2021).

frontiers | Frontiers in Microbiology

TYPE Original Research
PUBLISHED 11 August 2022
DOI 10.3389/fmicb.2022.940600



OPEN ACCESS

EDITED BY
Tao Li,
Shanghai Veterinary Research Institute (CAAS), China

REVIEWED BY
Jian Sun,
South China Agricultural University, China
Miranda Kirchner,
Animal and Plant Health Agency, United Kingdom

*CORRESPONDENCE
Ana Carolina Ewbank
acarolewbank@gmail.com

SPECIALTY SECTION
This article was submitted to Antimicrobials, Resistance and Chemotherapy, a section of the journal Frontiers in Microbiology

RECEIVED 10 May 2022
ACCEPTED 14 July 2022
PUBLISHED 11 August 2022

CITATION
Ewbank AC, Fuentes-Castillo D, Sacristán C, Esposito F, Fuga B, Cardoso B, Godoy SN, Zamana RR, Gattamorta MA, Catão-Dias JL and Lincopan N (2022) World Health Organization critical priority *Escherichia coli* clone ST648 in magnificent frigatebird (*Fregata magnificens*) of an uninhabited insular environment.
*Front. Microbiol.* 13:940600.
doi: 10.3389/fmicb.2022.940600



# World Health Organization critical priority *Escherichia coli* clone ST648 in magnificent frigatebird (*Fregata magnificens*) of an uninhabited insular environment

Ana Carolina Ewbank[1]*, Danny Fuentes-Castillo[2,3], Carlos Sacristán[4], Fernanda Esposito[3,5], Bruna Fuga[3,5,6], Brenda Cardoso[3,5], Silvia Neri Godoy[7], Roberta Ramblas Zamana[1], Marco Aurélio Gattamorta[1], José Luiz Catão-Dias[1] and Nilton Lincopan[3,5,6]

[1]Laboratory of Wildlife Comparative Pathology, Department of Pathology, School of Veterinary Medicine and Animal Sciences, University of São Paulo, São Paulo, Brazil, [2]Departamento de Patología y Medicina Preventiva, Facultad de Ciencias Veterinarias, Universidad de Concepción, Chillán, Chile, [3]One Health Brazilian Resistance Project (OneBR), São Paulo, Brazil, [4]Centro de Investigación en Sanidad Animal (CISA-INIA), CSIC, Valdeolmos-Alalpardo, Spain, [5]Department of Clinical Analysis, School of Pharmacy, University of São Paulo, São Paulo, Brazil, [6]Department of Microbiology, Institute of Biomedical Sciences, University of São Paulo, São Paulo, Brazil, [7]Refúgio de Vida Silvestre do Arquipélago de Alcatrazes – Instituto Chico Mendes de Conservação da Biodiversidade, São Paulo, Brazil

Antimicrobial resistance is an ancient natural phenomenon increasingly pressured by anthropogenic activities. *Escherichia coli* has been used as markers of environmental contamination and human-related activity. Seabirds may be bioindicators of clinically relevant bacterial pathogens and their antimicrobial resistance genes, including extended-spectrum-beta-lactamase (ESBL) and/or plasmid-encoded AmpC (pAmpC), in anthropized and remote areas. We evaluated cloacal swabs of 20 wild magnificent frigatebirds (*Fregata magnificens*) of the Alcatrazes Archipelago, the biggest breeding colony of magnificent frigatebirds in the southern Atlantic and a natural protected area with no history of human occupation, located in the anthropized southeastern Brazilian coast. We characterized a highly virulent multidrug-resistant ST648 (O153:H9) pandemic clone, harboring $bla_{CTX-M-2}$, $bla_{CMY-2}$, *qnrB, tetB, sul1, sul2, aadA1, aac(3)-VIa* and *mdfA,* and virulence genes characteristic of avian pathogenic (APEC) (*hlyF, iroN, iss, iutA,* and *ompT*) and other extraintestinal *E. coli* (ExPEC) (*chuA, kpsMII,* and *papC*). To our knowledge, this is the first report of ST648 *E. coli* co-producing ESBL and pAmpC in wild birds inhabiting insular environments. We suggest this potentially zoonotic and pathogenic lineage was likely acquired through indirect anthropogenic contamination of the marine environment, ingestion of contaminated seafood, or by intra and/or interspecific contact. Our findings reinforce the role of wild birds as anthropization sentinels in insular environments and the importance of wildlife

surveillance studies on pathogens of critical priority classified by the World Health Organization.

KEYWORDS

pAmpC, ESBL, antimicrobial resistance, island, wildlife, One Health

# Introduction

Antimicrobial resistance result from a naturally occurring ancient phenomenon that has been severely affected by anthropogenic activities such as use, misuse and overuse of antimicrobials in human and veterinary medicine, aquaculture and agriculture, and release of pharmaceutical manufacturing, domestic and agricultural waste into the environment (Wright, 2007; West et al., 2010; Yang et al., 2013; Michael et al., 2014). Worryingly, the issue of antimicrobial resistance leads to great healthcare, social and economical burdens worldwide, thus considered a quintessential One Health issue (Michael et al., 2014; Ewbank et al., 2021). *Escherichia coli* (order Enterobacterales) has been broadly suggested and used as a marker of environmental contamination and anthropogenic activity (Bonnedahl et al., 2009; Tenaillon et al., 2010). Extended-spectrum-ß-lactamase (ESBL)- and plasmid-encoded AmpC (pAmpC)-producing *E. coli* are classified as critical priority pathogens within the One health interface by the World Health Organization (WHO) (Tacconelli et al., 2018; Mughini-Gras et al., 2019).

Seabirds have been used as environmental bioindicators of ESBL/pAmpC-positive *E. coli* in remote locations due to their potential as sentinels of natural and anthropogenic-related changes to the marine ecosystem health (Hernandez et al., 2010; Hernández and González-Acuña, 2016; Ewbank et al., 2022). Given that clinically-relevant antimicrobial resistance genes are considered environmental pollutants and markers of environmental anthropization (Pruden et al., 2006; Jobbins and Alexander, 2015), most ESBL/pAmpC-producing *E. coli* studies have focused in synanthropic seabird species inhabiting anthropized environments (e.g., urban areas and dumpsites) (Bonnedahl et al., 2009; Atterby et al., 2016; Ahlstrom et al., 2018). Yet, insular biomes not inhabited by humans represent an informative setting in the study of the One Health chain of antimicrobial resistance by providing valuable insight into: (i) the occurrence, diversity, and dissemination of antimicrobial resistance genes (ARGs) and antimicrobial-resistant bacteria (ARB), such as ESBL/pAmpC-producing *E. coli*; (ii) the indirect anthropogenic effects over the environment (e.g., marine pollution); and (iii) the potential influence of biological and ecological characteristics of their local avian fauna (e.g., migration, use of coastal areas) (Hernandez et al., 2010; Ewbank et al., 2021, 2022).

Herein we analyzed cloacal swabs of 20 wild magnificent frigatebirds (*Fregata magnificens*; family Fregatidae) from an uninhabited archipelago located in southeastern Brazil, using microbiological techniques and whole genome sequencing (WGS) to investigate the occurrence, and phenotypic and genotypic characteristics of ESBL- and pAmpC-producing *E. coli* classified by WHO as critical priority pathogens (Tacconelli et al., 2018), and further identify and characterize their bacterial lineages, serotypes, resistome, plasmidome and virulome.

# Materials and methods

## Study area

The Alcatrazes Island is the principal, among the five islands and four islets forming the Alcatrazes Archipelago (24° 05′ 44.69″ S 45° 41′ 52.92″ W), located at 36 km off the coast of São Sebastião, in São Paulo state, southeastern Brazil (**Figure 1**). The archipelago, including the Alcatrazes Island, have no records of onshore human occupation or tourist visitation, the latter limited to the offshore territory. In 1979, the Brazilian Navy started using the northeastern face of Alcatrazes Island as target for artillery practice. Later on, in 1987, the Tupinambás Ecological Station (Esec Tupinambás) was created, partially including the archipelago, and restricting visitation even more. In 2013, the Brazilian Navy moved its training grounds to a smaller island of Alcatrazes. Finally, in 2016, the archipelago and adjacent marine area (approximately 273 km$^2$) were declared a conservation area - the Alcatrazes Archipelago Wildlife Refuge (Refuìgio de Vida Silvestre do Arquipeìlago de Alcatrazes - Refuìgio de Alcatrazes), focused specifically on the conservation of its local wildlife and flora, administered by the Chico Mendes Institute for Biodiversity Conservation (ICMBio), Brazilian Ministry of Environment (Instituto Chico Mendes de Conservação da Biodiversidade (ICMBio), 2017). This study was performed in full compliance with the Biodiversity Information and Authorization System (SISBIO 59150-4), Brazilian

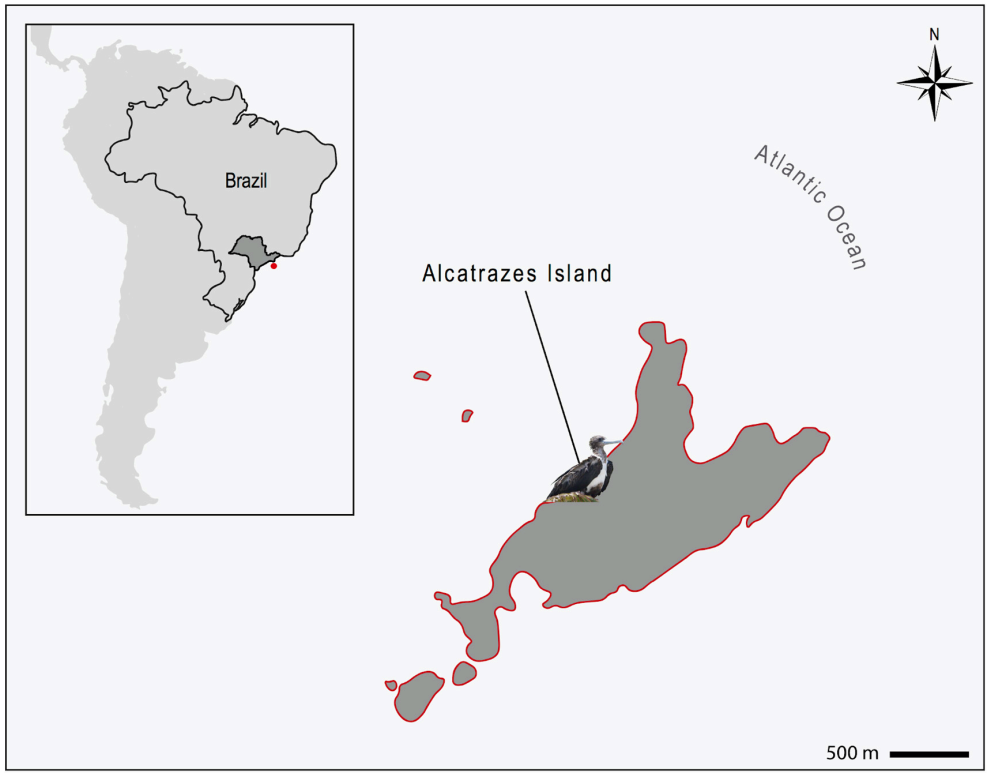


FIGURE 1
Location of the Alcatrazes Archipelago (red dot), territory of São Paulo state (dark gray), southeastern Brazil (inserted map). Magnificent frigatebird (*Fregata magnificens*) sampled in Alcatrazes island, part of the Alcatrazes Archipelago (lined in red). Scale: 500 m.

Ministry of Environment and the Ethical Committee in Animal Research of the School of Veterinary Medicine and Animal Sciences, University of São Paulo (Process number 1753110716).

## Sampling and bacterial identification

Twenty magnificent frigatebirds (17 adults and 3 juveniles) were sampled in the main island (Alcatrazes Island), in January 2020. The evaluated birds comprised nine males, eight females and three individuals of undetermined sex. All birds were captured with a butterfly net, manually restrained and immediately released after sample collection. The cloacal swabs were maintained in Amies transport medium containing charcoal and maintained at room temperature until processed (within 7 days). In order to select ESBL- and pAmpC-producing *E. coli* strains, cloacal samples were streaked onto ceftriaxone (CRO, 2 mg/L)-supplemented MacConkey agar plates) and incubated overnight at 35 ± 2°C. Bacterial isolates were identified by Matrix Assisted Laser Desorption Ionization Time of Flight Mass Spectrometry (MALDI-TOF MS, Bruker Daltonik, Germany).

## Antimicrobial susceptibility testing

Antimicrobial susceptibility was evaluated by the disc diffusion method using the following human and veterinary antimicrobials (Clinical and Laboratory Standards Institute [CLSI], 2018, 2019): amoxicillin/clavulanate, ceftriaxone, cefotaxime, ceftiofur, ceftazidime, cefepime, cefoxitin, imipenem, meropenem, ertapenem, enrofloxacin, ciprofloxacin, gentamicin, amikacin, chloramphenicol, trimethoprim-sulfamethoxazole, and tetracycline. The double-disc synergy test (DDST) was used for ESBL screening (EUCAST, 2017).

## Whole genome sequence analysis

The genomic DNA of the ESBL/pAmpC-positive *E. coli* strain was extracted using a PureLinkTM Quick Gel Extraction Kit (Life Technologies, Carlsbad, CA, United States) and a genomic paired-end library (75 × 2 bp), prepared using a Nextera XT DNA Library Preparation Kit (Illumina Inc., Cambridge, United Kingdom), according to the manufacturer's instructions. The whole genome was sequenced on the NextSeq platform (Illumina). *De novo* genome assembly was performed with CLC Genomics Workbench 12.0.3. The draft

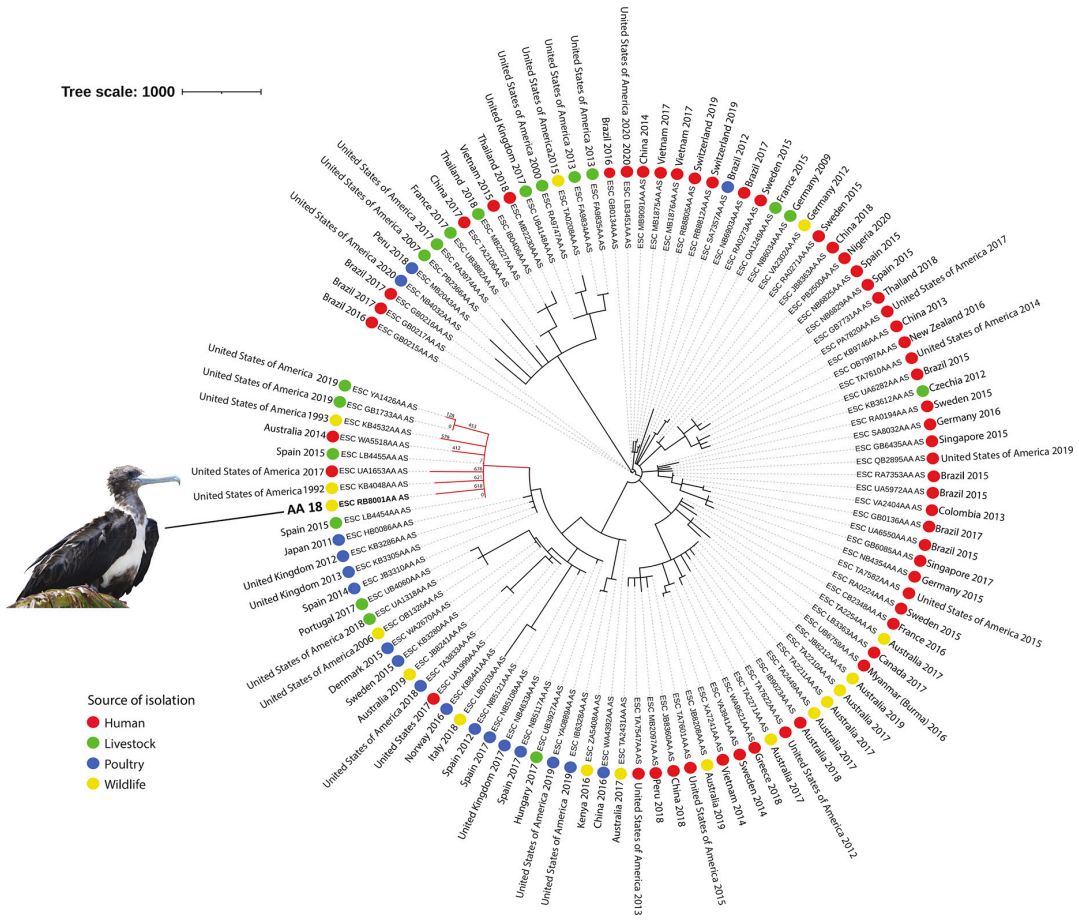


FIGURE 2
Phylogeny of CTX-M-2 and CMY-2-producing ST648 *E. coli* isolated from a magnificent frigatebird (*Fregata magnificens*) and global *E. coli* ST648. Each genome is shown in accordance to the source of isolation (colored circles), and country and year of isolation. In the red branch are the genomes that were phylogenetically closer to sample AA18. Tree scale: 1000.

genome sequence was automatically annotated using the NCBI Prokaryotic Genome Annotation Pipeline v.3.2. The MLST 2.0, PlasmidFinder 2.0, ResFinder 4.1, VirulenceFinder 2.0 and SerotypeFinder 2.0 databases available at the Centre for Genomic Epidemiology[1] were used to identify, respectively, the multilocus sequence type (MLST), plasmid replicons, resistome, virulome and serotype. A prediction filter of ≥98 and 100% were set for sequence identity and coverage thresholds, respectively. Additionally, phylogroup analysis was performed using the ClermonTyping database[2]. The nucleotide sequence data reported is available in the DDBJ/EMBL/GenBank databases under accession number NZ_JAGYFD010000000. The *E. coli* AA18 strain genomic information is available on the OneBR platform under ID number ONE119[3].

The MSTree V2 tool from Enterobase[4] was used to generate a minimum spanning tree based on the wgMLST scheme and 25,002 loci considering our *E. coli* isolate and an international collection of 107 *E. coli* strains belonging to ST648, selected according to source of isolation (colored circles), and country and year of isolation (**Figure 2**). iTOL v.6[5] was used to edit and visualize the phylogenetic tree. An interactive version of the tree is available at https://itol.embl.de/tree/17911376811006716172295 08.

## Results

Overall, we found an ESBL/pAmpC-producing *E. coli* prevalence of 5% (1/20) in the evaluated individuals.

1 http://genomicepidemiology.org/
2 http://clermontyping.iame-research.center/
3 http://onehealthbr.com
4 http://enterobase.warwick.ac.uk/species/index/ecoli
5 https://itol.embl.de

Phenotypically, the *E. coli* isolate (designated AA18 strain) presented a multidrug resistant (MDR) profile to amoxicillin/clavulanic acid, ceftiofur, cefoxitin, cefepime, aztreonam, trimethoprim-sulfamethoxazole, gentamicin, and tetracycline; remaining susceptible to carbapenems ertapenem, imipenem and meropenem (Clinical and Laboratory Standards Institute [CLSI], 2018, 2019). Regarding to genomic data, trimmed paired-end reads were assembled into 137 contigs, with 425,81 x coverage, and a G + C content of 49% (Andrews, 2010). Briefly, strain AA18 presented a genome size calculated as 5.4 million base pairs (bp), with 5,145 protein-coding sequences, 87 pseudogenes, 83 tRNAs, 3 rRNAs and 10 non-coding RNAs genomic analysis revealed that the isolate harbored genes $bla_{CTX-M-2}$, $bla_{CMY-2}$, *qnrB*, *tetB*, *sul1*, *sul2*, *aadA1*, *aac(3)-VIa* and *mdfA* in its resistome (**Table 1**).

Multilocus sequence typing (MLST) and serotype analyses revealed that the isolate corresponded to ST648 and belonged to the O153:H9 group, respectively. Our isolate presented several relevant virulence genes characteristic of avian pathogenic (APEC) and other extraintestinal pathogenic *E. coli* (ExPEC), such as *chuA* (outer membrane hemin receptor), *kpsMII* (group 2 capsule synthesis), *fimC* (fimbriae type I), *sitA* (iron transport protein), and *traT* (transfer protein). Additionally, WGS analysis also identified genes encoding resistance to disinfectants (i.e., acridines, chlorhexidine, crystal violet, ethidium bromide, quaternary ammonium compounds, sodium dodecyl sulphate), heavy metals (i.e., lead, arsenic, copper, silver, antimony, zinc, tellurium, tungsten, cobalt, nickel, manganese, cadmium, mercury, iron, molybdenum, chromium, and vanadium), acid or basidic environment (i.e., $H_2O_2$, HCl and NaOH), and pesticide (glyphosate). The resistome, plasmidome and virulome are listed in **Table 1**.

Upon phylogenetic analysis, strain AA18 clustered with genomes from *E. coli* strains recovered from humans (Australia), livestock (Spain and United States), poultry (United States of America), and European herring gulls (*Larus argentatus*; United States of America), with a high variability ranging from 2 to 628 SNPs (**Figure 2**).

TABLE 1 Genomic and epidemiological data of *E. coli* strain AA18.

| Characteristics | *E. coli* strain AA18 |
|---|---|
| Source | Cloacal swab |
| Genome size (Mbp) | 5,4 |
| No. of CDS[a] | 5,145 |
| G + C content (%) | 57,25 |
| tRNA (*n*) | 83 |
| rRNA (*n*) | 3 |
| Non-coding RNA (*n*) | 10 |
| Pseudogenes | 87 |
| CRISPR | 2 |
| MLST (ST)[b] | 648 |
| Serotype | O153:H9 |
| Resistome | |
| β-lactams | $bla_{CXT-M-2}$, $bla_{CMY-2}$ |
| Aminoglycosides | *aa(3)-VIa*, *aadA1* |
| Fluoroquinolones | *qnrB* |
| Sulphonamides | *sul1*, *sul2* |
| Tetracyclines | *tetB* |
| Macrolides | *mdfA* |
| Heavy metal | *bhsA, cusF, cutA, dsbAB, fetAB, fieF, glpF, mntPR, modE, nfsA, phnE, pitA, rcnR, robA, sitBCD, tehB, sodAB, ychH, yieF, yodD, zinT, znuA, zur* |
| Biocides | *cba, chuA, cma, cvaC, eilA, etsC, gad, hlyF, hra, ireA, iroN, iss, iucC, iutA, kpsE, kpsMII, lpfA, mchF, ompT, papC, sitA, terC, traT, tsh, yfcV* |
| Virulome | *acrE, cpxA, mdtEF, tehB, sugE, ydeOP* |
| Plasmidome | Col, IncFIB, IncFII |
| OneBR ID | ONE119 |
| GenBank accession number | NZ_JAGYFD010000000 |

[a]CDSs, coding sequences. [b]MLST, multilocus sequence type; ST, sequence type.

## Discussion

Herein, we found an overall prevalence of 5% (1/20) of ESBL/AmpC-positive *E. coli* isolates in magnificent frigatebirds of Alcatrazes Archipelago, southeastern Brazilian coast: a highly virulent MDR avian pathogenic *E. coli* (APEC) isolate of the pandemic high-risk ST648 clone (serotype O153:H9) harboring genes $bla_{CTX-M-2}$ and $bla_{CMY-2}$. To the authors' knowledge, this is the first report of the ST648 clone and pAmp-EC in wild birds inhabiting insular environments.

The CTX-M-2 and CMY-2 enzymes are, respectively, the most prevalent CTX-M ESBL in South America and pAmpC beta-lactamase worldwide (Jacoby, 2009; Rocha et al., 2015), reported in a variety of epidemiological settings in Brazil (Rocha et al., 2015; Cunha et al., 2017; Melo et al., 2018; de Carvalho et al., 2020; Fernandes et al., 2020b). Among wild birds, $bla_{CTX-M-2}$ and $bla_{CMY-2}$ genes have been described in bacterial pathogens colonizing gulls, corvids and Eurasian magpie (*Pica pica*) in Europe (Loncaric et al., 2013; Stedt et al., 2015; Alcalá et al., 2016; Jamborova et al., 2017; Athanasakopoulou et al., 2021), and in gulls and bald eagles (*Haliaeetus leucocephalus*) from the Americas (Poirel et al., 2012; Báez et al., 2015; Atterby et al., 2016; Liakopoulos et al., 2016; Ahlstrom et al., 2018). In Brazil, $bla_{CTX-M-2}$-positive bacteria have been detected in wild birds of prey and parrots, and in Magellanic penguin (*Spheniscus magellanicus*); whereas $bla_{CMY-2}$-positive bacteria have been described in birds of prey (Sellera et al., 2017; Batalha de Jesus et al., 2019; de Carvalho et al., 2020).

The international clone ST648 is predominantly MDR and virulent, and one of the most commonly reported international sequence types (STs) in the human–animal–environmental interface worldwide, suggesting great host adaptation (Hu et al., 2013; Fernandes et al., 2018; de Carvalho et al., 2020). Of note, ST648 has been detected in wild birds from almost all continents, including Europe (Guenther et al., 2010;

Schaufler et al., 2019), the Americas (Poirel et al., 2012; Báez et al., 2015), Asia (Hasan et al., 2012; Yang et al., 2016), and Oceania (Mukerji et al., 2019). In South America, this clone has been described in wild birds of prey in Brazil (Batalha de Jesus et al., 2019; de Carvalho et al., 2020) and gulls in Chile (Báez et al., 2015).

Strain AA18 carried several virulence genes of concern characteristic of highly pathogenic avian pathogenic *E. coli* (APEC) isolates: *cvaC* (colicin V), *fimC* (fimbriae type I), *hlyF* (hemolysin F), *iroN* (salmochelin), *iss* (increased serum survival), *iucC* (aerobactin production) *iut*A (ferric aerobactin receptor), *ompT* (outer membrane protein), *sitA* (iron transport protein), *tsh* (temperature-sensitive hemagglutinin) and *traT* (transfer protein) (Ewers et al., 2007; Sarowska et al., 2019). Additionally, we also found virulence genes characteristic of the other ExPEC: *chuA* (outer membrane hemin receptor), *kpsMII*, *papC* (outer membrane usher protein), and *yfcV* (major subunit of a putative chaperone-usher fimbria) (Grimwood et al., 2000; Kim, 2002; Sarowska et al., 2019). APEC strains may cause colibacillosis – multiple systemic and localized avian infection that may lead to high mortality and decreased production, capable of imposing severe economic losses to the poultry industry worldwide (Kemmett et al., 2014). Of note, some of the virulence factors found in our isolate were previously reported in ExPEC sampled from magnificent frigatebirds from the Alcatrazes Archipelago: *cvaC, fimH, hlyF, iroN, iss, iutA, ompT* and *papC* (Saviolli et al., 2016). Although APEC and other ExPEC strains are phylogenetically close, sharing some of the same virulence genes, APEC may carry other genes not common in other ExPEC isolates, such as those present in the colicin V (ColV) plasmid (Rodriguez-Siek et al., 2005; Bélanger et al., 2011). These characteristics suggest that APEC strains are potentially zoonotic, and could be a reservoir and source of virulence genes for other ExPEC strains (Ewers et al., 2007; Bélanger et al., 2011). In humans, APEC infections could take place through consumption of undercooked food from animal origin (especially retail poultry products), and direct contact with birds and their feces (Dziva and Stevens, 2008). Yet, despite the hypothetical zoonotic and pathogenic potential of our isolate (Ewers et al., 2014; Maluta et al., 2014; Sarowska et al., 2019), our findings must be carefully interpreted in light of the low prevalence of ESBL/AmpC-positive *E. coli* found herein (5%; 1/20) and the apparently healthy condition (with no signs of disease) presented by frigatebirds in Alcatrazes (also described by Saviolli et al., 2016). Furthermore, our strain also harbored genes encoding resistance to heavy metals, QACs and pesticides (**Table 1**), which may promote the development of AMR and co-selection of ARGs (Zou et al., 2014; Ramakrishnan et al., 2019; Mazhar et al., 2021).

Anthropization has been suggested as a driving factor in the epidemiology of ARGs in wildlife (Ahlstrom et al., 2018; Sacristaìn et al., 2020; Ewbank et al., 2021). Although occasionally visited or exploited for commercial guano harvesting until the mid-20$^{th}$ century, to this date, there are no reports of human occupation or settlements in the archipelago (Instituto Chico Mendes de Conservação da Biodiversidade (ICMBio), 2017). Nevertheless, Alcatrazes is located in the highly anthropized southeastern Brazilian coast, subjected to intense tourism activities, fishing, and oil exploitation, that also harbors the largest port complex (Santos Port), and oil and derivatives terminal in Latin America (Almirante Barroso Maritime Terminal - TEBAR). Of note, recent studies assessing antimicrobial resistance pollution in the marine ecosystem of the southeastern Brazilian coast showed that the local resistome is indeed under severe anthropogenic pressure (Fernandes et al., 2017, 2020a,b; Sellera et al., 2018a,b).

The Alcatrazes Archipelago is the largest insular bird breeding site of the southeastern Brazilian coast and the biggest breeding colony of magnificent frigatebirds in the southern Atlantic (Alcatrazes Island) (Instituto Chico Mendes de Conservação da Biodiversidade (ICMBio), 2017). Magnificent frigatebirds are non-synanthropic, non-migratory, and highly colonial seabird species that prefer insular over coastal environments, and also known for their particular feeding techniques (e.g., kleptoparasitism and fisheries interaction) (Saviolli et al., 2016; BirdLife International, 2021). Such characteristics infer that the studied Alcatrazes individuals most likely sustain very limited to no direct contact with humans, but that due to their philopatric (site fidelity) behavior, and limited roosting and nesting area of the island, are continuously interacting with the other frigatebird specimens and bird species using the area (especially with brown boobies (*Sula leucogaster*) and black vultures (*Coragyps atratus*), A.C. Ewbank, personal observation). Consequently, such close contact and active exchange of body fluids may be a possible route of infection by ESBL/pAmpC-positive *E. coli*, as seen in other avian pathogens (de Thoisy et al., 2009; Niemeyer et al., 2017).

Thus, in light of the above, we suggest that our isolate was likely acquired through one or more of the following: (i) indirect colonization by a bacterium released from human sources into the local marine environment (e.g., sewage) (Fernandes et al., 2017, 2018, 2020a,b); (ii) ingestion of contaminated seafood (Brahmi et al., 2015; Sellera et al., 2018a,b); and (iii) direct intra and/or interspecies contact (Ewbank et al., 2022).

Interestingly, according to the phylogenetic results, our isolate was not closely related to the selected ST648 isolates from other geographical regions or ecological sources included in the analysis. This indicates that, even though the origin of our isolate was likely related to human sources, this phylogenetic cluster seems to be restricted to the specific coastal/insular geographical area of Alcatrazes, southeastern Brazil. Nevertheless, additional studies in the region are necessary in order to confirm this hypothesis.

Previous studies have discussed the hypothetical potential of wild birds as reservoirs and disseminators of ARGs and ARB to insular biomes (Hernandez et al., 2010;

Ewbank et al., 2021, 2022). Nevertheless, in spite of experimental studies assessing the shedding, contamination and potential transmission of ARGs and ARB by wild birds (Sandegren et al., 2018; Franklin et al., 2020), their potential role as dispersers under real-world conditions is still unknown. Our findings demonstrate that even in the absence of regular human presence, insular resistomes are indirectly pressured by anthropogenic activities, suggesting that contamination of the marine ecosystem and inter and/or intraspecific bird interactions should also be considered in the study of antimicrobial resistance in these biomes.

Herein we reported the genomic background of a critical priority *E. coli* strain belonging to the pandemic high-risk clone ST648 *E.coli* with a hypothetical zoonotic and avian pathogenic potential colonizing a wild magnificent frigatebird of an insular biome. Our findings reinforce, within a One Health perspective, the importance of surveillance studies of WHO critical priority pathogens in wildlife and the role of wild birds as anthropization sentinels in insular environments. Future studies evaluating the occurrence and diversity of ESBL/pAmpC-positive *E. coli* in magnificent frigatebirds on the Alcatrazes Archipelago should rely on continuous temporal sampling to assess a larger number of specimens, evaluate interacting species (i.e., brown boobies and black vultures), and environmental samples (i.e., sea water and soil), including local marine life (i.e., fish), in order to monitor these populations through a One Health approach and further elucidate the epidemiology of ESBL/pAmpC-positive *E. coli* in this insular environment.

## Data availability statement

The data presented in this study are deposited in the DDBJ/EMBL/GenBank repository, accession number NZ_JAGYFD010000000. The sequence has been released and is available at the repository: https://www.ncbi.nlm.nih.gov/nuccore/NZ_JAGYFD000000000.1.

## Ethics statement

This study was performed in full compliance with the Biodiversity Information and Authorization System (SISBIO 59150-4), Brazilian Ministry of Environment and the Ethical Committee in Animal Research of the School of Veterinary Medicine and Animal Sciences, University of São Paulo (Process no. 1753110716).

## Author contributions

AE: conceptualization, methodology, investigation, writing original draft, supervision, project administration, and funding acquisition. DF-C: methodology, investigation, writing original draft, and supervision. CS: conceptualization, methodology, investigation, funding acquisition, and writing original draft. FE: methodology, formal analysis, and writing original draft. BF and BC: methodology and formal analysis. SG: conceptualization, investigation, resources, and funding acquisition. RZ and MG: investigation and resources. JC-D and NL: conceptualization, methodology, resources, writing–review and editing, supervision, project administration, and funding acquisition. All authors contributed to the article and approved the submitted version.

## Funding

This study was supported by the Bill & Melinda Gates Foundation (Grand Challenges Explorations Brazil OPP1193112). Under the grant conditions of the Foundation, a CC BY or equivalent license is applied to the Author Accepted Manuscript version arising from this submission. Additionally, this study was financed by the Coordination for the Improvement of Higher Education Personnel (CAPES), National Council for Scientific and Technological Development (CNPq) (AMR 443819/2018-1, 433128/2018-6), and the São Paulo State Research Foundation (FAPESP) (2020/08224-9). AE and FE receive doctoral fellowships from FAPESP (process no. 2018/20956-0 and 2019/15578-4, respectively), BC from CAPES (88882.333054/2019-01), and RZ from CNPq (process no. 165364/2018-1). BF was a recipient of a post-doctoral fellowship from CAPES (88887.358057/2019-00). CS was the recipient of a Juan the la Cierva Incorporation Fellowship IJC2020-046019-I. JC-D was the recipient of a professorship from CNPq (304999-18) and NL was a research fellow of CNPq (314336/2021-4)].

## Acknowledgments

We thank the staff of the Refúgio de Vida Silvestre do Arquipélago de Alcatrazes – Institute Chico Mendes for Biodiversity Conservation (ICMBio), José F. Delgado-Blas, Marcos Paulo Vieira Cunha and Terezinha Knöbl for the logistical and scientific support. We also thank Chris H. Gardiner, for contributing in the review of this manuscript.

## Conflict of interest

The authors declare that the research was conducted in the absence of any commercial or financial relationships that could be construed as a potential conflict of interest.

## Publisher's note



## References

Ahlstrom, C. A., Bonnedahl, J., Woksepp, H., Hernandez, J., Olsen, B., and Ramey, A. M. (2018). Acquisition and dissemination of cephalosporin-resistant *E. coli* in migratory birds sampled at an Alaska landfill as inferred through genomic analysis. *Sci. Rep.* 8:7361. doi: 10.1038/s41598-018-25474-w

Alcalá, L., Alonso, C. A., Simón, C., González-Esteban, C., Orós, J., Rezusta, A., et al. (2016). Wild birds, frequent carriers of extended-spectrum β-lactamase (ESBL) producing *Escherichia coli* of CTX-M and SHV-12 Types. *Microb. Ecol.* 72, 861–869. doi: 10.1007/s00248-015-0718-0

Andrews, S. (2010). *FastQC: A Quality Control Tool for High Throughput Sequence Data*. Available online at: https://github.com/s-andrews/FastQC (accessed on June 10, 2010).

Athanasakopoulou, Z., Tsilipounidaki, K., Sofia, M., Chatzopoulos, D. C., Giannakopoulos, A., Karakousis, I., et al. (2021). Poultry and wild birds as a reservoir of CMY-2-producing *Escherichia coli*: the first large-scale study in Greece. *J. Antibiot.* 10:235. doi: 10.3390/antibiotics10030235

Atterby, C., Ramey, A. M., Hall, G. G., Jarhult, J., Borjesson, S., and Bonnedahl, J. (2016). Increased prevalence of antibiotic-resistant *E. coli* in gulls sampled in Southcentral Alaska is associated with urban environments. *Infect. Ecol. Epidemiol.* 6:32334. doi: 10.3402/iee.v6.32334

Báez, J., Hernández-Gracía, M., Guamparito, C., Díaz, S., Olave, A., Guerrero, K., et al. (2015). Molecular characterization and genetic diversity of ESBL-producing *Escherichia coli* colonizing the migratory Franklin's gulls (*Leucophaeus pipixcan*) in Antofagasta, North of Chile. *Microb. Drug Resist.* 21, 111–116. doi: 10.1089/mdr.2014.0158

Batalha de Jesus, A. A., Freitas, A. A. R., de Souza, J. C., Martins, N., Botelho, L. A. B., Girão, V. B. C., et al. (2019). High-level multidrug-resistant *Escherichia coli* isolates from wild birds in a large urban environment. *Microb. Drug Resist.* 25, 167–172. doi: 10.1089/mdr.2018.0180

Bélanger, L., Garenaux, A., Harel, J., Boulianne, M., Nadeau, E., and Dozois, C. M. (2011). Escherichia coli from animal reservoirs as a potential source of human extraintestinal pathogenic *E. coli*. *FEMS Immunol. Med. Microbiol.* 62, 1–10. doi: 10.1111/j.1574-695X.2011.00797.x

BirdLife International (2021). *Species factsheet: Fregata magnificens*. Available online at: http://datazone.birdlife.org/species/factsheet/magnificent-frigatebird-fregata-magnificens (accessed on May 9, 2021).

Bonnedahl, J., Drobni, M., Gauthier-Clerc, M., Hernandez, J., Granholm, S., Kayser, Y., et al. (2009). Dissemination of *Escherichia coli* with CTX-M type ESBL between humans and yellow-legged gulls in the south of France. *PLoS One* 4:e5958. doi: 10.1371/journal.pone.0005958

Brahmi, S., Dunyach-Rémy, C., Touati, A., and Lavigne, J.-P. (2015). CTX-M-15-producing *Escherichia coli* and the pandemic clone O25b-ST131 isolated from wild fish in Mediterranean Sea. *Clin. Microbiol. Infect.* 21, e18–e20. doi: 10.1016/j.cmi.2014.09.019

Clinical and Laboratory Standards Institute [CLSI] (2018). *Performance Standards for Antimicrobial Disk and Dilution Susceptibility Tests for Bacteria Isolated From Animals*. CLSI supplement VET08. Philadelphia: CLSI.

Clinical and Laboratory Standards Institute [CLSI] (2019). *Performance Standards for Antimicrobial Susceptibility Testing* CLSI supplement M100. Philadelphia: CLSI.

Cunha, M. P., Lincopan, N., Cerdeira, L., Esposito, F., Dropa, M., Franco, L. S., et al. (2017). Coexistence of CTX-M-2, CTX-M-55, CMY-2, FosA3, and QnrB19 in extraintestinal pathogenic *Escherichia coli* from poultry in Brazil. *Antimicrob Agents Chemother* 61:e02474-16. doi: 10.1128/AAC.02474-16

de Carvalho, M. P. N., Fernandes, M. R., Sellera, F. P., Lopes, R., Monte, D. F., Hippólito, A. G., et al. (2020). International clones of extended-spectrum β-lactamase (CTX-M)-producing *Escherichia coli* in peri-urban wild animals, Brazil. *Transbound Emerg. Dis.* 67, 1804–1815. doi: 10.1111/tbed.13558

de Thoisy, B., Lavergne, A., Semelin, J., Pouliquen, J. F., Blanchard, F., Hansen, E., et al. (2009). Outbreaks of disease possibly due to a natural avian herpesvirus infection in a colony of young Magnificent Frigatebirds (Fregata magnificens) in French Guiana. *J. Wildl. Dis.* 45, 802–807. doi: 10.7589/0090-3558-45.3.802

Dziva, F., and Stevens, M. P. (2008). Colibacillosis in poultry: unravelling the molecular basis of virulence of avian pathogenic *Escherichia coli* in their natural hosts. *Avian Pathol.* 37, 355–366. doi: 10.1080/03079450802216652

EUCAST (2017). *Guidelines for Detection of Resistance Mechanisms and Specific Resistances of Clinical and/or Epidemiological Importance*. Sweden: European Comittee of Antimicrobial Susceptibility Testing.

Ewbank, A. C., Esperón, F., Sacristán, C., Sacristán, I., Krul, R., Cavalcante de Macedo, E., et al. (2021). Seabirds as anthropization indicators in two different tropical biotopes: a One Health approach to the issue of antimicrobial resistance genes pollution in oceanic islands. *Sci. Total Environ.* 754:142141. doi: 10.1016/j.scitotenv.2020.142141

Ewbank, A. C., Fuentes-Castillo, D., Sacristán, C., Cardoso, B., Esposito, F., Fuga, B., et al. (2022). Extended-spectrum β-lactamase (ESBL)-producing *Escherichia coli* survey in wild seabirds at a pristine atoll in the southern Atlantic Ocean, Brazil: first report of the O25b-ST131 clone harboring $bla_{CTX-M-8}$. *Sci. Total Environ.* 806:150539. doi: 10.1016/j.scitotenv.2021.150539

Ewers, C., Bethe, A., Stamm, I., Grobbel, M., Kopp, P. A., Guerra, B., et al. (2014). CTX-M-15-D-ST648 *Escherichia coli* from companion animals and horses: another pandemic clone combining multiresistance and extraintestinal virulence? *J. Antimicrobial. Chemother.* 69, 1224–1230. doi: 10.1093/jac/dkt516

Ewers, C., Li, G., Wilking, H., Kiessling, S., Alt, K., Antáo, E. M., et al. (2007). Avian pathogenic, uropathogenic, and newborn meningitis-causing *Escherichia coli*: how closely related are they? *Int. J. Med. Microbiol.* 297, 163–176. doi: 10.1016/j.ijmm.2007.01.003

Fernandes, M. R., Sellera, F. P., Moura, Q., Esposito, F., Sabino, C. P., and Lincopan, N. (2020b). Identification and genomic features of halotolerant extended-spectrum-β-lactamase (CTX-M)-producing *Escherichia coli* in urban-impacted coastal waters, Southeast Brazil. *Mar. Pollut. Bull.* 150:110689. doi: 10.1016/j.marpolbul.2019.110689

Fernandes, M. R., Sellera, F. P., Cunha, M. P. V., Lopes, R., Cerdeira, L., and Lincopan, N. (2020a). Emergence of CTX-M-27-producing *Escherichia coli* of ST131 and clade C1-M27 in an impacted ecosystem with international maritime traffic in South America. *J. Antimicrob. Chemother.* 75, 1647–1649. doi: 10.1093/jac/dkaa069

Fernandes, M. R., Sellera, F. P., Esposito, F., Sabino, C. P., Cerdeira, L., and Lincopan, N. (2017). Colistin-resistant *mcr-1*-positive *Escherichia coli* on public beaches, an infectious threat emerging in recreational waters. *Antimicrob. Agents Chemother.* 61:e00234-17. doi: 10.1128/AAC.00234-17

Fernandes, M. R., Sellera, F. P., Moura, Q., Gaspar, V. C., Cerdeira, L., and Lincopan, N. (2018). International high-risk clonal lineages of CTX-M-producing *Escherichia coli* F-ST648 in free-roaming cats, South America. *Infect. Genet. Evol.* 66, 48–51. doi: 10.1016/j.meegid.2018.09.009

Franklin, A. B., Ramey, A. M., Bentler, K. T., Barrett, N. L., McCurdy, L. M., Ahlstrom, C. A., et al. (2020). Gulls as sources of environmental contamination by colistin-resistant bacteria. *Sci. Rep.* 10:4408. doi: 10.1038/s41598-020-61318-2

Grimwood, K., Anderson, P., Anderson, V., Tan, L., and Nolan, T. (2000). Twelve year outcomes following bacterial meningitis: further evidence for persisting effects. *Arch. Dis. Child* 83, 111–116. doi: 10.1136/adc.83.2.111

Guenther, S., Grobbel, M., Beutlich, J., Bethe, A., Friedrich, N. D., Goedecke, A., et al. (2010). CTX-M-15-type extended-spectrum beta-lactamases-producing

*Escherichia coli* from wild birds in Germany. *Environ. Microbiol. Rep.* 2, 641–645. doi: 10.1111/j.1758-2229.2010.00148.x

Hasan, B., Sandegren, L., Melhus, A., Drobni, M., Hernandez, J., Waldenström, J., et al. (2012). Antimicrobial drug-resistant *Escherichia coli* in wild birds and free-range poultry, Bangladesh. *Emerg. Infect. Dis.* 18, 2055–2058. doi: 10.3201/eid1812.120513

Hernández, J., and González-Acuña, D. (2016). Anthropogenic antibiotic resistance genes mobilization to the polar regions. *Infect. Ecol. Epidemiol.* 6:32112. doi: 10.3402/iee.v6.32112

Hernandez, J., Bonnedahl, J., Eliasson, I., Wallensten, A., Comstedt, P., Johansson, A., et al. (2010). Globally disseminated human pathogenic *Escherichia coli* of O25b-ST131 clone, harbouring $bla_{CTX-M-15}$, found in Glaucous-winged gull at remote Commander Islands, Russia. *Environ. Microbiol. Rep.* 2, 329–332. doi: 10.1111/j.1758-2229.2010.00142.x

Hu, Y. Y., Cai, J. C., Zhou, H. W., Chi, D., Zhang, X. F., Chen, W. L., et al. (2013). Molecular typing of CTX-M-producing *Escherichia coli* isolates from environmental water, swine feces, specimens from healthy humans, and human patients. *Appl. Environ. Microbiol.* 79, 5988–5996. doi: 10.1128/AEM.01740-13

Instituto Chico Mendes de Conservação da Biodiversidade (ICMBio) (2017). *Plano de Manejo da Estação Ecológica Tupinambás e Refúgio de Vida Silvestre do Arquipélago de Alcatrazes*. Brasília, DF: Instituto Chico Mendes de Conservação da Biodiversidade.

Jacoby, G. A. (2009). AmpC beta-lactamases. *Clin. Microbiol. Rev.* 22, 161–182.

Jamborova, I., Dolejska, M., Zurek, L., Townsend, A. K., Clark, A. B., Ellis, J. C., et al. (2017). Plasmid-mediated resistance to cephalosporins and quinolones in *Escherichia coli* from American crows in the USA. *Environ. Microbiol.* 19, 2025–2036. doi: 10.1111/1462-2920.13722

Jobbins, S. E., and Alexander, K. A. (2015). From whence they came: antibiotic-resistant *Escherichia coli* in African wildlife. *J. Wildl. Dis.* 51, 811–820. doi: 10.7589/2014-11-257

Kemmett, K., Williams, N. J., Chaloner, G., Humphrey, S., Wigley, P., and Humphrey, T. (2014). The contribution of systemic *Escherichia coli* infection to the early mortalities of commercial broiler chickens. *Avian Pathol.* 43, 37–42. doi: 10.1080/03079457.2013.866213

Kim, K. S. (2002). Strategy of *Escherichia coli* for crossing the blood-brain barrier. *J. Infect. Dis.* 1, S220–S224. doi: 10.1086/344284

Liakopoulos, A., Olsen, B., Geurts, Y., Artursson, K., Berg, C., Mevius, D. J., et al. (2016). Molecular characterization of extended-spectrum-cephalosporin-resistant *Enterobacteriaceae* from wild kelp gulls in South America. *Antimicrob. Agents Chemother.* 60, 6924–6927. doi: 10.1128/AAC.01120-16

Loncaric, I., Stalder, G. L., Mehinagic, K., Rosengarten, R., Hoelzl, F., Knauer, F., et al. (2013). Comparison of ESBL and AmpC producing *Enterobacteriaceae* and methicillin-resistant *Staphylococcus aureus* (MRSA) isolated from migratory and resident population of rooks (*Corvus frugilegus*) in Austria. *PLoS One* 8:e84048. doi: 10.1371/journal.pone.0084048

Maluta, R. P., Logue, C. M., Casas, M. R., Meng, T., Guastalli, E. A., Rojas, T. C., et al. (2014). Overlapped sequence types (STs) and serogroups of avian pathogenic (APEC) and human extra-intestinal pathogenic (ExPEC) *Escherichia coli* isolated in Brazil. *PLoS One* 9:e105016. doi: 10.1371/journal.pone.0105016

Mazhar, S. H., Li, X., Rashid, A., Su, J., Xu, J., Brejnrod, A. D., et al. (2021). Co-selection of antibiotic resistance genes, and mobile genetic elements in the presence of heavy metals in poultry farm environments. *Sci. Total Environ.* 755:142702. doi: 10.1016/j.scitotenv.2020.142702

Melo, L. C., Oresco, C., Leigue, L., Netto, H. M., Melville, P. A., Benites, N. R., et al. (2018). Prevalence and molecular features of ESBL/pAmpC-producing *Enterobacteriaceae* in healthy and diseased companion animals in Brazil. *Vet. Microbiol.* 221, 59–66. doi: 10.1016/j.vetmic.2018.05.017

Michael, C. A., Dominey-Howes, D., and Labbate, M. (2014). The antimicrobial resistance crisis: causes, consequences, and management. *Front. Public Health* 2:145. doi: 10.3389/fpubh.2014.00145

Mughini-Gras, L., Dorado-García, A., van Duijkeren, E., van den Bunt, G., Dierikx, C. M., Bonten, M. J. M., et al. (2019). ESBL Attribution Consortium. Attributable sources of community-acquired carriage of *Escherichia coli* containing β-lactam antibiotic resistance genes: a population-based modelling study. *Lancet Planet Health* 3, e357–e369. doi: 10.1016/S2542-5196(19)30130-5

Mukerji, S., Stegger, M., Truswell, A. V., Laird, T., Jordan, D., Abraham, R. J., et al. (2019). Resistance to critically important antimicrobials in Australian silver gulls (*Chroicocephalus novaehollandiae*) and evidence of anthropogenic origins. *J. Antimicrob. Chemother.* 74, 2566–2574. doi: 10.1093/jac/dkz242

Niemeyer, C., Favero, C. M., Shivaprasad, H. L., Uhart, M., Musso, C. M., Rago, M. V., et al. (2017). Genetically diverse herpesviruses in South American Atlantic coast seabirds. *PLoS One* 12:e0178811. doi: 10.1371/journal.pone.0178811

Poirel, L., Potron, A., de La Cuesta, C., Cleary, T., Nordmann, P., and Munoz-Price, L. S. (2012). Wild coastline birds as reservoirs of broad-spectrum-β-lactamase-producing *Enterobacteriaceae* in Miami Beach, Florida. *Antimicrob. Agents Chemother.* 56, 2756–2758. doi: 10.1128/AAC.05982-11

Pruden, A., Pei, R., Storteboomm, H., and Carlson, K. H. (2006). Antibiotic resistance genes as emerging contaminants: studies in Northern Colorado. *Environ. Sci. Technol.* 40, 7445–7450. doi: 10.1021/es060413l

Ramakrishnan, B., Venkateswarlu, K., Sethunathan, N., and Megharaj, M. (2019). Local applications but global implications: can pesticides drive microorganisms to develop antimicrobial resistance? *Sci. Total Environ.* 654, 177–189. doi: 10.1016/j.scitotenv.2018.11.041

Rocha, F. R., Pinto, V. P. T., and Barbosa, F. C. B. (2015). The spread of CTX-M-type extended-spectrum β-lactamases in Brazil: a systematic review. *Microb. Drug Resist.* 22, 301–311. doi: 10.1089/mdr.2015.0180

Rodriguez-Siek, K. E., Giddings, C. W., Doetkott, C., Johnson, T. J., Fakhr, M. K., and Nolan, L. K. (2005). Comparison of *Escherichia coli* isolates implicated in human urinary tract infection and avian colibacillosis. *Microbiology* 151, 2097–2110. doi: 10.1099/mic.0.27499-0

Sacristaìn, I., Esperoìn, F., Acuna, F., Aguilar, E., Garciìa, S., Loìpez, M. J., et al. (2020). Antibiotic resistance genes as landscape anthropization indicators: using a wild felid as sentinel in Chile. *Sci. Total Environ.* 703:134900. doi: 10.1016/j.scitotenv.2019.134900

Sandegren, L., Stedt, J., Lustig, U., Bonnedahl, J., Andersson, D. I, and Järhult, J. D. (2018). Long-term carriage and rapid transmission of extended spectrum beta-lactamase-producing *E. coli* within a flock of Mallards in the absence of antibiotic selection. *Environ. Microbiol. Rep.* 10, 576–582. doi: 10.1111/1758-2229.12681

Sarowska, J., Futoma-Koloch, B., Jama-Kmiecik, A., Frej-Madrzak, M., Ksiazczyk, M., Bugla-Ploskonska, G., et al. (2019). Virulence factors, prevalence and potential transmission of extraintestinal pathogenic *Escherichia coli* isolated from different sources: recent reports. *Gut Pathog.* 21:10. doi: 10.1186/s13099-019-0290-0

Saviolli, J. Y., Cunha, M. P., Guerra, M. F., Irino, K., Catão-Dias, J. L., and de Carvalho, V. M. (2016). Free-ranging frigates (*Fregata magnificens*) of the southeast coast of Brazil harbor extraintestinal pathogenic *Escherichia coli* resistant to antimicrobials. *PLoS One* 11:e0148624. doi: 10.1371/journal.pone.0148624

Schaufler, K., Semmler, T., Wieler, L. H., Trott, D. J., Pitout, J., Peirano, G., et al. (2019). Genomic and functional analysis of emerging virulent and multidrug-resistant *Escherichia coli* lineage sequence type 648. *Antimicrob. Agents Chemother.* 63, e243–e219. doi: 10.1128/AAC.00243-19

Sellera, F. P., Fernandes, M. R., Moura, Q., Carvalho, M. P. N., and Lincopan, N. (2018a). Extended-spectrum-β-lactamase (CTX-M)-producing *Escherichia coli* in wild fishes from a polluted area in the Atlantic Coast of South America. *Mar. Pollut. Bull.* 135, 183–186.

Sellera, F. P., Fernandes, M. R., Moura, Q., Lopes, R. B., Souza, T. A., Cerdeira, L., et al. (2018b). Draft genome sequence of a $bla_{CMY-2}$/IncI1-harbouring *Escherichia coli* D:ST457 isolated from coastal benthic organisms. *J. Glob. Antimicrob. Resist.* 14, 83–84. doi: 10.1016/j.jgar.2018.06.010

Sellera, F. P., Fernandes, M. R., Sartori, L., Carvalho, M. P., Esposito, F., Nascimento, C. L., et al. (2017). *Escherichia coli* carrying IncX4 plasmid-mediated *mcr-1* and $bla_{CTX-M}$ genes in infected migratory Magellanic penguins (*Spheniscus magellanicus*). *J. Antimicrob. Chemother.* 72, 1255–1256. doi: 10.1093/jac/dkw543

Stedt, J., Bonnedahl, J., Hernandez, J., Waldenström, J., McMahon, B. J., Tolf, C., et al. (2015). Carriage of CTX-M type extended spectrum β-lactamases (ESBLs) in gulls across Europe. *Acta Vet. Scand.* 57:74. doi: 10.1186/s13028-015-0166-3

Tacconelli, E., Carrara, E., Savoldi, A., Harbarth, S., Mendelson, M., Monnet, D. L., et al. (2018). WHO Pathogens Priority List Working Group. Discovery, research, and development of new antibiotics: the WHO priority list of antibiotic-resistant bacteria and tuberculosis. *Lancet Infect Dis.* 18, 318–327. doi: 10.1016/S1473-3099(17)30753-3

Tenaillon, O., Skurnik, D., Picard, B., and Denamur, E. (2010). The population genetics of commensal *Escherichia coli*. *Nat. Rev. Microbiol.* 8, 207–217. doi: 10.1038/nrmicro2298

West, B. M., Liggit, P., Clemans, D. L., and Francoeur, S. N. (2010). Antibiotic resistance, gene transfer, and water quality patterns observed in waterways near

CAFO farms and wastewater treatment facilities. *Water Air Soil Pollut.* 217, 473–489. doi: 10.1007/s11270-010-0602-y

Wright, G. D. (2007). The antibiotic resistome: the nexus of chemical and genetic diversity. *Nat. Rev. Microbiol.* 5, 175–186. doi: 10.1038/nrmicro 1614

Yang, J., Wang, C., Shu, C., Liu, L., Geng, J., Hu, S., et al. (2013). Marine sediment bacteria harbor antibiotic resistance genes highly similar to those found in human pathogens. *Microb. Ecol.* 65, 975–981. doi: 10.1007/s00248-013-0187-2

Yang, R. S., Feng, Y., Lv, X. Y., Duan, J. H., Chen, J., Fang, L. X., et al. (2016). Emergence of NDM-5- and MCR-1-producing *Escherichia coli* clones ST648 and ST156 from a single muscovy duck (*Cairina moschata*). *Antimicrob. Agents Chemother.* 60, 6899–6902. doi: 10.1128/AAC.01365-16

Zou, L., Meng, J., McDermott, P. F., Wang, F., Yang, Q., Cao, G., et al. (2014). Presence of disinfectant resistance genes in *Escherichia coli* isolated from retail meats in the USA. *J. Antimicrob. Chemother.* 69, 2644–2649. doi: 10.1093/jac/dku197

frontiers | Frontiers in Microbiology

TYPE Original Research
PUBLISHED 12 August 2022
DOI 10.3389/fmicb.2022.941259



OPEN ACCESS

EDITED BY
Haihong Hao,
Huazhong Agricultural University, China

REVIEWED BY
Chang-Wei Lei,
Sichuan University, China
Xiaona Zhao,
Shandong Agricultural University, China

*CORRESPONDENCE
Keyu Zhang
z_cole@sina.com

†These authors have contributed equally to this work

SPECIALTY SECTION
This article was submitted to Antimicrobials, Resistance and Chemotherapy, a section of the journal Frontiers in Microbiology

RECEIVED 11 May 2022
ACCEPTED 01 July 2022
PUBLISHED 12 August 2022

CITATION
Cheng X, Zheng H, Wang C, Wang X, Fei C, Zhou W and Zhang K (2022) Effects of salinomycin and ethanamizuril on the three microbial communities *in vivo* and *in vitro*. *Front. Microbiol.* 13:941259. doi: 10.3389/fmicb.2022.941259



# Effects of salinomycin and ethanamizuril on the three microbial communities *in vivo* and *in vitro*

Xiaolei Cheng†, Haihong Zheng†, Chunmei Wang, Xiaoyang Wang, Chenzhong Fei, Wen Zhou and Keyu Zhang*

Key Laboratory of Veterinary Chemical Drugs and Pharmaceutics, Ministry of Agriculture and Rural Affairs, Shanghai Veterinary Research Institute, Chinese Academy of Agricultural Sciences, Shanghai, China

The fate of a drug is not only the process of drug metabolism *in vivo* and *in vitro* but also the homeostasis of drug-exposed microbial communities may be disturbed. Anticoccidial drugs are widely used to combat the detrimental effects of protozoan parasites in the poultry industry. Salinomycin and ethanamizuril belong to two different classes of anticoccidial drugs. The effect of salinomycin and ethanamizuril on the microbiota of cecal content, manure compost, and soil remains unknown. Our results showed that although both salinomycin and ethanamizuril treatments suppressed some opportunistic pathogens, they failed to repair the great changes in chicken cecal microbial compositions caused by coccidia infection. Subsequently, the metabolite5 profiling of cecal content by LC-MS/MS analyses confirmed the great impact of coccidia infection on chicken cecum and showed that histidine metabolism may be the main action pathway of salinomycin, and aminoacyl tRNA biosynthesis may be the major regulatory mechanism of ethanamizuril. The microbial community of manure compost showed a mild response to ethanamizuril treatment, but ethanamizuril in soil could promote *Actinobacteria* reproduction, which may inhibit other taxonomic bacteria. When the soil and manure were exposed to salinomycin, the *Proteobacteria* abundance of microbial communities showed a significant increase, which suggested that salinomycin may improve the ability of the microbiota to utilize carbon sources. This hypothesis was confirmed by a BIOLOG ECO microplate analysis. In the animal model of coccidia infection, the treatment of salinomycin and ethanamizuril may reconstruct a new equilibrium of the intestinal microbiota. In an *in vitro* environment, the effect of ethanamizuril on composting and soil microbiota seems to be slight. However, salinomycin has a great impact on the microbial communities of manure composting and soil. In particular, the promoting effect of salinomycin on *Proteobacteria* phylum should be further concerned. In general, salinomycin and ethanamizuril have diverse effects on various microbial communities.

KEYWORDS

**microbial community, salinomycin, ethanamizuril, metabolite profile, physiological profiling**

# Introduction

The microbiome is a unique ecosystem. Surfaces of animals, plants, and soil are colonized by complex microbial communities whose structure and function are seriously affected by microbe–microbe, microbe–host, and microbe–environmental factors interactions. Growing attention has been paid to the factors that influence the assembly and stability of host-associated microbiomes and their impact on host phenotype, ecology, and evolution over the last decades (McDonald et al., 2020). The animal gut microbiome is a dynamic collection of bacteria, archaea, fungi, and phages that plays numerous roles in immune development, pathogen colonization resistance, and food metabolism. Although the ecology of the gut microbiome is relatively stable, it could be impacted by various factors, such as food, pathogens, and drugs (Schwartz et al., 2020). The soil microbiome is clearly a key component of natural ecosystems. A large amount of evidence highlights that the survival and growth of soil microorganisms are seriously limited by abiotic stressors (e.g., acidic conditions) and frequent interference of other soil microbial groups (antibiotic-producing bacteria) (Islam et al., 2020). Composting is an environmental-friendly approach to transform animal manure into high-quality agricultural organic fertilizer (Wan et al., 2021). During composting, microbiota are an important driver of organic matter depolymerization and are influenced by physicochemical and other factors.

Coccidiosis is a serious protozoal infectious disease and is estimated to cause global economic losses of up to $3 billion annually only in the poultry industry (Kadykalo et al., 2018; Zhang et al., 2020a). The main method of controlling coccidiosis relies heavily on the use of the highly effective coccidiostats reasonably and correctly. Predominant drugs in controlling coccidiosis are polyether ionophore antibiotics and triazines compounds. Polyether ionophore antibiotics have the activity of facilitating the transport of cations through the cell membranes of target organisms (including protozoa and Gram-positive bacteria) and are important coccidiostats (Antoszczak et al., 2019). Salinomycin, a monocarboxylic polyether antibiotic, is an important member of the ionophore anticoccidials in poultry production. As broad-spectrum ionophore anticoccidials with activity against Gram-positive bacteria, fungi, and coccidia, salinomycin is widely used in veterinary medicine worldwide (Zhou et al., 2013). In addition, triazine compounds have been safely and effectively used to combat the detrimental effects of protozoan parasites, especially poultry coccidiosis, in the global veterinary community for years. Triazines have been reported to inhibit the nuclear division of protozoan parasites, thereby interfering with the development and growth of schizonts and gametocytes (Stock et al., 2018). Ethanamizuril is a novel triazine compound that has shown excellent effectiveness against coccidiosis at a dosage of 10 mg/L in drinking water (Wang et al., 2020; Zhang et al., 2020b). It has been approved for usage in broiler chickens since 2020 in China.

The resistance and resilience of a microbiome to external stress and perturbation are among the potential properties that characterize a healthy microbiome (Lloyd-Price et al., 2016). Accumulating evidence suggests that antibiotics play complex roles by reshaping the intestinal microbiota. Deep sequencing of the bacterial 16S rRNA gene revealed that the richness of the cecal microbiota was significantly reduced while the evenness increased after the male Cobb broilers had been supplemented with subtherapeutic salinomycin as antimicrobial growth promoters for 14 days (Robinson et al., 2019). The interaction between microbiota and used agents is complex and bidirectional (Weersma et al., 2020). The metabolic fates of drugs in the intestinal tract, manure compost, and soil environment have always been widely concerned. Understanding the microbial community profile is also important for predicting the fate of drugs in the environment. However, so far, the effect of coccidiostats on the gut microbiota of coccidial-infected chickens remains unknown. Moreover, excretion of the prototype drug through feces is the main metabolic pathway for ethanamizuril and salinomycin *in vivo* after chickens are administered (Henri et al., 2012; Liu et al., 2020). To the best of our knowledge, there is no research data on the effects of salinomycin and ethanamizuril on manure composting and soil microbial communities.

In the present study, we investigated and compared the effects of salinomycin and ethanamizuril on the microbiota of coccidia-infected broilers' cecal content, manure composting, and soil using the bacterial 16S rRNA gene sequencing. The two coccidiostats were chosen because they belong to different classes of anticoccidial drugs and are known to have different antiprotozoan mechanisms. Furthermore, the effects of salinomycin and ethanamizuril on the metabolism of the chicken cecum and on soil microbiota function were revealed by LC-tandem mass spectrometry and BIOLOG ECO microplates, respectively. Identification of a number of bacterial compositions that are altered in response to salinomycin and ethanamizuril sheds new light on their anticoccidial mechanism *in vivo* and harmless elimination *in vitro* and may contribute to the use of microbiota to improve anticoccidial efficiency and environmental protection in the future.

# Materials and methods

## Drugs and parasites

Salinomycin sodium was purchased from China Institute of Veterinary Drug Control (Beijing, China). Ethanamizuril and *E. tenella* strain (CAAS2111606) was obtained from Shanghai Veterinary Research Institute, Chinese Academy of Agriculture

Sciences (Shanghai, China). The oocysts of *E. tenella* were sporulated and purified according to the methods described in our previous studies (Li et al., 2019). Analytical grade chemicals and solvents for extraction and analysis were purchased from local chemical suppliers.

## Experimental design

### Exposure to the cecum *in vivo*

All the research was approved by the Shanghai Veterinary Research Institutional Animal Care Committee and in accordance with the National Institutes of Health Guide on the Care and Use of Laboratory Animals. Then, 1-day-old healthy Pudong yellow broiler chickens were obtained from the same hatch of a local commercial hatchery and reared in wire cages sterilized by dry heat sterilization. Feed and water were supplied *ad libitum,* and no additive drugs were used. At 8 days of age, a total of 120 chickens were weighed and randomly divided into four groups of 10 birds per cage. Each group was separated to prevent accidental cross-infection. The four groups were the control group (Mock), the non-medicated control group (NC), the ethanamizuril group (L1), and the salinomycin group (S). Then, the ethanamizuril group (L1) was treated with 10 mg/L of ethanamizuril in drinking water for 3 days, and the salinomycin group (S) was treated with 60 mg/kg salinomycin in feed for 7 days. Except for the chickens in the control group, all chickens were inoculated with $8 \times 10^4$ *E. tenella* sporulated oocysts per chicken at 10 days of age. The chickens in every group were all sacrificed 7 days post-infection. The cecal contents of each individual were aseptically collected and immediately immersed in liquid nitrogen. Ten samples randomly selected from each group were used for microbiota diversity analysis and six for metabolomic analysis.

### Exposure on manure composting

At 12 days of age, chickens were randomly assigned to three groups: the control group (BLANK), the ethanamizuril group (EZL), and the salinomycin group (SAL). Each group was reared in wire cages and separated to prevent accidental cross-infection. The control group was not given any antibiotics or anticoccidial drugs. The ethanamizuril group was treated with 10 mg/L of ethanamizuril in drinking water, and the salinomycin group was treated with 60 mg/kg of salinomycin in feed every day. Fresh fecal samples from 10 individuals in each group were collected at 1–3 days and were mixed well. About 80.0 g of fecal sample was weighed into a 250-ml sterile bottle, and the bottle was sealed with a breathable film and placed in an incubator. To simulate manure composting in the laboratory, the temperature of the incubator was set to be constant at 45°C after ramping up (30°C on day 1, 40°C on day 2, 50°C on days 3–7, and 45°C on days 7–11). The samples of manure composting on days 0, 7, and 11 were aseptically collected and immediately immersed into liquid nitrogen for microbiota diversity analysis. Meanwhile, the water content, pH, and electrical conductivity of samples were detected. Each treatment was replicated three times.

### Exposure on soil

Loam soil (pH 8.1, electrical conductivity 70.52 μS/cm) was obtained from a farmland (Huai'an, China). After passing through a 2-mm sieve, the fresh loam was divided into the three groups: the control group, the ethanamizuril group, and the salinomycin group. The control group was not given any antibiotics or anticoccidial drugs. The loam of the ethanamizuril group and the salinomycin group was fully mixed with ethanamizuril and salinomycin. The final concentrations of ethanamizuril and salinomycin in the mixture were 2.5 and 0.1 mg/kg, respectively. Each 2 kg of loam was placed in a flowerpot and placed in the same natural environment for 20 days. The samples of loam were aseptically collected with the five-point sampling method and immediately immersed in liquid nitrogen for a microbiota diversity analysis. The samples included the day 0 control group (BLANK 0day), the day 20 control group (BLANK 20day), the day 20 ethanamizuril group (ZEL 20day), and the day 20 salinomycin group (SAL 20day). Each treatment was replicated three times.

## Microbiome profiling by 16S rRNA

To evaluate microbial profile, total genome DNA from samples was extracted using the TIANamp Soil DNA Kit (TIANGEN BIOTECH, China). Agarose gel electrophoresis was used to monitor DNA concentration and purity. Qualified DNA was diluted to 1 μg/μl using sterile water. A pair of primers (338F: 5'-ACTCCTRCGGGAGGCAGCAG-3' and 806R: 5'-GGACTACCVGGGTATCTAAT-3') was used to amplify the V3-V4 hypervariable region of the 16S rRNA gene (Huang et al., 2018). According to the manufacturer's recommendations, the TruSeq® DNA PCR-Free Sample Preparation Kit (Illumina, USA) was used to generate sequencing libraries. The quality of the sequencing libraries was assessed and sequenced on an Illumina NovaSeq platform.

A sequence analysis was conducted as previously described (Zhou et al., 2020). Briefly, FLASH was used for assembling the paired-end raw reads obtained from the 16S ribosomal amplicon sequencing and barcode identification for de-multiplexing. To obtain the high-quality clean tags, the raw tags were filtered according to the QIIME quality-controlled process. Next, chimeric sequences were identified and removed using the UCHIME algorithm, and the finally obtained effective tags were clustered into operational taxonomic units (OTUs). According to the sequence analysis with UPARSE software, the sequences with a similarity greater than a threshold (97%) were assigned to

the same OTUs. Furthermore, based on the Mothur algorithm, each representative sequence of each OTU was annotated using the Silva database. Multiple sequence alignments were conducted using the MUSCLE software. To assess the impacts of two anticoccidials on the microbiota, both alpha diversity analysis and beta diversity analysis were performed based on the normalized OTUs abundance information. All indices in alpha diversity analyses including Observed-species, Chao1, Shannon and Simpson indices, ACE, and Good's coverage were obtained using QIIME software (version 1.9.1) and displayed with R software (version 2.15.3). Beta diversity on both weighted and unweighted UniFrac was analyzed in QIIME software (version 1.9.1).

## Cecal metabolomic profiling

We used the mixed solvent extraction method to obtain metabolites from the cecal contents. Briefly, a 25-mg sample was mixed with 500 μl of fresh-made LC/MS-grade extract solution in an EP tube (methanol/ acetonitrile/ water = 2: 2: 1, with the isotopically-labeled internal standard mixture). The mixture was homogenized at 35 Hz for 4 min and sonicated for 5 min in an ice-water bath 3 times repeatedly. Then, the mixture was incubated for 1 h at −40°C and centrifuged at 12,000 rpm for 15 min at 4°C. Afterward, each supernatant was moved to a fresh EP tube for the LC–MS/MS analysis. The quality control (QC) sample was prepared by mixing an equal aliquot of the supernatants from all samples.

To detect the metabolites of cecal contents, 3 μl of the extracted supernatant was injected into an LC-MS/MS system which consisted of a UHPLC system (Vanquish, Thermo Fisher Scientific) with a UPLC BEH Amide column (2.1 × 100 mm, 1.7 μm) coupled to Q-Exactive HFX mass spectrometer (Orbitrap MS, Thermo Fisher Scientific). The mobile phase of the system was a binary solvent mode consisting of 25 mmol/L ammonium acetate and 25 mmol/L ammonia hydroxide in water (pH = 9.75) (A) and acetonitrile (B). The auto-sampler temperature was set at 4°C.

According to the ability to acquire MS/MS spectra on information-dependent acquisition (IDA) mode in the control of the acquisition software (Xcalibur, Thermo), mass spectrometry of metabolites was performed using a Q-Exactive HFX mass spectrometer. In IDA mode, the acquisition software continuously evaluated the full scan MS spectrum. Furthermore, the ESI conditions were set as follows: sheath gas flow rate as 30 Arb, Aux gas flow rate as 25 Arb, full MS resolution as $6.0 \times 10^4$, MS/MS resolution as $7.5\times 10^3$, capillary temperature 350°C, collision energy as 10/30/60 in NCE mode, and spray voltage as 3.6 kV (positive) or −3.2 kV (negative), respectively.

After the LC–MS/MS analysis, the raw mass spectrometry data were converted to the mzXML format by ProteoWizard software and processed with an in-house program (BiotreeDB), which was developed using R and based on XCMS for peak detection, extraction, alignment, and integration. The information of normalized total peak intensity was then exported to SIMCA (version 16.0.2) software package where principal component analysis (PCA) and orthogonal partial least squares discriminant analysis (OPLS-DA) of the multivariate data were performed. The threshold for visualizing the distribution and the grouping of the samples was located at 97% in PCA. The importance of each variable in the OPLS-DA model in the projection (VIP) value was further calculated to show its contribution to the classification. Metabolites meeting VIP > 1 and $p \leq 0.05$ were considered to be significantly differentially expressed metabolites (DEMs). Kyoto Encyclopedia of Genes and Genomes (KEGG) database (http://www.kegg.jp/) was used to further analyze the pathways of the metabolites.

## Analysis on physiological profiling of soil microbial community

To investigate the metabolic functional diversity of loam microbial communities which exposed salinomycin and ethanamizuril, the BIOLOG ECO microplate method was applied in this study. The fresh loam of the same origin was divided into three groups: the control group (BLANK), the ethanamizuril group (EZL), and the salinomycin group (SAL). The final concentrations of ethanamizuril and salinomycin in loam reached 10 and 60 mg/kg, respectively. A total of 300 g of loam sample was weighed into a 500-ml sterile bottle, and the bottle was sealed with a breathable film and placed in a dark incubator at 25°C. In total 12.5 g sample was evenly drawn from each bottle and placed in a new 250-ml sterile glass on 7, 14, 21, 28, and 35 days and then added into 90 ml of stroke-physiological saline solution. The mixture was oscillated and shaken at 200 rpm for 30 min at 4°C and then stewed for 15 min. In total 5 ml of the supernatant was transferred to 45 ml of sterile saline. This process was repeated two times to dilute the soil suspension to a $10^{-3}$ gradient. To each well of the BIOLOG ECO microplates (BIOLOG, United States), 150 μl of diluent was added, and the microplates were cultured at a constant temperature (25°C) for 10 days. During cultivation, the absorbance values of ECO microplates were read at 590 nm wavelength every 24 h using an enzyme label tester (Thermo Fisher, USA). Each treatment was replicated three times. Average well-color development (AWCD) on microplates indicated the metabolic activity of microorganisms in loam (Ge et al., 2018).

## Statistical analysis

All experimental data were presented as mean ± standard deviation. All data were statistically analyzed by Student's *t*-test. A $p < 0.05$ indicated significant differences.

# Results

## Impact on the cecal microbiota of infected chickens

The effect of salinomycin and ethanamizuril on the microbiota profiles of chicken cecum contents was analyzed by 16S ribosomal amplicon sequencing. In total, 3,013 OTUs were observed in the four experimental groups, of which 321 OTUs were common to every group (Figure 1A). Both the numbers of total and unique OTUs in the ethanamizuril group (L1) were the most, while those in the salinomycin group (S) were the least. Based on the OTUs, all alpha diversity indicators were calculated to evaluate the microbial richness and species biodiversity. All of Good's coverage index was >99%. As presented in Figures 1B–E, the Shannon and Simpson indices of the control group (Mock) were significantly higher than those of the other three groups ($p < 0.05$). There was no significant difference observed in the Chao1 and ACE indices. The beta diversity indicators [principal coordinates analysis (PCoA), non-metric multidimensional scaling (NMDS)] were computed to reflect the intragroup and intergroup distances. As shown in Figures 1F,G, the PCoA and NMDS plot revealed that there was remarkable discrimination in the cecal microorganism between the control group and the other three groups. The other three groups seemed to be closer to forming a loose cluster, but the points of the salinomycin group were still scattered.

The heat map of the top 35 most abundant compositions in the microbiome community combined with their cluster analysis showed that there were wide variations in the bacterial taxa among groups (Figure 2A). The top 35 genera in relative abundance belong to five phyla, namely, *Firmicutes, Bacteroidota, Campilobacterota, Cyanobacteria, and Proteobacteria.* The relative abundance of genera was also compared predominantly (Figure 2B). Compared with the control group (Mock), the abundances of *Proteobacteria* (phylum level) and *Escherichia-Shigella* (genus level) increased significantly in the other three groups ($p < 0.05$), and the abundances of *Faecalibacterium* of *Firmicutes* and *Bacteroidota* of *Alistipes* decreased significantly ($p < 0.05$). In addition, it was worth noting that the abundance of some bacteria of *Firmicutes* such as *Tyzzerella* and *Enterococcus*, *Proteobacteria* such as *Acinetobacter,* and *Lampropedia* tended to be consistent with that of the healthy group after coccidiostats treatment. There was no significant difference in bacterial abundance between the salinomycin group and the ethanamizuril group. Furthermore, to distinguish the contribution of bacterial taxa to the difference in bacterial clustering, a *t*-test was performed to examine whether there was a significant difference between the non-medicated control group (NC) and the two coccidiostats treatment groups. As presented in Figures 2C,D, compared to the non-medicated control group (NC), the abundances of *unidentified Chloroplast*, *Rothia*, *Streptococcus, Terrisporobacter, Aerococcus,* and *Corynebacterium* were significantly increased in the ethanamizuril group, whereas *Lampropedia*, *Paracoccus*, *Neomegalonema, Gemmobacter,* and *Brevundimonas* decreased; *[Ruminococcus] torques group* in the salinomycin group were significantly increased and *Enterobacter*, *Acinetobacter*, *Lampropedia*, *Paracoccus*, *Neomegalonema*, *Thauera*, *Gemmobacter,* and *Brevundimonas* decreased. The significant difference between these bacteria made the top ten contributions to the significant difference between the two coccidiostats treatment groups and the control group.

The microbial function prediction analysis was conducted to determine the differences in the functions of microbiota among groups. According to Figure 2E, the top 10 functions include chemoheterotrophy, fermentation, animal parasites or symbionts, human gut, mammal gut, human pathogens, human pathogens diarrhea, xylanolysis, aerobic chemoheterotrophy, and nitrate reduction. The chemoheterotrophy and fermentation played a major role in the microbial function of cecal contents in the control group, which were significantly higher than those of the other three groups.

## Impact on the cecal metabolites of infected chickens

The effect of salinomycin and ethanamizuril on the metabolite profiles of chicken cecum contents was analyzed by an untargeted LC–MS-based metabolomics platform. Both PCA and OPLS-DA score models showed significant differences in the distribution of metabolites among each group. According to the VIP > 1 and $p < 0.05$, detailed information about the DEM has been distinguished. As presented in Figure 3A, there were dramatic metabolic changes among the control group (Mock) vs. the non-medicated control group (NC), which indicated that coccidia infection led to a sharp increase in the number of DEM. Similar dramatic metabolic changes were also related to the control group (Mock) vs. the drug treatment groups. There were relatively few DEMs among the non-medicated control group (NC) and the drug treatment groups.

Compared to the non-medicated control group, there were 49 DEMs increased and 26 decreased in the ethanamizuril group (Figures 3B,C). These metabolites included glycerophospholipids {PC(14:0/14:0), lysoPC[18:1(9Z)]}, fatty acyls (oleic acid and elaidic carnitine), amines (1-butylamine, diethanolamine), amino acids, peptides, analogs (L-methionine, N6-acetyl-l-lysine, tyrosyl-lysine), pyrazoles (demethylated antipyrine), eicosanoids (11-dehydro-thromboxane B2), quaternary ammonium salts (phosphorylcholine), sesquiterpenoids (xanthorrhizol), pyrrolidinylpyridines (nicotine), aldehydes (acetamidopropanal), and others

10.3389/fmicb.2022.941259

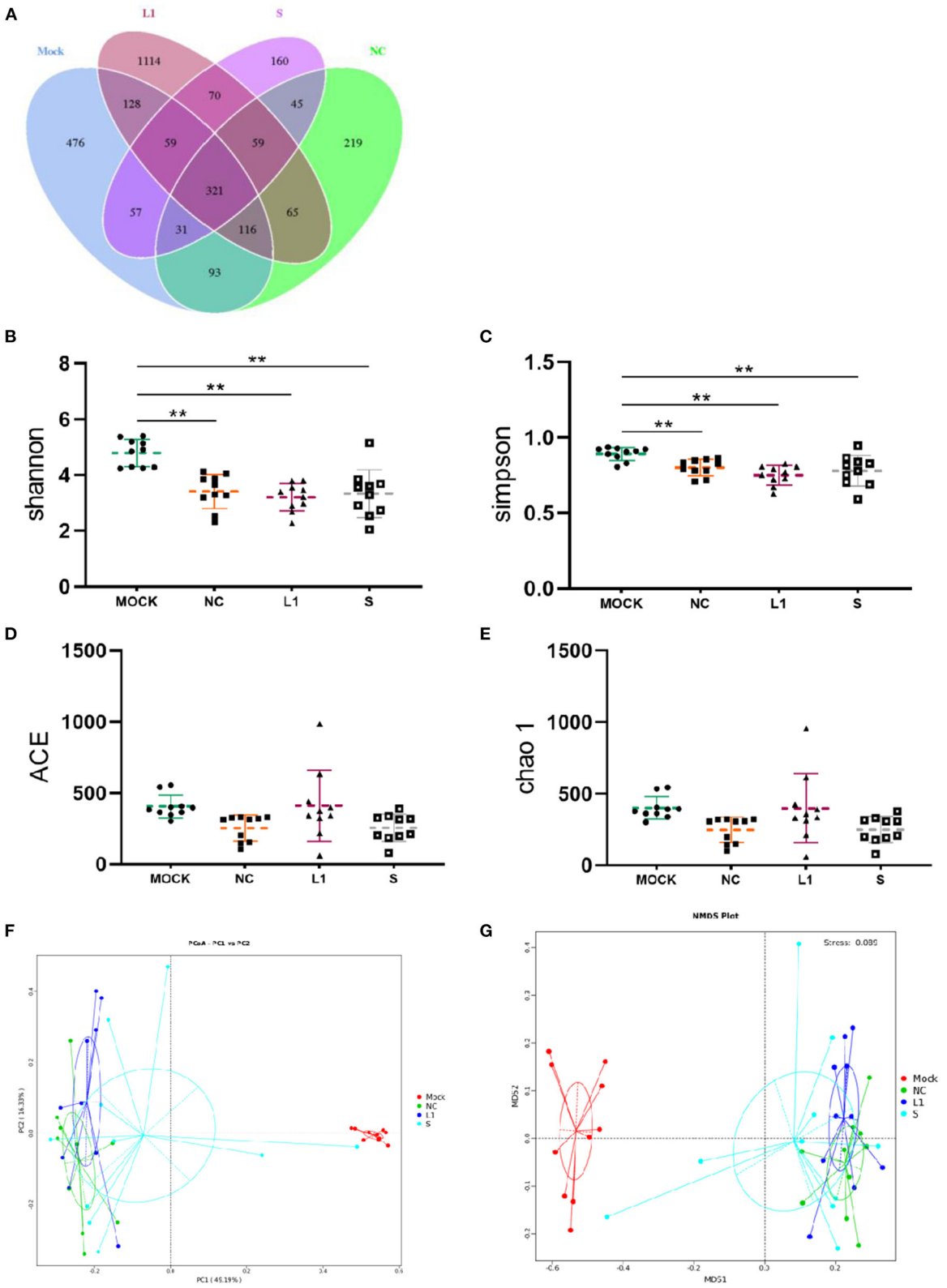


FIGURE 1
Venn diagram of shared OTUs of the different groups, as well as alpha diversity analysis and beta diversity analysis for the cecal microbiota of infected chickens. **(A)** for Venn diagram; **(B–E)** were the indices of Shannon, Simpson, ACE and Chao1, respectively. **(F)** for PCoA, **(G)** for NMDS. Mock for control group; NC for non-medicated control group; L1 for ethanamizuril group; S for salinomycin group. **Shows the significantly different ($P < 0.01$) when the treated groups compared with control group.

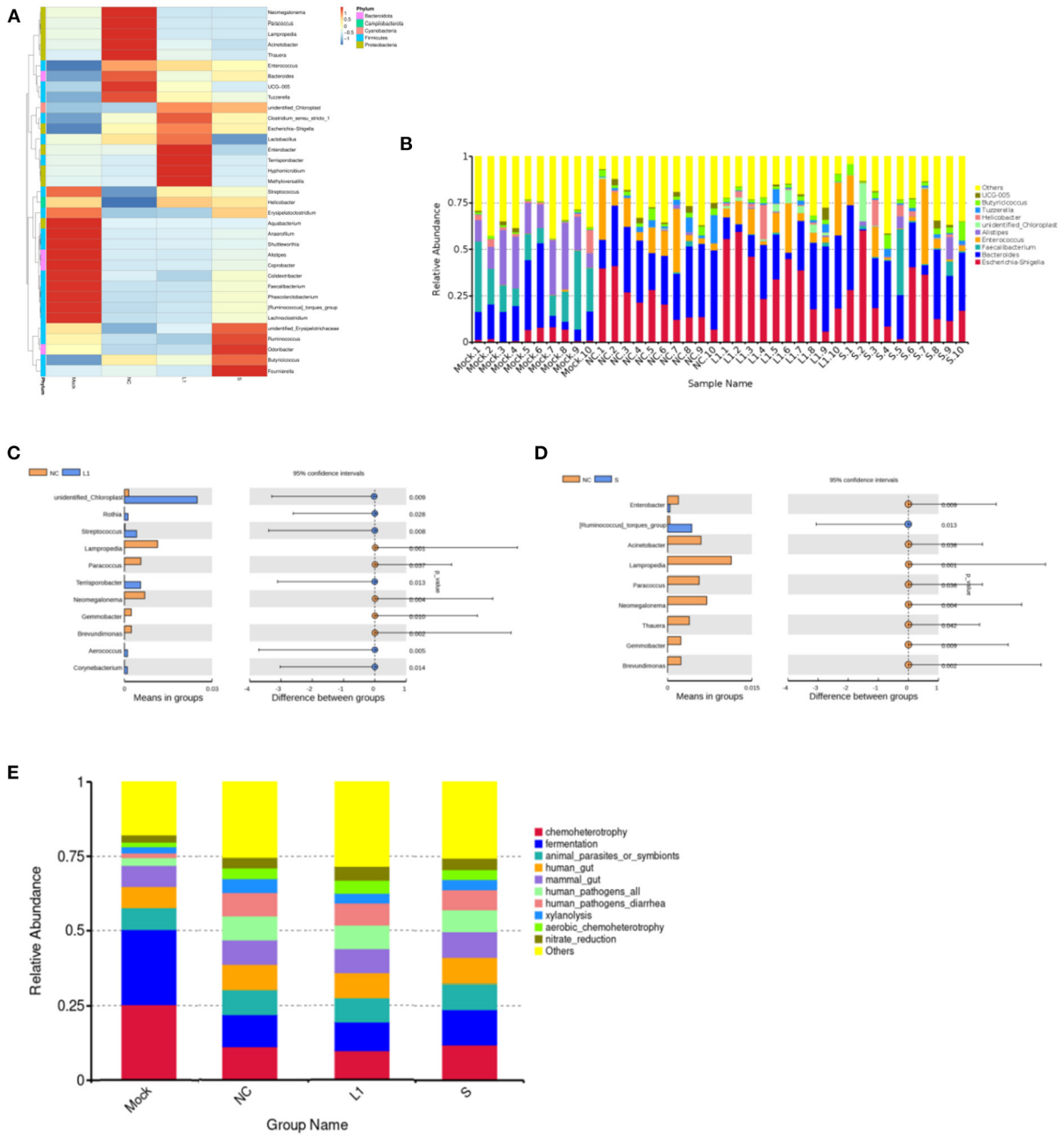


FIGURE 2
Analysis of the differences species and functions based on the OTUs abundant compositions for the cecal microbiota of infected chickens. **(A)** was the heat map of cluster analysis based on the level of genus. **(B)** was the composition of the top 10 microorganisms in the cecum at genus level. **(C)** was the analysis of significant differences species between ethanamizuril group vs. the non-medicated control group. **(D)** was the analysis of significant differences species between salinomycin group vs. the non-medicated control group. **(E)** was the analysis of microbial functions based on KEGG pathway of groups. Mock for control group; NC for non-medicated control group; L1 for ethanamizuril group; S for salinomycin group.

(o-cresol). The most up- and downregulated metabolites were xanthine and saccharin in the ethanamizuril group, respectively. Compared to the non-medicated control group, there were 51 metabolites increased and 14 decreased in the salinomycin group (Figures 3D,E). These metabolites included peptidomimetics (carnosine), amines (histidine), guanidines (methylguanidine), fatty acyls (ethyl stearate), purines and purine derivatives

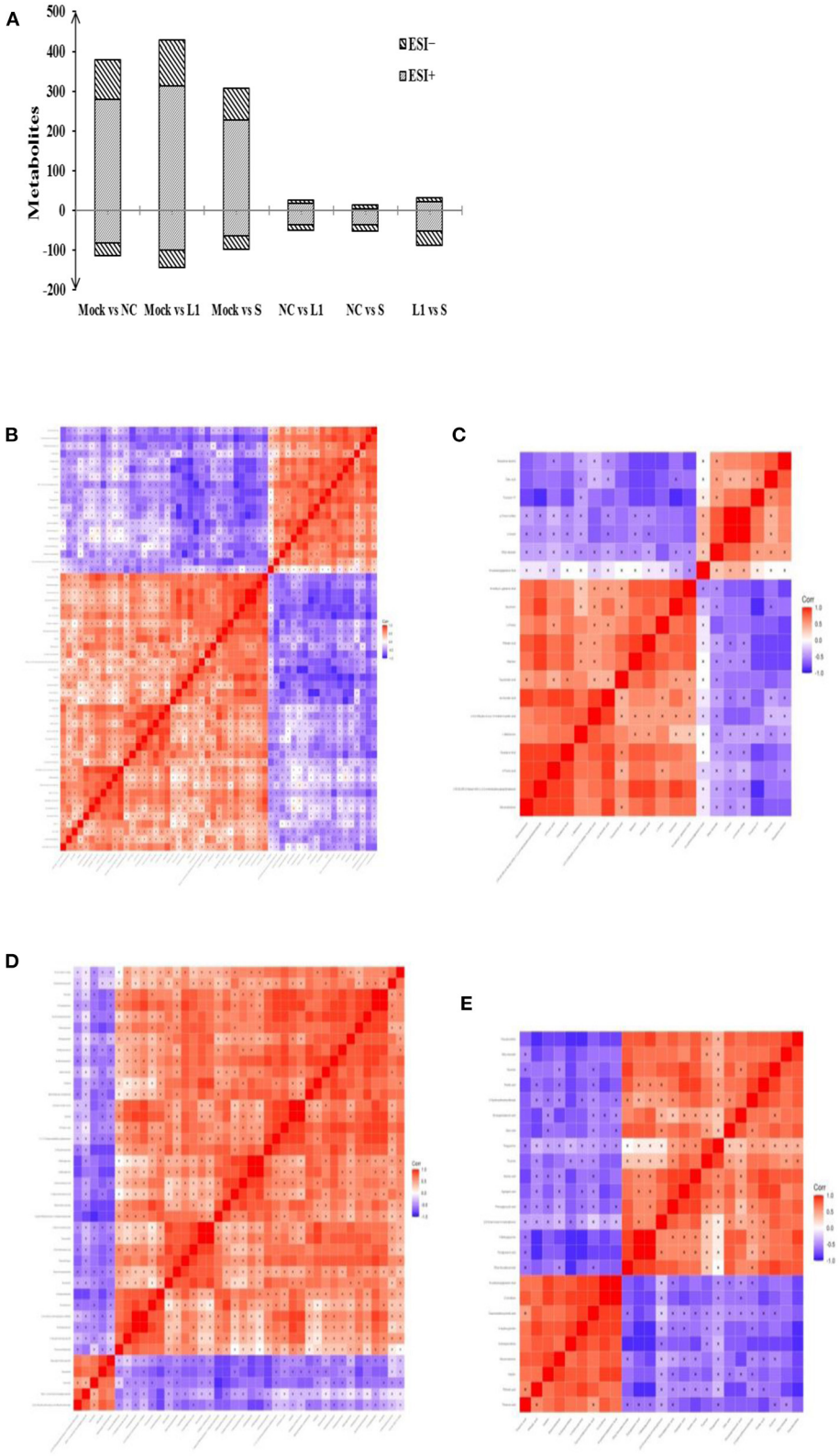


FIGURE 3
Total number of differentially expressed metabolites (DEM) in pairwise comparison and the heat map of correlation analysis for the cecal metabolites of infected chickens. **(A)** was the DEM distribution in pairwise comparison. **(B,C)** for the pairwise comparison of ethanamizuril group vs. the non-medicated control group in positive and negative mode, respectively; **(D,E)** for the pairwise comparison of salinomycin group vs. the non-medicated control group in positive and negative mode, respectively. Mock for control group; NC for non-medicated control group; L1 for ethanamizuril group; S for salinomycin group.

(guanine, 3-methyladenine), and others. The most up- and downregulated metabolites were porphobilinogen and daidzin in the salinomycin group, respectively. In addition, compared with the changes induced by ethanamizuril, the number of glycerophospholipids induced by salinomycin decreased.

The pathway enrichment analysis was used to find the key pathway with the highest correlation of metabolite differences. Table 1 shows the pathways of two coccidiostats that affect the metabolism of cecal contents in infected chickens. There were 8 most perturbed metabolic pathways including purine metabolism, aminoacyl-tRNA biosynthesis, glyoxylate and dicarboxylate metabolism, pentose phosphate pathway, TCA cycle, cysteine and methionine metabolism, arginine and proline metabolism, and glycerophospholipid metabolism in the comparison between the ethanamizuril group and the non-medicated control group. A total of 10 metabolic pathways, such as histidine metabolism, purine metabolism, and vitamin B6 metabolism, were disturbed in the comparison of the salinomycin group vs. the non-medicated control group. The metabolic pathways revealed by metabolomic profiling may be related to nitrate reduction, chemoheterotrophy, and fermentation functions which were revealed in microbiome profiling.

## Impact on the fecal microbiota during manure composting

During manure composting, the values of pH and electrical conductivity of fecal samples were significantly increased, but the water content had no significant change (Supplementary Table 1). The 16S rRNA gene-based sequencing generated from fecal samples on days 0, 7, and 11 yielded a total of 2,108,973 high-quality reads. The average assembled 16S (V3–V4) length was 428 nucleotides, ranging from 215 bp to 433 bp. In total, 19,779 OTUs were observed in the three treatment groups, of which 979 OTUs were common to every group (Figure 4A). Both the numbers of total and unique OTUs in the control group (BLANK) were the most, while those in the salinomycin group (SAL) were the least.

As presented in Table 2 all of Good's coverage index was >99%. On day 0, the Shannon index of the control group (BLANK) was significantly higher than those of the ethanamizuril group (EZL) and salinomycin group (SAL) ($p < 0.05$), and Faith's PD index of the control group and salinomycin group (SAL) was significantly higher than those of th ethanamizuril group (EZL) ($p < 0.05$). There was no significant difference observed in other indices and other days. PCoA was used to evaluate sample grouping tendency on the same day in taxa (Figure 4). The PCoA score plot showed the

TABLE 1 Pathway analysis of different metabolites in the salinomycin group vs. non-medicated control group and the ethanamizuril group vs. non-medicated control group for the cecal microbiota of infected chickens.

| Group | Pathway | Total | Hits | Raw *p* | Impact |
|---|---|---|---|---|---|
| Ethanamizuril group vs. non-medicated control group | Purine metabolism | 63 | 3 | 0.026769 | 0.03958 |
| | Aminoacyl-tRNA biosynthesis | 44 | 2 | 0.042226 | 0 |
| | Glyoxylate and dicarboxylate metabolism | 19 | 1 | 0.13706 | 0.14286 |
| | Pentose phosphate pathway | 20 | 1 | 0.14378 | 0 |
| | Citrate cycle (TCA cycle) | 20 | 1 | 0.14378 | 0.05354 |
| | Cysteine and methionine metabolism | 27 | 1 | 0.18952 | 0.09849 |
| | Arginine and proline metabolism | 38 | 1 | 0.25697 | 0.07211 |
| | Glycerophospholipid metabolism | 33 | 1 | 0.30299 | 0.04037 |
| Salinomycin group vs. non-medicated control group | Histidine metabolism | 16 | 2 | 0.015352 | 0.0641 |
| | Cyanoamino acid metabolism | 6 | 1 | 0.071584 | 0 |
| | Vitamin B6 metabolism | 9 | 1 | 0.10555 | 0 |
| | beta-Alanine metabolism | 20 | 1 | 0.22037 | 0.07065 |
| | Porphyrin and chlorophyll metabolism | 27 | 1 | 0.28608 | 0 |
| | Arginine and proline metabolism | 38 | 1 | 0.37895 | 0.02677 |
| | Pentose phosphate pathway | 20 | 1 | 0.20808 | 0 |
| | Biosynthesis of unsaturated fatty acids | 22 | 1 | 0.22649 | 0 |
| | Glutathione metabolism | 26 | 1 | 0.26213 | 0.00835 |
| | Purine metabolism | 63 | 1 | 0.52645 | 0.00396 |

Total, the number of all metabolites in the pathway; Hits, the number of differential metabolites hitting the pathway; Raw p, p-value obtained by enrichment analysis; Impact, impact factor obtained from topology analysis.

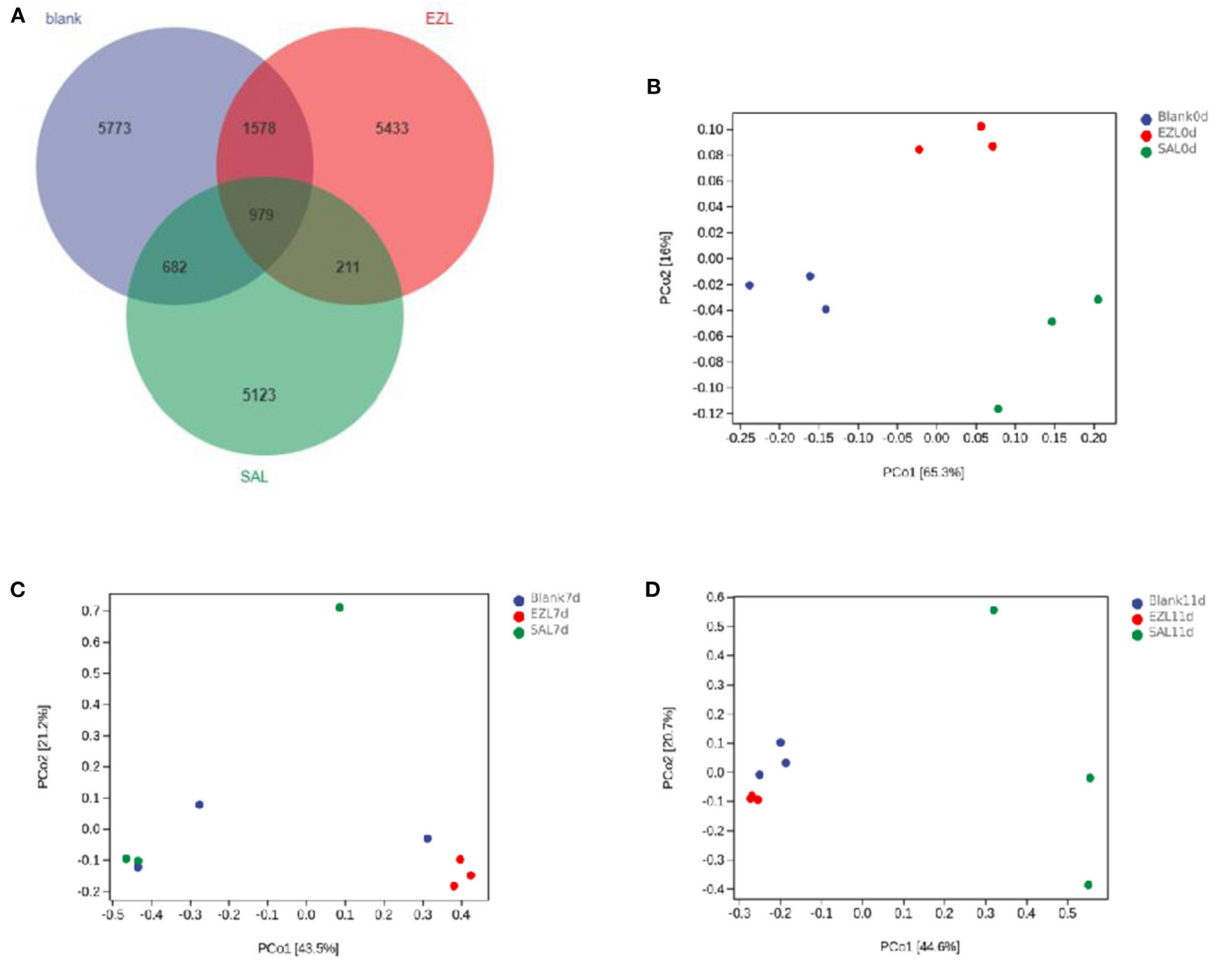


FIGURE 4
Venn diagram of shared OTUs of the different groups, and Principal coordinates analysis (PCoA) of days 0, 7 and 11 of the structure of the microbiota during manure composting. Blank was the control group; SAL was the salinomycin group; ZEL is the ethanamizuril group. **(A)** for Venn diagram; **(B–D)** were PCoA for the day 0, 7 and 11, respectively.

clear separation of the control group, the ethanamizuril group, and salinomycin group on day 0 (Figure 4A). Similar separation of groups was also seen in the research of ethanamizuril and salinomycin on cecal microbiota (Figures 1F,G). On days 7 and 11, the plot of the ethanamizuril group was gradually close to the control group (Figure 4C), which meant great variation occurred during manure composting.

To elucidate the effect of two coccidiostats on the composition of the manure microbiota, we analyzed the bacteria at the phylum and family levels to characterize the dynamics of microbial taxonomic distribution (Figure 5). At the phylum level, *Proteobacteria* (55.8%), *Firmicutes* (40.4%), and *Bacteroidetes* (3.3%) dominated the manure microbial community in all three groups on day 0. Compared to the control group, the relative abundance of *Proteobacteria* (80.4%) was significantly increased ($p < 0.05$) and *Firmicutes* (17.4%) was significantly decreased in the salinomycin group ($p < 0.05$), whereas *Bacteroidetes* was significantly decreased both in the ethanamizuril group (1.6%) and in the salinomycin group (1.9%) ($p < 0.05$) (Figure 5A). On days 7 and 11, *Firmicutes* were the absolutely dominant bacteria in all groups (98.7% in the control group, 98% in the ethanamizuril group, and 85.4% in the salinomycin group). The relative abundance of *Proteobacteria* in the salinomycin groups was 9.1% on day 7 and 12.2% on day 11, where both were significantly higher than those of the other groups ($p < 0.05$) (Figures 5B,C). At the family level, the bacterial composition was further compared in the manure. *Enterobacteriaceae*, *Lactobacillaceae*, *Leuconostocaceae*, *Ruminococcaceae,* and *Bacteroidaceae* dominated the manure microbial community on day 0. Compared to the control group, the relative abundance of *Enterobacteriaceae* was significantly increased ($p < 0.05$), whereas *Lactobacillaceae*,

TABLE 2 Alpha diversity indexes of the fecal microbiota during manure composting.

| Time (day) | Group | Observed_species | Shannon | Simpson | Chao1 | Faith_pd | Goods_coverage |
|---|---|---|---|---|---|---|---|
| 0 | Blank | 1,209.73 ± 109.70 | 4.68 ± 0.17[a] | 0.77 ± 0.03 | 1,396.23 ± 139.10 | 59.53 ± 2.50[a] | 0.9932 ± 0.0010 |
| | EZL | 744.67 ± 43.85 | 3.27 ± 0.21[b] | 0.61 ± 0.04 | 877.55 ± 47.23 | 43.56 ± 1.45[b] | 0.9956 ± 0.0002 |
| | SAL | 1,115.90 ± 52.21 | 3.84 ± 0.50[b] | 0.64 ± 0.07 | 1,313.27 ± 41.51 | 56.16 ± 3.18[a] | 0.9931 ± 0.0001 |
| 7 | Blank | 1,260.67 ± 1,377.22 | 5.72 ± 2.79 | 0.88 ± 0.14 | 1,338.92 ± 1,369.88 | 36.96 ± 25.83 | 0.9955 ± 0.0034 |
| | EZL | 1,955.47 ± 642.28 | 7.16 ± 1.28 | 0.93 ± 0.07 | 2,103.72 ± 616.12 | 59.51 ± 15.38 | 0.9909 ± 0.0014 |
| | SAL | 938.33 ± 845.39 | 4.80 ± 2.09 | 0.86 ± 0.09 | 1,078.57 ± 972.97 | 52.99 ± 59.15 | 0.9946 ± 0.0052 |
| 11 | Blank | 1,260.67 ± 1,377.22 | 7.45 ± 0.52 | 0.97 ± 0.01 | 2,216.01 ± 450.91 | 61.52 ± 13.18 | 0.9907 ± 0.0026 |
| | EZL | 1,955.47 ± 642.28 | 6.70 ± 0.42 | 0.94 ± 0.01 | 1,834.17 ± 392.71 | 61.54 ± 7.16 | 0.9910 ± 0.0026 |
| | SAL | 938.33 ± 845.39 | 5.80 ± 1.24 | 0.90 ± 0.09 | 1,389.14 ± 550.43 | 59.11 ± 39.38 | 0.9933 ± 0.0023 |

Blank, control group; EZL, ethanamizuril group; SAL, salinomycin group. Differentt letters in the same column showed statistically significant difference on the same day ($p < 0.05$).

*Leuconostocaceae,* and *Ruminococcaceae* were significantly decreased ($p < 0.05$) in the ethanamizuril group and the salinomycin group (Figure 5D). On days 7 and 11, *Bacillaceae* was the absolutely dominant bacteria in all groups, and there was no significant difference in microbial abundance among the groups.

## Impact on the loam microbiota

The effect of salinomycin and ethanamizuril on the microbiota profiles of loam soil was analyzed by 16S ribosomal amplicon sequencing. Following bacterial DNA isolation and sequencing of the V3–V4 region of the 16S rRNA gene, a total of 7,767,847 high-quality reads were obtained. The average assembled 16S (V3–V4) length was 420 nucleotides, ranging from 208 to 442 bp. In total, 31,769 OTUs were observed in the four experimental groups, of which 444 OTUs were common to every group (Figure 6A). Both the numbers of total and unique OTUs in the control group on day 0 (BLANK 0 day) were the most, while those in the control group on day 20 group (BLANK 20 day) were the least.

As presented in Table 3, compared with the control group on day 0 (BLANK 0day), all alpha diversity indicators related to richness, diversity, and evenness (BLANK 20 day) were decreased significantly after 20 days ($p < 0.05$). The Shannon index and the Simpson index of the loam microbiota treated with salinomycin (SAL 20 day) were decreased significantly too ($p < 0.05$), but there was no significant difference in the control group on day 20 group (BLANK 20 day). On the other hand, the Shannon index and Simpson index of the loam microbiota treated with ethanamizuril (ZEL 20 day) were significantly higher than those of the control group on day 20 (BLANK 20 day), but there was no significant difference from the control group on day 0 group (BLANK 0 day). To further reveal the differences in soil microbiota composition among individual treatments, beta diversity indicators were determined using PCoA and NMDS plot. As shown in Figures 6B,C, the PCoA and NMDS score plots revealed that there was remarkable segregation in the soil microorganism between the control group on day 0 (BLANK 0day) vs. the control group on day 20 group (BLANK 20 day) and the salinomycin group (SAL 20 day). Similarly, the plots of the control group on day 20 group (BLANK 20 day) were significantly separated from those of the ethanamizuril group (ZEL 20 day). The results of beta diversity confirmed the earlier observation on alpha diversity.

To elucidate the effect of two coccidiostats on the composition of the loam soil microbiota, we analyzed the bacteria at the phylum and genus levels to characterize the dynamics of microbial taxonomic distribution (Figure 7). At the phylum level (Figure 7A), *Proteobacteria, Actinobacteria, Chloroflexi, Acidobacteria,* and *Bacteroidetes* dominated the soil microbial community in the control group on day 0 (BLANK 0 day), and the relative abundance of *Proteobacteria, Actinobacteria, Chloroflexi,* and *Acidobacteria* were 39, 24, 12, and 9%, respectively. The relative abundance of *Proteobacteria* in the control group on day 20 (BLANK 20 day) and the salinomycin group (SAL 20 day) sharply increased to 79% ($p < 0.05$) and 71% ($p < 0.05$) and decreased to 20% ($p < 0.05$) in the ethanamizuril group (ZEL 20 day). The relative abundance of *Actinobacteria* in the control group on day 20 (BLANK 20 day) and the salinomycin group (SAL 20 day) sharply decreased to 5 ($p < 0.05$) and 15% ($p < 0.05$) and increased to 55% ($p < 0.05$) in the ethanamizuril group (ZEL 20 day). The relative abundance of *Chloroflexi* and *Acidobacteria* all decreased in the other three groups. At the genus level (Figure 7B), there was no bacteria genus of which relative abundance exceeded 5% in the control group on day 0 (BLANK 0 day). Similarly, only *Nocardioides* exceeded 5% in the ethanamizuril group (ZEL 20 day). However, the proportion of *Methylotenera* reached 22 ($p < 0.05$) and 43% ($p < 0.05$) in the control group on day 20 (BLANK 20 day) and the salinomycin group (SAL 20 day) respectively, and *Methylobacillus* were increased significantly too ($p < 0.05$).

Furthermore, we tried to use sequence abundance to predict the metabolic functional abundance of significant differences in samples. According to Figure 8, compared with

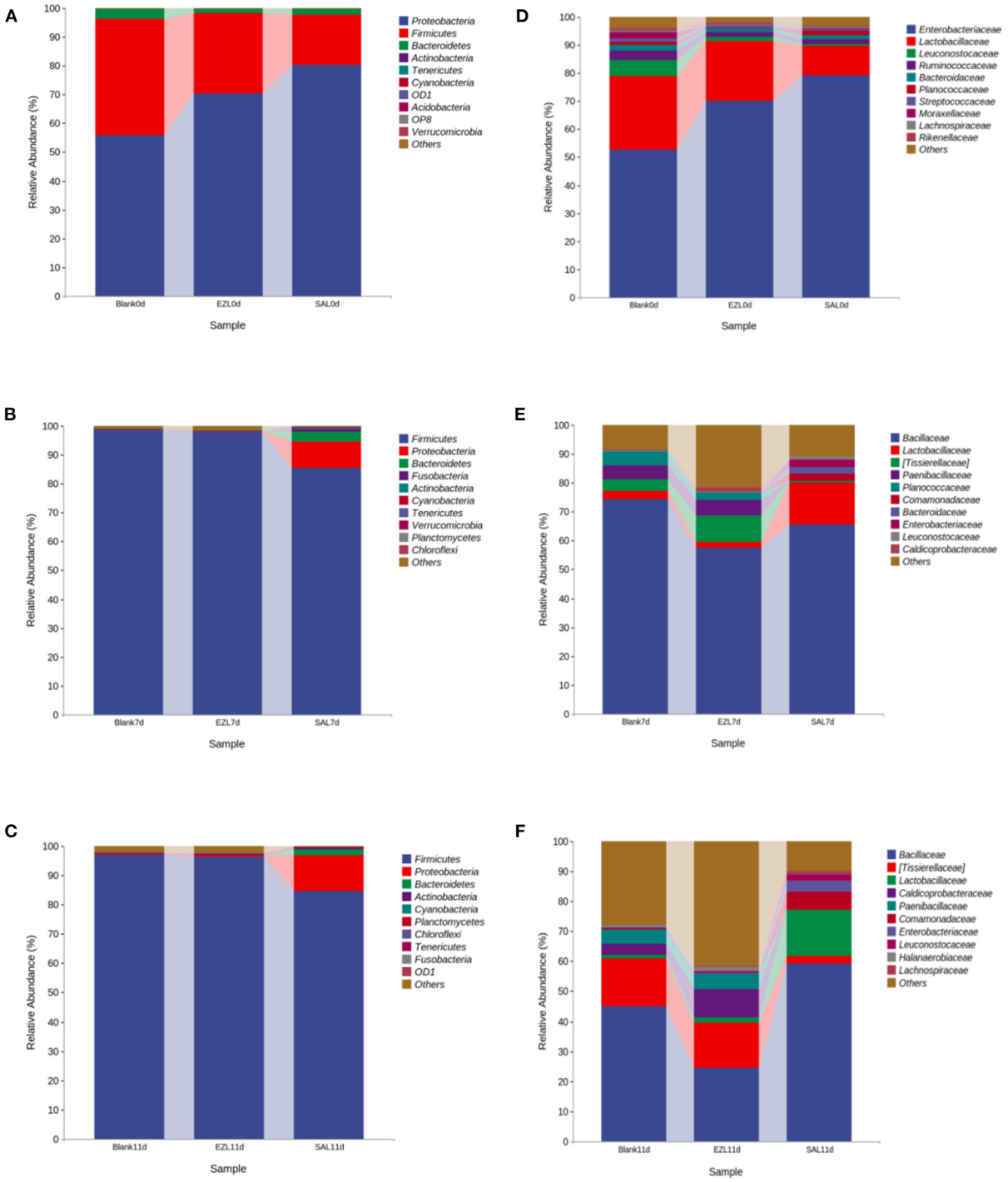


FIGURE 5
The dynamic relative abundance of the top 10 bacteria in taxonomic distribution at the phylum and the family levels during manure composting. **(A–C)** were the abundances in the phylum level; **(D–F)** were the abundances in the family level; **(A,D)** were the day 0; **(B,D)** were the day 7; **(C,F)** were the day 11, respectively. Blank was the control group; SAL was the salinomycin group; ZEL was the ethanamizuril group.

the control group on day 0 (BLANK 0 day), benzoyl-CoA degradation II (anaerobic) (CENTBENZCOA-PWY) was upregulated significantly in the control group on day 20 (BLANK 20day). Compared with the control group on day 20 (BLANK 20 day), methanogenesis from $H_2$ and $CO_2$ (METHANOGENESIS-PWY) was upregulated significantly in

TABLE 3 Alpha diversity indexes of the loam soil microbiota.

| Group | Chao1 | Faith_pd | Goods_coverage | Observed_species | Pielou_e | Shannon | Simpson |
|---|---|---|---|---|---|---|---|
| BLANK0day | 5,174.8 ± 1,264.5$^{a}$ | 331.65 ± 57.39$^{a}$ | 0.99 ± 0.00 | 4,959.7 ± 1,132.6$^{a}$ | 0.85 ± 0.06$^{a}$ | 10.37 ± 0.94$^{a}$ | 0.99 ± 0.01$^{a}$ |
| BLANK20day | 2,142.6 ± 1,418.6$^{b}$ | 189.15 ± 80.75$^{b}$ | 0.99 ± 0.01 | 1,987.7 ± 1,272.7$^{b}$ | 0.61 ± 0.08$^{b}$ | 6.48 ± 0.54$^{b}$ | 0.94 ± 0.03$^{b}$ |
| SAL20day | 4,005.8 ± 427.2$^{ab}$ | 279.59 ± 18.41$^{ab}$ | 0.99 ± 0.00 | 3,674.4 ± 373.6$^{ab}$ | 0.66 ± 0.03$^{b}$ | 7.83 ± 0.50$^{b}$ | 0.96 ± 0.01$^{b}$ |
| ZEL20day | 3,979.4 ± 153.1$^{ab}$ | 254.12 ± 11.22$^{ab}$ | 0.99 ± 0.00 | 3,860.9 ± 174.8$^{a}$ | 0.83 ± 0.01$^{a}$ | 9.88 ± 0.11$^{a}$ | 0.99 ± 0.00$^{a}$ |

BLANK0day, control group on day 0; BLANK20day, control group on day 20; ZEL20day, ethanamizuril group; SAL20day, salinomycin group. Differentt letters in the same column showed statistically significant difference in the same index ($p < 0.05$).

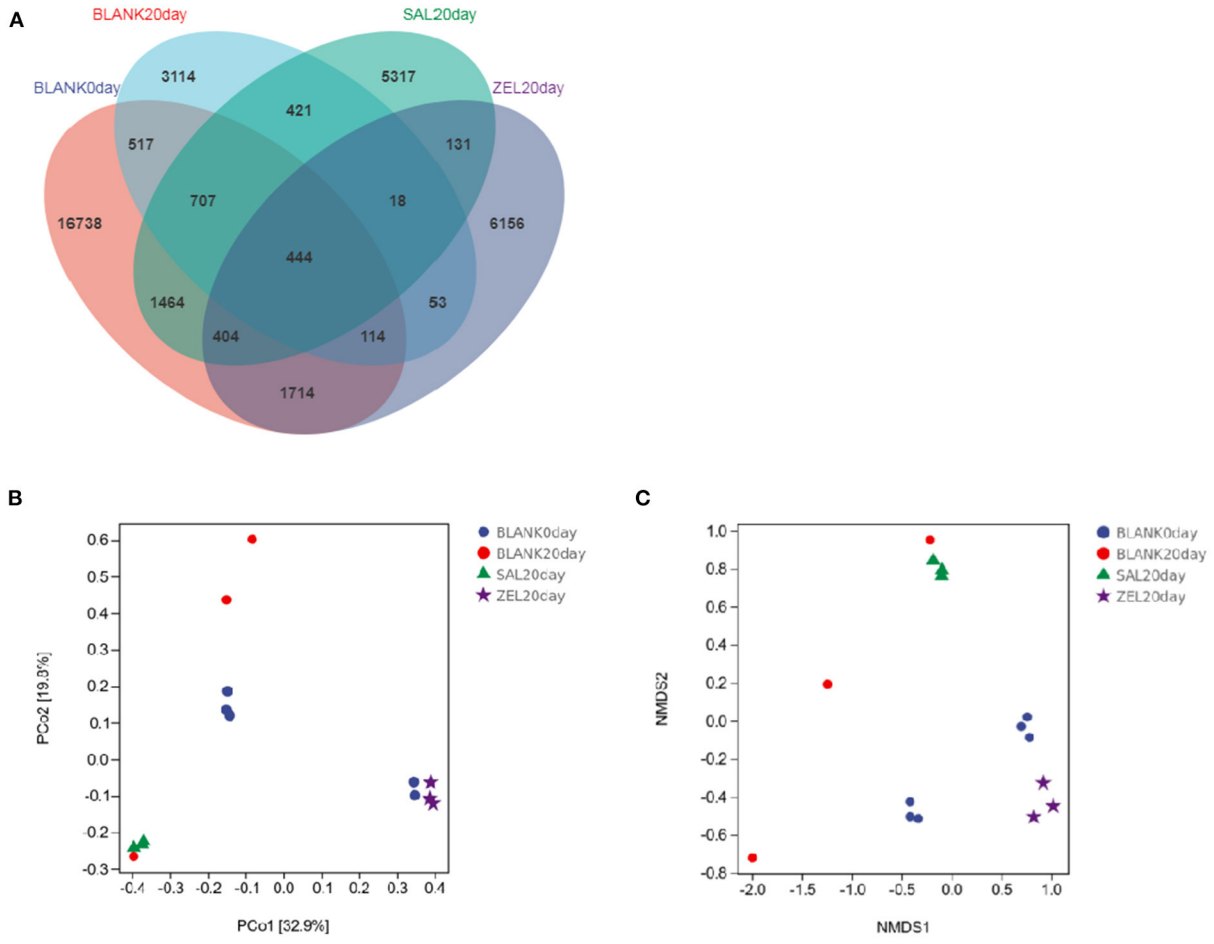


FIGURE 6
Venn diagram of shared OTUs of the different groups, and Principal coordinates analysis (PCoA) and Non-Metric Multi-Dimensional Scaling (NMDS) of the structure of the loam soil microbiota. **(A)** for Venn diagram; **(B)** for PCoA; **(C)** for NMDS, respectively. Blank 0 day was the control group on day 0; Balnk 20 day was the control group on day 20; SAL 20 day was the salinomycin group; ZEL 20 day was the ethanamizuril group.

the salinomycin group (SAL 20 day). When the ethanamizuril group was compared with the control group on day 20 (BLANK 20 day), there were 23 significant upregulation and 19 significant downregulation pathways, including creatinine degradation II, methanogenesis from $H_2$ and $CO_2$, lactose and galactose degradation I, and so on. In the ethanamizuril group vs. the salinomycin group, there were 50 significantly different metabolic pathways too.

## Impact on physiological profiling of soil microbial community

To evaluate the metabolic activity of loam microbial communities exposed to salinomycin and ethanamizuril, the development of AWCD of all carbon sources was investigated. All samples showed an increase in AWCD at all stages, indicating that microbial communities from the loam

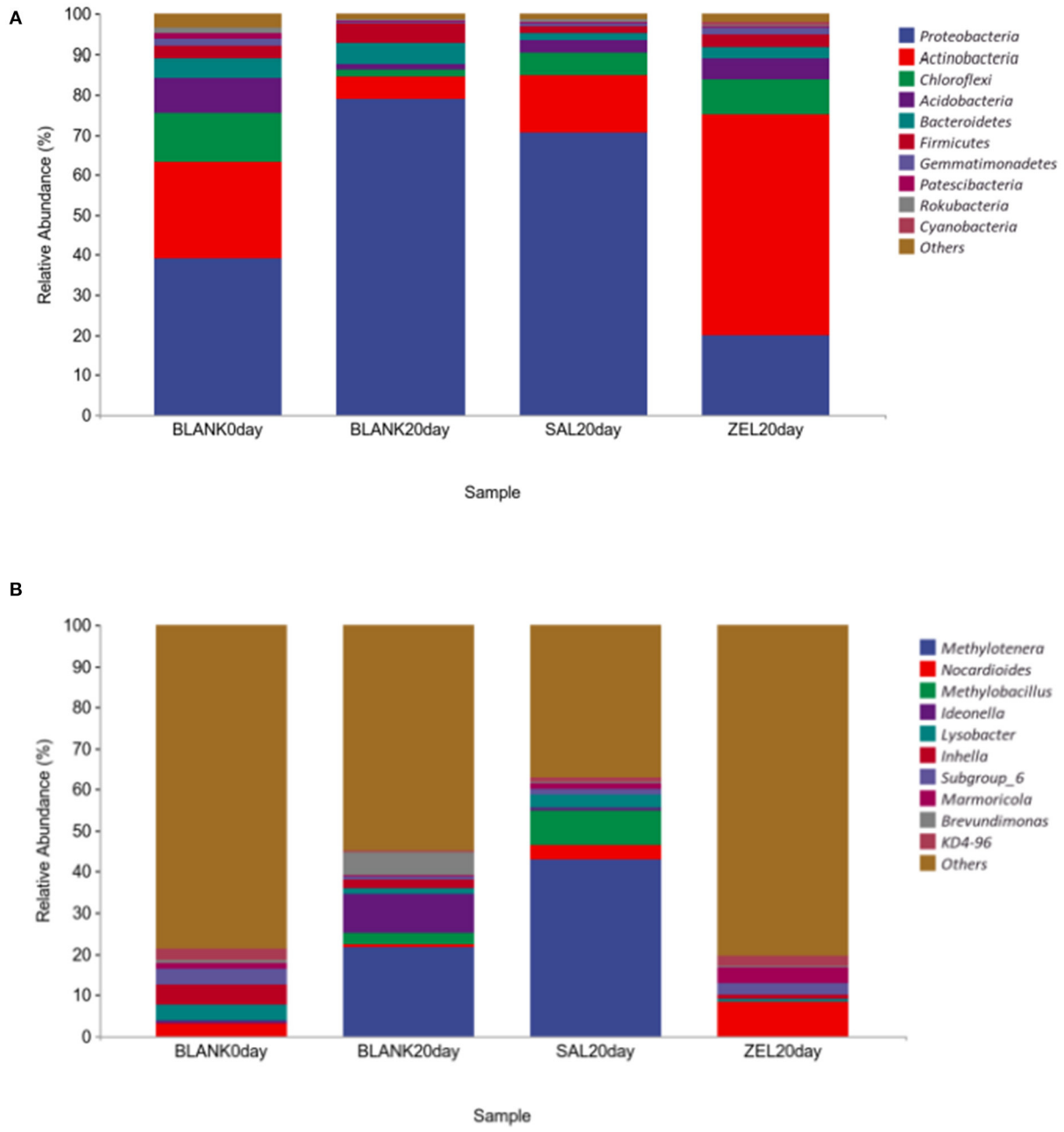


FIGURE 7
The relative abundance of the top 10 bacteria in microbial taxonomic distribution at the phylum and the genus levels in loam soil. **(A)** was the abundance in the phylum level; **(B)** was the abundance in the genus level. The same color in each diagram represented the same bacteria, and different areas represented different proportions. Blank 0 day was the control group on day 0; Balnk 20 day was the control group on day 20; SAL 20 day was the salinomycin group; ZEL 20 day was the ethanamizuril group, respectively.

samples could metabolize carbon substrates in BIOLOG ECO microplates. As shown in Figure 9, the AWCD value of the salinomycin group was the highest at all five time points and significantly higher than that of the control group and the ethanamizuril group on days 14, 21, and 28 ($p < 0.05$). There was no significant difference between the ethanamizuril group and the control group concerning AWCD at all stages ($p > 0.05$). Overall, the AWCD values of each group showed a downward trend with the extension of the incubation time of the loam sample. Furthermore, the utilization of L-serine, L-asparagine, γ-hydroxybutyric acid, N-acetyl-D-glucamine, 4-hydroxybenzoic acid, and D-galactose in the salinomycin group,

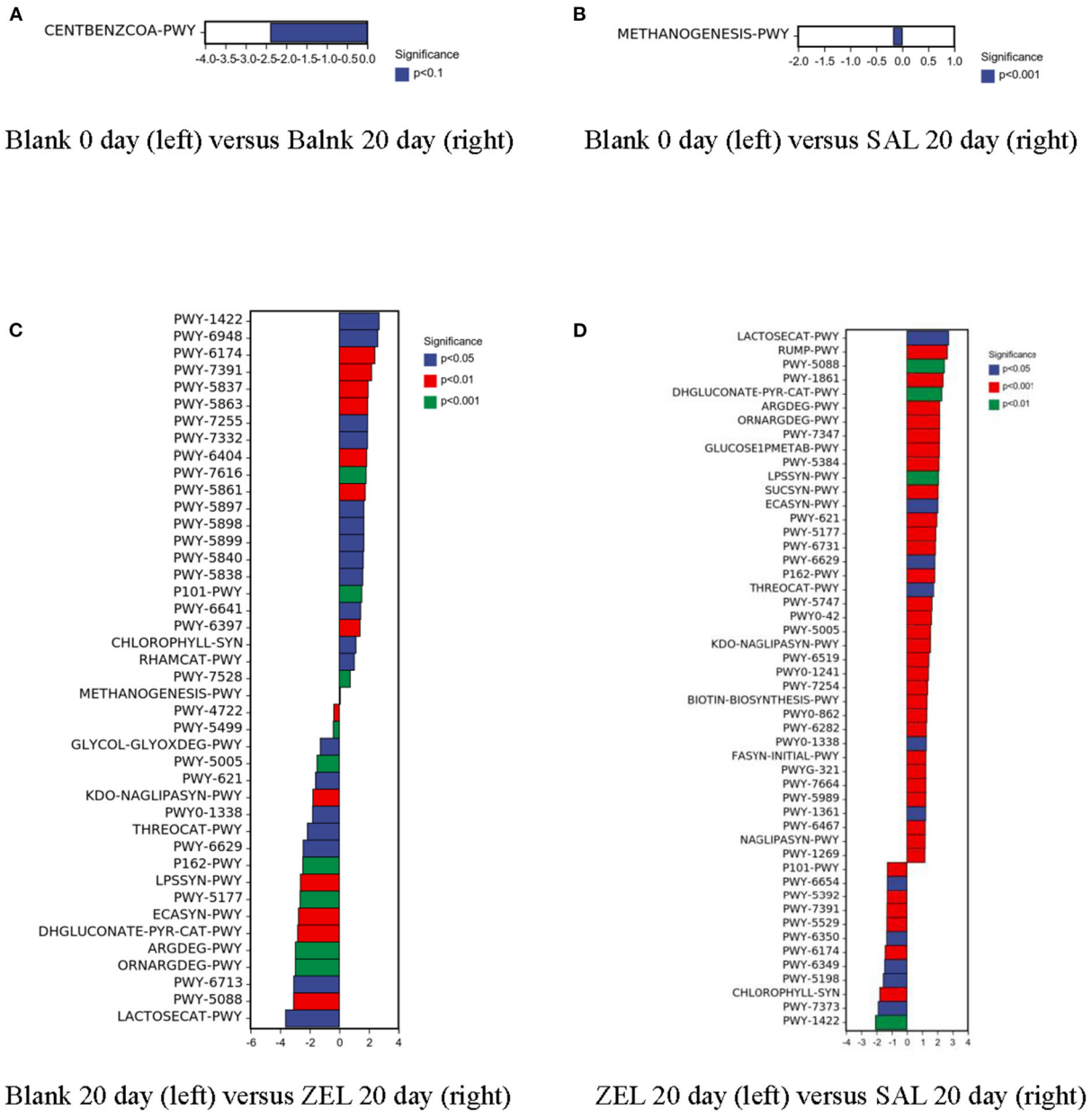


FIGURE 8
Predicted analysis for metabolic functional abundance of significant differences in samples based on sequence abundance in loam soil. Blank 0 day was the control group on day 0; Balnk 20 day was the control group on day 20; SAL 20 day was the salinomycin group; ZEL 20 day was the ethanamizuril group. **(A)** for Balnk 20 day (right) vs. Blank 0 day (left); **(B)** for Balnk 20 day vs. SAL 20 day; **(C)** for ZEL 20 day vs. Balnk 20 day; **(D)** for SAL 20 day vs. ZEL 20 day, respectively.

and L-asparagine and putrescine in the ethanamizuril group were significantly greater than those in the control group on some days ($p < 0.05$). However, the utilization of the L-arginine, γ-hydroxybutyric acid, D-galacturonic acid, D-glucuronic acid, and N-acetyl-D-glucamine in the ethanamizuril group was significantly lower than those in the control group on some days ($p < 0.05$).

The metabolic functional diversity after different treatments was evaluated by the Shannon, Simpson, and McIntosh indices. As presented in Table 4, the three indices of the salinomycin group were the highest at each sampling time among the three groups. Except on day 35, both the Shannon and Simpson indices of the salinomycin group were significantly higher than the control group ($p < 0.05$). There was no significant

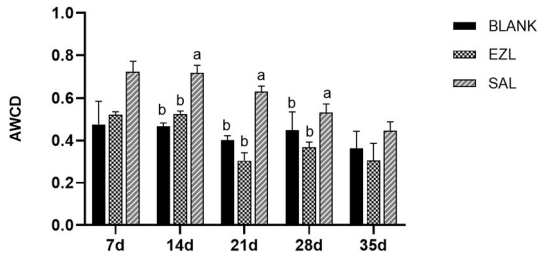


FIGURE 9
Average well-color development (AWCD) of BIOLOG ECO microplates within incubation time of microbial communities from loam of control group (BLANK), ethanamizuril group (EZL) and salinomycin group (SAL) for days 7, 14, 21, 28 and 35. Different letters on the column showed statistically significant differences on the same day ($p < 0.05$).

difference between the ethanamizuril group and the control group. Moreover, PCA revealed significant different positions among groups on carbon utilization characteristics. Figure 10 indicates that the point distributions of the ethanamizuril group and the control group in the PCA plot were relatively scattered and overlapped with each other. The point position of the salinomycin group was obviously clustered in one sector and distinct from the other groups on days 14 and 21.

## Discussion

This study was the first to investigate and compare the effects of salinomycin and ethanamizuril on the microbiota of coccidia-infected broilers' cecal content, manure composting, and loam soil. The current research results figure out that salinomycin and ethanamizuril have different effects on the composition of different microbial flora. Furthermore, the change in microbial composition could affect the micro-ecological function.

*Firmicutes*, *Actinobacteria*, *Bacteroidetes*, and *Proteobacteria* are the main phyla in poultry intestines (Waite and Taylor, 2015). Coccidia is the major intestinal protozoa of birds, which directly or indirectly affects the health of the host and significantly decreases microbiota diversity in the host intestine, and changes in the intestinal microbiota may also influence the infectivity of coccidian (Lu et al., 2021). The intestinal microbiome composition can be influenced by drugs too. It has been also reported that salinomycin and other ionophores could lead to a significant increase in evenness and a drastic decrease in the richness of the cecal content microbiota in broilers (Trela et al., 2020). Infection with *E. tenella* would lead to a decrease in the abundance of most bacterial taxa in chicken intestines except for members of the family Enterobacteriaceae (Kimura et al., 1976). In this study, the Shannon and Simpson indices of the cecum contents were significantly decreased, and the abundance of *Escherichia-Shigella* was obviously increased, whereas *Faecalibacterium* of *Firmicutes* and *Bacteroidota* of *Alistipes* decreased in response to the *E. tenella* infection. These data indicate that the *Eimeria* infection might strongly cause dysbiosis or disruption of resident microbiota and contribute to subsequent infection by other pathogens. It did not reverse the disturbance of cecal content microbiota, although the treatments of ethanamizuril or salinomycin significantly reduced chicken cecal lesions and oocyst shedding with showing high anticoccidial activity (data were not shown). Strikingly, some bacteria of *Firmicutes* such as *UCG-005*, *Enterococcus,* and *Streptococcus* tended to be consistent with that of the healthy group after ethanamizuril and salinomycin treatment. Compared to the non-medicated control group, *Lampropedia*, *Paracoccus*, *Neomegalonema, Gemmobacter,* and *Brevundimonas* were significantly decreased both in the salinomycin group and the ethanamizuril group. Furthermore, *Enterobacter* and *Acinetobacter* that have been reported as opportunistic pathogens in plants, animals, and humans and contain the major resistant bacterial pathogens (Davin-Regli et al., 2019; Shin et al., 2020), were significantly decreased in the salinomycin group. The similarity of the contribution of bacterial taxa to the difference of bacterial clustering suggested that the treatment of salinomycin and ethanamizuril may have similar effects on coccidia-infected cecal microbiota. However, salinomycin had better inhibitory effect on opportunistic pathogenic bacteria because of its extensive and strong antibacterial activity. It is generally accepted that the microbiota associated with health must have a degree of resilience to external or internal disturbances. Given that coccidiostats treatment showed the high therapeutic effects on coccidian infection and decreased some pathogenic bacteria in this study, we believe that salinomycin and ethanamizuril promoted the transformation of chicken cecal microbiota into a new equilibrium state that is facilitated by the different anticoccidial mechanisms of salinomycin and ethanamizuril.

Intestinal contents include gut flora metabolites and host metabolites, which are the key substances connecting the host metabolome and microbiome (Matsumoto et al., 2012). *Eimeria* infection could result in the alterations of key metabolites related to fatty acid metabolism, nucleotide metabolism, amino acid metabolism, and inflammatory reaction (Aggrey et al., 2019). Based on the microbiota results of 16S RNA sequencing, we predicted that the chemoheterotrophy and fermentation in the control group were significantly greater than those of the other three groups. This hypothesis had been confirmed in metabolomic research that showed the number of differential metabolites of the cecum contents in all chickens infected with *E. tenella* increased surprisingly when compared to the healthy group. Treatments of both salinomycin and ethanamizuril failed to improve the trend of the number increasing in differential metabolites, which indicated that *Eimeria* infection

TABLE 4 Metabolic functional diversity index of microbial community of soil.

| Index | Group | Sampling time (day) | | | | |
|---|---|---|---|---|---|---|
| | | 7 | 14 | 21 | 28 | 35 |
| Shannon | BLANK | $2.79 \pm 0.20^{b}$ | $2.75 \pm 0.03^{b}$ | $2.58 \pm 0.08^{b}$ | $2.68 \pm 0.36^{ab}$ | $2.55 \pm 0.38$ |
| | EZL | $2.86 \pm 0.06^{b}$ | $2.74 \pm 0.04^{b}$ | $2.38 \pm 0.14^{b}$ | $2.40 \pm 0.10^{b}$ | $2.47 \pm 0.31$ |
| | SAL | $3.30 \pm 0.18^{a}$ | $3.16 \pm 0.04^{a}$ | $3.05 \pm 0.06^{a}$ | $2.96 \pm 0.07^{a}$ | $2.94 \pm 0.05$ |
| Simpson | BLANK | $0.93 \pm 0.02^{b}$ | $0.93 \pm 0.00^{b}$ | $0.91 \pm 0.01^{ab}$ | $0.92 \pm 0.03^{ab}$ | $0.90 \pm 0.04$ |
| | EZL | $0.93 \pm 0.00^{ab}$ | $0.93 \pm 0.00^{b}$ | $0.89 \pm 0.02^{b}$ | $0.89 \pm 0.02^{b}$ | $0.89 \pm 0.03$ |
| | SAL | $0.95 \pm 0.00^{a}$ | $0.95 \pm 0.00^{a}$ | $0.95 \pm 0.00^{a}$ | $0.94 \pm 0.00^{a}$ | $0.94 \pm 0.00$ |
| Mclntosh | BLANK | $3.90 \pm 0.96$ | $3.91 \pm 0.22^{b}$ | $3.62 \pm 0.15^{b}$ | $3.79 \pm 0.49$ | $3.27 \pm 0.83$ |
| | EZL | $4.13 \pm 0.29$ | $4.38 \pm 0.22^{ab}$ | $3.07 \pm 0.50^{b}$ | $3.75 \pm 0.24$ | $2.93 \pm 0.91$ |
| | SAL | $4.94 \pm 0.79$ | $4.83 \pm 0.40^{a}$ | $4.52 \pm 0.32^{a}$ | $3.99 \pm 0.40$ | $3.42 \pm 0.58$ |

Blank, control group; EZL, ethanamizuril group; SAL, salinomycin group. Differentt letters in the same column showed statistically significant difference in the same index ($P < 0.05$).

has a great impact on cecum flora metabolism and host metabolism. Furthermore, the metabolites of chicken infected with coccidia changed by ethanamizuril were also different from that of salinomycin. Ethanamizuril mainly promoted o-cresol and other 48 metabolites increased, and L-methionine and other 25 metabolites decreased. These differential metabolites were mainly involved in purine metabolism, aminoacyl-tRNA biosynthesis, and other 6 metabolic pathways, which suggested that ethanamizuril may play an anticoccidian role by inhibiting the biosynthesis of cellular protein components. Moreover, metabolites such as peptidomimetics, amines, guanidine, fatty acyls interfered with salinomycin, and histidine metabolism and the other 9 metabolic pathways were perturbed. The involvement of the histidine metabolism pathway suggested that salinomycin may act against coccidia invasion by promoting intestinal innate immune response (Yamaki et al., 1998).

Over the past decades, composting has been increasingly recognized as one of the "best available techniques" for the on-farm processing of manure (Esperon et al., 2020). It is estimated that ~75% of the drugs are not absorbed by animals and are excreted with feces, which has prompted an interest on their fate and their impact on manure and soil microbiota communities (Chee-Sanford et al., 2009). *Firmicutes*, *Proteobacteria*, *Bacteroidetes,* and *Actinobacteria* are the four dominated bacterial phyla in initial composting microbiota, which represent at least three-quarters of the total bacterial community. The microbiota state of initial composting could have persistent effects for later phases of composting. Nevertheless, the compositions of the bacterial community were mainly influenced by redox potential, pH, and moisture, whereas temperature was another main environmental factor (Mao et al., 2020). Drastic changes in community composition and a clear reduction in bacterial and fungal diversity were observed during composting, which were strongly linked with both physicochemical compost properties and microbial community composition. Using classical microbiology methods, some key bacteria (*Salmonella spp*., *Campylobacter spp*., and *Escherichia coli*) were found to be reduced, which may be attributed to the high temperatures generated during composting that are lethal for most pathogenic bacteria (Erickson et al., 2015). In this study, *Firmicutes*, *Proteobacteria,* and *Bacteroidetes* dominated in manure microbiota during the initial composting, whereas the relative abundance of *Proteobacteria* was substantially increased and *Bacteroidota* was decreased compared with the chicken cecal bacterial composition of the control group. This phenomenon may be attributed to the contamination and rapid reproduction of *Proteobacteria* caused by the excreted feces being exposed to the breeding environment. *Firmicutes* gradually gained absolute dominance in the community composition of each treatment group following composting progress. This could be explained by conditions (pH, temperature program, moisture, and electrical conductivity) of this study were more suitable for the reproduction of *Firmicutes* phylum, and the ability to form endospores that can help it to survive high temperatures and harsh environments (Bello et al., 2020). A rise in pH and electrical conductivity indicated that the microbiota decompose the organic substance of manure and release various small molecules during the composting process. Strikingly, *Proteobacteria* always occupied a certain dominant proportion in the salinomycin group during the composting process. *Proteobacteria* phylum is formed by Gram-negative bacteria and includes a wide variety of pathogenic species such as *Escherichia spp., Campylobacter spp., Salmonella spp., and Pseudomonas spp.* A recent study has shown that some members of *Proteobacteria* can act as a reservoir for the dissemination of resistance to antibiotics in other pathogenic bacteria (Macdonald et al., 2017). The high percentage of *Proteobacteria* phylum in the salinomycin group may indicate that salinomycin is detrimental to the composting environment and may induce the risk of pathogen transmission. Furthermore, *Bacteroidetes* and microbiota richness were significantly decreased in both salinomycin and ethanamizuril groups at the initial composting.

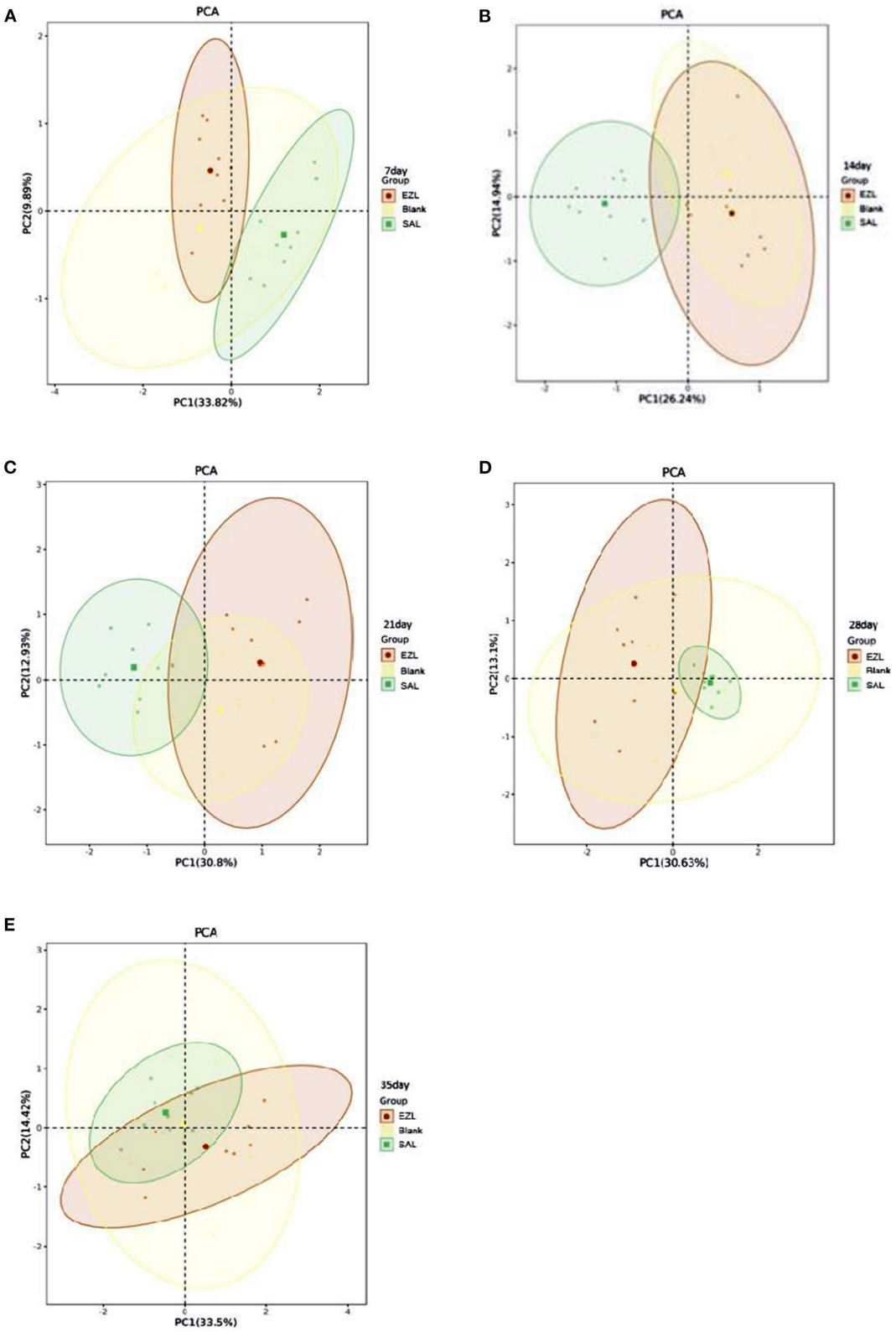


FIGURE 10
The plot of principal component analysis for the soil microbial carbon source utilization. Blank: control group; EZL: ethanamizuril group; SAL: salinomycin group. **(A–E)** were incubation time for 7, 14, 21, 28 and 35 days, respectively.

*Bacteroidetes* phyla are considered the primary degraders of polysaccharides (Lapebie et al., 2019). These data suggested that the decomposition of polysaccharide substances in the feces excreted by the two coccidiostats-treated chickens may be briefly inhibited during manure composting, but the influence on long-term composting is limited.

Soil microorganisms are the main drivers of organic substance transformation in soil, which have a significant impact on the level of soil fertility. The disparity in soil properties has a considerable impact on soil microbiome constituents. It has been reported that the introduction of pesticides into the soil environment can initiate processes that promote or inhibit soil microbial activity and alter the structure of the microbial community (Medo et al., 2021). The evenness and richness of the microbiota in the control group and the salinomycin group decreased significantly under natural conditions, indicating that the composition of the soil microbial community is a dynamic process and is affected by multiple factors. *Proteobacteria* phylum possesses a robust capacity to respond to carbon deficiencies and is reckoned as an abundant bacterial group in soil (Muller et al., 2016). *Proteobacteria* sharply increased in the control group on day 20, and the salinomycin group indicated that the carbon source in the soil may be relatively deficient, and other bacterial phyla have difficulty in growing with limited carbon. It was confirmed by the upregulation of benzoyl-CoA degradation II and methanogenesis from $H_2$ and $CO_2$ in functional predictions based on the sequence abundance. Interestingly, combined with the inhibition of *Proteobacteria* by salinomycin in the manure composting, we speculate that salinomycin may have a mechanism to promote its reproduction. Referring to the development of the control group, the progression of taxonomic abundance was obviously delayed by the ethanamizuril treatment. The *Actinobacteria* phylum is one of the oldest bacterial phyla and is a well-recognized biosynthetic factory that produces abundant antibiotics (Jose et al., 2021). *Actinobacteria* increased significantly with the ethanamizuril treatment, suggesting that ethanamizuril may promote the growth of *Actinobacteria* and may produce certain secondary metabolites, which compete and inhibit the reproduction of other taxonomic bacteria.

The 16S ribosomal amplicon sequencing focuses on characterizing the species, number, structure, and diversity of soil microbial communities, but is limited in terms of physiological profiling. The BIOLOG ECO microplate is a relatively simple and quick method for characterizing the ecological diversity and community-level status of microbial populations, which is based on metabolic functions using a redox system with 31 different sole carbon sources (Gryta et al., 2014). It has been reported that the BIOLOG ECO microplate was used to reveal the ecological status of environmental samples, such as soils, activated sludge, and sediments (Al-Dhabaan and Bakhali, 2017). The versatility derived from the BIOLOG ECO microplate has the potential to distinguish the effects of salinomycin and ethanamizuril on the metabolic activity of loam microbial communities. In this study, the AWCD decreased with the extension of incubation time, implying that the carbon and nitrogen sources in the loam were gradually depleted and the metabolic activity of loam microbiota declined gradually. However, AWCD of the salinomycin group exhibited obviously increased, which may be attributed to the improvement of metabolic capacity by salinomycin treatment. This result was consistent with the significant increase of *Proteobacteria* phylum in the salinomycin group observed in rDNA amplicon analysis. Based on the clustering of different carbon source utilization, alpha diversity analysis showed that the evenness and the richness were significantly increased in the salinomycin group, and the PCA calculation showed that the carbon source utilization mode of salinomycin treatment was different from that of the control group and the ethanamizuril group at an early stage. These data indicated that salinomycin may interfere with the metabolic function of soil microbiota, which should be attributed to its disruptive effects on soil microbiota composition in rDNA amplicon analysis. It is noteworthy that there was almost no significant difference between the ethanamizuril group and the control group in all assessment indicators, such as AWCD and alpha diversity, indicating that ethanamizuril has a very mild effect on the metabolism of soil microbiota.

Previous studies have confirmed that salinomycin exhibits a broad-spectrum antibiotic activity by destroying cell membrane ion transport (Miyazaki et al., 1974), whereas ethanamizuril has only anticoccidial activities but no antibacterial potential (data were not shown). The differences in antibacterial activity contribute to revealing that the interactions between salinomycin and various microbial communities were more violent than those of ethanamizuril. In addition, the degradation rate of salinomycin is relatively rapid in manure and soil (Sun et al., 2014), whereas ethanamizuril is insoluble in water and is stable in soil and manure (data were not shown). Therefore, these potential biological and physicochemical characteristics may support this perspective that the interaction between salinomycin and bacterial community led to the decrease of salinomycin concentration, and the influence on microbiota was limited to the early stage.

Our study reveals that salinomycin and ethanamizuril have different action patterns on various microbial communities for the first time. In the animal model of coccidia infection, the pathogen is the main driving force that affects the microbiota and metabolites of the chicken cecum, whereas the treatment of salinomycin and ethanamizuril may reconstruct a new equilibrium of the intestinal microbiota. In an *in vitro* environment, the effect of ethanamizuril on composting and soil microbiota seems to be slight. However, salinomycin has a great impact on the microbial communities of manure composting and soil, which promote the utilization of carbon sources. In particular, the promoting effect of salinomycin on the *Proteobacteria* phylum should be further researched. In conclusion, all the data of this study will contribute to

elucidating the interaction between anticoccidial drugs and microbial communities and contribute to the using and dealing of salinomycin and ethanamizuril in the poultry industry scientifically.

## Data availability statement

The datasets presented in this study can be found in online repositories. The names of the repository/repositories and accession number(s) can be found at: NCBI - PRJNA865872, PRJNA848967.

## Ethics statement

The animal study was reviewed and approved by Shanghai Veterinary Research Institutional Animal Care Committee and in accordance with the National Institutes of Health Guide on the Care and Use of Laboratory Animals.

## Author contributions

KZ: conceptualization and funding acquisition. XW and WZ: project administration and resources. HZ, KZ, and XC: roles/writing the original draft, reviewing, and editing. CW and CF: validation. XC and CF: investigation and methodology. KZ and HZ: data curation and formal analysis. All authors contributed to the article and approved the submitted version.

## Funding

The work was supported by the National Key R&D Program of China (2018YFE0192600, 2018YFD0500302).

## Conflict of interest

The authors declare that the research was conducted in the absence of any commercial or financial relationships that could be construed as a potential conflict of interest.

## Publisher's note

All claims expressed in this article are solely those of the authors and do not necessarily represent those of their affiliated organizations, or those of the publisher, the editors and the reviewers. Any product that may be evaluated in this article, or claim that may be made by its manufacturer, is not guaranteed or endorsed by the publisher.

## Supplementary material

The Supplementary Material for this article can be found online at: https://www.frontiersin.org/articles/10.3389/fmicb.2022.941259/full#supplementary-material

## References

Aggrey, S. E., Milfort, M. C., Fuller, A. L., Yuan, J., and Rekaya, R. (2019). Effect of host genotype and *Eimeria acervulina* infection on the metabolome of meat-type chickens. *PLoS ONE* 14, e0223417. doi: 10.1371/journal.pone.0223417

Al-Dhabaan, F. A. M., and Bakhali, A. H. (2017). Analysis of the bacterial strains using Biolog plates in the contaminated soil from Riyadh community. *Saudi. J. Biol. Sci*. 24, 901–906. doi: 10.1016/j.sjbs.2016.01.043

Antoszczak, M., Steverding, D., and Huczynski, A. (2019). Anti-parasitic activity of polyether ionophores. *Eur. J. Med. Chem*. 166, 32–47. doi: 10.1016/j.ejmech.2019.01.035

Bello, A., Han, Y., Zhu, H., Deng, L., Yang, W., Meng, Q., et al. (2020). Microbial community composition, co-occurrence network pattern and nitrogen transformation genera response to biochar addition in cattle manure-maize straw composting. *Sci. Total Environ*. 721, 137759. doi: 10.1016/j.scitotenv.2020.137759

Chee-Sanford, J. C., Mackie, R. I., Koike, S., Krapac, I. G., Lin, Y. F., Yannarell, A. C., et al. (2009). Fate and transport of antibiotic residues and antibiotic resistance genes following land application of manure waste. *J. Environ. Qual*. 38, 1086–1108. doi: 10.2134/jeq2008.0128

Davin-Regli, A., Lavigne, J. P., and Pages, J. M. (2019). *Enterobacter spp.*: update on taxonomy, clinical aspects, and emerging antimicrobial resistance. *Clin. Microbiol. Rev*. 32, e00002–e00019. doi: 10.1128/CMR.00002-19

Erickson, M. C., Smith, C., Jiang, X., Flitcroft, I. D., and Doyle, M. P. (2015). Manure source and age affect survival of zoonotic pathogens during aerobic composting at sublethal temperatures. *J. Food Prot*. 78, 302–310. doi: 10.4315/0362-028X.JFP-14-288

Esperon, F., Albero, B., Ugarte-Ruiz, M., Dominguez, L., Carballo, M., Tadeo, J. L., et al. (2020). Assessing the benefits of composting poultry manure in reducing antimicrobial residues, pathogenic bacteria, and antimicrobial resistance genes: a field-scale study. *Environ. Sci. Pollut. Res. Int*. 27, 27738–27749. doi: 10.1007/s11356-020-09097-1

Ge, Z., Du, H., Gao, Y., and Qiu, W. (2018). Analysis on metabolic functions of stored rice microbial communities by BIOLOG ECO microplates. *Front. Microbiol*. 9, 1375. doi: 10.3389/fmicb.2018.01375

Gryta, A., Frac, M., and Oszust, K. (2014). The application of the Biolog EcoPlate approach in ecotoxicological evaluation of dairy sewage sludge. *Appl. Biochem. Biotechnol*. 174, 1434–1443. doi: 10.1007/s12010-014-1131-8

Henri, J., Maurice, R., Postollec, G., Dubreil-Cheneau, E., Roudaut, B., Laurentie, M., et al. (2012). Comparison of the oral bioavailability and tissue disposition of monensin and salinomycin in chickens and turkeys. *J. Vet. Pharmacol. Ther*. 35, 73–81. doi: 10.1111/j.1365-2885.2011.01285.x

Huang, G., Tang, X., Bi, F., Hao, Z., Han, Z., Suo, J., et al. (2018). Eimeria tenella infection perturbs the chicken gut microbiota from the onset of oocyst shedding. *Vet. Parasitol*. 258, 30–37. doi: 10.1016/j.vetpar.2018.06.005

Islam, W., Noman, A., Naveed, H., Huang, Z., and Chen, H. Y. H. (2020). Role of environmental factors in shaping the soil microbiome. *Environ. Sci. Pollut. Res. Int*. 27, 41225–41247. doi: 10.1007/s11356-020-10471-2

Jose, P. A., Maharshi, A., and Jha, B. (2021). Actinobacteria in natural products research: Progress and prospects. *Microbiol. Res*. 246, 126708. doi: 10.1016/j.micres.2021.126708

Kadykalo, S., Roberts, T., Thompson, M., Wilson, J., Lang, M., and Espeisse, O. (2018). The value of anticoccidials for sustainable global poultry production. *Int. J. Antimicrob. Agents* 51, 304–310. doi: 10.1016/j.ijantimicag.2017.09.004

Kimura, N., Mimura, F., Nishida, S., and Kobayashi, A. (1976). Studies on the relationship between intestinal flora and cecal coccidiosis in chicken. *Poult. Sci*. 55, 1375–1383. doi: 10.3382/ps.0551375

Lapebie, P., Lombard, V., Drula, E., Terrapon, N., and Henrissat, B. (2019). Bacteroidetes use thousands of enzyme combinations to break down glycans. *Nat. Commun*. 10, 2043. doi: 10.1038/s41467-019-10068-5

Li, X. Y., Liu, L. L., Zhang, M., Zhang, L. F., Wang, X. Y., Wang, M., et al. (2019). Proteomic analysis of the second-generation merozoites of *Eimeria tenella* under nitromezuril and ethanamizuril stress. *Parasit. Vectors* 12, 592. doi: 10.1186/s13071-019-3841-9

Liu, Y., Zhao, X., Wang, C., Zhang, L., Zhang, K., Fei, C., et al. (2020). Metabolism, distribution, and excretion of ethanamizuril in chickens. *J. Agric. Food Chem*. 68, 1563–1570. doi: 10.1021/acs.jafc.9b05065

Lloyd-Price, J., Abu-Ali, G., and Huttenhower, C. (2016). The healthy human microbiome. *Genome Med*. 8, 51. doi: 10.1186/s13073-016-0307-y

Lu, C., Yan, Y., Jian, F., and Ning, C. (2021). Coccidia-microbiota interactions and their effects on the host. *Front. Cell Infect. Microbiol*. 11, 751481. doi: 10.3389/fcimb.2021.751481

Macdonald, S. E., Nolan, M. J., Harman, K., Boulton, K., Hume, D. A., Tomley, F. M., et al. (2017). Effects of Eimeria tenella infection on chicken caecal microbiome diversity, exploring variation associated with severity of pathology. *PLoS ONE* 12, e0184890. doi: 10.1371/journal.pone.0184890

Mao, H., Wang, K., Wang, Z., Peng, J., and Ren, N. (2020). Metabolic function, trophic mode, organics degradation ability and influence factor of bacterial and fungal communities in chicken manure composting. *Bioresour Technol* 302, 122883. doi: 10.1016/j.biortech.2020.122883

Matsumoto, M., Kibe, R., Ooga, T., Aiba, Y., Kurihara, S., Sawaki, E., et al. (2012). Impact of intestinal microbiota on intestinal luminal metabolome. *Sci. Rep*. 2, 233. doi: 10.1038/srep00233

McDonald, J. E., Marchesi, J. R., and Koskella, B. (2020). Application of ecological and evolutionary theory to microbiome community dynamics across systems. *Proc. Biol. Sci*. 287, 20202886. doi: 10.1098/rspb.2020.2886

Medo, J., Makova, J., Medova, J., Lipkova, N., Cinkocki, R., Omelka, R., et al. (2021). Changes in soil microbial community and activity caused by application of dimethachlor and linuron. *Sci. Rep*. 11, 12786. doi: 10.1038/s41598-021-91755-6

Miyazaki, Y., Shibuya, M., Sugawara, H., Kawaguchi, O., and Hirsoe, C. (1974). Salinomycin, a new polyether antibiotic. *J. Antibiot*. 27, 814–821. doi: 10.7164/antibiotics.27.814

Muller, D. B., Vogel, C., Bai, Y., and Vorholt, J. A. (2016). The plant microbiota: systems-level insights and perspectives. *Annu. Rev. Genet*. 50, 211–234. doi: 10.1146/annurev-genet-120215-034952

Robinson, K., Becker, S., Xiao, Y., Lyu, W., Yang, Q., Zhu, H., et al. (2019). Differential impact of subtherapeutic antibiotics and ionophores on intestinal microbiota of broilers. *Microorganisms*. 7, 282. doi: 10.3390/microorganisms7090282

Schwartz, D. J., Langdon, A. E., and Dantas, G. (2020). Understanding the impact of antibiotic perturbation on the human microbiome. *Genome Med*. 12, 82. doi: 10.1186/s13073-020-00782-x

Shin, B., Park, C., and Park, W. (2020). Stress responses linked to antimicrobial resistance in Acinetobacter species. *Appl. Microbiol. Biotechnol*. 104, 1423–1435. doi: 10.1007/s00253-019-10317-z

Stock, M. L., Elazab, S. T., and Hsu, W. H. (2018). Review of triazine antiprotozoal drugs used in veterinary medicine. *J. Vet. Pharmacol. Ther*. 41, 184–194. doi: 10.1111/jvp.12450

Sun, P., Cabrera, M. L., Huang, C. H., and Pavlostathis, S. G. (2014). Biodegradation of veterinary ionophore antibiotics in broiler litter and soil microcosms. *Environ. Sci. Technol*. 48, 2724–2731. doi: 10.1021/es404619q

Trela, J., Kieronczyk, B., Hautekiet, V., and Jozefiak, D. (2020). Combination of *Bacillus licheniformis* and *Salinomycin*: effect on the growth performance and git microbial populations of broiler chickens. *Animals* 10, 889. doi: 10.3390/ani10050889

Waite, D. W., and Taylor, M. W. (2015). Exploring the avian gut microbiota: current trends and future directions. *Front. Microbiol*. 6, 673. doi: 10.3389/fmicb.2015.00673

Wan, J., Wang, X., Yang, T., Wei, Z., Banerjee, S., Friman, V. P., et al. (2021). Livestock manure type affects microbial community composition and assembly during composting. *Front. Microbiol*. 12, 621126. doi: 10.3389/fmicb.2021.621126

Wang, C., Liu, Y., Zheng, H., Li, Y., He, J., Wang, X., et al. (2020). Safety pharmacology assessment of Ethanamizuril, a novel triazines coccidiostat. *Res. Vet. Sci*. 132, 271–278. doi: 10.1016/j.rvsc.2020.07.003

Weersma, R. K., Zhernakova, A., and Fu, J. (2020). Interaction between drugs and the gut microbiome. *Gut* 69, 1510–1519. doi: 10.1136/gutjnl-2019-320204

Yamaki, K., Thorlacius, H., Xie, X., Lindbom, L., Hedqvist, P., and Raud, J. (1998). Characteristics of histamine-induced leukocyte rolling in the undisturbed microcirculation of the rat mesentery. *Br. J. Pharmacol*. 123, 390–399. doi: 10.1038/sj.bjp.0701614

Zhang, K., Wang, C., Li, Y., He, J., Wang, M., Wang, X., et al. (2020a). Rat two-generation reproductive toxicity and teratogenicity studies of a novel coccidiostat - Ethanamizuril. *Regul. Toxicol. Pharmacol*. 113, 104623. doi: 10.1016/j.yrtph.2020.104623

Zhang, K., Zheng, H., Wei, S., Wang, X., Fei, C., Wang, C., et al. (2020b). Beagle dog 90-day oral toxicity study of a novel coccidiostat - ethanamizuril. *BMC Vet. Res*. 6, 444. doi: 10.1186/s12917-020-02655-2

Zhou, B. H., Jia, L. S., Wei, S. S., Ding, H. Y., Yang, J. Y., and Wang, H. W. (2020). Effects of Eimeria tenella infection on the barrier damage and microbiota diversity of chicken cecum. *Poult. Sci*. 99, 1297–1305. doi: 10.1016/j.psj.2019.10.073

Zhou, S., Wang, F., Wong, E. T., Fonkem, E., Hsieh, T. C., Wu, J. M., et al. (2013). Salinomycin: a novel anti-cancer agent with known anti-coccidial activities. *Curr. Med. Chem*. 20, 4095–4101. doi: 10.2174/15672050113109990199

frontiers | Frontiers in Microbiology

TYPE Original Research
PUBLISHED 06 September 2022
DOI 10.3389/fmicb.2022.960728



OPEN ACCESS

EDITED BY
Xiaolin Hou,
Beijing University of Agriculture, China

REVIEWED BY
Alaguvel Valliammai,
Ben-Gurion University of the Negev, Israel
Hong-Ning Wang,
Sichuan University, China
Arunachalam Kannappan,
Shanghai Jiao Tong University, China

*CORRESPONDENCE
Zhiwen Xu
abtcxzw@126.com
Lizi Yin
yinlizi@siacu.edu.cn

†These authors have contributed equally to this work

SPECIALTY SECTION
This article was submitted to Antimicrobials, Resistance and Chemotherapy, a section of the journal Frontiers in Microbiology

RECEIVED 03 June 2022
ACCEPTED 16 August 2022
PUBLISHED 06 September 2022

CITATION
Gu K, Ouyang P, Hong Y, Dai Y, Tang T, He C, Shu G, Liang X, Tang H, Zhu L, Xu Z and Yin L (2022) Geraniol inhibits biofilm formation of methicillin-resistant *Staphylococcus aureus* and increase the therapeutic effect of vancomycin *in vivo*. *Front. Microbiol.* 13:960728. doi: 10.3389/fmicb.2022.960728



# Geraniol inhibits biofilm formation of methicillin-resistant *Staphylococcus aureus* and increase the therapeutic effect of vancomycin *in vivo*

Kexin Gu†, Ping Ouyang†, Yuxin Hong, Yuyun Dai, Ting Tang, Changliang He, Gang Shu, Xiaoxia Liang, Huaqiao Tang, Ling Zhu, Zhiwen Xu* and Lizi Yin*

College of Veterinary Medicine, Sichuan Agriculture University, Chengdu, China

Methicillin-resistant *Staphylococcus aureus* (MRSA) is among the common drug resistant bacteria, which has gained worldwide attention due to its high drug resistance and infection rates. Biofilms produced by *S. aureus* are known to increase antibiotic resistance, making the treatment of *S. aureus* infections even more challenging. Hence, inhibition of biofilm formation has become an alternative strategy for controlling persistent infections. In this study, we evaluated the efficacy of geraniol as a treatment for MRSA biofilm infection. The results of crystal violet staining indicated that 256 μg/mL concentration of geraniol inhibited USA300 biofilm formation by 86.13% and removed mature biofilms by 49.87%. Geraniol exerted its anti-biofilm effect by influencing the major components of the MRSA biofilm structure. We found that geraniol inhibited the synthesis of major virulence factors, including staphyloxanthin and autolysins. The colony count revealed that geraniol inhibited staphyloxanthin and sensitized USA300 cells to hydrogen peroxide. Interestingly, geraniol not only reduced the release of extracellular nucleic acids (eDNA) but also inhibited cell autolysis. Real-time polymerase chain reaction data revealed the downregulation of genes involved in biofilm formation, which verified the results of the phenotypic analysis. Geraniol increased the effect of vancomycin in eliminating USA300 biofilms in a mouse infection model. Our findings revealed that geraniol effectively inhibits biofilm formation *in vitro*. Furthermore, in combination with vancomycin, geraniol can reduce the biofilm adhesion to the implant in mice. This suggests the potential of geraniol as an anti-MRSA biofilm drug and can provide a solution for the clinical treatment of biofilm infection.

KEYWORDS

**geraniol, MRSA, biofilm, PIA, eDNA, sarA, staphyloxanthin, implant model**

## Introduction

*Staphylococcus aureus* is a common gram-positive bacterium that remains the main cause of healthcare-associated infections (Tenover et al., 2006). Due to the unreasonable use of antibiotics, many antibiotic-resistant strains have been found (Catalano et al., 2022). Methicillin-resistant *Staphylococcus aureus* (MRSA) is a well-known drug-resistant bacterium. In adults, MRSA is the main pathogen that causes bacteremia, pneumonia, and endocarditis (Turner et al., 2019). To date, vancomycin has always been the drug of choice for the treatment of MRSA infections and the last line of defense against MRSA. Unfortunately, vancomycin-resistant strains have been isolated since the beginning of the twenty-first century, worsening the current situation (Cong et al., 2020). Therefore, finding novel drugs that exhibit antibacterial activity but do not cause antibiotic resistance has attracted increasing attention worldwide.

Numerous infections caused by MRSA are closely related to biofilms. The biofilm structure prevents the complete eradication of pathogenic bacteria using antibiotics. MRSA biofilms mainly comprise polysaccharide intercellular adhesin (PIA), extracellular nucleic acids (eDNA), and proteins called extracellular polymeric substances (EPS). EPS provide protection against bacteria wrapped in biofilms, including evading the immune system and avoiding exposure to antibiotics (Sharma et al., 2019). Biofilm formation is an extremely complex and closely regulated process. SarA, a well-known *S. aureus* regulatory system, regulates the expression of many important virulence factors and induces *S. aureus* to produce biofilms, mainly by inhibiting the secretion of proteases (Trotonda et al., 2005; Abdelhady et al., 2014). It has been reported that not only is the biofilm-forming ability of *sarA* mutants seriously damaged but it also leads to changes in the expression levels of at least 120 genes (Mauro et al., 2016; Oriol et al., 2021). Numerous natural compounds, including thymol, carvacrol, and hesperidin, have been found to combat MRSA biofilms by targeting SarA (Selvaraj et al., 2020; Yuan et al., 2020; Vijayakumar et al., 2022). Taken together, these results indicated that *sarA* is a promising anti-biofilm target.

Geraniol is a terpenoid compound that is well known as the main component of many essential oils (Xu et al., 2022). Geraniol is found mainly in aromatic herbaceous plants and is cost-effective and easy to produce (Prasad and Muralidhara, 2017; Younis et al., 2021). In previous studies, geraniol was found to have anti-neurotoxicity properties (Lin et al., 2021), inhibit gastric cancer cell proliferation (Yang et al., 2021), and relieve arthritis (Wu et al., 2020). In recent years, geraniol has been proven to have significant antibacterial activity against gram-negative bacteria, such as *Escherichia coli* and *Salmonella* Typhimurium, (Friedman et al., 2002), and *Streptococcus pneumoniae* and *S. aureus* (Inouye et al., 2001). It has also been reported that geraniol can inhibit the growth of MRSA and relieve the symptoms of systemic infection caused by MRSA in mice (Lin et al., 2021). Furthermore, geraniol inhibits biofilm production by a variety of bacteria (Gupta et al., 2021; Kwiatkowski et al., 2022; Yu et al., 2022). However, the inhibitory effect and mechanism of action of geraniol on MRSA biofilms have rarely been reported. This study shows that geraniol inhibits the formation of MRSA biofilms by regulating the expression of the sarA system regulatory genes, genes related to virulence factors, and other genes that regulate biofilm formation. Vancomycin is clinically used in the treatment of MRSA infections. However, it causes nephrotoxicity and large doses may cause bacterial drug resistance. In an aim to establish the efficacy of geraniol in combination with vancomycin and reduce the dose of vancomycin, we conducted the current study.

## Results

### Geraniol has an effect on the growth of USA300

Geraniol exhibited antibacterial activity against USA300 with minimum inhibitory concentration (MIC) and minimum bactericidal concentration values of 512 and 1,024 μg/mL, respectively. The MIC optical density values at 600 nm ($OD_{600\ nm}$) are shown in **Supplementary Table 1**. The growth curve (**Figure 1A** and **Supplementary Table 2**) showed that geraniol did not inhibit the growth of USA300 at concentrations of 0, 16, 32, 64, 128, and 256 μg/mL.

### Biofilm formation inhibition effects of geraniol against USA300 and several other *Staphylococcus aureus* strains

Biofilm experiments were performed at sub-inhibitory concentrations of geraniol. The results of the Alamar Blue test (**Figure 1B**) showed that there was a negligible difference in the fluorescence intensity between the drug treatment group and untreated group, indicating that the activity of USA300 was hardly affected by the sub-MICs of geraniol. Geraniol significantly inhibited biofilm formation induced by USA300. When the concentration of geraniol was 128 and 256 μg/mL, biofilm formation decreased by 70.29 ± 7.58% and 86.13 ± 5.22%, respectively (**Figure 2A**). **Figure 2B** shows that the slides containing samples from the untreated group were densely covered with cells. However, as the geraniol concentration increased, the number of cells decreased, and PIAs had exuded. Only a small number of unaggregated cells was observed in the group treated with 256 μg/mL geraniol. These results indicated that the sub-MICs of geraniol (16, 32, 64, 128, and 256 μg/mL) significantly inhibited USA300 biofilm formation in a dose-dependent manner. In addition to USA300,

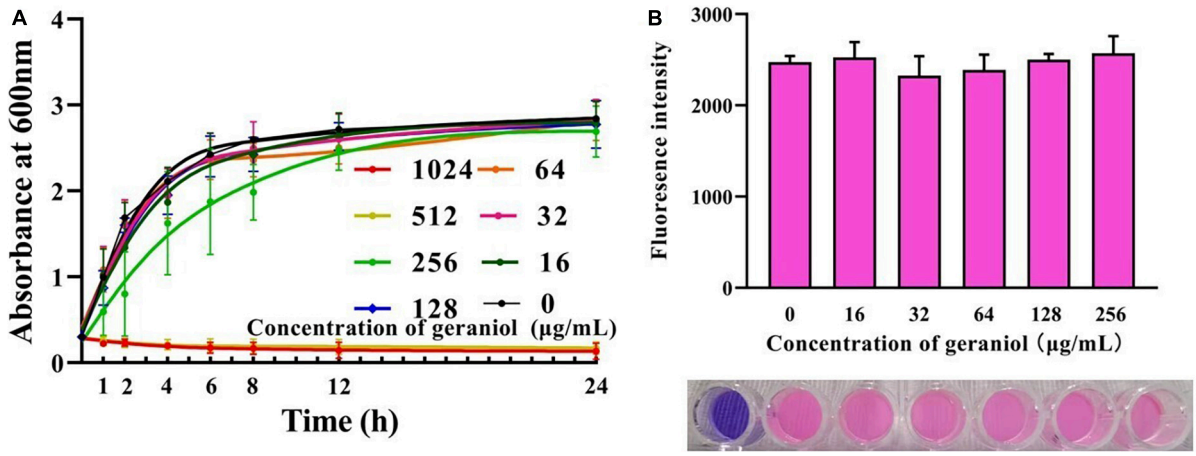


FIGURE 1
Effects of geraniol at different concentrations on the activity of USA300 assessed by the **(A)** growth curve assay and **(B)** Alamar blue analysis.

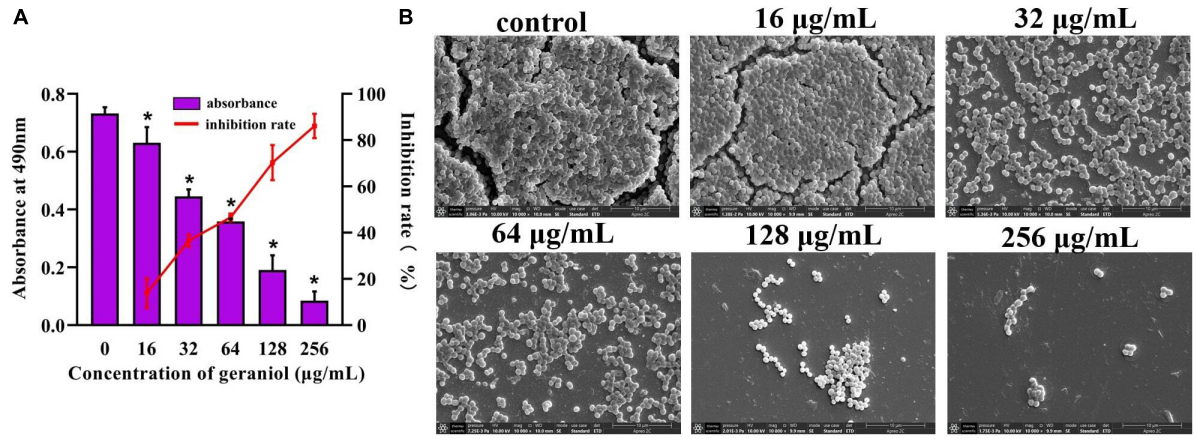


FIGURE 2
Effect of geraniol with sub-minimum inhibitory concentrations on the formation of USA300 biofilms assessed by **(A)** crystal violet staining and **(B)** scanning electron microscopy images at 10,000 × magnification. *$p < 0.05$ compared with the 0 μg/mL group.

the effect of geraniol on biofilm formation of several other *S. aureus* strains was also evaluated (**Supplementary Figure 1**). The biofilm inhibition rate of geraniol on these strains was more than 50%. The MIC of geraniol on these strains is shown in **Supplementary Table 3**.

## Geraniol removed preformed USA300 biofilms and several other *Staphylococcus aureus* strains

The biofilm removal assay revealed that geraniol, at concentrations of 256 μg/mL, effectively disrupted preformed biofilms, decreasing them by 49.87 ± 5.11% (**Figure 3A**). The scanning electron microscopy (SEM) observations (**Figure 3B**) showed that the slides without geraniol treatment were completely covered by bacteria and the bacterial cells were closely arranged like pavers blocks. As the concentration increased, bacteria gradually decreased, and the distribution of bacterial cells became scattered. Geraniol destroyed the structure of the biofilm. Geraniol also had different scavenging effects on preformed biofilms of other *S. aureus* strains. However, the effect on 26FS31, YFC18 and 2ZG3 clinical strains was not significant (**Supplementary Figure 2**).

## Qualitative analysis of polysaccharide intercellular adhesin production

In the Congo Red (CR) plate, the production of PIA was indicated by the number of black colonies, with the PIA-positive

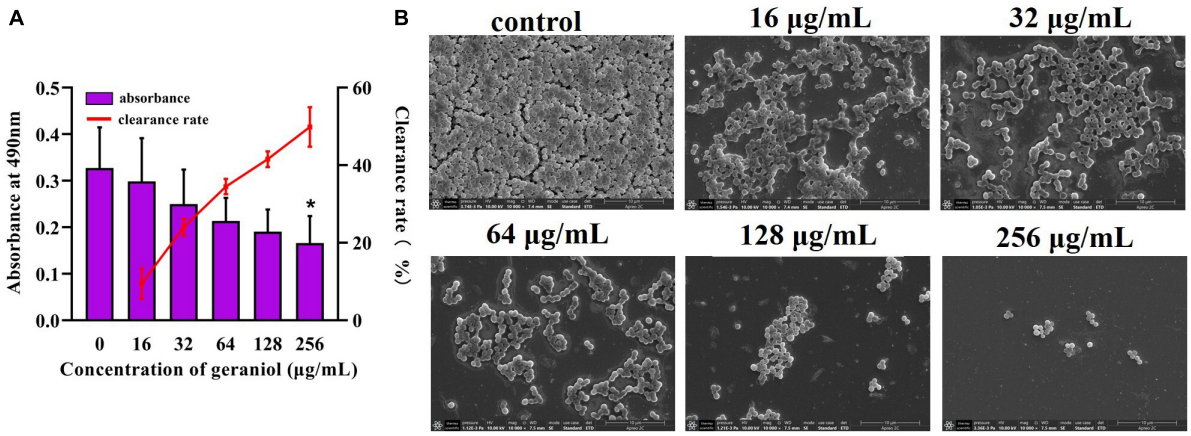


FIGURE 3
Effect of geraniol with sub-minimum inhibitory concentrations removing on preformed biofilms of USA300. **(A)** Crystal violet quantification and **(B)** scanning electron microscopy images at 10,000 × magnification. *$p < 0.05$ compared with the 0 μg/mL group.

bacterial strain being completely black. The results presented in Figure 4 show that as the geraniol concentration increased, the PIA synthesis gradually inhibited (observed as reduced color intensity of the black colonies). This suggests that geraniol inhibited USA300 biofilms by reducing the synthesis of PIA.

## Qualitative analysis of extracellular DNA release

The amount of eDNA released by USA300 cells was evaluated in the absence and presence of geraniol. As shown in Figure 5A, at low concentrations of geraniol, the release of eDNA from MRSA biofilms was significantly inhibited. Compared to that in the untreated group, eDNA release was decayed by 42.50 ± 1.57% and 57.10 ± 4.59% after treatment with 128 and 256 mg/mL geraniol, respectively.

## Cell autolysis assay

Autolysis of USA300 with 128 μg/mL geraniol was negligible in the first 30 min, whereas autolysis of USA300 treated with 256 μg/mL geraniol was effectively inhibited (Figure 5B).

## Geraniol inhibited the synthesis of staphyloxanthin and sensitized USA300 to $H_2O_2$

In geraniol-treated cells, the color of the bacteria turned pale (Figure 5C), and staphyloxanthin production (Figure 5D) was inhibited up to 70.70 ± 12.34%, with this inhibition being concentration-dependent. As shown in Figure 5E, the sensitivity of USA300 to $H_2O_2$ increased significantly in the 256 μg/mL geraniol-treated group (the number of live bacteria was $4.12 \times 10^7$ CFU/mL) compared with the untreated group (the number of live bacteria was $9.72 \times 10^7$ CFU/mL).

## Effect of geraniol on the expression of genes

The results of the quantitative polymerase chain reaction (qPCR) (Figure 6) showed the effect of 256 μg/mL geraniol on the genes involved in biofilm formation and virulence factor production in USA300. Geraniol downregulated the expression of *sarA*, *fnbA*, *fnbB*, *clfA*, *icaA*, *icaB*, *atlA*, and *crtM*.

## Vancomycin combined with geraniol reduced intraperitoneal foreign-body biofilm infection caused by methicillin-resistant *Staphylococcus aureus* in mice

### Vancomycin combination with geraniol removed preformed biofilms

The microscopic analysis showed that biofilms were removed to varying degrees. As shown in Figure 7, in the physiological saline group,the implant was tightly covered with dense biofilm bacteria, and many bacteria adhered to each other in clumps. A reticular structure was observed between the bacteria. In the high-dose combination group, the preformed biofilms were almost completely removed, and only a few bacteria were observed. A completely disrupted biofilm

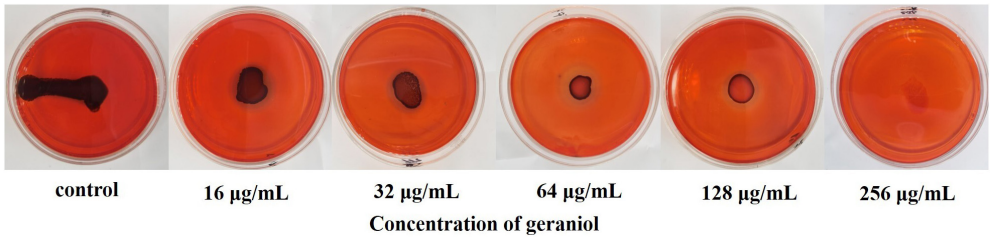


FIGURE 4
Qualitative analysis of the polysaccharide intercellular adhesin of USA300 upon geraniol treatment.

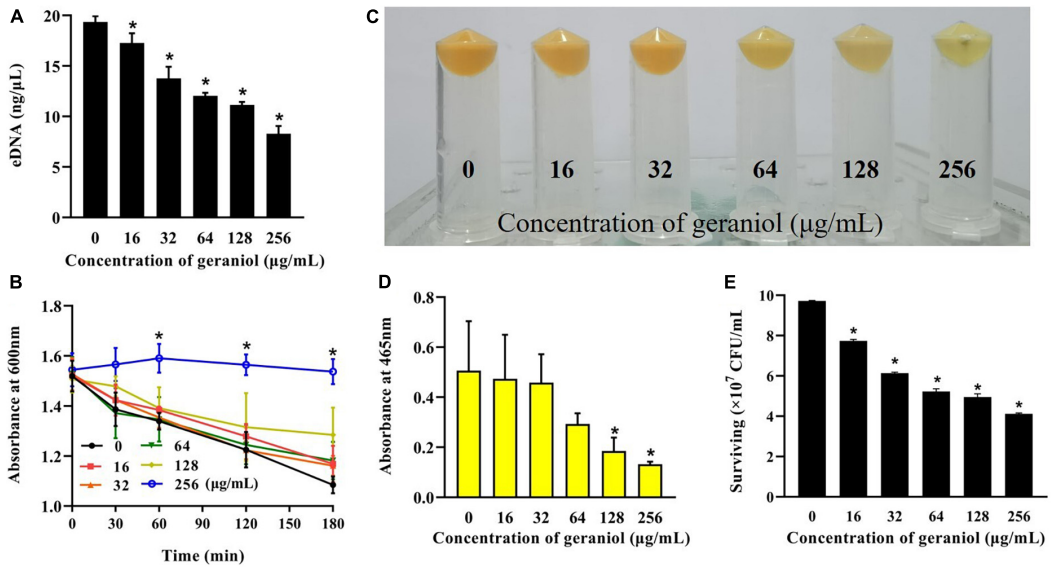


FIGURE 5
Inhibitory effects of geraniol on the release of extracellular nucleic acids and staphyloxanthin biosynthesis of USA300. **(A)** eDNA release, **(B)** autolysis, **(C)** cell color, **(D)** qualitative analysis of staphyloxanthin, and **(E)** effect of geraniol treatment on the survival of USA300 in $H_2O_2$. *$p < 0.05$ compared with the 0 μg/mL group.

architecture was observed, with reticula-connecting bacteria that had already been destroyed.

### Vancomycin combined with geraniol reduced bacterial adhesion

The bacterial burden on the implants was calculated using colony counting. The implants treated with a combination of geraniol (40 mg/kg) and vancomycin (40 mg/kg), which showed the most significant effect, exhibited minimal bacterial adhesion, and bacterial counts (Figure 8A) were lower than those observed in the physiological saline group (99.94% ± 0.06%).

### Vancomycin combined with geraniol reduced the inflammatory responses in mice

In all treatment groups, the white blood cell (WBC) count decreased to a normal level, and the levels of TNF-α and IL-6 were inhibited. Particularly, compared with the physiological saline group, the WBC count in the high-dose group (geraniol 40 mg/kg + vancomycin 40 mg/kg) decreased by 70.11% ± 10.70% (Figure 8B), and the levels of TNF-α and IL-6 were significantly lower by 46.33 ± 7.45% and 41.01 ± 7.90%, respectively (Figures 8C,D).

## Discussion

The limitation of antibiotic resistance caused by drug-resistant bacteria, such as MRSA and vancomycin-resistant *S. aureus*, has raised widespread concern worldwide. MRSA can cause chronic nosocomial infections and adhere to medical devices, especially implantable medical devices, by forming biofilms. Therefore, the demand for compound-targeted biofilms has increased in recent years. Anti-biofilm is a promising strategy for the treatment of MRSA-induced

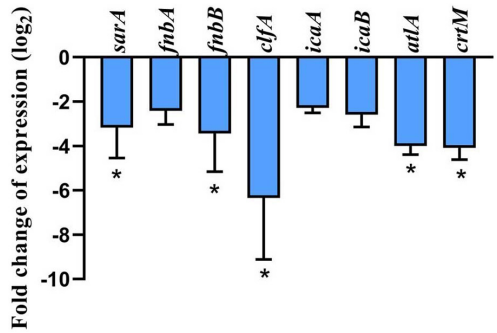


FIGURE 6
Effect of geraniol at 256 μg/mL concentration (half of the minimum inhibitory concentration) on the expression of genes involved in biofilm formation and related virulence factors of USA300. *$p < 0.05$ compared with the 0 μg/mL group.

infections (Roy et al., 2018). Several natural compounds, such as limonene, andrographolide sulfonate, and luteolin, have been found to inhibit biofilm formation (Zhang et al., 2021; Gambino et al., 2022; Yuan et al., 2022). In this study, the growth curves and Alamar Blue assay indicated that the tested concentration of geraniol did not affect the activity of bacteria. Indicating that the drug concentration will not have an effect on subsequent biofilm formation. This property is not easy to cause drug resistance in bacteria (Roy et al., 2018). Moreover, we found that geraniol has a transcendent activity of inhibiting MRSA biofilm formation and has a superior mature biofilms elimination effect.

Furthermore, to evaluate the inhibitory activity of geraniol on biofilm as comprehensively as possible, we observed the effect of geraniol on biofilm formation of methicillin-sensitive *S. aureus* (MSSA) and several other MRSA strains *in vitro*. Geraniol also has an apparent biofilm formation effect on these strains, which indicates that geraniol has a wide range of effects.

The PIA produced by *S. aureus* is an important contributor to biofilm formation. PIA contributes to stabilizing the interaction between bacterial cells and the adhesion of *S. aureus* to medical devices (Schilcher and Horswill, 2020). Nguyen et al. (2020) reported that wild-type strains cause more severe infections and show higher survival rates than PIA mutant strains in infected mouse models. Overall, determining the effect of geraniol on PIA production is important for exploring the potential mechanisms of geraniol. Our findings indicated that geraniol reduced PIA production in USA300 cells, as qualitatively evaluated using the CR plate method. PIA biosynthesis is regulated by the icaADBC operon. *icaA* encodes the main PIA synthesis, *icaB* is critical to the PIA adhesion function because it introduces a positive charge into the PIA via deacetylation, allowing the bacteria to adhere stably to surfaces (Nuryastuti and Krom, 2017; Lerch et al., 2019; Schilcher and Horswill, 2020). However, *icaA* cannot be expressed without *sarA*, since the promoter of the ica operon requires binding to *sarA* (Tamber and Cheung, 2009). *sarA* is an anti-biofilm target that has been discovered recently. It was reported that for individual strains, *ica* is not necessary for biofilm formation (Trotonda et al., 2005; Dengler Haunreiter et al., 2019). However, in *ica*-independent strains, *sarA* regulates

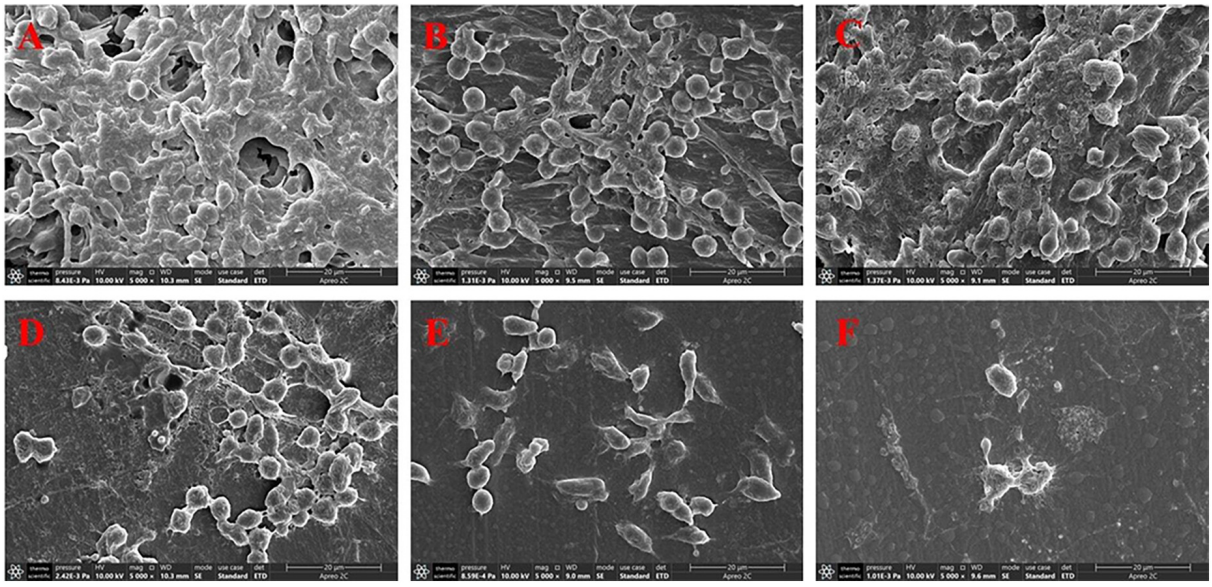


FIGURE 7
Scanning electron microscopy images at 5,000 × magnification of biofilms in peritoneal implants from mice. The doses of the drug were **(A)** physiological saline, **(B)** 40 mg/kg geraniol, **(C)** 40 mg/kg vancomycin, **(D)** 10 mg/kg geraniol + 40 mg/kg vancomycin, **(E)** 20 mg/kg geraniol + 40 mg/kg vancomycin, and **(F)** 40 mg/kg geraniol + 40 mg/kg vancomycin.

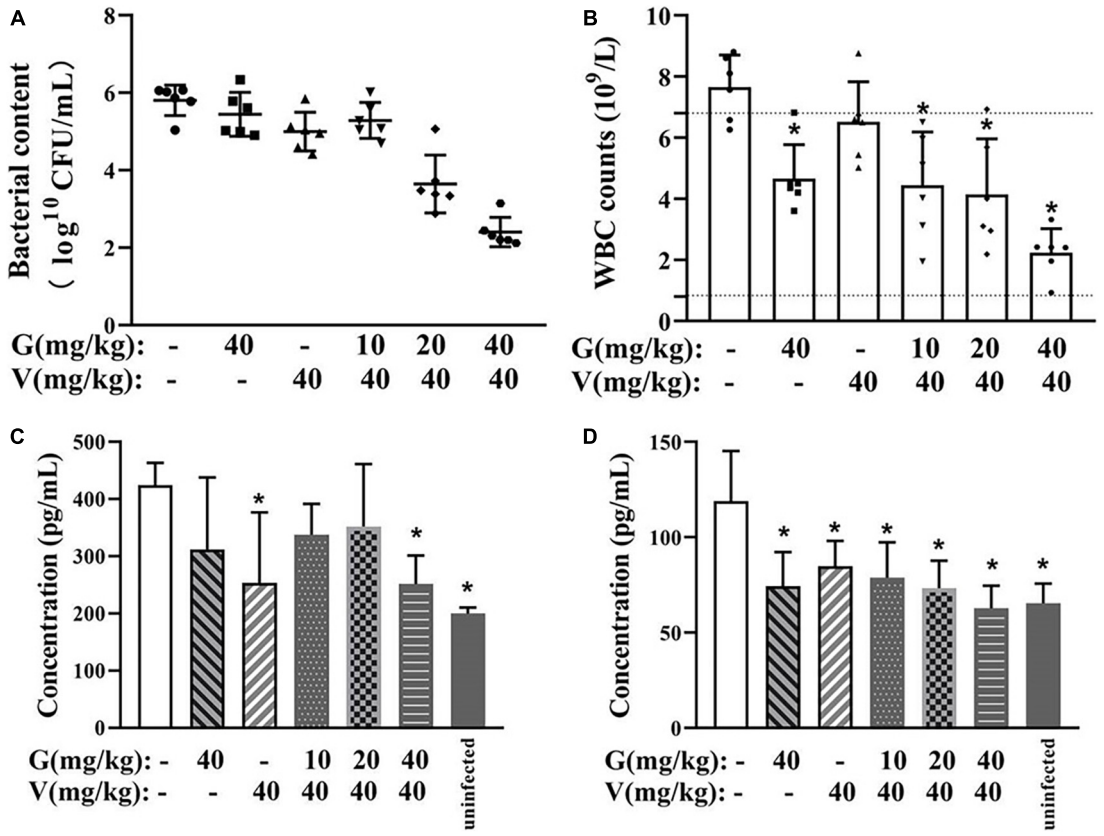


FIGURE 8
Therapeutic effect of combinations of vancomycin and/or geraniol on the mice infection model. **(A)** Bacterial count in implants, **(B)** white blood cell counts in mice, serum **(C)** TNF-α and **(D)** IL-6 levels in model mice after treatment. *$p < 0.05$ compared with the 0 μg/mL group.

biofilm formation in other ways. For instance, *sarA* positively regulates *fnbA*, *fnbB*, and *clfA* (determinants of *S. aureus* surface adhesins) (Pantrangi et al., 2015; Swarupa et al., 2018). Therefore, we selected several core genes for this study and found that they were significantly downregulated under the influence of geraniol. This is in agreement with phenotypic experiments (Zhang et al., 2021; Yehia et al., 2022).

In addition to PIA, eDNA is another major constituent of MRSA biofilms. The addition of DNase I (an enzyme that degrades eDNA) significantly reduces the formation of biofilms and facilitates its eradication (Nagasawa et al., 2017; Soler-Arango et al., 2019). The amount of eDNA released in this study (**Figure 5A**) supported the biofilm results, that is, geraniol inhibited the formation of biofilms and decreased the release of eDNA. Similar to apoptosis, *S. aureus* undergoes a cleavage process regulated by conserved genes, which is called autolysis (Rice et al., 2007). Autolysin is encoded by *atlA* and is involved in bacterial cell wall homeostasis and peptidoglycan conversion. Previous studies have shown that the release of eDNA by *S. aureus* is mediated by autolysis and biofilm formation (Rice et al., 2007; Houston et al., 2011). When the expression level of *atlA* was downregulated, the biofilm formation ability of *S. aureus* decreased sharply (Biswas et al., 2006). Therefore, we studied the autolysis of USA300 cells treated with geraniol, and found that geraniol significantly inhibited cell autolysis. This is consistent with the results of previous studies (Selvaraj et al., 2019; Valliammai et al., 2019) and suggests that geraniol reduces the release of eDNA by inhibiting cell autolysis. The gene expression level also confirmed that geraniol downregulated *atlA* gene. Hence, geraniol affected the USA300 biofilm architecture by modulating the expression of *atlA*.

Notably, geraniol changed the color of USA300 in this experiment. We speculate that this was associated with staphyloxanthin biosynthesis. Staphyloxanthin is the main component of the bacterial pigment that provides *S. aureus* its unique yellow or orange appearance. Staphyloxanthin protects *S. aureus* from escaping the immune system and from the bactericidal effect of oxides, which promotes bacterial survival (Liu and Nizet, 2009). This is due to the fact that the alternate bonds in the staphyloxanthin structure can absorb excess energy from reactive oxygen species (El-Agamey et al., 2004). Previous studies have shown that mutants encoding staphyloxanthin synthase CrtM not only cause *S. aureus* to lose its yellow

TABLE 1 Primer sequence.

| Primer | Sequence (5′→3′) |
|---|---|
| 16s-f | GCTGCCCTTTGTATTGTC |
| 16s-r | AGATGTTGGGTTAAGTCCC |
| sarA-f | TTGTTTTCGCTGATGTAT |
| sarA-r | CAATGGTCACTTATGCTG |
| fnbA-f | ATCAGCAGATGTAGCGGAAG |
| fnbA-r | TTTAGTACCGCTCGTTGTCC |
| fnbB-f | AAGAAGCACCGAAAACTGTG |
| fnbB-r | TCTCTGCAACTGCTGTAACG |
| clfA-f | ATTGGCGTGGCTTCAGTGCT |
| clfA-r | CGTTTCTTCCGTAGTTGCATTTG |
| icaA-f | TTTCGGGTGTCTTCACTCTAT |
| icaA-r | CGTAGTAATACTTCGTGTCCC |
| icaB-f | ATGGTCAAGCCCAGACAGAG |
| icaB-r | AGTATTTTCAATGTTTAAAGCA |
| atlA-f | TGTCGAAGTATTTGCCGACTTCGC |
| atlA-r | TGGAATCCTGCACATCCAGGAAC |
| crtM-f | ATCCAGAACCACCCGTTTTT |
| crtM-r | GCGATGAAGGTATTGGCATT |

appearance but are also more likely to be killed by peroxides in whole blood (Clauditz et al., 2006). The results of the lethal analysis and qPCR showed that geraniol could improve the sensitivity of USA300 to $H_2O_2$ and downregulate *crtM* gene expression, further verifying the results of phenotypic experiments. These results suggest that geraniol may be beneficial in the clinical treatment of MRSA.

Despite many preventive measures, medical device infections caused by biofilms still occur often, particularly implanted device infections. It is especially important to evaluate the biofilm scavenging activity of drugs *in vivo*. Therefore, we explored the therapeutic effects of geraniol combined with vancomycin on foreign body infections in mice. After 24 h of treatment, the pathological damage in mice was significantly alleviated. The therapeutic effect was the most obvious in the high-dose group. Neither geraniol nor vancomycin effectively killed bacteria that adhered to the surface. However, the number of bacteria significantly decreased with the addition of geraniol. Based on these results, we presumed that geraniol could effectively destroy the biofilm structure in mice and increase the effect of vancomycin. Infection with *S. aureus* causes an increase in WBCs and a large release of proinflammatory factors. In this study, the WBC count and the release of TNF-α and IL-6 in the dosing group were downregulated. Due to the high bacteriostatic concentration of geraniol (MIC = 512 μg/mL), we speculate that the anti-inflammatory effect of geraniol alleviates inflammatory symptoms in mice (Li et al., 2018; Toiu et al., 2019; Yuan et al., 2020). Owing to vancomycin's non-negligible toxicity, the dosage of vancomycin should not be increased in clinical practice. The *in vivo* results indicated that the combination of geraniol and vancomycin could effectively treat biofilm infection, which is critical for the treatment of MRSA biofilms.

In summary, geraniol not only effectively prevented MRSA biofilm formation but also removed mature MRSA biofilms. Geraniol inhibited the secretion of PIA and released eDNA, mainly by inhibiting the gene expression of *sarA* and *atlA*. Furthermore, geraniol reduced staphyloxanthin production by downregulating *crtM*, thereby increasing the sensitivity of MRSA to peroxides. In this study, the ability of geraniol in combination with vancomycin to remove biofilms *in vivo* was also evaluated. Although geraniol alone did not significantly remove the biofilm from the implant in mice, it is speculated that geraniol improved the therapeutic effect of vancomycin by destroying the structure of the biofilms, relieving inflammatory symptoms. In conclusion, geraniol is a potential drug for treating MRSA biofilms. However, the pharmacodynamics, pharmacokinetics, and toxicity of geraniol require further exploration.

# Materials and methods

## Bacterial strain and drug reagent

The MRSA strain USA300 (ATCC® BAA-1717™) [obtained from the American Type Culture Collection (ATCC)] was used in the current study and was cultivated in brain heart infusion (BHI) broth (Hopebio, Qingdao, China). The bacteria were cultured in an air bath constant temperature oscillator (BS-2F, Ningbo Jingda Formal Equipment Co., Ltd., Jintan, China) at a temperature of 37°C and a rotational speed of 150–200 rpm. Geraniol (>98% HPLC purity; CAS No. 106-24-1) was purchased from Shanghai McLean Biochemical Technology Co., Ltd. (Shanghai, China) and dissolved in dimethyl sulfoxide to obtain a stock solution. Vancomycin was purchased from Beijing Solarbio Science and Technology Co., Ltd. MSSA (ATCC® 25923, ATCC® 29213) were obtained from the ATCC. MRSA (ATCC® 43300, PHY6, 26FS18, C2Y, 2ZG3, YFC31) were presented by Professor Yanhua Li, School of Animal Medicine, Northeast Agricultural University.

## Ethics statement

All animal studies were performed in accordance with the approved experimental practices and standards of the Animal Ethics Committee of Sichuan Agricultural University (Chengdu, China), and the experimental protocols were approved and conducted under the supervision of the Animal Care Committee (permitnumberDKY-B2020203001; date of approval: June 11, 2021).

## Effect of geraniol on the activity of USA300

### Susceptibility testing and growth curve assay

The MIC of geraniol for *S. aureus* strains was determined using the double dilution method according to the Clinical and Laboratory Standards Institute (Arendrup et al., 2017). For USA300, after the bacteria were static cultured at 37°C for 18 h, the $OD_{600\ nm}$ of each bacteria group was determined. In the determination of the growth curve according to Yuan's experimental method (Yuan et al., 2019), the $OD_{600\ nm}$ was measured at different time points, which indicated the growth of USA300 (at 37°C and 200 rpm shaking speed) co-cultured with different concentrations (0, 16, 32, 64, 128, 256, 512, and 1,024 μg/mL) of geraniol. An appropriate amount of DMSO was used instead of geraniol as the control group in all experiments.

### Alamar blue assay

Cell viability was evaluated using the Alamar Blue (Solaibao, Beijing, China) assay according to Khan's experimental method (Khan et al., 2022). Briefly, Alamar Blue reagent was mixed with USA300 cells treated with sub-MIC (0, 16, 32, 64, 128, and 256 μg/mL) of geraniol. Samples were incubated in opaque 96-well plates (BKMAM BIOTECHNOLOGY Co., Ltd., Hunan, China) for 30 min at 37°C, before the fluorescence intensity was determined.

## Effect on biofilm formation

### The effect of geraniol on the formation of methicillin-resistant *Staphylococcus aureus* biofilms

Referring to the method of Peng et al. (2020), MSSA and MRSA strains cells (treated with sub-MICs of geraniol or appropriate concentration of DMSO) were cultured in 96-well plates (BKMAM BIOTECHNOLOGY Co., Ltd., Hunan, China) under anaerobic condition at 37°C for 18 h, and the mature biofilm was gently washed with non-heat source phosphate-buffered saline (PBS) to remove planktonic bacteria. Then the cultures were fixed by formaldehyde solution for more than 8 h and mature biofilms were stained with crystal violet for 2 h. Acetic acid (290 μL/well) was added to each well to dissolve the adhered dye, and the $OD_{490\ nm}$ was determined. SEM was used to observe morphological and structural changes in biofilms. The biofilms were cultured on slides (2 × 2 cm) using the same method as that used by Yuan et al. (2020). Finally, the biofilms were visualized using SEM (Apreo 2; Thermo Fisher Scientific Inc., Waltham, MA, United States).

### Biofilm removal assay

Preformed biofilms were treated with sub-MICs of geraniol or appropriate concentration of DMSO (diluted with PBS) for 24 h at 37°C. Then, similar to the steps in the previous experiment, the supernatant was removed and the planktonic bacteria were gently washed out with non-heat source PBS once. After crystal violet staining, the $OD_{490\ nm}$ was determined. SEM samples were prepared using the same method as previously described (Selvaraj et al., 2019).

### Polysaccharide intercellular adhesin analysis

To determine the effect of geraniol PIA production, the overnight (12 h) cultured USA300 suspension was inoculated on CR agar plates containing sub-MIC geraniol, and colony color was observed after incubation at 37°C for 24 h (Freeman et al., 1989).

### Extraction of extracellular DNA

USA300 was diluted to $10^7$ CFU/mL, and fresh BHI broth (Hopebio) with sub-MICs of geraniol was added to a 6-well plate (NEST Biotechnology Co., Ltd., Zhejiang, China), co-cultured for 18 h to construct a mature biofilm, and extracted according to the Rice method (Rice et al., 2007). Briefly, the mature biofilm was re-suspended by TEN buffer and the supernatant was absorbed for centrifugation (4°C, 18,000 rpm, 5 min). The supernatant was mixed with TE buffer and mixed solution of organic reagent (phenol, chloroform, and isoamyl alcohol) and extracted. After the extract was centrifuged (4°C, 12,000 rpm, 10 min), the supernatant was re-extracted by chloroform and isoamyl alcohol. Finally, eDNA release was detected using an ultra-micro spectrophotometer (NanoDrop One, Thermo Fisher Scientific Inc., Waltham, MA, United States).

### Autolysis analysis

USA300 cells were cultured overnight (12 h) in the presence of sub-MICs of geraniol. After washing thrice with PBS, the cells were resuspended in PBS containing 0.02% Triton Xmur100 (Solaibao, Beijing, China). These cells were cultured at 37°C and the $OD_{600\ nm}$ value of the bacterial suspension was determined every 30 min (Valliammai et al., 2019).

### Pigment production assay

Overnight (12 h) cultured USA300 was added to BHI broth containing sub-MICs of geraniol at 37°C and 180 rpm shaking speed for 24 h. Suspended cells were collected and extracted with methanol for more than 8 h. Thereafter, the supernatant was collected, and the $OD_{465\ nm}$ value was determined (Yuan et al., 2020).

### $H_2O_2$ killing assay

USA300 cells treated with sub-MICs of geraniol were added to PBS with $H_2O_2$ (1 mM) and incubated at 37°C for 1 h. The cells were then washed twice with PBS, diluted, evenly coated on BHI agar plates (Hopebio, Qingdao, China), cultured at 37°C for 24 h, and the colony count was performed (Valliammai et al., 2019).

### Quantitative real-time PCR

Total RNA was extracted from USA300 cells grown in BHI broth to the late-logarithmic phase in the absence and presence of geraniol (256 μg/mL) using an RNA kit (Tianmo Biotech, Beijing, China) and converted to cDNA using 5X RT Mix (Beijing Biomed Gene Technology Co., Ltd., China). PCR was performed in a 20 μL reaction volume containing BlasTaq$^{TM}$ 2XqPCR MasterMix (abm, Vancouver, Canada) according to the manufacturer's instructions. Real-time PCR was performed on a CFX Connect$^{TM}$ Real-Time PCR System (Bio-Rad Laboratories, Hercules, CA, United States) using specific primers (**Table 1**) designed using Primer 5.0. (PREMIER Biosoft, Canada) The levels of the target transcripts were calculated relative to those of 16S rRNA (housekeeping gene) using the $2^{-\Delta\Delta Ct}$ method (Schmittgen and Livak, 2008).

## Animals

### Establishment of a murine intraperitoneal foreign-body biofilm infection model in murine

The murine model was constructed according to the method by Yuan et al. (2020). Briefly, a USA300 biofilm was grown on the implants (a 1 mm in length medical PVC tubes, Yongkang, Shandong, China). Then, in the sterile environment, the mice were anesthetized with pentobarbital (40 mg/kg), a small incision was made in the left groin, the implants were placed carefully, and a professional sutured the incision. The process of establishing the mouse model is shown in **Supplementary Figure 3**. Finally, the mice were randomly divided into four groups with eight mice in each group, and the mice were injected with 0.1 mL of the drugs (40 mg/kg geraniol, 40 mg/kg vancomycin, 10 mg/kg geraniol + 40 mg/kg vancomycin, 20 mg/kg geraniol + 40 mg/kg vancomycin, 40 mg/kg geraniol + 40 mg/kg vancomycin, and physiological saline). All drugs were injected intraperitoneally twice daily (24 h) with a 12 h interval.

### Colony counting

The implants were removed from the mouse and gently rinsed with non-heat source PBS to remove the attached impurities. Thereafter, the colonies on the implants were counted (Tursi et al., 2020).

### Scanning electron microscopy

The implants were removed from the mice and fixed with 2.5% glutaraldehyde (Solaibao, Beijing, China) for 24 h; then the SEM (Apreo 2; Thermo Fisher Scientific Inc., Waltham, MA, United States) was used to observe the morphology and structure of the biofilms (Inoue et al., 2017).

### White blood cell counts

At 12 h after the second administration, the blood of the mice was collected, and a blood cell analyzer (BC-5120; Mindray, Shenzhen, China) was used to count the WBCs.

### Enzyme-linked immunosorbent assay

Blood was collected from the mice, and the serum was prepared according to the instructions of the enzyme-linked immunosorbent assay (ELISA) kit (Jiangsu Meimian industrial Co., Ltd., Yancheng, China) for ELISA.

## Statistical analysis

All *in vitro* experiments were performed in triplicate, and the values are presented as mean ± standard deviation. Two-tailed Student's *t*-tests and analysis of variance were used to analyze statistically significant differences. GraphPad Prism 8 software was used for the analysis. Differences with *p*-values less than 0.05 were considered statistically significant.

# Data availability statement

The raw data supporting the conclusions of this article will be made available by the authors, without undue reservation.

# Ethics statement

The animal study was reviewed and approved by the Animal Ethics Committee of Sichuan Agricultural University (Chengdu, China).

# Author contributions

LY and ZX conceived and designed the experiments. KG, YH, YD, CH, XL, GS, and TT performed the experiments. TT and LZ contributed to preparing the reagents, materials, and analysis tools. KG and OP wrote the manuscript. All authors have read and agreed to the published.

# Funding

This study was supported by the Sichuan Science and Technology Program (Grant no. 2021YFH0156), the National Natural Science Foundation of China (Grant no. 31702284), and the Central Government Funds of Guiding Local Scientific and Technological Development for Sichuan Province (Grant no. 2021ZYD0071).

## Acknowledgments

We sincerely thank Prof. Yanhua Li for providing the strains. We are grateful the Editage (www.editage.cn) for English language editing.

## Conflict of interest

The authors declare that the research was conducted in the absence of any commercial or financial relationships that could be construed as a potential conflict of interest.

## Publisher's note

All claims expressed in this article are solely those of the authors and do not necessarily represent those of their affiliated organizations, or those of the publisher, the editors and the reviewers. Any product that may be evaluated in this article, or claim that may be made by its manufacturer, is not guaranteed or endorsed by the publisher.

## Supplementary material

The Supplementary Material for this article can be found online at: https://www.frontiersin.org/articles/10.3389/fmicb.2022.960728/full#supplementary-material

SUPPLEMENTARY FIGURE 1
Inhibition rate of geraniol with sub-minimum inhibitory concentrations on the formation of MSSA standard strains **(A)** ATCC 29213, **(B)** ATCC 25923 and MRSA strains **(C)** ATCC 43300, **(D)** HYP6, **(E)** 26FS31, **(F)** C2Y, **(G)** 2ZG3, **(H)** YFC18.

SUPPLEMENTARY FIGURE 2
Clearance rate of geraniol with sub-minimum inhibitory concentrations on preformed biofilms of MSSA standard strains **(A)** ATCC 29213, **(B)** ATCC 25923 and MRSA strains **(C)** ATCC 43300, **(D)** HYP6, **(E)** 26FS31, **(F)** C2Y, **(G)** 2ZG3, **(H)** YFC18.

## References

Abdelhady, W., Bayer, A., Seidl, K., Moormeier, D., Bayles, K., Cheung, A., et al. (2014). Impact of vancomycin on sarA-mediated biofilm formation: role in persistent endovascular infections due to methicillin-resistant Staphylococcus aureus. *J. Infect. Dis.* 209, 1231–1240. doi: 10.1093/infdis/jiu007

Arendrup, M. C., Anupam, P., Joseph, M., Cheshta, S., and Anuradha, C. (2017). Comparison of EUCAST and CLSI reference microdilution MICs of eight antifungal compounds for candida auris and associated tentative epidemiological cutoff values. *Antimicrob. Agents Chemother.* 61:e00485-17. doi: 10.1128/AAC.00485-17

Biswas, R., Voggu, L., Simon, U., Hentschel, P., Thumm, G., and Götz, F. (2006). Activity of the major staphylococcal autolysin Atl. *FEMS Microbiol. Lett.* 259, 260–268. doi: 10.1111/j.1574-6968.2006.00281.x

Catalano, A., Iacopetta, D., Ceramella, J., Scumaci, D., Giuzio, F., Saturnino, C., et al. (2022). Multidrug Resistance (MDR): a widespread phenomenon in pharmacological therapies. *Molecules* 27:616. doi: 10.3390/molecules27030616

Clauditz, A., Resch, A., Wieland, K., Peschel, A., and Götz, F. (2006). Staphyloxanthin plays a role in the fitness of *Staphylococcus aureus* and its ability to cope with oxidative stress. *Infect. Immun.* 74, 4950–4953. doi: 10.1128/iai.00204-06

Cong, Y., Yang, S., and Rao, X. (2020). Vancomycin resistant Staphylococcus aureus infections: a review of case updating and clinical features. *J. Adv. Res.* 21, 169–176. doi: 10.1016/j.jare.2019.10.005

Dengler Haunreiter, V., Boumasmoud, M., Häffner, N., Wipfli, D., Leimer, N., Rachmühl, C., et al. (2019). In-host evolution of *Staphylococcus epidermidis* in a pacemaker-associated endocarditis resulting in increased antibiotic tolerance. *Nat. Commun.* 10:1149. doi: 10.1038/s41467-019-09053-9

El-Agamey, A., Lowe, G., McGarvey, D., Mortensen, A., Phillip, D., Truscott, T., et al. (2004). Carotenoid radical chemistry and antioxidant/pro-oxidant properties. *Arch. Biochem. Biophys.* 430, 37–48. doi: 10.1016/j.abb.2004.03.007

Freeman, D., Falkiner, F., and Keane, C. (1989). New method for detecting slime production by coagulase negative staphylococci. *J. Clin. Pathol.* 42, 872–874. doi: 10.1136/jcp.42.8.872

Friedman, M., Henika, P., and Mandrell, R. (2002). Bactericidal activities of plant essential oils and some of their isolated constituents against *Campylobacter jejuni*, *Escherichia coli*, *Listeria monocytogenes*, and *Salmonella enterica*. *J. Food Prot.* 65, 1545–1560. doi: 10.4315/0362-028x-65.10.1545

Gambino, E., Maione, A., Guida, M., Albarano, L., Carraturo, F., Galdiero, E., et al. (2022). Evaluation of the pathogenic-mixed biofilm formation of *Pseudomonas aeruginosa*/*Staphylococcus aureus* and treatment with limonene on three different materials by a dynamic model. *Int. J. Environ. Res. Public Health* 19:3741. doi: 10.3390/ijerph19063741

Gupta, P., Gupta, H., and Poluri, K. (2021). Geraniol eradicates *Candida glabrata* biofilm by targeting multiple cellular pathways. *Appl. Microbiol. Biotechnol.* 105, 5589–5605. doi: 10.1007/s00253-021-11397-6

Houston, P., Rowe, S., Pozzi, C., Waters, E., and O'Gara, J. (2011). Essential role for the major autolysin in the fibronectin-binding protein-mediated *Staphylococcus aureus* biofilm phenotype. *Infect. Immun.* 79, 1153–1165. doi: 10.1128/iai.00364-10

Inoue, D., Kabata, T., Ohtani, K., Kajino, Y., Shirai, T., and Tsuchiya, H. (2017). Inhibition of biofilm formation on iodine-supported titanium implants. *Int. Orthop.* 41, 1093–1099. doi: 10.1007/s00264-017-3477-3

Inouye, S., Takizawa, T., and Yamaguchi, H. (2001). Antibacterial activity of essential oils and their major constituents against respiratory tract pathogens by gaseous contact. *J. Antimicrob. Chemother.* 47, 565–573. doi: 10.1093/jac/47.5.565

Khan, M., Butt, S., Chaudhry, A., Rashid, A., Ijaz, K., Majeed, A., et al. (2022). Osteogenic induction with silicon hydroxyapatite using modified autologous adipose tissue-derived stromal vascular fraction: in vitro and qualitative histomorphometric analysis. *Materials* 15:1826. doi: 10.3390/ma15051826

Kwiatkowski, P., Sienkiewicz, M., Pruss, A., Łopusiewicz, Ł, Arszyńska, N., Wojciechowska-Koszko, I., et al. (2022). *Klebsiella pneumoniae*antibacterial and anti-biofilm activities of essential oil compounds against New Delhi Metallo-β-lactamase-1-producing uropathogenic strains. *Antibiotics* 11:147. doi: 10.3390/antibiotics11020147

Lerch, M., Schoenfelder, S., Marincola, G., Wencker, F., Eckart, M., Förstner, K., et al. (2019). A non-coding RNA from the intercellular adhesion (ica) locus of *Staphylococcus* epidermidis controls polysaccharide intercellular adhesion (PIA)-mediated biofilm formation. *Mol. Microbiol.* 111, 1571–1591. doi: 10.1111/mmi.14238

Li, S., Chen, L., Wang, G., Xu, L., Hou, S., Chen, Z., et al. (2018). Anti-ICAM-1 antibody-modified nanostructured lipid carriers: a pulmonary vascular endothelium-targeted device for acute lung injury therapy. *J. Nanobiotechnol.* 16:105. doi: 10.1186/s12951-018-0431-5

Lin, L., Long, N., Qiu, M., Liu, Y., Sun, F., and Dai, M. (2021). The inhibitory efficiencies of geraniol as an anti-inflammatory, antioxidant, and antibacterial, natural agent against methicillin-resistant *Staphylococcus aureus* infection in vivo. *Infect. Drug Resist.* 14, 2991–3000. doi: 10.2147/IDR.S318989

Liu, G., and Nizet, V. (2009). Color me bad: microbial pigments as virulence factors. *Trends Microbiol.* 17, 406–413. doi: 10.1016/j.tim.2009.06.006

Mauro, T., Rouillon, A., and Felden, B. (2016). Insights into the regulation of small RNA expression: SarA represses the expression of two sRNAs in Staphylococcus aureus. *Nucleic Acids Res.* 44, 10186–10200. doi: 10.1093/nar/gkw777

Nagasawa, R., Sato, T., and Senpuku, H. (2017). Raffinose induces biofilm formation by *Streptococcus mutans* in low concentrations of sucrose by increasing production of extracellular DNA and fructan. *Appl. Environ. Microbiol.* 83:e00869-17. doi: 10.1128/aem.00869-17

Nguyen, H. T. T., Nguyen, T. H., and Otto, M. (2020). The staphylococcal exopolysaccharide PIA – Biosynthesis and role in biofilm formation, colonization, and infection. *Comput. Struct. Biotechnol. J.* 18, 3324–3334. doi: 10.1016/j.csbj.2020.10.027

Nuryastuti, T., and Krom, B. (2017). Ica-status of clinical *Staphylococcus epidermidis* strains affects adhesion and aggregation: a thermodynamic analysis. *Antonie Van Leeuwenhoek* 110, 1467–1474. doi: 10.1007/s10482-017-0899-2

Oriol, C., Cengher, L., Manna, A., Mauro, T., Pinel-Marie, M., Felden, B., et al. (2021). Expanding the *Staphylococcus aureus* SarA regulon to small RNAs. *mSystems* 6:e0071321. doi: 10.1128/mSystems.00713-21

Pantrangi, M., Singh, V., and Shukla, S. (2015). Regulation of staphylococcal superantigen-like gene, ssl8, expression in *Staphylococcus aureus* strain, RN6390. *Clin. Med. Res.* 13, 7–11. doi: 10.3121/cmr.2014.1226

Peng, Q., Lin, F., and Ling, B. (2020). In vitro activity of biofilm inhibitors in combination with antibacterial drugs against extensively drug-resistant *Acinetobacter baumannii*. *Sci. Rep.* 10:18097. doi: 10.1038/s41598-020-75218-y

Prasad, S. N., and Muralidhara, M. (2017). Analysis of the antioxidant activity of geraniol employing various in-vitro models: relevance to neurodegeneration in diabetic neuropathy. *Asian J. Pharmaceutical Clin. Res.* 10, 101–105.

Rice, K., Mann, E., Endres, J., Weiss, E., Cassat, J., Smeltzer, M., et al. (2007). The cidA murein hydrolase regulator contributes to DNA release and biofilm development in *Staphylococcus aureus*. *Proc. Natl. Acad. Sci. U S A.* 104, 8113–8118. doi: 10.1073/pnas.0610226104

Roy, R., Tiwari, M., Donelli, G., and Tiwari, V. (2018). Strategies for combating bacterial biofilms: a focus on anti-biofilm agents and their mechanisms of action. *Virulence* 9, 522–554. doi: 10.1080/21505594.2017.1313372

Schilcher, K., and Horswill, A. R. (2020). Staphylococcal biofilm development: structure, regulation, and treatment strategies. *Microbiol. Mol. Biol. Rev. MMBR* 84:e00026-19. doi: 10.1128/MMBR.00026-19

Schmittgen, T., and Livak, K. (2008). Analyzing real-time PCR data by the comparative C(T) method. *Nat. Protocols* 3, 1101–1108. doi: 10.1038/nprot.2008.73

Selvaraj, A., Jayasree, T., Valliammai, A., and Pandian, S. K. (2019). Myrtenol attenuates MRSA biofilm and virulence by suppressing sarA expression dynamism. *Front. Microbiol.* 10:2027. doi: 10.3389/fmicb.2019.02027

Selvaraj, A., Valliammai, A., Muthuramalingam, P., Priya, A., Suba, M., Ramesh, M., et al. (2020). Carvacrol targets SarA and CrtM of methicillin-resistant *Staphylococcus aureus* to mitigate biofilm formation and staphyloxanthin synthesis: an in vitro and in vivo approach. *ACS Omega* 5, 31100–31114. doi: 10.1021/acsomega.0c04252

Sharma, D., Misba, L., and Khan, A. (2019). Antibiotics versus biofilm: an emerging battleground in microbial communities. *Antimicrobial Resistance Infect. Control* 8:76. doi: 10.1186/s13756-019-0533-3

Soler-Arango, J., Figoli, C., Muraca, G., Bosch, A., and Brelles-Marino, G. (2019). The *Pseudomonas aeruginosa* biofilm matrix and cells are drastically impacted by gas discharge plasma treatment: a comprehensive model explaining plasma-mediated biofilm eradication. *PLoS One* 14:e0216817. doi: 10.1371/journal.pone.0216817

Swarupa, V., Chaudhury, A., and Sarma, P. (2018). Staphylococcus aureusIron enhances the peptidyl deformylase activity and biofilm formation in. *3 Biotech* 8:32. doi: 10.1007/s13205-017-1050-9

Tamber, S., and Cheung, A. (2009). SarZ promotes the expression of virulence factors and represses biofilm formation by modulating SarA and agr in *Staphylococcus aureus*. *Infect. Immun.* 77, 419–428. doi: 10.1128/iai.00859-08

Tenover, F. C., McDougal, L. K., Goering, R. V., Killgore, G., Projan, S. J., Patel, J. B., et al. (2006). Characterization of a strain of community-associated methicillin-resistant *Staphylococcus aureus* widely disseminated in the United States. *J. Clin. Microbiol.* 44, 108–118. doi: 10.1128/JCM.44.1.108-118.2006

Toiu, A., Mocan, A., Vlase, L., Pârvu, A., Vodnar, D., Gheldiu, A., et al. (2019). In VivoComparative phytochemical profile, antioxidant, antimicrobial and anti-inflammatory activity of different extracts of traditionally used romanian L. and L. (Lamiaceae). *Molecules* 24:1597. doi: 10.3390/molecules24081597

Trotonda, M., Manna, A., Cheung, A., Lasa, I., and Penadés, J. (2005). SarA positively controls bap-dependent biofilm formation in *Staphylococcus aureus*. *J. Bacteriol.* 187, 5790–5798. doi: 10.1128/jb.187.16.5790-5798.2005

Turner, N. A., Sharma-Kuinkel, B. K., Maskarinec, S. A., Eichenberger, E. M., Shah, P. P., Carugati, M., et al. (2019). Methicillin-resistant *Staphylococcus aureus*: an overview of basic and clinical research. *Nat. Rev. Microbiol.* 17, 203–218. doi: 10.1038/s41579-018-0147-4

Tursi, S. A., Puligedda, R. D., Szabo, P., Nicastro, L. K., Miller, A. L., Qiu, C., et al. (2020). *Salmonella Typhimurium* biofilm disruption by a human antibody that binds a pan-amyloid epitope on curli. *Nat. Commun.* 11:1007. doi: 10.1038/s41467-020-14685-3

Valliammai, A., Sethupathy, S., Priya, A., Selvaraj, A., Bhaskar, J., Krishnan, V., et al. (2019). 5-Dodecanolide interferes with biofilm formation and reduces the virulence of methicillin-resistant *Staphylococcus aureus* (MRSA) through up regulation of agr system. *Sci. Rep.* 9:13744. doi: 10.1038/s41598-019-50207-y

Vijayakumar, K., Muhilvannan, S., and Arun Vignesh, M. (2022). Hesperidin inhibits biofilm formation, virulence and staphyloxanthin synthesis in methicillin resistant *Staphylococcus aureus* by targeting SarA and CrtM: an in vitro and in silico approach. *World J. Microbiol. Biotechnol.* 38:44. doi: 10.1007/s11274-022-03232-5

Wu, Y., Wang, Z., Fu, X., Lin, Z., and Yu, K. (2020). Geraniol-mediated osteoarthritis improvement by down-regulating PI3K/Akt/NF-κB and MAPK signals: in vivo and in vitro studies. *Int. Immunopharmacol.* 86:106713. doi: 10.1016/j.intimp.2020.106713

Xu, L., Liu, M., Yang, Y., Wang, Y., Hua, X., Du, L., et al. (2022). Geraniol enhances inhibitory inputs to the paraventricular thalamic nucleus and induces sedation in mice. *Phytomedicine* 98:153965. doi: 10.1016/j.phymed.2022.153965

Yang, H., Liu, G., Zhao, H., Dong, X., and Yang, Z. (2021). Inhibiting the JNK/ERK signaling pathway with geraniol for attenuating the proliferation of human gastric adenocarcinoma AGS cells. *J. Biochem. Mol. Toxicol.* 35:e22818. doi: 10.1002/jbt.22818

Yehia, F., Yousef, N., and Askoura, M. (2022). Celastrol mitigates staphyloxanthin biosynthesis and biofilm formation in *Staphylococcus aureus* via targeting key regulators of virulence; in vitro and in vivo approach. *BMC Microbiol.* 22:106. doi: 10.1186/s12866-022-02515-z

Younis, N., Elsewedy, H., Soliman, W., Shehata, T., and Mohamed, M. (2021). Geraniol isolated from lemon grass to mitigate doxorubicin-induced cardiotoxicity through Nrf2 and NF-κB signaling. *Chem. Biol. Interact.* 347:109599. doi: 10.1016/j.cbi.2021.109599

Yu, H., Liu, Y., Yang, F., Xie, Y., Guo, Y., Cheng, Y., et al. (2022). The combination of hexanal and geraniol in sublethal concentrations synergistically inhibits quorum sensing in *Pseudomonas fluorescens*-in vitro and in silico approaches. *J. Appl. Microbiol.* Online ahead of print. doi: 10.1111/jam.15446

Yuan, Q., Feng, W., Wang, Y., Wang, Q., Mou, N., Xiong, L., et al. (2022). Luteolin attenuates the pathogenesis of *Staphylococcus aureus* by interfering with the agr system. *Microb. Pathog.* 165:105496. doi: 10.1016/j.micpath.2022.105496

Yuan, Z., Dai, Y., Ouyang, P., Rehman, T., Hussain, S., Zhang, T., et al. (2020). Thymol inhibits biofilm formation, eliminates pre-existing biofilms, and enhances clearance of methicillin-resistant *Staphylococcus aureus* (MRSA) in a mouse peritoneal implant infection model. *Microorganisms* 8:99. doi: 10.3390/microorganisms8010099

Yuan, Z., Ouyang, P., Gu, K., Rehman, T., Zhang, T., Yin, Z., et al. (2019). The antibacterial mechanism of oridonin against methicillin-resistant *Staphylococcus aureus* (MRSA). *Pharm. Biol.* 57, 710–716. doi: 10.1080/13880209.2019.1674342

Zhang, L., Wen, B., Bao, M., Cheng, Y., Mahmood, T., Yang, W., et al. (2021). *Staphylococcus aureus*andrographolide sulfonate is a promising treatment to combat methicillin-resistant and its biofilms. *Front. Pharmacol.* 12:720685. doi: 10.3389/fphar.2021.720685

frontiers | Frontiers in Microbiology

TYPE Original Research
PUBLISHED 09 September 2022
DOI 10.3389/fmicb.2022.948188



OPEN ACCESS

EDITED BY
Xiaolin Hou,
Beijing University of Agriculture, China

REVIEWED BY
Rahul Bhadouria,
University of Delhi, India
Li Lin,
Anhui Agricultural University, China

*CORRESPONDENCE
Oscar Cardenas Alegria
oscar.alegria@icb.ufpa.br

†These authors have contributed equally to this work and share first authorship

SPECIALTY SECTION
This article was submitted to Antimicrobials, Resistance and Chemotherapy, a section of the journal Frontiers in Microbiology

RECEIVED 19 May 2022
ACCEPTED 16 August 2022
PUBLISHED 09 September 2022

CITATION
Cardenas Alegria O, Pires Quaresma M, Dias Dantas CW, Silva Guedes Lobato EM, de Oliveira Aragão A, Patroca da Silva S, Costa Barros da Silva A, Ribeiro Cruz AC, Ramos RTJ and Carneiro AR (2022) Impacts of soybean agriculture on the resistome of the Amazonian soil. *Front. Microbiol.* 13:948188. doi: 10.3389/fmicb.2022.948188



# Impacts of soybean agriculture on the resistome of the Amazonian soil

Oscar Cardenas Alegria[1*†], Marielle Pires Quaresma[1†], Carlos Willian Dias Dantas[2], Elaine Maria Silva Guedes Lobato[3], Andressa de Oliveira Aragão[1], Sandro Patroca da Silva[4], Amanda Costa Barros da Silva[1], Ana Cecília Ribeiro Cruz[4], Rommel Thiago Jucá Ramos[1,2] and Adriana Ribeiro Carneiro[1]

[1]Laboratory of Genomic and Bioinformatics, Center of Genomics and System Biology, Institute of Biological Sciences, Federal University of Pará, Belém, Brazil, [2]Institute of Biological Sciences, Federal University of Minas Gerais, Belo Horizonte, Brazil, [3]Department of Soil Science, Federal Rural University of the Amazon, Paragominas, Brazil, [4]Department of Arbovirology and Hemorrhagic Fevers, Evandro Chagas Institute-IEC/SVS/MS, Ananindeua, Brazil

The soils of the Amazon are complex environments with different organisms cohabiting in continuous adaptation processes; this changes significantly when these environments are modified for the development of agricultural activities that alter the chemical, macro, and microbiological compositions. The metagenomic variations and the levels of the environmental impact of four different soil samples from the Amazon region were evaluated, emphasizing the resistome. Soil samples from the organic phase from the different forest, pasture, and transgenic soybean monocultures of 2–14 years old were collected in triplicate at each site. The samples were divided into two groups, and one group was pre-treated to obtain genetic material to perform sequencing for metagenomic analysis; another group carried out the chemical characterization of the soil, determining the pH, the content of cations, and heavy metals; these were carried out in addition to identifying with different databases the components of the microbiological communities, functional genes, antibiotic and biocide resistance genes. A greater diversity of antibiotic resistance genes was observed in the forest soil. In contrast, in monoculture soils, a large number of biocide resistance genes were evidenced, highlighting the diversity and abundance of crop soils, which showed better resistance to heavy metals than other compounds, with a possible dominance of resistance to iron due to the presence of the *acn* gene. For up to 600 different genes for resistance to antibiotics and 256 genes for biocides were identified, most of which were for heavy metals. The most prevalent was resistance to tetracycline, cephalosporin, penam, fluoroquinolone, chloramphenicol, carbapenem, macrolide, and aminoglycoside, providing evidence for the co-selection of these resistance genes in different soils. Furthermore, the influence of vegetation cover on the forest floor was notable as a protective factor against the impact of human contamination. Regarding chemical characterization, the presence of heavy metals, different stress response

mechanisms in monoculture soils, and the abundance of mobile genetic elements in crop and pasture soils stand out. The elimination of the forest increases the diversity of genes for resistance to biocides, favoring the selection of genes for resistance to antibiotics in soils.

KEYWORDS

antibiotic resistance genes, biocide resistance genes, heavy metals, metagenomic, Amazonia soils

## Introduction

The use of land for agriculture has grown proportionally with the world population over time, increasing food production and the areas of cultivation. Among the widely developed cultures, the one with the most significant demand due to its application in different processes of the food industry is the soybean crop, with Brazil being the world's largest producer of soybeans, accounting for more than a third of production—followed by the United States and China (Voora et al., 2020).

In the northern region of the Brazilian territory, there are the most extensive areas of tropical Amazon forest. In the case of the state of Pará, it presents different ecological characteristics of forest, pasture, and the development of cassava, oil palm, soybean, corn, and others (Toloi et al., 2021). The expansion of agricultural frontiers makes it possible to modify the ecosystem by eliminating plant cover and applying chemical compounds, such as fertilizers, pesticides, antibiotics, salts, and others (Basso et al., 2021).

On the other hand, the soil is one of the largest and most diverse microbial habitats, having a vast reservoir of antibiotic resistance genes. Approximately 80% of soil microorganisms resist multiple antimicrobials, so these genes are naturally present in different ecological environments (Berg and Martinez, 2015; Chen et al., 2019). From this perspective, using fertilizers in the soil positively correlates with changing microbial composition and increases the abundance of resistance genes (Udikovic-Kolic et al., 2014; Sun et al., 2019). Thus, these environmental changes increase horizontal genetic transfer in microorganisms and accelerate adaptation to different stress mechanisms (Bottery et al., 2021). The antibiotic resistance genes (ARG) identified in the soil were tetracycline, fluoroquinolones, sulfonamides, β-lactams, aminoglycosides, erythromycin, and others (Jutkina et al., 2018; Armalyte et al., 2019; Brevik et al., 2020).

In this scenario, due to the effects of chemical and organic fertilizers, soil microbial communities are modified and become different from the original communities (Li et al., 2018; Chen et al., 2019). Soil microbial composition is complex and dynamic, as there are cooperative and competitive relationships within the same population, which can strengthen the diversity and stability of the environment (Yang et al., 2018; Qu et al., 2019). Furthermore, they may favor the co-selection of genes associated with adaptation, such as genes associated with resistance to antibiotics, heavy metals, biocides, and detergents, among others (Destoumieux-Garzón et al., 2018; Durso and Cook, 2019; Brevik et al., 2020). Natural levels of biocides such as heavy metals vary according to the type of soil (Costa et al., 2017), as well as cadmium (Cd), zinc (Zn), nickel (Ni), and mercury (Hg) are involved in the co-selection processes of multidrug-resistant bacteria (Heydari et al., 2022). Additionally, in the presence of horizontal transfer genes (HGT), the transfer of these genes is influenced by different abiotic and biotic factors (Hu et al., 2017; Jutkina et al., 2018).

While resistance and tolerance are considered properties of a population, interspecies interactions can have a significant effect on antibiotic and biocide treatment: communities or subpopulations of bacterial communities can survive exposure to antimicrobials due to interactions between species, and various mechanisms can act simultaneously within a community, many of which are widely known, such as antibiotic inactivation, biofilm formation, and quorum sensing activated responses (Bottery et al., 2021). In the case of the toxic effect of heavy metals, many microorganisms have developed efficient mechanisms of resistance to biocides, configuring three main types of proteins normally involved with flow pumps: (i) resistance-nodulation-cell division proteins (RND superfamily), (ii) cation diffusion facilitators (CDF family), and (iii) P-type ATPases (Romaniuk et al., 2018).

Otherwise, various biotic and abiotic stressors can affect agricultural productivity and crop yields, eventually leading to global food shortages (Bhagat et al., 2021). The need to adopt environmentally friendly methods to combat these stressors and improve crop yields is increasingly accentuating due to current agricultural practices' negative impacts (Salam et al., 2020). Plant health is closely linked to soil health, both of which are influenced by microbial communities, which significantly impact agricultural productivity and human health (Altier and Abreo, 2020). Thus, it is currently inevitable to associate human-mediated loss of biodiversity with the transformation of natural ecosystems and how they affect human health (Cook et al., 2020).

The monoculture production model, such as soybean production, requires extensive land use, a high level of mechanization, and intensive use of pesticides—compromising

the environment and human health (Belo et al., 2012; Pignati et al., 2017; Basso et al., 2021). Likewise, bacteria usually coexist in complex communities in the soil and present different interactions—including competition, exploitation, commensalism, and mutualism—these respond to exposure to different biotic and abiotic factors, which can alter the strength of selection acting on resistance mechanisms (Bottery et al., 2021), for example, soil pH and heavy metal pollution change the composition of bacterial communities (Chodak et al., 2013). Likewise, gene transfer processes can increase resistance in the different pathogenic organisms that reside in the soil, emphasizing the resistome's clinical importance (Forsberg et al., 2012).

The metagenomic analysis makes it possible to accurately describe the composition of microbial communities and the resistome genes under the environment's selective pressure and the effect of the alteration of ecosystems by agricultural production (Durso and Cook, 2019). In this context, we aimed (i) to evaluate the chemical characteristics of soils with and without tillage, which were exposed to agricultural compounds, (ii) to establish the relationship between soils used for tillage and changes in soil bacterial communities, and (iii) to elucidate the influence of soil properties on the disposition of genes associated with antibiotic and biocide resistance in soils in the Amazon region with different cultures and management times.

# Materials and methods

## Description of the study sites

The study site is in the Amazon, Paragominas-PA, Brazil. The area has been explored for 35 years for intensive grain farming and beef cattle. The predominant soil classified as Oxisol (Rodrigues et al., 2003) and the Aw climate (Alvares et al., 2013), hot and humid tropical, and was divided into four collection sites, being secondary forest (lat 2°58'34.46"S; long 47°18'0.72"W), Patagem (lat 2°58'52.88"S; long 47°18'1.332"W), soybean crop (Glycine max, P98 YH51 RR) 2 years (lat 2°59'2.54"S; long 47°17'18.77"W) and a 14-years-old soybean crop (lat 3°0'3.07"S; long 47°16'59"W). The soils were covered with native tropical forest, but after commercial timber was removed around 30 years ago, these were used for planting transgenic soybean crops and pasture; limestone was used, and chemical fertilizers were added to the cultivated sites [phosphate mono ammonium (MAP), potassium chloride (KCl), and Super triple phosphate]; herbicides; fungicides, and insecticides. As for the 14-years-old monoculture soil, ∼20 years ago, it was used for cultivation; at first, rice (*Oryza sativa*) was sown, and later three consecutive crops of corn (*Zea mays*) were used only for soybean cultivation. Samples were collected at a depth of up to 30 cm of soil (topsoil; Bach et al., 2018), and the collection was carried out in triplicate for each type of forest soils, pastures, and places where soybeans were developed for 2–14 continuous years. The collected samples were separated for chemical characterization and molecular analysis. Samples for chemical analysis were stored in 500 g plastic bags and kept at 4°C, whereas for molecular evaluation, the samples were stored in falcon tubes with a capacity of 15 ml and deposited immediately in liquid nitrogen.

## Soil chemical characterization

Raij et al. (2001) described the methodology used for chemical characterization. The samples were dehydrated in an oven with air circulation at 40°C and then sieved with a 2 mm mesh sieve. The pH was determined with water. The micronutrient contents of boro (B), copper (Cu), iron (Fe), manganese (Mn), cadmium (Cd), lead (Pb), cobalt (Co), mercury (Hg), nickel (Ni), and zinc (Zn) were determined by Inductively Coupled Plasma—Atomic Emission Spectrometry (ICP-AES, Thermo Fisher ICAP 7600). The cations were extracted with the chloride solution by the ion exchange process, using the EDTA titration method for the determination of calcium ($Ca^{2+}$), magnesium ($Mg^{2+}$), and potassium ($K^{+}$) cations.

## DNA isolation

The collected soil samples were first treated with sodium phosphate buffer solutions (500 mM $Na_2HPO_4$ and 500 mM $NaH_2PO_4$; pH 7.2), according to the protocol of Högfors-Rönnholm et al. (2018). Then, genetic material was extracted with the Dneasy PowerSoil DNA Isolation Kit (Qiagen, USA). DNA concentrations were measured by a NanoDrop spectrophotometer (Thermo Scientific), and quality was determined by horizontal electrophoresis in a 1% agarose gel with 0.5 ug $ul^{-1}$ of ethidium bromide.

## Next-generation sequencing

For the construction of the DNA libraries, the samples were processed in compliance with the manufacturer's protocol, Nextera XT DNA Library (Illumina). Sequencing was performed with the NextSeq 550 System High-Output kit, generating paired readings of 150 bp using the Illumina NextSeq 500/550 HighOutput platform.

The quality of the reads was analyzed using the FASTQC-Version 0.11.9 software (Andrew, 2019), later trimmed and filtered with a minimum quality standard of Phred 20 and a minimum size of 36 bp by the Trimmomatic software (Bolger et al., 2014).

## Microbial diversity analysis

Data in triplicates were analyzed by Kraken2 (Wood et al., 2019) to identify operational taxonomic units (OTU) and use the Pavian platform (Breitwieser and Salzberg, 2020) to perform diversity analysis. Then, Shannon's alpha diversity indices were calculated using the MicrobiomeAnalyst program (Dhariwal et al., 2017).

## Resistome assembly and analysis

Data assembly was performed using the Megahit program (Li et al., 2015), with a "meta-large" pattern, and the resulting contigs were analyzed using the Metaquast software (Mikheenko et al., 2016). Shortly after the assembly, contigs with sizes smaller than 350 pb were removed to reduce the number of artifacts in the assembly. Next, Prokka (Seemann, 2014) was used to identify the coding regions used later to identify antibiotic resistance genes by the Comprehensive Antibiotic Resistance Database (CARD) and Resistance Gene Identifier (RGI) databases (Alcock et al., 2020), in addition to the identification of resistance genes to biocides and heavy metals using the BacMet software (Pal et al., 2014). After that, the contigs were submitted to the public database of the metagenomic data analysis platform MG-RAST (Meyer et al., 2008), identifying functional genes using the SEED Subsystems database, with an alignment of 90%, a size of 20 bp, and an *e*-value of $10^{-5}$.

## Statistical analysis

The normality analysis of the variables was performed using the Shapiro–Wilk normality test, with a significance of $\alpha = 0.05$. The difference between the means was evaluated with the ANOVA and Kruskal–Wallis tests, while the Bonferroni correction was performed using the Tukey and Mann–Witney tests. Principal component analysis (PCA), ANOSIM, and cluster analysis were performed using the PAST program (Hammer et al., 2001). The Infogrames were developed with the Orange Data Mine tool (Demšar et al., 2013). The k-means method was used to create a heat map that picked 50 program clusters.

# Results

## Physicochemical analysis

The soils collected showed significant differences in terms of pH, with values varying between 5.7 and 6.9; the 2-years forest and culture sites were considered to have "high acidity" and "very low acidity," which was different among all sites (Tukey's test, $p < 0.05$), except for pasture and 14-years sites (Tukey; $Q = 0.471$; $p = 0.986$). The levels of cations in the different sites were similar for potassium and calcium. However, for magnesium, significant differences were observed between sites about everything on the 2-years site and the other sites (Tukey's test, $p <$ 0,05). The concentrations of micronutrients and heavy metals were found in the following decreasing order Fe$\gg$ Cr > Mn > Ni > Zn > Co > Cu > As, with the highest retention of these elements in the 14-years-old culture sites. However, the iron content was higher in the forest site, without significant differences between the other sites; the arsenic, cobalt, chromium, copper, and nickel contents were also similar; in the case of manganese, there were differences between the sites with the highest content in the pasture site e 2 years (Tukey's test; $Q =$ 5,516; $p = 0.019$), zinc showed significant differences with higher values in the 14-years-old culture and pasture sites, the 14-years-old site with forest and 2 years (Tukey's test, $p <$ 0.05), pasture with 2 years (Tukey's test; $Q =$ 5,821; $p = 0.014$; Table 1). Lead was identified only at the 14-years-old site (0.04 $\pm$ 0.07 mg $kg^{-1}$), and mercury was found at 2-years pasture and culture sites up to 0.02 mg $kg^{-1}$ but was not identified. Of cadmium anywhere.

## Microbial diversity

The most abundant bacterial phyla present in different soils are Proteobacteria and Actinobacteria. The prevalence of bacterial species was *Bradyrhizobium* sp. and *Rhodoplanes* sp. in the forest samples, and *Conexibacter* sp., *Enterobacter cloacae*, *Pseudomonas aeroginosa*, and *P. putida* in the other soils, in addition to *Bradyrhizobium* sp., and *Rhodoplanes* sp. (Figure 1). Shannon's alpha diversity index is high in all soils, with similar values between them (ANOVA; $F = 0.44$; $p$-value $= 0.73$).

## Abundance of functional genes

The relative abundance of functional genes according to the grouping of the SEED Subsystems database at its first level demonstrates similarities between the samples (Kruskal–Wallis; $\chi^2 = 5.823$; $p$-value $= 0.12$), with the highest relative number of genes being from functional classes related to protein, carbohydrate, and amino acid metabolism, RNA synthesis, stress response, transport of elements, dormancy, among others (Figure 2A).

The number of gene groups associated with adaptation and stress processes at a second level was higher in crop and pasture soils. Furthermore, it is possible to observe that the abundance of genes associated with DNA metabolism showed significant differences between soils (Kruskal–Wallis; $\chi^2 = 36.61$; $p$-value $= 1.27 \times 10^{-5}$), with a higher overall proportion of genes involved in repair and replication mechanisms (Figure 2B).

TABLE 1 Chemical characteristics were obtained from soil analysis, pH values, micronutrient contents, and heavy metals.

| | pH | $K^+$ | $Ca^{2+}$ | $Mg^{2+}$ | As | Co | Cr | Cu | Fe | Mn | Ni | Zn |
|---|---|---|---|---|---|---|---|---|---|---|---|---|
| | | $cmol_C\ dm^{-3}$ | | | $mg\ Kg^{-1}$ | | | | | | | |
| Forest | 5.73 ± 0.06 | 0.1 ± 0.02 | 4.59 ± 0.91 | 0.94 ± 0.09 | 0.34 ± 0.44 | 0.75 ± 0.34 | 70.71 ± 5.27 | 0.27 ± 0.06 | 86.67 ± 15.04 | 17.83 ± 4.76 | 2.45 ± 2.21 | 0.9 ± 0.1 |
| Pasture | 6.2 ± 0.2 | 0.34 ± 0.27 | 4.21 ± 0.4 | 1.00 ± 0.08 | 0.51 ± 0.16 | 0.62 ± 0.23 | 72.46 ± 11.33 | 0.47 ± 0.15 | 85.67 ± 44.64 | 25.47 ± 8.55 | 2.55 ± 0.95 | 1.47 ± 0.4 |
| 2 years | 6.93 ± 0.11 | 0.12 ± 0.01 | 4.47 ± 0.21 | 1.68 ± 0.25 | 0.37 ± 0.05 | 0.43 ± 0.15 | 70.81 ± 8.18 | 0.33 ± 0.06 | 61.33 ± 9.61 | 9.5 ± 0.46 | 1.88 ± 1.38 | 0.67 ± 0.15 |
| 14 years | 6.17 ± 0.06 | 0.4 ± 0.11 | 3.71 ± 0.18 | 1.k01 ± 0.1 | 0.69 ± 0.38 | 0.71 ± 0.48 | 88.39 ± 1.83 | 1 ± 0.56 | 67 ± 13.74 | 15.43 ± 2.14 | 4.62 ± 3.72 | 1.9 ± 0.17 |
| *p*-value | $1.6 \times 10^{-5}$* | 0.085 | 0.241 | 0.001* | 0.359 | 0.648 | 0.055 | 0.055 | 0.527 | 0.027* | 0.529 | 0.001* |

$K^+$, potassium cation; $Ca^{2+}$, calcium cation; $Mg^{2+}$, magnesium cation; As, arsenic; Cd, cadmium; Co, cobalt; Cr, chromium; Cu, copper; Fe, iron; Hg, mercury; Mn, manganese; Ni, nickel; Pb, lead; Zn, zinc.
*p-value $< 0.05$.

The composition of genes associated with the stress response process showed significant differences between soils (Kruskal–Wallis; $\chi^2 = 46.33$; $p$-value $= 1.29 \times 10^{-11}$): In forest soil, the genes responsible for the stress response were more prevalent than the heat shock response genes, constituting a response to oxidative stress and cold shock, respectively; in monoculture soils, in addition to the previously mentioned genes, there were genes for osmotic stress response and detoxification; and in pasture soil, a dominance of genes responding to oxidative stress and desiccation was observed, followed by genes from the functional classes mentioned above (Figure 2C).

Similarly, the number of genes associated with cell regulation and signaling showed significant differences between the samples (Kruskal–Wallis; $\chi^2 = 38.37$; $p$-value $= 2.36 \times 10^{-8}$), with crop and pasture soils demonstrating a prevalence of genes for quorum sensing, biofilm formation, programmed death, and toxin-antitoxin, while in forest soil there is a prevalence of genes for quorum sensing, biofilm formation, and virulence regulation (Figure 2D).

## Mobile elements and pathogenicity islands

The number of genes related to pathogenicity islands and mobile elements (phages, prophages, plasmids, transposons, and transfer genes) showed significant differences between soils (Kruskal–Wallis; $\chi^2 = 13.39$; $p$-value $= 0.001$). The prevalence of genes associated with phages and prophages increased in tilled soils, while the amounts in forest and pasture soils decreased. Similar to the previous one, the genes related to the most prevalent pathogenicity islands in different soils, especially in pasture samples (Figures 3A,B).

## Antibiotic and biocide resistance genes

A large number of resistance genes were identified in different soils, with significant differences (Figure 4A) between pasture and crop soils (Kruskal–Wallis; $\chi^2 = 72.22$; $p$-value $= 7.98 \times 10^{-18}$). In this context, up to 600 distinct genes were identified in the analyzed samples, among which 43% displayed multidrug resistance.

The presence of antibiotic resistance genes was observed at all sites. Comparatively, 24 genes are shared between the sites. As for the total number of genes identified in each soil, the forest had 122 genes, followed by pasture with 90 genes and crop soils with up to 73 genes (Figure 4B).

Regarding biocide resistance genes, a total of 256 genes were identified, of which 53% showed multi-resistance, especially to different heavy metals. A higher prevalence was detected in soils with 2–14 years of monoculture and pasture, making it possible to observe 31 genes in common in all analyzed soils. The 14-years-old soil crop had the highest number of unique biocide resistance genes, with 32 genes (Figure 4C).

The relative abundance of antibiotic resistance genes in the analyzed samples was of 32 different antibiotics, without showing significant differences between the soils (Kruskal–Wallis; $\chi^2 = 1.242$; $p$-value $= 0.742$), among which the resistance to classes of antibiotics. The most prevalent was resistance to tetracycline, cephalosporin, penam, fluoroquinolone, chloramphenicol, carbapenem, macrolide, and aminoglycoside (Figure 5A). Regarding the occurrence of the resistance mechanisms identified, there is a similarity between the soils (ANOVA; $F = 0.076$; $p$-value $= 0.972$), with the most common mechanisms being flow pumps, inactivation of antibiotics, and alteration of targets. Among these, efflux pumps were more abundant in 2- and 14-years-old monoculture soils, while in forest soil, the most abundant was antibiotic inactivation (Figure 5B).

As for biocide resistance, 94 genes associated with resistance to different chemical compounds were identified, and it was possible to observe significant differences between the genes found in each soil (Kruskal–Wallis; $\chi^2 = 9.405$; $p$-value $= 0.023$). Among them, heavy metals were the most abundant, followed by phenolic compounds, quaternary ammonium (QACs), and aromatic hydrocarbons, which are more prevalent in soils (Figure 6A). There was also evidence of resistance to

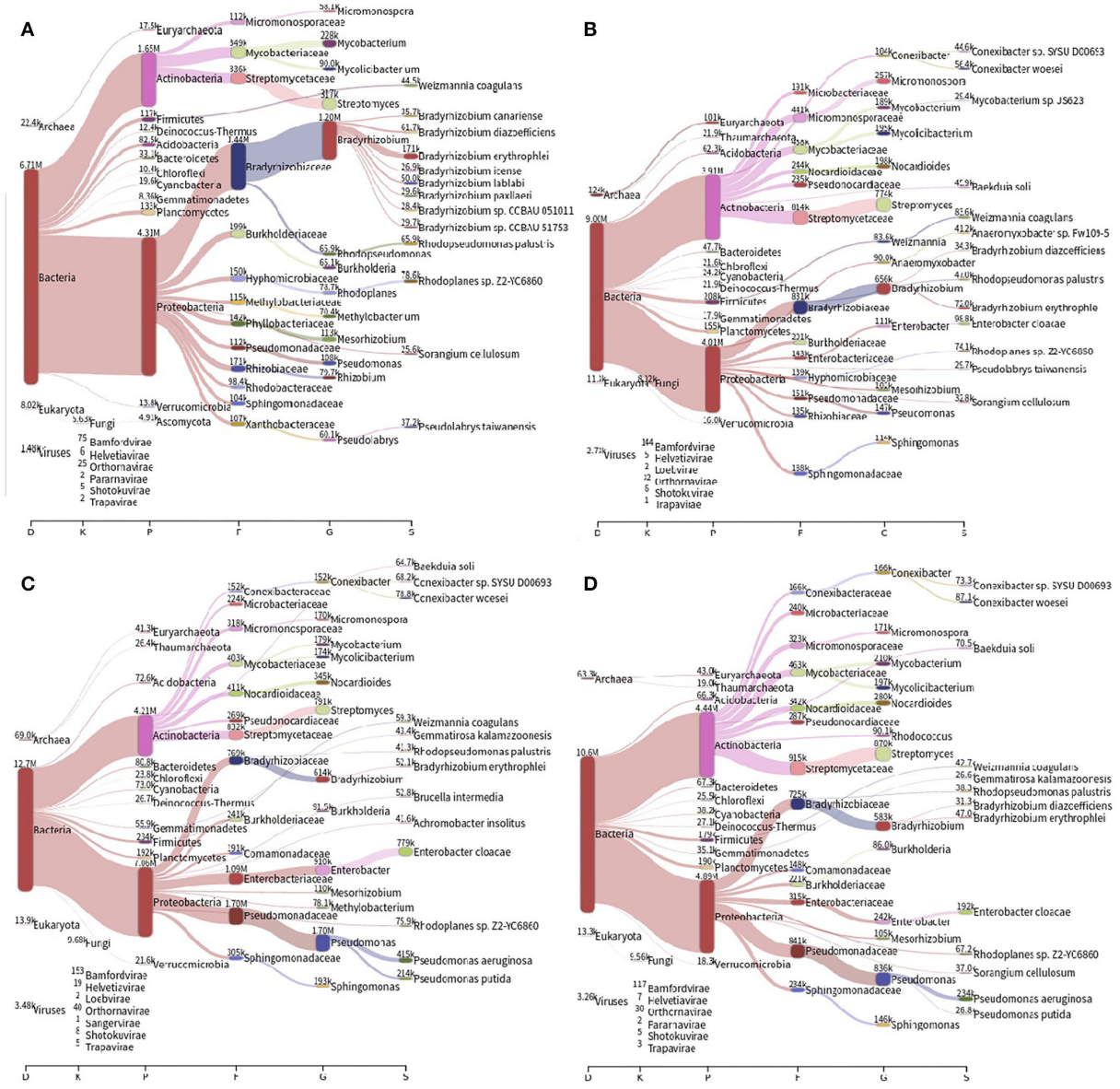


FIGURE 1
Distribution of the different bacterial taxonomic groups identified in the soils of **(A)** forest, **(B)** pasture, **(C)** 2-years soybean monoculture, and **(D)** 14-years soybean monoculture. The number of readings is classified as K, kingdom; P, phylum; F, family; G, genus; S, species.

heavy metals and a significant difference between the samples (Kruskal–Wallis; $\chi^2 = 11.11$; $p$-value $= 0.011$), with pasture and crop soils showing the greatest abundance of iron resistance genes, iron, copper, arsenic, and zinc (Figure 6B).

The distribution of resistance mechanisms was similar between soils (Kruskal–Wallis; $\chi^2 = 7.648$; $p$-value $= 0.053$), with the efflux pump and enzymatic inactivation being the most frequent.

Similarities between crop and pasture soils were observed during the distribution of the groups of antibiotic and biocide resistance genes according to their relative abundance. The diversity of these genes was observed, especially in the forest soil. The most prevalent genes in this soil were *dfrA42* (trimethoprim-resistant dihydrofolate reductase), *chrB* (23S ribosomal RNA methyltransferase), *MCR7.1* (Phosphoethanolamine transferase), *THIN-B* (Beta-lactamase), *OpmH* (resistance-nodulation-cell division (RND, efflux pump), *BEL3* (beta-lactamase) and *adeF* (RND). In crop soils, the most abundant genes were *MuxC* (RND), *rpsL* (mutations that confer resistance to streptomycin), *cpxA* (RND), *rpoB2* [rifamycin-resistant RNA polymerase beta subunit (rpoB)], *tet(52)* (Tetracycline inactivating enzyme), *carA* (ABC-F ATP-binding

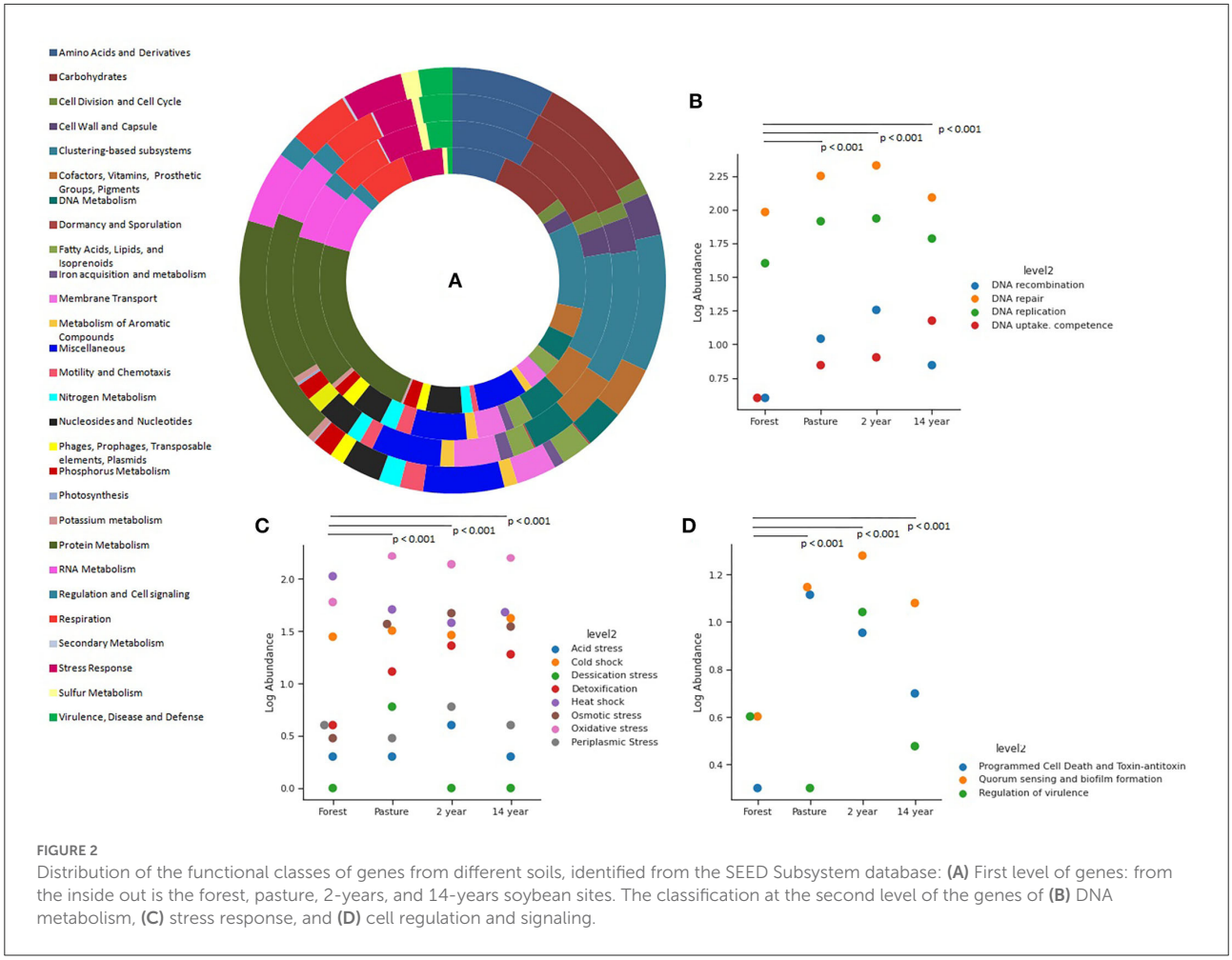


FIGURE 2
Distribution of the functional classes of genes from different soils, identified from the SEED Subsystem database: **(A)** First level of genes: from the inside out is the forest, pasture, 2-years, and 14-years soybean sites. The classification at the second level of the genes of **(B)** DNA metabolism, **(C)** stress response, and **(D)** cell regulation and signaling.

cassette ribosomal protection protein), *ParS* [RND; outer membrane porin (Opr)] and *rsmA* (RND) (Figure 7A).

Likewise, the analysis of the relative abundance of biocide resistance genes showed a similar grouping between cropland and pasture soils, with the composition of the genes with the highest prevalence being *acn* (Aconitato hydratase) in all soils, followed by genes *actP* (Copper transporter P-type ATPase), *chrC* (Fe-dependent superoxide dismutase), *mexF* (RND; MexF permeases protein), *mdtB* (MdtB multidrug-resistant protein), *aioA/aoxB* (Arsenite oxidase subunit), *actR* (Regulator protein ActR acid tolerance), *arsM* (Arsenite S-adenosylmethyltransferase), *mdtB/yegN* (MdtB multidrug-resistant protein), *FurA* (Transcriptional regulator), and *arsT* (Thioredoxin reductase) (Figure 7B).

## Association of genes and chemical characteristics

Principal component analysis (PCA) showed an accumulated variability of 99% in three components, represented by the first component (PC1) with 53% and the second component (PC2) with 34%, explaining the variability of the data. Further, the clustering of resistance genes with higher relative abundance was different in all soils (ANOSIM; $R = 0.984$; $p$-value $= 0.000$), especially in the 2-years monoculture soil. Thus, an association of the variables of heavy metal content was observed in the soils of 14-years-old culture and pasture, while the mobile elements identified are associated with magnesium cation, and the pH is relevant to the 2-years-old culture soil (Figure 8).

The resistance genes for antibiotics and biocides with the highest relative abundance according to the variables previously used were grouped into different dendrograms for each soil, and the most prevalent genes were in the formation of the outgroups. In forest soil, biocide resistance genes (*aioA/aoxB, mdtB/yegN, chrC,* and *actP*) are related to heavy metals, strong acids, and organic compounds, while pasture and crop soils presented the *acn* gene as an outgroup and iron resistance (Figure 9).

In the clades that presented the combinations of biocide and antibiotic resistance genes, there was a higher prevalence

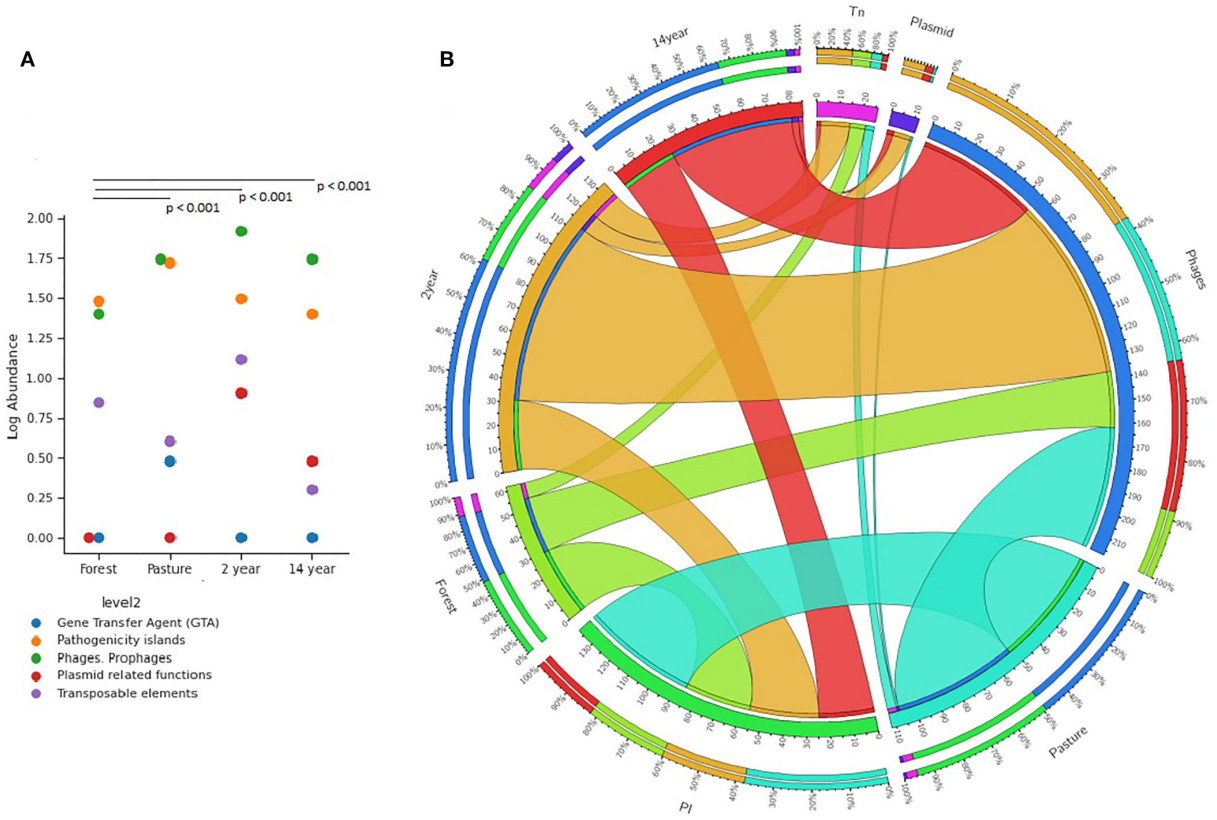


FIGURE 3
Distribution of the relative abundance of genes identified from the SUB Systems database of the MG-RAST platform for gene transfer agents (GTA), pathogenicity islands (PI), phages and prophages, plasmids, and transposons (Tn); **(A)** distribution in the different soils, the *p*-values obtained from Mann–Witney were corrected by Bonferroni analysis; **(B)** graphic representation of this distribution in circles.

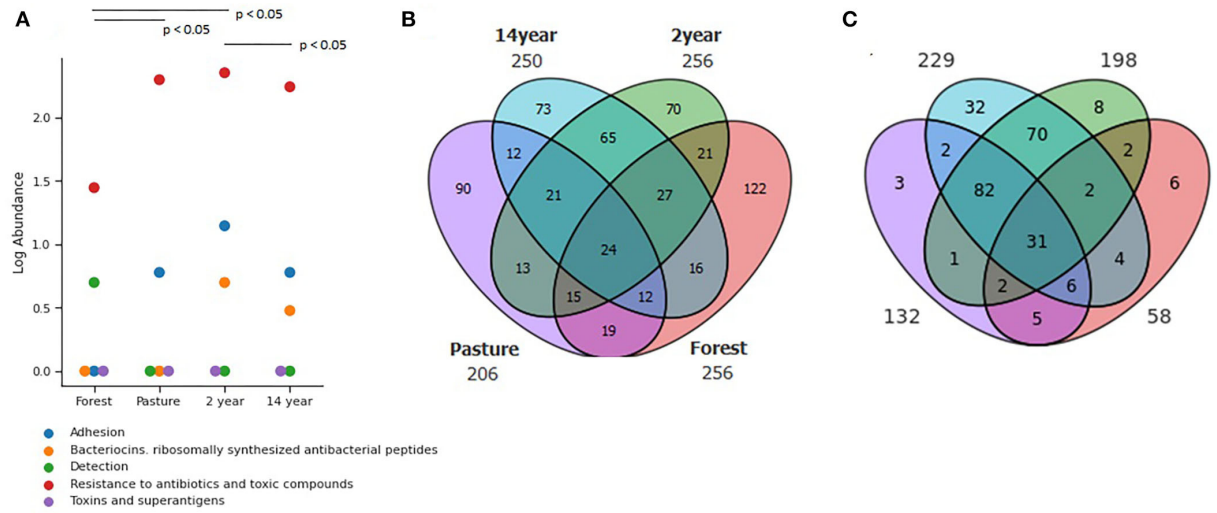


FIGURE 4
Distribution of **(A)** Functional genes in different soils identified from the SEED Subsystems database, demonstrating clustered genes of virulence, disease, and defense at its second level. Venn diagram of identified genes from **(B)** Antimicrobial resistance identified from CARD database and **(C)** Biocide resistance in different soils identified from BacMet database.

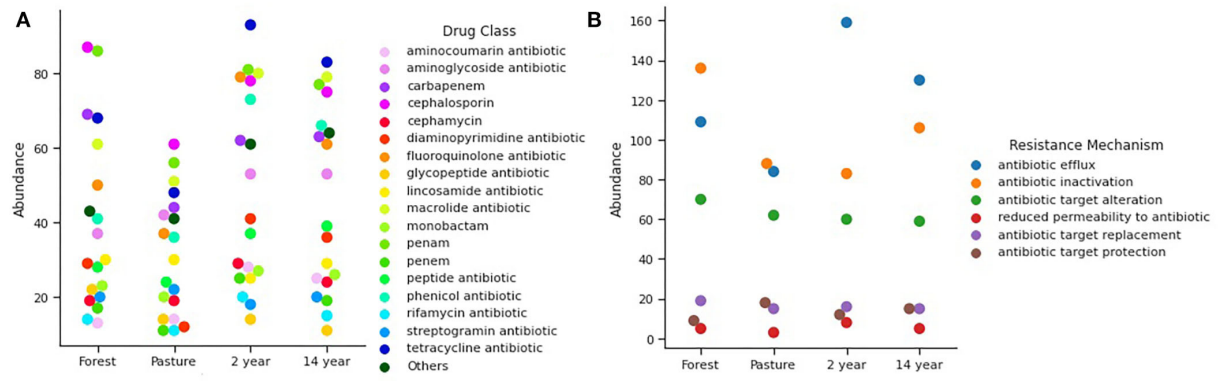


FIGURE 5
Relative abundance of **(A)** antibiotic classes according to the genes found for antimicrobial resistance. **(B)** Mechanisms of resistance found according to the genes identified.

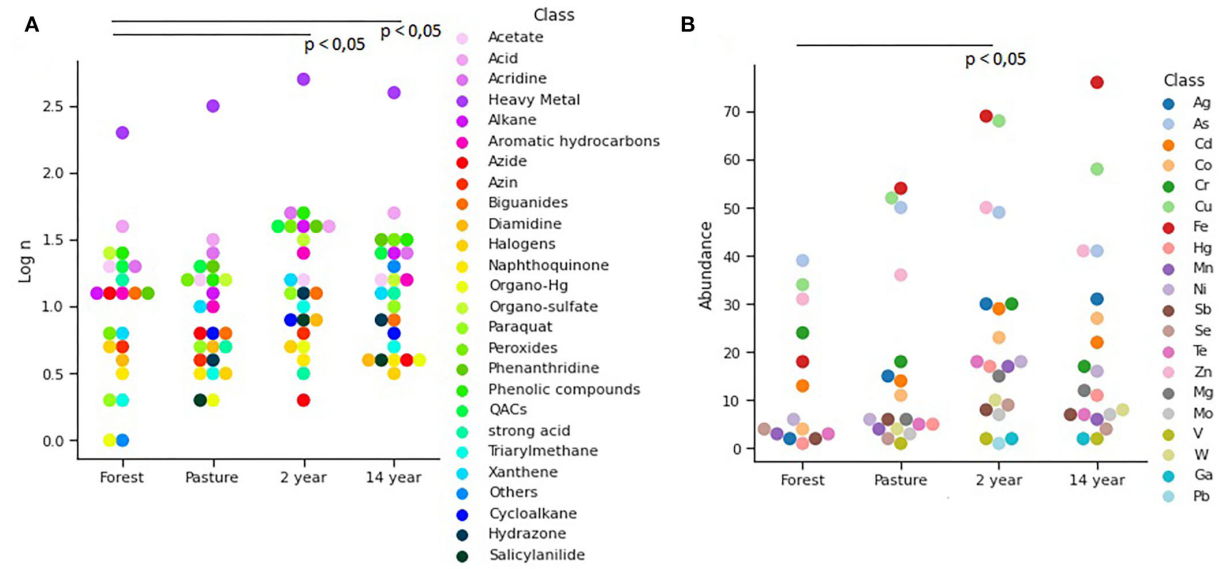


FIGURE 6
The distribution of **(A)** biocides and **(B)** heavy metals identified from the BacMet database showed significant differences ($p < 0.05$) between soils.

of resistance genes for iron and arsenic in the forest soil, in addition to the resistance to the fluoroquinolone, tetracycline, aminoglycoside, macrolide, and chloramphenicol classes of antibiotics (Figure 9A). In the pasture soil, the genes for triclosan and resistance to the tetracycline, aminoglycoside, fluoroquinolone, and monobactam classes of antibiotics were predominant (Figure 9B). In the 2-years-old monoculture soil, the prevalence occurred in the iron and arsenic resistance genes, as well as for the tetracycline, aminoglycoside, macrolide, and fluoroquinolone antibiotic classes (Figure 9C). In contrast, in the 14-years-old monoculture soil, the following were identified as resistance genes to arsenic, iron, chromium, triclosan, and the macrolide and monobactam classes of antibiotics (Figure 9D). Furthermore, multi-resistance genes to antibiotics, such as *ParS* and *carA*, are highlighted in different sites.

# Discussion

## Chemical characteristics and bacterial communities

The expansion of the agricultural frontier by using fire occurs by eliminating the vegetation cover of the soils, which favors changes in chemical components, as well as the increase in the levels of heavy metals, such as nickel, manganese, cobalt, cádmium, and arsenic (Stefanowicz et al., 2012; Popovych and Gapalo, 2021). However, the chemical characteristics of

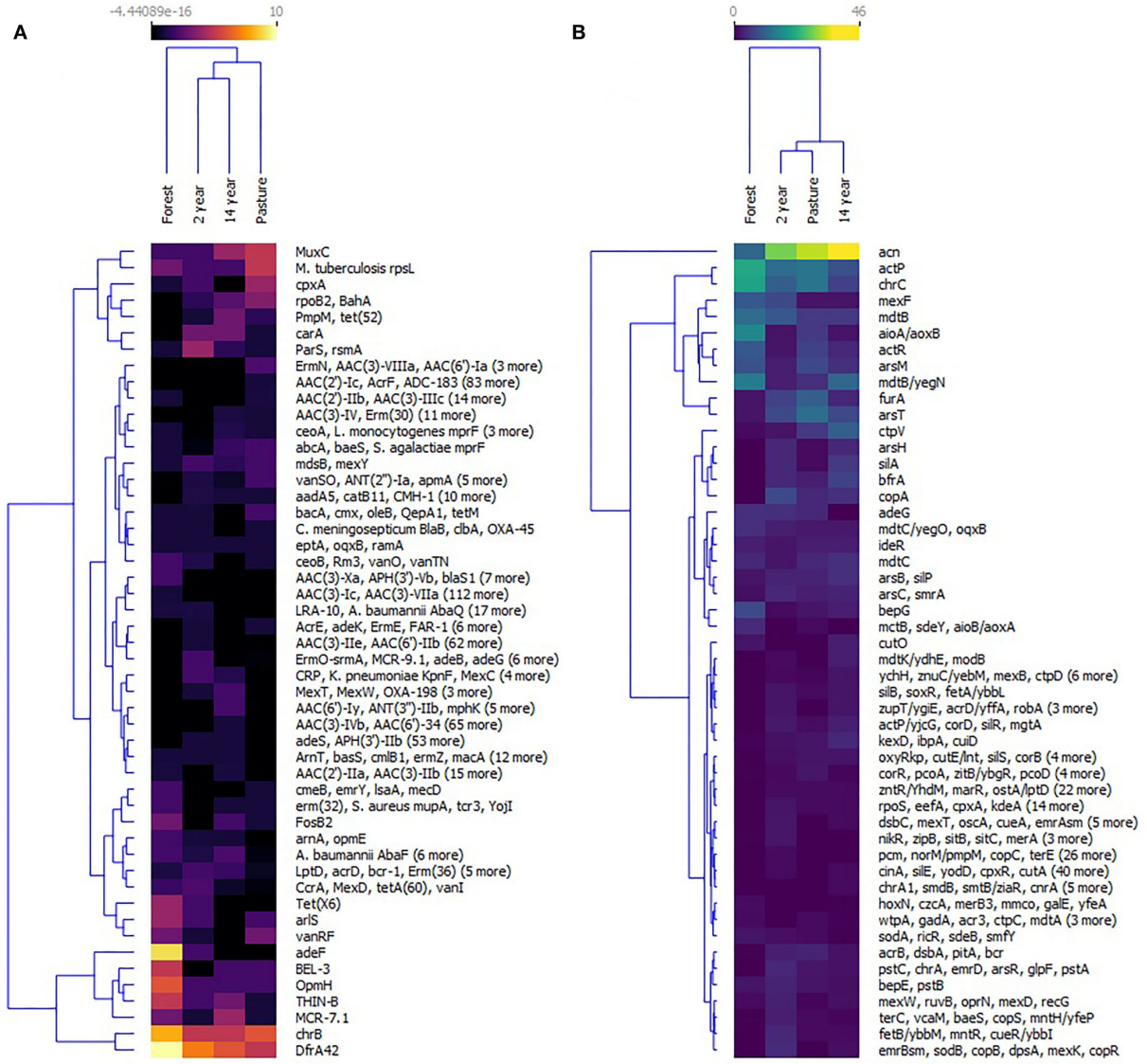


FIGURE 7
Heat map of **(A)** antibiotic resistance genes and **(B)** biocides resistance genes identified at collection sites—grouped using the k-means algorithm.

Amazonian soils vary according to the type of terrain and region, with specific contents of native chemical compounds (Costa et al., 2017).

In this work, it was possible to observe the variation of chemical characteristics in all analyzed soils, with higher pH, cations, and some heavy metals analyzed in monoculture soils. On the forest site, higher iron content was found, which reflects the presence of this element natively in this place. The accumulation of heavy metals can decrease the quality of soils, which can affect the health of consumers in the long term through bioaccumulation in vegetables (Salam et al., 2020).

Furthermore, although changes in the ecosystem can significantly influence the composition of soil bacterial communities (Meng et al., 2019; Salam et al., 2020), in this work, the diversity index values did not show significant changes due to chemical variations in soils, as reported by Thomas et al. (2020), but the change in the structure of microbial communities was observed, causing enrichment and recruitment of beneficial microorganisms for cultivation (Zhou et al., 2021).

In general, the bacterial communities in Amazonian soils are mainly composed of the phylum Proteobacteria and Acidobacteria, Actinobacteria, Bacteroidetes, and Firmicutes (Chodak et al., 2013; Shen et al., 2019; Thomas et al., 2020).

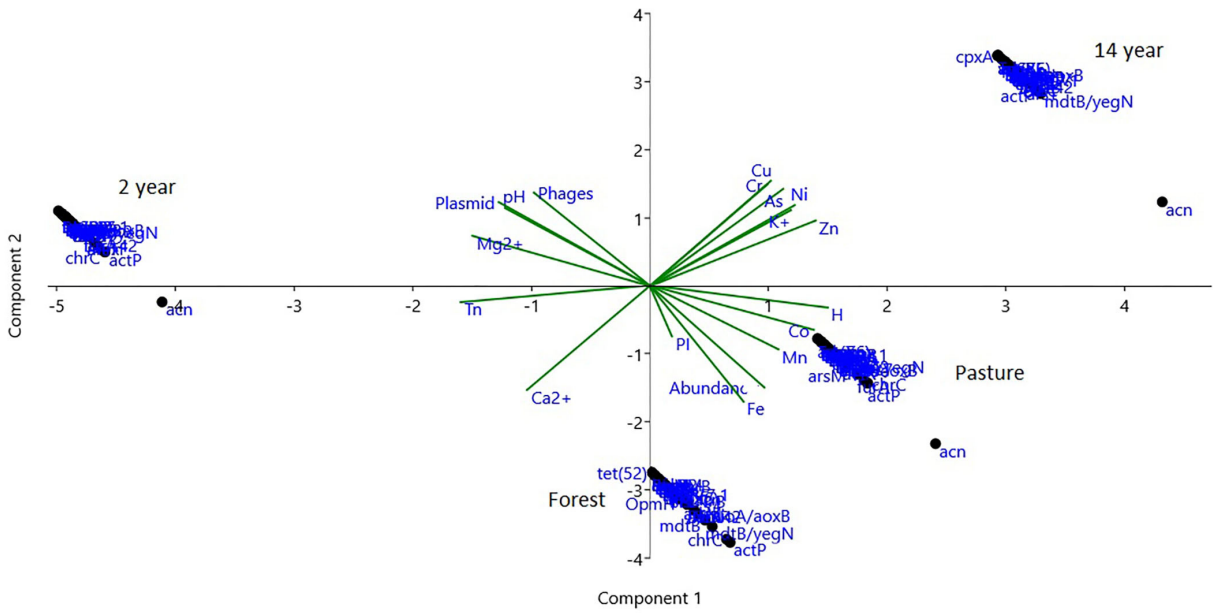


FIGURE 8
PCA analysis of genes with a greater abundance of antibiotic and biocide resistance genes, Shannon's alpha diversity index (H) also of plasmid mobile elements, phages, and transposons (Tn), pathogenicity islands (PI) with the chemical characteristics of pH, cations, and heavy metals.

However, the results of this work reveal a different composition between the sampled environments, with the forest floor showing the prevalence of different species of *Bradirhyzobium* sp.; it was in contrast to crop and pasture soils, in which *Enterobacter cloacae* and different species were relevant species of *Pseudomonas* sp., these data can be explained by the very conservation of soils for crops, which favor the development of these types of bacteria (Forsberg et al., 2012; Armalyte et al., 2019; Macedo et al., 2021; Yasir et al., 2022).

## Analysis of the composition of functional genes and soil resistome

The analysis of the diversity of functional genes identified in all soils reveals similarities in composition, but the relative abundance of these was different for the samples from each site, with the highest values found in genes associated with the metabolism of proteins, carbohydrates, amino acids, synthesis of RNA, stress response, and transport of elements, and it is possible to observe a more significant presence of these genes in soils where vegetation cover was removed, as reported in other works (Castañeda and Barbosa, 2017; Yasir et al., 2022).

The different communities of microorganisms that coexist in a given ecosystem are subject to the pressure of different stress factors inherent to their environment, such as climate and environmental change, and the presence of anthropic contaminants, among others. Soil microbial communities are generally sensitive to these disturbances from abiotic factors (drought, low/high temperature, salinity, and acidic conditions, light intensity, submersion, anaerobiosis, and nutrient deficiency) and biotic factors, but these microorganisms have several mechanisms that allow their adaptation in the environment, being able to maintain their main physiological functions (Pérez-Valera et al., 2020).

Thus, in this work, genes associated with the response to these environmental disturbances were identified, as well as genes involved with DNA repair mechanisms, which are more significant than replication genes, especially in soils of culture and pasture. In the case of genes associated with the response to defense mechanisms against abiotic stress, the composition of the forest soil was different from that of other soils, which possibly reflects the consequences of the removal of vegetation cover, in addition to the possibility that the type of forest management soil alters genetic diversity (Meena et al., 2017).

Soils without forests showed a prevalence of genes involved in quorum sensing and biofilm formation, which may be advantageous for the local vegetation due to the nutrient absorption capacity (Bhagat et al., 2021) or probably due to the application of agro-compound chemicals. Microorganisms show their ability to biodegrade in response to stress (Chen et al., 2021). Different bacterial communities have different mechanisms that help them recover quickly, returning to their microbial functions and activities as soon as the stress factor ends (Schimel, 2018; Bremer and Krämer, 2019; Schnecker et al., 2021).

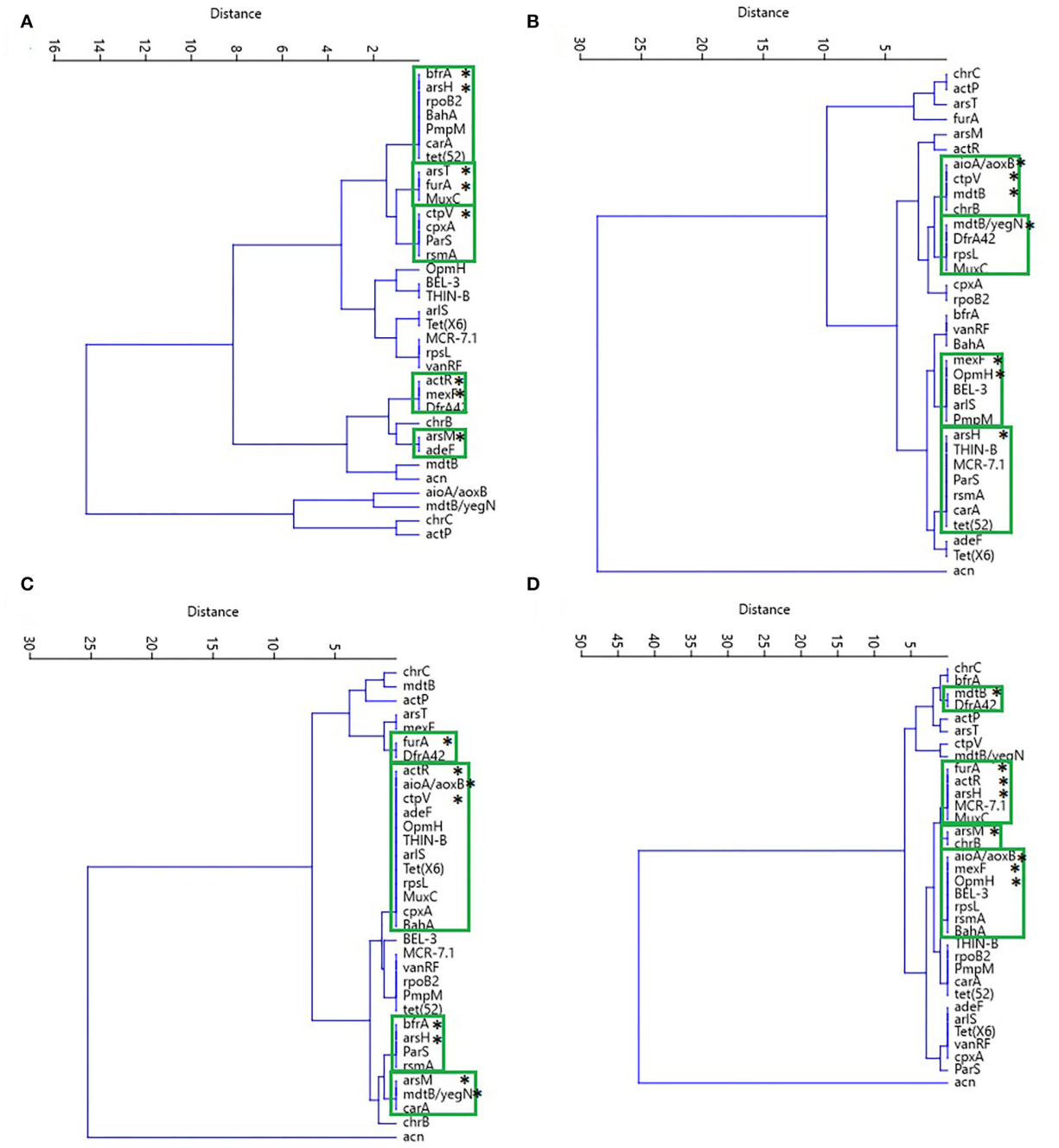


FIGURE 9
Cluster analysis performed by the UPGMA algorithm and the Euclidean similarity index of the most abundant resistance genes to antibiotics and biocides and the characteristics analyzed in soils from **(A)** forest, **(B)** pasture, **(C)** 2-years crop, and **(D)** culture of 14 years. In the green boxes are grouped the genes of resistance to antibiotics and biocides (*).

Likewise, the conditions of these environments can promote the selection of genetic components and their dissemination through mobile genetic elements (MGE), which can carry pathogenicity genes and antibiotic and biocide resistance genes (Martins and Rabinowitz, 2020). Thus, in crop soils, the presence of pathogenicity islands, phages, prophages, transposons, and plasmids was predominant, especially in the soil after 2 years of cultivation. As for antibiotic and biocide resistance genes, there was a more significant amount in pasture and crop soils, although the forest soil showed a greater diversity of antibiotic resistance genes. In crop soils, the resistance genes were more diverse to biocides.

Natural forest soils are a significant source of antibiotic ARG, and their large-scale distribution is regulated by the diversity of microorganisms and herbaceous plants (Hu et al., 2018; Qian et al., 2021). In this way, native ARGs in different soils can be shared with plants, becoming a potential route for the transfer of these genes to the human microbiome and the potential for transferring pathogens through the food chain (Zhang et al., 2019).

However, it remains unclear whether traditional agricultural activities affect the soil resistome (Qian et al., 2021), although data on sewage sludge contamination constitutes a vast repository of antibiotic, biocide, and MGE resistance genes that can affect the soil resistome (Markowicz et al., 2021).

The native antibiotic resistance profile of soil is varied but always presents high gene diversity (Qian et al., 2021; Zheng et al., 2021), as shown in forest soil. As for the profile of the resistome of the crop soils, a strong association was not found; it is possibly affected by the addition of compounds, such as fertilizers, and manure, among others (Martins and Rabinowitz, 2020; Macedo et al., 2021).

Analysis of soil resistance to antimicrobials and biocides shows that the most frequently used resistance mechanisms are efflux pumps and antibiotic inactivation, which reflects the evolution of microorganisms that have adapted to survive in ecosystems regardless of certain conditions. Changes likely serve as buffers for ecological niches (Walsh and Duffy, 2013; Armalyte et al., 2019). In this work, levels of different heavy metals were identified in the soil after 14 years of culture, while in the soil, after 2 years of culture, a more significant variation in pH, magnesium cation content, and the different EGM components were highlighted. Bivalent cations such as magnesium influence soil quality and plant development, in addition to being a metallic cofactor for different enzymatic processes for microorganisms (Sissi and Palumbo, 2009; Gerendás and Führs, 2013; Shin et al., 2014).

However, the results of this work suggest that, even in areas with low levels of heavy metals (Arsenic, copper, zinc, cobalt, and chromium), there is an induction to the selection of resistance to these elements, which could also be selecting resistance genes. Antibiotic resistance genes are ubiquitous. In addition, human activities also influence the selection of the composition of microbial communities, resistance genes, mobile elements, and other markers (Thomas et al., 2020).

Additionally, the presence of mobile genetic elements increases the spread of resistance genes through HGT, which can also be affected by environmental conditions and other stressors (Shen et al., 2019). In this study, it was possible to observe the presence of resistance genes to antimicrobials and widely used biocides, which makes the presence of MGEs in soils an indication of the potential of these molecules to promote the conjugative transfer of resistance at concentrations below the minimum inhibitory concentration, as previously stated. Identified in another work on tetracycline resistance, which is a potent inducer of conjugation (Jutkina et al., 2018). Likewise, nickel exposure has been reported to increase the horizontal transfer potential of ARG (Hu et al., 2017); in our work, the high levels of iron found in the forest could be a factor in the selective pressure on native microbial communities; this pressure would increase with the change of ecosystems for the development of pasture and culture and would be reflected in the diversity and abundance of resistance genes, and the presence of mobile elements.

## Co-selection of resistance genes

The metagenomic analysis allows a correlation between antibiotic and biocide resistance genes, providing additional information on heavy metal-induced ARG co-selection (Wang et al., 2020). Cross-resistance and co-resistance are the main drivers for ARG co-selection. However, other mechanisms are also involved in this phenomenon, such as the presence of a single regulatory gene for several resistance genes (Maurya et al., 2020).

In the results of this work, a correlation between resistance to antibiotics and biocides was identified between the genes of resistance to the classes of antibiotics: tetracycline, aminoglycoside, macrolide, and fluoroquinolone and the metals iron, arsenic, and copper.

Amazon deforestation has increased the amount of ARG in the soil and, like other anthropogenic disturbances, can exert selective pressure on microbial communities, expanding soil resistome and increasing microbial diversity in response to deforestation, along with changes in soil chemical properties, such as pH and the presence of aluminum (Lemos et al., 2021). This work observed no significant change in ARG diversity or abundance of these genes after long-term continuous cultivation. An increase in the diversity and abundance of biocide resistance genes was evidenced.

The analysis of resistance genes among the soil samples of this study suggests the development of resistance to antibiotics and biocides under different selection pressures in different environments. However, our data are limited by the number of sampling at the sites and the lack of longitudinal analysis. Despite these limitations, our results can be applied to other related studies, such as a comparative analysis of the soil microbiome and other environments to explore the diversity of ARG between different sites. For studies about the transfer of these genes from the environment to the human commensal microbiota, more sampling sites should be considered, in addition to the collection at different times to identify the soil microbiome and its resistome, thus making it possible to obtain more information about the development and ARG broadcasts. Even so, an analysis beyond genes, such as identifying ARG transcripts by metatranscriptomic sequencing, can provide a

more comprehensive understanding of their dynamics (Zheng et al., 2021).

## Conclusion

The analysis carried out on the different soils highlights the differences in chemical composition, bacterial communities, and genetic composition between different cultivation soils. These ecosystems presented a differentiated abundance of genetic composition and mobile genetic elements in other sites. Above all, the sites eliminated the vegetal cover.

On the other hand, it was demonstrated that antibiotic resistance genes were diverse in the forest site and more abundant in the crop soils. In contrast to the genes of resistance to biocides, especially for heavy metals, they were diverse and more abundant in the cultivation sites. As for antibiotic resistance, the most frequent were the antimicrobials aminoglycosides, macrolides, tetracyclines, and fluoroquinolones. In contrast, the most prevalent resistance to biocides is related to iron in different sites with high levels. Eliminating vegetative cover may alter the selection of other animals and genes that have the potential to affect human health.

## Data availability statement

The datasets presented in this study can be found in online repositories. The names of the repository/repositories and accession number(s) can be found at: NCBI-PRJNA841936.

## Author contributions

OC, MP, ACB, RR, and ARC contributed to conception and design of the study. ES, AO, ACR, and OC performed the statistical analysis manuscript. All authors contributed to manuscript revision, read, and approved the submitted version.

## Funding

Funded National Research Council (CNPq), Alliance Program for Education and Training—PAEC-OEA-GCUB 2017, within the scope of the Cooperation Agreement between the Organization of American States (OAS) and the Coimbra Group of Brazilian Universities (CGUB) and L'Oréal Brasil-UNESCO-ABC For Women in Science.

## Acknowledgments

We thank the PROPESP/UFPA (Pró-Reitoria de Pesquisa e Pós-Graduação / Universidade Federal do Pará for the financial support on this work.

## Conflict of interest

The authors declare that the research was conducted in the absence of any commercial or financial relationships that could be construed as a potential conflict of interest.

## Publisher's note

All claims expressed in this article are solely those of the authors and do not necessarily represent those of their affiliated organizations, or those of the publisher, the editors and the reviewers. Any product that may be evaluated in this article, or claim that may be made by its manufacturer, is not guaranteed or endorsed by the publisher.

## References

Alcock, B. P., Raphenya, A. R., Lau, T. T. Y., Tsang, K. K., Bouchard, M., Edalatmand, A., et al. (2020). CARD 2020: antibiotic resistome surveillance with the comprehensive antibiotic resistance database. *Nucl. Acids Res.* 48, D517–D525. doi: 10.1093/nar/gkz935

Altier, N. A., and Abreo, E. (2020). One health considerations in the international year of plant health. *Agrociencia Uruguay* 24, 1–14. doi: 10.31285/AGRO.24.422

Alvares, C. A., Stape, J. L., and Sentelhas, P. C. (2013). Köppen's climate classification map for Brazil. *Meteorol. Z.* 19, 14968–14969. doi: 10.1127/0941-2948/2013/0507

Andrew, S. (2019). *FastQC. Babraham Bioinformatics*. Available online at: http://www.bioinformatics.babraham.ac.uk/projects/fastqc/ (accessed May 4, 2021).

Armalyte, J., Skerniškyte, J., Bakiene, E., Krasauskas, R., Šiugždiniene, R., Kareiviene, V., et al. (2019). Microbial diversity and antimicrobial resistance profile in microbiota from soils of conventional and organic farming systems. *Front. Microbiol.* 10, 892. doi: 10.3389/fmicb.2019.00892

Bach, E. M., Williams, R. J., Hargreaves, S. K., Yang, F., and Hofmockel, K. S. (2018). Greatest soil microbial diversity found in micro-habitats. *Soil Biol. Biochem.* 118, 217–226. doi: 10.1016/j.soilbio.2017.12.018

Basso, C., Siqueira, A. C. F., and Richards, N. S. P. S. (2021). Impactos na saúde humana e no meio ambiente relacionados ao uso de agrotóxicos: Uma revisão integrativa. *RSD* 10, e43110817529. doi: 10.33448/rsd-v10i8.17529

Belo, M. S. S. P., Pignati, W., Dores, E. F. G. C., Moreira, J. C., and Peres, F. (2012). Uso de agrotóxicos na produção de soja do estado do Mato Grosso: um estudo preliminar de riscos ocupacionais e ambientais. *Rev. Bras. Saúde Ocup.* 37, 78–88. doi: 10.1590/S0303-76572012000100011

Berg, G., and Martinez, J. L. (2015). Friends or foes: can we make a distinction between beneficial and harmful strains of the *Stenotrophomonas maltophilia* complex? *Front. Microbiol.* 6, 241. doi: 10.3389/fmicb.2015.00241

Bhagat, N., Raghav, M., Dubey, S., and Bedi, N. (2021). Bacterial exopolysaccharides: insight into their role in plant abiotic stress tolerance. *J. Microbiol. Biotechnol.* 31, 1045–1059. doi: 10.4014/jmb.2105.05009

Bolger, A. M., Lohse, M., and Usadel, B. (2014). Trimmomatic: a flexible trimmer for Illumina sequence data. *Bioinformatics* 30, 2114–2120. doi: 10.1093/bioinformatics/btu170

Bottery, M. J., Pitchford, J. W., and Friman, V.-P. (2021). Ecology and evolution of antimicrobial resistance in bacterial communities. *ISME J.* 15, 939–948. doi: 10.1038/s41396-020-00832-7

Breitwieser, F. P., and Salzberg, S. L. (2020). Pavian: interactive analysis of metagenomics data for microbiome studies and pathogen identification. *Bioinformatics* 36, 1303–1304. doi: 10.1093/bioinformatics/btz715

Bremer, E., and Krämer, R. (2019). Responses of microorganisms to osmotic stress. *Annu. Rev. Microbiol.* 73, 313–334. doi: 10.1146/annurev-micro-020518-115504

Brevik, E. C., Slaughter, L., Singh, B. R., Steffan, J. J., Collier, D., Barnhart, P., et al. (2020). Soil and human health: current status and future needs. *Air Soil Water Res.* 13, 117862212093444. doi: 10.1177/1178622120934441

Castañeda, L. E., and Barbosa, O. (2017). Metagenomic analysis exploring taxonomic and functional diversity of soil microbial communities in Chilean vineyards and surrounding native forests. *PeerJ* 5, e3098. doi: 10.7717/peerj.3098

Chen, Q. L., Cui, H. L., Su, J. Q., Penuelas, J., and Zhu, Y. G. (2019). Antibiotic resistomes in plant microbiomes. *Trends Plant Sci.* 24, 530–541. doi: 10.1016/j.tplants.2019.02.010

Chen, X., Wicaksono, W. A., Berg, G., and Cernava, T. (2021). Bacterial communities in the plant phyllosphere harbour distinct responders to a broad-spectrum pesticide. *Sci. Total Environ.* 751, 141799. doi: 10.1016/j.scitotenv.2020.141799

Chodak, M., Gołebiewski, M., Morawska-Płoskonka, J., Kuduk, K., and Niklińska, M. (2013). Diversity of microorganisms from forest soils differently polluted with heavy metals. *Appl. Soil Ecol.* 64, 7–14. doi: 10.1016/j.apsoil.2012.11.004

Cook, J. A., Arai, S., Armién, B., Bates, J., Bonilla, C. A. C., Cortez, M. B. S., et al. (2020). Integrating biodiversity infrastructure into pathogen discovery and mitigation of emerging infectious diseases. *BioScience* 70, 531–534. doi: 10.1093/biosci/biaa064

Costa, R. D. S., Paula Neto, P., Campos, M. C. C., Nascimento, W. B., Nascimento, C. W. A., Silva, L. S., et al. (2017). Natural contents of heavy metals in soils of the southern Amazonas state, Brazil. *SCA* 38, 3499. doi: 10.5433/1679-0359.2017v38n6p3499

Demšar, J., Curk, T., Erjavec, A., Demsar, J., Curk, T., Erjave, A., et al. (2013). Orange: data mining toolbox in Python. *J. Mach. Learn. Res.* 8, 2349–2353. Available online at: https://www.jmlr.org/papers/volume14/demsar13a/demsar13a.pdf

Destoumieux-Garzón, D., Mavingui, P., Boetsch, G., Boissier, J., Darriet, F., Duboz, P., et al. (2018). The one health concept: 10 years old and a long road ahead. *Front. Vet. Sci.* 5, 14. doi: 10.3389/fvets.2018.00014

Dhariwal, A., Chong, J., Habib, S., King, I. L., Agellon, L. B., and Xia, J. (2017). MicrobiomeAnalyst: a web-based tool for comprehensive statistical, visual and meta-analysis of microbiome data. *Nucl. Acids Res.* 45, W180–W188. doi: 10.1093/nar/gkx295

Durso, L. M., and Cook, K. L. (2019). One health and antibiotic resistance in agroecosystems. *EcoHealth* 16, 414–419. doi: 10.1007/s10393-018-1324-7

Forsberg, K. J., Reyes, A., Wang, B., Selleck, E. M., Sommer, M. O. A., and Dantas, G. (2012). The shared antibiotic resistome of soil bacteria and human pathogens. *Science* 337, 1107–1111. doi: 10.1126/science.1220761

Gerendás, J., and Führs, H. (2013). The significance of magnesium for crop quality. *Plant Soil* 368, 101–128. doi: 10.1007/s11104-012-1555-2

Hammer, D. A. T., Ryan, P. D., Hammer, Ø., and Harper, D. A. T. (2001). Past: paleontological statistics software package for education and data analysis. *Palaeontol. Elect.* 4, 178. Available online at: http://palaeo-electronica.org/2001_1/past/issue1_01.htm

Heydari, A., Kim, N. D., Horswell, J., Gielen, G., Siggins, A., Taylor, M., et al. (2022). Co-selection of heavy metal and antibiotic resistance in soil bacteria from agricultural soils in New Zealand. *Sustainability* 14, 1790. doi: 10.3390/su14031790

Högfors-Rönnholm, E., Christel, S., Engblom, S., and Dopson, M. (2018). Indirect DNA extraction method suitable for acidic soil with high clay content. *MethodsX* 5, 136–140. doi: 10.1016/j.mex.2018.02.005

Hu, H., Wang, J., Singh, B. K., Liu, Y., Chen, Y., Zhang, Y., et al. (2018). Diversity of herbaceous plants and bacterial communities regulates soil resistome across forest biomes. *Environ. Microbiol.* 20, 3186–3200. doi: 10.1111/1462-2920.14248

Hu, H.-W., Wang, J.-T., Li, J., Shi, X.-Z., Ma, Y.-B., Chen, D., et al. (2017). Long-term nickel contamination increases the occurrence of antibiotic resistance genes in agricultural soils. *Environ. Sci. Technol.* 51, 790–800. doi: 10.1021/acs.est.6b03383

Jutkina, J., Marathe, N. P., Flach, C.-F., and Larsson, D. G. J. (2018). Antibiotics and common antibacterial biocides stimulate horizontal transfer of resistance at low concentrations. *Sci. Total Environ.* 616–617, 172–178. doi: 10.1016/j.scitotenv.2017.10.312

Lemos, L. N., Pedrinho, A., Vasconcelos, A. T. R., Tsai, S. M., and Mendes, L. W. (2021). Amazon deforestation enriches antibiotic resistance genes. *Soil Biol. Biochem.* 153, 108110. doi: 10.1016/j.soilbio.2020.108110

Li, D., Liu, C.-M., Luo, R., Sadakane, K., and Lam, T.-W. (2015). MEGAHIT: an ultra-fast single-node solution for large and complex metagenomics assembly via succinct de Bruijn graph. *Bioinformatics* 31, 1674–1676. doi: 10.1093/bioinformatics/btv033

Li, J., Wu, X., Gebremikael, M. T., Wu, H., Cai, D., Wang, B., et al. (2018). Response of soil organic carbon fractions, microbial community composition and carbon mineralization to high-input fertilizer practices under an intensive agricultural system. *PLoS ONE* 13, e0195144. doi: 10.1371/journal.pone.0195144

Macedo, G., van Veelen, H. P. J., Hernandez-Leal, L., van der Maas, P., Heederik, D., Mevius, D., et al. (2021). Targeted metagenomics reveals inferior resilience of farm soil resistome compared to soil microbiome after manure application. *Sci. Total Environ.* 770, 145399. doi: 10.1016/j.scitotenv.2021.145399

Markowicz, A., Bondarczuk, K., Wiekiera, A., and Sułowicz, S. (2021). Is sewage sludge a valuable fertilizer? A soil microbiome and resistome study under field conditions. *J. Soils Sedim.* 21, 2882–2895. doi: 10.1007/s11368-021-02984-1

Martins, A. F., and Rabinowitz, P. (2020). The impact of antimicrobial resistance in the environment on public health. *Fut. Microbiol.* 15, 699–702. doi: 10.2217/fmb-2019-0331

Maurya, A. P., Rajkumari, J., Bhattacharjee, A., and Pandey, P. (2020). Development, spread and persistence of antibiotic resistance genes (ARGs) in the soil microbiomes through co-selection. *Rev. Environ. Health* 35, 371–378. doi: 10.1515/reveh-2020-0035

Meena, K. K., Sorty, A. M., Bitla, U. M., Choudhary, K., Gupta, P., Pareek, A., et al. (2017). Abiotic stress responses and microbe-mediated mitigation in plants: the omics strategies. *Front. Plant Sci.* 8, 172. doi: 10.3389/fpls.2017.00172

Meng, M., Lin, J., Guo, X., Liu, X., Wu, J., Zhao, Y., et al. (2019). Impacts of forest conversion on soil bacterial community composition and diversity in subtropical forests. *CATENA* 175, 167–173. doi: 10.1016/j.catena.2018.12.017

Meyer, F., Paarmann, D., D'Souza, M., Olson, R., Glass, E., Kubal, M., et al. (2008). The metagenomics RAST server: a public resource for the automatic phylogenetic and functional analysis of metagenomes. *BMC Bioinform.* 9, 386. doi: 10.1186/1471-2105-9-386

Mikheenko, A., Saveliev, V., and Gurevich, A. (2016). MetaQUAST: evaluation of metagenome assemblies. *Bioinformatics* 32, 1088–1090. doi: 10.1093/bioinformatics/btv697

Pal, C., Bengtsson-Palme, J., Rensing, C., Kristiansson, E., and Larsson, D. G. J. (2014). BacMet: antibacterial biocide and metal resistance genes database. *Nucl. Acids Res.* 42, D737–D743. doi: 10.1093/nar/gkt1252

Pérez-Valera, E., Verdú, M., Navarro-Cano, J. A., and Goberna, M. (2020). Soil microbiome drives the recovery of ecosystem functions after fire. *Soil Biol. Biochem.* 149, 107948. doi: 10.1016/j.soilbio.2020.107948

Pignati, W. A., Lima, F. A. N. S., Lara, S. S., Correa, M. L. M., Barbosa, J. R., Leão, L. H. C., et al. (2017). Distribuição espacial do uso de agrotóxicos no Brasil: uma ferramenta para a Vigilância em Saúde. *Ciênc. Saúde Coletiva* 22, 3281–3293. doi: 10.1590/1413-812320172210.17742017

Popovych, V., and Gapalo, A. (2021). Monitoring of ground forest fire impact on heavy metals content in edafic horizons. *J. Ecol. Eng.* 22, 96–103. doi: 10.12911/22998993/135872

Qian, X., Gunturu, S., Guo, J., Chai, B., Cole, J. R., Gu, J., et al. (2021). Metagenomic analysis reveals the shared and distinct features of the soil resistome across tundra, temperate prairie, and tropical ecosystems. *Microbiome* 9, 108. doi: 10.1186/s40168-021-01047-4

Qu, K., Guo, F., Liu, X., Lin, Y., and Zou, Q. (2019). Application of machine learning in microbiology. *Front. Microbiol.* 10, 827. doi: 10.3389/fmicb.2019.00827

Raij, B. V., Andrade, J., Cantarella, H., and Quaggio, J. A. (2001). *Análise Química para Avaliação da Fertilidade de Solos Tropicais*. Campinas: Instituto Agronômico.

Rodrigues, T. E., Silva, R. D. C., Da Silva, J. M. L., De Oliveira, R. C., Gama, J. R. N. F., and Valente, M. A. (2003). *Carcterização e Calssificação dos solos do Município de Paragominas, Estado do Pará, 1st Edn*. Belem, PA: Embrapa Amazônia Oriental.

Romaniuk, K., Ciok, A., Decewicz, P., Uhrynowski, W., Budzik, K., Nieckarz, M., et al. (2018). Insight into heavy metal resistome of soil psychrotolerant bacteria

originating from King George Island (Antarctica). *Polar Biol.* 41, 1319–1333. doi: 10.1007/s00300-018-2287-4

Salam, L. B., Obayori, O. S., Ilori, M. O., and Amund, O. O. (2020). Effects of cadmium perturbation on the microbial community structure and heavy metal resistome of a tropical agricultural soil. *Bioresour. Bioprocess.* 7, 25. doi: 10.1186/s40643-020-00314-w

Schimel, J. P. (2018). Life in dry soils: effects of drought on soil microbial communities and processes. *Annu. Rev. Ecol. Evol. Syst.* 49, 409–432. doi: 10.1146/annurev-ecolsys-110617-062614

Schnecker, J., Meeden, D. B., Calderon, F., Cavigelli, M., Lehman, R. M., Tiemann, L. K., et al. (2021). Microbial activity responses to water stress in agricultural soils from simple and complex crop rotations. *Soil* 7, 547–561. doi: 10.5194/soil-7-547-2021

Seemann, T. (2014). Prokka: rapid prokaryotic genome annotation. *Bioinformatics* 30, 2068–2069. doi: 10.1093/bioinformatics/btu153

Shen, Y., Stedtfeld, R. D., Guo, X., Bhalsod, G. D., Jeon, S., Tiedje, J. M., et al. (2019). Pharmaceutical exposure changed antibiotic resistance genes and bacterial communities in soil-surface- and overhead-irrigated greenhouse lettuce. *Environ. Int.* 131, 105031. doi: 10.1016/j.envint.2019.105031

Shin, J.-H., Wakeman, C. A., Goodson, J. R., Rodionov, D. A., Freedman, B. G., Senger, R. S., et al. (2014). Transport of magnesium by a bacterial nramp-related gene. *PLoS Genet.* 10, e1004429. doi: 10.1371/journal.pgen.1004429

Sissi, C., and Palumbo, M. (2009). Effects of magnesium and related divalent metal ions in topoisomerase structure and function. *Nucl. Acids Res.* 37, 702–711. doi: 10.1093/nar/gkp024

Stefanowicz, A. M., Kapusta, P., Szarek-Łukaszewska, G., Grodzińska, K., Niklińska, M., and Vogt, R. D. (2012). Soil fertility and plant diversity enhance microbial performance in metal-polluted soils. *Sci. Total Environ.* 439, 211–219. doi: 10.1016/j.scitotenv.2012.09.030

Sun, Y., Qiu, T., Gao, M., Shi, M., Zhang, H., and Wang, X. (2019). Inorganic and organic fertilizers application enhanced antibiotic resistome in greenhouse soils growing vegetables. *Ecotoxicol. Environ. Saf.* 179, 24–30. doi: 10.1016/j.ecoenv.2019.04.039

Thomas, J. C., Oladeinde, A., Kieran, T. J., Finger, J. W., Bayona-Vásquez, N. J., Cartee, J. C., et al. (2020). Co-occurrence of antibiotic, biocide, and heavy metal resistance genes in bacteria from metal and radionuclide contaminated soils at the Savannah River Site. *Microb. Biotechnol.* 13, 1179–1200. doi: 10.1111/1751-7915.13578

Toloi, M. N. V., Bonilla, S. H., Toloi, R. C., Silva, H. R. O., and Nääs, I. A. (2021). Development indicators and soybean production in Brazil. *Agriculture* 11, 1164. doi: 10.3390/agriculture11111164

Udikovic-Kolic, N., Wichmann, F., Broderick, N. A., and Handelsman, J. (2014). Bloom of resident antibiotic-resistant bacteria in soil following manure fertilization. *Proc. Natl. Acad. Sci. U. S. A.* 111, 15202–15207. doi: 10.1073/pnas.1409836111

Voora, V., Larrea, C., and Bermúdez, S. (2020). *Global Market Report: Soybeans. Sustainable Commodities Marketplace*, 20. Available online at: www.iisd.org (accessed March 18, 2022).

Walsh, F., and Duffy, B. (2013). The culturable soil antibiotic resistome: a community of multi-drug resistant bacteria. *PLoS ONE* 8, e65567. doi: 10.1371/journal.pone.0065567

Wang, X., Lan, B., Fei, H., Wang, S., and Zhu, G. (2020). Heavy metal-induced co-selection for antibiotic resistance in terrestrial subsurface soils. *Res. Squa.* 1, 1–21. doi: 10.21203/rs.3.rs-41493/v1

Wood, D. E., Lu, J., and Langmead, B. (2019). Improved metagenomic analysis with Kraken 2. *Genome Biol.* 20, 257. doi: 10.1186/s13059-019-1891-0

Yang, G., Wagg, C., Veresoglou, S. D., Hempel, S., and Rillig, M. C. (2018). How soil biota drive ecosystem stability. *Trends Plant Sci.* 23, 1057–1067. doi: 10.1016/j.tplants.2018.09.007

Yasir, M., Khan, R., Ullah, R., Bibi, F., Khan, I., Mustafa Karim, A., et al. (2022). Bacterial diversity and the antimicrobial resistome in the southwestern highlands of Saudi Arabia. *Saudi J. Biol. Sci.* 29, 2138–2147. doi: 10.1016/j.sjbs.2021.11.047

Zhang, Y.-J., Hu, H.-W., Chen, Q.-L., Singh, B. K., Yan, H., Chen, D., et al. (2019). Transfer of antibiotic resistance from manure-amended soils to vegetable microbiomes. *Environ. Int.* 130, 104912. doi: 10.1016/j.envint.2019.104912

Zheng, Y., Yu, S., Wang, G., Xie, F., Xu, H., Du, S., et al. (2021). Comparative microbial antibiotic resistome between urban and deep forest environments. *Environ. Microbiol. Rep.* 13, 503–508. doi: 10.1111/1758-2229.12942

Zhou, Y., Tang, Y., Hu, C., Zhan, T., Zhang, S., Cai, M., et al. (2021). Soil applied Ca, Mg and B altered phyllosphere and rhizosphere bacterial microbiome and reduced huanglongbing incidence in gannan navel orange. *Sci. Total Environ.* 791, 148046. doi: 10.1016/j.scitotenv.2021.148046

frontiers | Frontiers in Microbiology

TYPE Review
PUBLISHED 23 September 2022
DOI 10.3389/fmicb.2022.976657



OPEN ACCESS

EDITED BY
Xia Jiang,
The Chinese University of Hong Kong, China

REVIEWED BY
Yujie Shi,
Northeast Normal University, China
Bingjian Zhu,
Institute of Mountain Hazards and Environment (CAS), China

*CORRESPONDENCE
Shiheng Zhang
zhangshiheng@cqtgmc.edu.cn
Huan Li
lihuanzky@163.com

†These authors have contributed equally to this work

SPECIALTY SECTION
This article was submitted to Antimicrobials, Resistance and Chemotherapy, a section of the journal Frontiers in Microbiology

RECEIVED 23 June 2022
ACCEPTED 05 September 2022
PUBLISHED 23 September 2022

CITATION
Han B, Ma L, Yu Q, Yang J, Su W, Hilal MG, Li X, Zhang S and Li H (2022) The source, fate and prospect of antibiotic resistance genes in soil: A review. *Front. Microbiol.* 13:976657. doi: 10.3389/fmicb.2022.976657



# The source, fate and prospect of antibiotic resistance genes in soil: A review

Binghua Han[1†], Li Ma[1†], Qiaoling Yu[2], Jiawei Yang[1], Wanghong Su[1], Mian Gul Hilal[1], Xiaoshan Li[3], Shiheng Zhang[3]* and Huan Li[1,2]*

[1]Institute of Occupational and Environmental Health, School of Public Health, Lanzhou University, Lanzhou, China, [2]State Key Laboratory of Grassland Agro-Ecosystems, Center for Grassland Microbiome, Lanzhou University, Lanzhou, China, [3]Chongqing Key Laboratory of Development and Utilization of Genuine Medicinal Materials in Three Gorges Reservoir Area, Faculty of Basic Medical Sciences, Chongqing Three Gorges Medical College, Wanzhou, China

Antibiotic resistance genes (ARGs), environmental pollutants of emerging concern, have posed a potential threat to the public health. Soil is one of the huge reservoirs and propagation hotspot of ARGs. To alleviate the potential risk of ARGs, it is necessary to figure out the source and fate of ARGs in the soil. This paper mainly reviewed recent studies on the association of ARGs with the microbiome and the transmission mechanism of ARGs in soil. The compositions and abundance of ARGs can be changed by modulating microbiome, soil physicochemical properties, such as pH and moisture. The relationships of ARGs with antibiotics, heavy metals, polycyclic aromatic hydrocarbons and pesticides were discussed in this review. Among the various factors mentioned above, microbial community structure, mobile genetic elements, pH and heavy metals have a relatively more important impact on ARGs profiles. Moreover, human health could be impacted by soil ARGs through plants and animals. Understanding the dynamic changes of ARGs with influencing factors promotes us to develop strategies for mitigating the occurrence and dissemination of ARGs to reduce health risks.

KEYWORDS

**antibiotic resistance genes, resistomes, microbiome, horizontal gene transfer, heavy metals**

## Introduction

Antibiotic resistance refers to the mechanism in which microorganisms can resist a high concentration of antibiotics, while other organisms are susceptible to these antibiotics (Martinez et al., 2007). The sum of all ARGs in soil environment is called "soil resistome" (Gorovtsov et al., 2018). ARGs are considered as environmental pollutants of emerging concern (Tan et al., 2018), and its global spread and dissemination pose a great threat to human health. Human pathogens carrying various ARGs can generate superbugs, which persist after antibiotic treatment and eventually lead to human death. Antibiotic resistance

is reported to cause 700,000 people deaths a year, more seriously, it is estimated to account for 10 million deaths by 2050 if uncontrolled (O'Neill, 2016).

Most antibiotics are natural compounds or originate from natural compounds, produced by different kinds of bacteria, fungi or plants (Davies and Davies, 2010). Before the introduction of synthetic antibiotics, the existence of natural antibiotics may exert continuous selective pressure on microorganisms, but most microorganisms were susceptible to antibiotics before the era of antibiotics discovery (Davis and Anandan, 1970; Hughes and Datta, 1983). From 2010 to 2030, it is estimated that the use of antibiotics in animal production worldwide will increase by 67%, and China is predicted to increase by 99% (Van Boeckel et al., 2015). The huge market demand for antibiotics and its inappropriate use globally have promoted the increase and spread of ARGs in soil microorganisms (Cheng et al., 2013; Gorecki et al., 2019).

Soil is one of the largest environmental reservoirs for ARGs (Forsberg et al., 2012), accounting for about 30% of the known ARGs, and it is also one of the most complex ecosystems in terms of niches and biodiversity. At present, several main antibiotics used by humans are screened and cultured from soil (30%), and more than 80% of antibiotics used clinically come from soil bacteria. ARGs are indigenous in soil (World Bank, 2017), which may resist to β-lactam, tetracycline and glycopeptide, and these ARGs are detected in 30,000-year-old Beringian permafrost sediments, and exogenous ARGs can also be introduced into the soil by applying organic manure, sewage discharge, and irrigation of wastewater treatment plants (WWTPs) in densely populated areas. Thus, soil can act as a reservoir and potential source of ARGs, which poses a threat to the environment and human health.

The influencing factors on ARGs profiles are different depending on soil types. Microbial community structure, antibiotic type and concentration, soil physicochemical properties (such as pH, humidity, nutrition and temperature), heavy metals, polycyclic aromatic hydrocarbons (PAHs) and pesticides can exert selective pressure on the soil resistomes (Figure 1) and interact with each other. Given that the potential transmission of environmental ARGs to human commensals and pathogens, investigating the source and transmission mechanism of antibiotic resistance in soil, their relationships with microorganisms, mobile genetic elements (MGEs), soil physicochemical properties and various pollutants will contribute to managing antibiotic resistome in soil, and develop effective mitigation strategies to improve human health.

Despite these advances mentioned above, many knowledge gaps still remain in the field of soil antibiotic resistance, as described below. What inexpensive and easy-to-operate technologies can effectively treat emissions of ARGs-containing substances? What are the mechanisms that affect soil ARGs by soil special substrates, such as clay and humic acid? What are the complex interactions and molecular mechanisms between soil ARGs and environment and human health? What are the individual and compound effects of various environmental and biological factors on soil ARGs? More researches are needed to address these questions.

## Antibiotic resistance gene classes distribution across soil

Some ARGs are indigenous in soil, and may originate from soil indigenous bacteria. β-Lactam, tetracycline and vancomycin resistance genes can be detected in some relatively primitive environments with no or limited human impacts (Martinez et al., 2015), such as permafrost (Mindlin et al., 2008; Perron et al., 2015), Antarctic soil (Van Goethem et al., 2018) and Qinghai-Tibet Plateau (Yang et al., 2019; Li B. et al., 2020). Therefore, ARGs are natural and ancient, preceding the selective pressure exerted by man-made antibiotics. ARGs detected in the relatively primitive Qinghai-Tibet plateau soil with high altitude and limited human activities are mainly uncommon glycopeptides (such as vancomycin), rifamycin (Van Bambeke, 2004; Damodaran and Madhan, 2011) and a small part of β-Lactamase resistance genes (LRA-3, LRA-9 and LRA-5). Amycolatopsis in the soil can secrete vancomycin and rifamycin (McIntyre et al., 1996; Tan et al., 2006). Although β-Lactam antibiotics are widely used in clinical treatment, the three genotypes of LRA-3, LRA-9 and LRA-5 have not been reported in clinical pathogens (Li B. et al., 2020). Seven kinds of ARGs, including quinolones, aminoglycosides, β-Lactam, macrolide-lincomycin-streptomycin B (MLSB), multidrug, sulfonamides and tetracycline resistance genes, were detected in 24 pristine forest soils in China, in which aminoglycosides and quinolones resistance genes were dominant (Song et al., 2021). Thirty classes of ARGs resisting to the sulfonamides, tetracyclines, aminoglycosides, quinolones, macrolides and β-Lactam were detected in polar sediments. Among these ARGs, *sul* genes were the most common, and the abundance ($10^{-8} \sim 10^{-6}$ copies/16S rRNA gene copies) was about 2 to 5 orders of magnitude lower than that other areas having higher anthropogenic activities ($10^{-4} \sim 10^{-2}$ copies/16S rRNA gene copies; Tan et al., 2018). In the relatively primitive Qinghai-Tibet plateau wetlands, FCAs (fluoroquinolone, quinolone, florfenicol, chloramphenicol, and amphenicol resistance genes), β-Lactamase, MLSBs, aminoglycoside and tetracycline resistance genes were dominant (Yang et al., 2019). In conclusion, the types of dominant ARGs detected in different soil types are distinct (Table 1).

Tetracycline resistance genes are generally dominant in various soil types, such as agricultural soil (Durso et al., 2012; Cadena et al., 2018), and ~60% of soil-derived strains are resistant to tetracycline (D'Costa et al., 2006). The possible reason is that tetracycline is widely used in animal husbandry and is one of the top five antibiotics most commonly used in China (Zhang et al., 2015). Tetracycline, an indigenous and ancient antibiotic, exerts strong selection pressure on ARGs, which have been detected in Beringian permafrost formed 30,000 years ago (D'Costa et al., 2011) and polar sediments (Tan et al., 2018).

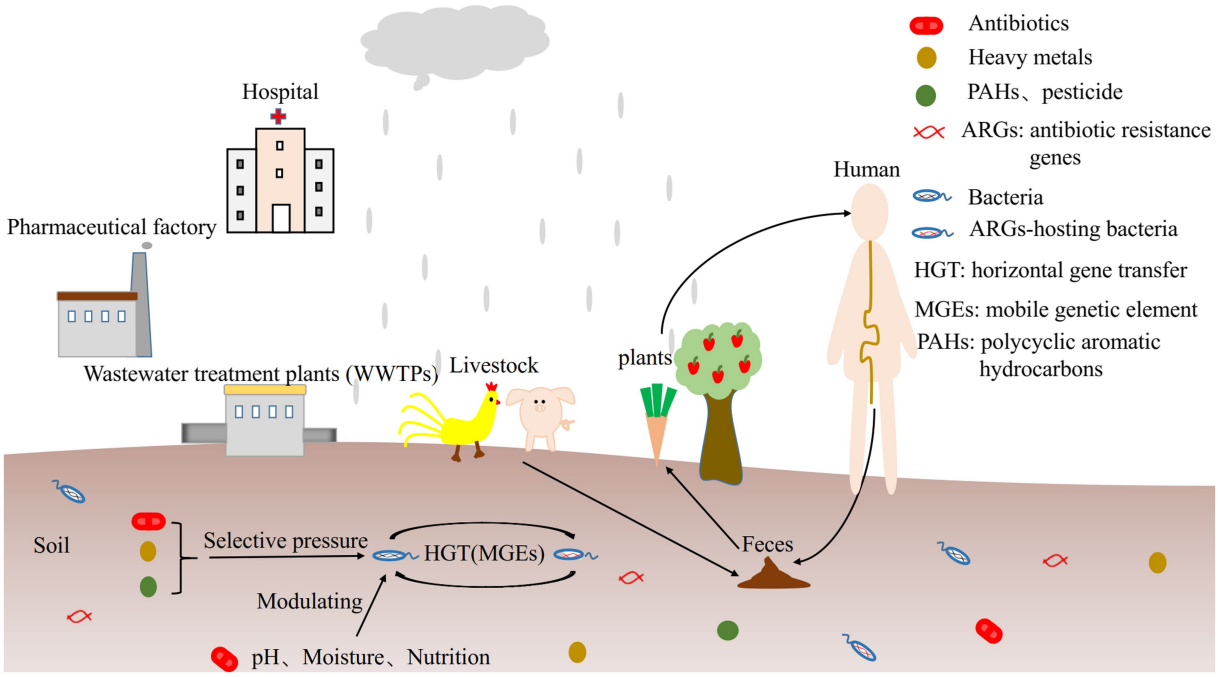


FIGURE 1
The influencing factors of ARGs.

Vancomycin resistance genes are widely distributed and detected in most wetlands of relatively primitive Qinghai-Tibet Plateau (Yang et al., 2019) and other types of soils (D'Costa et al., 2011), which pose a great threat to public health because vancomycin is the last resort against Gram-positive bacteria (some strains are resistant to most antibiotics; Hubbard and Walsh, 2003).

Multidrug resistance genes, one of the dominant ARGs in soil, explain the emergence of multidrug-resistant bacteria in the clinic. Several common ARGs have been detected in the river beach soils of Port Philip Bay and Yarra River in Victoria, Australia, among which multidrug resistance genes were the most abundant, accounting for 32.7% of the total number of detected ARGs (Zhang Y. et al., 2019).

# The origin of antibiotic resistance genes

## Natural antibiotic resistance genes in soil

Microorganisms in soil secrete some antibiotics to compete for resources (high concentration antibiotics; Newman et al., 2003) or communicate (low concentration antibiotics; Linares et al., 2006). Microorganisms resist antibiotics to protect themselves from "suicide" (i.e., the "producer hypothesis"; Cundliffe, 1989; Wright, 2007; Davies and Davies, 2010; Cordero et al., 2012). Microorganisms without resistance can be killed or inhibited by antibiotics. Therefore, according to Darwin's "arms-shields race" hypothesis, in order not to be killed or inhibited by antibiotics, microorganisms adjacent to antibiotics producers acquire antibiotic resistance through gene mutation and expression of latent genes under the selective pressure of antibiotics (Cytryn, 2013). Therefore, some ARGs are indigenous in the soil itself. And it is estimated that the origin of natural antibiotics is before 2 Gyr ~ 40 Myr, thereby the antibiotic resistance should also be equally ancient (Hall and Barlow, 2004).

## Antibiotic resistance genes with composting

In addition to the indigenous resistome, resistome obtained through various ways are called the "acquired resistome." As common drugs and feed additives, antibiotics are widely used and even abused to treat diseases and promote animal growth. Even after taking antibiotics for a long time, antibiotic-resistant bacteria (ARB) can continue to exist in the intestine for many years (Clemente et al., 2015). Up to 30 ~ 90% of antibiotics are not fully absorbed or metabolized after ingestion and excreted through faeces in the form of original drugs, conjugates and by-products (Johnson et al., 2016; Qian et al., 2018). After animal manure is applied to soil, the residual antibiotics exert selective pressure on microorganisms, then conferring antibiotic resistance (Guo et al., 2018). A large number of ARGs were detected in human faeces and animal intestines and faeces. For the sake of amending soil and increasing soil nitrogen source and organic matter

TABLE 1 Antibiotic resistance genes (ARGs) and mainly influencing factors in different soil types.

| Soil type | ARG numbers | Dominant ARGs | ARG abundance | Mainly influencing factors | Reference |
|---|---|---|---|---|---|
| 24 Pristine forest soils (broadleaf forests) | 25 Subtypes of the 30 target ARGs | Aminoglycoside (36.3%), quinolone (27.7%), MLSB[a] (17.5%) resistance genes | Average absolute abundance: $1.78 \times 10^5$ copies/g soil Average relative abundance: $7.22 \times 10^{-3}$ ARG copy numbers/16S rRNA gene copy numbers | Physicochemical factors (e.g., temperature, total phosphorus) (65.8%), microbiota (48.3%), spatial factors (longitude) (26.79%), and MGE (3.6%). | Song et al. (2021) |
| 5 Forest soil from north to south (boreal forest, temperature mixed coniferous forest, temperate deciduous forest, subtropical (evergreen broadleaf) forest and tropical (rainforest) forest) | 160 ARGs | Multidrug (22.4%), β-lactam (21.8%), aminoglycoside (13.5%), MLSB (14.1%), tetracycline (11.2%) and vancomycin (8.2%) resistance genes | – | MGEs, microbiota, herbs and pH | Hu H-W. et al. (2018) |
| Amazon rainforest soils | 215 ARG subtypes | Multidrug resistance genes | 0.243 Copies/16S rRNA gene | Bacterial community composition | Qian et al. (2021) |
| Deciduous forest | 7 ARGs | Sul1, ermB, vanA, aph(3′)-IIa, aph(3′)-IIIa, tet(W) and blaTEM-1 | – | – | Radu et al. (2021) |
| Deep forest in Yunnan | – | Multidrug, MLS (macB) resistance genes | – | – | Zheng et al. (2021) |
| Paddy soil in South China | 16 ARGs, corresponding to 110 ARG subtypes | Multidrug (38–47.5%), acriflavine (16.4–21%), MLS (13.2–20.7%), bacitracin (5.4–12.5%) resistance genes | 7–10 ppm | Microbial communities, pH | Xiao et al. (2016) |
| Paddy soil in Shaoxing City | 5 ARGs | TetB, tetC, tetW, sul1, sul2 | 2.37 ~ 5.01 log10-transformed copies/g dry weight | Microbial community | Lin et al. (2016) |
| Paddy soil in the Lake Tai Basin | >6 ARGs | Multidrug (>90%) resistance genes | – | MGEs | Zhang et al. (2021) |
| Paddy soil in Hunan province | 119 ARGs | Multidrug (17.6%), tetracycline (16.8%), aminoglycoside (16.0%), MLSB (15.1%) and β lactam (14.3%) resistance genes | $10^9 \sim 1.2 \times 10^{12}$copies/g dry soil | Bacteria, MGEs, As | Zhao et al. (2020) |
| Urban soil in Belfast, Northern Ireland | 164 ARGs | β-lactams (23%) and multidrug (23%) resistance genes | $6.8 \times 10^2 \sim 1.7 \times 10^8$ copies/g soil | MGEs, heavy metals (Cu, Zn, etc), pH | Zhao Y. et al. (2019) |
| Urban soil in Victoria, Australia | 40 ARGs | β-lactam (>23%), MLSB (16.34%), and quinolones and fluoroquinolones (11.76%) resistance genes | – | Reclaimed water irrigation, MGEs, bacterial community composition, pH, total nitrogen | Han et al. (2016) |
| Urban soil in Greater Melbourne, Australia | 217 ARGs | Multidrug (52.22%), MLSB (18.50%) and β-lactamase (12.30%) resistance genes | Around $10^{-3}$ copies/16S rRNA gene | MGEs, industrial distribution | Yan et al. (2019) |

[a]Macrolide-lincosamide-streptogramin B.
tet, tetracycline resistance genes; sul, sulfonamide resistance genes; erm, macrolide resistance genes; bla, β-lactam resistance genes; van, vancomycin resistance genes; aph (3′)-IIa, aminoglycoside resistance genes.

(Garcia-Pausas et al., 2017), applying manure has become a routine operation. However, this operation introduces fecal ARGs into the soil (Graham et al., 2016; Peng et al., 2017). It is reported that there were no significant differences in ARGs abundance and types between soil and animal faeces in a relatively primitive Tibetan environment (Chen B. et al., 2016). Long term application of livestock manure can increase the diversity and abundance of ARGs (Li S. et al., 2020). The number of observed ARGs in manured soil increased significantly and continuously during the three consecutive years of fertilization from 2015 to 2017 compared with the treatment without manure application (fertilized pig manure 68–92, fertilized chicken manure 70–84, fertilized cow manure 69–83; Liu et al., 2021). However, other researchers have pointed out that long-term application of organic fertilizer does not always increase the abundance of ARGs. Firstly, the composting process and high temperature (the temperature above 70°C can completely and directly degrade bacterial DNA) can reduce the abundance of ARGs by killing the bacterial hosts (Guo et al., 2019). The total abundance of ARGs decreased by 90.19–91.87% on the 17th day of composting (Guo et al., 2019). Secondly, the exogenous ARG-containing bacteria cannot acclimatize to soil environment and can be inhibited by soil native bacteria; thus, some faecal ARG-containing bacteria can only survive temporally in the soil. After the application of manure, the abundance of ARGs may subsequently decreased (Sun et al., 2015c). The total relative abundance of ARGs decreased gradually with composting, from 2,910 ppm at day 0 to 1,200 ppm and 700 ppm in day-71 and day-171 composting, respectively (Zhang et al., 2020). In addition to manure, the decomposition of animal carcasses, especially fish, livestock and poultry, will also introduce ARGs into the soil. For example, the absolute and relative abundance of total ARGs were enriched 536.96 and 18.16 folds in the Crucian carps carcass soil, respectively (Feng et al., 2021).

## Antibiotic resistance genes in WWTPs

As the interface between humans and the environment, WWTPs in densely populated cities contain various antibiotics, ARBs and ARGs discharged from farms, hospitals and pharmaceutical industries. Microorganisms are subjected to multiple selection pressures in WWTPs, making it possible for horizontal gene transfer (HGT) between environmental bacteria and pathogenic bacteria (Rizzo et al., 2013), and microbial opportunists such as multidrug-resistant bacteria occur after exposure to various toxic compounds (Tello et al., 2012). The WWTPs aim to remove carbonaceous materials, nutrients, and pathogenic bacteria, and are not explicitly used to remove antibiotics and ARGs. The wastewater discharged from the WWTPs introduces and enriches many antibiotics and ARGs, which may pollute soil. High concentration of sulfamethoxazole ($18\,\mu g\,kg^{-1}$) was detected in the soil adjacent to WWTP of Puchukollo, while sulfamethoxazole has not been observed in other soil sampling sites staying away from WWTP (Archundia et al., 2017). Therefore, WWTPs can act as a source of pollutants (Guo J. et al., 2017), which contains plenty of resistance genes.

# The impacting factors of antibiotic resistance genes

## The association between antibiotic resistance genes and microorganisms

Soil microorganisms are main producers of antibiotics and their derivatives, which can equip themself to compete for limited resources. Actinomycetes are well-known bacteria that produce antibiotics (Lima-Mendez et al., 2015; Zhang et al., 2020; Song et al., 2021). Approximately 5–6% of soil bacteria are actinomycetes, most of which can secrete tetracycline. Soil microorganisms are also potential hosts of ARGs. In the study of soil metagenomics, Proteobacteria and Actinobacteria are the most common predictive hosts of multidrug resistance genes (D'Costa et al., 2006; Rafiq et al., 2017; Guo et al., 2019; Yang et al., 2019). All isolates carrying gram-negative *sulI*/*sulII* genes belong to Proteobacteria (Razavi et al., 2017).

Previous studies have shown that bacterial community structure mainly determines the soil ARGs profiles (Forsberg et al., 2014), and bacterial phylogenetic and taxonomic structure significantly affect resistant components in the soil (Chen Q. et al., 2016). Therefore, ARGs profiles can be affected by changing bacterial communities (Xie et al., 2018). Microbial diversity is negatively linked to the abundance of resistance genes (Van Goethem et al., 2018; Chen et al., 2019b; Li B. et al., 2020). After controlling for other potential drivers such as culture time and microbial abundance, this correlation still exists. The reason may be that high biodiversity as a biological barrier can resist the spread of antibiotic resistance (Chen et al., 2017b), or microbial communities with high ARGs abundance compete with susceptible species to reduce soil diversity (Van Goethem et al., 2018). Thereby, increasing microbial diversity can slow down the propagation of ARGs in the soil (Chen et al., 2019b).

## Transmission mechanism of antibiotic resistance genes and their relationships with MGEs

ARGs are highly diverse because they can move between microbes (Gorecki et al., 2019). There are two main ways for ARGs to spread in the environment, vertical gene transfer (VGT) and horizontal gene transfer (HGT). VGT refers to that the genomic content passes from generation to generation. Generally, these ARGs are located on the chromosomes. HGT refers to the transfer of MGEs such as plasmids, integrons and transposons carrying ARGs between two strains through transformation, transduction and conjugation, so that the recipient bacteria can obtain new metabolic ability to adapt to the new niche (D'Costa

et al., 2007). These ARGs are usually located on plasmids. These three HGT mechanisms are shown in Figure 2. Transformation refers to that the competent receptor bacterial cells embed the free ARGs absorbed from the external environment (ARBs are released into the environment after dissolution) into the bacterial chromosome, then obtain a new phenotype. Transformation is the most common way of HGT in bacteria (Wang, 2019). Transduction refers to the process of transferring ARGs from donor bacteria to recipient bacteria by phage (Barlow, 2009), then conducting gene recombination. Penadés and his colleagues found that phages were active in transmission of ARGs related to MGEs (Penades et al., 2015). Conjugation refers to ARG transfer to recipient cells through sexual pili during direct contact between donor and recipient cells (Abe et al., 2020).

Most MGEs before the antibiotic era did not carry ARGs (Davis and Anandan, 1970; Hughes and Datta, 1983), but with the selective pressure posed by the increased use of antibiotics, more and more MGEs were accompanied with resistance genes. Studies have shown that the total relative abundance of ARGs and the relative abundance of several individual ARGs are significantly positively correlated with total transposase genes and total integrase genes (Pehrsson et al., 2016; Guo et al., 2019; Zhang Y-J. et al., 2019; Li S. et al., 2020). Moreover, we can observe the correlation of antibiotic resistance genes and MGEs after controlling various influencing factors such as pH and temperature. The variation of ARGs can be explained mainly by MGEs, accounting for 36.41%; 10 of 16 ARGs were associated positively with MGEs (Guo et al., 2019). *IntI1* (class I integron-integrase gene) was significantly positively correlated with *sulI*, *sulII* and *tetG* gene in manure-amended soil (Guo et al., 2019). Quinolone resistance genes are prevalent, probably because they are located on plasmids and are easy to transfer between natural bacteria (Vaz-Moreira et al., 2016). In agriculture soils, HGT mediated by MGEs may enable nonpathogenic environmental bacteria and pathogens acquire resistance (Johnson et al., 2016), thus increasing the difficulty of clinical treatment. However, other studies have shown that the association of MGEs and ARGs does not always exist (Zhang et al., 2020), or MGEs cannot explain much about ARG variations (Xu et al., 2021). For example, the absolute abundance of ARGs was significantly correlated with the abundance of integrons, but not with the abundance of transposases in wetland soil on the Qinghai-Tibetan Plateau (Yang et al., 2019). These phenomena need to be studied further.

## The association between antibiotic resistance genes and soil physicochemical properties

The main factors shaping ARGs profiles are distinct in different geographical locations and soil types. Soil pH, moisture,

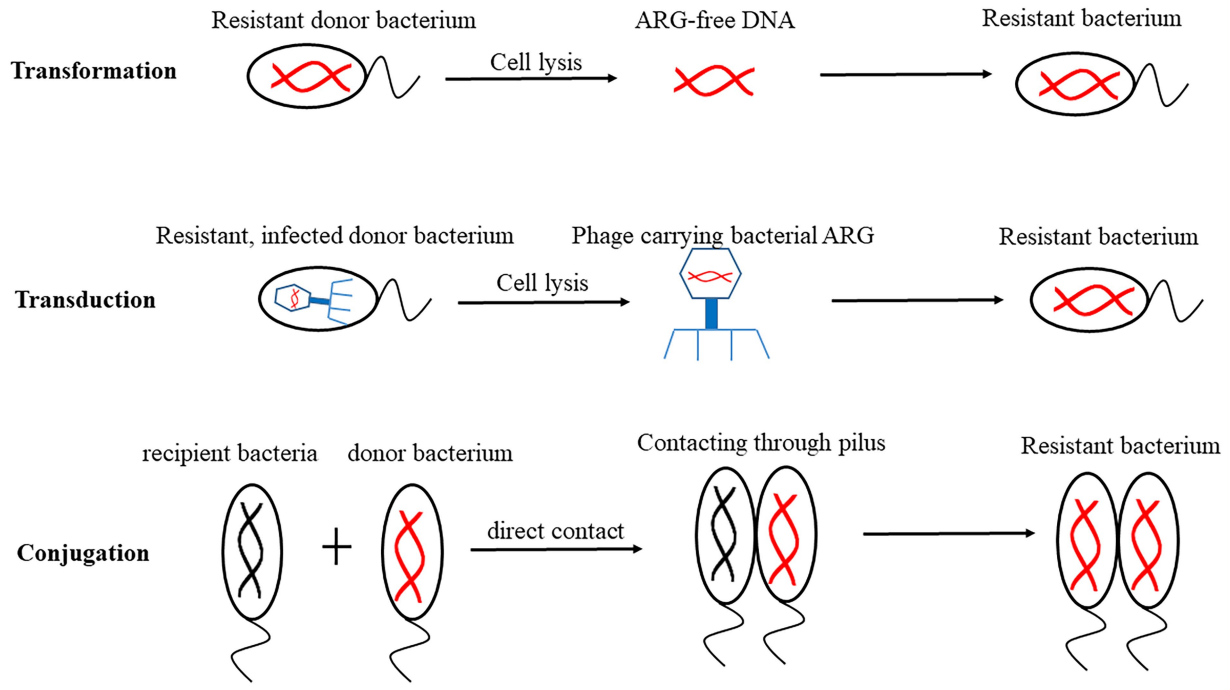


FIGURE 2
Mechanisms of horizontal gene transfer (HGT). Transformation refers to that the receptive receptor bacterial cells embed the free antibiotic resistance genes (ARGs) into the bacterial chromosome, integrate and stable express. Transduction refers to transfer ARGs from donor bacteria to recipient bacteria by phage. Conjugation refers to transfer of ARGs through sexual pili during direct contact between donor and recipient cells.

temperature, and C/N ratio all can affect ARGs profiles. Soil pH and moisture are common influencing factors in various soils.

Soil pH is one of the most vital factors affecting ARGs diversity and composition (Xie et al., 2018). ARGs diversity is highest when pH is neutral (Hu H-W. et al., 2018), and positively correlated with pH (pH: 4.0 ~ 5.5) in Amazon rainforest soil (Lemos et al., 2021). Soil pH was significantly and negatively correlated with ARGs abundance in bulk soil (Yan et al., 2021). For instance, the abundance of ARGs (*tetO*, *tetQ*, *tetC* and *tetX*) increased significantly under acidic conditions and decreased under alkaline conditions (Guo A. et al., 2017). Previous studies showed that soil pH is also the essential factor that influences the soil microbial diversity and community structure (Shen et al., 2013; Sun et al., 2015c), and soil pH can select microorganisms by affecting nutrient availability or physiological activity (Xiao et al., 2014). The certain pH levels may exert direct pressure on bacterial cells, selecting some bacterial population (e.g., Acidobacteria; McCaig et al., 1999, Zhang et al., 2014), and then indirectly affect the ARGs profiles. The optimal pH of most soil bacteria is narrow (the intracellular pH value is usually within 1 unit of near neutral pH; Xiao et al., 2016), and the growth of soil microorganisms is inhibited, if pH deviates from the optimal pH (Rousk et al., 2010).

In addition, soil moisture is another key factor driving the ARGs pattern (Hu H-W. et al., 2018; Yang et al., 2019; Zhang et al., 2020). Soil moisture is positively correlated with the relative abundance of ARGs encoding inactivation mechanism (Cheng et al., 2019; Song et al., 2021). The absolute copy numbers of *sulI* and *tetO* gene were positively correlated with moisture (Song et al., 2016), which might be explained that water is one of the main limitations for growth of the total microbial community in soils. Thus increased moisture will increase the microbial biomass, then increase the ARG content. In the thermophilic composting stage, the main factor affecting ARGs is moisture. Low moisture conditions are helpful to removing ARGs (Cheng et al., 2019), because high moisture promotes the propagation of ARGs by MGEs (Wang et al., 2016), or ARGs migrate with water flow. Moreover, the moisture level can also indirectly affect ARGs level by affecting microbial activity (Liang et al., 2003), free airspace (Awasthi et al., 2018), metabolic activity, physiological activity (Zhang M. et al., 2019), ARGs dissipation (Song et al., 2016) and increasing the sensitivity of microbial community to antibiotics (Reichel et al., 2014).

Nutrients in the soil are also correlated with ARGs. For instance, potassium is positively correlated with the relative abundance of ARGs with protective mechanisms or sulfonamides classes (Song et al., 2021). Total phosphorus is negatively correlated with the relative abundance of ARGs encoding efflux pump mechanism or tetracyclines classes (Zhang Y-J. et al., 2019). High C/N ratio and $NO_3^-$-N contents are positively correlated with the absolute abundance of ARGs (Guo et al., 2020). Moreover, the nitrogen conversion indicators (TKN: total Kjeldahl nitrogen, $NO_3^-$-N, $NH_4^+$-N) explain part of the variation of ARGs (24.21%; Guo et al., 2019). The nutrient is one of the most significant determinants for the direction of microbial interaction. In nutrient-rich environment, microorganisms show competition and increases the diversity of ARGs (Hammarlund and Harcombe, 2019).

Soil temperature shapes the distribution of resistome and it is negatively correlated with ARGs abundance. The reason may be that increasing soil temperature decreased microbial community diversity, then leaded to reduce ARGs abundance in soils (Dunivin and Shade, 2018). The diversity and abundance of *bla_A*, *bla_B*, *dfra12* and *tolC* gene decreases with soil temperature (Dunivin and Shade, 2018). High temperature can reduce the abundances of most ARGs (Banerjee et al., 2016), which is usually used to remove ARGs in the composting process.

## The association between antibiotic resistance genes and meteorological parameters

Meteorological parameters (e.g., precipitation and atmospheric temperature) have great effects on ARGs. The abundance, diversity and composition of ARGs increase substantially during rainfall (Jang et al., 2021). Total ARGs suddenly reached to the highest level ($4.5 \times 10^9$ copies/ml) at the 7th after rainfall (Jang et al., 2021). The average concentrations of *sulII* gene in the wet season ($9.04 \times 10^7$ copies/g sediments) were higher than those in the dry season ($3.78 \times 10^7$ copies/g sediments; Li et al., 2018). Moreover, the absolute abundances of the *sul1, sul2, tetA, tetQ, qepA, qnrB, qnrS, ampC,* and *aacC2* gene increased by nearly one order of magnitude during rainfall compared with before rainfall (approximately 12, 16, 3.6, 11, 1.1, 32, 7.5, 5.7, and 3.8 folds, respectively; Wang Q. et al., 2021). Several reasons can explain the phenomena. Firstly, almost 98% of airborne ARB particles fall to the ground surface through the scavenging action of rainwater, promoting the dissemination of ARGs from ambient air to soil during rainfall (Wang Q. et al., 2021). The relative contribution of rain to resistance genes was 16.34% (Hu J. et al., 2018). Secondly, wetter weather can lead to bacterial blooms, compared with drier conditions (Marti et al., 2014). Thirdly, rainwater increased the abundance of MGEs, especially the *intI*1 ($2.35 \times 10^6$ copies $m^{-3}$), which accelerated the propagation of ARGs (Wang Q. et al., 2021).

It appears that the effect of atmospheric temperature on ARGs was less important than that of precipitation (Meyers et al., 2020). Previously, some studies found that ARGs were positively associated with air temperature. The absolute abundance of resistance genes was highest in summer ($2.81 \times 10^9$ copies/L on average), and the ARG abundance in four seasons fluctuated along with local air temperature (Zheng et al., 2018). For example, temperature was positively associated with vancomycin and sulfonamide resistance genes (Yang et al., 2019). This may be attributed to the warming climate, which will very likely contribute to increased soil temperature, alter the ARGs-containing microbial community structure and then increase the background levels of ARGs. Climate warming is one of the severe

environmental challenges of the world today, and this may contribute to increasing ARGs abundance, especially high risk ARGs. If high-risk ARGs are transferred to human pathogens, this could pose a huge burden for public health. Conversely, the absolute abundances of seven types of ARGs (*tetM*, *tetO*, *tetW*, *ermB*, *ermQ*, *mphE* and *aph (3′)-IIIa*) showed little correlations with temperature (Ouyang et al., 2020). Therefore, the association of ARGs and temperature remains elusive.

## The association between antibiotic resistance genes and antibiotic use

The relationship between antibiotics and ARGs is unclear (Tan et al., 2006; Zhang et al., 2015). Traditionally, according to Darwin's "arms-shields race" evolutionary hypothesis, antibiotics directly select ARGs. The concentration of antibiotics are positively correlated with the abundance of ARGs (Su et al., 2014; Zhang et al., 2020) and negatively correlated with the diversity of ARGs (Zhao R. et al., 2019). Moreover, high concentrations of antibiotics are associated with class 1 integrons and can accelerate the spread of ARGs (Andersson and Hughes, 2014).

However, the effect of antibiotics on ARGs is not always strong, sometimes weaker than other drivers, such as MGEs and metals. The reason may be that antibiotics can inactivate rapidly through adsorption, photolysis and biodegradation, so the effect of antibiotics on ARGs profiles may be temporal. The effect of antibiotic concentration on ARGs abundance is insignificant in paddy soil (Zhao et al., 2020). Moreover, antibiotics and their corresponding ARGs do not always appear synchronously, and ARGs can persist even without antibiotic selection pressure. In a remote Alaskan soil that was not contaminated by antibiotics, $bla_{LRA\text{-}13}$ gene (β-Lactamase resistance genes) was detected (Allen et al., 2009). The direct selection pressure of given antibiotics leads to the enrichment of corresponding and non-corresponding ARGs, which reveals the collateral effect of antibiotics on the development of resistance. Although sulfonamides were not detected in soils, *sul* gene (sulfonamides resistance genes) with high abundance was detected in all soil samples (Wang et al., 2015).

## The association between antibiotic resistance genes and heavy metals

The content of heavy metals in soils is generally positively correlated with ARGs, but the soil type should be considered. Cu is positively correlated with aminoglycosides (*aadA* and *aac*) and MLSB (*mefA*) resistance genes detected in Belfast, Northern Ireland soil (Zhao Y. et al., 2019). Zn, Cu and Cd are positively associated with vancomycin resistance genes in the soil of gold tails (Qiao et al., 2021). The strong correlation between heavy metals and ARGs implicates that heavy metals (not easy to degrade) impose continuous selective pressure on metal resistance genes (MRGs). ARGs and MRGs may be located in the same DNA fragment (Kiran et al., 2015). Class I integrons (*intI*) generally exist in metal-polluted environment (Poole, 2017). Heavy metals can combine antibiotics to promote the transmission of ARGs through co-selection by *intI* (Seiler and Berendonk, 2012). For example, Cd/Zn resistance gene (*cadD*) and aminoglycoside resistance gene (*aph (3′) IIIA*) are located on the same plasmid, and β-Lactam resistance gene (*blaCTX-M*) and Cu resistance gene (*pcoA-E (5/25)*) are on the same *IncHI2* plasmid (Fang et al., 2016). Therefore, the transmission of corresponding resistance genes can be accelerated in metal-polluted environment. In turn, microbes may utilize similar mechanisms to fight antibiotics and heavy metals. Furthermore, to some extent, the use of metal-containing antimicrobial agents may promote the occurrence of multidrug resistance (Pal et al., 2017). However, heavy metals do not always correlate with ARGs depending on the concentration of heavy metals. Low heavy metal concentration has little or no effect on ARG profiles; On the contrary, high heavy metal concentration greatly impacts ARG profiles (Wang X. et al., 2021). Low concentration of Ni (the geo-accumulation index (Igeo) < 0 in some samples) is not related to most of the ARGs detected; High concentrations of As, Pb and Cd (Igeo>4 in some samples) are positively correlated with aminoglycoside and vancomycin resistance genes (Qiao et al., 2021).

## The association between antibiotic resistance genes and other pollutants

The PAHs in soils, including pyrene, benzopyrene, phenanthrene and naphthalene, can affect the pattern of ARGs. The expression of ARGs cassette elevated in PAHs-contaminated soil, and the fluctuation of the abundance of tetracycline resistance genes (*tetM*, *tetW*) and sulfonamide resistance genes (*sulII*, *sulIII*) was positively correlated with the pyrene concentration in soil (Sun et al., 2015a). The 100 mg $L^{-1}$ naphthalene and 10 mg $L^{-1}$ phenanthrene increased the abundances of sulfonamide resistance gene (*sulI*) and aminoglycoside resistance gene (*aadA2*; Wang et al., 2017). This is possibly because PAH directly enriches ARGs and produces mutagenic effect by triggering stress/repair system or changing DNA composition (Busch et al., 2018). In addition, the abundances of ARGs such as *macB*, *mexB* and *tolC* in PAHs-contaminated soil were about 15 times higher than those in lightly polluted soil. ARGs enriched in PAHs-contaminated soil are mostly in chromosomes rather than plasmids, so their frequencies of HGT among bacteria are low (Chen et al., 2017a). Phenanthrene, a small molecule, leaded to the reduction of ampicillin resistance gene (*Ampr*) transformation through noncovalent interaction; the transformation was not significant in the presence of macromolecule pyrene and benzopyrene, which further indicated the reduction of HGT in PAH-contaminated samples (Kang et al., 2015). However, the total amount of phenanthrene or pyrene in soil was not always related to ARGs abundance, but their bioavailability was significantly related to ARGs abundance (Sun et al., 2015b), thus, the relationship between PAHs and ARGs needs further study.

Pesticides and antibiotics together exert selective pressure on microorganisms to produce pesticide-antibiotic cross-resistance (Rangasamy et al., 2018). The application of pesticides increased the absolute and relative abundance of *ermB*, *aph (3′)-IIIa* and *tetW* gene in the soil quickly (Radu et al., 2021). The 20.0 mg $kg^{-1}$ chloropyrophos significantly increased the total abundance of *tetM*, *tetO*, *tetQ*, *tetW*, *tetX*, *sulI* and *sulII* gene (Guo et al., 2020). Furthermore, bacteria in pesticide-contaminated soil contained *IncP* plasmid, which further promoted the propagate of ARGs (Anjum et al., 2011).

## The association between antibiotic resistance genes and plants

Plants can acquire exogenous ARGs by soil. The dynamics and transfer of ARGs amongst plants are associated with soil. On one hand, plant phyllosphere and rhizosphere bacteria can absorb exogenous ARGs from soil (Chen et al., 2019a). Ten ARGs (*vanTC*, *vanC*, *vanYD*, *mexF*, *ttgA*, *oprJ*, *ampC*, *blaCTX-M*, *pncA*, *cmx (A)*) were absorbed into Brassica phyllosphere from soil (Chen et al., 2017c). On the other hand, soil ARGs can be horizontally transferred to microbiomes that parasitize or adhere to plants (Chen et al., 2019c). Moreover, the *intI1* and genes encoding transposases are common in vegetables (Wang et al., 2015; Chen et al., 2018). Some self-transmissible plasmids resisting tetracycline occur in arugula (Blau et al., 2018), which speeds up transferring ARGs from soil to plants. High risk ARGs in vegetables may be transferred to the human gut and may harm human health if ARGs reside in the body.

# The association between antibiotic resistance genes and human health

The relationship between antibiotic resistance and human health can be characterized by the soil–plant/animal-human cycle in soil. Antibiotics, ARGs or ARBs are brought into the soil by wastewater inflow, reclaimed water irrigation, composting and other ways. Then, plants can absorb ARGs from soil. Fortunately, most plant ARG-carrying microbes are non-pathogenic (Zhang et al., 2011), but their possible participating in the spread of ARGs to human pathogens by HGT *via* MGEs (Rossi et al., 2014). Endophytic bacteria of plants closely related to human pathogens or opportunistic human pathogens may potentially harm human health. In 2011, multidrug resistant enterohemorrhagic *Escherichia coli* (EHEC) broke out in Europe, causing 50 persons dead by eating raw fruits and vegetables contaminated by animal feces (Buchholz et al., 2011). Outbreaks of *Salmonella poona* infections in America associated with consuming melons were associated to unhygienic irrigation at the source farms (Lee and Gilmore, 2004). Therefore, ARGs in soil spread to vegetables and threaten human health if vegetables are not or rarely processed.

Animals intake ARGs from soil through contact, feedings, and other ways, acting as intermediate hosts for ARBs and becoming reservoirs for ARGs to transfer to human pathogens (Allen et al., 2010). Then, humans acquire ARGs by eating animal products (Winokur et al., 2001), which causes direct and indirect harm to human health. Mcr-1 myxin resistance genes were initially found in animals and meat and then detected in food samples and human intestinal flora (Hu et al., 2016), indicating that ARGs were transmitted from animals to humans. It is reported that the outbreak of quinolone-resistant *Campylobacter* infections in the United States is caused by humans consumption of chicken (Barza and Travers, 2002).

Antibiotics are one of the greatest discoveries before the Second World War. The mortality rate of infectious diseases drops sharply by antibiotics treatment (Rachakonda and Cartee, 2004). Therefore, the liberal use of antibiotics in clinical practice causes widely-distributed antibiotic resistance, which leads infectious diseases to be one of the leading causes of death in the world (Nathan, 2004). In Europe, the *Escherichia coli* resistance to the third generation cephalosporins increases (European Center for disease prevention and control, 2016). Cephalosporins, as a common over-the-counter drug in China, its resistance consequences have certain reference implications.

Moreover, the excessive use and abuse of various antibiotics by humans has led to the emergence of multidrug-resistant bacteria in the environment and human body, and even "superbacteria" such as NDM-1 (Ahammad et al., 2014; Nesme and Simonet, 2015). Then, the pathogens has become insensitive to most antibiotics used in the clinic (World Bank, 2017). Previously, highly pathogenic *Klebsiella pneumonia* was detected in Chinese hospitals, resistant to all tested antibiotics (Gu et al., 2018). These make us stand on the edge of the post-antibiotic era (Tyrrell et al., 2019). The American Centers for Disease Control and Prevention estimates that more than 70% of the bacteria causing the infection are resistant to at least one antibiotic commonly used for treatment (IDSA, 2004). This has greatly increased the treatment difficulty of clinical infectious diseases and increased infection mortality. By 2050, it is expected that 10 million people will die of antibiotic resistance every year (WHO, 2019), which will bring a substantial economic burden to patients and society. A WHO report point out that by 2050, the global financial burden caused by antibiotic resistance will be equivalent to that caused by the economic crisis in 2008 (WHO, 2019).

# Future perspectives

Since the discovery of ARGs in the last century, people constantly get the knowledge about it, from what to how to spread and then to harm. However, much remains unknown. Firstly, which technologies can reduce the source and presence of ARGs in soil? Secondly, what are the molecular mechanisms of environmental factors affecting soil ARGs transmission? Thirdly, how does soil ARGs affect human health, and how can it be mitigated? Some work

needs to be done to figure out these problems. The following initiatives are put forward for future research:

1. Develop highly efficient technologies to treat agricultural waste, waste water and minimize their ARGs input to soil. Materials introduced into soil, such as ARGs in compost and irrigation water, should be treated in advance to reduce input. Establish a sound surveillance system to reduce the release of ARG into the soil.
2. Investigate the influence mechanisms of special substrates in soil, such as clay minerals and humic acid, on the genetic transformation and horizontal gene transfer of ARGs; The effects of different ARGs in soil environment and their harm to human body may vary greatly, therefore, it is necessary to analyze the environmental and health effects of important ARGs in soil from the perspective of molecular mechanism.
3. Continue to deeply study the transfer and transformation regulation of ARGs in soil, clarify the individual and compound effects of various environmental and biological factors, establish biogeochemical models, predict the migration and fate of ARGs in soil, and provide scientific guidance for biological governance.
4. Develop strategies to regulate soil ARGs. Whether ARGs can be modified to reduce the impact on the environment and human health through cultivation, fertilization, irrigation and other measures.
5. Formulate reasonable and standardized antibiotic use measures and legal norms to reduce the abuse of antibiotics, especially in agriculture, so as to reduce ARGs in soil environment.

## Conclusion

ARGs are indigenous and ancient in soil, and soil can acquire exogenous ARGs from various ways. Microbiome, as the producer and potential host of ARGs, its composition and structure shape ARGs profiles, which acquire resistance by HGT *via* MGEs. ARG abundance are negatively correlated with pH, but are positively associated with moisture and rainfall amount. Antibiotics, heavy metals, PAHs and pesticides in high concentration can exert selective pressure on ARGs and enrich ARGs. Plants and animals can absorb ARGs from soil, then spread to humans and possibly pose a potential harm to human health. Our study systematically reviewed various influencing factors of soil resistome, such as microorganisms, MGEs. Although we have acquired these achievements of ARGs, there are still many unknowns that need to be further studied to protect humanity from ARGs. In the future, we need to study how soil ARGs are transmitted to the human body and affect human health and how this potential harm can be reduced.

## Author contributions

BH, LM, SZ, and HL led the drafting of the manuscript, with substantial input from the other authors. All authors contributed to the article and approved the submitted version.

## Funding

This work was supported by the National Natural Science Foundation of China (42007026), NSRP of CQTGMC (XJ2021000101), and Innovative Research Group Project of Chongqing municipal education commission (CXQT20030).

## Conflict of interest

The authors declare that the research was conducted in the absence of any commercial or financial relationships that could be construed as a potential conflict of interest.

## Publisher's note

All claims expressed in this article are solely those of the authors and do not necessarily represent those of their affiliated organizations, or those of the publisher, the editors and the reviewers. Any product that may be evaluated in this article, or claim that may be made by its manufacturer, is not guaranteed or endorsed by the publisher.

## References

Abe, K., Nomura, N., and Suzuki, S. (2020). Biofilms: hot spots of horizontal gene transfer (HGT) in aquatic environments, with a focus on a new HGT mechanism. *FEMS Microbiol. Ecol.* 96. doi: 10.1093/femsec/fiaa031

Ahammad, Z. S., Sreekrishnan, T. R., Hands, C. L., Knapp, C. W., and Graham, D. W. (2014). Increased waterborne Bla (NDM-1) resistance gene abundances associated with seasonal human pilgrimages to the upper Ganges River. *Environ. Sci. Technol.* 48, 3014–3020. doi: 10.1021/es405348h

Allen, H. K., Donato, J., Wang, H. H., Cloud-Hansen, K. A., Davies, J., and Handelsman, J. (2010). Call of the wild: antibiotic resistance genes in natural environments. *Nat. Rev. Microbiol.* 8, 251–259. doi: 10.1038/nrmicro2312

Allen, H. K., Moe, L. A., Rodbumrer, J., Gaarder, A., and Handelsman, J. (2009). Functional metagenomics reveals diverse beta-lactamases in a remote Alaskan soil. *ISME J.* 3, 243–251. doi: 10.1038/ismej.2008.86

Andersson, D. I., and Hughes, D. (2014). Microbiological effects of sublethal levels of antibiotics. *Nat. Rev. Microbiol.* 12, 465–478. doi: 10.1038/nrmicro3270

Anjum, R., Grohmann, E., and Malik, A. (2011). Molecular characterization of conjugative plasmids in pesticide tolerant and multi-resistant bacterial isolates from contaminated alluvial soil. *Chemosphere* 84, 175–181. doi: 10.1016/j.chemosphere.2011.02.002

Archundia, D., Duwig, C., Lehembre, F., Chiron, S., Morel, M. C., Prado, B., et al. (2017). Antibiotic pollution in the Katari subcatchment of the Titicaca Lake: major transformation products and occurrence of resistance genes. *Sci. Total Environ.* 576, 671–682. doi: 10.1016/j.scitotenv.2016.10.129

Awasthi, S. K., Wong, J. W. C., Li, J., Wang, Q., Zhang, Z., Kumar, S., et al. (2018). Evaluation of microbial dynamics during post-consumption food waste composting. *Bioresour. Technol.* 251, 181–188. doi: 10.1016/j.biortech.2017.12.040

Banerjee, G., Ray, A. K., and Kumar, R. (2016). Effect of temperature on lateral gene transfer efficiency of multi-antibiotics resistant bacterium, *Alcaligenes faecalis*. *Sains Malays.* 45, 909–914.

Barlow, M. (2009). "What antimicrobial resistance has taught us about horizontal gene transfer," in *Horizontal Gene Transfer*. eds. M. B. Gogarten, J. P. Gogarten and L. C. Olendzenski (Humana Press).

Barza, M., and Travers, K. (2002). Excess infections due to antimicrobial resistance: the "attributable fraction". *Clin. Infect. Dis.* 34, S126–S130. doi: 10.1086/340250

Blau, K., Bettermann, A., Jechalke, S., Fornefeld, E., Vanrobaeys, Y., Stalder, T., et al. (2018). The transferable Resistome of produce. *MBio* 9. doi: 10.1128/mBio.01300-18

Buchholz, U., Bernard, H., Werber, D., Böhmer, M. M., Remschmidt, C., Wilking, H., et al. (2011). German outbreak of Escherichia coli O104: H4 associated with sprouts. *N. Engl. J. Med.* 365, 1763–1770. doi: 10.1056/NEJMoa1106482

Busch, A., Mesa-Torres, N., and Krell, D. (2018). "The Family of two-component systems that regulate hydrocarbon degradation pathways," in *Cellular Ecophysiology of Microbe*. ed. T. Krell (Springer International Publishing), 1–21.

Cadena, M., Durso, L. M., Miller, D. N., Waldrip, H. M., Castleberry, B. L., Drijber, R. A., et al. (2018). Tetracycline and sulfonamide antibiotic resistance genes in soils from Nebraska organic farming operations. *Front. Microbiol.* 9:1283. doi: 10.3389/fmicb.2018.01283

Chen, Q., An, X., Li, H., Su, J., Ma, Y., and Zhu, Y. G. (2016). Long-term field application of sewage sludge increases the abundance of antibiotic resistance genes in soil. *Environ. Int.* 92-93, 1–10. doi: 10.1016/j.envint.2016.03.026

Chen, Q.-L., An, X. L., Li, H., Zhu, Y. G., Su, J. Q., and Cui, L. (2017b). Do manure-borne or indigenous soil microorganisms influence the spread of antibiotic resistance genes in manured soil? *Soil Biol. Biochem.* 114, 229–237. doi: 10.1016/j.soilbio.2017.07.022

Chen, Q.-L., An, X. L., Zheng, B. X., Gillings, M., Peñuelas, J., Cui, L., et al. (2019b). Loss of soil microbial diversity exacerbates spread of antibiotic resistance. *Soil Ecol. Lett.* 1, 3–13. doi: 10.1007/s42832-019-0011-0

Chen, Q.-L., An, X. L., Zheng, B. X., Ma, Y. B., and Su, J. Q. (2018). Long-term organic fertilization increased antibiotic resistome in phyllosphere of maize. *Sci. Total Environ.* 645, 1230–1237. doi: 10.1016/j.scitotenv.2018.07.260

Chen, Q.-L., An, X. L., Zhu, Y. G., Su, J. Q., Gillings, M. R., Ye, Z. L., et al. (2017c). Application of struvite alters the antibiotic Resistome in soil, rhizosphere, and Phyllosphere. *Environ. Sci. Technol.* 51, 8149–8157. doi: 10.1021/acs.est.7b01420

Chen, Q.-L., Cui, H. L., Su, J. Q., Penuelas, J., and Zhu, Y. G. (2019c). Antibiotic Resistomes in plant microbiomes. *Trends Plant Sci.* 24, 530–541. doi: 10.1016/j.tplants.2019.02.010

Chen, B., He, R., Yuan, K., Chen, E., Lin, L., Chen, X., et al. (2017a). Polycyclic aromatic hydrocarbons (PAHs) enriching antibiotic resistance genes (ARGs) in the soils. *Environ. Pollut.* 220, 1005–1013. doi: 10.1016/j.envpol.2016.11.047

Chen, C., Pankow, C. A., Oh, M., Heath, L. S., Zhang, L., du, P., et al. (2019a). Effect of antibiotic use and composting on antibiotic resistance gene abundance and resistome risks of soils receiving manure-derived amendments. *Environ. Int.* 128, 233–243. doi: 10.1016/j.envint.2019.04.043

Chen, B., Yuan, K., Chen, X., Yang, Y., Zhang, T., Wang, Y., et al. (2016). Metagenomic analysis revealing antibiotic resistance genes (ARGs) and their genetic compartments in the Tibetan environment. *Environ. Sci. Technol.* 50, 6670–6679. doi: 10.1021/acs.est.6b00619

Cheng, W., Chen, H., Su, C., and Yan, S. (2013). Abundance and persistence of antibiotic resistance genes in livestock farms: a comprehensive investigation in eastern China. *Environ. Int.* 61, 1–7. doi: 10.1016/j.envint.2013.08.023

Cheng, D., Feng, Y., Liu, Y., Xue, J., and Li, Z. (2019). Dynamics of oxytetracycline, sulfamerazine, and ciprofloxacin and related antibiotic resistance genes during swine manure composting. *J. Environ. Manag.* 230, 102–109. doi: 10.1016/j.jenvman.2018.09.074

Clemente, J. C., Pehrsson, E. C., Blaser, M. J., Sandhu, K., Gao, Z., Wang, B., et al. (2015). The microbiome of uncontacted Amerindians. *Sci. Adv.* 1. doi: 10.1126/sciadv.1500183

Cordero, O. X., Wildschutte, H., Kirkup, B., Proehl, S., Ngo, L., Hussain, F., et al. (2012). Ecological populations of bacteria act as socially cohesive units of antibiotic production and resistance. *Science* 337, 1228–1231. doi: 10.1126/science.1219385

Cundliffe, E. (1989). How antibiotic-producing organisms avoid suicide. *Annu. Rev. Microbiol.* 43, 207–233. doi: 10.1146/annurev.mi.43.100189.001231

Cytryn, E. (2013). The soil resistome: the anthropogenic, the native, and the unknown. *Soil Biol. Biochem.* 63, 18–23. doi: 10.1016/j.soilbio.2013.03.017

Damodaran, S. E., and Madhan, S. (2011). Telavancin: A novel lipoglycopeptide antibiotic. *J. Pharmacol. Pharmacother.* 2, 135–137. doi: 10.4103/0976-500x.81918

Davies, J., and Davies, D. (2010). Origins and evolution of antibiotic resistance. *Microbiol. Mol. Biol. Rev.* 74, 417–433. doi: 10.1128/MMBR.00016-10

Davis, C. E., and Anandan, J. (1970). The evolution of r factor. A study of a "preantibiotic" community in Borneo. *N. Engl. J. Med.* 282, 117–122. doi: 10.1056/nejm197001152820302

D'Costa, V. M., Griffiths, E., and Wright, G. D. (2007). Expanding the soil antibiotic resistome: exploring environmental diversity. *Curr. Opin. Microbiol.* 10, 481–489. doi: 10.1016/j.mib.2007.08.009

D'Costa, V. M., King, C. E., Kalan, L., Morar, M., Sung, W. W., Schwarz, C., et al. (2011). Antibiotic resistance is ancient. *Nature* 477, 457–461. doi: 10.1038/nature10388

D'Costa, V. M., McGrann, K. M., Hughes, D. W., and Wright, G. D. (2006). Sampling the antibiotic resistome. *Science* 311, 374–377. doi: 10.1126/science.1120800

Dunivin, T. K., and Shade, A. (2018). Community structure explains antibiotic resistance gene dynamics over a temperature gradient in soil. *FEMS Microbiol. Ecol.* 94. doi: 10.1093/femsec/fiy016

Durso, L. M., Miller, D. N., and Wienhold, B. J. (2012). Distribution and quantification of antibiotic resistant genes and bacteria across agricultural and non-agricultural metagenomes. *PLoS One* 7:e48325. doi: 10.1371/journal.pone.0048325

Fang, L., Li, X., Li, L., Li, S., Liao, X., Sun, J., et al. (2016). Co-spread of metal and antibiotic resistance within ST3-Inc HI2 plasmids from *E. coli* isolates of food-producing animals. *Sci. Rep.* 6:6. doi: 10.1038/srep25312

Feng, T., Su, W., Zhu, J., Yang, J., Wang, Y., Zhou, R., et al. (2021). Corpse decomposition increases the diversity and abundance of antibiotic resistance genes in different soil types in a fish model. *Environ. Pollut.* 286:117560. doi: 10.1016/j.envpol.2021.117560

Forsberg, K. J., Patel, S., Gibson, M. K., Lauber, C. L., Knight, R., Fierer, N., et al. (2014). Bacterial phylogeny structures soil resistomes across habitats. *Nature* 509, 612–616. doi: 10.1038/nature13377

Forsberg, K. J., Reyes, A., Wang, B., Selleck, E. M., Sommer, M. O. A., and Dantas, G. (2012). The shared antibiotic Resistome of soil bacteria and human pathogens. *Science* 337, 1107–1111. doi: 10.1126/science.1220761

Garcia-Pausas, J., Rabissi, A., Rovira, P., and Romanyà, J. (2017). Organic fertilisation increases C and N stocks and reduces soil organic matter stability in mediterranean vegetable gardens. *Land Degrad. Dev.* 28, 691–698. doi: 10.1002/ldr.2569

Gorecki, A., Decewicz, P., Dziurzynski, M., Janeczko, A., Drewniak, L., and Dziewit, L. (2019). Literature-based, manually-curated database of PCR primers for the detection of antibiotic resistance genes in various environments. *Water Res.* 161, 211–221. doi: 10.1016/j.watres.2019.06.009

Gorovtsov, A. V., Sazykin, I. S., and Sazykina, M. A. (2018). The influence of heavy metals, polyaromatic hydrocarbons, and polychlorinated biphenyls pollution on the development of antibiotic resistance in soils. *Environ. Sci. Pollut. Res.* 25, 9283–9292. doi: 10.1007/s11356-018-1465-9

Graham, D. W., Knapp, C. W., Christensen, B. T., McCluskey, S., and Dolfing, J. (2016). Appearance of β-lactam resistance genes in agricultural soils and clinical isolates over the 20th century. *Sci. Rep.* 16:21550. doi: 10.1038/srep21550

Gu, D., Dong, N., Zheng, Z., Lin, D., Huang, M., Wang, L., et al. (2018). A fatal outbreak of ST11 carbapenem-resistant hypervirulent *Klebsiella pneumoniae* in a Chinese hospital: a molecular epidemiological study. *Lancet Infect. Dis.* 18, 37–46. doi: 10.1016/s1473-3099(17)30489-9

Guo, H., Gu, J., Wang, X., Yu, J., Nasir, M., Peng, H., et al. (2019). Responses of antibiotic and heavy metal resistance genes to bamboo charcoal and bamboo vinegar during aerobic composting. *Environ. Pollut.* 252, 1097–1105. doi: 10.1016/j.envpol.2019.05.014

Guo, A., Gu, J., Wang, X., Zhang, R., Yin, Y., Sun, W., et al. (2017). Effects of superabsorbent polymers on the abundances of antibiotic resistance genes, mobile genetic elements, and the bacterial community during swine manure composting. *Bioresour. Technol.* 244, 658–663. doi: 10.1016/j.biortech.2017.08.016

Guo, J., Li, J., Chen, H., Bond, P. L., and Yuan, Z. (2017). Metagenomic analysis reveals wastewater treatment plants as hotspots of antibiotic resistance genes and mobile genetic elements. *Water Res.* 123, 468–478. doi: 10.1016/j.watres.2017.07.002

Guo, T., Lou, C., Zhai, W., Tang, X., Hashmi, M. Z., Murtaza, R., et al. (2018). Increased occurrence of heavy metals, antibiotics and resistance genes in surface soil after long-term application of manure. *Sci. Total Environ.* 635, 995–1003. doi: 10.1016/j.scitotenv.2018.04.194

Guo, A., Pan, C., Ma, J., and Bao, Y. (2020). Linkage of antibiotic resistance genes, associated bacteria communities and metabolites in the wheat rhizosphere from chlorpyrifos-contaminated soil. *Sci. Total Environ.* 741:140457. doi: 10.1016/j.scitotenv.2020.140457

Hall, B. G., and Barlow, M. (2004). Evolution of the serine beta-lactamases: past, present and future. *Drug Resist. Updat.* 7, 111–123. doi: 10.1016/j.drup.2004.02.003

Hammarlund, S. P., and Harcombe, W. R. (2019). Refining the stress gradient hypothesis in a microbial community. *Proc. Natl. Acad. Sci. U. S. A.* 116, 15760–15762. doi: 10.1073/pnas.1910420116

Han, X.-M., Hu, H. W., Shi, X. Z., Wang, J. T., Han, L. L., Chen, D., et al. (2016). Impacts of reclaimed water irrigation on soil antibiotic resistome in urban parks of Victoria, Australia. *Environ. Pollut.* 211, 48–57. doi: 10.1016/j.envpol.2015.12.033

Hu, Y., Liu, F., Lin, I. Y. C., Gao, G. F., and Zhu, B. (2016). Dissemination of the mcr-1 colistin resistance gene. *Lancet Infect. Dis.* 16, 146–147. doi: 10.1016/s1473-3099(15)00533-2

Hu, H.-W., Wang, J. T., Singh, B. K., Liu, Y. R., Chen, Y. L., Zhang, Y. J., et al. (2018). Diversity of herbaceous plants and bacterial communities regulates soil resistome across forest biomes. *Environ. Microbiol.* 20, 3186–3200. doi: 10.1111/1462-2920.14248

Hu, J., Zhao, F., Zhang, X. X., Li, K., Li, C., Ye, L., et al. (2018). Metagenomic profiling of ARGs in airborne particulate matters during a severe smog event. *Sci. Total Environ.* 615, 1332–1340. doi: 10.1016/j.scitotenv.2017.09.222

Hubbard, B. K., and Walsh, C. T. (2003). Vancomycin assembly: nature's way. *Angew. Chem. Int. Ed. Engl.* 42, 730–765. doi: 10.1002/anie.200390202

Hughes, V. M., and Datta, N. (1983). Conjugative plasmids in bacteria of the 'pre-antibiotic' era. *Nature* 302, 725–726. doi: 10.1038/302725a0

Jang, J., Kim, M., Baek, S., Shin, J., Shin, J., Shin, S. G., et al. (2021). Hydrometeorological influence on antibiotic-resistance genes (ARGs) and bacterial Community at a Recreational Beach in Korea. *J. Hazard. Mater.* 403:123599. doi: 10.1016/j.jhazmat.2020.123599

Johnson, T. A., Stedtfeld, R. D., Wang, Q., Cole, J. R., Hashsham, S. A., Looft, T., et al. (2016). Clusters of antibiotic resistance genes enriched together stay together in swine agriculture. *MBio* 7, e02214–e02215. doi: 10.1128/mBio.02214-15

Kang, F., Hu, X., Liu, J., and Gao, Y. (2015). Noncovalent binding of polycyclic aromatic hydrocarbons with genetic bases reducing the in vitro lateral transfer of antibiotic resistant genes. *Environ. Sci. Technol.* 49, 10340–10348. doi: 10.1021/acs.est.5b02293

Kiran, S., Swarnkar, M. K., Pal, M., Thakur, R., Tewari, R., Singh, A. K., et al. (2015). Complete genome sequencing of protease-producing novel *Arthrobacter* sp. strain IHBB 11108 using PacBio single-molecule real-time sequencing technology. *Genome. Announc.* 3:e00346-15. doi: 10.1128/genomeA.00346-15

Lee, K., and Gilmore, A. (2004). *Globalization and Infectious Diseases, A Review of the Linkages*, Training in Tropical Diseases, Switzerland.

Lemos, L. N., Pedrinho, A., Vasconcelos, A. T. R., Tsai, S. M., and Mendes, L. W. (2021). Amazon deforestation enriches antibiotic resistance genes. *Soil Biol. Biochem.* 153:108110. doi: 10.1016/j.soilbio.2020.108110

Li, B., Chen, Z., Zhang, F., Liu, Y., and Yan, T. (2020). Abundance, diversity and mobility potential of antibiotic resistance genes in pristine Tibetan plateau soil as revealed by soil metagenomics. *FEMS Microbiol. Ecol.* 96. doi: 10.1093/femsec/fiaa172

Li, A., Chen, L., Zhang, Y., Tao, Y., Xie, H., Li, S., et al. (2018). Occurrence and distribution of antibiotic resistance genes in the sediments of drinking water sources, urban rivers, and coastal areas in Zhuhai, China. *Environ. Sci. Pollut. Res.* 25, 26209–26217. doi: 10.1007/s11356-018-2664-0

Li, S., Yao, Q., Liu, J., Wei, D., Zhou, B., Zhu, P., et al. (2020). Profiles of antibiotic resistome with animal manure application in black soils of Northeast China. *J. Hazard. Mater.* 384:121216. doi: 10.1016/j.jhazmat.2019.121216

Liang, C., das, K. C., and McClendon, R. W. (2003). The influence of temperature and moisture contents regimes on the aerobic microbial activity of a biosolids composting blend. *Bioresour. Technol.* 86, 131–137. doi: 10.1016/s0960-8524(02)00153-0

Lima-Mendez, G., Faust, K., Henry, N., Decelle, J., Colin, S., Carcillo, F., et al. (2015). Determinants of community structure in the global plankton interactome. *Science* 348. doi: 10.1126/science.1262073

Lin, H., Sun, W., Zhang, Z., Chapman, S. J., Freitag, T. E., Fu, J., et al. (2016). Effects of manure and mineral fertilization strategies on soil antibiotic resistance gene levels and microbial community in a paddy-upland rotation system. *Environ. Pollut.* 211, 332–337. doi: 10.1016/j.envpol.2016.01.007

Linares, J. F., Gustafsson, I., Baquero, F., and Martinez, J. L. (2006). Antibiotics as intermicrobial signaling agents instead of weapons. *Proc. Natl. Acad. Sci. U. S. A.* 103, 19484–19489. doi: 10.1073/pnas.0608949103

Liu, W., Ling, N., Guo, J., Ruan, Y., Wang, M., Shen, Q., et al. (2021). Dynamics of the antibiotic resistome in agricultural soils amended with different sources of animal manures over three consecutive years. *J. Hazard. Mater.* 401:123399. doi: 10.1016/j.jhazmat.2020.123399

Marti, R., Tien, Y. C., Murray, R., Scott, A., Sabourin, L., and Topp, E. (2014). Safely coupling livestock and crop production systems: how rapidly do antibiotic resistance genes dissipate in soil following a commercial application of swine or dairy manure? *Appl. Environ. Microbiol.* 80, 3258–3265. doi: 10.1128/aem.00231-14

Martinez, J. L., Baquero, F., and Andersson, D. I. (2007). Predicting antibiotic resistance. *Nat. Rev. Microbiol.* 5, 958–965. doi: 10.1038/nrmicro1796

Martinez, J. L., Coque, T. M., and Baquero, F. (2015). What is a resistance gene? ranking risk in resistomes. *Nat. Rev. Microbiol.* 13, 116–123. doi: 10.1038/nrmicro3399

McCaig, A. E., Glover, L. A., and Prosser, J. I. (1999). Molecular analysis of bacterial community structure and diversity in unimproved and improved upland grass pastures. *Appl. Environ. Microbiol.* 65, 1721–1730. doi: 10.1128/AEM.65.4.1721-1730.1999

McIntyre, J. J., Bull, A. T., and Bunch, A. W. (1996). Vancomycin production in batch and continuous culture. *Biotechnol. Bioeng.* 49, 412–420. doi: 10.1002/(sici)1097-0290(19960220)49:4<412::Aid-bit8>3.0.Co;2-s

Meyers, M. A., Durso, L. M., Gilley, J. E., Waldrip, H. M., Castleberry, L., and Millmier-Schmidt, A. (2020). Antibiotic resistance gene profile changes in cropland soil after manure application and rainfall. *J. Environ. Qual.* 49, 754–761. doi: 10.1002/jeq2.20060

Mindlin, S. Z., Soina, V. S., Petrova, M. A., and Gorlenko, Z. M. (2008). Isolation of antibiotic resistance bacterial strains from eastern Siberia permafrost sediments. *Russ. J. Genet.* 44, 27–34. doi: 10.1134/s1022795408010043

Nathan, C. (2004). Antibiotics at the crossroads. *Nature* 431, 899–902. doi: 10.1038/431899a

Nesme, J., and Simonet, P. (2015). The soil resistome: a critical review on antibiotic resistance origins, ecology and dissemination potential in telluric bacteria. *Environ. Microbiol.* 17, 913–930. doi: 10.1111/1462-2920.12631

Newman, D. J., Cragg, G. M., and Snader, K. M. (2003). Natural products as sources of new drugs over the period 1981-2002. *J. Nat. Prod.* 66, 1022–1037c

O'Neill, J. (2016). *Tackling Drug-Resistant Infections Globally: Final Report and Recommendations*, 1–80.

Ouyang, W., Gao, B., Cheng, H., Zhang, L., Wang, Y., Lin, C., et al. (2020). Airborne bacterial communities and antibiotic resistance gene dynamics in PM2.5 during rainfall. *Environ. Int.* 134:105318. doi: 10.1016/j.envint.2019.105318

Pal, C., Asiani, K., Arya, S., Rensing, C., Stekel, D. J., Larsson, D. G. J., et al. (2017). Metal resistance and its association with antibiotic resistance. *Adv. Microb. Physiol.* 70, 261–313. doi: 10.1016/bs.ampbs.2017.02.001

Pehrsson, E. C., Tsukayama, P., Patel, S., Mejía-Bautista, M., Sosa-Soto, G., Navarrete, K. M., et al. (2016). Interconnected microbiomes and resistomes in low-income human habitats. *Nature* 533, 212–216. doi: 10.1038/nature17672

Penades, J. R., Chen, J., Quiles-Puchalt, N., Carpena, N., and Novick, R. P. (2015). Bacteriophage-mediated spread of bacterial virulence genes. *Curr. Opin. Microbiol.* 23, 171–178. doi: 10.1016/j.mib.2014.11.019

Peng, S., Feng, Y., Wang, Y., Guo, X., Chu, H., and Lin, X. (2017). Prevalence of antibiotic resistance genes in soils after continually applied with different manure for 30 years. *J. Hazard. Mater.* 340, 16–25. doi: 10.1016/j.jhazmat.2017.06.059

Perron, G. G., Whyte, L., Turnbaugh, P. J., Goordial, J., Hanage, W. P., Dantas, G., et al. (2015). Functional characterization of bacteria isolated from ancient Arctic soil exposes diverse resistance mechanisms to modern antibiotics. *PLoS One* 10:e0069533. doi: 10.1371/journal.pone.0069533

Poole, K. (2017). At the nexus of antibiotics and metals: the impact of cu and Zn on antibiotic activity and resistance. *Trends Microbiol.* 25, 820–832. doi: 10.1016/j.tim.2017.04.010

Qian, X., Gu, J., Sun, W., Wang, X. J., Su, J. Q., and Stedfeld, R. (2018). Diversity, abundance, and persistence of antibiotic resistance genes in various types of animal manure following industrial composting. *J. Hazard. Mater.* 344, 716–722. doi: 10.1016/j.jhazmat.2017.11.020

Qian, X., Gunturu, S., Guo, J., Chai, B., Cole, J. R., Gu, J., et al. (2021). Metagenomic analysis reveals the shared and distinct features of the soil resistome across tundra, temperate prairie, and tropical ecosystems. *Microbiome* 9:108. doi: 10.1186/s40168-021-01047-4

Qiao, L. K., Liu, X., Zhang, S., Zhang, L., Li, X., Hu, X., et al. (2021). Distribution of the microbial community and antibiotic resistance genes in farmland surrounding gold tailings: a metagenomics approach. *Sci. Total Environ.* 779:146502. doi: 10.1016/j.scitotenv.2021.146502

Rachakonda, S., and Cartee, L. (2004). Challenges in antimicrobial drug discovery and the potential of nucleoside antibiotics. *Curr. Med. Chem.* 11, 775–793. doi: 10.2174/0929867043455774

Radu, E., Woegerbauer, M., Rab, G., Oismüller, M., Strauss, P., Hufnagl, P., et al. (2021). Resilience of agricultural soils to antibiotic resistance genes introduced by agricultural management practices. *Sci. Total Environ.* 756:143699. doi: 10.1016/j.scitotenv.2020.143699

Rafiq, M., Hayat, M., Anesio, A. M., Jamil, S. U. U., Hassan, N., Shah, A. A., et al. (2017). Recovery of metallo-tolerant and antibiotic resistant psychrophilic bacteria from Siachen glacier, Pakistan. *PLoS One* 12:e0178180. doi: 10.1371/journal.pone.0178180

Rangasamy, K., Athiappan, M., Devarajan, N., Samykannu, G., Parray, J. A., Aruljothi, K. N., et al. (2018). Pesticide degrading natural multidrug resistance bacterial flora. *Microb. Pathog.* 114, 304–310. doi: 10.1016/j.micpath.2017.12.013

Razavi, M., Marathe, N. P., Gillings, M. R., Flach, C. F., Kristiansson, E., and Joakim Larsson, D. G. (2017). Discovery of the fourth mobile sulfonamide resistance gene. *Microbiome* 5:160. doi: 10.1186/s40168-017-0379-y

Reichel, R., Radl, V., Rosendahl, I., Albert, A., Amelung, W., Schloter, M., et al. (2014). Soil microbial community responses to antibiotic-contaminated manure under different soil moisture regimes. *Appl. Microbiol. Biotechnol.* 98, 6487–6495. doi: 10.1007/s00253-014-5717-4

Rizzo, L., Manaia, C., Merlin, C., Schwartz, T., Dagot, C., Ploy, M. C., et al. (2013). Urban wastewater treatment plants as hotspots for antibiotic resistant bacteria and genes spread into the environment: a review. *Sci. Total Environ.* 447, 345–360. doi: 10.1016/j.scitotenv.2013.01.032

Rossi, F., Rizzotti, L., Felis, G. E., and Torriani, S. (2014). Horizontal gene transfer among microorganisms in food: current knowledge and future perspectives. *Food Microbiol.* 42, 232–243. doi: 10.1016/j.fm.2014.04.004

Rousk, J., Bååth, E., Brookes, P. C., Lauber, C. L., Lozupone, C., Caporaso, J. G., et al. (2010). Soil bacterial and fungal communities across a pH gradient in an arable soil. *ISME J.* 4, 1340–1351. doi: 10.1038/ismej.2010.58

Seiler, C., and Berendonk, T. U. (2012). Heavy metal driven co-selection of antibiotic resistance in soil and water bodies impacted by agriculture and aquaculture. *Front. Microbiol.* 3. doi: 10.3389/fmicb.2012.00399

Shen, C., Xiong, J., Zhang, H., Feng, Y., Lin, X., Li, X., et al. (2013). Soil pH drives the spatial distribution of bacterial communities along elevation on Changbai Mountain. *Soil Biol. Biochem.* 57, 204–211. doi: 10.1016/j.soilbio.2012.07.013

Song, L., Li, L., Yang, S., Lan, J., He, H., McElmurry, S. P., et al. (2016). Sulfamethoxazole, tetracycline and oxytetracycline and related antibiotic resistance genes in a large-scale landfill, China. *Sci. Total Environ.* 551-552, 9–15. doi: 10.1016/j.scitotenv.2016.02.007

Song, M., Song, D., Jiang, L., Zhang, D., Sun, Y., Chen, G., et al. (2021). Large-scale biogeographical patterns of antibiotic resistome in the forest soils across China. *J. Hazard. Mater.* 403:123990. doi: 10.1016/j.jhazmat.2020.123990

Su, H.-C., Pan, C. G., Ying, G. G., Zhao, J. L., Zhou, L. J., Liu, Y. S., et al. (2014). Contamination profiles of antibiotic resistance genes in the sediments at a catchment scale. *Sci. Total Environ.* 490, 708–714. doi: 10.1016/j.scitotenv.2014.05.060

Sun, M., Ye, M., Wu, J., Feng, Y., Shen, F., Tian, D., et al. (2015a). Impact of bioaccessible pyrene on the abundance of antibiotic resistance genes during Sphingobium sp.- and sophorolipid-enhanced bioremediation in soil. *J. Hazard. Mater.* 300, 121–128. doi: 10.1016/j.jhazmat.2015.06.065

Sun, M., Ye, M., Wu, J., Feng, Y., Wan, J., Tian, D., et al. (2015b). Positive relationship detected between soil bioaccessible organic pollutants and antibiotic resistance genes at dairy farms in Nanjing, eastern China. *Environ. Pollut.* 206, 421–428. doi: 10.1016/j.envpol.2015.07.022

Sun, R., Zhang, X. X., Guo, X., Wang, D., and Chu, H. (2015c). Bacterial diversity in soils subjected to long-term chemical fertilization can be more stably maintained with the addition of livestock manure than wheat straw. *Soil Biol. Biochem.* 88, 9–18. doi: 10.1016/j.soilbio.2015.05.007

Tan, L., Li, L., Ashbolt, N., Wang, X., Cui, Y., Zhu, X., et al. (2018). Arctic antibiotic resistance gene contamination, a result of anthropogenic activities and natural origin. *Sci. Total Environ.* 621, 1176–1184. doi: 10.1016/j.scitotenv.2017.10.110

Tan, G. Y. A., Ward, A. C., and Goodfellow, M. (2006). Exploration of Amycolatopsis diversity in soil using genus-specific primers and novel selective media. *Syst. Appl. Microbiol.* 29, 557–569. doi: 10.1016/j.syapm.2006.01.007

Tello, A., Austin, B., and Telfer, T. C. (2012). Selective pressure of antibiotic pollution on bacteria of importance to public health. *Environ. Health Perspect.* 120, 1100–1106. doi: 10.1289/ehp.1104650

Tyrrell, C., Burgess, C. M., Brennan, F. P., and Walsh, F. (2019). Antibiotic resistance in grass and soil. *Biochem. Soc. Trans.* 47, 477–486. doi: 10.1042/bst20180552

Van Bambeke, F. (2004). Glycopeptides in clinical development: pharmacological profile and clinical perspectives. *Curr. Opin. Pharmacol.* 4, 471–478. doi: 10.1016/j.coph.2004.04.006

Van Boeckel, T. P., Brower, C., Gilbert, M., Grenfell, B. T., Levin, S. A., Robinson, T. P., et al. (2015). Global trends in antimicrobial use in food animals. *Proc. Natl. Acad. Sci. U. S. A.* 112, 5649–5654. doi: 10.1073/pnas.1503141112

Van Goethem, M. W., Pierneef, R., Bezuidt, O. K., Van De Peer, Y., Cowan, D. A., and Makhalanyane, T. P. (2018). A reservoir of 'historical' antibiotic resistance genes in remote pristine Antarctic soils. *Microbiome* 6. doi: 10.1186/s40168-018-0424-5

Vaz-Moreira, I., Varela, A. R., Pereira, T. V., Fochat, R. C., and Manaia, C. M. (2016). Multidrug resistance in quinolone-resistant gram-negative bacteria isolated from hospital effluent and the municipal wastewater treatment plant. *Microb. Drug Resist.* 22, 155–163. doi: 10.1089/mdr.2015.0118

Wang, L. (2019). *Study on Propagation Mechanism of Antibiotic Resistance Gene in Landfill Reactor and Effect of Leachate Recirculation*. Master, East China Normal University.

Wang, Q., Guo, S., Hou, Z., Lin, H., Liang, H., Wang, L., et al. (2021). Rainfall facilitates the transmission and proliferation of antibiotic resistance genes from ambient air to soil. *Sci. Total Environ.* 799:149260. doi: 10.1016/j.scitotenv.2021.149260

Wang, X., Lan, B., Fei, H., Wang, S., and Zhu, G. (2021). Heavy metal could drive co-selection of antibiotic resistance in terrestrial subsurface soils. *J. Hazard. Mater.* 411:124848. doi: 10.1016/j.jhazmat.2020.124848

Wang, F.-H., Qiao, M., Chen, Z., Su, J. Q., and Zhu, Y. G. (2015). Antibiotic resistance genes in manure-amended soil and vegetables at harvest. *J. Hazard. Mater.* 299, 215–221. doi: 10.1016/j.jhazmat.2015.05.028

Wang, J., Wang, J., Zhao, Z., Chen, J., Lu, H., Liu, G., et al. (2017). PAHs accelerate the propagation of antibiotic resistance genes in coastal water microbial community. *Environ. Pollut.* 231, 1145–1152. doi: 10.1016/j.envpol.2017.07.067

Wang, R., Zhang, J., Sui, Q., Wan, H., Tong, J., Chen, M., et al. (2016). Effect of red mud addition on tetracycline and copper resistance genes and microbial community during the full scale swine manure composting. *Bioresour. Technol.* 216, 1049–1057. doi: 10.1016/j.biortech.2016.06.012

Winokur, P. L., Vonstein, D. L., Hoffman, L. J., Uhlenhopp, E. K., and Doern, G. V. (2001). Evidence for transfer of CMY-2 amp C beta-lactamase plasmids between Escherichia coli and salmonella isolates from food animals and humans. *Antimicrob. Agents Chemother.* 45, 2716–2722. doi: 10.1128/aac.45.10.2716-2722.2001

World Bank, T. W. (2017). *Drug-Resistant Infections. A Threat to Our Economic Future*. Washington, DC: World Bank Group.

Wright, G. D. (2007). The antibiotic resistome: the nexus of chemical and genetic diversity. *Nat. Rev. Microbiol.* 5, 175–186. doi: 10.1038/nrmicro1614

Xiao, K.-Q., Bao, P., Bao, Q. L., Jia, Y., Huang, F. Y., Su, J. Q., et al. (2014). Quantitative analyses of ribulose-1, 5-bisphosphate carboxylase/oxygenase (Rubis CO) large-subunit genes (cbb L) in typical paddy soils. *FEMS Microbiol. Ecol.* 87, 89–101. doi: 10.1111/1574-6941.12193

Xiao, K.-Q., Li, B., Ma, L., Bao, P., Zhou, X., Zhang, T., et al. (2016). Metagenomic profiles of antibiotic resistance genes in paddy soils from South China. *FEMS Microbiol. Ecol.* 92. doi: 10.1093/femsec/fiw023

Xie, W.-Y., Yuan, S. T., Xu, M. G., Yang, X. P., Shen, Q. R., Zhang, W. W., et al. (2018). Long-term effects of manure and chemical fertilizers on soil antibiotic resistome. *Soil Biol. Biochem.* 122, 111–119. doi: 10.1016/j.soilbio.2018.04.009

Xu, S., Qasim, M. Z., Zhang, T., Wang, R., Li, C., and Ge, S. (2021). Diversity, abundance and expression of the antibiotic resistance genes in a Chinese landfill: effect of deposit age. *J. Hazard. Mater.* 417:126027. doi: 10.1016/j.jhazmat.2021.126027

Yan, Z.-Z., Chen, Q. L., Li, C. Y., Nguyen, B. A. T., Zhu, Y. G., He, J. Z., et al. (2021). Termite mound formation reduces the abundance and diversity of soil resistomes. *Environ. Microbiol.* 23, 7661–7670. doi: 10.1111/1462-2920.15631

Yan, Z.-Z., Chen, Q. L., Zhang, Y. J., He, J. Z., and Hu, H. W. (2019). Antibiotic resistance in urban green spaces mirrors the pattern of industrial distribution. *Environ. Int.* 132:105106. doi: 10.1016/j.envint.2019.105106

Yang, Y., Liu, G., Ye, C., and Liu, W. (2019). Bacterial community and climate change implication affected the diversity and abundance of antibiotic resistance genes in wetlands on the Qinghai-Tibetan plateau. *J. Hazard. Mater.* 361, 283–293. doi: 10.1016/j.jhazmat.2018.09.002

Zhang, Y., Cong, J., Lu, H., Li, G., Qu, Y., Su, X., et al. (2014). Community structure and elevational diversity patterns of soil Acidobacteria. *J. Environ. Sci.* 26, 1717–1724. doi: 10.1016/j.jes.2014.06.012

Zhang, M., He, L. Y., Liu, Y. S., Zhao, J. L., Liu, W. R., Zhang, J. N., et al. (2019). Fate of veterinary antibiotics during animal manure composting. *Sci. Total Environ.* 650, 1363–1370. doi: 10.1016/j.scitotenv.2018.09.147

Zhang, M., He, L. Y., Liu, Y. S., Zhao, J. L., Zhang, J. N., Chen, J., et al. (2020). Variation of antibiotic resistome during commercial livestock manure composting. *Environ. Int.* 136:105458. doi: 10.1016/j.envint.2020.105458

Zhang, Y.-J., Hu, H. W., Yan, H., Wang, J. T., Lam, S. K., Chen, Q. L., et al. (2019). Salinity as a predominant factor modulating the distribution patterns of antibiotic resistance genes in ocean and river beach soils. *Sci. Total Environ.* 668, 193–203. doi: 10.1016/j.scitotenv.2019.02.454

Zhang, L., Kinkelaar, D., Huang, Y., Li, Y., Li, X., and Wang, H. H. (2011). Acquired antibiotic resistance: are we born with it? *Appl. Environ. Microbiol.* 77, 7134–7141. doi: 10.1128/aem.05087-11

Zhang, W.-G., Wen, T., Liu, L. Z., Li, J. Y., Gao, Y., Zhu, D., et al. (2021). Agricultural land-use change and rotation system exert considerable influences on the soil antibiotic resistome in Lake Tai Basin. *Sci. Total Environ.* 771:144848. doi: 10.1016/j.scitotenv.2020.144848

Zhang, Q.-Q., Ying, G. G., Pan, C. G., Liu, Y. S., and Zhao, J. L. (2015). Comprehensive evaluation of antibiotics emission and fate in the river basins of China: source analysis, multimedia modeling, and linkage to bacterial resistance. *Environ. Sci. Technol.* 49, 6772–6782. doi: 10.1021/acs.est.5b00729

Zhao, Y., Cocerva, T., Cox, S., Tardif, S., Su, J. Q., Zhu, Y. G., et al. (2019). Evidence for co-selection of antibiotic resistance genes and mobile genetic elements in metal polluted urban soils. *Sci. Total Environ.* 656, 512–520. doi: 10.1016/j.scitotenv.2018.11.372

Zhao, R., Feng, J., Liu, J., Fu, W., Li, X., and Li, B. (2019). Deciphering of microbial community and antibiotic resistance genes in activated sludge reactors under high selective pressure of different antibiotics. *Water Res.* 151, 388–402. doi: 10.1016/j.watres.2018.12.034

Zhao, X., Shen, J. P., Zhang, L. M., du, S., Hu, H. W., and He, J. Z. (2020). Arsenic and cadmium as predominant factors shaping the distribution patterns of antibiotic resistance genes in polluted paddy soils. *J. Hazard. Mater.* 389:121838. doi: 10.1016/j.jhazmat.2019.121838

Zheng, Y., Yu, S., Wang, G., Xie, F., Xu, H., du, S., et al. (2021). Comparative microbial antibiotic resistome between urban and deep forest environments. *Environ. Microbiol. Rep.* 13, 503–508. doi: 10.1111/1758-2229.12942

Zheng, J., Zhou, Z., Wei, Y., Chen, T., Feng, W., and Chen, H. (2018). High-throughput profiling of seasonal variations of antibiotic resistance gene transport in a peri-urban river. *Environ. Int.* 114, 87–94. doi: 10.1016/j.envint.2018.02.039

frontiers | Frontiers in Microbiology

TYPE Original Research
PUBLISHED 24 October 2022
DOI 10.3389/fmicb.2022.1018682



OPEN ACCESS

EDITED BY
Haihong Hao,
Huazhong Agricultural University,
China

REVIEWED BY
Tao He,
Jiangsu Academy of Agricultural Sciences (JAAS), China
Basil Britto Xavier,
University of Antwerp,
Belgium

*CORRESPONDENCE
Zhangnv Yang
znyang@cdc.zj.cn
Biao Tang
tangbiao@zaas.ac.cn
Min Yue
myue@zju.edu.cn

†These authors have contributed equally to this work

SPECIALTY SECTION
This article was submitted to Antimicrobials, Resistance and Chemotherapy, a section of the journal Frontiers in Microbiology

RECEIVED 13 August 2022
ACCEPTED 06 October 2022
PUBLISHED 24 October 2022

CITATION
Zhou W, Lin R, Zhou Z, Ma J, Lin H, Zheng X, Wang J, Wu J, Dong Y, Jiang H, Yang H, Yang Z, Tang B and Yue M (2022) Antimicrobial resistance and genomic characterization of *Escherichia coli* from pigs and chickens in Zhejiang, China. *Front. Microbiol.* 13:1018682. doi: 10.3389/fmicb.2022.1018682



# Antimicrobial resistance and genomic characterization of *Escherichia coli* from pigs and chickens in Zhejiang, China

Wei Zhou[1†], Rumeng Lin[2,3,4†], Zhijin Zhou[1], Jiangang Ma[2], Hui Lin[2,5], Xue Zheng[2], Jingge Wang[2], Jing Wu[2], Yuzhi Dong[2,4], Han Jiang[4], Hua Yang[2], Zhangnv Yang[6*], Biao Tang[2*] and Min Yue[7*]

[1]Zhejiang Provincial Center for Animal Disease Prevention and Control, Hangzhou, China, [2]State Key Laboratory for Managing Biotic and Chemical Threats to the Quality and Safety of Agro-Products, Institute of Agro-Product Safety and Nutrition, Zhejiang Academy of Agricultural Sciences, Hangzhou, China, [3]School of Food Science and Technology, Jiangnan University, Wuxi, China, [4]Key Laboratory of Marine Food Quality and Hazard Controlling Technology of Zhejiang Province, China Jiliang University, Hangzhou, China, [5]The Institute of Environment, Resource, Soil and Fertilizers, Zhejiang Academy of Agricultural Sciences, Hangzhou, China, [6]Zhejiang Provincial Center for Disease Control and Prevention, Hangzhou, China, [7]Department of Veterinary Medicine, Institute of Preventive Veterinary Sciences, Zhejiang University College of Animal Sciences, Hangzhou, Zhejiang, China

*Escherichia coli* is considered an opportunistic pathogen and an indicator for antimicrobial resistance (AMR) monitoring. Despite many reports on its AMR monitoring, studies based on genome-based analysis of AMR genes are still insufficient. Here, 181 *E. coli* strains were isolated from anal swab samples collected from pigs and chickens of animal farms located in Eastern China and sequenced through the Illumina platform. The results showed that 87.85% (159/181) of the *E. coli* isolates were multidrug-resistant (MDR). Ampicillin (AMP)- spectinomycin (SPT)- tetracycline (TET)- florfenicol (FFC)- sulfisoxazole (SF)- trimethoprim/sulfamethoxazole (SXT) was the predominant AMR pattern. By whole-genome sequencing, we found that ST10 (10.49%, 19/181) and ST48 (7.18%, 13/181) were major sequence types. IncFIB and IncX1 were the most prevalent plasmid replicons. The AMR genes $bla_{NDM-5}$ (1.10%, 2/181), *mcr*-1 (1.10%, 2/181), *tet*(X4) (1.10%, 2/181), and *cfr* (6.08%, 11/181) were also found in these isolates. In addition, among the 169 virulence genes detected, we identified *ast*A (37.02%, 67/181), *hly*A (1.66%, 3/181), *hly*B (1.66%, 3/181) and *hly*D (1.66%, 3/181), which were closely related to heat-stable enterotoxin 1 and α-hemolysin. In addition, there were 33 virulence genes associated with the iron uptake system, and 46 were adhesion-related genes. Our study highlighted the need for routine surveillance of AMR with advanced genomic approaches, providing up-to-date data on the prevalence of AMR for the development and execution of antimicrobial stewardship policy.

KEYWORDS

***Escherichia coli*, animal origin, antimicrobial resistance, genomic characterization, virulence genes**

# Introduction

The recent emergence and rapid increase of multi-drug resistant (MDR, resistance to more than three kinds of antibiotics) bacteria have caused public concern, represented by *Escherichia coli* resistant to carbapenem, colistin and tigecycline which were recognized as the last line of resort (Li et al., 2017; He et al., 2019; Ma et al., 2022). Due to incorrect use and misuse of antibiotics, the spread of antimicrobial resistance (AMR) is accelerating (Wang et al., 2022; Tang et al., 2022a,b). The continuous spread of AMR not only increases the difficulty of preventing and controlling livestock and poultry diseases but also seriously threatens livestock products' safety and endangers consumers' health (Xu et al., 2022; Li et al., 2022a).

*E. coli* is a commonly used AMR indicator in human and food animal (Brisola et al., 2019; Ma et al., 2022). There have been many reports on the study in *E. coli* and monitoring of the spread of AMR. The emergence of plasmid-mediated carbapenem resistance genes, especially $bla_{NDM}$, has seriously affected the efficacy of meropenem (0.4%, 1/219; Tang et al., 2019, 2021b). Colistin resistance mediated by a plasmid-encoded *mcr*-1 was first documented in China during routine surveillance of food animals (21%, 166/804; Liu et al., 2016). A retrospective survey showed that *mcr*-1 was first traced back to 1980 but was not prevalent among bacteria until 2009 (Shen et al., 2016). With the detection rate of *mcr*-1 in bacteria increasing year by year, a relatively high occurrence rate of the *mcr*-1 gene (1%) was detected from *E. coli* in human (Wang et al., 2017). Tigecycline resistance are mediated by two novel genes, *tet*(X3) and *tet*(X4), both of which can significantly reduce the efficacy of tigecycline (He et al., 2019; Sun et al., 2019; Guan et al., 2022). Additionally, bacterial strains carrying the *cfr* gene encoding 23S rRNA methylase, which is resistant to five classes of antimicrobials, including phenols, lincosamides, oxazolidinones, pleuromutilin, and streptomycin A,allowing bacteria to develop MDR (Deng et al., 2014; Tang et al., 2022c).

Whole genome sequencing (WGS) played a vital role in AMR study (Tang et al., 2020b; Peng X. et al., 2022; Li et al., 2022b). We can obtain the tested strains' AMR and virulence genes by combining them with the antimicrobial sensitivity test (AST). It is helpful to better understand AMR's development and transmission (Teng et al., 2022). WGS has become an indispensable and reliable tool for revealing the AMR mechanism in global pathogen surveillance (Boolchandani et al., 2019; Tang et al., 2021a; Yang et al., 2022).

In this study, we investigated the prevalence of AMR *E. coli* in pigs and chickens from animal farms in Eastern China and evaluated the AMR phenotypes, genotypes, virulence genes, and plasmids replicons. This study helps understand the AMR situation and provides a reference to formulate livestock AMR control policies to better protect food safety in China.

# Materials and methods

## Sample collection and strain isolation

A total of 200 anal swab samples were collected from three cities (Lishui, Jinhua, and Quzhou) located in Zhejiang Province, Eastern China, from March to April 2021. The samples were randomly collected from 110 chickens and 90 pigs in 5 poultry farms and 4 swine farms, respectively (Table 1; Figure 1A). All experiment activities in this study were approved by the Institutional Review Board of Zhejiang Academy of Agricultural Sciences.

Anal swab samples were enriched in 10 ml of buffered peptone solution (BPW, Land Bridge, Beijing, China). After initial pre-enrichment in BPW, 0.1 ml of enriched samples were streaked on MacConkey Agar (Land Bridge, Beijing, China) or Eosin Methylene Blue Agar (Land Bridge, Beijing, China) and incubated at 37°C for 24 h. Only one suspicious colony (round, moist, and show pink color on MacConkey Agar; purple-black color with green metallic sheen on EMB Agar) were selected and further cultured on Luria-Bertani (LB) Agar (Land Bridge, Beijing, China). Bacteria identification was carried out by MALDI-TOF MS. Confirmed isolates were stored at −80°C.

## Antimicrobial sensitivity testing

Micro-broth dilution method was used (Bio Fosun, Fosun Diagnostics, Shanghai, China) to determine the AMR profile of *E. coli* isolates (Tang et al., 2022b). The panel of antimicrobial compounds tested included ampicillin (AMP), augmentin (amoxicillin/clavulanic acid, A/C), gentamicin (GEM), tetracycline (TET), spectinomycin (SPT), florfenicol (FFC), sulfisoxazole (SF), trimethoprim/sulfamethoxazole (SXT), ceftiofur (CEF), ceftazidime (CAZ), enrofloxacin (ENR), ofloxacin (OFL), meropenem (MEM), ampicillin (APR), colistin (CL) and mequindox (MEQ). The 14 tested antibiotics are grouped into 9 classes (Figure 1B), including penicillins (AMP and A/C), aminoglycosides (GEM、SPT, and CEF), cephalosporins (CAZ), carbapenems (MEM), sulfonamides (SF and SXT), quinolones (ENR and OFL),

TABLE 1 Source of 200 samples and isolation of 181 *E. coli* strains.

| City | Number of farm | Animal | Number | Isolated strains | Separation rate (%) |
|---|---|---|---|---|---|
| Lishui | 2 | Chicken | 50 | 46 | 92.00 |
| | 1 | Pig | 25 | 21 | 84.00 |
| Quzhou | 1 | Chicken | 20 | 19 | 95.00 |
| | 2 | Pig | 40 | 39 | 97.50 |
| Jinhua | 2 | Chicken | 40 | 31 | 77.50 |
| | 1 | Pig | 25 | 25 | 100.00 |

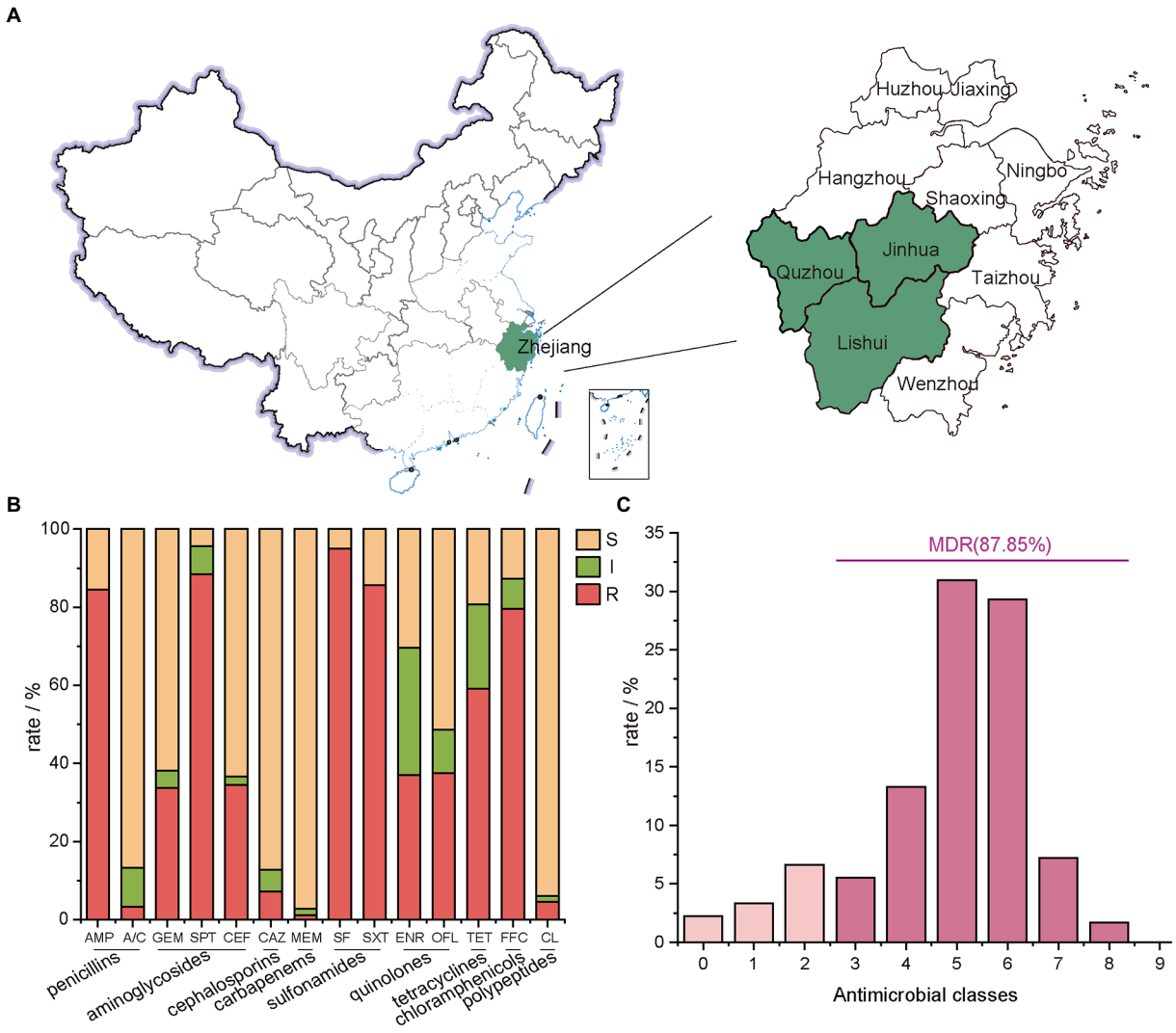


FIGURE 1
Geographical distribution of the sampling areas in Zhejiang Provinces, China, and AMR rates of *E. coli* isolates. **(A)** Sample sources of 181 strains of *E. coli*, Zhejiang Province in this study are shaded in green; **(B)** the number of *E. coli* isolates from farms in Zhejiang Province resistant to different antibiotics. In this experiment, 14 antibiotics with inflection points were divided into 9 categories; **(C)** the distribution of MDR strains.

tetracyclines (TET), chloramphenicols (FFC) and polypeptides (CL). The breakpoint for each antimicrobial was from the Clinical and Laboratory Standards Institute (CLSI, 2016:M100-S30). *E. coli* ATCC 25922 was used as quality control.

## Whole genome sequencing and bioinformatics analysis

The genomic DNA extraction of *E. coli* was performed using a bacterial DNA extraction kit (Generay, Shanghai, China). The whole genome sequencing was performed on the Novaseq 6,000 (Illumina, SanDiego, CA, United States). Clean reads were assembled using SPAdesv3.12.0 (Bankevich et al., 2012). Genome annotation was performed using the NCBI Prokaryotic Genome Annotation Pipeline (Tatusova et al., 2016). ABRicate 1.0.1 tool[1] and VFDB database were applied to predict the virulence genes and AMR genes. Replicons and sequence type (ST) were determined at the Center for Genomic Epidemiology (CGE).[2] Phylogenetic analysis of the genome and plasmids was performed by kSNP 3.1 software based on the maximum-likelihood method (Gardner et al., 2015). Easyfig 2.2.5 was used for comparative analysis of the plasmids (Sullivan et al., 2011).

1 https://github.com/tseemann/abricate
2 http://www.genomicepidemiology.org/services/

## Statistical analysis

TBtools was used for clustering heat map analysis of AMR genes, AMR phenotypes, virulence genes, and plasmid replicons (Chen et al., 2020).

# Results

## Prevalence and AMR of *Escherichia coli* isolates

A total of 181 *E. coli* strains were isolated from all 200 anal swab samples with a detection rate of 90.50%. Among them, 96 isolates were from chickens, and 85 isolates were from pigs (Table 1).

*E. coli* isolates showed the lowest resistance rate to MEM at 2.76%, followed by A/C at 3.31%, CL at 5.52%, and CAZ at 7.18% (Figure 1B). A high resistance rate was shown for five antibiotics in descending order. They were SF (95.03%), SPT (88.40%), SXT (85.64%), AMP (84.53%) and FFC (79.56%). Except for TET with a resistance rate of 59.12%, the resistance rates of *E. coli* isolates to OFL, ENR, CEF and GEM ranged between 35.0%~40.0% (Figure 2).

The 14 tested antibiotics are grouped into 9 classes (Figure 1B), including penicillins (AMP and A/C), aminoglycosides (GEM、SPT, and CEF), cephalosporins (CAZ), carbapenems (MEM), sulfonamides (SF and SXT), quinolones (ENR and OFL), tetracyclines (TET), chloramphenicols (FFC) and polypeptides (CL). Carbapenems class of antibiotics, which in this study is MEM had the lowest resistance rate. Meanwhile, the sulfonamides class of antibiotics had the highest resistance rate with 181 resistant isolates, of which 172 were resistant to SF.

87.85% of isolates were MDR (Figure 1C; Supplementary Table S1), and the predominant MDR pattern (19.50%, 31/159) was resistance to AMP-SPT-TET-FFC-SF-SXT. Notably, three strains were determined to be resistant to 12 types of antibiotics. The patterns were AMP-A/C-GEM-SPT-TET-FFC-SF-SXT-CEF-CAZ-ENR-OFL and AMP-GEM-SPT-TET-FFC-SF-SXT-CEF-CAZ-ENR-OFL-CL, respectively.

## Genomic characterization of *Escherichia coli* isolates

Sixty-five different sequence types (STs) were generated in 181 *E. coli* isolates (Figure 3), which were further grouped into 16 clonal complexes (CCs) and 38 singletons. Among them, ST10 was most prevalent with 19 isolates (10.50%), followed by ST48 with 13 isolates (7.18%), ST58 and ST162 both with 9 isolates (4.97%).

The plasmid replicon analysis (Figure 4) showed that a total of 40 types of plasmid replicons were detected in all 181 *E. coli* isolates, of which 107 (59.12%) carried the IncFIB (AP001918) replicon, followed by IncX1 replicon existing in 86 isolates (47.51%). 94.48% (171/181) of the isolates carried 2~6 replicons. Similar plasmid replicon types can be found in different cities and animals, suggesting that plasmids carrying AMR genes may be widely spread through horizontal gene transfer.

As shown in Figure 5, 72 acquired AMR genes were detected in this study, among which *mdf*(A) was carried by all isolates. Notably, two isolates carried carbapenem resistance gene $bla_{\text{NDM-5}}$, two isolates carried colistin resistance gene *mcr*-1, six isolates carried tigecycline resistance gene *tet*(X4), and eleven isolates carried linezolid resistance gene *cfr*.

One hundred and sixty-nine virulence genes were found (Figure 6). Ten including *ent*A, *ent*B, *ent*D, *ent*E, *ent*F, *fep*A, *fep*C, *fep*D, *fes* and *omp*A were detected in all isolates. The virulence genes carried by the other isolates ranged from 25 to 77. The encoding gene *ast*A of heat-stable enterotoxin1 (East1) was detected in 37.02% (67/181) of the isolates. Three α-hemolysin encoding genes: *hly*A, *hly*B and *hly*D, were present simultaneously in isolates ECLSZ21-06, ECQZZ21-39, and ECJHZ21-15. Thirty-three virulence genes detected here were related to the iron uptake system, and 46 were adhesion-associated genes.

In this study, we found that strains ECJHJ21-07 and ECJHJ21-14 carry the $bla_{\text{NDM-5}}$ gene and have the same genetic context $bla_{\text{NDM-5}}$-*ble-trpF-dsbD*. Strains ECLSZ21-04, ECLSZ21-15, ECQZZ21-02, ECQZZ21-05, ECQZZ21-04, and ECQZZ21-15 contain the *tet*(X4) gene, which is all adjacent to the *estX* gene. In the latter two strains, the *tet*(X4) gene is located in the gene arrangement *estX*-*tet*(X4)-IS*Vsa3* based on better sequencing quality. In addition, we found two strains carrying the *mcr-1* gene, which have different genetic environments. The *mcr-1*-carrying plasmid in strain ECJHJ21-13 is homologous with plasmids pMCR4D31–3 and pHNSHP45 with an IncI2 type; the fragment harboring *mcr-1* gene in strain ECQZJ21-13 is homologous with the IncHI2 plasmid (Figure 7).

Strains from different cities can gather on the same branch. As the last line of drugs, the AMR genes *mcr*-1, $bla_{\text{NDM}}$, and *tet*(X4) are distributed in different branches, showing different genetic relationships (Figure 8). In the present study, these AMR genes are more likely to be horizontal gene transfer between *E. coli* strains. In addition, the *cfr* gene mainly exists in two branches, which may be the clonal transmission (Figure 8).

## Analysis of genotypes and phenotypes of AMR *Escherichia coli* isolates

The highest concordance between genotype and phenotype was detected for carbapenems (100.00%), followed by polypeptides (93.92%), and tetracyclines (90.61%; Supplementary Table S2). In addition, two isolates carrying $bla_{\text{NDM-5}}$ gene were found resistant to AMP, CEF, TET, FFC, SF, SXT, ENR, and OFL. All eleven isolates carrying the *cfr* gene showed resistance to AMP, SF, and SXT. Similarly, the isolates carrying *mcr*-1 showed resistance to AMP, TET, FFC, SF, CEF, ENR, and OFL, and the isolates carrying *tet*(X4) showed resistance to SPT, TET, FFC, SF, and SXT. These

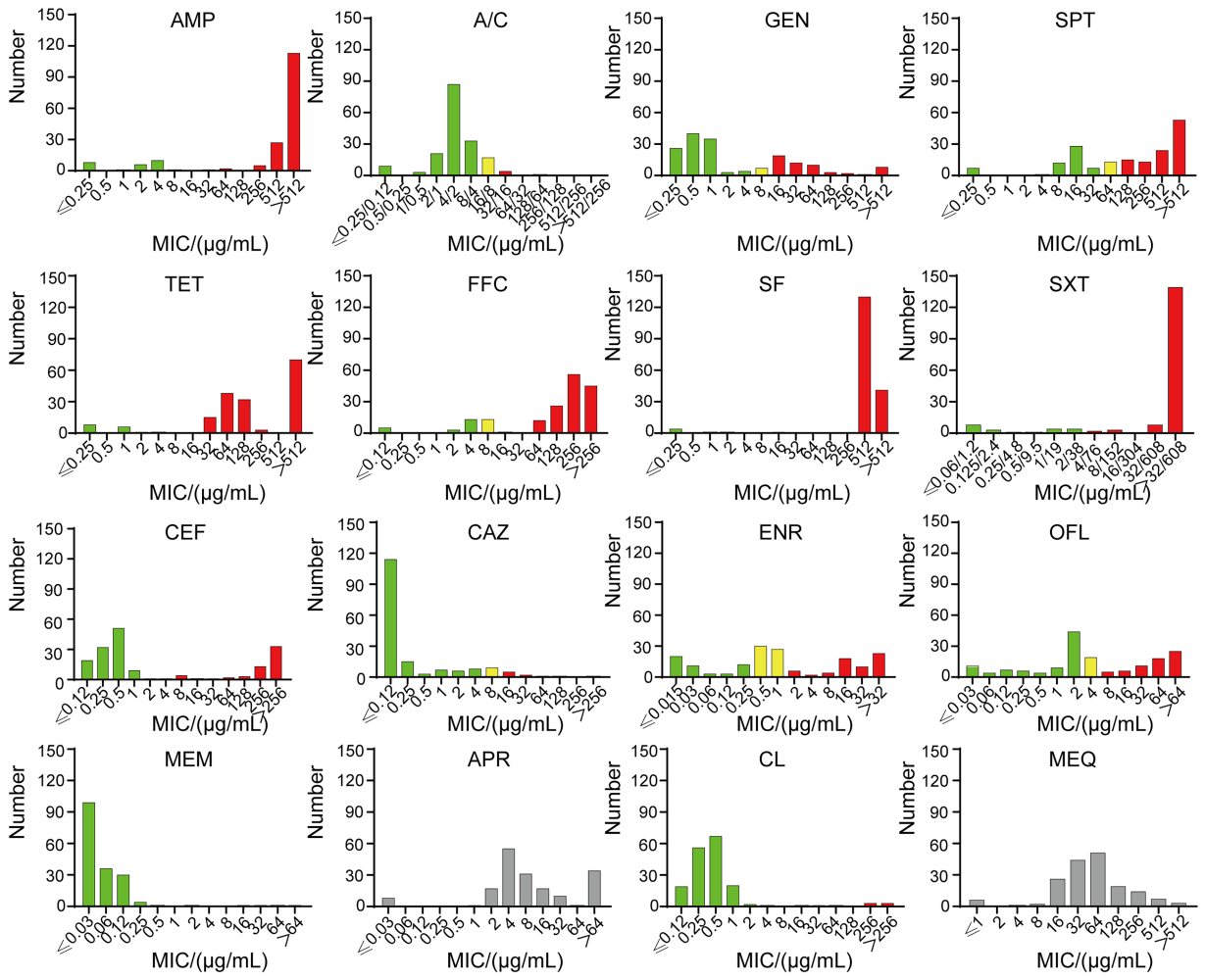


FIGURE 2
The MICs of 181 strains. Green indicates sensitivity, yellow indicates intermediary, and red indicates resistance. SF and SXT have no intermediate value, and APR and MEQ have no breakpoint. Ampicillin (AMP), amoxicillin/clavulanic acid (A/C), gentamicin (GEM), tetracycline (TET), spectinomycin (SPT), florfenicol (FFC), sulfisoxazole (SF), trimethoprim/sulfamethoxazole (SXT), ceftiofur (CEF), ceftazidime (CAZ), enrofloxacin (ENR), ofloxacin (OFL), meropenem (MEM), apramycin (APR), colistin (CL) and mequindox (MEQ).

provide supporting evidence for AMR genes to explain drug resistance. The AMR gene *cfr* mainly existed in two STs, ST2161 and ST162. Two isolates carrying the $bla_{NDM-5}$ were both assigned ST93. Isolates carrying *mcr*-1 belonged to ST2973 (ECJHJ21-13) and ST354 (ECQZJ21-13), respectively (Figure 3). Meanwhile, the isolates carrying *tet*(X4) demonstrated sequence type diversity, ST195, ST48, ST5873 and ST7136 were included.

## Discussion

The AMR of *E. coli* has become a worldwide public health problem (Rutuja et al., 2018). Pigs and poultry products may have a cross infection of AMR *E.coli* during processing and subsequent sale, which increases the risk of transmission and poses a significant threat to the sale of products and people's health (Chang et al., 2020). To understand the current situation of AMR of *E. coli*, we analyzed AMR, MLST and virulence genes of *E. coli* isolated from anal swab samples of pigs and chickens in farms in Lishui, Quzhou and Jinhua, Zhejiang Province, Eastern China. In this study, relatively high AMR rates of FFC (79.56%), SXT (85.64%), SF (95.03%), SPT (88.40%) and AMP (84.53%) were detected that were consistent with the previously published results (Ma et al., 2022; Peng Z. et al., 2022). At the same time, the AMR rates of A/C (3.31%), MEM (2.76%), CL (5.52%) and CAZ (7.18%) were low. CL and MEM are recognized as the last line of defense against gram-negative bacteria (Lin et al., 2022; Wang et al., 2022) and low AMR rates reveal their resistance's effectiveness is decreasing.

Genomic analysis revealed that the *E. coli* isolates harbored various AMR genes, which could be consistent with the AMR phenotype. All *E. coli* isolates contained the AMR gene *mdf*(A), and most of them also carried *tet*(A) (68.51%, 124/181), *flo*R (62.98%, 114/181) and *sul*2 (56.35%, 102/181). These genes

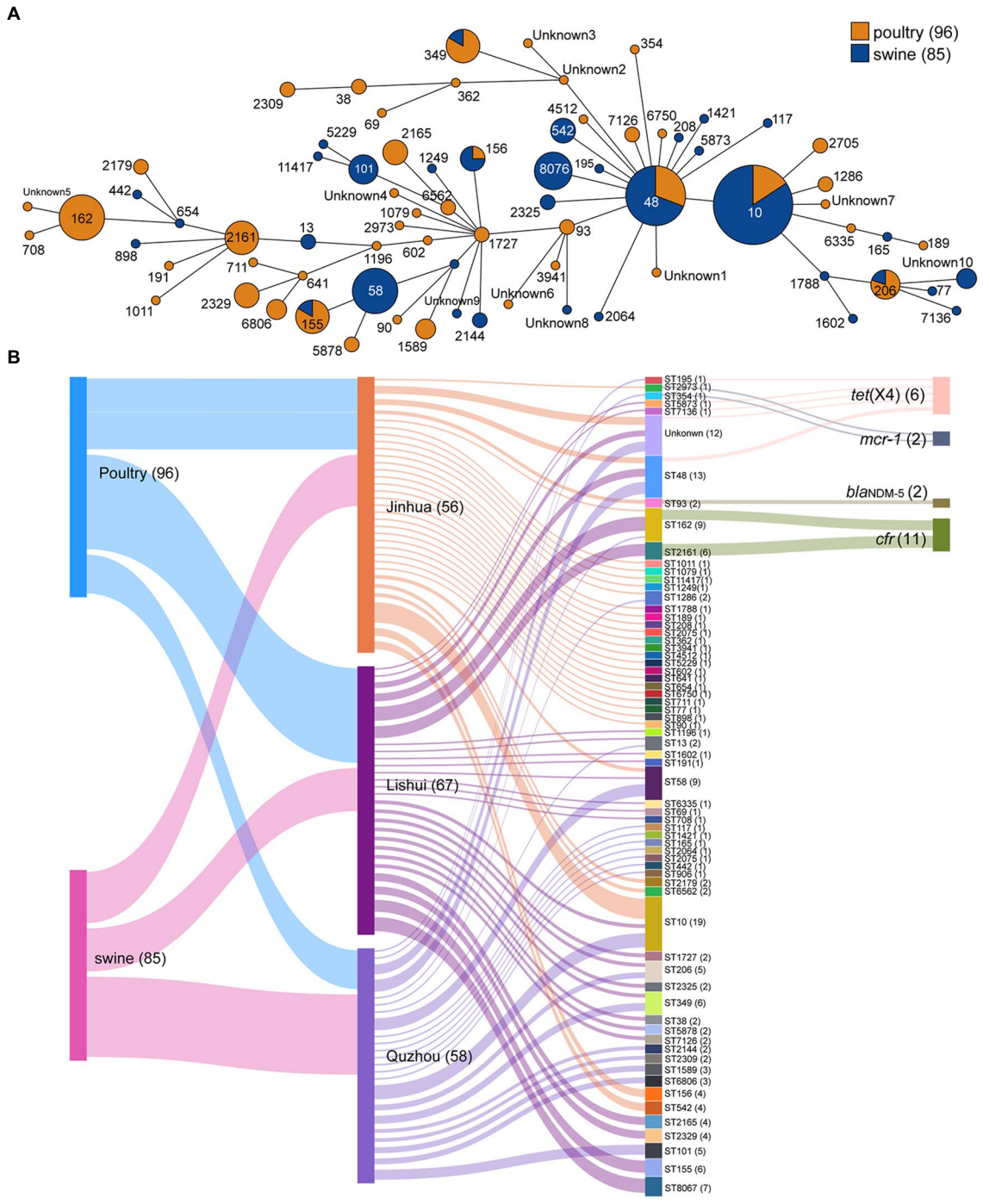


FIGURE 3
Minimum spanning tree of *E. coli* strains based on MLST and Sankey diagram combining the provinces, STs, farms, and sampling sources based on 181 *E. coli* isolates. **(A)** Each node represents a single ST. The size of the nodes is proportional to the number of isolates. The length of branches between each node is proportional to the number of different alleles that differ between two linked nodes; **(B)** the diameter of the line is directly proportional to the number of isolates, which is also marked with numbers. The lines are colored according to the city and the sampling source.

mediate resistance to tetracycline, chloramphenicol, and sulfonamide antibiotics. These critical AMR genes in *E. coli* isolates from food animals present a tremendous public health concern. It's important to mention that the acquired AMR genes in bacterial genomes do not inevitably confer phenotypic resistance and vice versa (Boolchandani et al., 2019; Tang et al., 2022a). Other mechanisms such as SNPs and MDRtransporter also significantly contribute to the phenotypic resistance (Boolchandani et al., 2019). The phenotypic confirmation is still essential for validating of AMR profiles. As we found in this study,

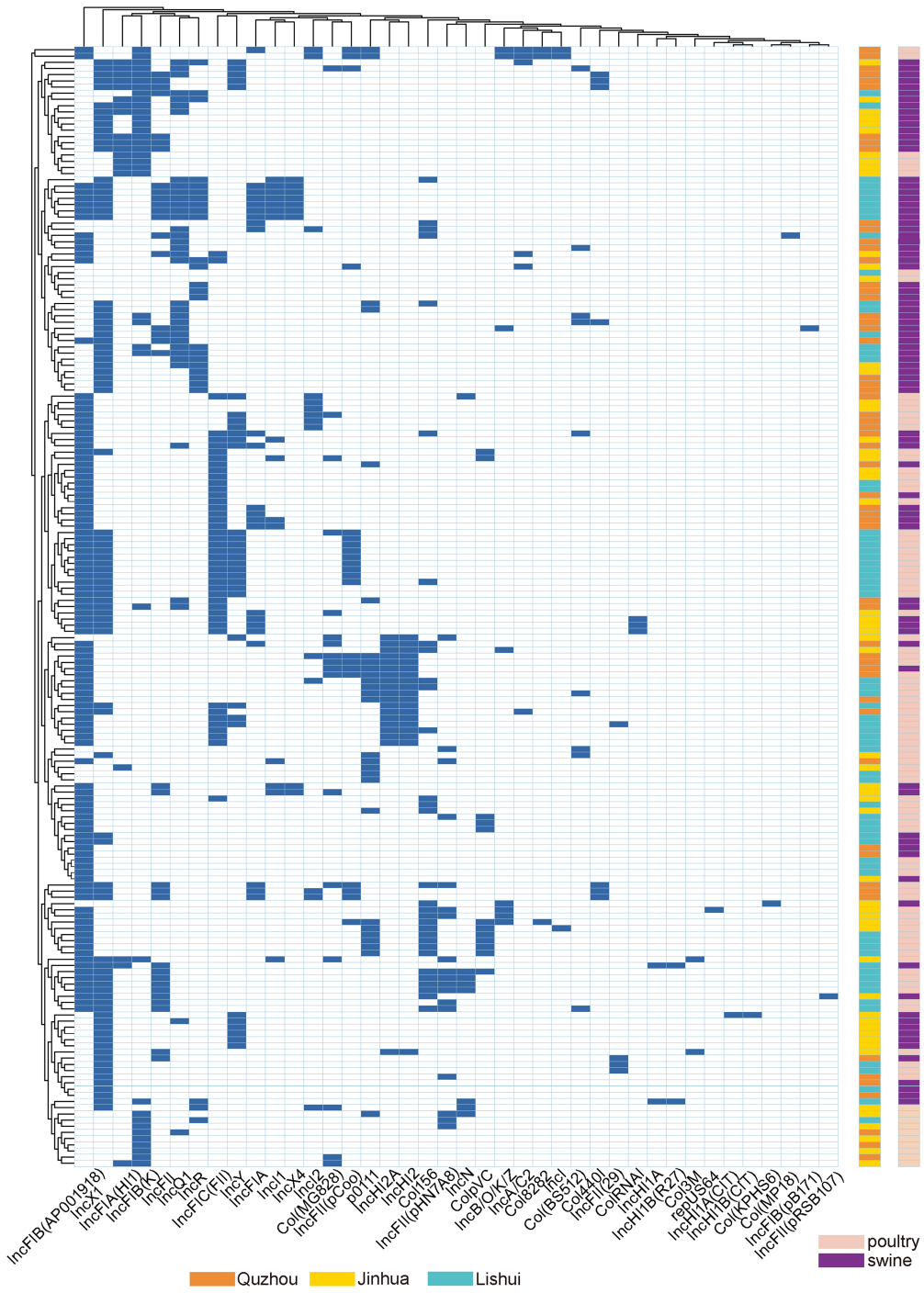


FIGURE 4
Dendrogram of hierarchical clustering heatmap of the 181 isolates and 40 plasmid replicons. Y-axis is the isolate number, and x-axis is the selected resistance genes identified. Non-expression of resistance is a white background and resistance phenotype is a blue background. Orange indicates isolates were isolated from Quzhou samples, aqua blue indicates isolates were isolated from Lishui, and bright yellow indicates isolates were isolated from Jinhua. Purple indicates that the strain is isolated from pig anal swab samples, and green indicates that the strain is isolated from bird anal swab samples.

only the acquired genes of carbapenem, colistin and tetracycline resistance have the highest consistency with the AMR phenotypes. While other acquired AMR genes can not predict the resistance phenotype of the bacteria very well.

Sixty-five different STs were determined in all *E. coli* isolates. Among them, ST10 accounted for the largest proportion, up to 10.50% (19/181). Next was ST48, and 13 isolates (7.18%) were tested for this ST type. ST10 *E. coli* has been seen repeatedly in

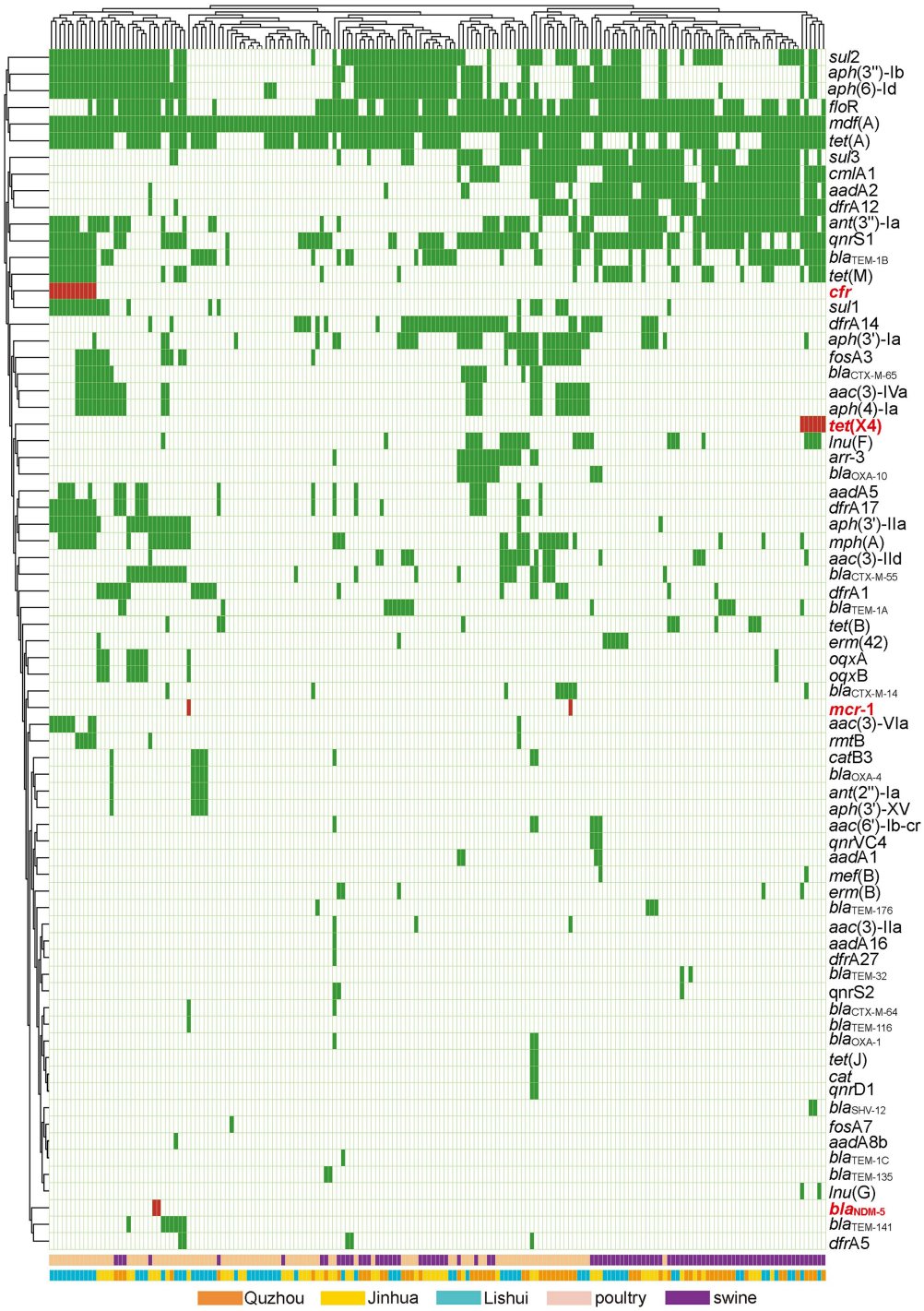


FIGURE 5
Antibiotic resistance patterns of *E. coli* isolates. Y-axis is the number of isolated strains, and x-axis is the selected AMR genes identified. Green indicates that the isolate is isolated from Quzhou sample, light blue indicates that it is isolated from Lishui, and light yellow indicates that it is isolated from Jinhua. Flesh color indicates that the isolate is isolated from poultry anal swab samples, and cinnabar indicates that it is isolated from pig anal swab samples. Dark green in the small grid indicates the presence of AMR genes, white indicates no, and red indicates the presence of risk AMR genes. The risk AMR genes mentioned here refer to the genes that have been focused on, such as *tet*(X4) (resistant to tigecycline), *mcr-1* (resistant to colistin), $bla_{NDM-5}$ (meropenem) or *cfr* (resistant to oxazolidinone, amphenicol, lincosamide), which pose a serious threat to public health and safety. Rifamycin (*arr-3*), Aminoglycoside (*aac(3)-Iia*, *aac(3)-IId*, *aac(3)-IVa*, *aac(3)-VIa*, *aac(6')-Ib-cr*, *aadA16*, *aadA1*, *aadA2*, *aadA5*, *aadA8b*, *ant(2'')-Ia*, *ant(3'')-Ia*, *aph(3'')-Ib*, *aph(3')-Iia*, *aph(3')-Ia*, *aph(3')-XV*, *aph(4)-Ia*, *aph(6)-Id*, *rmtB*), Beta-lactam ($bla_{CTX-M-14}$, $bla_{CTX-M-55}$, $bla_{CTX-M-64}$, $bla_{CTX-M-65}$, $bla_{NDM-5}$, $bla_{OXA-10}$, $bla_{OXA-1}$, $bla_{OXA-4}$, $bla_{SHV-12}$, $bla_{TEM-116}$, $bla_{TEM-135}$, $bla_{TEM-141}$, $bla_{TEM-176}$, $bla_{TEM-1A}$, $bla_{TEM-1B}$, $bla_{TEM-1C}$, $bla_{TEM-32}$), Amphenicol (*catB3*, *cat*, *cmlA1*, *floR*, *cfr*), Folate pathway antagonist (*dfrA12*, *dfrA14*, *dfrA17*, *dfrA1*, *dfrA27*, *dfrA5*, *sul1*, *sul2*, *sul3*), Macrolide (*erm(42)*, *erm(B)*, *mdf(A)*, *mef(B)*, *mph(A)*), Fosfomycin (*fosA3*, *fosA7*), Lincosamide (*lnu(F)*, *lnu(G)*), Polypeptides (*mcr-1*), Quinolone (*oqxA*, *oqxB*, *qnrD1*, *qnrS1*, *qnrS2*, *qnrVC4*), Tetracycline (*tet*(A), *tet*(B), *tet*(J), *tet*(M), *tet*(X)).


FIGURE 6
Dendrogram of the hierarchical clustering heat map of isolates and virulence genes. The figure shows the predicted virulence genes factor profile of the studied isolates. Y-axis is the isolate number and x-axis is the selected virulence genes identified. The red color in the small cells indicates virulence genes associated with toxin production, the orange color indicates genes editing other virulence factors, and the white color indicates no virulence expression. Withered grass color indicates isolates isolated from Quzhou samples, yellow indicates isolates from Jinhua, and blue color indicates isolates from Lishui. Incarnadine pink indicates that the isolates were isolated from pig anal swab samples, and bright green indicates that they were isolated from birds.

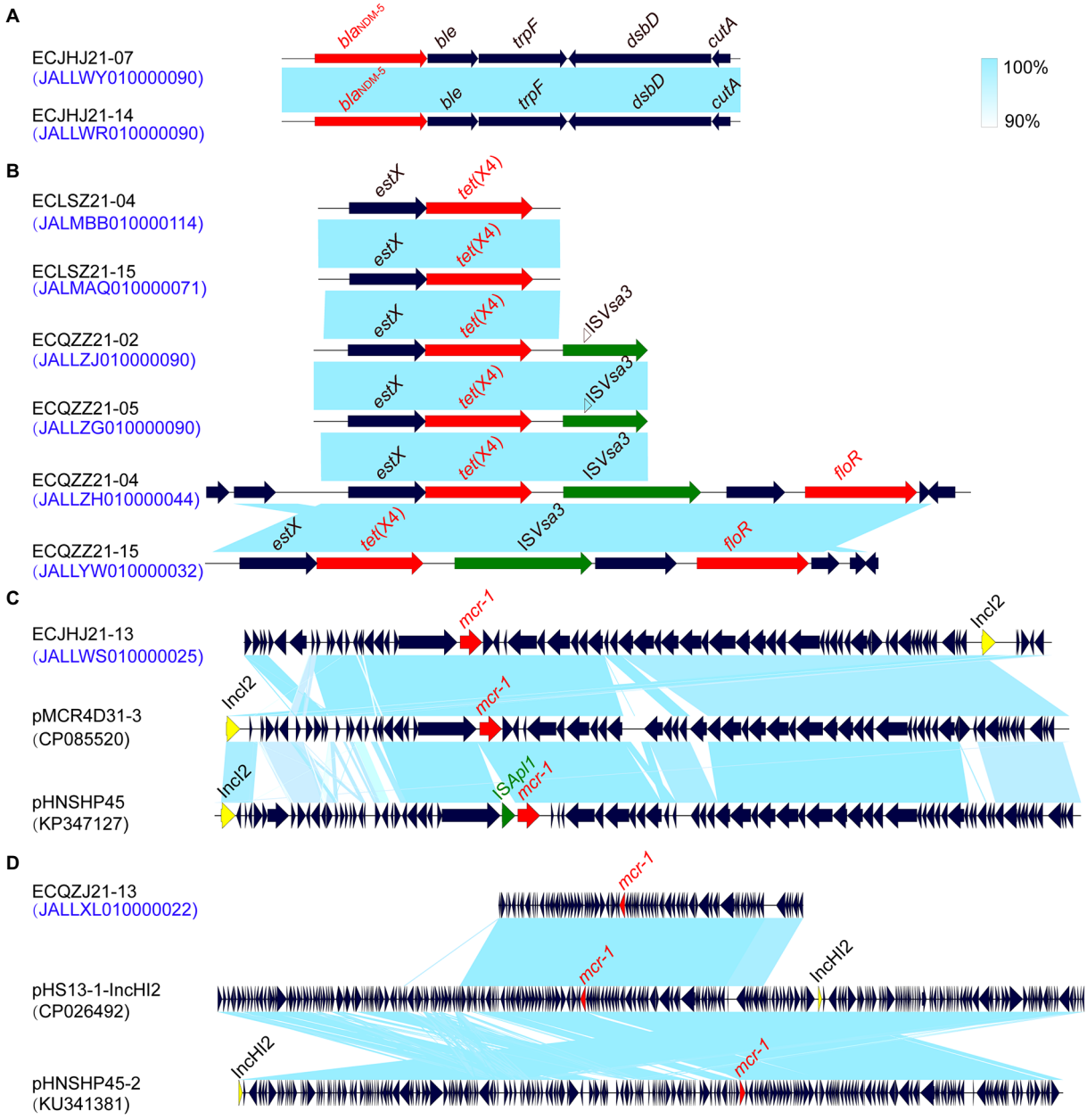


FIGURE 7
Comparison of the risk AMR gene environments in *E. coli* strains. **(A)** the $bla_{NDM-5}$ gene environment. **(B)** the *tet*(X4) gene environment. **(C)** the *mcr-1* gene environment of IncI2 plasmids. **(D)** the *mcr-1* gene environment of IncHI2 plasmids.

related pathogenicity studies, with multiple disease outbreaks associated with ST10 in a broiler production unit by testing over 18 months (Bojesen et al., 2022).

Nine of the ST10 *E. coli* isolates detected in our study carried the virulence gene *ast*A, which plays an essential role in causing diarrhea and affecting the survival of animals (Meng et al., 2014; Paixão et al., 2016). In recent years, multiple researchers have found that some virulence genes can promote the AMR of bacteria strains (Fu et al., 2022). At the same time, some toxins will be enhanced under the pressure of antibiotics (Wangkheimayum et al., 2022). In our study, the prevalance of *ast*A is up to 36.81%. The *ast*A gene does not sufficiently lead to disease and is also found in healthy pigs, but when it cooperates with F pili or other virulence genes such as *sta* and *stb*, it will lead to diarrhea and pose a potential threat to food safety. Hemolysin is an important pathogenic factor of pathogenic *E. coli*. It not only plays a role in cracking cells but also promotes cell death by activating typical inflammatory bodies in cells. Hemolysin A (HlyA) toxin is important for triggering cell death in human macrophages(Verma et al., 2019; Gu et al., 2021). Our

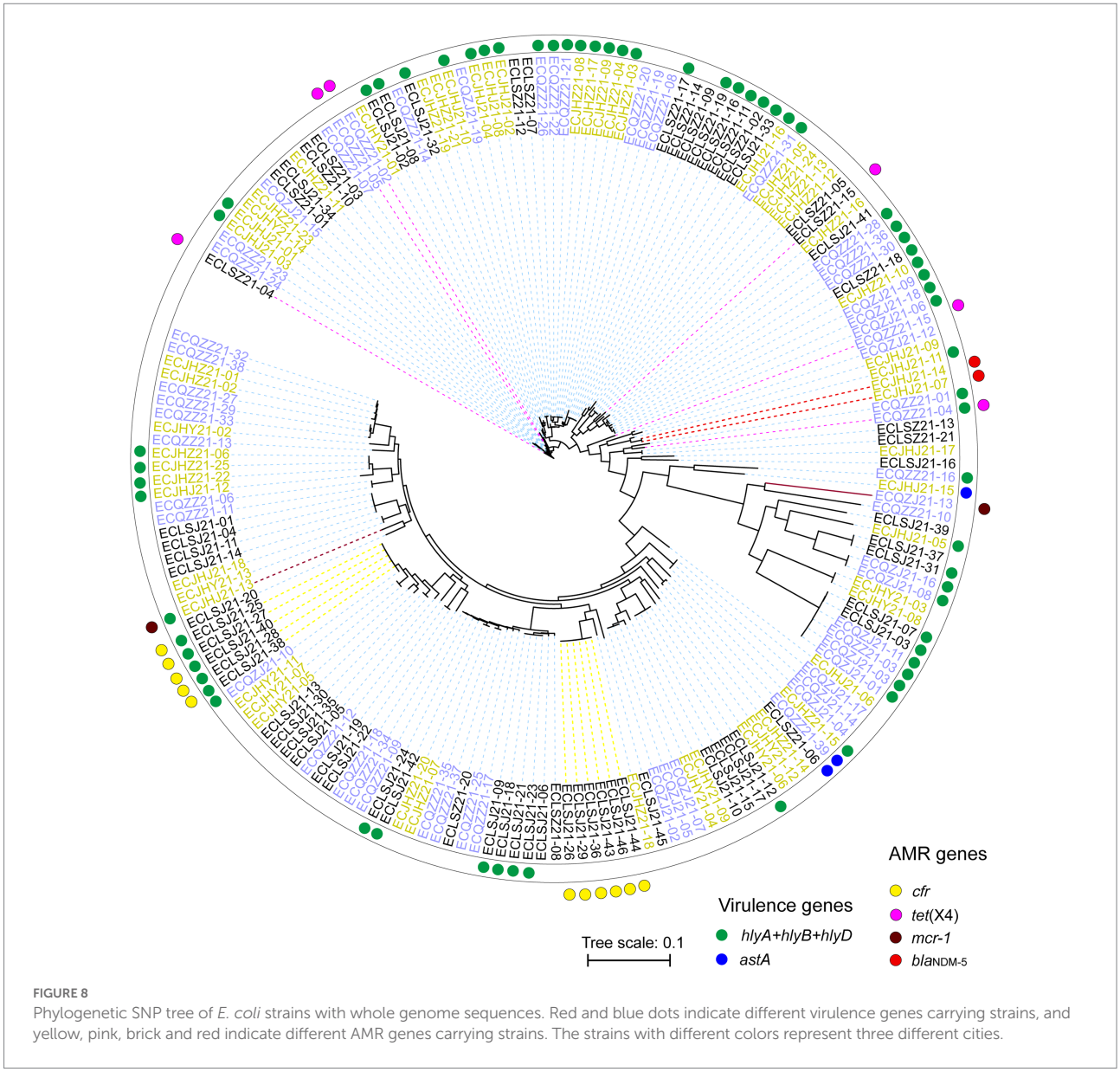


FIGURE 8
Phylogenetic SNP tree of *E. coli* strains with whole genome sequences. Red and blue dots indicate different virulence genes carrying strains, and yellow, pink, brick and red indicate different AMR genes carrying strains. The strains with different colors represent three different cities.

study obtained three isolates carrying encoding genes of three kinds of α-hemolysin, *hly*A, *hly*B, and *hly*D. Here, we would also like to note the proportion of virulence genes associated with the iron uptake system (33/169, 19.53%) and adhesion (46/169, 27.22%). Adhesins are usually a class of glycoprotein or glycolipid biomolecules that are mainly distributed on the surface of bacteria (Berne et al., 2015). The adhesins identified in this study included F1C hairs, K88 hairs, type I hairs, and *E. coli* common hairs.

*E. coli* isolates harbored several kinds of plasmids, with the dominance of IncFIB (AP001918) followed by IncX1. These plasmids have been verified linked to resistance to several antimicrobial classes, including *β*-lactams, aminoglycosides, sulfonamides, tetracyclines, etc. Our research also showed that these plasmids were carried by isolates originating from chickens and pigs in Zhejiang provinces, indicating that these plasmids could disseminate widely among different hosts (Hu et al., 2016; Tang et al., 2019, 2020a).

## Conclusion

In summary, a comprehensive study of AMR and genomic characterization of *E. coli* isolated from pigs and chickens anal swab samples in Eastern China was conducted. A high prevalence of MDR *E. coli* and many virulence determinants in the isolates posed a potential risk to food safety. This is a significant warning for public health safety in Zhejiang Province. It is essential to continue monitoring the MDR *E. coli* and implement antimicrobial stewardship programs for rational use of essential antimicrobials in animal farms to improve food safety and prevent the emergence of MDR bacteria.

## Data availability statement

The datasets presented in this study can be found in online repositories. The names of the repository/repositories and accession number(s) can be found in the article/Supplementary material.

## Author contributions

WZ, BT, ZY, and MY: conceptualization. HY, MY, and BT: funding acquisition. WZ, ZZ, HL, JWu, YD, HY, HJ, and BT: investigation. WZ, ZZ, and BT: methodology. ZY, BT, and MY: supervision. RL, JWa, XZ, and BT: visualization. RL and WZ: writing–original draft. All authors have read and agreed to the published version of the manuscript.

## Funding

This work was supported by the Key Research and Development Program of Zhejiang Province (2020C02031), the Key Research and Development Program of Hangzhou (202203A08), the earmarked fund for China Agriculture Research System (CARS-42-27), the State Key Laboratory for Managing Biotic and Chemical Threats to the Quality and Safety of Agro-Products (2010DS700124-ZZ2102), and Collaborative Extension Plan of Major Agricultural Technologies in Zhejiang Province (2021XTTGXM03).

## Conflict of interest

The authors declare that the research was conducted in the absence of any commercial or financial relationships that could be construed as a potential conflict of interest.

## Publisher's note

All claims expressed in this article are solely those of the authors and do not necessarily represent those of their affiliated organizations, or those of the publisher, the editors and the reviewers. Any product that may be evaluated in this article, or claim that may be made by its manufacturer, is not guaranteed or endorsed by the publisher.

## Supplementary material

The Supplementary material for this article can be found online at: https://www.frontiersin.org/articles/10.3389/fmicb.2022.1018682/full#supplementary-material

## References

Bankevich, A., Nurk, S., Antipov, D., Gurevich, A. A., Dvorkin, M., Kulikov, A. S., et al. (2012). SPAdes: a new genome assembly algorithm and its applications to single-cell sequencing. *J. Comput. Biol.* 19, 455–477. doi: 10.1089/cmb.2012.0021

Berne, C., Ducret, A., Hardy, G. G., and Brun, Y. V. (2015). Adhesins involved in attachment to abiotic surfaces by gram-negative bacteria. *Microbiol Spectr* 3:10. doi: 10.1128/microbiolspec.MB-0018-2015

Bojesen, A. M., Ahmed, U., Skaarup, H., and Espinosa-Gongora, C. (2022). Recurring outbreaks by the same *Escherichia coli* ST10 clone in a broiler unit during 18 months. *Vet. Res.* 53:2. doi: 10.1186/s13567-021-01017-6

Boolchandani, M., D'Souza, A. W., and Dantas, G. (2019). Sequencing-based methods and resources to study antimicrobial resistance. *Nat. Rev. Genet.* 20, 356–370. doi: 10.1038/s41576-019-0108-4

Brisola, M. C., Crecencio, R. B., Bitner, D. S., Frigo, A., Rampazzo, L., Stefani, L. M., et al. (2019). *Escherichia coli* used as a biomarker of antimicrobial resistance in pig farms of southern Brazil. *Sci. Total Environ.* 647, 362–368. doi: 10.1016/j.scitotenv.2018.07.438

Chang, J., Tang, B., Chen, Y., Xia, X., Qian, M., and Yang, H. (2020). Two IncHI2 plasmid-mediated Colistin-resistant *Escherichia coli* strains from the broiler chicken supply chain in Zhejiang Province, China. *J. Food Prot.* 83, 1402–1410. doi: 10.4315/jfp-20-041

Chen, C., Chen, H., Zhang, Y., Thomas, H. R., Frank, M. H., He, Y., et al. (2020). TBtools: an integrative toolkit developed for interactive analyses of big biological data. *Mol. Plant* 13, 1194–1202. doi: 10.1016/j.molp.2020.06.009

Deng, H., Sun, J., Ma, J., Li, L., Fang, L. X., Zhang, Q., et al. (2014). Identification of the multi-resistance gene cfr in *Escherichia coli* isolates of animal origin. *PLoS One* 9:e102378. doi: 10.1371/journal.pone.0102378

Fu, D., Wu, J., Gu, Y., Li, Q., Shao, Y., Feng, H., et al. (2022). Corrigendum to the response regulator OmpR contributes to the pathogenicity of avian pathogenic *Escherichia coli*. *Poult. Sci.* 101:101876. doi: 10.1016/j.psj.2022.101876

Gardner, S. N., Slezak, T., and Hall, B. G. (2015). kSNP3.0: SNP detection and phylogenetic analysis of genomes without genome alignment or reference genome. *Bioinformatics* 31, 2877–2878. doi: 10.1093/bioinformatics/btv271

Gu, H., Cai, X., Zhang, X., Luo, J., Zhang, X., Hu, X., et al. (2021). A previously uncharacterized two-component signaling system in uropathogenic *Escherichia coli* coordinates protection against host-derived oxidative stress with activation of hemolysin-mediated host cell pyroptosis. *PLoS Pathog.* 17:e1010005. doi: 10.1371/journal.ppat.1010005

Guan, C., Tang, B., Yang, H., Ma, J., Huang, Y., and Liu, C. (2022). Emergence of plasmid-mediated tigecycline resistance gene, *tet*(X4), in *Escherichia fergusonii* from pigs. *J Glob Antimicrob Resist* 30, 249–251. doi: 10.1016/j.jgar.2022.06.029

He, T., Wang, R., Liu, D., Walsh, T. R., Zhang, R., Lv, Y., et al. (2019). Emergence of plasmid-mediated high-level tigecycline resistance genes in animals and humans. *Nat. Microbiol.* 4, 1450–1456. doi: 10.1038/s41564-019-0445-2

Hu, Y., Yang, X., Li, J., Lv, N., Liu, F., Wu, J., et al. (2016). The bacterial mobile resistome transfer network connecting the animal and human microbiomes. *Appl. Environ. Microbiol.* 82, 6672–6681. doi: 10.1128/aem.01802-16

Li, Y., Ed-Dra, A., Tang, B., Kang, X., Müller, A., Kehrenberg, C., et al. (2022a). Higher tolerance of predominant *Salmonella* serovars circulating in the antibiotic-free feed farms to environmental stresses. *J. Hazard. Mater.* 438:129476. doi: 10.1016/j.jhazmat.2022.129476

Li, Y., Kang, X., Ed-Dra, A., Zhou, X., Jia, C., Müller, A., et al. (2022b). Genome-based assessment of antimicrobial resistance and virulence potential of isolates of non-pullorum/gallinarum *Salmonella* serovars recovered from dead poultry in China. *Microbiol Spectr* 10:e0096522. doi: 10.1128/spectrum.00965-22

Li, R., Xie, M., Zhang, J., Yang, Z., Liu, L., Liu, X., et al. (2017). Genetic characterization of *mcr-1*-bearing plasmids to depict molecular mechanisms underlying dissemination of the colistin resistance determinant. *J. Antimicrob. Chemother.* 72, 393–401. doi: 10.1093/jac/dkw411

Lin, J., Tang, B., Zheng, X., Chang, J., Ma, J., He, Y., et al. (2022). Emergence of Incl2 plasmid-mediated colistin resistance in avian *Escherichia fergusonii*. *FEMS Microbiol. Lett.* 369:fnac016. doi: 10.1093/femsle/fnac016

Liu, Y. Y., Wang, Y., Walsh, T. R., Yi, L. X., Zhang, R., Spencer, J., et al. (2016). Emergence of plasmid-mediated colistin resistance mechanism MCR-1 in animals and human beings in China: a microbiological and molecular biological study. *Lancet Infect. Dis.* 16, 161–168. doi: 10.1016/s1473-3099(15)00424-7

Ma, J., Zhou, W., Wu, J., Liu, X., Lin, J., Ji, X., et al. (2022). Large-scale studies on antimicrobial resistance and molecular characterization of *Escherichia coli* from food animals in developed areas of eastern China. *Microbiol Spectr* 10:e0201522. doi: 10.1128/spectrum.02015-22

Meng, Q., Bai, X., Zhao, A., Lan, R., Du, H., Wang, T., et al. (2014). Characterization of Shiga toxin-producing *Escherichia coli* isolated from healthy pigs in China. *BMC Microbiol.* 14:5. doi: 10.1186/1471-2180-14-5

Paixão, A. C., Ferreira, A. C., Fontes, M., Themudo, P., Albuquerque, T., Soares, M. C., et al. (2016). Detection of virulence-associated genes in pathogenic and commensal avian *Escherichia coli* isolates. *Poult. Sci.* 95, 1646–1652. doi: 10.3382/ps/pew087

Peng, X., Ed-Dra, A., and Yue, M. (2022). Whole genome sequencing for the risk assessment of probiotic lactic acid bacteria. *Crit. Rev. Food Sci. Nutr.* 1–19. doi: 10.1080/10408398.2022.2087174

Peng, Z., Hu, Z., Li, Z., Zhang, X., Jia, C., Li, T., et al. (2022). Antimicrobial resistance and population genomics of multidrug-resistant *Escherichia coli* in pig farms in mainland China. *Nat. Commun.* 13:1116. doi: 10.1038/s41467-022-28750-6

Rutuja, D., Ragini, M., Dhananjaya, S., Kayzad, N., Appasaheb, G., and Tannaz, B. (2018). Antibiotic resistance characterization of Environmental *E. coli* isolated from river Mula-Mutha, Pune District, India. *Int. J. Environ. Res. Public Health* 15:1247. doi: 10.3390/ijerph15061247

Shen, Z., Wang, Y., Shen, Y., Shen, J., and Wu, C. (2016). Early emergence of *mcr-1* in *Escherichia coli* from food-producing animals. *Lancet Infect. Dis.* 16:293. doi: 10.1016/s1473-3099(16)00061-x

Sullivan, M. J., Petty, N. K., and Beatson, S. A. (2011). Easyfig: a genome comparison visualizer. *Bioinformatics* 27, 1009–1010. doi: 10.1093/bioinformatics/btr039

Sun, J., Chen, C., Cui, C. Y., Zhang, Y., Liu, X., Cui, Z. H., et al. (2019). Plasmid-encoded *tet*(X) genes that confer high-level tigecycline resistance in *Escherichia coli*. *Nat. Microbiol.* 4, 1457–1464. doi: 10.1038/s41564-019-0496-4

Tang, B., Chang, J., Cao, L., Luo, Q., Xu, H., Lyu, W., et al. (2019). Characterization of an NDM-5 carbapenemase-producing *Escherichia coli* ST156 isolate from a poultry farm in Zhejiang, China. *BMC Microbiol.* 19:82. doi: 10.1186/s12866-019-1454-2

Tang, B., Chang, J., Chen, Y., Lin, J., Xiao, X., Xia, X., et al. (2022a). *Escherichia fergusonii*, an underrated repository for antimicrobial resistance in food animals. *Microbiol Spectr* 10:e0161721. doi: 10.1128/spectrum.01617-21

Tang, B., Chang, J., Luo, Y., Jiang, H., Liu, C., Xiao, X., et al. (2022b). Prevalence and characteristics of the *mcr-1* gene in retail meat samples in Zhejiang Province, China. *J. Microbiol.* 60, 610–619. doi: 10.1007/s12275-022-1597-y

Tang, B., Chang, J., Zhang, L., Liu, L., Xia, X., Hassan, B. H., et al. (2020a). Carriage of distinct *mcr-1*-harboring plasmids by unusual serotypes of *Salmonella*. *Adv. Biosyst.* 4:e1900219. doi: 10.1002/adbi.201900219

Tang, B., Tang, Y., Zhang, L., Liu, X., Chang, J., Xia, X., et al. (2020b). Emergence of *fexA* in mediating resistance to Florfenicols in *Campylobacter*. *Antimicrob. Agents Chemother.* 64:e00260-20. doi: 10.1128/AAC.00260-20

Tang, B., Wang, Y., Luo, Y., Zheng, X., Qin, X., Yang, H., et al. (2021a). Coexistence of *optrA* and *fexA* in *Campylobacter*. *mSphere* 6:e00125-21. doi: 10.1128/mSphere.00125-21

Tang, B., Wang, J., Zheng, X., Chang, J., Ma, J., Wang, J., et al. (2022c). Antimicrobial resistance surveillance of *Escherichia coli* from chickens in the Qinghai plateau of China. *Front. Microbiol.* 13:885132. doi: 10.3389/fmicb.2022.885132

Tang, B., Yang, H., Jia, X., and Feng, Y. (2021b). Coexistence and characterization of Tet(X5) and NDM-3 in the MDR-*Acinetobacter indicus* of duck origin. *Microb. Pathog.* 150:104697. doi: 10.1016/j.micpath.2020.104697

Tatusova, T., DiCuccio, M., Badretdin, A., Chetvernin, V., Nawrocki, E. P., Zaslavsky, L., et al. (2016). NCBI prokaryotic genome annotation pipeline. *Nucleic Acids Res.* 44, 6614–6624. doi: 10.1093/nar/gkw569

Teng, L., Liao, S., Zhou, X., Jia, C., Feng, M., Pan, H., et al. (2022). Prevalence and genomic investigation of multidrug-resistant *Salmonella* isolates from companion animals in Hangzhou, China. *Antibiotics (Basel)* 11:625. doi: 10.3390/antibiotics11050625

Verma, V., Gupta, S., Kumar, P., Rawat, A., Singh Dhanda, R., and Yadav, M. (2019). Efficient production of endotoxin depleted bioactive α-hemolysin of uropathogenic *Escherichia coli*. *Prep. Biochem. Biotechnol.* 49, 616–622. doi: 10.1080/10826068.2019.1591993

Wang, J., Tang, B., Lin, R., Zheng, X., Ma, J., Xiong, X., et al. (2022). Emergence of *mcr-1*- and $bla_{NDM-5}$-harbouring IncHI2 plasmids in *Escherichia coli* strains isolated from meat in Zhejiang, China. *J. Glob. Antimicrob. Resist.* 30, 103–106. doi: 10.1016/j.jgar.2022.06.002

Wang, Y., Tian, G. B., Zhang, R., Shen, Y., Tyrrell, J. M., Huang, X., et al. (2017). Prevalence, risk factors, outcomes, and molecular epidemiology of *mcr-1*-positive *Enterobacteriaceae* in patients and healthy adults from China: an epidemiological and clinical study. *Lancet Infect. Dis.* 17, 390–399. doi: 10.1016/s1473-3099(16)30527-8

Wangkheimayum, J., Chanda, D. D., and Bhattacharjee, A. (2022). Expression of *itaT* toxin gene is enhanced under aminoglycoside stress in *Escherichia coli* harbouring aac(6′)-Ib. *Gene Reports* 26:101526. doi: 10.1016/j.genrep.2022.101526

Xu, L., Wan, F., Fu, H., Tang, B., Ruan, Z., Xiao, Y., et al. (2022). Emergence of Colistin resistance gene mcr-10 in *Enterobacterales* isolates recovered from fecal samples of chickens, slaughterhouse workers, and a nearby resident. *Microbiol Spectr* 10:e0041822. doi: 10.1128/spectrum.00418-22

Yang, L., Shen, Y., Jiang, J., Wang, X., Shao, D., Lam, M., et al. (2022). Distinct increase in antimicrobial resistance genes among *Escherichia coli* during 50 years of antimicrobial use in livestock production in China. *Nat. Food* 3, 197–205. doi: 10.1038/s43016-022-00470-6

frontiers | Frontiers in Microbiology

TYPE Correction
PUBLISHED 10 February 2023
DOI 10.3389/fmicb.2023.1102931



OPEN ACCESS

APPROVED BY
Frontiers Editorial Office,
Frontiers Media SA, Switzerland

*CORRESPONDENCE
Zhangnv Yang
✉ znyang@cdc.zj.cn
Biao Tang
✉ tangbiao@zaas.ac.cn
Min Yue
✉ myue@zju.edu.cn

†These authors have contributed equally to this work

SPECIALTY SECTION
This article was submitted to Antimicrobials, Resistance and Chemotherapy, a section of the journal Frontiers in Microbiology

RECEIVED 19 November 2022
ACCEPTED 23 January 2023
PUBLISHED 10 February 2023

CITATION
Zhou W, Lin R, Zhou Z, Ma J, Lin H, Zheng X, Wang J, Wu J, Dong Y, Jiang H, Yang H, Yang Z, Tang B and Yue M (2023) Corrigendum: Antimicrobial resistance and genomic characterization of *Escherichia coli* from pigs and chickens in Zhejiang, China. *Front. Microbiol.* 14:1102931. doi: 10.3389/fmicb.2023.1102931



# Corrigendum: Antimicrobial resistance and genomic characterization of *Escherichia coli* from pigs and chickens in Zhejiang, China

Wei Zhou[1†], Rumeng Lin[2,3,4†], Zhijin Zhou[1], Jiangang Ma[2], Hui Lin[2,5], Xue Zheng[2], Jingge Wang[2], Jing Wu[2], Yuzhi Dong[2,4], Han Jiang[4], Hua Yang[2], Zhangnv Yang[6]*, Biao Tang[2]* and Min Yue[7]*

[1]Zhejiang Provincial Center for Animal Disease Prevention and Control, Hangzhou, China, [2]State Key Laboratory for Managing Biotic and Chemical Threats to the Quality and Safety of Agro-Products, Institute of Agro-Product Safety and Nutrition, Zhejiang Academy of Agricultural Sciences, Hangzhou, China, [3]School of Food Science and Technology, Jiangnan University, Wuxi, China, [4]Key Laboratory of Marine Food Quality and Hazard Controlling Technology of Zhejiang Province, China Jiliang University, Hangzhou, China, [5]The Institute of Environment, Resource, Soil and Fertilizers, Zhejiang Academy of Agricultural Sciences, Hangzhou, China, [6]Zhejiang Provincial Center for Disease Control and Prevention, Hangzhou, China, [7]Department of Veterinary Medicine, Institute of Preventive Veterinary Sciences, Zhejiang University College of Animal Sciences, Hangzhou, Zhejiang, China

KEYWORDS

***Escherichia coli*, animal origin, antimicrobial resistance, genomic characterization, virulence genes**

A corrigendum on

Antimicrobial resistance and genomic characterization of *Escherichia coli* from pigs and chickens in Zhejiang, China

by Zhou, W., Lin, R., Zhou, Z., Ma, J., Lin, H., Zheng, X., Wang, J., Wu, J., Dong, Y., Jiang, H., Yang, H., Yang, Z., Tang, B., and Yue, M. (2022). *Front. Microbiol.* 13:1018682. doi: 10.3389/fmicb.2022.1018682

A correction has been made to **Abstract**. This sentence previously stated:

"The AMR genes $bla_{NDM-5}$ (1.10%, 2/181), *mcr-1* (1.10%, 2/181), *tet*(X4) (1.10%, 2/181), and *cfr* (6.08%, 2/181) were also found in these isolates."

The corrected sentence appears below:

"The AMR genes $bla_{NDM-5}$ (1.10%, 2/181), *mcr-1* (1.10%, 2/181), *tet*(X4) (1.10%, 2/181), and *cfr* (6.08%, 11/181) were also found in these isolates."

The authors apologize for this error and state that this does not change the scientific conclusions of the article in any way. The original article has been updated.

## Publisher's note

All claims expressed in this article are solely those of the authors and do not necessarily represent those of their affiliated organizations, or those of the publisher, the editors and the reviewers. Any product that may be evaluated in this article, or claim that may be made by its manufacturer, is not guaranteed or endorsed by the publisher.

frontiers | Frontiers in Microbiology

TYPE Original Research
PUBLISHED 27 January 2023
DOI 10.3389/fmicb.2022.991352



OPEN ACCESS

EDITED BY
Xiaolin Hou,
Beijing University of Agriculture, China

REVIEWED BY
Jinhu Huang,
Nanjing Agricultural University, China
Ana P. Tedim,
Institute of Health Sciences Studies of Castilla y León (IECSCYL), Spain

*CORRESPONDENCE
Daofeng Qu
✉ daofeng@mail.zjgsu.edu.cn

SPECIALTY SECTION
This article was submitted to Antimicrobials, Resistance and Chemotherapy, a section of the journal Frontiers in Microbiology

RECEIVED 11 July 2022
ACCEPTED 01 December 2022
PUBLISHED 27 January 2023

CITATION
Zhang E, Zong S, Zhou W, Zhou J, Han J and Qu D (2023) Characterization and comparative genomics analysis of RepA_N multi-resistance plasmids carrying *optrA* from *Enterococcus faecalis*. *Front. Microbiol.* 13:991352. doi: 10.3389/fmicb.2022.991352



# Characterization and comparative genomics analysis of RepA_N multi-resistance plasmids carrying *optrA* from *Enterococcus faecalis*

Enbao Zhang[1], Shuaizhou Zong[1], Wei Zhou[2], Jinzhi Zhou[2], Jianzhong Han[1] and Daofeng Qu[1]*

[1]Key Laboratory of Food Quality and Safety, School of Food Science and Biotechnology, Zhejiang Gongshang University, Hangzhou, China, [2]Zhejiang Provincial Center for Animal Disease Prevention and Control, Hangzhou, China

**Introduction:** This research aimed to investigate the antibiotic resistance of *Enterococcus faecalis* from swine farms in Zhejiang Province and the prevalence and transmission mechanism of oxazolidone resistance gene *optrA*.

**Method:** A total of 226 *Enterococcus faecalis* were isolated and their resistance to 14 antibiotics was detected by broth microdilution. The resistance genes were detected by PCR.

**Results:** The antibiotic resistance rate of 226 isolates to nearly 57% (8/14) of commonly used antibiotics was higher than 50%. The resistance rate of tiamulin was highest (98.23%), that of tilmicosin, erythromycin, tetracycline and florfenicol was higher than 80%, and that of oxazolidone antibiotic linezolid was 38.49%. The overall antibiotics resistance in Hangzhou, Quzhou and Jinhua was more serious than that in the coastal cities of Ningbo and Wenzhou. The result of PCR showed that *optrA* was the main oxazolidinone and phenicols resistance gene, with a detection rate of 71.68%, and *optrA* often coexisted with *fexA* in the isolates. Through multi-locus sequence typing, conjugation transfer, and replicon typing experiments, it was found that the horizontal transmission mediated by RepA_N plasmid was the main mechanism of *optrA* resistance gene transmission in E. faecalis from Zhejiang Province. Two conjugative multi-resistance plasmids carrying *optrA*, RepA_N plasmid pHZ318-*optrA* from Hangzhou and Rep3 plasmid from Ningbo, were sequenced and analyzed. pHZ318-*optrA* contain two multidrug resistance regions (MDR), which contributed to the MDR profile of the strains. *optrA* and *fexA* resistance genes coexisted in IS*1216*E-*fexA*-*optrA*-*ferr*-*erm*(A)-IS*1216*E complex transposon, and there was a partial sequence of Tn*554* transposon downstream. However, pNB304-optrA only contain *optrA*, *fexA* and an insertion sequence IS*Vlu1*. The presence of mobile genetic elements at the boundaries can possibly facilitate transfer among *Enterococcus* through inter-replicon gene transfer.

**Discussion:** This study can provide theoretical basis for ensuring the quality and safety of food of animal origin, and provide scientific guidance for slowing down the development of multi-antibiotic resistant *Enterococcus*.

KEYWORDS

**plasmid, antibiotic resistance, *optrA*, MDR, mobile elements**

# 1. Introduction

The livestock and poultry breeding industry in China is gradually changing from decentralized breeding to intensive breeding, and antibiotics are widely used as growth promoters and treatment antibiotics for bacterial diseases (Wang et al., 2021). The unreasonable use of antibiotics leads to the enhancement of bacterial antibiotic resistance and the diffusion of antibiotic resistance genes, which brings great harm to public health (Sun, 2014). *Enterococcus faecalis* is one of the common pathogens causing infectious diseases in humans or animals, and oxazolidinone antibiotics are the "last line of defense" in the treatment of vancomycin-resistant *Enterococcus*, so monitoring its antibiotic resistance is of great health significance (Senior, 2000; Yasufuku et al., 2011). However, there are few studies on the antibiotic resistance of *Enterococcus faecalis* from swine in Zhejiang Province. Previous studies mainly focused on clinical *Enterococcus* or gram-negative bacteria such as *Escherichia coli* and *Salmonella* from swine (Falagas et al., 2011; Anjum et al., 2016).

Linezolid is the first class of oxazolidinones, which is a fully synthetic antibiotic that binds to the initial complex and inhibits protein synthesis (Bender et al., 2018). Linezolid is active against a wide range of Gram-positive bacteria, including methicillin-resistant *Staphylococcus aureus* (MRSA) and Vancomycin-resistant *Enterococcus* (VRE), and has been the "last line of defense" against gram-positive multidrug-resistant bacteria following vancomycin (Carmen et al., 2018). Most bacteria, including *Enterococcus*, have multiple copies of genes encoding 23S rRNA, and the level of resistance to linezolid expression depends on the number of these genes containing relevant mutations (Pillai et al., 2002). Currently, three different groups of acquired resistance genes which can product cross-resistance to linezolid and florfenicol have been identified. These genes include *cfr*, *optrA*, and *poxtA* (Liu et al., 2012; Yang et al., 2015; Hao et al., 2019). *cfr* resistance gene modifies A2503 methyltransferase in bacterial 23S rRNA, and was first identified in *Staphylococcus sciuri* of animal origin (Schwarz et al., 2000). The gene *optrA* encodes a ribosomal protection protein of the ABC-F family, and imparts transferable resistance to oxazolidone (linezolid and tedizolid) and phenicols (chloramphenicol and florfenicol; Wang et al., 2015). *poxtA* also encodes a ribosomal protection protein of the ABC-F family and has recently been identified in MRSA (Antonelli et al., 2018).

Oxazolidinones antibiotics are not allowed to be used in foodborne animal farming, however, linezolid-resistant *Enterococcus* carrying *optrA* gene in transferable plasmids have been detected in these animals (Carmen et al., 2018). This gene coexists with antibiotic resistance genes of commonly used animal antibiotics (penicillins, tetracyclines, lincosamides, and aminoglycosides), indicating their role in co-selection of multidrug resistant bacteria, which poses a risk to public health (Carmen et al., 2018). Although oxazolidinones are not used in the swine industry, florfenicol is widely used to treat bacterial infections in swine, which may promote the spread of *cfr*, *optrA*, and *poxtA* genes in swine farms (Zhao et al., 2016). Moreover, it is still unknown how frequently *optrA* gene occurs in the *Enterococcus* in Zhejiang Province, and the number of related multi-resistance plasmids containing *optrA* is not very high in the NCBI database. Moreover, the genetic background of *optrA* also needs to be further studied.

In this study, the antibiotic resistance of the 14 common antibiotics in *Enterococcus faecalis* from swine farms was determined. This research provided resistance profile of *Enterococcus faecalis* and comparison analysis of multiple antibiotic resistance from swine farms in five cities of Zhejiang Province. In addition, the presence, transferability and related mobile elements of the *optrA* gene in *Enterococcus* of swine origin was investigated. Furthermore, two conjunctive plasmids harboring *optrA* were analyzed to clarify the basis for dissemination. This research enriched the study of plasmids containing *optrA* resistance genes in the NCBI database.

# 2. Materials and methods

## 2.1. Bacterial strains

A total of 226 non-duplicate *Enterococcus faecalis* isolates were collected from 15 swine farms in Hangzhou, Ningbo, Jinhua, Quzhou and Wenzhou of Zhejiang Province, China in 2020. A list of collected fecal samples from swine was presented in Table 1. Colonies of red to purple growing on *Enterococcus* Chromogenic medium were initially considered *Enterococcus* strains. The isolates were further identified as *Enterococcus faecalis* by VITEK-2 Compact and 16S rRNA gene identification using the universal 16 s primers 27F and 1492R (Lane, 1991). *Enterococcus faecalis* JH2-2 served as the recipient strain in conjugal transfer experiments. JH2-2 was resistant to rifampicin and fusidic acid, but sensitive to other antibiotics.

## 2.2. Antimicrobial susceptibility testing

Antibiotic susceptibility testing of *Enterococcus faecalis* strains was performed by broth microdilution method (MIC) and classified as resistant, intermediate, or susceptible according to the

TABLE 1 The results of *Enterococcus* isolation from fecal samples in Zhejiang.

| Source | Number of samples | Number of isolates | Isolated rate (%) |
|---|---|---|---|
| Hangzhou | 105 | 41 | 39.05 |
| Ningbo | 100 | 18 | 18.00 |
| Jinhua | 120 | 68 | 56.67 |
| Quzhou | 100 | 37 | 37.00 |
| Wenzhou | 120 | 62 | 51.67 |
| Total | 545 | 226 | 41.47 |

CLSI criteria for *Enterococcus* as the breakpoints were shown in Supplementary Table S2. *Enterococcus faecalis* strains exhibiting resistance to three or more classes of antimicrobials were considered to be multi-drug resistant (MDR). *Enterococcus faecalis* ATCC 29212 served as the control strain.

## 2.3. PCR analysis

*Enterococcus faecalis* strains were screened for the presence of the antibiotic resistance genes and for the type of plasmid replicon by PCR using the primers listed in Supplementary Table S3 [*cfr, cfr(B), optrA, poxtA, fexA, fexB, floR, cmlA and lsa*(E)] and Supplementary Table S4 (including 10 plasmid *rep* genes, such as pIP501, pRE25, pS86), as described previously (Jensen et al., 2010). PCR amplification consisted of denaturation at 95°C for 5 min followed by denaturation at 94°C for 30 s, annealing at their respective annealing temperature for 30 s, and polymerization at 72°C for 40 s for a total of 30 cycles, and a final extension at 72°C for 10 min. All the PCR products were subjected to Sanger sequencing.

## 2.4. Multilocus sequencing typing

Multilocus sequencing typing (MLST) of 30 oxazolidone resistance gene positive *Enterococcus faecalis* strains isolated from five cities in Zhejiang province was studied by PCR method. Seven pair primers of housekeeping genes of *Enterococcus faecalis* were searched from pubmlst website[1] and synthesized by Shanghai Biological Engineering Co., Ltd. (Supplementary Table S5). The PCR amplification condition was as described previously (Ruiz-Garbajosa et al., 2006). The positive PCR products were sent to biological companies for sequencing, and the sequences were submitted to *Enterococcus* MLST database[2] to analyze the housekeeping genes number and the Sequence type of each strain was determined.

## 2.5. Conjugal transfer experiments

Conjugal transfer experiments were performed with rifampin and fusidic acid resistant *Enterococcus faecalis* JH2-2 used as a recipient and each of the 20 *optrA*-positive *Enterococcus faecalis* isolates as a donor. Brain Heart Infusion (BHI) was supplemented with 64 μg/ml rifampicin, 64 μg/ml fusidic acid and 16 μg/ml florfenicol to screen transconjugants. After incubation at 37°C for 24 h, colonies growing on these selective plates were further confirmed by antimicrobial sensitivity experiments and VITEK-2 Compact.

## 2.6. Sequencing and analysis

The two conjugatable plasmids of the transconjugants HZ318-JH2-2 and NB304-JH2-2 were sequenced by the Illumina MiSeq platforms. The two plasmids DNA was extracted from the transconjugants HZ318-JH2-2 and NB304-JH2-2 using the Qiagen Large-Construct Kit. After extraction, the mate-pair library was constructed. Then MiSeq (Illumina, CA, United States) was used to sequence the plasmids, and Newbler 2.6 was used to assemble the illumina read sets straight off the MiSeq. Quality control and removing low-quality data were performed with TrimMomatic 0.36 (Bolger Anthony et al., 2014). Gapfiller V1.11 is used to fill gaps (Nederbragt, 2014). Finally, Cytoscape was used to spline the sequence to obtain the final cyclized plasmids. The plasmid sequences were submitted to Rast, Genemarks, Glimmer, and Prodigal library for preliminary gene prediction then submitted to ISFinder, Integrall, ResFinder, and TN Number Registry for mobile elements (Boetzer and Pirovano, 2012). Gene organization diagrams were drawn by running a gene alignment program in Perl language (Supplementary material) with Ubuntu 18.04 LTS[3] and Inkscape 0.48.1.[4]

## 2.7. Determination of plasmid stability

The *optrA* positive transconjugants HZ318-JH2-2, NB304-JH2-2 and the control strain JH2-2 were inoculated into BHI plate and cultured in a constant temperature incubator at 37°C for 12~18 h, and a single colony of each strain was inoculated into 5 ml LB broth medium for 12 h. Absorb 5 μl overnight culture solution and add sterilized BHI broth to 5 ml, dilute it by 1,000 times, then subculture for 14 days. The bacterial solution was diluted by 10 times gradient series, and 100 μl suitable diluted bacterial solution was coated on LB plate without antibiotics for overnight culture. Transfer the single colony on the plate to LB-florfenicol resistant plate and non-resistant LB plate, respectively. Plasmid retention ratio = number of single colonies on florfenicol resistant plate/number of single colonies on non-resistant plate. The stability curve of plasmid was drawn with the retention ratio (%) of plasmid in *Enterococcus faecalis* as ordinate and the passage days (d) as abscissa.

# 3. Results

## 3.1. Analysis of antibiotic resistance of *Enterococcus faecalis*

In this study, 226 strains of *Enterococcus faecalis* were identified by VITEK-2 Compact and the amplification of 16S

1 http://www.mlst.net
2 https://pubmlst.org/organisms/
3 https://ubuntu.com/
4 https://inkscape.org/en/

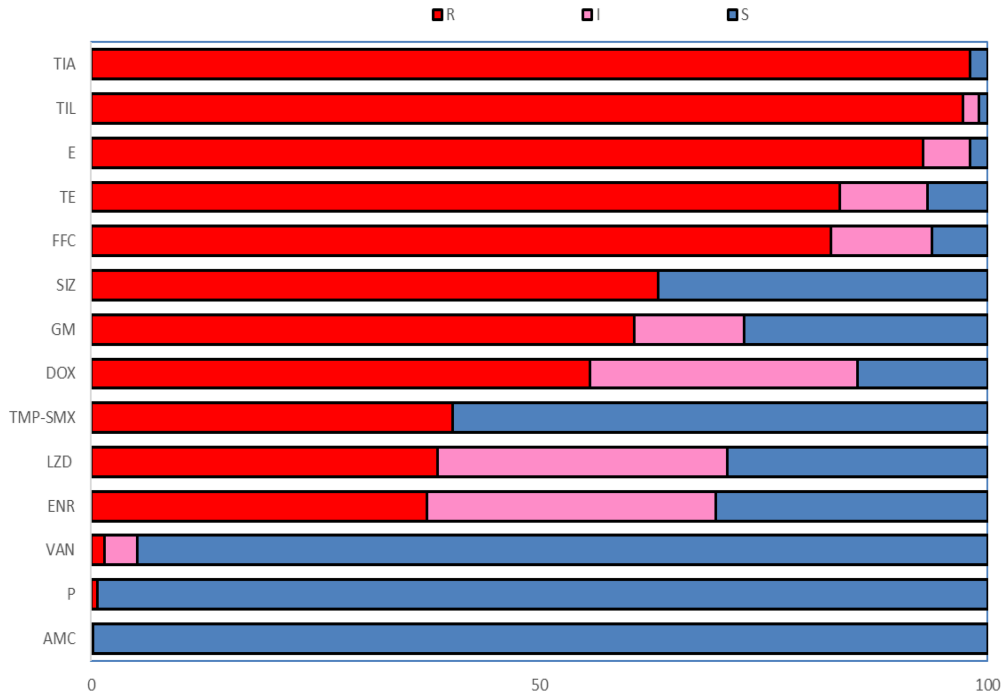


FIGURE 1
The resistance rate to 14 antibiotics of *Enterococcus faecalis* from swine. R, Resistant; I, Intermediate; S, Susceptible; P, Penicillin; AMC, Amoxicillin/clavulanic acid; GM, Gentamicin; E, Erythromycin; TIL, Tilmicosin; FFC, Florfenicol; SIZ, Sulfisoxazole; TMP-SME, Trimethoprim/Sulfamethoxazole; VAN, Vancomycin; DOX, Doxycycline; TE, Tetracycline; ENR, Enrofloxacin; LZD, Linezolid; TIA, Tiamulin.

rRNA gene (Supplementary Table S6). Table 1 showed the isolation of *Enterococcus faecalis* in Hangzhou, Ningbo, Jinhua, Quzhou and Wenzhou of Zhejiang Province, in which the highest isolation rate of *Enterococcus faecalis* was 56.67% in Jinhua, and the lowest in Ningbo was 18%. It can be seen from Figure 1 that among the 14 antibiotics, 226 strains of *Enterococcus faecalis* isolated from swine developed strong resistance to nearly 57% of the commonly used antibiotics, their resistance rates were all higher than 50%, and maintained high sensitivity to penicillin, vancomycin and amoxicillin/clavulanic acid. Strains resistant to amoxicillin/clavulanic acid (AMC) were not detected, but producing varying degrees of resistance to the other 13 antibiotics.

The resistance rates of 226 *Enterococcus faecalis* isolates to tiamulin, tilmicosin and erythromycin were 98.23%, 97.78%, and 92.92%, respectively, and the resistance rates to tetracycline and florfenicol were 83.50% and 82.51%, which were all higher than 80%. *Enterococcus faecalis* produced resistance to 1 to 11 antibiotics of these 14 antibiotics, and no strains resistant to 12 or more antibiotics were found. As can be seen from Figure 2, the antibiotic resistance grade of *Enterococcus faecalis* is concentrated in 7R~10R, accounting for 90%, respectively, and the proportion of multiple antibiotic resistant bacteria (3R–14R) is as high as 97.79%.

## 3.2. Comparison of multiple antibiotic resistance in five cities

As shown in Figure 2B, the antibiotic resistance characteristics of *Enterococcus faecalis* isolates from different regions were compared. It was found that the isolates in each region were highly resistant to erythromycin, florfenicol, tiamulin, tilmicosin, and tetracycline, and some of them were even 100% resistant. *Enterococcus faecalis* in Hangzhou, Quzhou and Wenzhou were completely resistant to erythromycin, while *Enterococcus faecalis* in Hangzhou, Ningbo and Jinhua were completely resistant to tiamulin and tilmicosin. Hangzhou and Ningbo are completely resistant to tetracycline.

There were significant differences in antibiotic resistance rates of enrofloxacin, sulfamethoxazole, trimethoprim/sulfamethoxazole, gentamicin and linezolid antibiotics in five different cities ($p < 0.05$). One strain of *Enterococcus faecalis* resistant to penicillin was found in Quzhou, and one strain and two strains of *Enterococcus faecalis* resistant to vancomycin were found in Hangzhou and Quzhou, respectively.

## 3.3. Detection of the resistance genes in *Enterococcus faecalis strains*

The resistance genes of oxazolidinone, phenicols, and lincoamine-pleuromutilin-streptomycin A were searched in 226

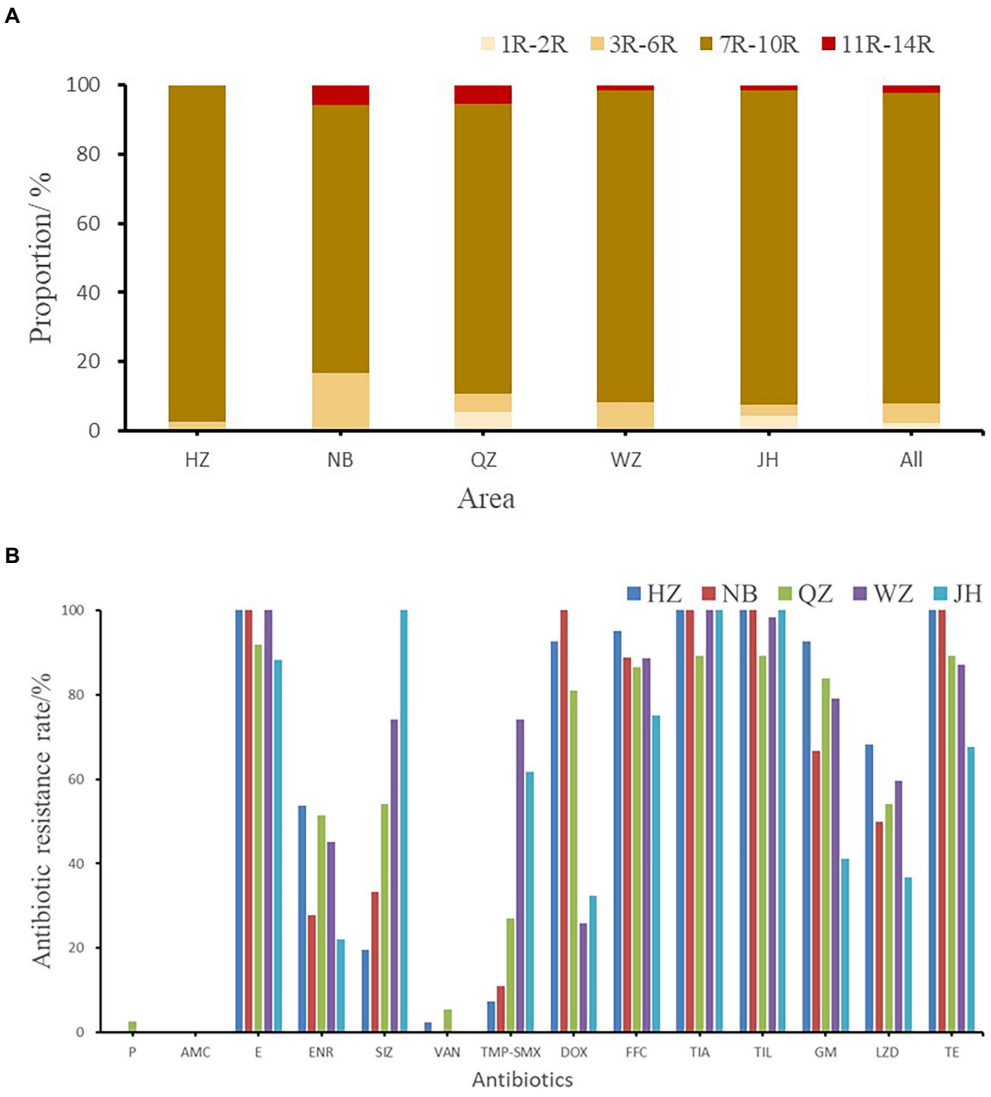


FIGURE 2
**(A)** The multi-drug resistance of *Enterococcus faecalis* from swine in Zhejiang. **(B)** The resistance rate of *E. faecalis* from five cities. HZ, Hangzhou; NB, Ningbo; QZ, Quzhou; WZ, Wenzhou; JH, Jinhua; All, Zhejiang Province.

resistant strains. 38.49% (87/226) strains was resistant to oxazolidinone and 82.30% (186/226) was resistant to phenicols. The results showed that only two oxazolidinone resistance genes were detected in these antibiotic resistant strains, including *optrA* and *poxtA* (Figure 3). A total of 173 strains contained oxazolidinones resistance genes (*optrA* and *poxtA*). The detection rates of *optrA* and *poxtA* were 71.68% (162/226) and 7.08% (16/226), respectively. The detection rates of *optrA* in Hangzhou, Ningbo, Quzhou, Wenzhou and Jinhua were 80.49% (33/41), 55.56% (10/18), 70.27% (26/37), 69.35% (43/62), and 73.53% (50/68), respectively. The detection rate of *optrA* in Hangzhou was significantly higher than that in Ningbo ($p < 0.05$). *optrA* and *fexA* were the main phenicols resistance genes, and the detection rates were 71.68% (162/226) and 69.47% (157/226), respectively. A total of 121 strains of *Enterococcus faecalis* containing lincoamine-pleuromutilin-streptomycin A resistance gene *lsa*(E) were detected, with a detection rate of 53.54% (121/226).

## 3.4. MLST analysis of *Enterococcus faecalis*

Through MLST analysis of 30 strains of oxazolidinone resistance gene positive *Enterococcus faecalis*, the evolution and genetic relationship among different strains were studied, and the transmission mechanism of *optrA* resistance gene in *Enterococcus faecalis* was inferred. The results showed that the distribution of different strains of *Enterococcus faecalis* was scattered. There were 19 different types of *Enterococcus faecalis* in 30 strains, of which 6 strains were dominant ST714 type, 3 strains were ST16 type, and the rest ST types contained 1 or 2 strains of *Enterococcus faecalis* (Supplementary Table S6). The ST type of each strain was shown in Supplementary Table S6. There are a small number of strains of *Enterococcus faecalis* with same ST type, but the ST types of most strains are different, indicating that horizontal transmission may

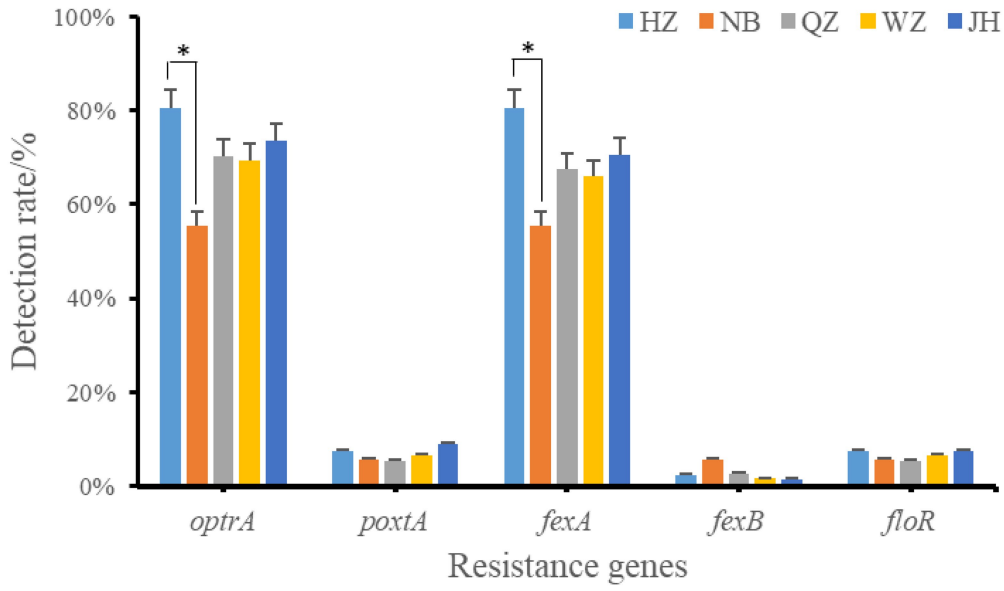


FIGURE 3
Positive rate of oxazolidinones and phenicoles resistance genes. *indicates that there is a significant difference between the two groups. HZ, Hangzhou; NB, Ningbo; QZ, Quzhou; WZ, Wenzhou; JH, Jinhua.

TABLE 2 Major features of plasmids analyzed.

| Type | Plasmid Name | | | |
|---|---|---|---|---|
| | pHZ318-optrA | plasmid2 | pNB304-optrA | N48037F-3 |
| Sequence Type | RepA_N | RepA_N | Rep3 | Rep3 |
| The total length(kb) | 87,785 | 78,419 | 36,331 | 40,269 |
| The number of ORF | 112 | 93 | 40 | 48 |
| Average GC content (%) | 34.53 | 34.77 | 34.34 | 34.01 |
| Accessory modules | MDR-1 region and MDR-2 region | MDR-1 region and *ant* (6)-I related region | *fexA-optrA* and IS*Vlu1* | *fexA-optrA* and IS*Vlu1* |

be the main mechanism of the prevalence of oxazolidinone resistance gene *optrA* in *Enterococcus faecalis*.

## 3.5. The *optrA* gene is transferable

The transconjugants isolated by mating *optrA* positive strains with JH2-2 were resistant to rifampicin and florfenicol antibiotics. 20 *optrA* positive strains were conjugated and transferred successfully, which indicated that some of the *optrA* genes were located on plasmids and could be transmitted by conjugation transfer. The highest conjugation transfer efficiency of HZ318 was $5.8 \times 10–4$, and the lowest conjugation efficiency was NB304, which was only $6.8 \times 10^{-6}$. According to the MIC results of wild strains and transconjugant, the resistant plasmid has been successfully introduced into the recipient bacteria (Supplementary Table S7). Among the 12 isolates of *Enterococcus faecalis*, 7 strains were RepA-N type plasmid with replicon type of Rep 9 family, 3 strains were lnc18 type plasmid with replicon type of rep2 family, and 2 strains were Rep_3 Small_theta type plasmid with replicon type of rep18 and repUS40, respectively. The results showed that the horizontal transmission of oxazolidone resistance gene *optrA* may be dominated by RepA_N type plasmid in swine farms of Zhejiang Province.

## 3.6. Characterization of plasmids pHZ318-optrA and pNB304-optrA

Plasmid pHZ318-optrA belonged to RepA_N plasmid with a total length of 87,785 bp, and 112 ORFs (Table 2; Figure 4). The replication initiation proteins of pHZ318-optrA belong to rep9 family, contains replicons *repA* and *repB*. Plasmid2 was also RepA_N and the backbone sequence was highly similar to pHZ318-optrA, so chosen as a reference (Figure 5). The entire backbone area of the plasmid pHZ318-optrA was inserted by

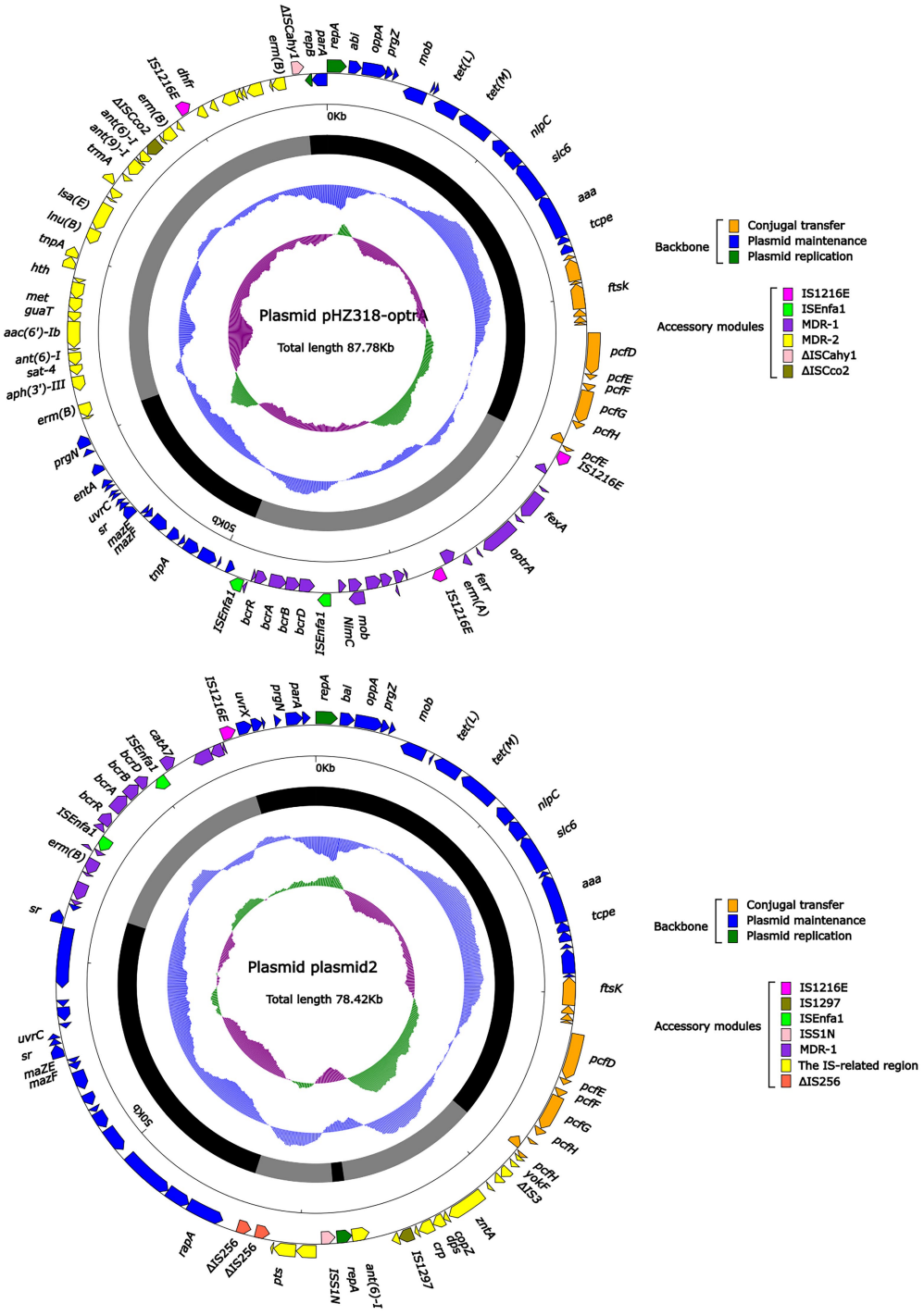


FIGURE 4
The complete sequence diagram of pHZ318-optrA and plasmid2. In the figure, the innermost ring represents (G – C)/(G+C); the blue ring indicates GC content, and the outward depression indicates that the GC content is higher than the mean value. Black area in the outer circle represents the backbone area and gray area represents the accessory modules. The outermost circle shows the distribution of genes represented by colored arrows in the plasmid.

MDR-1 and MDR-2, while that of plasmid2 was interrupted by a multidrug resistance region MDR-1 and *ant* (6)-I related region with multiple IS sequences (Figure 6). The MDR-1 region of pHZ318-optrA consisted of the following mobile elements: IS*1216*E-*fexA*-*optrA*-*ferr*-*erm*(A)-IS*1216*E, IS*1216*E and The IS*Enfa1*-*bcr*RABD-IS*Enfa1* unit (Figure 7). IS*1216*E was a complete insertion sequence with a full length of 808 bp, flanked by 24 bp reverse repeats and interspersed with 681 bp IS*6* family

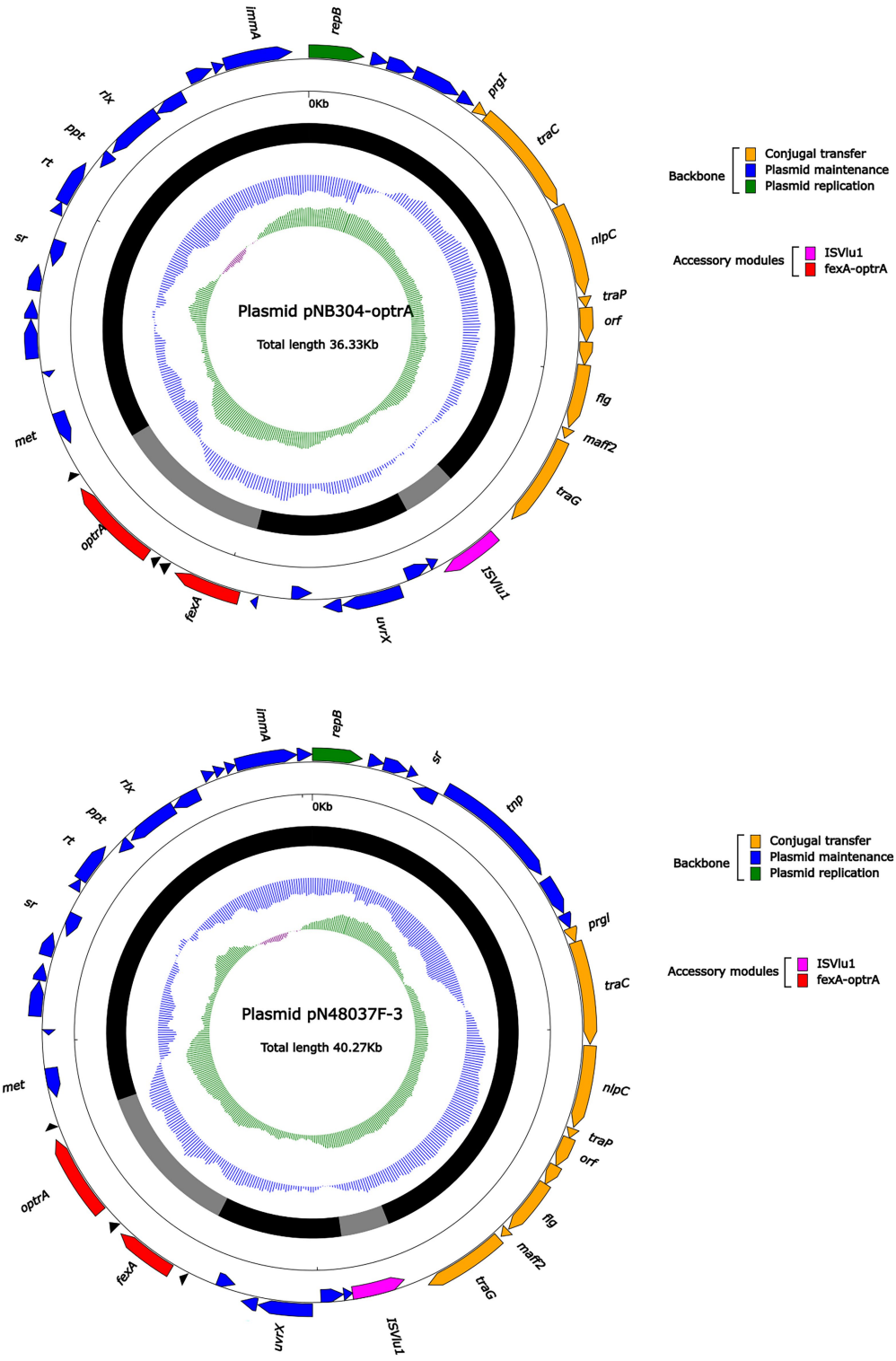


FIGURE 5
The complete sequence diagram of pNB304-optrA and N48037F-3.

transposable enzymes. Two IS*1216*E and *fexA-optrA-ferr-erm*(A) gene clusters together formed a transposable unit, which was found to be identical to the transposition unit in plasmidpc25-1 (CP030043.1) through comparison. Multidrug resistance region MDR-2 was mainly composed of some intermediate sequences of Tn*554* transposon, IS insertion sequence and antibiotic resistance gene clusters including erm (B) and *lsa* (E).

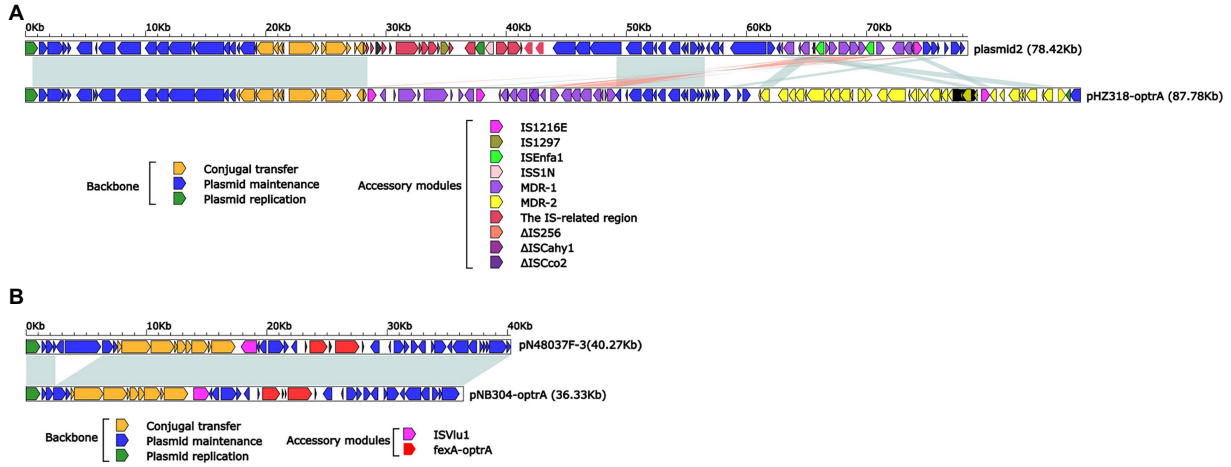


FIGURE 6
**(A)** Linear comparison of pHZ318-optrA and plasmid2. **(B)** Linear comparison of pNB304-optrA and pN48037F-3.

Plasmid pNB304-optrA belonged to Rep3 plasmid with a total length of 36,331 bp and 40 ORFs. The plasmid also contained two accessory modules, comprising *fexA-optrA* and IS*Vlu1* regions, without no other transposons and mobile elements. The antibiotic resistance gene only contain aminol resistance gene *fexA* and oxazolidinone resistance gene *optrA*. The main difference of plasmid pNB304-optrA and the reference plasmid N48037F-3 (Genbank Number: CP028723.1) was that pNB304-optrA lost part of the backbone area due to specific recombination in the downstream of *sr* gene after the initiation of plasmid replication.

By comparing the flanking sequences of *optrA* in pHZ318-optrA and pNB304-optrA, it was found that there was a phenicols resistance gene *fexA* in the upstream of *optrA* and a macrolide resistance gene *erm*(B) in the downstream of *optrA* in pHZ318-optrA. Figure 8 showed the flanking genetic environment of *optrA* in different strains, indicating genetic diversity. The plasmid-mediated oxazolidone resistance gene *optrA* was mostly related to IS insertion sequence, especially IS*1216E* mobile element. Other researchers also found similar genetic background IS*1216*E-*fexA*-*optrA*-*erm*(A)-IS*1216*E in many different *optrA* vectors, suggesting that IS*1216*E may promote the common transfer of *optrA*, *fexA*, and *erm* (A) among different plasmids.

## 3.7. Stability analysis of *optrA* resistant plasmids

The plasmids stability of transconjugants of HZ318 and NB304 strains without antibiotic selection pressure was analyzed. Results as shown in Figure 9, a small part of plasmid were lost in transconjugant HZ318-JH2-2 under no antibiotic selection pressure, while most of plasmids were lost in transconjugant NB304-JH2-2, in which plasmid HZ318-JH2-2 was lost by 16.3% ± 1.1% in 12 days. NB304-JH2-2 plasmid was lost by 85.0% ± 1.2% in 12 days. This indicated that there was some difference in the stability of the two plasmids.

# 4. Discussion

In this study, 226 *Enterococcus faecalis* strains isolated from swine farms in Zhejiang Province showed high-level resistance to nearly 57% (8/14) of commonly used antibiotics, and their antibiotic resistance rates were all higher than 50%. This showed that the traditional antibiotics were no longer suitable for the treatment of bacterial diseases in swine farms, especially tiamulin, which was widely used in livestock and poultry breeding as veterinary antibiotic and feed additives. More importantly, the resistance rate of linezolid, known as the "last line of defense" of Gram-positive bacteria, was as high as 38.49% (87/226), and the intermediary rate of antibiotic resistance was 32.30% (73/226). In this study, it was found that the antibiotic resistance of strains resistant to linezolid was often more serious. According to multiple antibiotic resistance analysis, it was basically concentrated in 7 or more multiple antibiotic resistance strains.

In this study, the resistance rate of *Enterococcus faecalis* to florfenicol was 82.51%, which was higher than 16.1% in Tibet (Peng et al., 2014). This may be directly related to the antibiotic use level of swine in Tibetan. Swine in Tibetan are generally in the form of stocking or semi-stocking, and the antibiotic use level is relatively low, but the swine industry is more developed in Zhejiang, the antibiotic use level is higher, resulting in the selection pressure of bacterial antibiotic resistance. In view of the high antibiotic resistance of linezolid, oxazolidinone antibiotic resistance genes *cfr*, *cfr*(B), *optrA*, and *poxtA* were detected in this study. *optrA* resistance gene made strains resistant to linezolid and also produced cross-resistance to phenicols antibiotics. Through further detection of other phenicols resistance genes *fexA*, *fexB*,

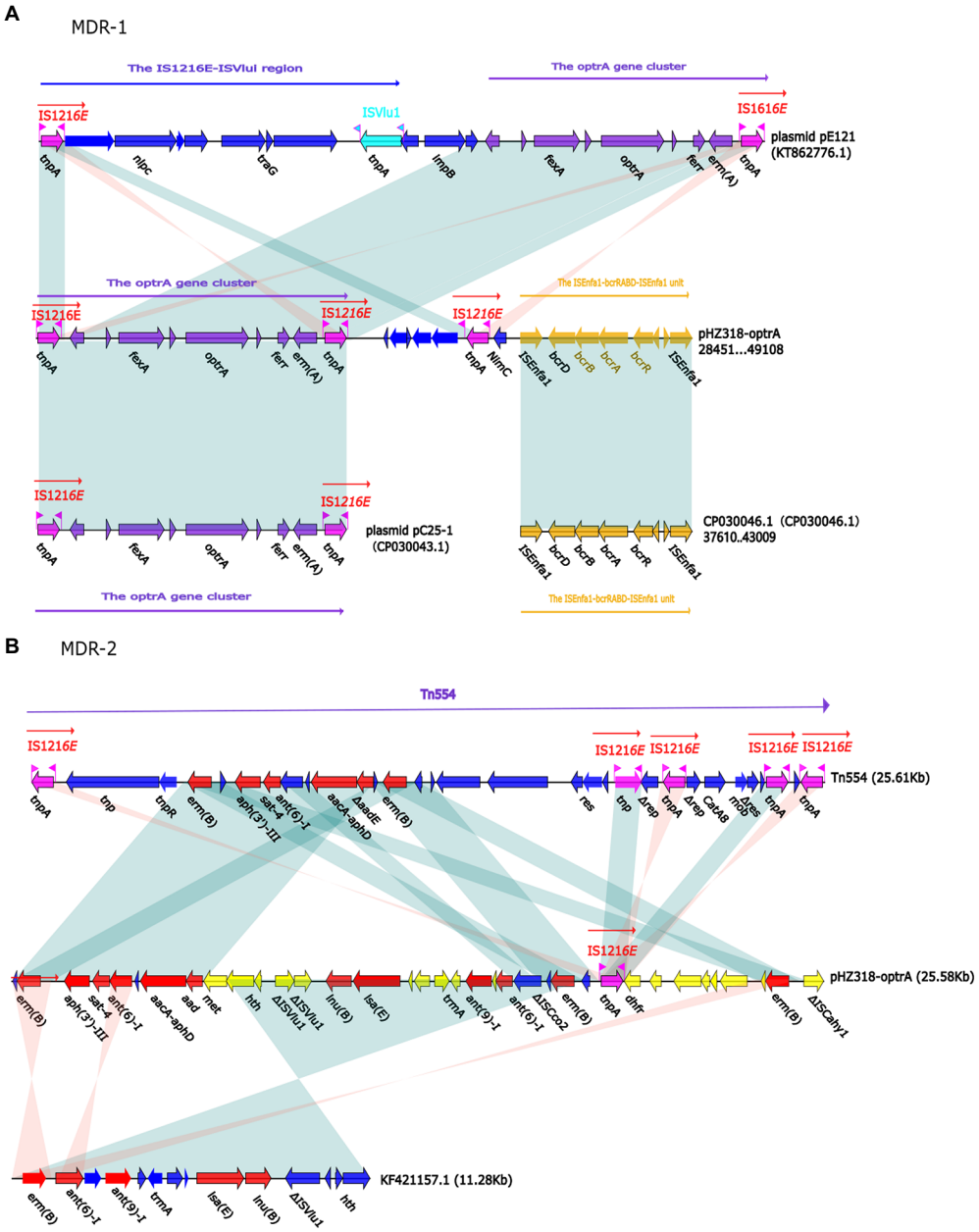


FIGURE 7
**(A)** The organization and alignment of MDR-1 region of pHZ318-optrA. **(B)** The organization and alignment of MDR-2 region of pHZ318-optrA. Genes are indicated by arrows. Genes, mobile elements, and other features are colored based on functional classification. Shadows indicate nucleotide homology is greater than 95%. The number in parentheses indicates the location of the fragment in the plasmid.

*cmlA*, and *floR*, it was found that *optrA* + *fexA* genotype was the main mechanism of resistance of *Enterococcus* to oxazolidone and phenicols antibiotics. The emergence of *optrA* multidrug resistance gene and its prevalence in *Enterococcus* have weakened the efficacy of linezolid in the treatment of clinical antibiotic resistant strains to a certain extent, posing a huge potential threat to human health.

Insertion sequence, transposon and integron can assist the horizontal transfer of antibiotic resistance genes among bacteria, which is an important reason for the widespread existence of antibiotic resistance genes in different environments and microorganisms (Stokes and Gillings, 2011). Plasmids are important vectors for carrying these Mobile Genetic Elements (MGEs) and acquired antibiotic resistance genes, and these MGEs provide a mechanism for intracellular movement, so that antibiotic resistance genes have the opportunity to "escape" to host chromosomes or other plasmids (Partridge et al., 2018). In the presence of antibiotic selection pressure, the interaction between different types of MGEs promotes the evolution of a variety of antibiotic resistant bacteria (Partridge et al., 2010).

We identified two conjunctive multi-resistance plasmids carrying *optrA* and analyzed the genetic context of *optrA* and MDR region. IS*1216*E could be reassembled to form a circular

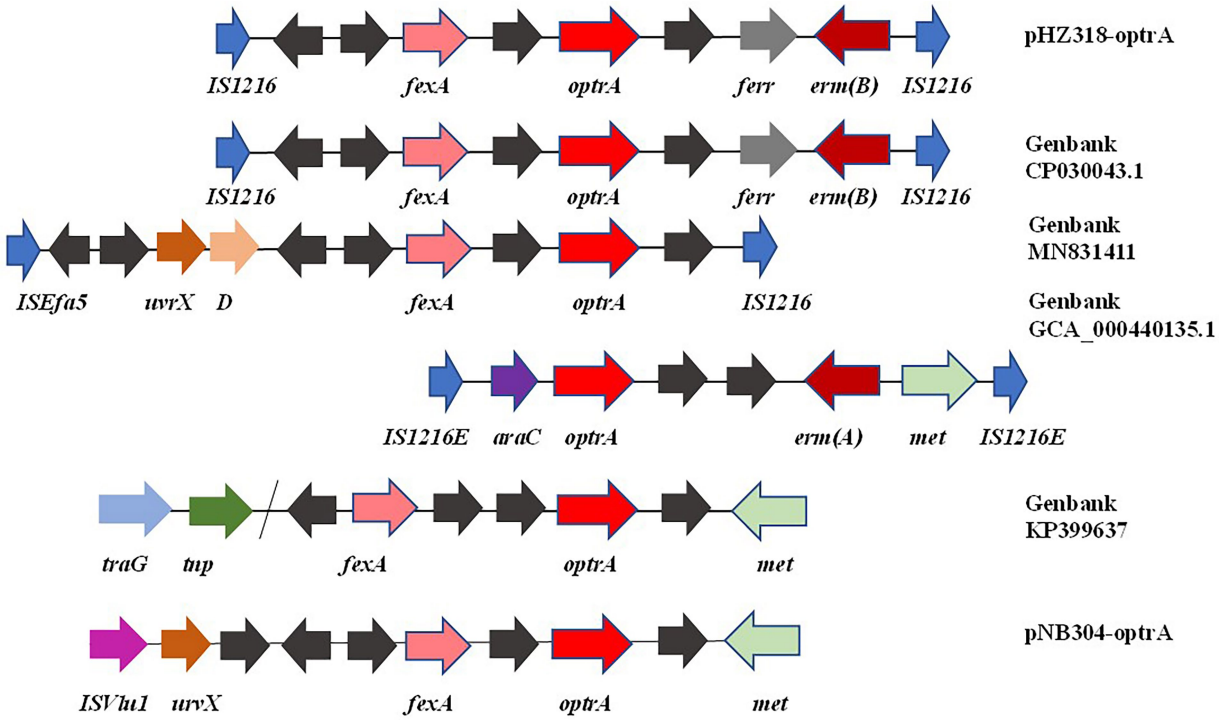


FIGURE 8
Diversity of flanking genetic environment of *optrA* gene on plasmids.

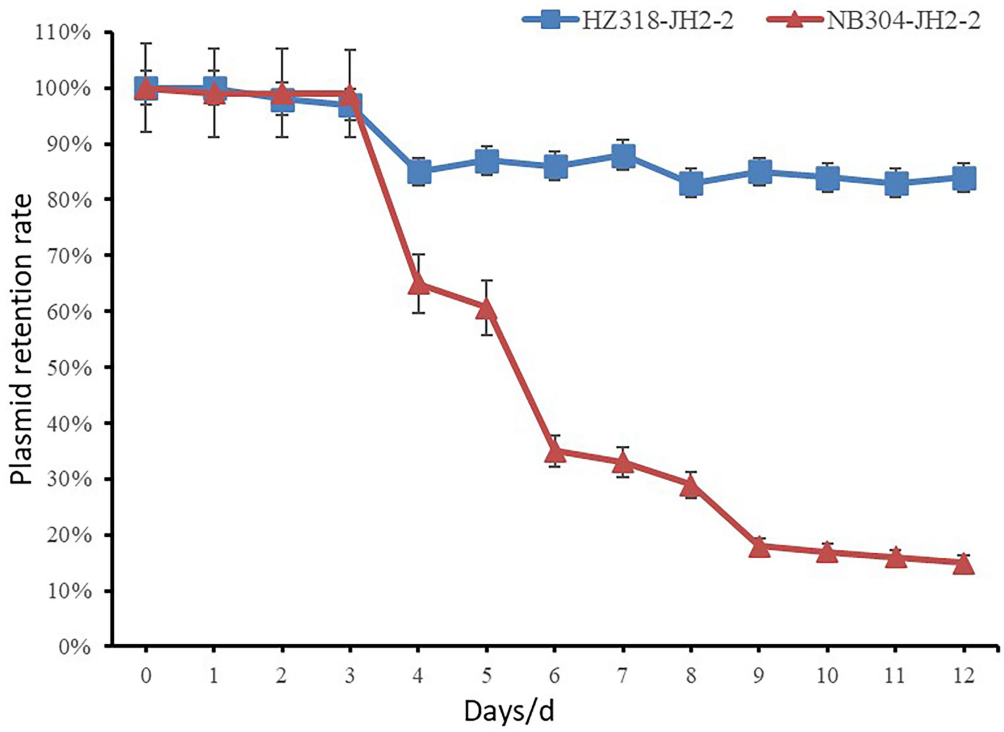


FIGURE 9
Stability of the plasmids in conjugants.

intermediate, which could integrate *optrA* into the plasmid or chromosome and spread among different bacterial species. In addition, there was a partial complete sequence of Tn*554* transposon downstream of the plasmid *optrA*, which endows the strain with resistance to macrolides and streptomycin. And studies have shown that IS*1216*E, Tn*554* and Tn*558* may promote the horizontal transmission of *optrA* and *poxtA* (Kang et al., 2019). The existence of other antibiotic resistance genes, including *fexA*, *fexB* and *erm*(A), may lead to the common selection of *optrA* and *poxtA*, which makes it widely spread in *Enterococcus*.

IS*1216*E has also been reported in previous literature, such as vancomycin resistance gene *VanA* in *Enterococcus* and multidrug resistance genes *poxtA*, *optrA*, and *cfr* in *Enterococcus* and *Staphylococci* (Darini et al., 2000; Liu et al., 2013; Antonelli et al., 2018). This shows that IS*1216*E plays an important role in the transmission of antibiotic resistance genes in Gram-positive bacteria. In this experiment, a partial complete sequence of transposon Tn*554* was also found downstream of IS*1216*E-*fexA*-*optrA*-*ferr*-*erm*(A)-IS*1216*E transposon of plasmid pHZ318-optrA. We should pay more attention to the transmission of transferable oxazolidinone resistance genes in foodborne Gram-positive bacteria, because livestock and poultry farms may become a repository of transferable oxazolidinone resistance genes, and these antibiotic resistance genes may be transmitted to humans through the food chain.

## 5. Conclusion

The presence of multiple mobile elements in a *optrA*-carrying multi-resistance plasmid makes it flexible. These elements aid its persistence and dissemination among *Enterococcus faecalis* and potentially other Gram-positive bacteria. This study demonstrated the abundance of oxazolidinone and phenicols resistance genes of swine origin in Zhejiang Province. It also upgraded the research on plasmids containing *optrA* antibiotic resistance genes. This research also provided the antibiotic profile of bacteria isolated from swine farms in Zhejiang Province, indicating that local farmers can possibly reduce the use of specific antibiotics to reduce the evolution of multi-resistant strains.

## Data availability statement

The data presented in the study are deposited in the NCBI repository, accession numbers OQ181208 and OQ181209.

## Author contributions

EZ: visualization, data curation, software, and writing-original draft preparation. SZ: conceptualization, methodology, formal analysis, and writing-original draft preparation. WZ: visualization and investigation. JZ: software and writing—review and editing. JH: formal analysis and resources. DQ: conceptualization, resources, supervision, and writing-review and editing. All authors contributed to the article and approved the submitted version.

## Funding

This work was supported by National Natural Science Foundation of China (no. 32172188) and the Key R&D projects in Zhejiang Province (nos. 2018C02024 and 2020C02031).

## Acknowledgments

We gratefully acknowledge the reviewers for their constructive comments and suggestions.

## Conflict of interest

The authors declare that the research was conducted without any commercial or financial relationships that could be construed as a potential conflict of interest.

## Publisher's note



## Supplementary material

The Supplementary material for this article can be found online at: https://www.frontiersin.org/articles/10.3389/fmicb.2022.991352/full#supplementary-material

## References

Anjum, M. F., Duggett, N. A, AbuOun, M., Randall, L., Nunez-Garcia, J., Ellis, R. J., et al. (2016). Colistin resistance in Salmonella and Escherichia coli isolates from a pig farm in Great Britain. *J. Antimicrob. Chemother.* 71, 2306–2313. doi: 10.1093/jac/dkw149

Antonelli, A., D'Andrea, M., Brenciani, A., Galeotti, A,, Morroni, C. L., Pollini, S., et al. (2018). Characterization of *poxtA*, a novel phenicol-oxazolidinone-tetracycline resistance gene from an MRSA of clinical origin. *J. Antimicrob. Chemother.* 73, 1763–1769. doi: 10.1093/jac/dky 088

Bender, J. K., Cattoir, V., Hegstad, K., Sadowy, E., Coque, T. M., Westh, H., et al. (2018). Update on prevalence and mechanisms of resistance to linezolid, tigecycline and daptomycin in enterococci in Europe: towards a common nomenclature. *Drug Resist. Updat.* 40, 25–39. doi: 10.1016/j.drup.2018.10.002

Boetzer, M., and Pirovano, W. (2012). Toward almost closed genomes with GapFiller. *Genome Biol.* 13:R56. doi: 10.1186/gb-2012-13-6-r56

Bolger Anthony, M., Lohse, M., and Usadel, B. (2014). Trimmomatic: a flexible trimmer for Illumina sequence data. *Bioinformatics*. 30, 2114–2120. doi: 10.1093/bioinformatics/btu170

Carmen, T., Andrea, A. C., Laura, R. R., Ricardo, L.-S., Rosa, D. C., and Coque, T. M. (2018). Antimicrobial resistance in enterococcus spp. of animal origin. *Microbiol. Spectr.* 6. doi: 10.1128/microbiolspec.ARBA-0032-2018

Darini, A. L., Palepou, M. F., and Woodford, N. (2000). Effects of the movement of insertion sequences on the structure of VanA glycopeptide resistance elements in *enterococcus faecium*. *Antimicrob. Agents Chemother.* 44, 1362–1364. doi: 10.1128/aac.44.5.1362-1364.2000

Falagas, M. E., Karageorgopoulos, D. E., and Nordmann, P. (2011). Therapeutic options for infections with *Enterobacteriaceae* producing carbapenem-hydrolyzing enzymes. *Future Microbiol.* 6, 653–666. doi: 10.2217/fmb.11.49

Hao, W., Shan, X., Li, D., Schwarz, S., Zhang, S. M., Li, X. S., et al. (2019). Analysis of a *poxtA*- and optrA-co-carrying conjugative multiresistance plasmid from enterococcus faecalis. *J. Antimicrob. Chemother.* 74, 1771–1775. doi: 10.1093/jac/dkz109

Jensen, L. B., Garcia-Migura, L., Valenzuela, A. J., Løhr, M., Hasman, H., and Aarestrup, F. M.. (2010). A classification system for plasmids from *enterococci* and other gram-positive bacteria. *J. Microbiol. Methods* 80, 25–43. doi: 10.1016/j.mimet.2009.10.012

Kang, Z. Z., Lei, C. W., Kong, L. H., Wang, Y. L., Ye, X. L., Ma, B. H., et al. (2019). Detection of transferable oxazolidinone resistance determinants in *enterococcus faecalis* and *enterococcus faecium* of swine origin in Sichuan Province, China. *J. Glob. Antimicrob. Resist.* 19, 333–337. doi: 10.1016/j.jgar.2019.05.021

Lane, D. J. (1991). "16S/23S rRNA sequencing" in *Nucleic Acid Techniques in Bacterial Systematics*. eds. E. Stackebrandt and M. Goodfellow (New York, NY: John Wiley and Sons), 115–175.

Liu, Y., Wang, Y., Schwarz, S., Li, Y., Shen, Z., Zhang, Q., et al. (2013). Transferable multiresistance plasmids carrying cfr in enterococcus spp. from swine and farm environment. *Antimicrob. Agents Chemother.* 57, 42–48. doi: 10.1128/AAC.01605-12

Liu, Y., Wang, Y., Wu, C., Shen, Z., Schwarz, S., Du, X. D., et al. (2012). First report of the multidrug resistance gene cfr in *enterococcus faecalis* of animal origin. *Antimicrob. Agents Chemother.* 56, 1650–1654. doi: 10.1128/AAC.06091-11

Nederbragt, A. J. (2014). On the middle ground between open source and commercial software - the case of the Newbler program. *Genome Biol.* 15, 1–2. doi: 10.1186/gb4173

Partridge, S. R., Guy, T., Enrico, C., and Iredell, J. R. (2010). Gene cassettes and cassette arrays in mobile resistance integrons. *FEMS Microbiol. Rev.* 4, 757–784. doi: 10.1111/j.1574-6976.2009.00175.x

Partridge, S. R., Kwong, S. M., Neville, F., and Jensen, S. O. (2018). Mobile genetic elements associated with antimicrobial resistance. *Clin. Microbiol. Rev.* 31. doi: 10.1128/CMR.00088-17

Peng, L., Dongfang, W., Kunyao, L., Sizhu, S., Tao, H., Xuan, L., et al. (2014). Investigation of antimicrobial resistance in Escherichia coli and enterococci isolated from Tibetan pigs. *PLoS One* 9:e95623. doi: 10.1371/journal.pone.0095623

Pillai, S. K., Sakoulas, G., Wennersten, C., Eliopoulos, G. M., Moellering, R. C. Jr., Ferraro, M. J., et al. (2002). Linezolid resistance in Staphylococcus aureus: characterization and stability of resistant phenotype. *J Infect Dis* 186, 1603–1607. doi: 10.1086/345368

Ruiz-Garbajosa, P., Bonten, M. J., Robinson, D. A., Top, J., Nallapareddy, S. R., Torres, C., et al. (2006). Multilocus sequence typing scheme for *enterococcus faecalis* reveals hospital-adapted genetic complexes in a background of high rates of recombination. *J. Clin. Microbiol.* 44, 2220–2228. doi: 10.1128/jcm.02596-05

Schwarz, S., Werckenthin, C., and Kehrenberg, C. (2000). Identification of a plasmid-borne chloramphenicol-florfenicol resistance gene in Staphylococcus sciuri. *Antimicrob. Agents Chemother.* 44, 2530–2533. doi: 10.1128/aac.44.9.2530-2533.2000

Senior, K. (2000). FDA approves first drug in new class of antibiotics. *Lancet* 355:1523. doi: 10.1016/s0140-6736(00)02173-5

Stokes, H. W., and Gillings, M. R. (2011). Gene flow, mobile genetic elements and the recruitment of antibiotic resistance genes into gram-negative pathogens. *FEMS Microbiol. Rev.* 35, 790–819. doi: 10.1111/j.1574-6976.2011.00273.x

Sun, T. (2014). The use of antibiotics and bacterial resistance. *Chin. J. Clin. Pharmacol.* 30, 151–155. doi: 10.3969/j.issn.1001-6821.2014.02.020

Wang, M. Y., Lu, X., Kan, B., Chen, S. E., and Fan, Y. B. (2021). Research progress on bacterial resistance and gene carrying resistance in migratory birds. *Zhonghua Yu Fang Yi Xue Za Zhi* 55, 271–276. doi: 10.3760/cma.j.cn112150-20200914-01199

Wang, Y., Lv, Y., Cai, J., Schwarz, S., Cui, L., Hu, Z., et al. (2015). A novel gene, optrA, that confers transferable resistance to oxazolidinones and phenicols and its presence in *enterococcus faecalis* and *enterococcus faecium* of human and animal origin. *J. Antimicrob. Chemother.* 70, 2182–2190. doi: 10.1093/jac/dkv116

Yang, W., Lv, Y., Cai, J., Stefan, S., Cui, L., Hu, Z., et al. (2015). A novel gene, optrA, that confers transferable resistance to oxazolidinones and phenicols and its presence in *enterococcus faecalis* and *enterococcus faecium* of human and animal origin. *J. Antimicrob. Chemother.* 8:2182. doi: 10.1093/jac/dkv116

Yasufuku, T., Shigemura, K., Shirakawa, T., Matsumoto, M., Nakano, Y., Tanaka, K., et al. (2011). Mechanisms of and risk factors for fluoroquinolone resistance in clinical *enterococcus faecalis* isolates from patients with urinary tract infections. *J. Clin. Microbiol.* 49, 3912–3916. doi: 10.1128/jcm.05549-11

Zhao, Q., Wang, Y., Wang, S., Wang, Z., Du, X.-D., Jiang, H., et al. (2016). Prevalence and abundance of Florfenicol and linezolid resistance genes in soils adjacent to swine feedlots. *Sci. Rep.* 6:32192. doi: 10.1038/srep32192

frontiers | Frontiers in Microbiology

TYPE Original Research
PUBLISHED 16 March 2023
DOI 10.3389/fmicb.2023.1135278



OPEN ACCESS

EDITED BY
Tao Li,
Shanghai Veterinary Research Institute (CAAS), China

REVIEWED BY
Yanan Yin,
Xi'an University of Architecture and Technology, China
Dong Yang,
Tianjin Institute of Environmental and Operational Medicine, China

*CORRESPONDENCE
Wei-Guo Zhang
✉ weiguozhang@jaas.ac.cn
Ya-Jun Chang
✉ changyj@cnbg.net

†These authors have contributed equally to this work

SPECIALTY SECTION
This article was submitted to Antimicrobials, Resistance and Chemotherapy, a section of the journal Frontiers in Microbiology

RECEIVED 31 December 2022
ACCEPTED 28 February 2023
PUBLISHED 16 March 2023

CITATION
Zhang M-S, Liang S-Z, Zhang W-G, Chang Y-J, Lei Z, Li W, Zhang G-L and Gao Y (2023) Field ponding water exacerbates the dissemination of manure-derived antibiotic resistance genes from paddy soil to surrounding waterbodies. *Front. Microbiol.* 14:1135278. doi: 10.3389/fmicb.2023.1135278



# Field ponding water exacerbates the dissemination of manure-derived antibiotic resistance genes from paddy soil to surrounding waterbodies

Ming-Sha Zhang[1†], Si-Zhou Liang[2,3†], Wei-Guo Zhang[1,3,4,5*], Ya-Jun Chang[2*], Zhongfang Lei[4], Wen Li[6], Guo-Liang Zhang[7] and Yan Gao[8]

[1]School of Resources and Environmental Sciences, Nanjing Agricultural University, Nanjing, China, [2]Jiangsu Key Laboratory for the Research and Utilization of Plant Resources, Institute of Botany, Jiangsu Province and Chinese Academy of Sciences (Nanjing Botanical Garden Memorial Sun Yat-Sen), Nanjing, China, [3]School of the Environment and Safety Engineering, Jiangsu University, Zhenjiang, China, [4]School of Life and Environmental Sciences, University of Tsukuba, Tsukuba, Japan, [5]Jiangsu Key Laboratory for Food Quality and Safety-State Key Laboratory Cultivation Base, Ministry of Science and Technology, Nanjing, China, [6]School of Life Sciences, Nanjing University, Nanjing, China, [7]Huaiyin Institute of Technology, Huaian, China, [8]Institute of Agricultural Resources and Environment, Jiangsu Academy of Agricultural Sciences, Nanjing, China

Farmlands fertilized with livestock manure-derived amendments have become a hot topic in the dissemination of antibiotic resistance genes (ARGs). Field ponding water connects rice paddies with surrounding water bodies, such as reservoirs, rivers, and lakes. However, there is a knowledge gap in understanding whether and how manure-borne ARGs can be transferred from paddy soil into field ponding water. Our studies suggest that the manure-derived ARGs *aadA1*, *bla1*, *catA1*, *cmlA1-01*, *cmx(A)*, *ermB*, *mepA* and *tetPB-01* can easily be transferred into field ponding water from paddy soil. The bacterial phyla Crenarchaeota, Verrucomicrobia, Cyanobacteria, Choloroflexi, Acidobacteria, Firmicutes, Bacteroidetes, and Actinobacteria are potential hosts of ARGs. Opportunistic pathogens detected in both paddy soil and field ponding water showed robust correlations with ARGs. Network co-occurrence analysis showed that mobile genetic elements (MGEs) were strongly correlated with ARGs. Our findings highlight that manure-borne ARGs and antibiotic-resistant bacteria in paddy fields can conveniently disseminate to the surrounding waterbodies through field ponding water, posing a threat to public health. This study provides a new perspective for comprehensively assessing the risk posed by ARGs in paddy ecosystems.

KEYWORDS

**antibiotic resistance genes, field ponding water, rice paddy, manure fertilized soil, public health**

## 1. Introduction

In recent years, the contamination of antibiotic resistance genes (ARGs) caused by misuse and overuse of antibiotics in healthcare and animal husbandry has attracted worldwide concern (Martínez, 2008; Zhu et al., 2013; Rodriguez-Mozaz et al., 2015; Zhang et al., 2022). Livestock manure is a hotspot that harbors abundant ARGs under selective pressure of antibiotics (Zhu

et al., 2013; Jia et al., 2017; Congilosi and Aga, 2021; Macedo et al., 2022). The overuse of chemical fertilizers results in severe soil hardening, agricultural nonpoint source pollution, and disruption of the ecological balance (Jiao et al., 2017; Zou et al., 2020). Therefore, in recent years, some policies have been formulated and implemented to alleviate these problems. Of these, the well-known one is that "organic fertilizers partially replace chemical fertilizers" (Jiao et al., 2017; Zhang et al., 2021b). Consequently, amounts of livestock manure or manure-derived amendments as organic fertilizer have been poured into farmland, but the contamination of antibiotics and ARGs in farmland has become increasingly severe, attracting increasing attention (Ding et al., 2019; Pu et al., 2020; Zhang et al., 2022). Farmlands fertilized with manure or manure-derived amendments have become important sources of ARG contamination in other environments (Zheng et al., 2018; Zhang et al., 2021b). ARGs can be transferred from soil to vegetables and fruits, posing a direct threat to human health (Marti et al., 2013; Zhu et al., 2017; Mei et al., 2021; Zhang et al., 2022). The emergence and spread of antibiotic resistance kill approximately 4.95 million people worldwide annually (Ding et al., 2022).

Paddy fields are among the largest farmlands in the world. Compared with other farmlands, paddy fields are more convenient for transferring substances in the soil to other environments through field ponding water. Due to irrigation with reclaimed wastewater and fertilization with livestock manure amendments, the rice paddy fields have become a hotspot of antibiotics and ARGs (Awad et al., 2015; Zhou et al., 2019; Guo et al., 2021; Zhang et al., 2021b). Although the abundance, diversity and environmental behaviors of ARGs were well investigated in these studies, the interaction between the paddy soil and field ponding water was poorly understood. If ARGs can be transferred into field ponding water from paddy soil, then they will easily disseminate to the surrounding waterbodies, such as reservoirs, rivers, and lakes, some of which are important sources of drinking water (Zhang et al., 2021a). Consequently, the main objective of this study was to elucidate whether and how ARGs could be transferred into field ponding water from paddy soils fertilized with livestock manure. Microbial community is the key factor which determines the environmental behavior of ARGs (Hu et al., 2017; Guo et al., 2018; Zheng et al., 2018; Zhang et al., 2021a). Therefore, the relationship between the microbiome and resistome was investigated in our study. Further, to evaluate the direct threat of ARGs to human health, we assessed the correlation between ARGs and opportunistic pathogens detected in paddy soil and field ponding water. Horizontal gene transfer (HGT) plays an important role in ARG dissemination among different bacterial species (Aguila-Arcos et al., 2017; Lerminiaux and Cameron, 2019; Schmidt et al., 2022). Finally, the correlation between the mobile genetic elements (MGEs) and ARGs was determined.

# 2. Materials and method

## 2.1. Sampling site and sample collection

Soil was collected from a rice paddy field located at the Jiangsu Academy of Agricultural Sciences, Nanjing, China (32°01N, 118°52E). The agricultural soil in this area is classified as yellow-brown soil according to the Chinese Soil Taxonomy and as Udalf according to the US Soil Taxonomy. Commercial chicken manure was purchased from a farmer's market in Nanjing. Fifty kilograms soil sample was mixed with 2.5 kg livestock manure thoroughly. This soil mixture was aged for 3 months from March 7, 2021 to June 6, 2021. In our study, six customized plastic pots were designed to conduct pot experiments (Supplementary Figure S1). Seven kilograms soil/manure mixture filled in each plastic pot. Six plastic pots were set as six repetitions. Sterile water without ARGs detection was used to steep the soil for 7 days. Eighteen healthy rice seedings with similar growth condition were selected to transplant. Before transplant, the roots of these rice seedings were washed with five times. The flushing water was collected. An inoculating loop was soaked in the flushing water, and then lined on the surface of solid plate of Luria-Bertani broth to detect the microbes. When bacteria were not detected, three rice seedings were transplanted in each pot. After transplant, the six repetitive plastic pots were placed in an artificial climate chamber ZRG-1000A (Binglin, China). Gas cylinders filled with sterile air were linked to an artificial climate chamber to continuously supply fresh air. This avoided contamination by airborne ARGs. During the experiment, the sterile water without ARGs detection was used to irrigate the soil keeping the water 5 cm above the soil surface. No organic or inorganic fertilizers were used during the whole experimental period. The temperature was kept at 30°C in daytime and 25°C in night. The photoperiod was kept 12 h form 6:00 A.M. to 18:00 P.M every day. The light intensity was 30,000 lux. Field ponding water and soil samples were collected on June 28, July 21, August 22, September 27, and October 22. Each time 200 ml of field ponding water was collected from each pot. The water samples were stored in plastic bottles and immediately transported to the laboratory and stored at 4°C. Nitrocellulose membranes (0.45 μm) were used to obtain the microorganisms through filtering the water sample. The obtained microbes were stored at −20°C. Each time 50 g of paddy soil from each pot was collected. After collection, the soil samples were immediately transported to the laboratory and stored at −20°C in Ziplock bags for extracting DNA. Eighteen ARGs and two MGEs were detected in the commercial chicken manure in this study (Supplementary Table S1). Among which, eight ARGs *aadA1*, *bla1*, *catA1*, *cmlA1-01*, *cmx(A)*, *ermB*, *mepA* and *tetPB-01*, and two MGEs *tnp-01* and *-02* were selected as target detecting genes. These eight manure-derived ARGs and two MGEs were not detected in the paddy soil before mixed with the chicken manure.

## 2.2. DNA extraction and real-time quantitative polymerase chain reaction (RT-qPCR)

DNA in paddy soil was extracted from 1.0 g of soil using the FastDNA Spin Kit for soil (MP Biomedical, United States), according to the manufacturer's instructions. Field ponding water DNA was extracted using a PowerWater DNA isolation kit (Mobio, United States), according to the manufacturer's instructions. The purity, quality, and quantity of extracted DNA were determined using the method described by Li et al. (2017). RT-qPCR was conducted using a CFX96 Touch Real-time PCR System (Bio-Rad, United States). The primers information of ARGs, MGEs, and 16S rRNA were shown in Supplementary Table S1. The mixtures were reacted in a 20 μl system. All qPCR reactions were conducted in triplicate for each

primer set, including the non-template negative control. PCR amplification was conducted according to the following program: 95°C for 10 min to activate enzymes, followed by 40 cycles at 95°C for 30 s to denature DNA, then annealing at 60°C for 30 s. When the Ct value was less than 31 for more than two positive replicates, amplification was considered valid (Su et al., 2015). The absolute copy numbers of ARGs and MGEs were normalized to the absolute 16S rRNA gene copy numbers (Looft et al., 2012; Wang et al., 2014; Guo et al., 2018; Zhang et al., 2021b).

## 2.3. Amplicon high-throughput sequencing and data processing

To characterize bacterial communities, the V4 region of the 16S rRNA gene was amplified using the primer set 515F/806R (Bates et al., 2011). The low-quality reads were trimmed using CUTADAPT version 1.9.1. According to the unique barcodes, the sample data were separated from the reads. After removing the barcodes and primers, raw reads were generated. The chimeric sequences of raw reads were identified and removed using the UCHIME algorithm (Edgar et al., 2011) to yield effective tags (clean reads). UPARSE, version 7.0.1001 was used to cluster the clean sample reads. Sequences with a threshold similarity of 97% were binned into operational taxonomic units. The National Center for Biotechnology Information (NCBI) database was selected to deposit all 16S rRNA gene sequences generated in this study under the accession number PRJNA934052.

## 2.4. Data analysis and visualization

All mathematical operations were performed in Microsoft Office 365. The Sankey diagram was depicted with Origin 9.0. The co-occurrence network was analyzed and visualized using R software with the graph package. To detect significant correlations, we constructed a correlation matrix by calculating all possible pairwise Spearman's rank correlations between the ARGs and bacterial taxa, ARGs and opportunistic pathogens, and ARGs and MGEs. The effective Spearman's correlation coefficient ($\rho$) was set at >0.8 on the premise of $p < 0.05$.

# 3. Results and discussion

## 3.1. Dynamic distribution of ARGs in rice paddy soil and field ponding water

Figure 1 shows that eight ARGs, *aadA1*, *bla1*, *catA1*, *cmlA1-01*, *cmx(A)*, *ermB*, *mepA*, and *tetPB-01*, were both detected in paddy soil and field ponding water. These genes confer resistance to aminoglycoside, beta-lactamase, MLSB (macrolide, lincosamide, and streptogramin B), multidrugs, and tetracycline. In addition, two MGEs, *tnp-01* and *-02*, were also detected in both paddy soil and field ponding water. These results indicate that ARGs can be easily transferred into field ponding water from paddy soils. Water bodies such as reservoirs, rivers, and lakes surrounded by paddy fields suffer from ARGs contamination (Yang et al., 2017; Wang et al., 2020; Zhang et al., 2021b). In these studies, the contamination sources mainly attributed to domestic sewage, livestock wastewater, aquaculture wastewater, and medical wastewater. Field ponding water is an important connection between paddy fields and surrounding waterbodies (Zhang et al., 2021a). Although the rice paddy fields have become a hotspot of antibiotics and ARGs because of irrigation with reclaimed wastewater and fertilization with livestock manure amendments, the rice paddy fields have become a hotspot of antibiotics and ARGs (Awad et al., 2015; Zhou et al., 2019; Guo et al., 2021; Zhang et al., 2021b), the interaction between the paddy soil and field ponding water has not been demonstrated yet. Our study verifies that field ponding water is also an important contamination source of ARGs to other large-scale water bodies, through facilitating the dissemination of manure-derived ARGs in paddy ecosystems.

The abundance of ARGs in paddy soil was three orders of magnitude higher than that in field ponding water (Figure2). The paddy soil fertilized with chicken manure was the source of the antibiotic resistome in field ponding water. The number of genes in paddy soil increased from June to October. Specifically, the abundances of *aadA1*, *bla1*, *catA1*, *cmlA1-01*, *cmx(A)*, *ermB*,

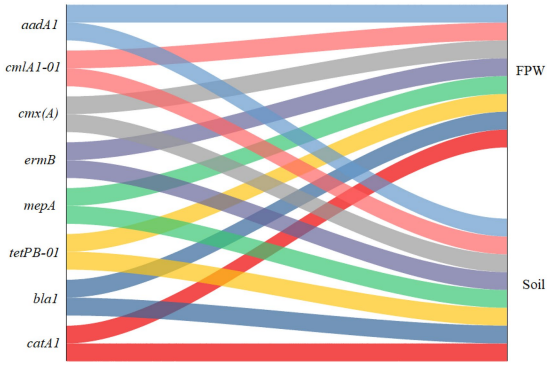


FIGURE 1
Sankey diagram depicting the distribution of antibiotic resistance genes (ARGs) in paddy soil fertilized with livestock manure and field ponding water (FPW).

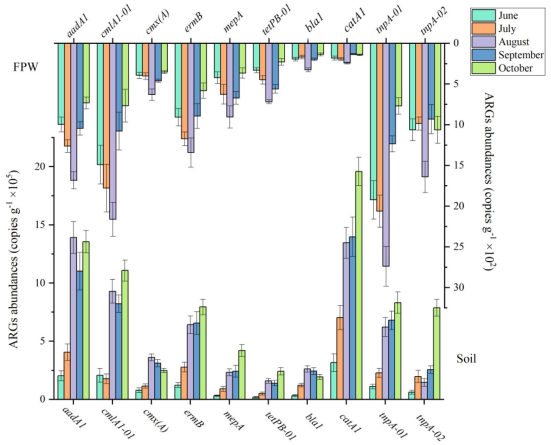


FIGURE 2
The dynamic abundances of ARGs in paddy soil fertilized with livestock manure amendment and field ponding water (FPW). The error bars represent±SD ($n$=6).

*mepA*, and *tetPB-01* in October were 5.68-, 5.03-, 5.22-, 4.35-, 2.18-, 5.49-, 12.27-, and 12.44-fold higher than those in June, respectively. Compared with other ARGs, the genes *catA1*, *aadA1* and *cmlA1-01* were more abundant in the paddy soil. The genes in field ponding water increased from June to August but decreased from August to October. The abundance of genes *cmlA1-01*, *aadA1* and *ermB* were higher than the other ARGs. The reasons for the two different tendencies of the antibiotic resistome in paddy soil and field ponding water are discussed in the following sections.

## 3.2. Microbial mechanisms driving the dynamic pattern of antibiotic resistome

Although ARGs can exist in the environment in the form of eDNA, microbes are predominant in the prevalence of antibiotic resistome (Beaber et al., 2004; Martínez, 2008). The microbiome determines the pattern of antibiotic resistome (Hu et al., 2017; Guo et al., 2018; Zheng et al., 2018; Zhang et al., 2021a). In this study, the absolute abundances of 16S rRNA in paddy soil and field ponding water showed a similar tendency to that of the total ARGs (Figure 3).

The core bacterial taxa that intensively influenced the ARGs pattern have been also investigated in several previous studies through co-occurrence network analysis. Hu et al. (2017) found that the phyla Cyanobacteria, Actinobacteria, Gemmatimonadetes, and Crenarchaeota were the most likely ARG hosts in farmland with wheat and maize rotation. Wang et al. (2018) reported that the genera *Bradyrhizobium*, *Acidobacteria* Gp1, and *Gemmatimonas* were strongly correlated with ARGs in a dryland located in Jiangxi, China, whereas the genus *Acidobacteria* Gp2 was significantly correlated with ARGs in a paddy field. Wang et al. (2020) explored the relationship between the microbiome and antibiotic resistome in an agriculturally disturbed lake and found that the phyla Firmicutes, Gemmatimonadetes, Proteobacteria, and Verrucomicrobia exhibited a significantly positive correlation with ARGs. The results of Zhang et al. (2021a) showed that Acidobacteria, Actinobacteria, Chloroflexi, Firmicutes, Nitrospirae, and Verrucomicrobia were mainly attributed to the prevalence of ARGs in paddy fields located in Lake Tai Basin, China. These studies indicated that the core bacteria influencing the pattern of ARGs varied between biotopes. In this study, although the microbial alpha- and beta-diversity showed a significant variance between the paddy soil and field ponding water (Supplementary Figures S2, S3), the core bacterial taxa influencing the pattern of ARGs were similar in the paddy soil and field ponding water. The phyla Crenarchaeota, Verrucomicrobia, Cyanobacteria, Choloroflexi, Acidobacteria, Firmicutes, Bacteroidetes, and Actinobacteria had a significantly positive relationship with ARGs (Figure 4), indicating that these bacterial taxa exerted key roles in the environmental behaviors of these ARGs. Interestingly, the phylum Proteobacteria, the predomination microbial taxa in both paddy soil and field ponding water (Supplementary Figure S3), showed no significant correlation with ARGs. Similar phenomena were reported by Hu et al. (2017) and Zhang et al. (2021b), in which the predomination bacterial taxa also built weak correlation with ARGs while non-domination bacterial taxa showed robust correlations.

## 3.3. Correlation between ARGs and opportunistic pathogens

Pathogens that carry ARGs pose a direct threat to human health (Sommer et al., 2009; Martínez et al., 2015; Crits-Christoph et al., 2022). If humans are infected with antibiotic-resistant pathogens, therapy will be intractable (Forsberg et al., 2012; Rajput et al., 2022). Numerous ARGs can be released into the environment, but not everyone having a higher risk. Recent studies proposed that the risk assessment of ARGs was decided based on three criteria: (1) enriched in human-related environments, (2) gene mobility, and (3) host pathogenicity (Zhang et al., 2021c; Yu et al., 2023). The genus which could be retrieved in the pathogenic bacteria database GlobalPPh and the previous references were identified as opportunistic pathogens.

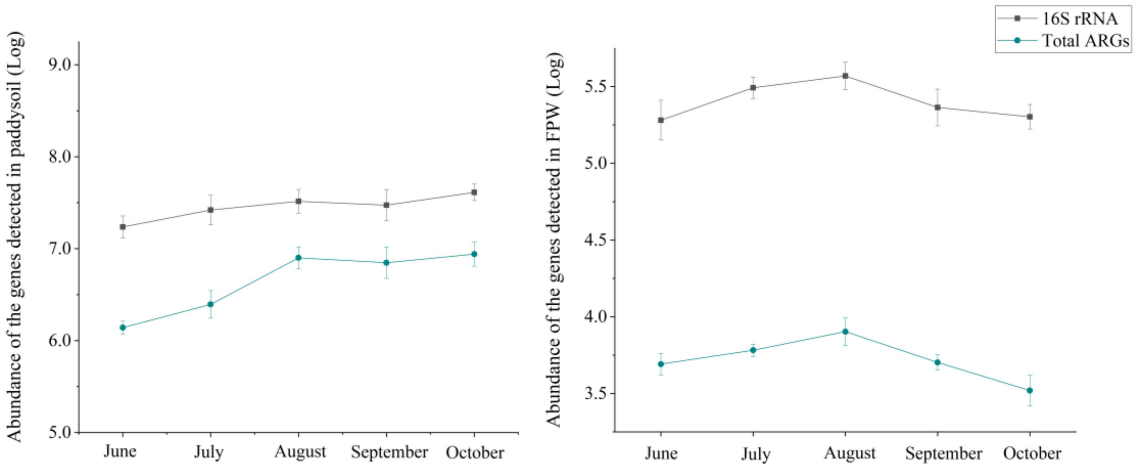


FIGURE 3
Abundances of 16S rRNA in paddy soil and field ponding water. The error bars represent±SD ($n$=6). FPW, field ponding water.

In this study, 18 opportunistic pathogens were identified in paddy soil and field ponding water. In paddy soil, *ermB*, *catA1*, *cmlA1-01*, *aadA1*, *cmx(A)*, *bla1*, *mepA*, and *tetPB-01* were positively correlated with eight, six, four, two, two, one, and one opportunistic pathogen, respectively; in field ponding water, *catA1*, *cmx(A)*, *aadA1*, *bla1*, *cmlA1-01*, *mepA*, *tetPB-01*, and *ermB* were positively correlated with six, six, five, five, four, four, three, and two opportunistic pathogens, respectively. These results suggest that field ponding water is an important pathway to disseminate potential antibiotic-resistant pathogens to the surrounding waterbodies (Figure 5).

## 3.4. Correlation between ARGs and MGEs

Vertical gene transfer (VGT) and horizontal gene transfer (HGT) are two ways of disseminating ARGs in nature. Compared with VGT, the risk of HGT is higher because of its ability to transfer ARGs between different bacterial species (Gogarten and Townsend, 2005; Partridge et al., 2018; Abe et al., 2020; Lu et al., 2020; Li et al., 2022). The process of HGT is regulated by various of MGEs, including plasmids, transposons, and integrons (Zhu et al., 2013; Forsberg et al., 2014; Guo et al., 2017; Zhang et al., 2022). In this study, two manure-derived MGEs *tnp 01* and *02*, were detected in both paddy soil and field ponding water. As shown in Figure 6, all detected ARGs were significantly correlated with the two MGEs, indicating a potential dissemination ability of ARGs in both paddy soil and field ponding water. More importantly, once these antibiotic resistance bacteria went into the ponds, reservoirs, rivers and lakes *via* field ponding water, ARGs will be transferred to the protogenetic microbes, exacerbating the ARGs contamination.

# 4. Conclusion

In this study, the environmental behavior and driving mechanisms of ARGs in rice paddies fertilized with livestock manure were demonstrated. Our results highlighted that field ponding water

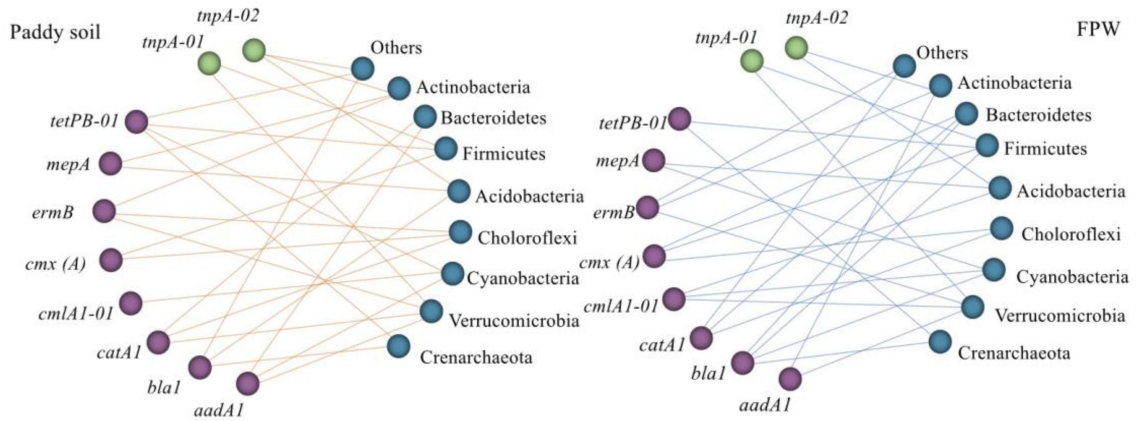


FIGURE 4
Correlation between ARGs and the major phyla. Spearman's rank correlation was used to test the significance. The effective correlation coefficient ($\rho$) was set as >0.8 on the premise of $p$<0.05. Graphics were generated in R using the graph package. FPW, field ponding water.

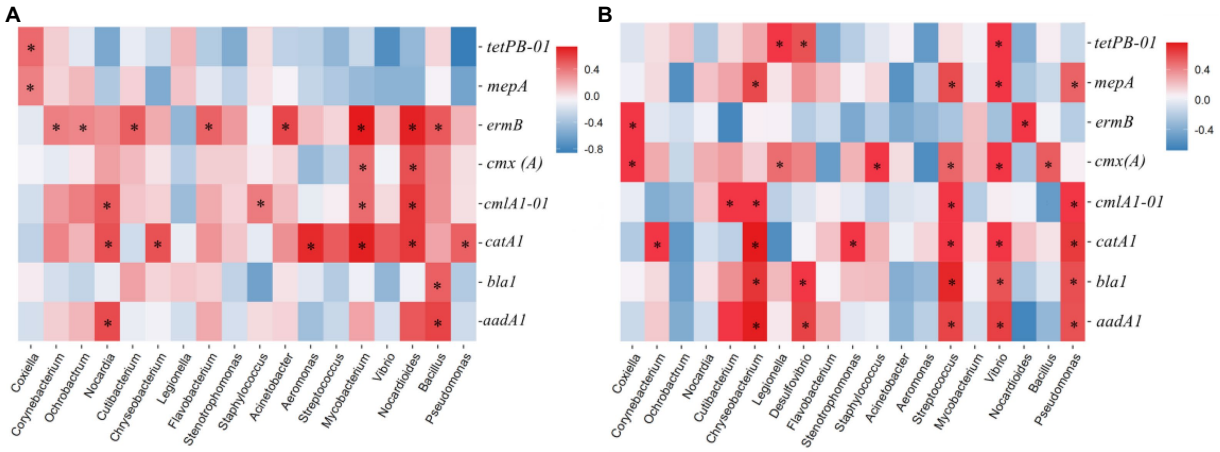


FIGURE 5
Heatmap showing the correlations between the opportunistic pathogens and ARGs detected in paddy soil **(A)** and field ponding water **(B)**. Spearman's rank correlation was used to test the significance. *$p$<0.05.

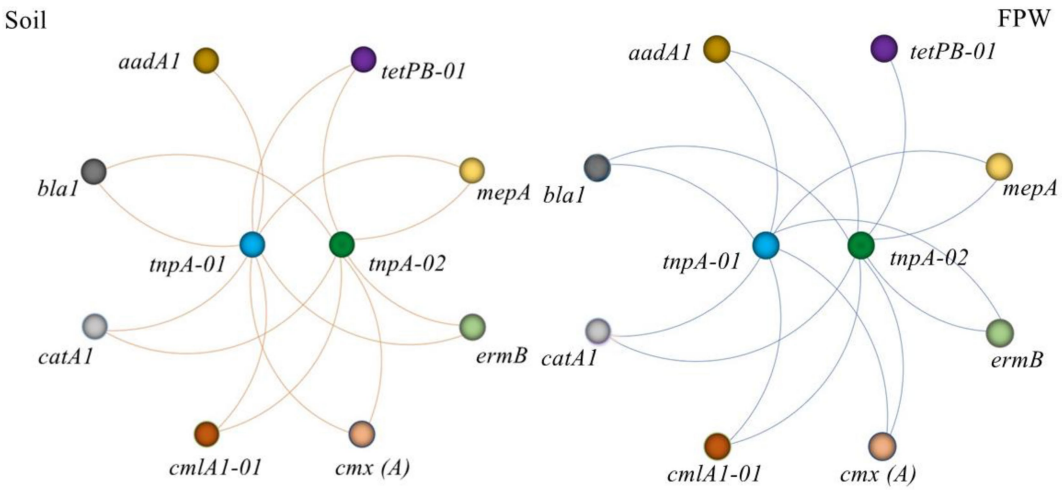


FIGURE 6
Network analysis depicting the correlations between antibiotic resistance genes and mobile genetic elements. Spearman's rank correlation was used to test the significance. Each connection represents a significant Spearman's correlation ($p$<0.05). FPW, field ponding water.

can easily obtain ARGs from rice paddy soil, indicating that ARGs can conveniently disseminate to the surrounding waterbodies. The abundance of ARGs increased from June to October in the paddy soil; while that increased from June to August, but decreased from August to October. Microbiomes play a vital role in the dynamic pattern of antibiotic resistance. The phyla Crenarchaeota, Verrucomicrobia, Cyanobacteria, Choloroflexi, Acidobacteria, Firmicutes, Bacteroidetes, and Actinobacteria were potential ARG hosts. Eighteen opportunistic pathogens detected in both paddy soil and field ponding were significantly correlated with the corresponding ARGs. Network co-occurrence analysis between MGEs and ARGs in field ponding water suggests that ARGs have a strong dissemination ability across different bacterial species.

## Data availability statement

The raw data supporting the conclusions of this article will be made available by the authors, without undue reservation.

## Author contributions

W-GZ and YG designed the research. M-SZ, S-ZL, W-GZ, and WL conducted the lab work. W-GZ, M-SZ, and S-ZL performed the data analysis and wrote the manuscript in close consultation with all authors. G-LZ and Y-JC provided professional advice. ZL provided constructional advice in the revising process. All authors contributed to the article and approved the submitted version.

## Funding

This work was supported by the Jiangsu Agriculture Science and Technology Innovation Fund (CX(22)3001) and (CX(20)1010); Independent Research Foundation of Jiangsu Key Laboratory for Food Quality and Safety-State Key Laboratory Cultivation Base (2022-SBGJZZ-9).

## Conflict of interest

The authors declare that the research was conducted in the absence of any commercial or financial relationships that could be construed as a potential conflict of interest.

## Publisher's note

All claims expressed in this article are solely those of the authors and do not necessarily represent those of their affiliated organizations, or those of the publisher, the editors and the reviewers. Any product that may be evaluated in this article, or claim that may be made by its manufacturer, is not guaranteed or endorsed by the publisher.

## Supplementary material

The Supplementary material for this article can be found online at: https://www.frontiersin.org/articles/10.3389/fmicb.2023.1135278/full#supplementary-material

## References

Abe, K., Nomura, N., and Suzuki, S. (2020). Biofilms: hot spots of horizontal gene transfer (HGT) in aquatic environments, with a focus on a new HGT mechanism. *FEMS Microbiol. Ecol.* 96:fiaa031. doi: 10.1093/femsec/fiaa031

Aguila-Arcos, S., Alvarez-Rodriguez, I., Garaiyurrebaso, O., Garbisu, C., Grohmann, E., and Alkorta, I. (2017). Biofilm-forming clinical *Staphylococcus* isolates harbor horizontal transfer and antibiotic resistance genes. *Front. Microbiol.* 8:2018. doi: 10.3389/fmicb.2017.02018

Awad, Y. M., Rae, K. K., Sung-Chul, K., Kangjoo, K., Ryong, L. S., Soo, L. S., et al. (2015). Monitoring antibiotic residues and corresponding antibiotic resistance genes in an agroecosystem. *J. Chem.* 2015, 1–7. doi: 10.1155/2015/974843

Bates, S. T., Berg-Lyons, D., Caporaso, J. G., Walters, W. A., Knight, R., and Fierer, N. (2011). Examining the global distribution of dominant archaeal populations in soil. *ISME J.* 5, 908–917. doi: 10.1038/ismej.2010.171

Beaber, J. W., Hochhut, B., and Waldor, M. K. (2004). SOS response promotes horizontal dissemination of antibiotic resistance genes. *Nature* 427, 72–74. doi: 10.1038/nature02241

Congilosi, J. L., and Aga, D. S. (2021). Review on the fate of antimicrobials, antimicrobial resistance genes, and other micropollutants in manure during enhanced anaerobic digestion and composting. *J. Hazard. Mater.* 405:123634. doi: 10.1016/j.jhazmat.2020.123634

Crits-Christoph, A., Hallowell, H. A., Koutouvalis, K., and Suez, J. (2022). Good microbes, bad genes? The dissemination of antimicrobial resistance in the human microbiome. *Gut Microbes* 14:2055944. doi: 10.1080/19490976.2022.2055944

Ding, P., Lu, J., Wan, Y., Schembri, M. A., and Guo, J. (2022). Antidepressants promote the spread of antibiotic resistance via horizontally conjugative gene transfer. *Environ. Microbiol.* 24, 5261–5276. doi: 10.1111/1462-2920.16165

Ding, J., Zhu, D., Hong, B., Wang, H. T., Li, G., Ma, Y. B., et al. (2019). Long-term application of organic fertilization causes the accumulation of antibiotic resistome in earthworm gut microbiota. *Environ. Int.* 124, 145–152. doi: 10.1016/j.envint.2019.01.017

Edgar, R. C., Haas, B. J., Clemente, J. C., Quince, C., and Knight, R. (2011). UCHIME improves sensitivity and speed of chimera detection. *Bioinformatics* 27, 2194–2200. doi: 10.1093/bioinformatics/btr381

Forsberg, K. J., Patel, S., Gibson, M. K., Lauber, C. L., Knight, R., Fierer, N., et al. (2014). Bacterial phylogeny structures soil resistomes across habitats. *Nature* 509, 612–616. doi: 10.1038/nature13377

Forsberg, K. J., Reyes, A., Wang, B., Selleck, E. M., Sommer, M. O., and Dantas, G. (2012). The shared antibiotic resistome of soil bacteria and human pathogens. *Science* 337, 1107–1111. doi: 10.1126/science.1220761

Gogarten, J. P., and Townsend, J. P. (2005). Horizontal gene transfer, genome innovation and evolution. *Nat. Rev. Microbiol.* 3, 679–687. doi: 10.1038/nrmicro1204

Guo, J., Li, J., Chen, H., Bond, P. L., Yuan, Z. (2017). Metagenomic analysis reveals wastewater treatment plants as hotspots of antibiotic resistance genes and mobile genetic elements. *Water Res.* 123, 468–478. doi: 10.1016/j.watres.2017.07.002

Guo, Y. Y., Liu, M., Liu, L. M., Liu, X., Chen, H. H., and Yang, J. (2018). The antibiotic resistome of free-living and particle-attached bacteria under a reservoir cyanobacterial bloom. *Environ. Int.* 117, 107–115. doi: 10.1016/j.envint.2018.04.045

Guo, Y. W., Xiao, X., Zhao, Y., Liu, J. G., Zhou, J. Z., Sun, B., et al. (2021). Antibiotic resistance genes in manure-amended paddy soils across eastern China: occurrence and influencing factors. *Front. Env. Sci. Eng.* 16:91. doi: 10.1007/s11783-021-1499-y

Hu, H. W., Wang, J. T., Li, J., Shi, X. Z., Ma, Y. B., Chen, D., et al. (2017). Long-term nickel contamination increases the occurrence of antibiotic resistance genes in agricultural soils. *Environ. Sci. Technol.* 51, 790–800. doi: 10.1021/acs.est.6b03383

Jia, S., Zhang, X. X., Miao, Y., Zhao, Y., Ye, L., Li, B., et al. (2017). Fate of antibiotic resistance genes and their associations with bacterial community in livestock breeding wastewater and its receiving river water. *Water Res.* 124, 259–268. doi: 10.1016/j.watres.2017.07.061

Jiao, W., Min, Q., and Fuller, A. M. (2017). Converting rice paddy to dry land farming in the tai Lake Basin, China: toward an understanding of environmental and economic impacts. *Paddy Water Environ.* 15, 171–179. doi: 10.1007/s10333-016-0538-y

Lerminiaux, N. A., and Cameron, A. (2019). Horizontal transfer of antibiotic resistance genes in clinical environments. *Can. J. Microbiol.* 65, 34–44. doi: 10.1139/cjm-2018-0275

Li, J., Zhang, Q., Li, Y., Liu, J., Pan, H., Guan, X., et al. (2017). Impact of mowing management on nitrogen mineralization rate and fungal and bacterial communities in a semiarid grassland ecosystem. *J. Soils Sediments* 17, 1715–1726. doi: 10.1007/s11368-016-1620-1

Li, W., Zhang, W. G., Zhang, M. S., Lei, Z. F., Li, P. F., Ma, Y., et al. (2022). Environmentally relevant concentrations of mercury facilitate the horizontal transfer of plasmid-mediated antibiotic resistance genes. *Sci. Total Environ.* 852:158272. doi: 10.1016/j.scitotenv.2022.158272

Looft, T., Johnson, T. A., Allen, H. K., Bayles, D. O., Alt, D. P., Stedtfeld, R. D., et al. (2012). In-feed antibiotic effects on the swine intestinal microbiome. *Proc. Natl. Acad. Sci. U. S. A.* 109, 1691–1696. doi: 10.1073/pnas.1120238109

Lu, J., Wang, Y., Jin, M., Yuan, Z., Bond, P., Guo, J., et al. (2020). Both silver ions and silver nanoparticles facilitate the horizontal transfer of plasmid-mediated antibiotic resistance genes. *Water Res.* 169:115229. doi: 10.1016/j.watres.2019.115229

Macedo, G., Olesen, A. K., Maccario, L., Hernandez Leal, L., V. D. Maas, P., Heederik, D., et al. (2022). Horizontal gene transfer of an IncP1 plasmid to soil bacterial community introduced by *Escherichia coli* through manure amendment in soil microcosms. *Environ. Sci. Technol.* 56, 11398–11408. doi: 10.1021/acs.est.2c02686

Marti, R., Scott, A., Tien, Y. C., Murray, R., Sabourin, L., Zhang, Y., et al. (2013). Impact of manure fertilization on the abundance of antibiotic-resistant bacteria and frequency of detection of antibiotic resistance genes in soil and on vegetables at harvest. *Appl. Environ. Microbiol.* 79, 5701–5709. doi: 10.1128/AEM.01682-13

Martínez, J. L. (2008). Antibiotics and antibiotic resistance genes in natural environments. *Science* 321, 365–367. doi: 10.1126/science.1159483

Martínez, J. L., Coque, T. M., and Baquero, F. (2015). What is a resistance gene? Ranking risk in resistomes. *Nat. Rev. Microbiol.* 13, 116–123. doi: 10.1038/nrmicro3399

Mei, Z., Xiang, L., Wang, F., Xu, M., Fu, Y., Wang, Z., et al. (2021). Bioaccumulation of manure-borne antibiotic resistance genes in carrot and its exposure assessment. *Environ. Int.* 157:106830. doi: 10.1016/j.envint.2021.106830

Partridge, S. R., Kwong, S. M., Firth, N., Jensen, S. O. (2018). Mobile genetic elements associated with antimicrobial resistance. *Clin. Microbiol. Rev.* 31, e00088–e00017. doi: 10.1128/CMR.00088-17

Pu, Q., Zhao, L. X., Li, Y. T., and Su, J. Q. (2020). Manure fertilization increase antibiotic resistance in soils from typical greenhouse vegetable production bases. *J. Hazard. Mater.* 391:122267. doi: 10.1016/j.jhazmat.2020.122267

Rajput, A., Tsunemoto, H., Sastry, A. V., Szubin, R., Rychel, K., Chauhan, S. M., et al. (2022). Advanced transcriptomic analysis reveals the role of efflux pumps and media composition in antibiotic responses of Pseudomonas aeruginosa. *Nucleic Acids Res.* 50, 9675–9688. doi: 10.1093/nar/gkac743

Rodriguez-Mozaz, S., Chamorro, S., Marti, E., Huerta, B., Gros, M., Sànchez-Melsió, A., et al. (2015). Occurrence of antibiotics and antibiotic resistance genes in hospital and urban wastewaters and their impact on the receiving river. *Water Res.* 69, 234–242. doi: 10.1016/j.watres.2014.11.021

Schmidt, S., Rodríguez-Rojas, A., Rolff, J., and Schreiber, F. (2022). Biocides used as material preservatives modify rates of de novo mutation and horizontal gene transfer in bacteria. *J. Hazard. Mater.* 437:129280. doi: 10.1016/j.jhazmat.2022.129280

Sommer, M., Dantas, G., and Church, G. M. (2009). Functional characterization of the antibiotic resistance reservoir in the human microflora. *Science* 325, 1128–1131. doi: 10.1126/science.1176950

Su, J. Q., Wei, B., Ouyang, W. Y., Huang, F. Y., Zhao, Y., Xu, H. J., et al. (2015). Antibiotic resistome and its association with bacterial communities during sewage sludge composting. *Environ. Sci. Technol.* 49, 7356–7363. doi: 10.1021/acs.est.5b01012

Wang, Z., Han, M., Li, E., Liu, X., Wei, H., Yang, C., et al. (2020). Distribution of antibiotic resistance genes in an agriculturally disturbed lake in China: their links with microbial communities, antibiotics, and water quality. *J. Hazard. Mater.* 393:122426. doi: 10.1016/j.jhazmat.2020.122426

Wang, F. H., Qiao, M., Su, J. Q., Chen, Z., Zhou, X., Zhu, Y. G. (2014). High throughput profiling of antibiotic resistance genes in urban park soils with reclaimed water irrigation. *Environ. Sci. Technol.* 48, 9079–9085.

Wang, F., Xu, M., Stedtfeld, R. D., Sheng, H., Fan, J., Liu, M., et al. (2018). Long-term effect of different fertilization and cropping systems on the soil antibiotic resistome. *Environ. Sci. Technol.* 52, 13037–13046. doi: 10.1021/acs.est.8b04330

Yang, Y. Y., Liu, W. Z., Xu, C., Wei, B. Q., and Wang, J. (2017). Antibiotic resistance genes in lakes from middle and lower reaches of the Yangtze River, China: effect of land use and sediment characteristics. *Chemosphere* 178, 19–25. doi: 10.1016/j.chemosphere.2017.03.041

Yu, Q., Han, Q., Shi, S., Sun, X., Wang, X., Wang, S., et al. (2023). Metagenomics reveals the response of antibiotic resistance genes to elevated temperature in the Yellow River. *Sci. Total Environ.* 859:60324. doi: 10.1016/j.scitotenv.2022.160324

Zhang, M. S., Li, W., Zhang, W. G., Li, Y. T., Li, J. Y., Gao, Y., et al. (2021a). Agricultural land-use change exacerbates the dissemination of antibiotic resistance genes via surface runoffs in Lake Tai Basin, China. *Ecotox. Environ. Safe* 220:112328. doi: 10.1016/j.ecoenv.2021.112328

Zhang, W. G., Wen, T., Liu, L. Z., Li, J. Y., Gao, Y., Zhu, D., et al. (2021b). Agricultural land-use change and rotation system exert considerable influences on the soil antibiotic resistome in Lake Tai Basin. *Sci. Total Environ.* 771:144848. doi: 10.1016/j.scitotenv.2020.144848

Zhang, A. N., Gaston, J. M., Dai, C. L., Zhao, S., Poyet, M., Groussin, M., et al. (2021c). An omics-based framework for assessing the health risk of antimicrobial resistance genes. *Nat. Commun.* 12:4765.

Zhang, W. G., Zhang, M. S., and Li, W. (2022). The antibiotic resistance genes contamination of strawberries with the long-term use of raw, aerobic composting, and anaerobic composting livestock manure: a comparative study. *Front. Environ. Sci.* 10:902321. doi: 10.3389/fenvs.2022.902321

Zheng, J., Zhou, Z., Wei, Y., Chen, T., Feng, W., and Chen, H. (2018). High-throughput profiling of seasonal variations of antibiotic resistance gene transport in a peri-urban river. *Environ. Int.* 114, 87–94. doi: 10.1016/j.envint.2018.02.039

Zhou, S. Y., Zhu, D., Giles, M., Yang, X. R., Daniell, T., Neilson, R., et al. (2019). Phyllosphere of staple crops under pig manure fertilization, a reservoir of antibiotic resistance genes. *Environ. Pollut.* 252, 227–235. doi: 10.1016/j.envpol.2019.05.098

Zhu, B., Chen, Q., Chen, S., and Zhu, Y. G. (2017). Does organically produced lettuce harbor higher abundance of antibiotic resistance genes than conventionally produced? *Environ. Int.* 98, 152–159. doi: 10.1016/j.envint.2016.11.001

Zhu, Y. G., Johnson, T. A., Su, J. Q., Qiao, M., Guo, G. X., Stedtfeld, R. D., et al. (2013). Diverse and abundant antibiotic resistance genes in Chinese swine farms. *Proc. Natl. Acad. Sci. U.S. A.* 110, 3435–3440. doi: 10.1073/pnas.1222743110

Zou, L., Liu, Y., Wang, Y., and Hu, X. (2020). Assessment and analysis of agricultural non-point source pollution loads in China: 1978-2017. *J. Environ. Manag.* 263:110400. doi: 10.1016/j.jenvman.2020.110400

frontiers | Frontiers in Microbiology

TYPE Original Research
PUBLISHED 30 March 2023
DOI 10.3389/fmicb.2023.1128905



OPEN ACCESS

EDITED BY
Tao Li,
Shanghai Veterinary Research Institute (CAAS), China

REVIEWED BY
Xiang-Dang Du,
Henan Agricultural University, China
Xi Li,
People's Hospital of Hangzhou Medical College, China

*CORRESPONDENCE
Zengqi Yang
✉ yzq8162@163.com
Biao Tang
✉ tangbiao@zaas.ac.cn

†These authors have contributed equally to this work and share first authorship

SPECIALTY SECTION
This article was submitted to Antimicrobials, Resistance and Chemotherapy, a section of the journal Frontiers in Microbiology

RECEIVED 21 December 2022
ACCEPTED 14 March 2023
PUBLISHED 30 March 2023

CITATION
Ma J, Wang J, Yang H, Su M, Li R, Bai L, Feng J, Huang Y, Yang Z and Tang B (2023) IncHI1 plasmids mediated the *tet*(X4) gene spread in *Enterobacteriaceae* in porcine. *Front. Microbiol.* 14:1128905. doi: 10.3389/fmicb.2023.1128905



# IncHI1 plasmids mediated the *tet*(X4) gene spread in *Enterobacteriaceae* in porcine

Jiangang Ma[1,2†], Juan Wang[2†], Hua Yang[1], Mengru Su[2], Ruichao Li[3], Li Bai[4], Jie Feng[2], Yuting Huang[1], Zengqi Yang[2*] and Biao Tang[1*]

[1]State Key Laboratory for Managing Biotic and Chemical Threats to the Quality and Safety of Agro-Products and Institute of Agro-Product Safety and Nutrition, Zhejiang Academy of Agricultural Sciences, Hangzhou, Zhejiang, China, [2]College of Veterinary Medicine, Northwest A&F University, Yangling, China, [3]College of Veterinary Medicine, Yangzhou University, Yangzhou, China, [4]National Health Commission Key Laboratory of Food Safety Risk Assessment, Food Safety Research Unit (2019RU014) of Chinese Academy of Medical Science, China National Center for Food Safety Risk Assessment, Beijing, China

The tigecycline resistance gene *tet*(X4) was widespread in various bacteria. However, limited information about the plasmid harboring the *tet*(X4) gene spread among the different species is available. Here, we investigated the transmission mechanisms of the *tet*(X4) gene spread among bacteria in a pig farm. The *tet*(X4) positive *Escherichia coli*, *Klebsiella pneumoniae*, *Enterobacter cloacae* and *Enterobacter hormaeche* were identified in the same farm. The whole genome sequencing (WGS) analysis showed that the *K. pneumoniae* belonged to ST727 (*n*=11) and ST3830 (*n*=1), *E. cloacae* and *E. hormaeche* belonged to ST524 (*n*=1) and ST1862 (*n*=1). All *tet*(X4) genes were located on the IncHI1 plasmids that could be conjugatively transferred into the recipient *E. coli* C600 at 30°C. Moreover, a fusion plasmid was identified that the IncHI1 plasmid recombined with the IncN plasmid mediated by IS*CR2* during the conjugation from strains B12L to C600 (pB12L-EC-1). The fusion plasmid also has been discovered in a *K. pneumoniae* (K1L) that could provide more opportunities to spread antimicrobial resistance genes. The *tet*(X4) plasmids in these bacteria are derived from the same plasmid with a similar structure. Moreover, all the IncHI1 plasmids harboring the *tet*(X4) gene in GenBank belonged to the pST17, the newly defined pMLST. The antimicrobial susceptibility testing was performed by broth microdilution method showing the transconjugants acquired the most antimicrobial resistance from the donor strains. Taken together, this report provides evidence that IncHI1/pST17 is an important carrier for the *tet*(X4) spread in *Enterobacteriaceae* species, and these transmission mechanisms may perform in the environment.

KEYWORDS

**tigecycline resistance, *tet*(X4), IncHI1, pMLST, *Enterobacteriaceae***

## Introduction

Tigecycline, a member of tetracyclines, is one of the last-resort antibiotics to treat infections caused by Carbapenem-Resistant *Enterobacteriaceae* (CRE). The tigecycline still exhibits antibacterial activities in the bacteria containing the earlier tetracyclines resistance genes. The plasmid-mediated *tet*(X3) and *tet*(X4) genes conferring tigecycline resistance were discovered in various Gram-negative bacteria, including carbapenem-resistant and colistin-resistant

bacterial strains (He T. et al., 2019; Sun et al., 2019; Tang et al., 2022a; Ma et al., 2022b). The *tet*(X) variant-positive isolates from animals, retail meat, and humans have been identified (Zheng et al., 2020; Tang et al., 2021; Umar et al., 2021). Despite the large numbers of *tet*(X) variant genes were discovered, *tet*(X3) and *tet*(X4) were the most popular tigecycline resistance genes, especially *tet*(X4) (Cheng et al., 2020; Guan et al., 2022). The *tet*(X4) gene was widelydetected in *Escherichia coli*, *Klebsiella pneumoniae*, *Aeromonas caviae*, *Citrobacter freundii*, *Acinetobacter indicus*, *Enterobacter cloacae* and so on (Chen et al., 2019; Fang et al., 2020; Li et al., 2021; Zeng et al., 2021; Wu et al., 2022; Zhai et al., 2022).

IncHI plasmid is an important vector for the *tet*(X4) gene, which belongs to the H incompatibility (IncH) group, including IncHI1 to IncHI5 subgroups (Phan and Wain, 2008; Cui et al., 2022). The IncHI1 plasmid is a conjugative plasmid usually larger than 200 kb. IncHI1 plasmid usually contains three replication genes (*repHI1A*, *repHI1B* and *repFIA-like*) (Liang et al., 2018). IncHI1 plasmids are thermosensitive for conjugative transfer, and the efficiency is optimal between 22 and 30°C (Phan and Wain, 2008). It is one of the most common plasmids carrying antimicrobial resistance genes (ARGs) in *Salmonella* (Kubasova et al., 2016). Moreover, IncHI1 plasmids also have been discovered in other *Enterobacteriaceae*, such as *E. coli*, *K. pneumoniae* and *C. freundii* (Dolejska et al., 2013; Hüttener et al., 2019). Significantly, the *tet*(X4) positive IncHI1 plasmids were discovered in several species of *Enterobacteriaceae* (Feng et al., 2022; Gao et al., 2022; Wu et al., 2022).

There are few reports about the mechanism of the *tet*(X4) gene spread between bacterial species. Here, we screened the tigecycline resistance bacteria from a large-scale pig farm in Guangxi province, China. The tigecycline-resistant *E. coli*, *K. pneumoniae*, *E. cloacae* and *Enterobacter hormaechei* were isolated at the same time. The mechanisms of the *tet*(X4) gene transferred among the spaces were unknown. We analyzed the characterization of these strains and compared the ability of conjugative transfer. To the best of our knowledge, this is the first evidence for the IncHI1 and IncHI1-N plasmid harboring the *tet*(X4) gene transferred in several bacteria spp. in a farm.

# Method

## Sample collection and bacterial isolation

Eighty-nine fecal samples were collected from a pig farm in Guangxi province, China, in 2019. These samples were distributed in several stages of the pig's life, including the piglets, weanling piglets, fattening pigs, and sows. The samples were sent to the laboratory in a cryogenic incubator and screened by the MacConkey agar containing the tigecycline (4 mg/l). The *tet*(X) gene was detected by PCR as the primer (F: 5'-TGGACCCGTTGGACTGACTA-3', R: 5'-CACTTC TTCTTACCAGGTTC-3') and sequenced by Sanger Sequencing for the tigecycline resistant strains. Then the *tet*(X)-positive strains were identified by 16S rDNA PCR and sequencing.

## Whole genome sequencing

Whole genome sequencing (WGS) of all isolates was performed using the Illumina HiSeq platform (Yu et al., 2018). The sequences were assembled with SPAdes and analyzed *via* the CGE server.[1] To further characterize the *tet*(X4) gene in the isolates, three *K. pneumoniae* strains, one *E. cloacae* strain and one *E. hormaechei* were sequenced by the Nanopore MinION platform and assembled by Unicycler. Then the sequence was annotated with the RAST server.[2] The novel plasmid multilocus sequence typing MLST (pMLST) of IncHI1 was assigned by PubMLST.

## Conjugation testing

The *tet*(X4) positive *K. pneumoniae*, *E. cloacae* and *E. hormaechei* were used as the donor strains, and the *E. coli* C600 (rifampin-resistant) was used as the recipient. In addition, *E. coli* J53 (sodium azide-resistant) was the recipient when the transconjugants used as the donor (Tang et al., 2019, Tang, B. et al., 2020; Lin et al., 2022). The cultures of donor and recipient strains were mixed in fresh LB stationary at 30°C or 37°C overnight. The mixed cultures were collected by centrifugation, then diluted with PBS. The transconjugants were selected by the LB plate containing 4 μg/ml of tigecycline with rifampin (100 μg/ml) at 37°C overnight. Each experiment was repeated three times.

## S1-nuclease digestion pulsed-field gel electrophoresis (S1-PFGE)

S1-PFGE was used to detect plasmid size in strains performed as previously described (Ma et al., 2022a,b; Tang et al., 2022b). In brief, the plugs were made from the fresh cultures embedded in 2% gold agarose and lysed with cell lysis buffer. Then S1 nuclease was used to cut the plugs, and the *Salmonella* H9812 was restricted with *Xba*I as the marker. The plasmids were separated with the CHEF Mapper XA system.

## Antimicrobial susceptibility testing

The minimum inhibitory concentrations (MICs) for 13 antimicrobial agents (ampicillin (AMP), amoxicillin-clavulanate (A/C), gentamicin (GEN), florfenicol (FFC), tetracycline (TET), tigecycline (TIG), ceftiofur (CEF), ceftazidime (CAZ), enrofloxacin (ENR), sulfisoxazole (SUL), imipenem (IMP), meropenem (MEM), colistin (COL)) were determined by the broth microdilution method according to the Clinical and Laboratory Standards Institute (CLSI) as previously described (Ma et al., 2020; Tang et al., 2022a). The wild strains and transconjugants were tested.

# Result

## Prevalence of *tet*(X4)-positive isolates

A total of twelve (13.48%) *K. pneumoniae*, one (1.12%) *E. cloacae* and one (1.12%) *E. hormaechei* were screened by MacConkey agar with

1 http://www.genomicepidemiology.org/
2 https://rast.nmpdr.org/rast.cgi

tigecycline (4 mg/l) from 89 swine feces samples in Guangxi Province in China. Furthermore, 26 (29.21%) *tet*(X4)-positive *E. coli* had been isolated and reported in a previous study (Feng et al., 2022). All of these strains carrying the *tet*(X4) genes were identified by PCR and sequencing.

## Genomic epidemiology of *tet*(X4)-positive *Klebsiella pneumoniae*, *Enterobacter cloacae* and *Enterobacter hormaechei*

The Multi-Locus Sequence Typing (MLST) analysis showed that 12 isolates of *K. pneumoniae* belong to ST727 (11/12) and ST3830 (1/12), the *E. cloacae* belong to ST524 and the *E. hormaechei* belongs to novel type (ST1862), respectively. The *K. pneumoniae* showed a clone spread with the ST727 type.

The ARGs prediction showed the strains have various resistance genes, including $bla_{\text{TEM-1}}$, $bla_{\text{OXA-10}}$, $bla_{\text{SHV-11}}$, *floR*, *cmlA1*, *fosA*, *mef*(B), *oqxA*, *oqxB*, *qnrS1*, *sul3*, *tet*(A), *tet*(X4), *aadA12*, *aph(3′)-Ia*, *dfrA14*, *arr-2* and so on (Figure 1). The *K. pneumoniae* strains 16 l, 29 l, 38 l, 39 l, 312 l, 313 l, 421 l, 423 l, K1L, 3Z1L and B12L belonged to ST727 that have a similar ARGs. They were different from the *K. pneumoniae* 3Z5L (ST3830), *E. cloacae* GX1Z-11 (ST524) and *E. hormaechei* GX4-8 l (ST1862).

## Genetic structures of tet(X4)-positive plasmids

All strains carried multiple replicons (IncHI1A, IncHI1B and IncFIA), and most *K. pneumoniae* strains carried IncN replicon (Table 1). The complete sequence of strains K1L, 3Z5L, B12L, GX1Z-11 and GX4-8 l showed that the tet(X4) gene are located on the IncHI1 plasmid and belongs to a novel pMLST. The IncHI1 plasmid was assigned to pST17, which contained two novel alleles, HCM1_043 (4) and HCM1_116 (5). Moreover, we analyzed 100 IncHI1 plasmid sequences from GenBank database that showed all *tet*(X4)-positive plasmids belonged to pST17. Although these plasmids were discovered in different spaces, more commonly *E. coli*, a small amount of *K. pneumoniae* (MW940615), *Salmonella enterica* (CP060586), and *Citrobacter* sp. (MW940627) that have relatively close consanguinity based on the core genes analysis. Similarly, the *mcr* and $bla_{\text{NDM}}$ positive plasmids have a closer relationship (Figure 2). This suggests that the *tet*(X4), *mcr*, and $bla_{\text{NDM}}$-positive IncHI1 plasmid in several species were mainly transmitted by cloning.

*Klebsiella pneumoniae* and *E. cloacae tet*(X4) positive plasmids have similar backbone structures (Figure 3A). All the IncHI1 plasmids contained the completed conjugation transfer elements including *oriT*, T4SS and T4CP, but without a conjugation transfer element was identified in IncN plasmid. IncHI1 plasmid-mediated *tet*(X4) transfer risk in different species is underestimated. The core genetic structures of *tet*(X4) remained in the conserved sequence as *abh-tet*(X4)-IS*CR2* (Li et al., 2020b). Interestingly, the pK1L (301 kb) is a complex plasmid (IncHI1-N) that is derived by homologous recombination of the IncHI1 (~190 kb) and IncN (~110 kb) from other *K. pneumoniae* strains. The fusion plasmid IncHI1-N was also detected in the transconjugant (pB12L-EC-1) harboring *tet*(X4) from the *K. pneumoniae* B12L (pB12L-1 and pB12L-2) to *E. coli* C600 mediated by IS*CR2* with a ~ 13 kb homologous sequence (IS*CR2-virD-floR-lysR-tet*(A)-$bla_{\text{TEM-1B}}$-IS*26-dfrA14-aadA1-*$bla_{\text{OXA-10}}$*-cmlA-aadA1-IntI1*-IS*26*) (Figure 3B). This is similar to the previously reported that the *mcr-1*-bearing plasmids pD72-mcr1 (IncF33: A-: B-) recombined with pD72-F33 (IncN) that was mediated by IS*26* (He D. et al., 2019). The fusion plasmid pB12L-EC-1 was highly similar to pK1L.

## Conjugation and S1-PFGE analysis of *tet*(X4)-positive strains

The conjugation assay was performed to investigate the transferability of the *tet*(X4) gene in *Enterobacteriaceae*. As with the

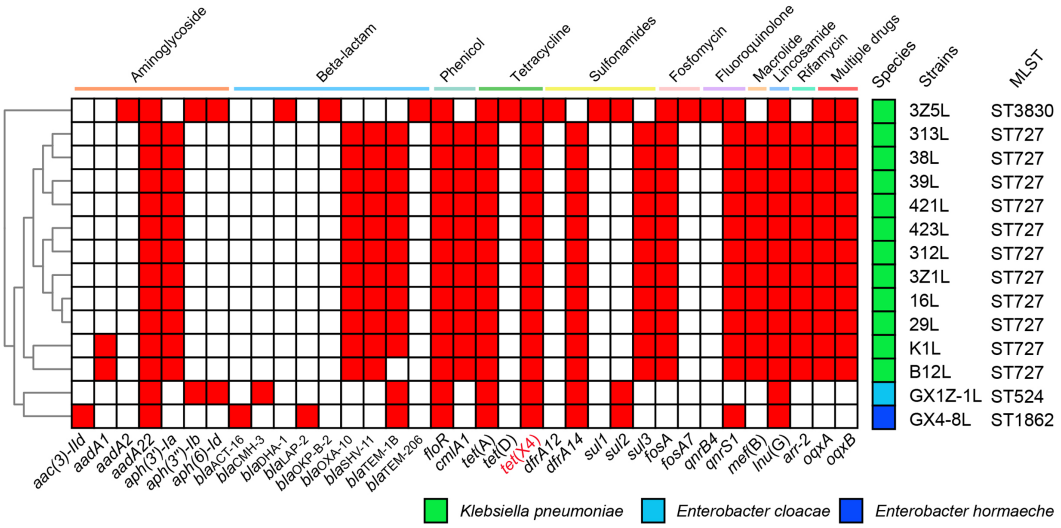


FIGURE 1
The heat map of antimicrobial resistance genes of 14 strains in this study. The positive genes in strains are marked with the red box. The names of genes are labeled below the heat map.

TABLE 1 The genome characteristics of the *K. pneumoniae*, *E. cloacae* and *Enterobacter hormaechei* strains.

| Strains | Species | MLST | Plasmids | Inc type | Size(−kb) | GC content (%) | *tet*(X4) position | Accession no. |
|---|---|---|---|---|---|---|---|---|
| 3Z5L | *K. pneumoniae* | ST3830 | - | - | 5,215,453 | 58 | No | CP072515 |
| | | | p3Z5L-1 | IncHI1B | 259,774 | 47.2 | No | CP072516 |
| | | | p3Z5L-2 | IncHI1 | 196,655 | 46.2 | Positive | CP072517 |
| | | | p3Z5L-3 | IncFIB(K) | 110,830 | 52.1 | No | CP072518 |
| | | | p3Z5L-4 | IncM2 | 59,397 | 51.9 | No | CP072519 |
| B12L | *K. pneumoniae* | ST727 | - | - | 5,419,314 | 57.3 | No | CP072456 |
| | | | pB12L-1 | IncHI1 | 185,386 | 46.5 | Positive | CP072457 |
| | | | pB12L-2 | IncN | 111,105 | 51.7 | No | CP072458 |
| K1L | *K. pneumoniae* | ST727 | - | - | 5,420,142 | 57.3 | No | CP072460 |
| | | | pK1L-1 | IncHI1-N | 301,103 | 48.3 | Positive | CP072461 |
| | | | pK1L-2 | - | 9,585 | 42.0 | No | CP072462 |
| GX1Z-1l | *E. cloacae* | ST524 | - | - | 4,798,859 | 54.9 | No | CP071861 |
| | | | pGX1Z-1l | IncHI1 | 296,468 | 48.7 | Positive | CP071862 |
| GX4-8l | *E. cloacae* | ST1862 | - | - | 4,754,790 | 55.2 | No | CP071876 |
| | | | pGX4-8l | IncHI1 | 195,884 | 46.2 | Positive | CP071877 |

characteristics of IncHI1 plasmids, conjugation experiments showed that all strains successfully transfer the *tet*(X4) gene to recipient strain *E. coli* C600 with a higher conjugation frequency at 30°C, and a significantly reduced conjugation frequency observed at 37°C (Figure 4A). This is consistent with the characteristics of the thermosensitive plasmids. As mentioned above, the fusion plasmid pB12L-C600-1 containing two replicons, IncHI1 and IncN generated by the conjugation transfer of the *K. pneumoniae* B12L to *E. coli* C600. The plasmid profiles of the donor and transconjugants detected by S1-PFGE showed the two sizes plasmids (about 200 kb and 300 kb) in the transconjugants (Figure 4B).

In order to analyze the ability of conjugation transfer of the IncHI1 and IncHI1-N plasmids. The transconjugants containing the pB12L-EC-1(IncHI1-N) and pB12L-EC-2(IncHI1) were further conjugated transfer to recipient *E. coli* J53 at 30°C or 37°C. The result showed that the pB12L-EC-1 and pB12L-EC-2 had no significant difference in conjugation frequency from EC600 to J53, both at 30°C and 37°C (Figure 4A).

## Antimicrobial susceptibility testing of donors and transconjugants

The *K. pneumoniae*, *E. cloacae* and *E. hormaechei*, as well as their transconjugants were detected the antimicrobial susceptibility. All of the wild-type strains exhibited resistance to AMP, A/C, FFC, TET, TIG, ENR and SUL, and sensitive to CAZ, IMP, MEM and COL. Only one strain GX4-8l was resistant to GEN. The transconjugants acquired the most of ARGs that have similar resistant profiles (Supplementary Table S1).

# Discussion

The *tet*(X4) is the critical resistant gene for the tetracycline family, especially tigecycline. An increasing number of *tet*(X4)-positive bacteria species have been discovered since it was first discovered in *E. coli* (He T. et al., 2019; Sun et al., 2019). The *E. coli* remains the most common carrier for the *tet*(X4) gene, and the *Citrobacter* sp., *Acinetobacter sp.*, *K. pneumoniae*, *E. cloacae* and *E. hormaechei* carrying *tet*(X4) gene were reported occasionally. The different bacteria spp. carrying *tet*(X4) gene were always isolated from different farms or regions. Here, we identified the *tet*(X4)-positive *K. pneumoniae*, *E. cloacae* and *E. hormaechei* in a pig farm at the same time. These strains carried the same plasmid that belonged to pST17 IncHI1 plasmid. The *tet*(X4)-positive IncHI1 plasmid was also identified in *E. coli* from this farm in our previous study (Feng et al., 2022). It is strong evidence that the IncHI1plasmid mediated the *tet*(X4) gene transfer among different *Enterobacteriaceae*.

The *tet*(X4) gene was always located on the plasmid in *Enterobacteriaceae* and on chromosomes in other bacteria. The IncX1 type plasmid was considered the most common vector for the *tet*(X4) gene, followed closely by the IncHI1 plasmid (Cui et al., 2022). The IncHI1 harbored *tet*(X4) gene is becoming increasingly common in *Enterobacteriaceae* (Fang et al., 2020; Gao et al., 2022). Notice that it has become the most important type for the spread of the *tet*(X4) gene among *Enterobacteriaceae*, except *E. coli*, which has been discovered in *K. pneumoniae* and *E. cloacae*.

pMLST is an important method for tracing the spread of plasmids based on molecular typing. Phan et al. established the typing method for IncHI1 plasmids using variation in six conserved loci (Phan et al., 2009). Seventeen types that have been identified in IncHI1 plasmids and recorded in PubMLST.[3] The *tet*(X4) gene is only located in the pST17 IncHI1 plasmid, and similar results were observed in *mcr*, $bla_{NDM}$ and $bla_{CTX-M}$ located in a specific plasmid (Valcek et al., 2021). This suggests that there is some association between resistance genes and plasmid typing. The probability of insertion of resistance genes into plasmids is much lower than plasmid transfer.

3 https://pubmlst.org/bigsdb?db=pubmlst_plasmidseqdef

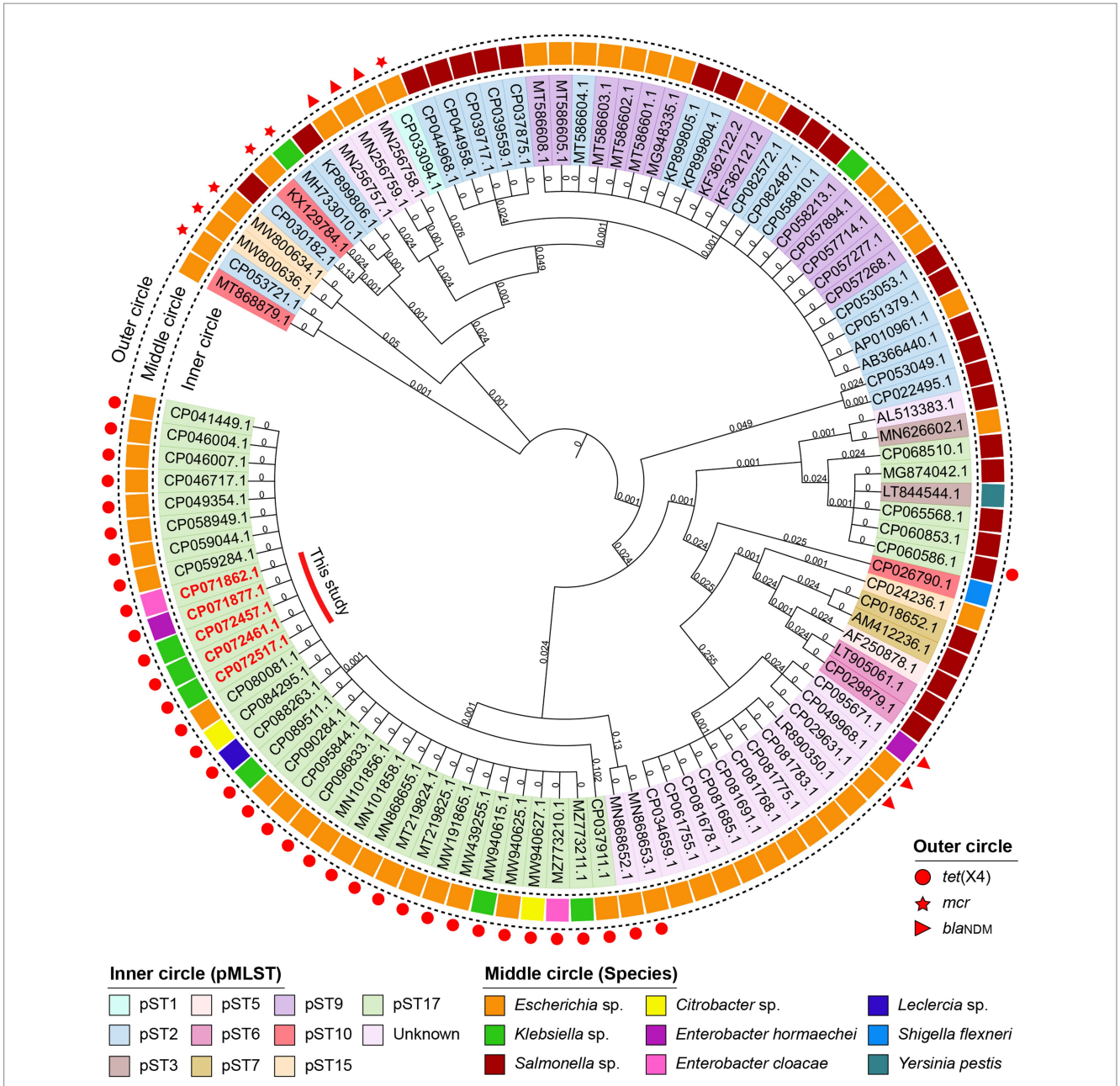


FIGURE 2
Phylogenetic tree of 100 IncHI1 plasmids with complete sequence from GenBank database. The accession numbers in red are discovered in this study. The innermost to outermost circles indicated the pMLST of plasmids, the species of isolates and the important ARGs on the plasmids.

The plasmid is the most important vector for transferring the ARGs. The ARGs and the virulence genes are always located on the specific Inc-type plasmids, such as the *mcr-1* mainly in IncX4, IncI2 and IncHI2 plasmid (Rodríguez-Santiago et al., 2021). Hybrid plasmids are becoming increasingly common, which could contribute to the ARGs and virulence genes co-translocation and assist the non-conjugative plasmids transferred (Li et al., 2020a; Tang, M. et al., 2020). The most of hybrid plasmids were derived during the conjugation transfer, and the insertion sequence IS*26* was the most common element for guided the plasmids recombination by the homologous sequence (Liu et al., 2020; Peng et al., 2022). Conversely, the doner plasmids containing the highly similar homologous sequences suggested that the small plasmids may be produced by decomposition of fusion plasmid from other hosts. The mechanism of initial fusion remains to be investigated. Note that the IncHI1 plasmid could remove the temperature restrictions for conjugative transfer by fusion with the IncN plasmid and obtain the resistance and virulence genes at the same time. This study is the first report of the IncHI1 fusion with IncN plasmid that may increase the ability to spread *tet*(X4).

## Conclusion

In summary, we reported the IncHI1 plasmid harboring the *tet*(X4) gene discovered in *K. pneumoniae*, *E. cloacae*, and

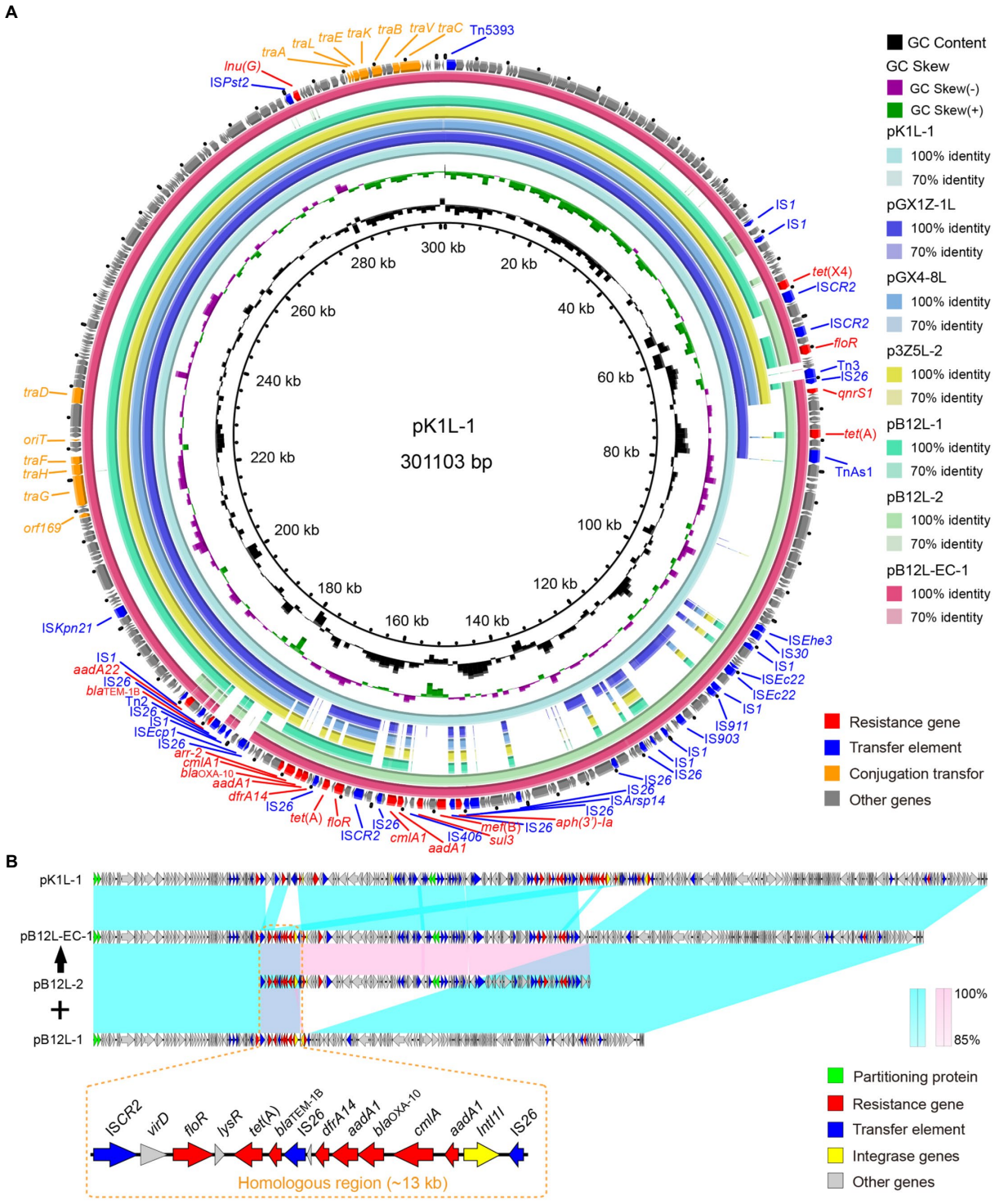


FIGURE 3
Sequence alignment of *tet*(X) harboring plasmids in this study. **(A)** The circular genetic map of plasmids pK1L, pGX1Z-1l, pGX4-8l, p3Z5L-2, pB12L-1, pB12L-2 and pB12L-EC-1. The pK1L is used as the reference. **(B)** Linear comparison of plasmids pK1L, pB12L-1 and pB12L-2 with the transconjugant plasmid pB12L-EC-1. The corresponding alignments are represented in wathet blue and pink. The orange dashed boxes indicated the genes in the homologous region. The arrows and triangles represent genes of different function categories (blue: transfer element; red: AMR gene; green: partitioning protein; golden: integrase and resolvase; gray: other functions).

*E. hormaechei* from the same farm. It provided further evidence that the *tet*(X4) gene transfer among bacteria by IncHI1 plasmid in livestock farm. The *tet*(X4)-positive IncHI1 plasmids belonged to pST17, a novel subtype. Furthermore, the IncHI1 and IncN plasmid tended to fuse by the IS*CR2*, which could increase the risk of co-transfer the ARGs among bacteria. The study highlights that the IncHI1 plasmid is a risk factor for transfer *tet*(X4) among *Enterobacteriaceae*.

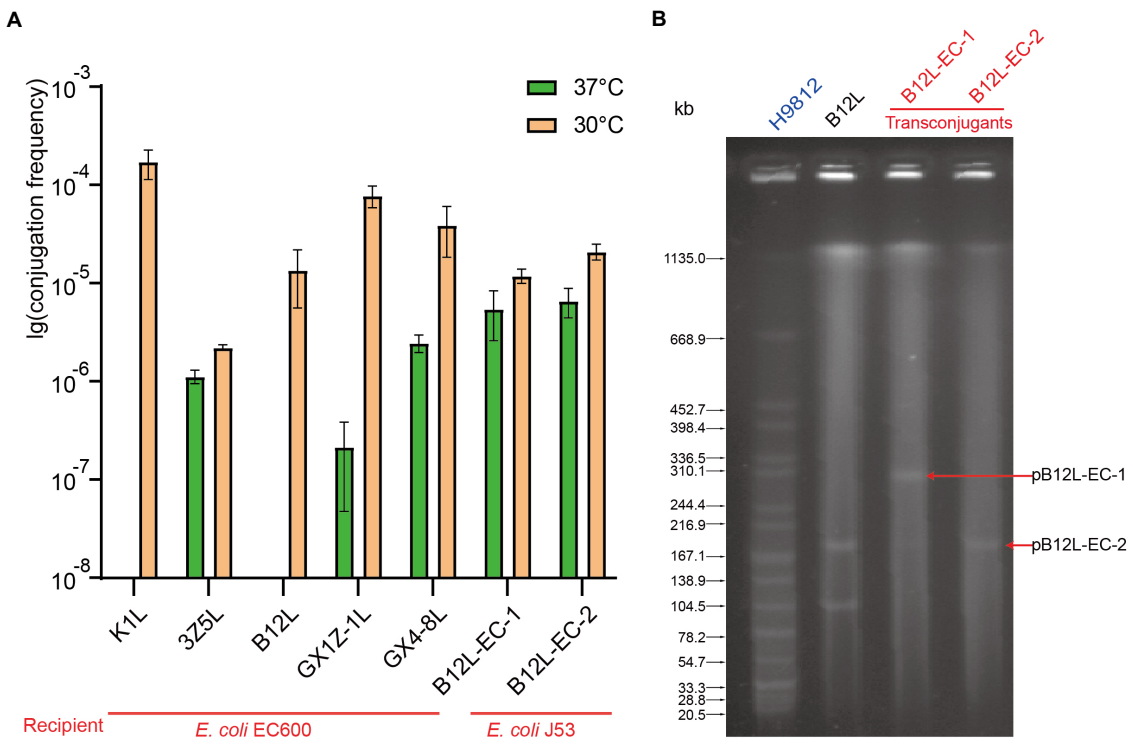


FIGURE 4
The conjugation transfer frequency of different bacteria and the plasmid profiles of fusion plasmid. **(A)** The conjugation transfer frequency of five *tet*(X4) positive strains and the transconjugants of B12L. **(B)** The S1-PFGE of the donor strain B12L and two types transconjugants (B12L-EC-1 and B12L-EC-2).

## Data availability statement

The datasets presented in this study can be found in online repositories. The names of the repository/repositories and accession number(s) can be found in the article/Supplementary material.

## Author contributions

JM and JW designed the study. BT, HY, MS, and JF collected the samples and conducted the experiments. RL, LB, and YH analyzed and interpreted the data. JM, BT, and ZY drafted the manuscript. All authors contributed to the article and approved the submitted version.

## Funding

This work was supported by the China Postdoctoral Science Foundation [grant number 2021 M702904], China Wool Sheep Industry and Technology System project [grant number CARS-39], the Natural Science Basic Research Plan in Shaanxi Province of China [grant number 2021KW-41], State Key Laboratory for Managing Biotic and Chemical Threats to the Quality and Safety of Agro-products [grant number 2010DS700124-ZZ2008 and 2021DG700024-KF202213], "Leading Goose" R&D Program of Zhejiang Province [2023C03045] and Key Research and Development Program of Zhejiang Province [LY23C180001].

## Conflict of interest

The authors declare that the research was conducted in the absence of any commercial or financial relationships that could be construed as a potential conflict of interest.

## Publisher's note

All claims expressed in this article are solely those of the authors and do not necessarily represent those of their affiliated organizations, or those of the publisher, the editors and the reviewers. Any product that may be evaluated in this article, or claim that may be made by its manufacturer, is not guaranteed or endorsed by the publisher.

## Supplementary material

The Supplementary material for this article can be found online at: https://www.frontiersin.org/articles/10.3389/fmicb.2023.1128905/full#supplementary-material

# References


Chen, C., Chen, L., Zhang, Y., Cui, C. Y., Wu, X. T., He, Q., et al. (2019). Detection of chromosome-mediated tet(X4)-carrying *Aeromonas caviae* in a sewage sample from a chicken farm. *J. Antimicrob. Chemother.* 74, 3628–3630. doi: 10.1093/jac/dkz387

Cheng, Y., Chen, Y., Liu, Y., Guo, Y., Zhou, Y., Xiao, T., et al. (2020). Identification of novel tetracycline resistance gene tet(X14) and its co-occurrence with tet(X2) in a tigecycline-resistant and colistin-resistant *Empedobacter stercoris*. *Emerg. Microbes Infect.* 9, 1843–1852. doi: 10.1080/22221751.2020.1803769

Cui, C. Y., Li, X. J., Chen, C., Wu, X. T., He, Q., Jia, Q. L., et al. (2022). Comprehensive analysis of plasmid-mediated tet(X4)-positive *Escherichia coli* isolates from clinical settings revealed a high correlation with animals and environments-derived strains. *Sci. Total Environ.* 806:150687. doi: 10.1016/j.scitotenv.2021.150687

Dolejska, M., Villa, L., Poirel, L., Nordmann, P., and Carattoli, A. (2013). Complete sequencing of an IncHI1 plasmid encoding the carbapenemase NDM-1, the ArmA 16S RNA methylase and a resistance-nodulation-cell division/multidrug efflux pump. *J. Antimicrob. Chemother.* 68, 34–39. doi: 10.1093/jac/dks357

Fang, L. X., Chen, C., Cui, C. Y., Li, X. P., Zhang, Y., Liao, X. P., et al. (2020). Emerging high-level tigecycline resistance: novel tetracycline destructases spread via the mobile tet(X). *BioEssays* 42:e2000014. doi: 10.1002/bies.202000014

Feng, J., Su, M., Li, K., Ma, J., Li, R., Bai, L., et al. (2022). Extensive spread of tet(X4) in multidrug-resistant *Escherichia coli* of animal origin in Western China. *Vet. Microbiol.* 269:109420. doi: 10.1016/j.vetmic.2022.109420

Gao, X., He, X., Lv, L., Cai, Z., Liu, Y. Y., and Liu, J. H. (2022). Detection of Tet(X4)-producing *Klebsiella pneumoniae* from the environment and wide spread of IncFIA-IncHI1A-IncHI1B plasmid carrying tet(X4) in China. *J. Glob. Antimicrob. Resist.* 30, 130–132. doi: 10.1016/j.jgar.2022.05.028

Guan, C., Tang, B., Yang, H., Ma, J., Huang, Y., and Liu, C. (2022). Emergence of plasmid-mediated tigecycline resistance gene, tet(X4), in *Escherichia fergusonii* from pigs. *J. Glob. Antimicrob. Resist.* 30, 249–251. doi: 10.1016/j.jgar.2022.06.029

He, T., Wang, R., Liu, D., Walsh, T. R., Zhang, R., Lv, Y., et al. (2019). Emergence of plasmid-mediated high-level tigecycline resistance genes in animals and humans. *Nat. Microbiol.* 4, 1450–1456. doi: 10.1038/s41564-019-0445-2

He, D., Zhu, Y., Li, R., Pan, Y., Liu, J., Yuan, L., et al. (2019). Emergence of a hybrid plasmid derived from IncN1-F33:A-:B- and mcr-1-bearing plasmids mediated by IS26. *J. Antimicrob. Chemother.* 74, 3184–3189. doi: 10.1093/jac/dkz327

Hüttener, M., Prieto, A., Aznar, S., Bernabeu, M., Glaría, E., Valledor, A. F., et al. (2019). Expression of a novel class of bacterial Ig-like proteins is required for IncHI plasmid conjugation. *PLoS Genet.* 15:e1008399. doi: 10.1371/journal.pgen.1008399

Kubasova, T., Cejkova, D., Matiasovicova, J., Sekelova, Z., Polansky, O., Medvecky, M., et al. (2016). Antibiotic resistance, core-genome and protein expression in IncHI1 plasmids in *Salmonella* Typhimurium. *Genome Biol. Evol.* 8, 1661–1671. doi: 10.1093/gbe/evw105

Li, R., Cheng, J., Dong, H., Li, L., Liu, W., Zhang, C., et al. (2020a). Emergence of a novel conjugative hybrid virulence multidrug-resistant plasmid in extensively drug-resistant *Klebsiella pneumoniae* ST15. *Int. J. Antimicrob. Agents* 55:105952. doi: 10.1016/j.ijantimicag.2020.105952

Li, R., Li, Y., Peng, K., Yin, Y., Liu, Y., He, T., et al. (2021). Comprehensive genomic investigation of tigecycline resistance gene tet(X4)-bearing strains expanding among different settings. *Microbiol. Spectr.* 9:e0163321. doi: 10.1128/spectrum.01633-21

Li, R., Lu, X., Peng, K., Liu, Z., Li, Y., Liu, Y., et al. (2020b). Deciphering the structural diversity and classification of the mobile tigecycline resistance gene tet(X)-bearing plasmidome among bacteria. *mSystems* 5, e00134–e00120. doi: 10.1128/mSystems.00134-20

Liang, Q., Jiang, X., Hu, L., Yin, Z., Gao, B., Zhao, Y., et al. (2018). Sequencing and genomic diversity analysis of IncHI5 plasmids. *Front. Microbiol.* 9:3318. doi: 10.3389/fmicb.2018.03318

Lin, J., Tang, B., Zheng, X., Chang, J., Ma, J., He, Y., et al. (2022). Emergence of Incl2 plasmid-mediated colistin resistance in avian *Escherichia fergusonii*. *FEMS Microbiol. Lett.* 369:fnac016. doi: 10.1093/femsle/fnac016

Liu, Z., Xiao, X., Liu, Y., Li, R., and Wang, Z. (2020). Recombination of NDM-5-producing plasmids mediated by IS26 among *Escherichia coli*. *Int. J. Antimicrob. Agents* 55:105815. doi: 10.1016/j.ijantimicag.2019.09.019

Ma, J., Tang, B., Lin, J., Ed-Dra, A., Lin, H., Wu, J., et al. (2022a). Genome assessment of carbapenem- and colistin-resistant *Escherichia coli* from patients in a sentinel hospital in China. *Cells* 11:3480. doi: 10.3390/cells11213480

Ma, J., Wang, J., Feng, J., Liu, Y., Yang, B., Li, R., et al. (2020). Characterization of three porcine *Acinetobacter towneri* strains co-harboring tet(X3) and Bla(OXA-58). *Front. Cell. Infect. Microbiol.* 10:586507. doi: 10.3389/fcimb.2020.586507

Ma, J., Zhou, W., Wu, J., Liu, X., Lin, J., Ji, X., et al. (2022b). Large-scale studies on antimicrobial resistance and molecular characterization of Escherichia coli from food animals in developed areas of eastern China. *Microbiol. Spectr.* 10:e0201522. doi: 10.1128/spectrum.02015-22

Peng, K., Yin, Y., Li, Y., Qin, S., Liu, Y., Yang, X., et al. (2022). QitanTech nanopore long-read sequencing enables rapid resolution of complete genomes of multi-drug resistant pathogens. *Front. Microbiol.* 13:778659. doi: 10.3389/fmicb.2022.778659

Phan, M. D., Kidgell, C., Nair, S., Holt, K. E., Turner, A. K., Hinds, J., et al. (2009). Variation in *Salmonella enterica* serovar typhi IncHI1 plasmids during the global spread of resistant typhoid fever. *Antimicrob. Agents Chemother.* 53, 716–727. doi: 10.1128/AAC.00645-08

Phan, M. D., and Wain, J. (2008). IncHI plasmids, a dynamic link between resistance and pathogenicity. *J. Infect. Dev. Ctries.* 2, 272–278. doi: 10.3855/jidc.221

Rodríguez-Santiago, J., Cornejo-Juárez, P., Silva-Sánchez, J., and Garza-Ramos, U. (2021). Polymyxin resistance in *Enterobacterales*: overview and epidemiology in the Americas. *Int. J. Antimicrob. Agents* 58:106426. doi: 10.1016/j.ijantimicag.2021.106426

Sun, J., Chen, C., Cui, C. Y., Zhang, Y., Liu, X., Cui, Z. H., et al. (2019). Plasmid-encoded tet(X) genes that confer high-level tigecycline resistance in *Escherichia coli*. *Nat. Microbiol.* 4, 1457–1464. doi: 10.1038/s41564-019-0496-4

Tang, B., Chang, J., Cao, L., Luo, Q., Xu, H., Lyu, W., et al. (2019). Characterization of an NDM-5 carbapenemase-producing Escherichia coli ST156 isolate from a poultry farm in Zhejiang, China. *BMC Microbiol.* 19:82. doi: 10.1186/s12866-019-1454-2

Tang, B., Chang, J., Luo, Y., Jiang, H., Liu, C., Xiao, X., et al. (2022a). Prevalence and characteristics of the mcr-1 gene in retail meat samples in Zhejiang Province, China. *J. Microbiol.* 60, 610–619. doi: 10.1007/s12275-022-1597-y

Tang, B., Chang, J., Zhang, L., Liu, L., Xia, X., Hassan, B. H., et al. (2020). Carriage of distinct mcr-1-harboring plasmids by unusual serotypes of *Salmonella*. *Adv Biosyst.* 4:e1900219. doi: 10.1002/adbi.201900219

Tang, M., Kong, X., Hao, J., and Liu, J. (2020). Epidemiological characteristics and formation mechanisms of multidrug-resistant hypervirulent *Klebsiella pneumoniae*. *Front. Microbiol.* 11:581543. doi: 10.3389/fmicb.2020.581543

Tang, B., Wang, J., Zheng, X., Chang, J., Ma, J., Wang, J., et al. (2022b). Antimicrobial resistance surveillance of *Escherichia coli* from chickens in the Qinghai plateau of China. *Front. Microbiol.* 13:885132. doi: 10.3389/fmicb.2022.885132

Tang, B., Yang, H., Jia, X., and Feng, Y. (2021). Coexistence and characterization of Tet(X5) and NDM-3 in the MDR-*Acinetobacter indicus* of duck origin. *Microb. Pathog.* 150:104697. doi: 10.1016/j.micpath.2020.104697

Umar, Z., Chen, Q., Tang, B., Xu, Y., Wang, J., Zhang, H., et al. (2021). The poultry pathogen *Riemerella anatipestifer* appears as a reservoir for Tet(X) tigecycline resistance. *Environ. Microbiol.* 23, 7465–7482. doi: 10.1111/1462-2920.15632

Valcek, A., Sismova, P., Nesporova, K., Overballe-Petersen, S., Bitar, I., Jamborova, I., et al. (2021). Horsing around: *Escherichia coli* ST1250 of equine origin harbouring epidemic IncHI1/ST9 plasmid with Bla(CTX-M-1) and an operon for short-chain fructooligosaccharides metabolism. *Antimicrob. Agents Chemother.* 65, e02556–e02520. doi: 10.1128/AAC.02556-20

Wu, Y., He, R., Qin, M., Yang, Y., Chen, J., Feng, Y., et al. (2022). Identification of plasmid-mediated tigecycline-resistant gene tet(X4) in *Enterobacter cloacae* from pigs in China. *Microbiol. Spectr.* 10:e0206421. doi: 10.1128/spectrum.02064-21

Yu, Y., Tang, B., Dai, R., Zhang, B., Chen, L., Yang, H., et al. (2018). Identification of the streptothricin and tunicamycin biosynthetic gene clusters by genome mining in *Streptomyces* sp. strain fd1-xmd. *Appl. Microbiol. Biotechnol.* 102, 2621–2633. doi: 10.1007/s00253-018-8748-4

Zeng, Y., Dong, N., Liu, C., Lu, J., and Zhang, R. (2021). Presence of tet(X4)-positive *Citrobacter freundii* in a cancer patient with chemotherapy-induced persistent diarrhoea. *J. Glob. Antimicrob. Resist.* 24, 88–89. doi: 10.1016/j.jgar.2020.11.007

Zhai, W., Tian, Y., Lu, M., Zhang, M., Song, H., Fu, Y., et al. (2022). Presence of mobile tigecycline resistance gene tet(X4) in Clinical *Klebsiella pneumoniae*. *Microbiol. Spectr.* 10:e0108121. doi: 10.1128/spectrum.01081-21

Zheng, X. R., Zhu, J. H., Zhang, J., Cai, P., Sun, Y. H., Chang, M. X., et al. (2020). A novel plasmid-borne tet(X6) variant co-existing with $bla_{NDM-1}$ and $bla_{OXA-58}$ in a chicken *Acinetobacter baumannii* isolate. *J. Antimicrob. Chemother.* 75, 3397–3399. doi: 10.1093/jac/dkaa342

frontiers | Frontiers in Microbiology

TYPE Original Research
PUBLISHED 30 March 2023
DOI 10.3389/fmicb.2023.1141952



OPEN ACCESS

EDITED BY
Dennis Lee Wright,
University of Connecticut,
United States

REVIEWED BY
Nayeem Ahmad,
Arabian Gulf University,
Bahrain
Vigyasa Singh,
University of Arizona,
United States

*CORRESPONDENCE
Xun Suo
✉ suoxun@cau.edu.cn
Xianyong Liu
✉ liuxianyong@cau.edu.cn

SPECIALTY SECTION
This article was submitted to Antimicrobials, Resistance and Chemotherapy, a section of the journal Frontiers in Microbiology

RECEIVED 11 January 2023
ACCEPTED 10 March 2023
PUBLISHED 30 March 2023

CITATION
Sun P, Wang C, Zhang Y, Tang X, Hu D, Xie F, Hao Z, Suo J, Yu Y, Suo X and Liu X (2023) Transcriptome profile of halofuginone resistant and sensitive strains of *Eimeria tenella*. *Front. Microbiol.* 14:1141952. doi: 10.3389/fmicb.2023.1141952



# Transcriptome profile of halofuginone resistant and sensitive strains of *Eimeria tenella*

Pei Sun[1], Chaoyue Wang[2], Yuanyuan Zhang[3], Xinming Tang[4], Dandan Hu[5], Fujie Xie[1], Zhenkai Hao[1], Jingxia Suo[1], Yonglan Yu[6], Xun Suo[1]* and Xianyong Liu[1]*

[1]National Key Laboratory of Veterinary Public Health Security, Key Laboratory of Animal Epidemiology and Zoonosis of Ministry of Agriculture, National Animal Protozoa Laboratory and College of Veterinary Medicine, China Agricultural University, Beijing, China, [2]Department of Pathogen Biology, Guangdong Provincial Key Laboratory of Tropical Disease Research, School of Public Health, Southern Medical University, Guangzhou, Guangdong, China, [3]Key Laboratory of Animal Genetics, Breeding and Reproduction of the Ministry of Agriculture and Beijing Key Laboratory of Animal Genetic Improvement, China Agricultural University, Beijing, China, [4]Institute of Animal Science, Chinese Academy of Agricultural Sciences, Beijing, China, [5]School of Animal Science and Technology, Guangxi University, Nanning, Guangxi, China, [6]Department of Clinic Veterinary Medicine, College of Veterinary Medicine, China Agricultural University, Beijing, China

The antiparasitic drug halofuginone is important for controlling apicomplexan parasites. However, the occurrence of halofuginone resistance is a major obstacle for it to the treatment of apicomplexan parasites. Current studies have identified the molecular marker and drug resistance mechanisms of halofuginone in *Plasmodium falciparum*. In this study, we tried to use transcriptomic data to explore resistance mechanisms of halofuginone in apicomplexan parasites of the genus *Eimeria* (Apicomplexa: Eimeriidae). After halofuginone treatment of *E. tenella* parasites, transcriptome analysis was performed using samples derived from both resistant and sensitive strains. In the sensitive group, DEGs associated with enzymes were significantly downregulated, whereas the DNA damaging process was upregulated after halofuginone treatment, revealing the mechanism of halofuginone-induced parasite death. In addition, 1,325 differentially expressed genes (DEGs) were detected between halofuginone resistant and sensitive strains, and the DEGs related to translation were significantly downregulated after halofuginone induction. Overall, our results provide a gene expression profile for further studies on the mechanism of halofuginone resistance in *E. tenella*.

KEYWORDS

***Eimeria tenella*, halofuginone, transcriptome analysis, DEG, resistance**

## Introduction

*Eimeria* is related to malarial parasites and is a major parasitic disease of the intestinal tract of animals and causes huge losses in the poultry industry (Dubey and Jenkins, 2018). Although the current medication against *Eimeria* is quite effective, it has adverse side effects, particularly with regard to the emergence and spread of resistance (Peek and Landman, 2003; Noack et al., 2019). However, there is not yet any unequivocal evidence regarding the drug resistance mechanisms in *Eimeria tenella*. The identification of drug resistance mechanisms is an essential step toward solving drug resistance problems.

Halofuginone, a synthetic derivative of the natural product febrifugine, exhibits potent inhibitory activities against both protozoan parasites and numerous cancer cells (Derbyshire et al., 2012; Zhang et al., 2012; McLaughlin et al., 2014; Herman et al., 2015; Bellini et al., 2020; Cheng et al., 2022). In *Eimeria*, it was shown that halofuginone inhibits the invasion of sporozoites into host cells at an early stage of the life cycle and later disrupts the development of schizonts (Zhang et al., 2012). At present, halofuginone-resistant cases have been reported among different species and have shown that halofuginone resistance is primarily associated with point mutations and copy number variants in the parasite prolyl-tRNA synthetase (PRS) enzyme of *P. falciparum* (Keller et al., 2012; Herman et al., 2014, 2015; Hewitt et al., 2017; Jain et al., 2017). In addition, reports on the mode of action have elucidated that halofuginone is an ATP-dependent inhibitor that simultaneously occupies two different substrate-binding sites in prolyl-transfer RNA synthetase (ProRS) (Zhou et al., 2013; Gill and Sharma, 2022; Tye et al., 2022). To date, halofuginone-resistant *Eimeria* strains have been reported, but there is no coherent picture of the mechanism of halofuginone resistance in *Eimeria* (Peek and Landman, 2003; Lan et al., 2017). Resistance hinders the control of coccidiosis in the field; hence, exploring the mechanism of halofuginone resistance would help us to design new anticoccidial drugs.

The development of multi-omics technology provides a bridge to study phenotype-function relationships (Volkman et al., 2012; Hu et al., 2018). To evade different drug pressures, *Eimeria* drug-resistant strains may depend on different mechanisms of gene regulation (Xie et al., 2020). Previous studies have suggested that the differential expression of regulated genes may lead to differences in drug-resistant and drug-sensitive strains, and the current series of studies using transcriptome analysis has been successful in dissecting drug resistance mechanisms (Antony et al., 2016; Ingham et al., 2018, 2020; Xie et al., 2020; Zhang et al., 2022). Here, we performed transcriptome analysis to explore the mechanism of halofuginone resistance in *E. tenella*.

# Materials and methods

## Ethics statement

All chickens in this experiment were performed in accordance with the China Agricultural University Institutional Animal Welfare and Animal Experimental Ethical Inspection [Approval number: AW22022202-1-1].

## Animals and parasites

One- to six-week-old Arbor Acres broilers, used for proliferation and halofuginone-resistant line, were purchased from Beijing Arbor Acres Poultry Breeding (Beijing, China). All birds were treated with a coccidia-free diet and water *ad libitum*. The sensitive *E. tenella* Xinjiang strain used was maintained in the laboratory, which is sensitive to the anticoccidial drug halofuginone and used as the parental line. The resistant strains were generated under halofuginone (30 mg/kg) through an experimental evolution strategy and verified through a drug resistance test (Sun et al., 2023). The procedures for collection, sporulation and purification of the parasite were carried out as the previous report (Duan et al., 2020). The cervical dislocation was performed for chickens necessary for sacrifice, which aims to lose consciousness of chickens rapidly.

## Isolation of sporozoites

Sporocysts were extracted from freshly sporulated oocysts after glass-bead grinding. The sporozoites of sensitive strains (HaloS) and halofuginone-resistant strains (HaloR) were purified by the Percoll (Sigma, United States) density gradient method (Dulski and Turner, 1988). To further purify the sporozoites, they were next purified by cellulose DE-52. The viability of sporozoites was tested before *in vitro* culture by trypan blue staining, and sporozoites with >95% viability were used.

## Invasion test of parasites after drug treatment *in vitro*

Madin-Darby bovine kidney (MDBK) cells were used as an infection model. MDBK cells were cultured at 37°C and 5% $CO_2$ in 24-well plates with Dulbecco's modified Eagle's medium (DMEM, Macgene) supplemented with 10% fetal bovine serum (Macgene, China). For evaluating the efficiency of halofuginone inhibition, approximately $5 \times 10^7$ sensitive sporozoites were incubated in DMEM with drug at different concentrations (0, 10, 100 nM, and 1, 5 μM) for 6 h. After the incubation, all samples were washed three times with ice-cold PBS (Solarbio, pH 7.4, Beijing, China). Then fresh MDBK monolayers were seeded into 24-well plates ($10^6$/well) and infected with sporozoites ($10^5$/well) with different concentrations. All assays were performed in triplicate. At 12 hpi, the cells were washed three times with sterile PBS to wash out uninvaded sporozoites, and new medium was added. Sporozoites were counted at 25 different locations in each well under a microscope. Then the samples were collected and immediately stored at −80°C in TRIzol reagent (Ambion, United States) for the following test using RT-qPCR.

## Comparison of endogenous development *in vivo*

Comparison of the reproductivity of sporozoites treated with halofuginone of different concentrations (0, 10, 100 nM and 1 μM) was tested by measuring oocyst output. For this experiment, 4 groups of 7-day-old chickens were infected with $2 \times 10^5$ sporozoites/bird for each strain. Each sample were performed twice.

## RNA-seq

Sporozoites were treated with halofuginone at different concentrations (0, 10, 100 nM and 1 μM) as before and immediately stored at −80°C in TRIzol (Ambion, United States) for the subsequent RNA-seq analysis. Each treatment consisted of three biological replicates. Samples were designated SC, S10, S100, SIU, RC and R1U. The number represents the exposure concentration, and the

letters "S" and "R" represent halofuginone-sensitive and halofuginone-resistant strains, respectively. RNA-Seq was performed using an Illumina HiSeq-PE150. The raw reads were subjected to quality control and filtered into clean reads using Trimmomatic-0.38 and then mapped against the *E. tenella* reference genome (pEimTen1.1) using STAR aligner (v.2.7.10a). The sorted BAM files were then used for read count *via* featherCounts (v2.0.3). Differentially expressed genes (DEGs) were identified using the R package DESeq2 (Anders and Huber, 2010). Adjusted *p* values were calculated using the Benjamini and Hochberg methods to control the false discovery rate. The standard for screening DEGs was an adjusted $p < 0.05$ and a $|\text{Log2 (fold change)}| \geq 1$. Functional enrichment analysis was mainly conducted through Gene Ontology (GO) annotation using ClusterProfiler (v 4.0.5).

## qRT–PCR

Total RNA was isolated by using TRIzol (Ambion, United States) according to the manufacturer's instructions. RNA purity was checked using a NanoPhotometer spectrophotometer (IMPLEN, Los Angeles, CA, United States). cDNA of different samples was also prepared from 100 to 500 ng total RNA using the HiScript III 1st Strand cDNA Synthesis Kit (+gDNA wiper) (Vazyme, Nanjing, China) and random hexamers. Quantitative PCR was performed on Stepone using PerfectStart Green qPCR SuperMix (+Dye I) (TransGen Biotech, Beijing, China). For the evaluation of the efficiency of invasion, transcription was quantified from cDNA (RT-qPCR) using specific primers for the sporozoite (Fw_SP and Pv_SP), together with actin (Marugan-Hernandez et al., 2020). For verification of the RNA-seq data, primers specific for 10 genes were designed for different exons to avoid the amplification of genomic DNA (Supplementary Table 1). The expression of each gene was normalized to the reference gene actin. Relative expression levels were calculated according to the $2^{-\Delta\Delta CT}$ method.

# Results

## The effects of halofuginone on invasion and endogenous development can be assessed *in vivo* and *in vitro*

To better investigate the effects of halofuginone on the development of *E. tenella*, we performed experiments *in vivo* and *in vitro* using different halofuginone concentrations (Figure 1A). Because halofuginone inhibits the invasion of sporozoites, we tested the efficiency of inhibition by counting the number of sporozoites and conducting RT-qPCR analysis *in vitro*. Our data showed that the number of sporozoites gradually decreased with increasing concentration of halofuginone and the number of transcripts per zoite corresponding to sporozoite-specific target SP25 also decreased after drug treatment (Figures 1B,C). To further evaluate whether endogenous development was inhibited, we also compared the number of oocyst outputs among different groups, and the trend was consistent with that *in vitro* (Figure 1D). Overall, halofuginone affected the invasion and endogenous development of *E. tenella*.

## Differential expression of genes related to invasion *in vitro* under different concentrations of halofuginone

As halofuginone primarily targets the sporozoite stage of *Eimeria*, we treated the sensitive strain with halofuginone *in vitro*. To screen the gene expression landscape under different halofuginone concentrations, sporozoites were preincubated with different concentrations and subsequently subjected to RNA-seq to track the dynamic change in genes (Figure 2A). The total clean paired-end reads were mapped to the reference genome (pEimTen1.1) (>90% uniquely mapped). Principle component analyses (PCA) of the transcriptomic profiles showed distinct variants among different groups (Figure 2B). The DEGs were counted, and we found that the number of differentially expressed genes increased gradually with increasing drug concentration (Figure 2C). DEG analysis, adjusting for drug concentrations as covariates, identified different numbers of DEGs among the groups (Figure 2C; Supplementary Datasets 1–3). We evaluated the gene expression pattern among different treatment groups. The comparison among the three groups showed considerable changes in gene expression profiles after drug treatment, although some genes had the same expression pattern between different treatment groups (Figure 2D).

Hierarchical clustering analysis of the differentially expressed transcripts allowed the identification of groups of co-expressed transcripts for each group. Interestingly, only 44 DEGs were shared among the different sensitive groups (Figure 3A; Supplementary Dataset 4). We hypothesized that the expression of these co-expressed genes was related to halofuginone damage in *E. tenella*.

With the exception of 16 genes that showed no significant pattern after halofuginone treatment, 27 genes were downregulated, and one gene related to programmed cell death was upregulated (Figure 3A). As a result of drug pressure, the parasite expression levels of some enzymes, such as those involved in cytoplasmic translation (GO:0002181) and ligase activity (GO:0016874), were significantly reduced (Figure 3B). Besides these enzymes, the expression of transmembrane transporter (GO:0055085, GO:0022857) also downregulates. Five genes were randomly selected to validate the transcriptome data by RT–qPCR analysis and the downregulated genes selected from the transcriptome had the same pattern in the RT–qPCR analysis (Figure 3C). Based on our data, the genes involved in important biological processes were repressed and programmed cell death was significantly activated, which led to parasite death after halofuginone treatment.

## Gene expression changes after halofuginone resistance induction

To identify novel mechanisms of resistance mediated at the level of transcription, we subjected halofuginone-resistant and halofuginone-sensitive strains of *E. tenella* to comparative transcriptomics using RNA sequencing (Figure 4A). We hypothesized that after obtaining a stable resistance phenotype, only a few gene expression levels change after drug treatment within a short time. Then we compared the transcriptomic data among halofuginone-resistant strains with

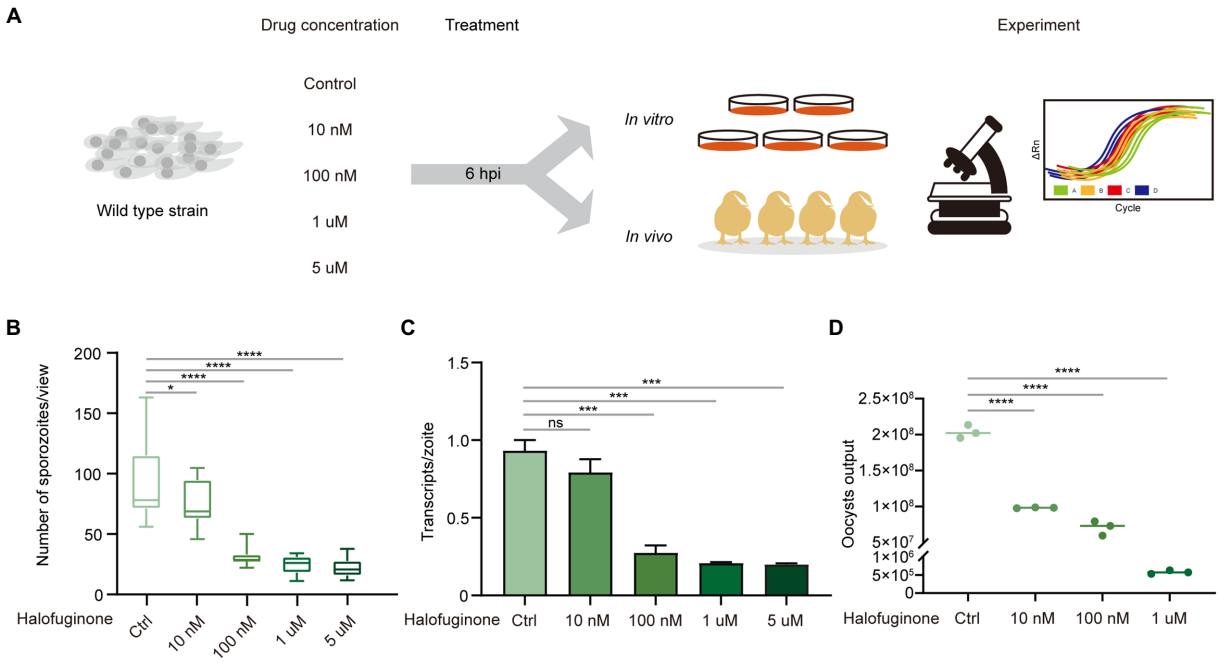


FIGURE 1
Halofuginone affects invasion and endogenous development in *E. tenella*. **(A)** Schematic illustration of the experimental design. The fresh sporozoites were extracted and treated with different concentrations (0, 10, 100nM and 1, 5μM) of halofuginone for 6h. Designed experiments to detect the difference between different groups *in vivo* and *in vitro*. **(B)** The effect of halofuginone on the invasion efficiency for *E. tenella* in MDBK cells. Sporozoites were counted at 25 different locations in each well under a microscope and each sample was performed with triplicates. ***$p$<0.001. **(C)** Detection of changes in invasion by RT-qPCR when sporozoites are preincubated with different concentrations of halofuginone (0, 10, 100nM and 1, 5μM). Values represent the mean±SEM from five independent experiments performed in triplicates. ***$p$<0.001. **(D)** Comparison of the number of oocysts output among different concentrations (0, 10, 100nM and 1μM). Each sample was performed twice. ***$p$<0.001.

different concentrations, and there were only 12 DEGs existed (Supplementary Dataset 6). We reasoned that the differences in gene expression among resistant and sensitive strains may drive mechanisms of resistance. PCA was performed to cluster the 6 samples based on gene expression level, and PC1 showed a distinct distance between halofuginone-resistant and -sensitive strains (Figure 4B). Based on our data, there were 1,325 DEGs between the resistant and sensitive groups (Supplementary Dataset 5). Thus, halofuginone had little effect on the gene expression pattern of the drug-resistant group.

To further explore the expression dynamics of DEGs, a volcano plot was generated, and the results showed that there were a total of 1,325 DEGs of which 1,018 DEGs were downregulated and 307 DEGs were upregulated (Figure 5A). RT–qPCR was performed to verify the transcriptome data (Figure 5B). To further understand the functions of DEGs after halofuginone induction, we performed a GO analysis (Figure 5C). Interestingly, among these downregulated genes, translation-related genes (GO:0016071) and structural constituents of ribosomes (GO:0005840, GO:0003735) were statistically significant, suggesting the downregulation of protein translation in resistant strains (Figure 5C). We also found that the expressions of some genes involved in ATP synthase were decreased (Supplementary Figure 1). These processes are all crucial for parasite protein translation, indicating that protein synthesis was inactive in the halofuginone-resistant strain.

## Discussion

Halofuginone, a traditional Chinese medicine, is used as an anticoccidial drug to control coccidiosis (Zhang et al., 2012). However, the therapeutic utility of halofuginone and its analogs have been stymied by resistance, and the previously unknown mode of action in the parasite has impeded the rational development of drugs with improved pharmacological properties (Peek and Landman, 2003). Our recent work has identified that *EtcPRS*$^{Mut}$ also confers halofuginone resistance in *E. tenella* (Sun et al., 2023). Here, we performed transcriptome analysis to explore the potential halofuginone resistance mechanism in *E. tenella*. As outlined above, we found that the expressions of genes involved in translation and ribosomal proteins were significantly decreased in resistant strain, which represents the potential resistance mechanism of halofuginone in *E. tenella*. In addition, hundreds of DEGs were detected after halofuginone treatment in sensitive groups, and the number of DEGs increased gradually with increasing the concentration of halofuginone. However, only 12 DEGs existed in the resistant group, which indicates that halofuginone has a more significant impact on sensitive strains. Furthermore, we provided a gene expression profile to explore the difference between halofuginone-sensitive and resistant strains, which could help us to further explore the mechanism of anticoccidial drugs in *E. tenella*.

Up to date, one of the great challenges is to identify the functional role of loci that are identified as genomically diverse or under selection

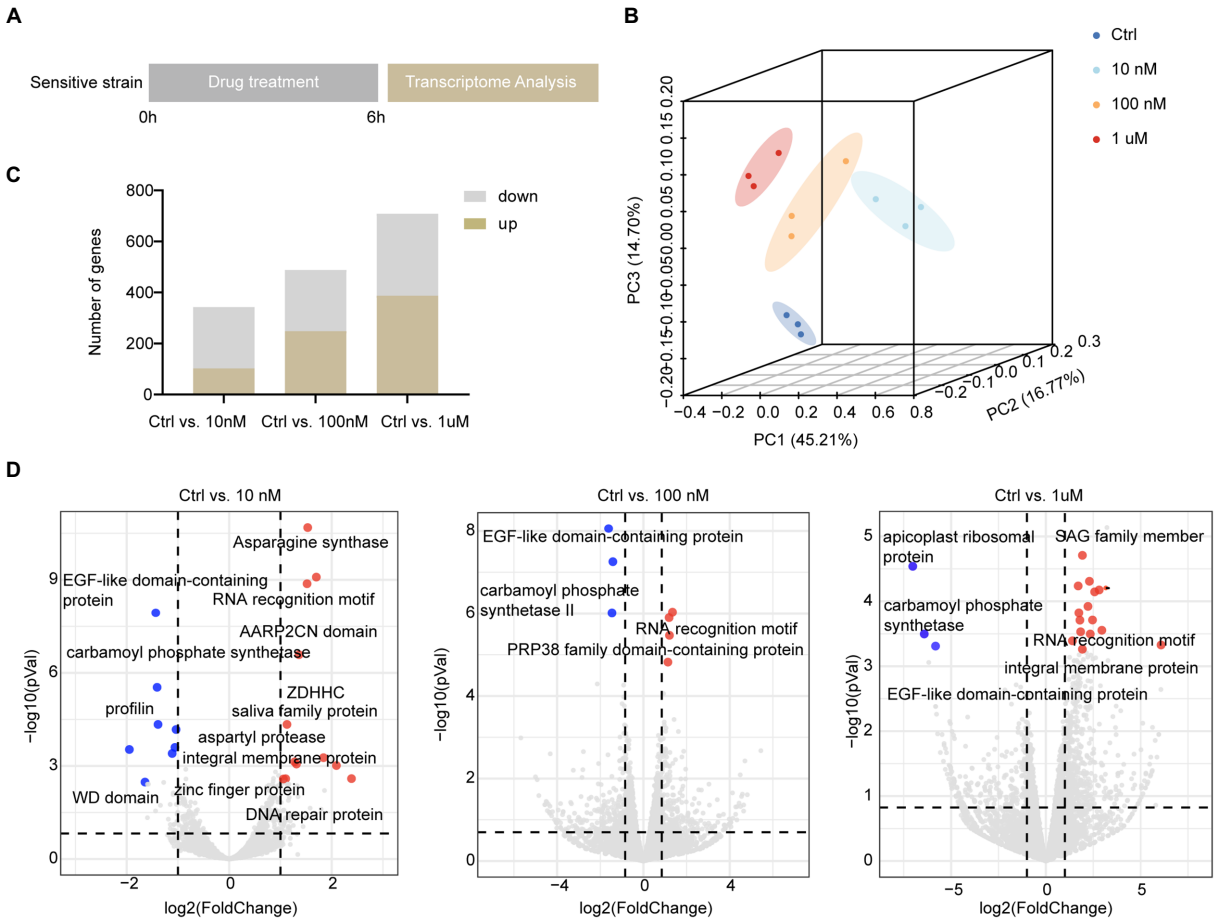


FIGURE 2
Overall description of transcriptome data among different concentrations in sensitive *E. tenella*. **(A)** Schematic illustration of the halofuginone treatment and sampling strategies. Fresh sporozoites of sensitive *E. tenella* strains were treated with different concentrations (0, 10, 100nM, and 1μM) of halofuginone 6h, respectively. Total RNA was then subjected to RNA-seq. **(B)** PCA plots for transcriptome samples labeled by different halofuginone concentrations. **(C)** Comparison of up-regulated and down-regulated numbers of DEGs under different concentrations, and a gene with a *value of p* less than 0.05 and a two-fold change was considered as a DEG. **(D)** Volcano plots showing the proportion of DEGs in different groups. The red dots represented up-regulated genes and the blue dots represented down-regulated genes, and the gray dots showed no significance.

in the parasite genome. To explore the further information between phenotype and genotype, additional insight can be obtained from transcriptome analysis (Richardson and Kaye, 2005; Volkman et al., 2012). To explain the mechanism of halofuginone inhibition, we performed transcriptome analysis to screen the gene profile under halofuginone treatment. By screening the transcriptome data in our study, we found that the expression of ATPase catalytic, SAG family member and several other enzymes (glutamine synthetase and pyridine nucleotide-disulfide oxidoreductase) involved in important biological processes were downregulated, and the expression of programmed cell death protein was upregulated. As we all know, enzymes participate in multiple metabolic processes; for example, detailed studies of glutamine synthetase (GS) have shown that it is an ATP-dependent enzyme found in most species, which synthesizes glutamine from glutamate and ammonia (Tardito et al., 2015; Ben Haim et al., 2021). Downregulation of GS may delay cell cycle progression and morphological alteration. In *Leishmania*, GS can be exploited as a potential drug target (Cruzat et al., 2018). In *Leishmania*, it can be exploited as a potential drug target (Kumar et al., 2021). Based on our data, the expression level of programmed cell death protein is upregulated, the result is consistent with our previous work (Figure 1). Previous work reported that autophagy was a potential mechanism for drug-induced parasite killing in *Toxoplasma* and *Eimeria*, and numerous *in vitro* studies have found that drug treatment-induced programmed cell death in trypanosomes and *Plasmodium* spp. (Lavine and Arrizabalaga, 2012; Proto et al., 2013; Charvat and Arrizabalaga, 2016; Zhang et al., 2022). Thus, many successful inhibitors to date have been designed to induce programmed cell death (Kepp et al., 2011). Our comprehensive results indicate that halofuginone damages biological pathways and induces autophagy in *E. tenella*.

Previous studies also found that differential expression of regulated genes may lead to differences in drug-resistant and drug-sensitive strains (Antony et al., 2016; Ingham et al., 2020; Xie et al., 2020; Laing et al., 2022; Okombo et al., 2022; Zhang et al., 2022). Hence, it was expected that long-term selection would lead to transcriptional changes in different genes in the resistant strain. Although there is no evidence regarding the resistance mechanism in *E. tenella*, several mechanisms of drug resistance exist in *P. falciparum* and *T. gondii* (Ariey et al., 2014; Herman et al., 2015; Amato et al., 2017; Palencia

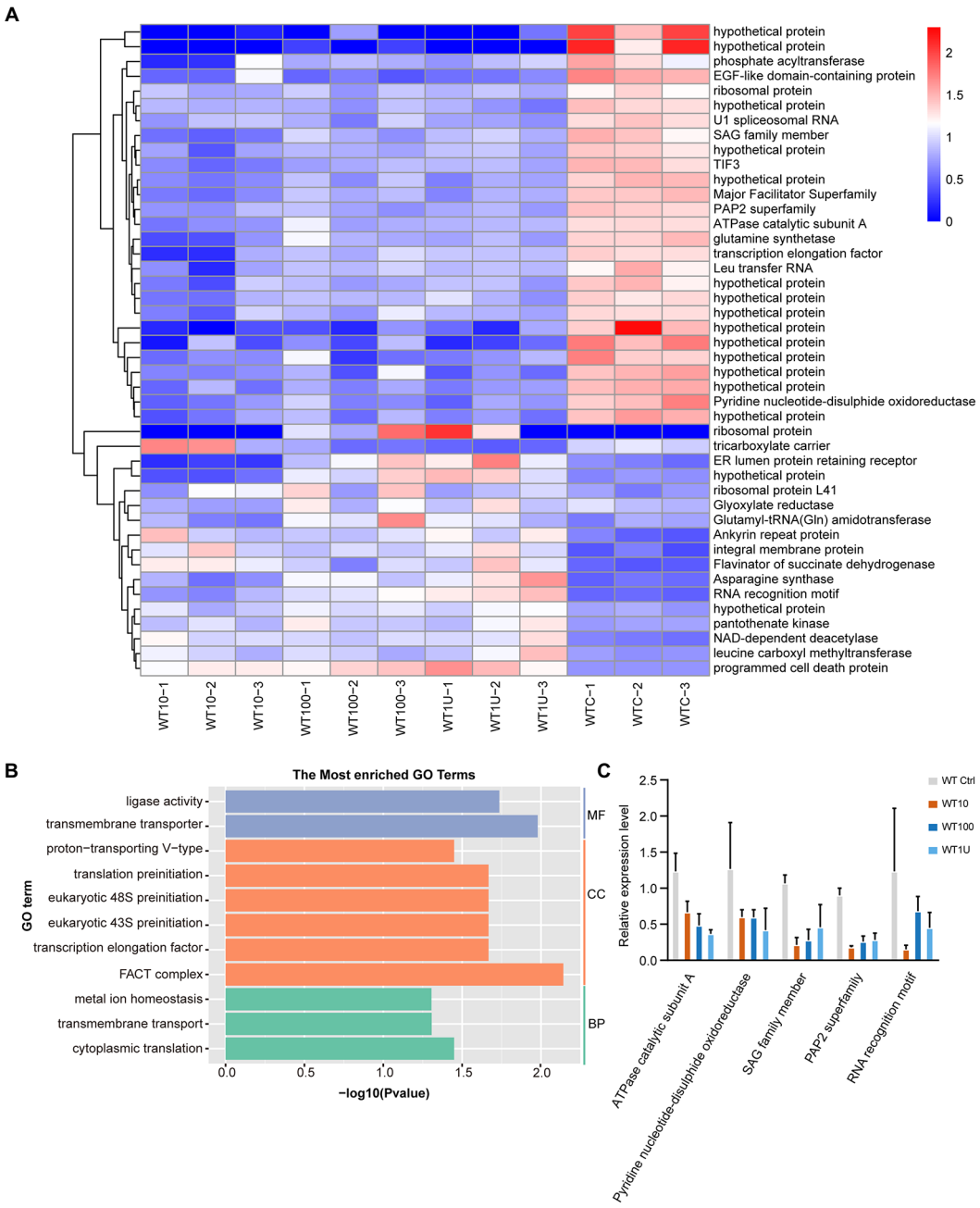


FIGURE 3
Differential expression of genes shared among sensitive strains after halofuginone treatment **(A)** Heat map of the $\log_2$ fold change of significantly different genes among three treatment groups. Each treatment consisted of three biological replicates **(B)** Functional enrichment of shared DEGs among sensitive groups with different concentrations of halofuginone. The 11 most extensive GO terms of the three GO categories "molecular function" (blue), "cellular component" (orange), and "biological process" (green) are shown. **(C)** Verification of gene expression by real-time quantitative PCR. The black bars with standard errors indicate fold changes based on the relative expression level determined by qPCR using the $2^{-\Delta\Delta CT}$ method for three biological replicates.

et al., 2017; Mishra et al., 2019; Rosenberg et al., 2019; Bellini et al., 2020; Rocamora et al., 2021). As discussed in the previous review, resistance development to toxic drugs in different species shows both important similarities and differences (Hughes and Andersson, 2015). With regard to similarities, it is striking that the mechanisms of resistance are often genetically and functionally similar between these different organisms and cells. In the reports on *P. falciparum* and *T. gondii*, the mechanism of resistance could be summarized as 1) reducing the interaction between the drug and target by mutation, modification, or protection; 2) restricting the internal concentration of

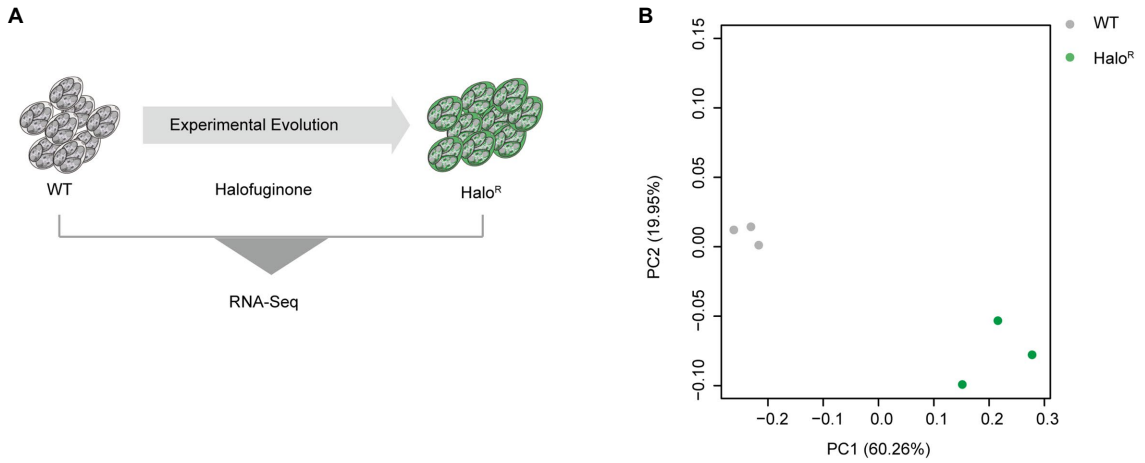


FIGURE 4
Overview of transcriptome analysis between halofuginone-sensitive strain and resistant *E. tenella* strains. **(A)** Schematic illustration of the induction of halofuginone-resistant strain. **(B)** PCA plots for transcriptome samples labeled by different strains. Gray dots represent wild-type strains while green dots represent halofuginone-resistant strains.

the drug by altering efflux or influx; and 3) reducing the concentration of the active drug by altering enzymatic activity (Hughes and Andersson, 2015). Comparing the expression landscape of the halofuginone-resistant and halofuginone-sensitive strains, 1,325 DEGs were identified. In our study, we found that genes involved in the mRNA metabolic process and ribosome proteins were downregulated in the halofuginone-resistant strain. Parasites need a powerful translation system to synthetic protein to complete the complex life cycle (Bennink and Pradel, 2019). In contrast, we found a significant reduction in transcription levels of translation-related genes in resistant strains, which also explains the poor fitness of resistant strains in the fields (Zhang et al., 2022). As previously described, one mechanism by which cells cope with environmental stressors is to downregulate the rate of protein synthesis and increase the selective expression of certain genes for stress adaptation (Han et al., 2020; Kusnadi et al., 2020). In accordance with previous findings, halofuginone acts as a prolyl-tRNA synthetase inhibitor, which ultimately impedes protein translation (Keller et al., 2012; Zhou et al., 2013; Jain et al., 2017). Furthermore, downregulating the process of translation may lead to resistance to halofuginone in *E. tenella*. We hypothesized that mutations that change gene expression can contribute to halofuginone resistance after drug induction. In other species, mutations in *cis*- or *trans*-regulatory elements in the promoter regions of genes of interest and/or changes in the expression level of transcription factors binding to these *cis*- or *trans*-regulatory elements may contribute to drug resistance (Liu et al., 2015; Hu et al., 2021). Unfortunately, detailed information about *cis*- or *trans*- regulatory elements in apicomplexan parasites is limited. Two conserved sequences (RPA: 5'CGGCTTATATTCG, RPB: 5'YGCATGCR) were found in *T. gondii* (Mullapudi et al., 2009). From the DEGs, we only found 7 genes related to translation may be regulated by RPB in *E. tenella* (Supplementary Figure 2). This is interesting for the further study.

In summary, this study highlights the remarkable transcriptome versatility displayed by *E. tenella* for both drug inhibition and resistance mechanisms. This may provide an effective approach to exploring drug resistance mechanisms in *Eimeria*.

## Data availability statement

The data presented in the study are deposited in the NCBI repository (https://www.ncbi.nlm.nih.gov/), accession number PRJNA921718.

## Ethics statement

The animal study was reviewed and approved by China Agricultural University Institutional Animal Welfare and Animal Experimental Ethical Inspection.

## Author contributions

PS: performed experiment, wrote the original draft, and data analysis. CW, XT, and DH: conceptualized project. YZ: data analysis. FX and ZH: generated some strains and cell lines. JS: helped with some general experiments. YY, XS, and XL: funding acquisition and supervision. All authors read and approved the final manuscript.

## Funding

This study was supported by the National Natural Science Foundation of China (31873007 and 32072884) and the National Key Research and Development Program of China (2018YFD0500300 and 2016YFD0501300). XL was supported by the 2115 Talent Development Program of China Agricultural University.

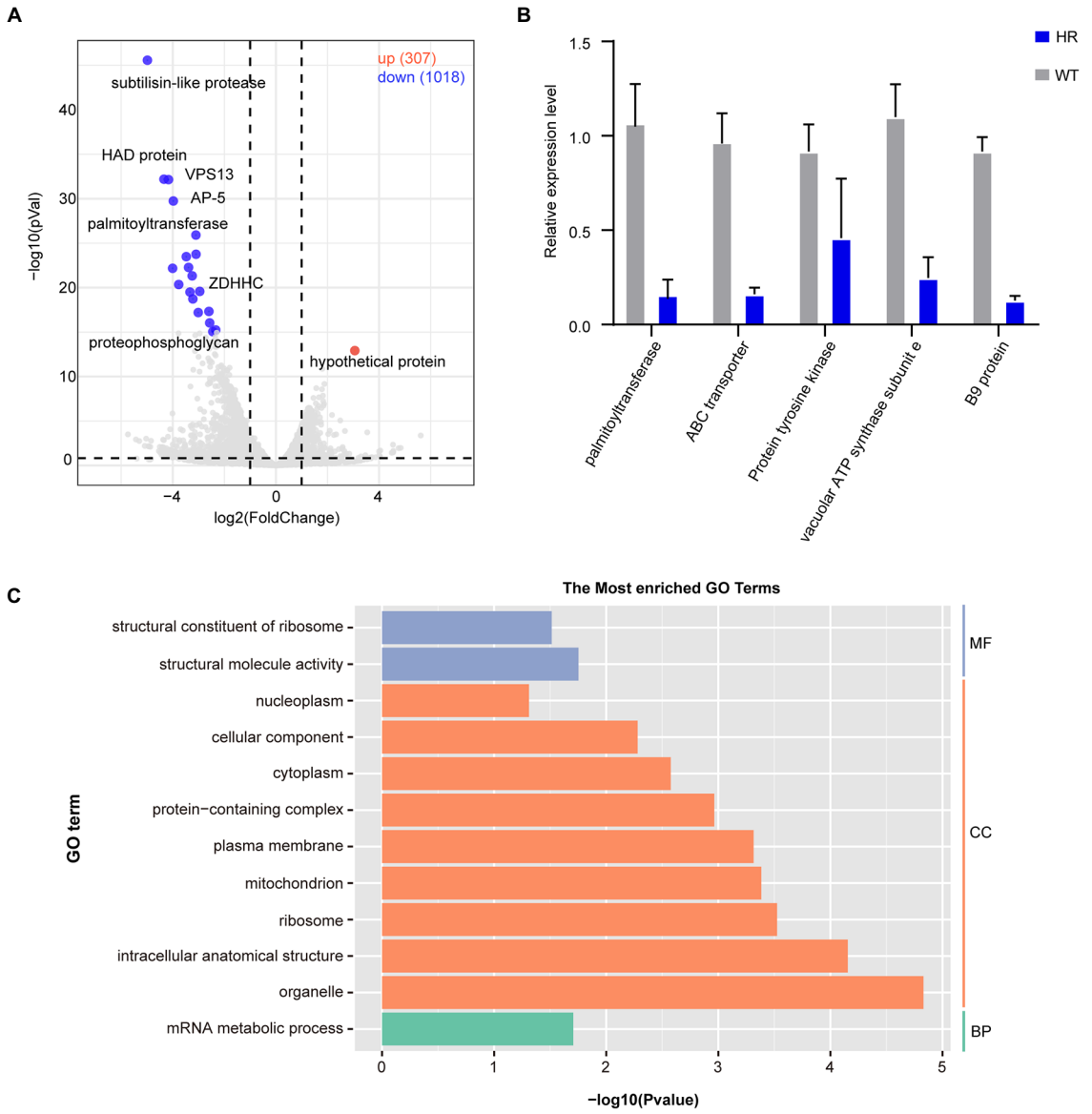


FIGURE 5
Differential gene expression after halofuginone induction. **(A)** Volcano plot showing the proportion of DEGs between the sensitive group and resistant group. The red dots represented up-regulated genes, the blue dots represented down-regulated genes, and the gray dots showed no significance. **(B)** Verification of gene expression by real-time quantitative PCR. The black bars with standard errors indicate fold changes based on the relative expression level determined by qPCR using the $2^{-\Delta\Delta CT}$ method for three biological replicates. **(C)** Functional enrichment of DEGs between halofuginone-sensitive and -resistant strains. The 12 most extensive GO terms of the three GO categories "molecular function" (blue), "cellular component" (orange), and "biological process" (green) are shown.

## Conflict of interest

The authors declare that the research was conducted in the absence of any commercial or financial relationships that could be construed as a potential conflict of interest.

## Publisher's note

All claims expressed in this article are solely those of the authors and do not necessarily represent those of their affiliated organizations, or those of the publisher, the editors and the reviewers. Any product that may be evaluated in this article, or claim that may be made by its manufacturer, is not guaranteed or endorsed by the publisher.

## Supplementary material

The Supplementary material for this article can be found online at: https://www.frontiersin.org/articles/10.3389/fmicb.2023.1141952/full#supplementary-material

# References


Amato, R., Lim, P., Miotto, O., Amaratunga, C., Dek, D., Pearson, R. D., et al. (2017). Genetic markers associated with dihydroartemisinin-piperaquine failure in *plasmodium falciparum* malaria in Cambodia: a genotype-phenotype association study. *Lancet Infect. Dis.* 17, 164–173. doi: 10.1016/S1473-3099(16)30409-1

Anders, S., and Huber, W. (2010). Differential expression analysis for sequence count data. *Genome Biol.* 11, 1–12. doi: 10.1186/gb-2010-11-10-r106

Antony, H. A., Pathak, V., Parija, S. C., Ghosh, K., and Bhattacherjee, A. (2016). Transcriptomic analysis of Chloroquine-sensitive and Chloroquine-resistant strains of *plasmodium falciparum*: toward malaria diagnostics and therapeutics for Global Health. *J. Integr. Biol.* 20, 424–432. doi: 10.1089/omi.2016.0058

Ariey, F., Witkowski, B., Amaratunga, C., Beghain, J., Langlois, A.-C., Khim, N., et al. (2014). A molecular marker of artemisinin-resistant *plasmodium falciparum* malaria. *Nature* 505, 50–55. doi: 10.1038/nature12876

Bellini, V., Swale, C., Brenier-Pinchart, M.-P., Pezier, T., Georgeault, S., Laurent, F., et al. (2020). Target identification of an antimalarial Oxaborole identifies AN13762 as AN alternative Chemotype for targeting CPSF3 in Apicomplexan parasites. *iScience* 23:101871. doi: 10.1016/j.isci.2020.101871

Ben Haim, L., Schirmer, L., Zulji, A., Sabeur, K., Tiret, B., Ribon, M., et al. (2021). Evidence for glutamine synthetase function in mouse spinal cord oligodendrocytes. *Glia* 69, 2812–2827. doi: 10.1002/glia.24071

Bennink, S., and Pradel, G. (2019). The molecular machinery of translational control in malaria parasites. *Mol. Microbiol.* 112, 1658–1673. doi: 10.1111/mmi.14388

Charvat, R. A., and Arrizabalaga, G. (2016). Oxidative stress generated during monensin treatment contributes to altered *toxoplasma gondii* mitochondrial function. *Sci. Rep.* 6:22997. doi: 10.1038/srep22997

Cheng, B., Cai, Z., Luo, Z., Luo, S., Luo, Z., Cheng, Y., et al. (2022). Structure-guided Design of Halofuginone Derivatives as ATP-aided inhibitors against bacterial Prolyl-tRNA Synthetase. *J. Med. Chem.* 65, 15840–15855. doi: 10.1021/acs.jmedchem.2c01496

Cruzat, V., Macedo Rogero, M., Noel Keane, K., Curi, R., and Newsholme, P. (2018). Glutamine: metabolism and immune function, supplementation and clinical translation. *Nutrients* 10:1564. doi: 10.3390/nu10111564

Derbyshire, E. R., Mazitschek, R., and Clardy, J. (2012). Characterization of *plasmodium* liver stage inhibition by halofuginone. *ChemMedChem* 7, 844–849. doi: 10.1002/cmdc.201200045

Duan, C., Tang, X., Hu, D., Zhang, S., Liu, J., Bi, F., et al. (2020). Nucleofection and *in vivo* propagation of chicken *Eimeria* parasites. *J. Visual. Exp.* 156:e60552. doi: 10.3791/60552

Dubey, J. P., and Jenkins, M. C. (2018). Re-evaluation of the life cycle of *Eimeria maxima* Tyzzer, 1929 in chickens (Gallus domesticus). *Parasitology* 145, 1051–1058. doi: 10.1017/S0031182017002153

Dulski, P., and Turner, M. (1988). The purification of sporocysts and sporozoites from *Eimeria tenella* oocysts using Percoll density gradients. *Avian Dis.* 32, 235–239. doi: 10.2307/1590810

Gill, J., and Sharma, A. (2022). Prospects of halofuginone as an antiprotozoal drug scaffold. *Drug Discov. Today* 27, 2586–2592. doi: 10.1016/j.drudis.2022.05.020

Han, N. C., Kelly, P., and Ibba, M. (2020). Translational quality control and reprogramming during stress adaptation. *Exp. Cell Res.* 394:112161. doi: 10.1016/j.yexcr.2020.112161

Herman, J. D., Pepper, L. R., Cortese, J. F., Estiu, G., Galinsky, K., Zuzarte-Luis, V., et al. (2015). The cytoplasmic prolyl-tRNA synthetase of the malaria parasite is a dual-stage target of febrifugine and its analogs. *Sci. Transl. Med.* 7:288ra77. doi: 10.1126/scitranslmed.aaa3575

Herman, J. D., Rice, D. P., Ribacke, U., Silterra, J., Deik, A. A., Moss, E. L., et al. (2014). A genomic and evolutionary approach reveals non-genetic drug resistance in malaria. *Genome Biol.* 15:511. doi: 10.1186/s13059-014-0511-2

Hewitt, S. N., Dranow, D. M., Horst, B. G., Abendroth, J. A., Forte, B., Hallyburton, I., et al. (2017). Biochemical and structural characterization of selective allosteric inhibitors of the *plasmodium falciparum* drug target, Prolyl-tRNA-synthetase. *ACS Infect. Dis.* 3, 34–44. doi: 10.1021/acsinfecdis.6b00078

Hu, B., Huang, H., Hu, S., Ren, M., Wei, Q., Tian, X., et al. (2021). Changes in both trans- and cis-regulatory elements mediate insecticide resistance in a lepidopteron pest Spodoptera exigua. *PLoS Genet.* 17:e1009403. doi: 10.1371/journal.pgen.1009403

Hu, D., Wang, C., Wang, S., Tang, X., Duan, C., Zhang, S., et al. (2018). Comparative transcriptome analysis of *Eimeria maxima* (Apicomplexa: Eimeriidae) suggests DNA replication activities correlating with its fecundity. *BMC Genomics* 19:699. doi: 10.1186/s12864-018-5090-2

Hughes, D., and Andersson, D. I. (2015). Evolutionary consequences of drug resistance: shared principles across diverse targets and organisms. *Nat. Rev. Genet.* 16, 459–471. doi: 10.1038/nrg3922

Ingham, V. A., Anthousi, A., Douris, V., Harding, N. J., Lycett, G., Morris, M., et al. (2020). A sensory appendage protein protects malaria vectors from pyrethroids. *Nature* 577, 376–380. doi: 10.1038/s41586-019-1864-1

Ingham, V. A., Wagstaff, S., and Ranson, H. (2018). Transcriptomic meta-signatures identified in Anopheles gambiae populations reveal previously undetected insecticide resistance mechanisms. *Nat. Commun.* 9:5282. doi: 10.1038/s41467-018-07615-x

Jain, V., Yogavel, M., Kikuchi, H., Oshima, Y., Hariguchi, N., Matsumoto, M., et al. (2017). Targeting Prolyl-tRNA Synthetase to accelerate drug discovery against malaria, Leishmaniasis, toxoplasmosis, cryptosporidiosis, and Coccidiosis. *Structure* 25, 1495–1505.e6. doi: 10.1016/j.str.2017.07.015

Keller, T. L., Zocco, D., Sundrud, M. S., Hendrick, M., Edenius, M., Yum, J., et al. (2012). Halofuginone and other febrifugine derivatives inhibit prolyl-tRNA synthetase. *Nat. Chem. Biol.* 8, 311–317. doi: 10.1038/nchembio.790

Kepp, O., Galluzzi, L., Lipinski, M., Yuan, J., and Kroemer, G. (2011). Cell death assays for drug discovery. *Nat. Rev. Drug Discov.* 10, 221–237. doi: 10.1038/nrd3373

Kumar, V., Ghosh, S., Roy, K., Pal, C., and Singh, S. (2021). Deletion of glutamine Synthetase gene disrupts the survivability and infectivity of *Leishmania donovani*. *Front. Cell. Infect. Microbiol.* 11:622266. doi: 10.3389/fcimb.2021.622266

Kusnadi, E. P., Trigos, A. S., Cullinane, C., Goode, D. L., Larsson, O., Devlin, J. R., et al. (2020). Reprogrammed mRNA translation drives resistance to therapeutic targeting of ribosome biogenesis. *EMBO J.* 39:e105111. doi: 10.15252/embj.2020105111

Laing, R., Doyle, S. R., McIntyre, J., Maitland, K., Morrison, A., Bartley, D. J., et al. (2022). Transcriptomic analyses implicate neuronal plasticity and chloride homeostasis in ivermectin resistance and response to treatment in a parasitic nematode. *PLoS Pathog.* 18:e1010545. doi: 10.1371/journal.ppat.1010545

Lan, L. H., Sun, B. B., Zuo, B. X. Z., Chen, X. Q., and Du, A. F. (2017). Prevalence and drug resistance of avian *Eimeria* species in broiler chicken farms of Zhejiang province China. *Poul. Sci.* 96, 2104–2109. doi: 10.3382/ps/pew499

Lavine, M. D., and Arrizabalaga, G. (2012). Analysis of monensin sensitivity in *toxoplasma gondii* reveals autophagy as a mechanism for drug induced death. *PLoS One* 7:e42107. doi: 10.1371/journal.pone.0042107

Liu, N., Li, M., Gong, Y., Liu, F., and Li, T. (2015). Cytochrome P450s--Their expression, regulation, and role in insecticide resistance. *Pestic. Biochem. Physiol.* 120, 77–81. doi: 10.1016/j.pestbp.2015.01.006

Marugan-Hernandez, V., Jeremiah, G., Aguiar-Martins, K., Burrell, A., Vaughan, S., Xia, D., et al. (2020). The growth of Eimeria tenella: characterization and application of quantitative methods to assess Sporozoite invasion and endogenous development in cell culture. *Front. Cell. Infect. Microbiol.* 10:579833. doi: 10.3389/fcimb.2020.579833

McLaughlin, N. P., Evans, P., and Pines, M. (2014). The chemistry and biology of febrifugine and halofuginone. *Bioorg. Med. Chem.* 22, 1993–2004. doi: 10.1016/j.bmc.2014.02.040

Mishra, S., Malhotra, N., Kumari, S., Sato, M., Kikuchi, H., Yogavel, M., et al. (2019). Conformational heterogeneity in apo and drug-bound structures of *toxoplasma gondii* prolyl-tRNA synthetase. *Acta Crystallographica Commun. Struct. Biol.* 75, 714–724. doi: 10.1107/S2053230X19014808

Mullapudi, N., Joseph, S. J., and Kissinger, J. C. (2009). Identification and functional characterization of cis-regulatory elements in the apicomplexan parasite *toxoplasma gondii*. *Genome Biol.* 10:R34. doi: 10.1186/gb-2009-10-4-r34

Noack, S., Chapman, H. D., and Selzer, P. M. (2019). Anticoccidial drugs of the livestock industry. *Parasitol. Res.* 118, 2009–2026. doi: 10.1007/s00436-019-06343-5

Okombo, J., Mok, S., Qahash, T., Yeo, T., Bath, J., Orchard, L. M., et al. (2022). Piperaquine-resistant PfCRT mutations differentially impact drug transport, hemoglobin catabolism and parasite physiology in *plasmodium falciparum* asexual blood stages. *PLoS Pathog.* 18:e1010926. doi: 10.1371/journal.ppat.1010926

Palencia, A., Bougdour, A., Brenier-Pinchart, M.-P., Touquet, B., Bertini, R.-L., Sensi, C., et al. (2017). Targeting CPSF3 as a new approach to control toxoplasmosis. *EMBO Mol. Med.* 9, 385–394. doi: 10.15252/emmm.201607370

Peek, H. W., and Landman, W. J. M. (2003). Resistance to anticoccidial drugs of Dutch avian Eimeria spp. field isolates originating from 1996, 1999 and 2001. *J. WVPA* 32, 391–401. doi: 10.1080/0307945031000121149

Proto, W. R., Coombs, G. H., and Mottram, J. C. (2013). Cell death in parasitic protozoa: regulated or incidental? *Nat. Rev. Microbiol.* 11, 58–66. doi: 10.1038/nrmicro2929

Richardson, A., and Kaye, S. B. (2005). Drug resistance in ovarian cancer: the emerging importance of gene transcription and spatio-temporal regulation of resistance. *Rev. Comment. Antimicrob. Anticancer Chemother.* 8, 311–321. doi: 10.1016/j.drup.2005.09.001

Rocamora, F., Gupta, P., Istvan, E. S., Luth, M. R., Carpenter, E. F., Kümpornsin, K., et al. (2021). PfMFR3: A Multidrug-Resistant Modulator in *Plasmodium falciparum*. *ACS Infect. Dis.* 7, 811–825. doi: 10.1021/acsinfecdis.0c00676

Rosenberg, A., Luth, M. R., Winzeler, E. A., Behnke, M., and Sibley, L. D. (2019). Evolution of resistance *in vitro* reveals mechanisms of artemisinin activity in *toxoplasma gondii*. *Proc. Natl. Acad. Sci. U. S. A.* 116, 26881–26891. doi: 10.1073/pnas.1914732116

Sun, P., Zhang, Y., Wang, C., Hu, D., Liu, J., Chen, L., et al. (2023). *EtcPRS*$^{Mut}$ as a molecular marker of halofuginone resistance in *Eimeria tenella* and *toxoplasma gondii*. *iScience* 26:106334. doi: 10.1016/j.isci.2023.106334

Tardito, S., Oudin, A., Ahmed, S. U., Fack, F., Keunen, O., Zheng, L., et al. (2015). Glutamine synthetase activity fuels nucleotide biosynthesis and supports growth of glutamine-restricted glioblastoma. *Nat. Cell Biol.* 17, 1556–1568. doi: 10.1038/ncb3272

Tye, M. A., Payne, N. C., Johansson, C., Singh, K., Santos, S. A., Fagbami, L., et al. (2022). Elucidating the path to *plasmodium* prolyl-tRNA synthetase inhibitors that overcome halofuginone resistance. *Nat. Commun.* 13:4976. doi: 10.1038/s41467-022-32630-4

Volkman, S. K., Neafsey, D. E., Schaffner, S. F., Park, D. J., and Wirth, D. F. (2012). Harnessing genomics and genome biology to understand malaria biology. *Nat. Rev. Genet.* 13, 315–328. doi: 10.1038/nrg3187

Xie, Y., Huang, B., Xu, L., Zhao, Q., Zhu, S., Zhao, H., et al. (2020). Comparative Transcriptome analyses of drug-sensitive and drug-resistant strains of *Eimeria tenella* by RNA-sequencing. *J. Eukaryot. Microbiol.* 67, 406–416. doi: 10.1111/jeu.12790

Zhang, D. F., Sun, B. B., Yue, Y. Y., Yu, H. J., Zhang, H. L., Zhou, Q.-J., et al. (2012). Anticoccidial effect of halofuginone hydrobromide against *Eimeria tenella* with associated histology. *Parasitol. Res.* 111, 695–701. doi: 10.1007/s00436-012-2889-7

Zhang, H., Zhang, L., Si, H., Liu, X., Suo, X., and Hu, D. (2022). Early transcriptional response to Monensin in sensitive and resistant strains of *Eimeria tenella*. *Front. Microbiol.* 13:934153. doi: 10.3389/fmicb.2022.934153

Zhou, H., Sun, L., Yang, X.-L., and Schimmel, P. (2013). ATP-directed capture of bioactive herbal-based medicine on human tRNA synthetase. *Nature* 494, 121–124. doi: 10.1038/nature11774

frontiers | Frontiers in Microbiology

TYPE Original Research
PUBLISHED 21 April 2023
DOI 10.3389/fmicb.2023.1167693



OPEN ACCESS

EDITED BY
Nagendran Tharmalingam,
Rhode Island Hospital, United States

REVIEWED BY
Adriana Morar,
Banat University of Agricultural Sciences and Veterinary Medicine, Romania
Garima Arvikar,
University of California, San Francisco, United States
Debasish Paul,
National Institutes of Health (NIH), United States

*CORRESPONDENCE
Maria Laura Breser
✉ laurabreser45@hotmail.com
Carina Porporatto
✉ cporporatto@unvm.edu.ar

RECEIVED 16 February 2023
ACCEPTED 03 April 2023
PUBLISHED 21 April 2023

CITATION
Breser ML, Tisera L, Orellano MS, Bohl LP, Isaac P, Bianco I and Porporatto C (2023) Chitosan can improve antimicrobial treatment independently of bacterial lifestyle, biofilm biomass intensity and antibiotic resistance pattern in non-aureus staphylococci (NAS) isolated from bovine clinical mastitis. *Front. Microbiol.* 14:1167693. doi: 10.3389/fmicb.2023.1167693



# Chitosan can improve antimicrobial treatment independently of bacterial lifestyle, biofilm biomass intensity and antibiotic resistance pattern in non-aureus staphylococci (NAS) isolated from bovine clinical mastitis

Maria Laura Breser[1,2]*, Lucia Tisera[1,2], Maria Soledad Orellano[2,3], Luciana Paola Bohl[1,2], Paula Isaac[1,2], Ismael Bianco[4] and Carina Porporatto[1,2]*

[1]Instituto Multidisciplinario de Investigación y Transferencia Agroalimentaria y Biotecnológica (IMITAB-CONICET), Universidad Nacional de Villa María, Villa María, Argentina, [2]Instituto Académico Pedagógico de Ciencias Básicas y Aplicadas, Universidad Nacional de Villa María, Villa María, Argentina, [3]University of the Basque Country UPV/EHU. Responsive Polymer Therapeutics Group (POLYMAT), San Sebastián, Spain, [4]Centro de Excelencia en Productos y Procesos de Córdoba (CEPROCOR), Ministerio de Industria, Comercio, Minería y Desarrollo Científico Tecnológico, Córdoba, Argentina

Bovine mastitis is the most frequent and costly disease that affects dairy cattle. Non-aureus staphylococci (NAS) are currently one of the main pathogens associated with difficult-to-treat intramammary infections. Biofilm is an important virulence factor that can protect bacteria against antimicrobial treatment and prevent their recognition by the host's immune system. Previously, we found that chronic mastitis isolates which were refractory to antibiotic therapy developed strong biofilm biomass. Now, we evaluated the influence of biofilm biomass intensity on the antibiotic resistance pattern in strong and weak biofilm-forming NAS isolates from clinical mastitis. We also assessed the effect of cloxacillin (Clx) and chitosan (Ch), either alone or in combination, on NAS isolates with different lifestyles and abilities to form biofilm. The antibiotic resistance pattern was not the same in strong and weak biofilm producers, and there was a significant association ($p \leq 0.01$) between biofilm biomass intensity and antibiotic resistance. Bacterial viability assays showed that a similar antibiotic concentration was effective at killing both groups when they grew planktonically. In contrast, within biofilm the concentrations needed to eliminate strong producers were 16 to 128 times those needed for weak producers, and more than 1,000 times those required for planktonic cultures. Moreover, Ch alone or combined with Clx had significant antimicrobial activity, and represented an improvement over the activity of the antibiotic on its own, independently of the bacterial lifestyle, the biofilm biomass intensity or the antibiotic resistance pattern. In conclusion, the degree of protection conferred by biofilm against antibiotics appears to be associated with the intensity of its biomass, but treatment with Ch might be able to help counteract it. These findings suggest that bacterial biomass should be considered when designing new antimicrobial therapies aimed at reducing antibiotic concentrations while improving cure rates.

KEYWORDS

biofilm, antibiotic resistance, chitosan, cloxacillin, biofilm and antibiotic resistance association, non-aureus staphylococcus

# 1. Introduction

Bovine mastitis (BM) is the most prevalent disease that affects dairy cattle. It compromises the health of dairy herds and leads to serious economic losses that can impact the entire production chain (Hogeveen et al., 2011; Aghamohammadi et al., 2018; Heikkilä et al., 2018). The costs are related to the intervention, treatment, and monitoring of infection, and are compounded by a significant reduction in the quality and quantity of the milk produced (Vissio et al., 2015; Aghamohammadi et al., 2018; Heikkilä et al., 2018). Coagulase-negative Staphylococcus, recently named non-aureus staphylococci (NAS), are one of the most prevalent pathogens associated with BM (De Visscher et al., 2016; Condas et al., 2017; Taponen et al., 2017). They are associated with persistent intramammary infection (IMI), decreased milk production (Heikkilä et al., 2018), and elevated somatic cell counts (SCC; Supré et al., 2011; Fry et al., 2014). In the absence of effective immunoprevention therapies, antibiotics have become the main means to deal with this pathology. However, their indiscriminate use and the high mutation rates of pathogens have led to the emergence of multiresistant bacteria, against which antibiotics are increasingly less effective (Chantziaras et al., 2014; Lhermie et al., 2017; De Jong et al., 2018; Kim et al., 2019; Van Boeckel et al., 2019). In fact, NAS are currently the most resistant mastitis-causing pathogens (de Oliveira et al., 2016; Dorneles et al., 2019; Kim et al., 2019), since they have higher mutation rates and are more capable of horizontal gene transfer than other species. This means they might act as reservoirs and help spread different virulence factors (Bal et al., 2010; Sampimon et al., 2011; Taponen et al., 2017). The highest cure rates for the clinical and subclinical forms of the disease are usually obtained when antibiotics are applied during dry-off (Rabiee and Lean, 2013). Nevertheless, only 66% of the udders infected before this period are clinically cured afterwards (Lipkens et al., 2019).

Bacterial biofilms may lessen exposure to antibiotics and offer general protection against adverse environmental factors, so they may further hamper the efficacy of antimicrobial therapies (Lebeaux et al., 2014; Tremblay et al., 2014; de Oliveira et al., 2016; Srednik et al., 2017; Breser et al., 2018). Biofilms not only prevent antibiotics from acting directly on bacterial growth, but can also allow the entry of low or suboptimal concentrations of these compounds into their structure (Flemming et al., 2016; Ster et al., 2017). Such concentrations may exert selection pressure and favor the development of resistance in the bacteria within the biofilm (Flemming et al., 2016). Moreover, strong biofilm-forming strains have been described to cause more severe tissue damage than weak producers. More than 85% of the NAS isolated from BM can reportedly grow in biofilms (Tremblay et al., 2014; Felipe et al., 2017; Srednik et al., 2017). Previously, we found that NAS isolates from chronic BM which were refractory to different antibiotic protocols were able to develop strong biofilm biomass (Breser et al., 2018). This indicates that biofilm growth could play an important role in IMI chronicity.

On the other hand, chitosan (Ch) is a natural, biocompatible, and biodegradable polymer with many well-documented biological applications. Its reported antimicrobial activity against a wide range of microorganisms is mainly attributed to its cationic nature (Muxika et al., 2017; Verlee et al., 2017). When we tested it on its own or combined with antibiotics, it had remarkable antimicrobial effects on *Staphylococcus* isolates from clinical and chronic IMIs, whether in their planktonic form, in preformed biofilms, or in intracellular infections (Breser et al., 2018; Felipe et al., 2019).

Given the continuous increase in antimicrobial resistance among mastitis pathogens and the associated reduction in clinical and bacteriological cure rates, chitosan and other similar materials could be useful for the design of new control strategies. These strategies should consider the role of well-established biofilms in the emergence of resistance, which so far remains unclear. Accordingly, the present study evaluated the influence of biofilm forming strength on the patterns of antibiotic resistance in NAS isolates from clinical mastitis. It also assessed the effectiveness of combining Ch with an antibiotic against different bacterial lifestyles.

# 2. Materials and methods

## 2.1. Bacterial isolate classification, growth conditions, and reagents

A total of 110 non-aureus staphylococci (NAS) isolates from clinical BM were collected at 14 independent local dairy farms. NAS were isolated from milk samples from quarters with clinical signs, a positive Californian Mastitis Test (CMT), and SCC ≥ 250.000 cells/ml. The samples were cultured at 37°C for 24 h on Trypticase soy agar (TSA) plates containing 5% sheep blood. All the experiments were carried out under the supervision and with the approval of the Institutional Ethics Committee at the National University of Villa María (UNVM) which monitors experiments with animals, as well as in accordance with international guidelines for the use and handling of pathogenic microorganism isolates from mastitis (Hogan et al., 1999). The identity of the isolates had been confirmed earlier by amplification and partial sequencing of the 16S rRNA gene and MALDI-TOF, and they were classified taxonomically as NAS species (Felipe et al., 2017).

To categorize the intensity of their biofilms, a biofilm formation assay was performed on an abiotic surface and the biomass produced was quantified as previously described (Breser et al., 2018). Briefly, 100 µl of bacterial suspensions ($1 \times 10^7$ CFU/ml) in Trypticase soy broth (TSB) were added into individual wells on flat polystyrene microtiter plates. The plates were statically incubated for 24 h at 37°C, to allow the cells to bind and biofilm to form. The supernatants were discarded and the biofilms were washed twice with sterile PBS to remove non-adherent bacteria, air dried, and stained with a crystal violet (CV) solution (0.5% w/v) for 5 min. The excess dye was washed and the plates were left to dry for 24 h. The dye bound to each well was

resuspended in 200 µl of 96% alcohol. After 20 min of incubation at room temperature, 100 µl were taken from each well and transferred into a new 96-well plate. The absorbance of the eluates was measured at 590 nm with a Multiskan GO microplate spectrophotometer reader (TermoFisher Scientifc), and expressed as optical density (OD) values. The OD values were used to assess the degree of biofilm adhesion to the contact surface. The negative control (NC) consisted of wells cultured with TSB. The $OD_{NC}$ value was obtained by considering three standard deviations above the mean value of the negative control. An isolate was considered a weak biofilm producer (WBP) when $OD_{NC} <$ OD of the isolate $\leq 4$ $OD_{NC}$. On the other hand, when the OD of the isolate >8 $OD_{NC}$ ($OD_{590nm}$ between 2 and 3.15), it was classified as a strong biofilm producer (SBP; Li et al., 2012). In all the assays, *S. epidermidis* strain ATCC 12288 was used as a negative control for biofilm formation (Zhang et al., 2003). Two different groups of 10 NAS isolates each were selected from the collection on the basis of their biofilm biomass intensity (strong vs. weak). To maintain homogeneous species distribution, each group included two isolates of each of the most frequently found species: *S. chromogenes*, *S. simulans*, *S. xylosus*, *S. epidermidis*, and *S. haemolyticus*.

As a quality control for the microbiological assays, the following *Staphylococcus aureus* (*S. aureus*) strains were used: ATCC 29213, ATCC 25923, methicillin-resistant (MRSA) ATCC 43300, and ATCC 35984. The isolates and the reference strains were stored at −80°C in a nutrient broth containing 20% glycerol. The inocula were prepared in TSB at 37°C, 18 to 24 h before carrying out the assays. They were adjusted with DensiCHEK Plus (bioMérieux SA, Marcy-l'Étoile, France) according to the McFarland scale, and the values were corroborated by plate counting.

Low molecular weight chitosan (Ch; 50–90 kDa powder with ≥85% deacetylation), cloxacillin (Clx) powder, and crystal violet (CV) were purchased from Sigma-Aldrich (St Louis, MO, USA). The antibiotic disks and the nutrient media were purchased from Britania (CABA, BA, Argentina).

## 2.2. Susceptibility test

The antimicrobial susceptibility of the isolates was determined by the standard disk diffusion method, following the guidelines by the guidelines of Clinical and Laboratory Standards Institute (CLSI) (2020). The isolates were recovered on fresh TSA 18–24 h prior to the test. The direct colonies were suspended and adjusted at 0.5 on the McFarland scale. The suspensions were swabbed across Mueller-Hilton agar plates; antibiotic disks were placed on the surface, and the plates were incubated for 18–20 h at 35°C. Afterwards, the zone of inhibition around the disks was measured with a calibrated ruler and interpreted according to CLSI breakpoints. The disks used were penicillin (PEN) 10 Units, ampicillin (AMP) 10 µg, cefoxitin (FOX) 30 µg, erythromycin (ERY) 15 µg, and rifampicin (RIF) 5 µg. A cefoxitin disk was used as an indicator of methicillin susceptibility.

## 2.3. Determination of MIC and MBC

The minimum inhibitory concentrations (MIC) of Clx and Ch were determined through a broth microdilution assay according to the CLSI guidelines [Clinical and Laboratory Standards Institute (CLSI), 2020]. Bacterial suspensions ($1\times10^5$ CFU/mL) were cultured for 24 h at 37°C in 96-well bottom-plates (Deltalab, Barcelona, Spain), with different concentrations of Clx (0.025 to 16 µg/ml), Ch (200 µg/ml), or combinations of both. The planktonic minimum bactericidal concentration (P-MBC) was found by seeding the bacteria on TSA plates with concentrations of the antimicrobial compounds which were equal to or greater than the MIC, and assessing viability after 24 h (Breser et al., 2018).

## 2.4. Bacterial viability in preformed biofilms

The viability of bacteria within biofilms was measured after different treatments as previously described (Breser et al., 2018). Briefly, 100 µl of bacterial suspensions ($1\times10^7$ CFU/mL) were placed into 96-well flat-plates (Deltalab), and a final volume of 200 µl in each well was obtained by adding TSB. The plates were statically incubated for 24 h at 37°C, to allow the cells to bind and biofilms to form. After that, the supernatants were discarded and the biofilms were washed twice with sterile PBS to remove non-adherent bacteria. These preformed biofilms were treated for 24 h at 37°C with different concentrations of Clx (64 to 2048 µg/mL), Ch (200 µg/ml), or combinations of both. The biofilm minimum bactericidal concentration (B-MBC) was determined by measuring bacterial viability within the biofilms biomass, after it was disaggregated and seeded on TSA plates.

## 2.5. Viability analysis by flow cytometry

Bacterial suspensions were obtained from planktonic cultures grown for 24 h at 37°C in TSB (control), or with the addition of different concentrations of Clx (4 to 0.065 µg/ml), Ch (200 µg/ml), or combinations of both. Homogeneous suspensions were also prepared with the preformed biofilms, which were disaggregated and filtered after growing for 24 h at 37°C in TSB (control), or in the presence of Clx (8 to 2048 µg/ml), Ch (200 µg/ml), or combinations of both. Bacterial viability was evaluated in both kinds of suspension with a LIVE/DEAD BacLight Bacterial Viability Kit (ThermoFisher Scientific, CA, USA), according to the manufacturer's instructions. The suspensions were analyzed with an ACCURI C6 cytometer (BD Bioscience, CA, USA), and the data were processed on FlowJo software (Tree Star, OR, USA; Breser et al., 2018).

## 2.6. Statistical analysis

The parametric data were statistically analyzed by one or two-way ANOVA, with a Bonferroni *post hoc* test, while non-parametric data were statistically analyzed with Kruskal Wallis one-way analysis of variance. The number of independent replicates in each assay has been specified in the corresponding figures. To control the variability of the isolates, some analyses were conducted with a two-factor factorial design, in which the first factor was the treatment and the second factor was the isolate. R software was used to process the information (R Core Team, 2020), and the graphs were made on GraphPad Prism 5.0 (GraphPad Software, Inc., CA, USA).

# 3. Results

## 3.1. Antimicrobial resistance pattern in strong and weak biofilm-producers NAS isolates

Even though biofilm formation can be an important virulence factor, not enough is known about its direct influence on antibiotic resistance. We evaluated the antimicrobial resistance pattern in NAS isolates in relation to their biofilm-forming ability. The isolates were selected from a collection and divided into two groups of 10 each, depending on whether they were strong biofilm producers (SBPs) or weak biofilm producers (WBPs; Felipe et al., 2017; Breser et al., 2018). The first step was to compare the extracellular components in mature SBP and WBP biofilms (Oniciuc et al., 2016). In both cases, over 88% of the biofilm was removed after treatment with sodium metaperiodate (NaIO4), which degrades exopolysaccharides, and about 20% was removed after treatment with Proteinase K, which degrades proteins. This means that the composition of the biofilm matrix was similar for the two groups (Supplementary Figure). We then assessed the susceptibility of the isolates to the main antibiotic families used to control mastitis, and found that SBPs and WBPs had different antimicrobial resistance patterns (Tables 1A,B; Figure 1). According to the antibiogram, 70, 50, 30, and 10% of the SBPs were, respectively, resistant to penicillin, ampicillin, cefoxitin, and erythromycin (Table 1A), while the percentages were 20, 20, 10, and 0% for WBPs (Table 1B). All the isolates were sensitive to rifampicin. Only 10% of the SBPs were sensitive to different antibiotic families; in the case of WBPs it was 70% (Figure 1). The relative frequency of resistance was 0.9 for SBPs; i.e., 9 to 10 of these isolates were resistant to one or more antibiotics. This value was 0.3 (3 to 10 isolates) for WBPs (Figure 1; Table 1). An odd-ratio analysis showed a significant association ($p \leq 0.01$) between biofilm biomass intensity and antibiotic resistance; and an individual association between biofilms intensity and penicillin resistance ($p \leq 0.01$).

## 3.2. Effect of cloxacillin on planktonic cultures and preformed biofilms

The minimum bactericidal concentration was determined by measuring the viability of SBPs and WBPs in planktonic cultures (P-MBC) and in preformed biofilms (B-MBC). The cloxacillin (Clx) concentration needed to kill bacteria in the biofilms (256 to 1,024 μg/

TABLE 1 Antibiotic susceptibility in SBP and WBP NAS isolates from clinical bovine mastitis.

| Isolates | PEN | AMP | FOX | ERY | RIF | Resistance(#) |
|---|---|---|---|---|---|---|
| A. Strong biofilms producer NAS | | | | | | |
| *SBP1* | R | R | R | S | S | 3 |
| SBP2 | R | S | R | S | S | 2 |
| SBP3 | R | R | S | S | S | 2 |
| SBP4 | R | S | S | S | S | 1 |
| SBP5 | R | R | S | S | S | 2 |
| SBP6 | S | S | S | R | S | 1 |
| SBP7 | S | S | S | S | S | 0 |
| SBP8 | S | S | R | S | S | 1 |
| SPB9 | R | R | S | S | S | 2 |
| SBP10 | R | R | S | S | S | 2 |
| Resistance (%) | 70 | 50 | 30 | 10 | 0 | |
| B. Weak biofilm producer NAS | | | | | | |
| WBP1 | S | S | S | S | S | 0 |
| WBP2 | S | S | S | S | S | 0 |
| WBP3 | S | S | S | S | S | 0 |
| WBP4 | S | S | S | S | S | 0 |
| WBP5 | S | S | S | S | S | 0 |
| WBP6 | I | I | S | S | S | 0 |
| WBP7 | R | R | S | S | S | 2 |
| WBP8 | S | S | S | S | S | 0 |
| WBP9 | R | S | R | S | S | 2 |
| WBP10 | S | R | S | S | S | 1 |
| Resistance (%) | 20 | 20 | 10 | 0 | 0 | |

R, resistant; S, susceptible. AMP, ampicillin; PEN, penicillin G; FOX, cefoxitin; ERY, erythromycin; and RYF, rifampicin. The number of antibiotics to which each NAS isolate was resistant is shown in the last column.The percentage of resistance to each antibiotic is shown in the last row. A. Strong biofilms producer NAS isolates. B. Weak biofilms producer NAS isolates.

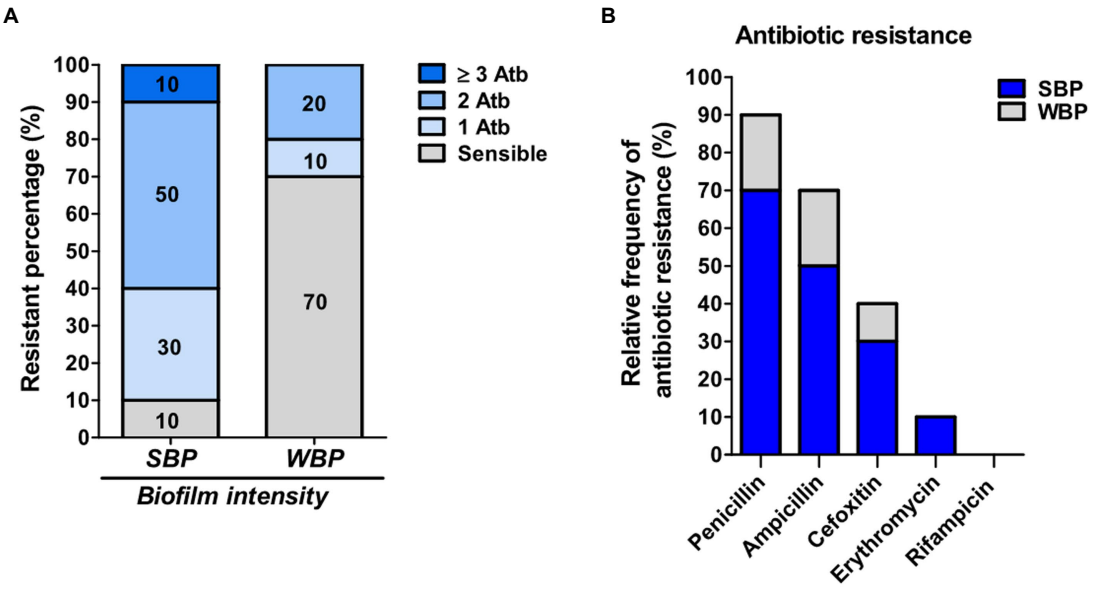


FIGURE 1
Antibiotic resistance in SBP and WBP NAS isolates from clinical bovine mastitis. **(A)** Percentage of resistance to antibiotics in SBP and WBP NAS isolates. **(B)** Relative frequency of resistance to penicillin, ampicillin, cefoxitin, erythromycin and rifampicinin SBP and WBP NAS isolates.

ml for SBPs; 16 to 32 μg/ml for WBPs) was significantly higher ($p \leq 0.001$, Kruskal-Wallis test) than for their planktonic counterparts (1 to 4 μg/ml for SBPs and WBPs; Table 2; Figure 2). In fact, the concentration required to kill SBPs in preformed biofilms was 128 to 1,024 times the one needed when they grew planktonically. For WBPs, the B-MBC was 8–16 times the P-MBC. The differences between the two groups were directly associated with their biofilm-forming ability ($p \leq 0.001$, Kruskal-Wallis test; Table 2; Figure 2).

A flow cytometry analysis with SYTO9 and PI dyes was performed to assess bacterial viability in terms of membrane integrity, after SBPs and WBPs in planktonic cultures and preformed biofilms were incubated with different Clx concentrations. An isolate from each group was selected to build the density plots (Figures 3A,C), and bar graphs show the percentages of bacterial viability for all the isolates in each group (Figures 3B,D). After exposure to different concentrations of the antibiotic, bacterial viability was similar for both groups in the planktonic cultures (Figures 3A,B). In contrast, viability was significantly higher for SBPs than for WBPs when they were treated with the same Clx concentration in the preformed biofilms (Figures 3C,D). Interestingly, SBPs appeared to be generally much more protected than WBPs inside the biofilms, regardless of their specific antibiotic resistance pattern (Figures 3C,D). The flow cytometry data confirm that the antibiotic concentrations needed to kill bacteria in preformed biofilms may be closely related to biofilm-forming ability (Figures 2, 3).

## 3.3. Chitosan and cloxacillin reduce the protection conferred by biofilm

Biofilms are known to protect bacteria against antimicrobial therapies, but more information is needed about the influence of biomass intensity on the degree of protection conferred. Earlier, we observed that combining Clx with Ch made it possible to reduce the concentration of the antibiotic required to kill NAS isolates within biofilms (Breser et al., 2018). Here, we used plate counting and flow cytometry to explore the effects of Clx and Ch (alone or combined) on NAS isolates with different biofilm-forming abilities. As before, the bacteria were evaluated in planktonic cultures and preformed biofilms. The combination of Clx and Ch enabled a significant reduction in the Clx concentration needed to kill both SBPs and WBPs, in planktonic cultures and in preformed biofilms (Table 3; Figure 4). In planktonic cultures, the antibiotic concentrations needed to kill SBPs and WBPs were, respectively, 8–32 times and 16–32 times those required to achieve the same purpose in combination with Ch (Table 3A). In the preformed biofilms, the combination of Clx and Ch resulted in a 4-to 16-fold reduction in the amount of the antibiotic needed to kill SBPs. For WBPs, this reduction was 4-to 8-fold (Table 3B; Figure 4). Furthermore, Ch had strong antimicrobial activity on its own, regardless of bacterial growth or the intensity of the biofilm (Figure 4). It reduced the viability of SBPs by 67% in planktonic cultures and by 30% in preformed biofilms. For WBPs, the percentages were, respectively, 52 and 48% (Figures 4B,D). In summary, we found that the Clx and Ch combination has significant antimicrobial activity and improves the treatment with Clx alone. This combination could enable a significant reduction in the antibiotic concentrations required to kill bacteria in different lifestyles, regardless of the biofilm biomass intensity and the antibiotic resistance pattern in NAS isolates.

# 4. Discussion

Until effective immunoprevention strategies are made available for this pathology, antibiotics will remain the main stay of treatment. Nevertheless, their progressive loss of effectiveness due to the speed at which bacteria develop virulence factors is becoming cause for global public health concern (WHO/FAO/OIE, 2016; Aidara-Kane et al., 2018). The ingrained belief that antimicrobials improve the overall

TABLE 2 Susceptibility of SBP and WBP NAS isolates to cloxacillin in planktonic cultures and preformed biofilms.

| Isolates | Planktonic cultures | | |
|---|---|---|---|
| | P-MBC [μg/ml] | B-MBC [μg/ml] | B-MBC/P-MBC |
| A. Strong biofilms producer NAS | | | |
| SBP1 | 1 | 1,024 | 1,024 |
| SBP2 | 2 | 1,024 | 512 |
| SBP3 | 2 | 1,024 | 512 |
| SBP4 | 2 | 1,024 | 512 |
| *SBP5* | 1 | 1,024 | 1,024 |
| SBP6 | 2 | 1,024 | 512 |
| SBP7 | 4 | 512 | 128 |
| SBP8 | 1 | 1,024 | 1,024 |
| SBP9 | 1 | 256 | 256 |
| SBP10 | 1 | 256 | 256 |
| B. Weak biofilms producer NAS | | | |
| WBP1 | 2 | 32 | 16 |
| WBP2 | 1 | 16 | 16 |
| WBP3 | 2 | 16 | 8 |
| WBP4 | 2 | 32 | 16 |
| WBP5 | 2 | 16 | 8 |
| WBP6 | 1 | 16 | 16 |
| WBP7 | 2 | 32 | 16 |
| WBP8 | 2 | 16 | 8 |
| WBP9 | 2 | 32 | 16 |
| WBP10 | 2 | 16 | 8 |

A. Strong biofilms producer bacteria. B. Weak biofilms producer bacteria. Minimum bactericidal concentration of cloxacillin in planktonic cultures (P-MBC), and in preformed biofilms (B-MBC). Bactericidal ratio between preformed biofilms and planktonic cultures (B-MBC/P-MBC). The breakpoint for the minimum inhibitory concentration (MIC) of cloxacillin was taken from the CLSI guidelines for penicillinase-stable penicillins in NAS (≥0.5 μg/ml).

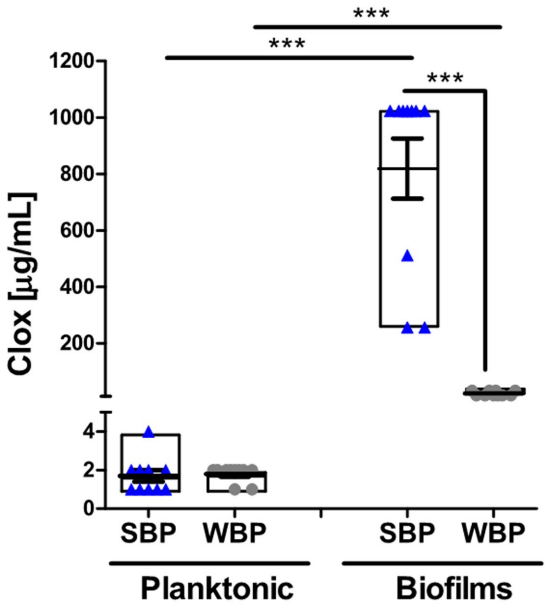


FIGURE 2
Minimum bactericidal concentration of cloxacillin for SBP and WBP NAS isolates in planktonic cultures and preformed biofilms. The bar graph shows the cloxacillin MBC in planktonic cultures and biofilms measured by a plate count assay. Data are shown as the mean of each isolate ± SEM and box plot distribution. These experiments were performed three independent times with three biological replicates of each of the 10 SBP and WBP isolates. The *p* values ***<0.001 were obtained with a Kruskal-Wallis test.

health of live stock and lead to higher yields and better quality products has triggered their overuse (Gross, 2013; Michael et al., 2014). According to official FDA and EU reports, more than the 75% of the antibiotics sold in the US and the European Union are for veterinary use [Food and Drug Administration (FDA), 2010, 2018]. In 2018 alone, more than 11,575 tons of antibiotics were administered in the US to food-producing animals; 42% of them were destined for cattle [Van Boeckel et al., 2015; Stevens et al., 2016; Food and Drug Administration (FDA), 2018].

NAS are one of the most prevalent pathogens of bovine IMIs. Although not always related to the severity of mastitis, they are usually associated with the persistence of infection and the worst antibiotic cure rates (Simojoki et al., 2012; Fry et al., 2014; Condas et al., 2017). Frequently, antibiotic therapy failures and persistent infections are not cannot be attributed to the presence of resistance genes in pathogens, which suggests that other mechanisms may play a relevant role in antibiotic cure rates (Lebeaux et al., 2014; Koo et al., 2017; Breser et al., 2018). Biofilm structures have been shown to act as protective shields against antibiotics (Hathroubi et al., 2017; Pedersen et al., 2021), and thus to favor the establishment of persistent and recurrent infections (Bjarnsholt et al., 2013; Flemming et al., 2016). NAS are more frequently capable than other mastitis-causing pathogens of producing biofilm biomass, which might therefore explain their high resistance rates (Tremblay et al., 2013; de Oliveira et al., 2016; Felipe et al., 2017; Srednik et al., 2017). Still, the influence of biofilm growth on antibiotic failure and infection chronicity and recurrence can be largely unpredictable (Flemming et al., 2016; Pedersen et al., 2021). In a murine IMI model, glands infected with a strong biofilm-forming *S. aureus* strain developed greater tissue inflammation, neutrophil recruitment, and functionality loss than those infected with a weak biofilm-forming strain (Gogoi-Tiwari et al., 2017). We found that NAS isolates from clinical BM, which were classified according to their biofilm biomass intensity, had significantly different antibiotic resistance patterns that were not species-dependent. A strong association was observed, in fact, between biofilm intensity and antibiotic resistance. Numerous other studies have determined that multiresistant bacteria isolated from different sources (burns, medical devices, chronic infections) are moderate or strong biofilm producers (Karigoudar et al., 2019; Mahmoudi et al., 2019; Folliero et al., 2021). This has not been observed for environmental bacteria of various origins (agricultural soils, surface water and sediments, plants, air, walls; Donadu et al., 2022; Sharan et al., 2023). Some authors contend that biofilm is synonymous with antibiotic resistance, because of its proficiency at transferring resistance genes and its innate phenotypic tolerance to antibiotics (Bowler et al., 2020; Trubenová et al., 2022). For this reason, new disease control strategies should focus on counteracting the protection offered by bacterial biofilms, since this could decrease resistance rates to the antimicrobials that are already in use. In this work, we found that the antimicrobial activity of the

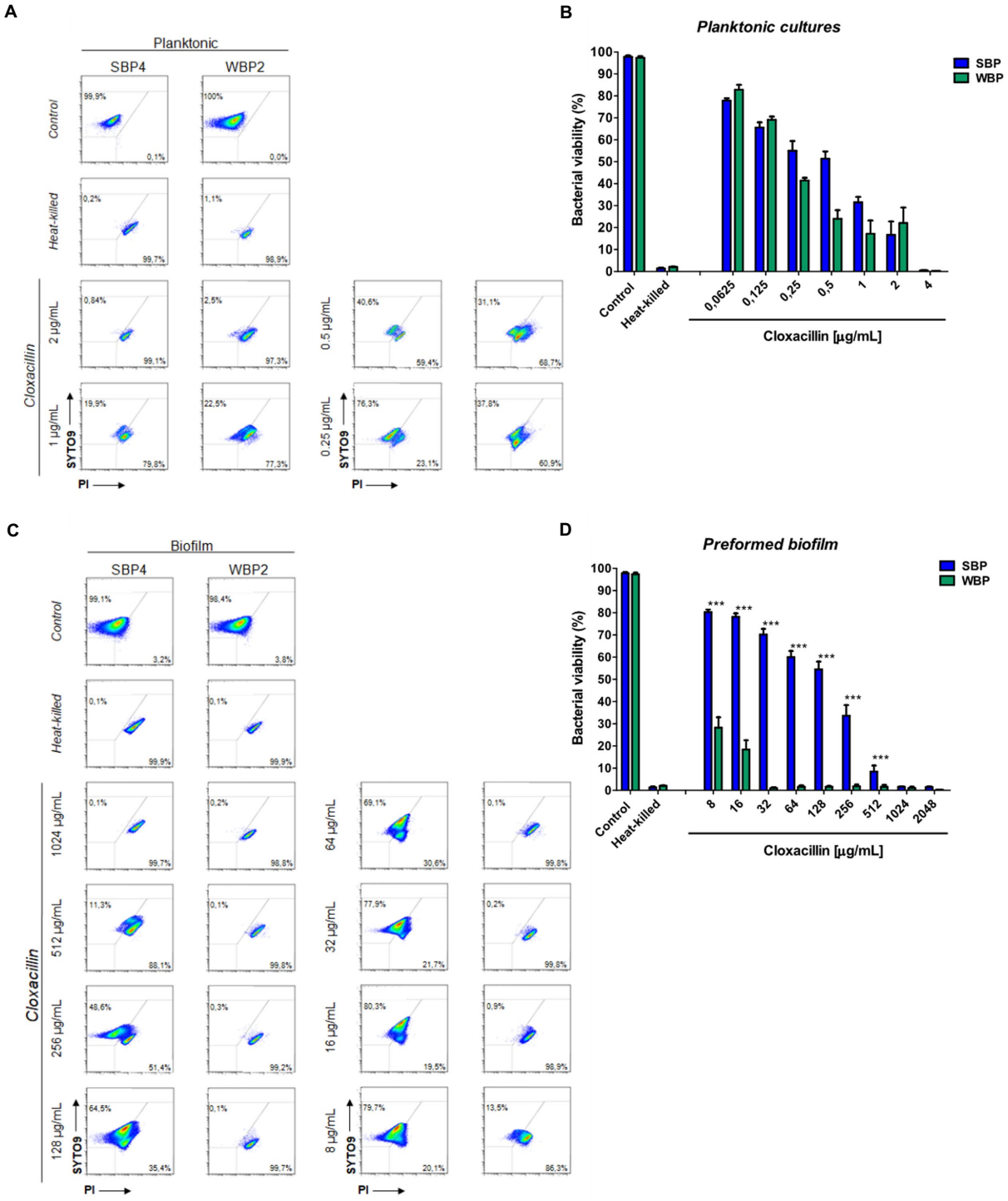


FIGURE 3
Bacterial viability of SBP and WBP NAS isolates in planktonic cultures and preformed biofilms after treatment with cloxacillin. **(A)** Bacterial viability of SBPs and WBPs in planktonic cultures grown in TSB or treated with different concentrations of cloxacillin, analyzed by flow cytometry using SYTO9 and PI dyes. **(B)** Bacterial viability percentages of SBPs and WBPs in planktonic cultures. **(C)** Bacterial viability of SBPs and WBPs in preformed biofilms grown in TSB or treated with different concentrations of cloxacillin, analyzed by flow cytometry using SYTO9 and PI dyes. **(D)** Bacterial viability percentages of SBPs and WBPs in preformed biofilms. These experiments were performed four independent times with three biological replicates of each of the 10 SBP and WBP isolates. Data were analyzed with one-way ANOVA followed by Bonferroni post-hoc, and are shown as mean±SEM. The *p* values *<0.05, **<0.01, and ***<0.001 were considered significant.

antibiotic Clx against the isolates was overall enhanced when it was combined with Ch, regardless of the bacterial lifestyle, the biofilm biomass intensity or the antibiotic resistance pattern. The data obtained suggest that the degree of protection conferred by biofilm against antibiotic treatment may depend on the intensity of its biomass, and that Ch could be useful to counteract this protection.

TABLE 3 Effect of combined chitosan and cloxacillin on SBP and WBP NAS isolates in planktonic cultures and preformed biofilms.

| Isolates | P-MBC[μg/ml] | | B-MBC[μg/ml] | |
|---|---|---|---|---|
| | Clox.+Ch. | Clox./Clox.+Ch. | Clox.+Ch. | Clox./Clox.+Ch. |
| A. Strong biofilm producer NAS | | | | |
| SBP1 | 0.0625 | 16 | 64 | 16 |
| SBP2 | 0.0625 | 32 | 64 | 16 |
| SBP3 | 0.125 | 16 | 64 | 16 |
| SBP4 | 0.0625 | 32 | 64 | 16 |
| SBP5 | 0.0625 | 16 | 64 | 16 |
| SBP6 | 0.125 | 16 | 64 | 16 |
| SBP7 | 0.125 | 32 | 64 | 8 |
| SBP8 | 0.0625 | 16 | 64 | 16 |
| SBP9 | 0.0625 | 16 | 64 | 4 |
| SBP10 | 0.125 | 8 | 64 | 4 |
| B. Weak biofilm producer NAS | | | | |
| | Planktonic cultures | | Preformed biofilms | |
| WBP1 | 0.0625 | 32 | 4 | 8 |
| WBP2 | 0.0625 | 16 | 2 | 4 |
| WBP3 | 0.0625 | 32 | 4 | 8 |
| WBP4 | 0.0625 | 32 | 4 | 8 |
| WBP5 | 0.0625 | 32 | 4 | 4 |
| WBP6 | 0.0625 | 16 | 2 | 4 |
| WBP7 | 0.0625 | 32 | 4 | 8 |
| WBP8 | 0.125 | 16 | 4 | 4 |
| WBP9 | 0.0625 | 32 | 4 | 8 |
| WBP10 | 0.125 | 16 | 4 | 4 |

A. Strong biofilms producer bacteria. B. Weak biofilms producer bacteria. Minimum bactericidal concentration of Clx + Ch in planktonic cultures (P-MBC), and in preformed biofilms (B-MBC). Bactericidal concentration ratio between Clx alone and Clx + Ch. Weak biofilm producer NAS.

The antimicrobial concentrations which are effective for bacteria growing within biofilms have been reported to be significantly higher than for bacteria in planktonic cultures (Tremblay et al., 2014; Claessens et al., 2015; Breser et al., 2018). To gain a deeper understanding of the effect of biofilms on antimicrobial resistance and therapy failure, comparative and standardized antimicrobial assays on preformed biofilms are needed. Thieme et al. (2019) reviewed different reports that explored antimicrobial effects on preformed biofilms, and noted that the results of the assays could be interpreted in many ways. Different parameters like minimum biofilm eradication concentration (MBEC) or bactericidal biofilm concentration (BBC) do not always represent the antimicrobial concentrations required to kill bacteria. In some cases, 3 Log10 bacterial reductions were described with respect to control conditions or untreated bacteria (Tremblay et al., 2013; Brady et al., 2017; Cruz et al., 2018; Thieme et al., 2019).This means that the findings of different studies might not render comparable conclusions about the influence of biofilms on therapy efficacy (Thieme et al., 2019).

However, a few studies have focused on the antibiotic concentrations required to kill bacteria in terms of the biomass of their biofilms, and in comparison with their planktonic form. We found that the Clx concentrations needed to kill strong and weak biofilm producers (SBPs and WBPs) were only similar when the bacteria were grown planktonically. In preformed biofilms, much higher concentrations were needed to kill SBPs than WBPs. The addition of Ch to the Clx treatment not only reduced the concentration of the antibiotic needed to kill bacteria in the planktonic cultures but also in the preformed biofilms, independently of the biofilm intensity and the antibiotic resistance pattern. The antimicrobial effects of Ch and its mode of action have been explored in many microorganisms including viruses, bacteria, and fungi (Muxika et al., 2017; Sahariah and Másson, 2017; Verlee et al., 2017; Matica et al., 2019; Ke et al., 2021). Its versatility makes it an ideal candidate for combination with other compounds (Matica et al., 2019; Meng et al., 2021) and for the design of micro/nano-structures (Divya et al., 2017; Sahariah and Másson, 2017; Kravanja et al., 2019; Orellano et al., 2019), and there is wide evidence of its ability to inhibit biofilm biomass and eradicate preformed biofilms (Felipe et al., 2019; Orellano et al., 2019; Khan et al., 2020). For these reasons, it has been proposed (alone or combined with different antibiotics) as an alternative to improve the cure rates of infections caused by bacterial biofilms or multiresistant bacteria (Asli et al., 2017; Breser et al., 2018; Zhang et al., 2019; Meng et al., 2021). Indeed, Asli et al. (2017) used Ch by itself or combined with tilmicosin to treat a mammary gland infected by *S. aureus* in a

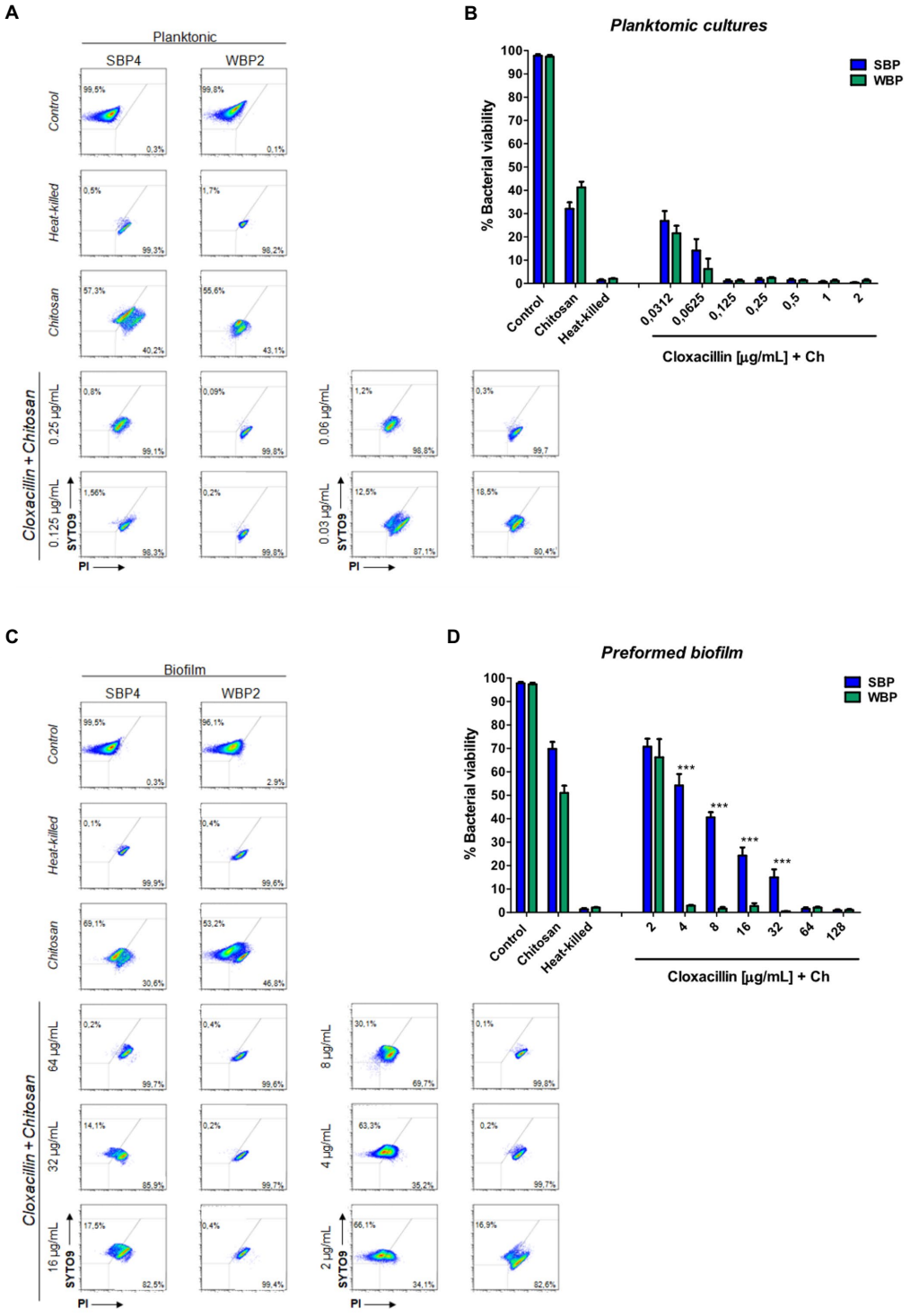


FIGURE 4
Minimum bactericidal concentration of combined chitosan and cloxacillin in SBP and WBP NAS isolates in planktonic cultures and preformed biofilms. **(A)** Bacterial viability of SBPs and WBPs in planktonic cultures grown in TSB or treated with different concentrations of cloxacillin and chitosan, analyzed by flow cytometry using SYTO9 and PI dyes. **(B)** Bacterial viability percentages of SBPs and WBPs in planktonic cultures. **(C)** Bacterial viability of SBPs and WBPs in preformed biofilms grown in TSB or treated with different concentrations of cloxacillin and chitosan, analyzed by flow cytometry using SYTO9 and PI dyes. **(D)** Bacterial viability percentages of SBPs and WBPs in preformed biofilms. These experiments were performed four independent times with three biological replicates of each of the 10 SBP and WBP isolates. Data were analyzed with one-way ANOVA followed by Bonferroni post-hoc, and are shown as mean±SEM. The *p* values *<0.05, **<0.01, and ***<0.001 were considered significant.

murine model. Both the polymer on its own and its association with the antibiotic significantly reduced bacterial colonization, and the combined treatment was significantly better at decreasing the bacterial load inside the tissue than tilmicosin by itself.

Even though further research is essential to fully comprehend the extent of the influence exerted by bacterial biofilms on antimicrobial therapies, the findings available so far suggest that combining Ch and antibiotics could be a promising alternative to minimize antibiotic concentrations while improving the cure rates of bovine IMIs (Asli et al., 2017; Breser et al., 2018). In any case, novel treatment strategies will have to contemplate the central role played by biofilm in the development and persistence of bacterial infections.

## 5. Conclusion

According to the results of this study, strong and weak biofilm-producing NAS isolates from bovine mastitis have significantly different antibiotic resistance patterns. Such patterns are not species-dependent, but rather associated to the intensity of the biofilm biomass. The minimum bactericidal concentration of cloxacillin (Clx) was similar for both groups (strong and weak producers) when they were growing planktonically. A significantly higher concentration was required to kill bacteria in preformed biofilms, and in turn, this concentration was much higher for strong producers than for weak producers. These data confirm that the antibiotic concentration needed to kill bacteria in preformed biofilms is closely related to biofilm-forming ability. On the other hand, the addition of chitosan (Ch) to the Clx treatment made it possible to significantly reduce the bactericidal concentration of the antibiotic required for the two different lifestyles, regardless of the intensity of the biofilm biomass or the antibiotic resistance pattern of each isolate. These findings shed light on the influence exerted by bacterial biofilms on antibiotic treatments and antimicrobial resistance. Moreover, they provide evidence in favor of a therapeutic strategy that can mitigate such influence, and which could therefore be explored further as an alternative treatment for intramammary infections.

## Data availability statement

The raw data supporting the conclusions of this article will be made available by the authors, without undue reservation.

## Author contributions

MB and LT designed and carried out the experiments and interpreted the data. IB, LB, and PI discussed the experiments and results. MB, IB, and CP participated in design and discussion, and supervised the final draft of the manuscript. All authors contributed to the article and approved the submitted version.

## Funding

This work was supported by grants from the Argentinian Agency for the Promotion of Science and Technology (ANPCyT) (PICT 2016-1024 and PICT 2017-0822) and the National University of Villa Maria.

## Acknowledgments

We thank Paola Traversa, Mariana Bonaterra, and Virginia Angiolini for their excellent technical assistance.

## Conflict of interest

The authors declare that the research was conducted in the absence of any commercial or financial relationships that could be construed as potential conflicts of interest.

## Publisher's note

All claims expressed in this article are solely those of the authors and do not necessarily represent those of their affiliated organizations, or those of the publisher, the editors and the reviewers. Any product that may be evaluated in this article, or claim that may be made by its manufacturer, is not guaranteed or endorsed by the publisher.

## Supplementary material

The Supplementary material for this article can be found online at: https://www.frontiersin.org/articles/10.3389/fmicb.2023.1167693/full#supplementary-material

## References

Aghamohammadi, M., Haine, D., Kelton, D. F., Barkema, H. W., Hogeveen, H., Keefe, G. P., et al. (2018). Herd-level mastitis-associated costs on Canadian dairy farms. *Front. Vet. Sci.* 5:100. doi: 10.3389/fvets.2018.00100

Aidara-Kane, A., Angulo, F. J., Conly, J. M., Minato, Y., Silbergeld, E. K., McEwen, S. A., Collignon, P. J., and WHO Guideline Development Group. (2018). World Health Organization (WHO) guidelines on use of medically important antimicrobials in food-producing animals. *Antimicrob. Resist. Infect. Control.* 7:7. doi: 10.1186/s13756-017-0294-9

Asli, A., Brouillette, E., Ster, C., Ghinet, M. G., Brzezinski, R., Lacasse, P., et al. (2017). Antibiofilm and antibacterial effects of specific chitosan molecules on Staphylococcus aureus isolates associated with bovine mastitis. *PLoS One* 12:e0176988. doi: 10.1371/journal.pone.0176988

Bal, E. B., Bayar, S., and Bal, M. A. (2010). Antimicrobial susceptibilities of coagulase-negative staphylococci (CNS) and streptococci from bovine subclinical mastitis cases. *J. Microbiol.* 48, 267–274. doi: 10.1007/s12275-010-9373-9

Bjarnsholt, T., Alhede, M., Alhede, M., Eickhardt-Sørensen, S. R., Moser, C., Kühl, M., et al. (2013). The in vivo biofilm. *Trends Microbial* 21, 466–474. doi: 10.1016/j.tim.2013.06.002

Bowler, P., Murphy, C., and Wolcott, R. (2020). Biofilm exacerbates antibiotic resistance: is this a current oversight in antimicrobial stewardship? *Antimicrob. Resist. Infect. Control* 9:162. doi: 10.1186/s13756-020-00830-6

Brady, A. J., Laverty, G., Gilpin, D. F., Kearney, P., and Tunney, M. (2017). Antibiotic susceptibility of planktonic- and biofilm-grown staphylococci isolated from implant-associated infections: should MBEC and nature of biofilm formation replace MIC? *J. Med. Microbiol.* 66, 461–469. doi: 10.1099/jmm.0.000466

Breser, M. L., Felipe, V., Bohl, L. P., Orellano, M. S., Isaac, P., Conesa, A., et al. (2018). Chitosan and cloxacillin combination improve antibiotic efficacy against different lifestyle of coagulase-negative staphylococcus isolates from chronic bovine mastitis. *Sci. Rep.* 23;8, 8:5081. doi: 10.1038/s41598-018-23521-0

Chantziaras, I., Boyen, F., Callens, B., and Dewulf, J. (2014). Correlation between veterinary antimicrobial use and antimicrobial resistance in food-producing animals: a report on seven countries. *J. Antimicrob. Chemother.* 69, 827–834. doi: 10.1093/jac/dkt443

Claessens, J., Roriz, M., Merckx, R., Baatsen, P., Van Mellaert, L., and Van Eldere, J. (2015). Inefficacy of vancomycin and teicoplanin in eradicating and killing Staphylococcus epidermidis biofilms in vitro. *Int. J. Antimicrob. Agents* 45, 368–375. doi: 10.1016/j.ijantimicag.2014.11.011

Clinical and Laboratory Standards Institute (CLSI) (2020). *Performance standards for antimicrobial susceptibility testing, CLSI M100, edition 30*. Clinical and Laboratory Standards Institute, Wayne, PA.

Condas, L. A. Z., De Buck, J., Nobrega, D. B., Carson, D. A., Naushad, S., De Vliegher, S., et al. (2017). Prevalence of non-aureus staphylococci species causing intramammary infections in Canadian dairy herds. *J. Dairy Sci.* 100, 5592–5612. doi: 10.3168/jds.2016-12478

Cruz, C. D., Shah, S., and Tammela, P. (2018). Defining conditions for biofilm inhibition and eradication assays for Gram-positive clinical reference strains. *BMC Microbiol.* 18:173. doi: 10.1186/s12866-018-1321-6

De Jong, A., Garch, F. E., Simjee, S., Moyaert, H., Rose, M., Youala, M., et al. (2018). Monitoring of antimicrobial susceptibility of udder pathogens recovered from cases of clinical mastitis in dairy cows across Europe: VetPath results. *Vet. Microbiol.* 213, 73–81. doi: 10.1016/j.vetmic.2017.11.021VetPath Study Group

de Oliveira, A., Cataneli Pereira, V., Pinheiro, L., Moraes Riboli, D. F., Benini Martins, K., Ribeiro De Souza Da Cunha, M., et al. (2016). Antimicrobial resistance profile of planktonic and biofilm cells of Staphylococcus aureus and coagulase-negative staphylococci. *Int. J. Mol. Sci.*. 1 17:1423. doi: 10.3390/ijms17091423

De Visscher, A., Piepers, S., Haesebrouck, F., and De Vliegher, S. (2016). Intramammary infection with coagulase-negative staphylococci at parturition: Species-specific prevalence, risk factors, and effect on udder health. *J. Dairy Sci.* 99, 6457–6469. doi: 10.3168/jds.2015-10458

Divya, K., Vijayan, S., George, T. K., and Jisha, M. S. (2017). Antimicrobial properties of chitosan nanoparticles: mode of action and factors affecting activity. *Fibers Polym.* 18, 221–230. doi: 10.1007/s12221-017-6690-1

Donadu, M. G., Ferrari, M., Mazzarello, V., Zanetti, S., Kushkevych, I., Rittmann, S. K. R., et al. (2022). No correlation between biofilm-forming capacity and antibiotic resistance in environmental *Staphylococcus* spp.: in vitro results. *Pathogens* 11:471. doi: 10.3390/pathogens11040471

Dorneles, E. M. S., Fonseca, M. D. A. M., Abreu, J. A. P., Lage, A. P., Brito, M. A. V. P., Pereira, C. R., et al. (2019). Genetic diversity and antimicrobial resistance in Staphylococcus aureus and coagulase-negative *Staphylococcus* isolates from bovine mastitis in Minas Gerais, Brazil. *Microbiologyopen* 8:e00736. doi: 10.1002/mbo3.736

Felipe, V., Breser, M. L., Bohl, L. P., Rodrigues da Silva, E., Morgante, C. A., Correa, S. G., et al. (2019). Chitosan disrupts biofilm formation and promotes biofilm eradication in *Staphylococcus* species isolated from bovine mastitis. *Int. J. Biol. Macromol.* 126, 60–67. doi: 10.1016/j.ijbiomac.2018.12.159

Felipe, V., Morgante, C. A., Somale, P. S., Varroni, F., Zingaretti, M. L., Bachetti, R. A., et al. (2017). Evaluation of the biofilm forming ability and its associated genes in *Staphylococcus* species isolates from bovine mastitis in Argentinean dairy farms. *Microb. Pathog.* 104, 278–286. doi: 10.1016/j.micpath.2017.01.047

Flemming, H. C., Wingender, J., Szewzyk, U., Steinberg, P., Rice, S. A., and Kjelleberg, S. (2016). Biofilms: an emergent form of bacterial life. *Nat. Rev. Microbiol.*. 11 14, 563–575. doi: 10.1038/nrmicro.2016.94

Folliero, V., Franci, G., Dell'Annunziata, F., Giugliano, R., Foglia, F., Sperlongano, R., et al. (2021). Evaluation of antibiotic resistance and biofilm production among clinical strain isolated from medical devices. *Int. J. Microbiol.* 2021, 9033278–9033211. doi: 10.1155/2021/9033278

Food and Drug Administration (FDA) (2010). CVM updates - CVM reports on antimicrobials sold or distributed for food-producing animals. Available at: https://www.fda.gov/media/79581/download

Food and Drug Administration (FDA) (2018), Antimicrobials sold or distributed for use in food-producing Animals. Available at: https://www.fda.gov/media/133411/download#:~:text=Of%20the%202018%20domestic%20sales,fluoroquinolones%20for%20less%20than%201

Fry, P. R., Middleton, J. R., Dufour, S., Perry, J., Scholl, D., and Dohoo, I. (2014). Association of coagulase-negative staphylococcal species, mammary quarter milk somatic cell count, and persistence of intramammary infection in dairy cattle. *J. Dairy Sci.* 97, 4876–4885. doi: 10.3168/jds.2013-7657

Gogoi-Tiwari, J., Williams, V., Waryah, C. B., Costantino, P., Al-Salami, H., Mathavan, S., et al. (2017). Mammary gland pathology subsequent to acute infection with strong versus weak biofilm forming *Staphylococcus aureus* bovine mastitis isolates: a pilot study using non-invasive mouse mastitis model. *PLoS One* 12:e0170668. doi: 10.1371/journal.pone.0170668

Gross, M. (2013). Antibiotics in crisis. *Curr. Biol.* 23, R1063–R1065. doi: 10.1016/j.cub.2013.11.057

Hathroubi, S., Mekni, M. A., Domenico, P., Nguyen, D., and Jacques, M. (2017). Biofilms: microbial shelters against antibiotics. *Microb. Drug Resist.* 23, 147–156. doi: 10.1089/mdr.2016.0087

Heikkilä, A. M., Liski, E., Pyörälä, S., and Taponen, S. (2018). Pathogen-specific production losses in bovine mastitis. *J. Dairy Sci.* 101, 9493–9504. doi: 10.3168/jds.2018-14824

Hogan, J.S., Harmon, R.J., González, R.N., Nickerson, S.C., Oliver, S.P., Pankey, J. W., et al. (1999). *Laboratory handbook on bovine mastitis*. National Mastitis Council (NMC). Madison, WI. Pg. 222.

Hogeveen, H., Huijps, K., and Lam, T. (2011). Economic aspects of mastitis: new developments. *N. Z. Vet. J.* 59, 16–23. doi: 10.1080/00480169.2011.547165

Karigoudar, R. M., Karigoudar, M. H., Wavare, S. M., and Mangalgi, S. S. (2019). Detection of biofilm among uropathogenic Escherichia coli and its correlation with antibiotic resistance pattern. *J. Lab. Phys.* 11, 017–022. doi: 10.4103/JLP.JLP_98_18

Ke, C.-L., Fu-Sheng, D., Chih-Yu, C., and Ching-Hsuan, L. (2021). Antimicrobial actions and applications of chitosan. *Polymers* 6:904. doi: 10.3390/polym13060904

Khan, F., Pham, D. T. N., Oloketuyi, S. F., Manivasagan, P., Oh, J., and Kim, Y. M. (2020). Chitosan and their derivatives: Antibiofilm drugs against pathogenic bacteria. *Colloids Surf. B: Biointerfaces* 185:110627. doi: 10.1016/j.colsurfb.2019.11062

Kim, S.-J., Moon, D. C., Park, S.-C., Kang, H. Y., Na, S. H., and Lim, S. K. (2019). Antimicrobial resistance and genetic characterization of coagulase-negative staphylococci from bovine mastitis milk samples in Korea. *J. Dairy Sci.* 102, 11439–11448. doi: 10.3168/jds.2019-17028

Koo, H., Allan, R. N., Howlin, R. P., Stoodley, P., and Hall-Stoodley, L. (2017). Targeting microbial biofilms: current and prospective therapeutic strategies. *Nat. Rev. Microbiol.* 15, 740–755. doi: 10.1038/nrmicro.2017.99

Kravanja, G., Primožič, M., Knez, Ž., and Leitgeb, M. (2019). Chitosan-based (Nano) materials for novel biomedical applications. *Molecules* 24:1960. doi: 10.3390/molecules24101960

Lebeaux, D., Ghigo, J.-M., and Beloin, C. (2014). Biofilm-related infections: bridging the gap between clinical management and fundamental aspects of recalcitrance toward antibiotics. *Microbiol. Mol. Biol. Rev.* 78, 510–543. doi: 10.1128/MMBR.00013-14

Lhermie, G., Gröhn, Y. T., and Raboisson, D. (2017). Addressing antimicrobial resistance: an overview of priority actions to prevent suboptimal antimicrobial use in food-animal production. *Front. Microbiol.* 7:2114. doi: 10.3389/fmicb.2016.02114

Li, L., Yang, H. J., Cheng Liu, D., He, H. B., Wang, C. F., Zhong, J. F., et al. (2012). Analysis of biofilms formation and associated genes detection in staphylococcus isolates from bovine mastitis. *Int. J. Appl Res. Vet. Med* 10:62. doi: 10.5897/AJB11.081

Lipkens, Z., Piepers, S., Verbeke, J., and De Vliegher, S. (2019). Infection dynamics across the dry period using dairy herd improvement somatic cell count data and its effect on cow performance in the subsequent lactation. *J. Dairy Sci.* 102, 640–651. doi: 10.3168/jds.2018-15130

Mahmoudi, H., Pourhajibagher, M., Chiniforush, N., Soltanian, A. R., Alikhani, M. Y., and Bahador, A. (2019). Biofilm formation and antibiotic resistance in meticillin-resistant and meticillin-sensitive Staphylococcus aureus isolated from burns. *J. Wound Care* 28, 66–73. doi: 10.12968/jowc.2019.28.2.66

Matica, M. A., Aachmann, F. L., Tøndervik, A., Sletta, H., and Ostafe, V. (2019). Chitosan as a wound dressing starting material: antimicrobial properties and mode of action. *Int. J. Mol. Sci.* 20:5889. doi: 10.3390/ijms20235889

Meng, Q., Sun, Y., Cong, H., Hu, H., and Xu, F. J. (2021). An overview of chitosan and its application in infectious diseases. *Drug Deliv. Transl. Res.* 11, 1340–1351. doi: 10.1007/s13346-021-00913-w

Michael, C. A., Dominey-Howes, D., and Labbate, M. (2014). The antimicrobial resistance crisis: causes, consequences, and management. *Front. Public Health* 2:145. doi: 10.3389/fpubh.2014.00145

Muxika, A., Etxabide, A., Uranga, J., Guerrero, P., and de la Caba, K. (2017). Chitosan as a bioactive polymer: processing, properties and applications. *Int. J. Biol. Macromol.* 105, 1358–1368. doi: 10.1016/j.ijbiomac.2017.07.087

Oniciuc, E. A., Cerca, N., and Nicolau, A. I. (2016). Compositional analysis of biofilms formed by *Staphylococcus aureus* isolated from food sources. *Front. Microbiol.* 30, 7:390. doi: 10.3389/fmicb.2016.00390

Orellano, M. S., Isaac, P., Breser, M. L., Bohl, L. P., Conesa, A., Falcone, R. D., et al. (2019). Chitosan nanoparticles enhance the antibacterial activity of the native polymer against bovine mastitis pathogens. *Carbohydr. Polym.* 213, 1–9. doi: 10.1016/j.carbpol.2019.02.016

Pedersen, R. R., Krömker, V., Bjarnsholt, T., Dahl-Pedersen, K., Buhl, R., and Jørgensen, E. (2021). Biofilm research in bovine mastitis. *Front. Vet. Sci.* 8:656810. doi: 10.3389/fvets.2021.656810

R Core Team (2020). R: A language and environment for statistical computing. R Foundation for Statistical Computing, Vienna, Austria. Available at: http://mirror.fcaglp.unlp.edu.ar/CRAN/

Rabiee, A. R., and Lean, I. J. (2013). The effect of internal teat sealant products (Teatseal and Orbeseal) on intramammary infection, clinical mastitis, and somatic cell counts in lactating dairy cows: a meta-analysis. *J. Dairy Sci.* 96, 6915–6931. doi: 10.3168/jds.2013-6544

Sahariah, P., and Másson, M. (2017). Antimicrobial chitosan and chitosan derivatives: a review of the structure–activity relationship. *Biomacromolecules* 18, 3846–3868. doi: 10.1021/acs.biomac.7b01058

Sampimon, O., Lam, T., Mevius, D., Schukken, Y., and Zadoks, R. (2011). Antimicrobial susceptibility of coagulase-negative staphylococci isolated from bovine milk samples. *Vet. Microbiol.* 150, 173–179. doi: 10.1016/j.vetmic.2011.01.017

Sharan, M., Dhaka, P., Bedi, J. S., Singh, R., and Mehta, N. (2023). Characterization of chicken eggs associated Escherichia coli and Staphylococcus aureus for biofilm production and antimicrobial resistance traits. *Anim. Biotechnol.*, 1–12. doi: 10.1080/10495398.2023.2171423

Simojoki, H., Hyvönen, P., Plumed Ferrer, C., Taponen, S., and Pyörälä, S. (2012). Is the biofilm formation and slime producing ability of coagulase-negative staphylococci associated with the persistence and severity of intramammary infection? *Vet. Microbiol.* 158, 344–352. doi: 10.1016/j.vetmic.2012.02.031

Srednik, M. E., Tremblay, Y. D. N., Labrie, J., Archambault, M., Jacques, M., Fernández Cirelli, A., et al. (2017). Biofilm formation and antimicrobial resistance genes of coagulase-negative staphylococci isolated from cows with mastitis in Argentina. *FEMS Microbiol. Lett.* 364. doi: 10.1093/femsle/fnx001

Ster, C., Lebeau, V., Leclerc, J., Fugère, A., Veh, K. A., Roy, J. P., et al. (2017). In vitro antibiotic susceptibility and biofilm production of Staphylococcus aureus isolates recovered from bovine intramammary infections that persisted or not following extended therapies with cephapirin, pirlimycin or ceftiofur. *Vet. Res.* 21, 48:56. doi: 10.1186/s13567-017-0463-0

Stevens, M., Piepers, S., Supré, K., Dewulf, J., and De Vliegher, S. (2016). Quantification of antimicrobial consumption in adult cattle on dairy herds in Flanders, Belgium, and associations with udder health, milk quality, and production performance. *J Dairy Sci.* 99, 2118–2130. doi: 10.3168/jds.2015-10199

Supré, K., Haesebrouck, F., Zadoks, R. N., Vaneechoutte, M., Piepers, S., and De Vliegher, S. (2011). Some coagulase-negative staphylococcus species affect udder health more than others. *J. Dairy Sci.* 94, 2329–2340. doi: 10.3168/jds.2010-3741

Taponen, S., Liski, E., Heikkilä, A. M., and Pyörälä, S. (2017). Factors associated with intramammary infection in dairy cows caused by coagulase-negative staphylococci, Staphylococcus aureus, *Streptococcus uberis*, *Streptococcus dysgalactiae*, *Corynebacterium bovis*, or *Escherichia coli*. *J. Dairy Sci.* 100, 493–503. doi: 10.3168/jds.2016-11465

Thieme, L., Hartung, A., Tramm, K., Klinger-Strobel, M., Jandt, K. D., Makarewicz, O., et al. (2019). MBEC versus MBIC: the lack of differentiation between biofilm reducing and inhibitory effects as a current problem in biofilm methodology. *Biol. Proced.* 18, 21–18. doi: 10.1186/s12575-019-0106-0

Tremblay, Y. D. N., Caron, V., Blondeau, A., Messier, S., and Jacques, M. (2014). Biofilm formation by coagulase-negative staphylococci: impact on the efficacy of antimicrobials and disinfectants commonly used on dairy farms. *Vet. Microbiol.* 172, 511–518. doi: 10.1016/j.vetmic.2014.06.007

Tremblay, Y. D. N., Lamarche, D., Chever, P., Haine, D., Messier, S., and Jacques, M. (2013). Characterization of the ability of coagulase-negative staphylococci isolated from the milk of Canadian farms to form biofilms. *J. Dairy Sci.* 96, 234–246. doi: 10.3168/jds.2012-5795

Trubenová, B., Roizman, D., Moter, A., Rolff, J., and Regoes, R. R. (2022). Population genetics, biofilm recalcitrance, and antibiotic resistance evolution. *Trends Microbiol.* 30, 841–852. doi: 10.1016/j.tim.2022.02.005

Van Boeckel, T. P., Brower, C., Gilbert, M., Grenfell, B. T., Levin, S. A., Robinson, T. P., et al. (2015). Global trends in antimicrobial use in food animals. *Proc. Natl. Acad. Sci. U. S. A.* 112, 5649–5654. doi: 10.1073/pnas.1503141112

Van Boeckel, T. P., Pires, J., Silvester, R., Zhao, C., Song, J., Criscuolo, N. G., et al. (2019). Global trends in antimicrobial resistance in animals in low- and middle-income countries. *Science* 20;365:eaaw1944. doi: 10.1126/science.aaw1944

Verlee, A., Mincke, S., and Stevens, C. V. (2017). Recent developments in antibacterial and antifungal chitosan and its derivatives. *Carbohydr. Polym.* 164, 268–283. doi: 10.1016/j.carbpol.2017.02.001

Vissio, C., Agüero, D. A., Raspanti, C. G., Odierno, L. M., and Larriestra, A. J. (2015). Productive and economic daily losses due to mastitis and its control expenditures in dairy farms in Córdoba, Argentina. *Arch. Med. Vet.* 47, 7–14. doi: 10.4067/S0301-732X2015000100003

WHO/FAO/OIE (2016). Antimicrobial resistance: a manual for developing national action plans. Available at: https://apps.who.int/iris/bitstream/handle/10665/204470/9789241549530_eng.pdf?sequence=1&isAllowed=y

Zhang, R., Li, Y., Zhou, M., Wang, C., Feng, P., Miao, W., et al. (2019). Photodynamic chitosan Nano-assembly as a potent alternative candidate for combating antibiotic-resistant bacteria. *ACS Appl. Mater. Interfaces* 11, 26711–26721. doi: 10.1021/acsami.9b09020

Zhang, Y. Q., Ren, S. X., Li, H. L., Wang, Y. X., Fu, G., Yang, J., et al. (2003). Genome-based analysis of virulence genes in a non-biofilm-forming *Staphylococcus epidermidis* strain (ATCC 12228). *Mol. Microbiol.* 49, 1577–1593. doi: 10.1046/j.1365-2958.2003.03671.x

frontiers | Frontiers in Microbiology

TYPE Original Research
PUBLISHED 26 April 2023
DOI 10.3389/fmicb.2023.1155956



OPEN ACCESS

EDITED BY
Tao Li,
Chinese Academy of Agricultural Sciences, China

REVIEWED BY
Rachelle E. Beattie,
United States Geological Survey, United States
Milena Dropa,
University of São Paulo, Brazil

*CORRESPONDENCE
Dominic Frigon
✉ dominic.frigon@mcgill.ca

RECEIVED 01 February 2023
ACCEPTED 03 April 2023
PUBLISHED 26 April 2023

CITATION
Gibson C, Kraemer SA, Klimova N, Guo B and Frigon D (2023) Antibiotic resistance gene sequencing is necessary to reveal the complex dynamics of immigration from sewers to activated sludge.
*Front. Microbiol.* 14:1155956.
doi: 10.3389/fmicb.2023.1155956



# Antibiotic resistance gene sequencing is necessary to reveal the complex dynamics of immigration from sewers to activated sludge

Claire Gibson[1], Susanne A. Kraemer[1,2], Natalia Klimova[1], Bing Guo[3] and Dominic Frigon[1]*

[1]Department of Civil Engineering and Applied Mechanics, McGill University, Montreal, QC, Canada, [2]Aquatic Contaminants Research Division, Environment and Climate Change Canada, Montreal, QC, Canada, [3]Department of Civil and Environmental Engineering, Centre for Environmental Health and Engineering, University of Surrey, Surrey, United Kingdom

Microbial community composition has increasingly emerged as a key determinant of antibiotic resistance gene (ARG) content. However, in activated sludge wastewater treatment plants (AS-WWTPs), a comprehensive understanding of the microbial community assembly process and its impact on the persistence of antimicrobial resistance (AMR) remains elusive. An important part of this process is the immigration dynamics (or community coalescence) between the influent and activated sludge. While the influent wastewater contains a plethora of ARGs, the persistence of a given ARG depends initially on the immigration success of the carrying population, and the possible horizontal transfer to indigenously resident populations of the WWTP. The current study utilized controlled manipulative experiments that decoupled the influent wastewater composition from the influent microbial populations to reveal the fundamental mechanisms involved in ARG immigration between sewers and AS-WWTP. A novel multiplexed amplicon sequencing approach was used to track different ARG sequence variants across the immigration interface, and droplet digital PCR was used to quantify the impact of immigration on the abundance of the targeted ARGs. Immigration caused an increase in the abundance of over 70 % of the quantified ARGs. However, monitoring of ARG amplicon sequence variants (ARG-ASVs) at the immigration interface revealed various immigration patterns such as (i) suppression of the indigenous mixed liquor ARG-ASV by the immigrant, or conversely (ii) complete immigration failure of the influent ARG-ASV. These immigration profiles are reported for the first time here and highlight the crucial information that can be gained using our novel multiplex amplicon sequencing techniques. Future studies aiming to reduce AMR in WWTPs should consider the impact of influent immigration in process optimisation and design.

KEYWORDS

**immigration, community coalescence, antimicrobial resistance, wastewater, activated sludge, community assembly**

# 1. Introduction

Antimicrobial resistance (AMR) is recognized as one of the greatest threats to public health worldwide (Abadii et al., 2019). Each year 700,000 deaths are attributed to AMR and without action this number is predicted to rise to 10 million by 2050 (O'Neill, 2014). The United Nations Environment Assembly (UNEA-3) have recognized the importance of the environment in the development, spread and transmission of AMR to humans and animals (United Nations Environment Programme, 2022). Of particular interest are wastewater treatment plants (WWTPs), which have been identified as hotspots of AMR (Rizzo et al., 2013) and gateways to the environmental spread. Although a reduction in the load is observed, the wastewater treatment process does not effectively remove all phylogenetically mobile antibiotic resistance genes (ARGs) and resistant bacteria (ARB) before release into the environment (Lapara et al., 2011). Consequently, effluent wastewater has been shown to contribute to antibiotic resistance in surface waters and sediments downstream of effluent discharge points (Quintela-Baluja et al., 2019; Reichert et al., 2021). ARGs are also disseminated in the waste biosolids produced during the treatment process (Munir et al., 2011; Gao et al., 2012), which are often applied to agricultural land as fertilizers which creates another route of AMR dissemination. To minimize the spread of AMR, wastewater treatment plant design requires urgent optimization for the removal of ARB and ARGs.

With increasing knowledge of emerging contaminants in wastewater and the benefits of water resource recovery, the need for new wastewater treatment technologies is widely recognized. In this context, studies have aimed to minimize ARG release into the environment with novel design. However, results are often variable. For example, some studies of anoxic-aerobic membrane bioreactor observed a reduction in the abundance of ARGs (Le et al., 2018; Zhu et al., 2018), whilst others found the abundance of genes such as *tet*C to increase (Xia et al., 2012). The use of ozonation to reduce ARG loads resulted in removal efficiencies which varied between ARG classes (Staley et al., 2019). Similarly, some found chlorination to cause large reductions in the abundance of ARGs (Zhang et al., 2019) and increases in the abundance of cell free ARGs (Liu et al., 2018), whilst others reported no impact on genes such as *bla*TEM-1 (Pang et al., 2016). These contradictory results exemplify our lack of understanding of the drivers in the persistence and proliferation of ARBs and ARGs in WWTPs, which remains one of the greatest hurdles in developing appropriate treatment strategies to reduce AMR.

Influent wastewater contains a plethora of ARB which harbor several ARGs with specific amplicon sequence variants (ASVs) often associated with the genetic context of the gene (Gibson et al., 2023b). Each ARG variant is likely to obey different elimination or persistence mechanisms following their immigration into the biological treatment process from the sewer. The characterization of these mechanisms, however, requires the identification and quantification of ARG amplicon sequence variants across the influent and activated sludge (AS-WWTP) interface with high resolutions and sensitivity (Smith et al., 2022; Gibson et al., 2023b). Although quantitative PCR is sensitive, it is uninformative with regards to ARG sequence variants. Conversely, metagenomic shotgun sequencing can provide information on the genetic context of the most abundant variants, but it has limited capabilities in the identification of variants occurring in low abundance, and is less sensitive than qPCR for ARG detection (Bharti and Grimm, 2021). In environmental samples such as soil and activated sludge, metagenomic sequencing depth is insufficient to represent all diversity within these complex communities (Zaheer et al., 2018; Jankowski et al., 2022). Numerous studies have used data on ARG occurrence in the influent and activated sludge to infer the origin of AMR. However, more recent studies demonstrate that ARGs can vary at the sequence level based upon their origin (Zhang et al., 2021). The development of specific approaches to address this knowledge gap is the main goal of the current study.

The fate of immigrating ARB and ARGs is related to the complex ecological dynamics occurring at the interface between the influent and AS-WWTP. Firstly, the persistence of a given ARG depends on the immigration and success of its carrying population in the downstream community (Gibson et al., 2023a). Some ARGs may persist because the carrying population is already an indigenous resident of the AS-WWTP community. In this case, the ARG may not even be present in the influent community. Secondly, the persistence of a given ARG may also be impacted by its phylogenetic mobility. Horizontal gene transfer has been demonstrated to play a pivotal role in the spread of ARG across species (Von Wintersdorff et al., 2016). Although a given ARB may be unsuccessful in the AS-WWTP community, processes such as conjugation, transformation and transduction enable the movement of ARGs and increase the likelihood of ARG persistence by transferring to other, better adapted, hosts. For example, conjugative plasmids have been shown to play a significant role in facilitating the persistence of multidrug resistant ARB in WWTPs (Che et al., 2019). To determine the contributions of these mechanisms, ARG amplicon sequence variants (ARG-ASVs) need to be tracked across the immigration interface between the influent wastewater and the activated sludge. The current study employed a novel multiplex amplicon sequencing approach (Smith et al., 2022; Gibson et al., 2023b) to study ARG amplicon sequence variant dynamics with the required sensitivity and resolution. Such a technique will likely provide valuable insights into the contradictory results on the persistence of ARGs.

The compounded impact of complex immigration dynamics, community composition drifts and horizontal gene transfers on the fate of ARGs are better studied in highly controlled and replicated reactor experiments. In full-scale WWTP, the influent substrate compositions, bacterial population, and ARGs vary on a daily basis (Guo et al., 2019; Sun et al., 2021). These variations, even when small, limit our ability to accurately assess the exact mechanisms behind influent immigration and AMR in AS-WWTPs. Therefore, this study utilized triplicated lab-scale reactors fed with a synthetic wastewater, which allowed for a high level of control on the immigration process and the possibility of reproducing similar conditions in subsequent manipulative experiments. Among the operated reactors, the only varying factor was immigration, which was simulated by the addition of naturally occurring microbial communities (i.e., suspended solids) harvested in municipal wastewaters to the synthetic wastewater.

The ARG analyses presented here expand upon previous observations on the population dynamics and community assembly

obtained with the same experimental set-up and published previously (Gibson et al., 2023a). Droplet digital PCR was used to quantify the variation in abundance of the ARGs across the immigration interface. Due to influent wastewater containing ARGs originating from several sources [e.g., clinical waste, sewer biofilms, and agricultural runoff (Guo et al., 2019; Qin et al., 2020)], it was hypothesized that ARG-ASVs from the influent wastewater would be different than the ones occurring endogenously in the activate sludge. Thus, multiplex amplicon sequencing was used for ARG source tracking.

## 2. Materials and methods

### 2.1. Samples

Samples for analysis were collected from reactors previously operated as described by Gibson et al. (2023a). Briefly, small scale activated sludge (AS) reactors were inoculated with mixed liquor taken from three full scale AS-WWTPs (**Figure 1**: Block A-La Prairie AS, Block B-Cowansville AS, and Block C-Pincourt AS). Reactors were operated with a hydraulic retention time of 1.8 days and a solid retention time of 5 days, and fed with a synthetic wastewater (Syntho; Boeije et al., 1999). A synthetic wastewater was utilized to ensure a stable wastewater composition was maintained over time, this could not be achieved using wastewater obtained from a full-scale WWTP which is impacted by numerous factors. Synthetic wastewater (Syntho) was produced in the laboratory using the recipe developed by Boeije et al. (1999) and autoclaved at 121°C and 5 PSI for 30 min to sterilize. The main carbon sources within Syntho were sodium acetate, starch, glycerol, and milk powder. During Phase 1 of reactor operation, all reactors received Syntho only to ensure that a stable community was formed and any existing immigrants were removed. In Phase 2, to investigate the impact of immigration, in one third of the reactors the synthetic wastewater was supplemented with influent solids (i.e., an influent wastewater community) taken from a full-scale AS-WWTP. Two control groups were also included, the first was a substrate control, that received Syntho supplemented with sterile influent solids (autoclaved at 121°C, 15 psi for 30 min). The final nine reactors received Syntho only to act as a continuity control. Finally, during Phase 3 of reactor operation, influent solids were removed from the feeds to determine if the impact of immigration was maintained over time.

This experiment was repeated with the use of three different sources of influent wastewater community. It was observed that the impact of immigration was similar in each set of reactors, thus only one set of reactors was selected for ARG analysis (27 reactors). The chosen reactors received influent solids from Cowansville AS-WWTP (Set B; Gibson et al., 2023a). For ARG analysis, samples from each Block (with the same inoculum; Block A-La Prairie AS, Block B-Cowansville AS and Block C-Pincourt AS), receiving the same feed were pooled (three biological replicates pooled). A total of 12 samples collected during Phase 2 of reactor operation were analyzed: three groups with immigration, three groups with sterilized influent solids, three with synthetic wastewater only, and three influent wastewater samples as shown in **Figure 1**.

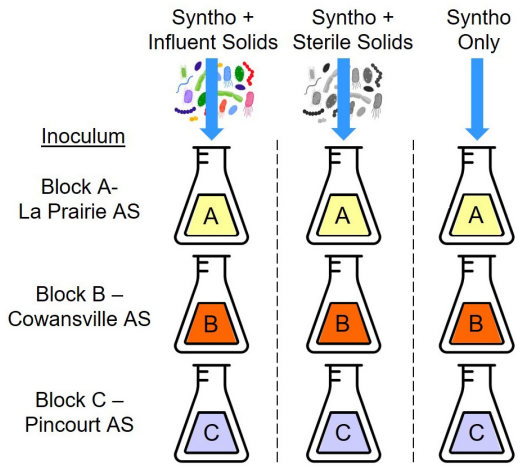


FIGURE 1
One set of reactors which received one source of influent solids (27 reactors). Reactors were inoculated with three different activated sludge communities (Block A-C). One third of the reactors received synthetic wastewater (Syntho) supplemented with influent solid which was the group with immigration (9 reactors). Another third of the reactors received Syntho and sterile solids which acted as a substrate control (9 reactors). The final third of reactors received Syntho only and acted as a continuity control (9 reactors).

### 2.2. Sample collection and processing

Mixed liquor biomass samples were collected from the reactors and centrifuged in 2 mL microcentrifuge tubes for 5 min at 16,000 × *g*. The supernatant was discarded and biomass was stored immediately at -80°C until nucleic acid extraction (approximately 3 months). Three aliquots were stored per reactor sample. DNA was extracted from approximately 0.25 g of each stored biomass sample using DNeasy PowerSoil Kit (Qiagen, Germantown, MD, USA) following the manufacturer's instructions with a final elution volume of 100 µl. One blank was included per batch of extractions (approximately 24 samples). Samples were extracted in duplicate, and DNA aliquots were immediately stored at -80°C until future use.

The quality of nucleic acids was assessed using the ratio of absorbance at 260 nm and 280 nm (260/280) obtained using NanoDrop™ One. DNA extracts with a 260/280 value between 1.8 and 2.0 were considered to have good purity. Quant-iT™ PicoGreen™ dsDNA Assay kit (Invitrogen, ON, Canada) was used to accurately quantify the double-stranded DNA concentration of the extracts prior to droplet digital PCR.

### 2.3. Droplet digital PCR

A total of 15 different antibiotic resistance genes were analyzed using droplet digital PCR and multiplexed amplicon sequencing (**Supplementary Table 1**). Clinically relevant ARGs were selected which displayed resistance to five classes of antimicrobials; beta-lactams (*bla*MOX, *bla*TEM, *bla*OXA), fluoroquinolones (*qnr*S, *qnr*B), diaminopyrimidines (*dfr*A), macrolides (*mph*E, *ere*A) and tetracyclines (*tet*O, *tet*Q, *tet*E) to investigate whether the impact of immigration varied between ARG classes. In addition, four

multidrug resistance genes were included (*rob*A, *msr*D, *qac*L, and *mar*R). Primers were designed and *in silico* verification was conducted by Swift Biosciences, Ann Arbor and manufactured by Integrated DNA Technologies, USA. Appropriate DNA dilutions were determined using a standard quantitative PCR reaction (Powerup SYBR green master mix) performed using three DNA dilutions to check for PCR inhibition. The fold dilution for digital droplet PCR was calculated using *Eq*.1. Samples were diluted to the appropriate concentration using DNase/RNase free water.

$$Dilution\ (fold)\ =\ 2^{24-Cq} \tag{1}$$

A 20 μl reaction mix was prepared for each droplet digital PCR reaction, which included 1 × QX200™ ddPCR™ Evagreen® Supermix (Bio-Rad, CA, USA; catalogue number 1864033), 100 nM of the forward and reverse primers, template DNA as determined using equation 1, and RNase/DNase-free water. For quality control purposes, a positive control obtained from wastewater samples was used in each run to ensure the matrix was representative of the actual samples to be analyzed. In addition, a no template control was included. Droplets were generated using the Bio-Rad QX200™ Droplet Generator and DG8™ Cartridges with 20 μl of reaction mix and 70 μl of Droplet Generation Oil for Evagreen. Following droplet generation, droplets were transferred to a 96 well plate and sealed with foil using a Bio-Rad PX1 PCR Plate Sealer. A Bio-Rad C100 Touch Thermal Cycler was used for thermal cycling of all plates. Reaction conditions used were as follows; 95°C for 5 min., followed by 50 cycles of 95°C for 30 s., *x*°C for 60 s, and 72°C for 30 s. whereby *x* is the annealing temperature (**Supplementary Table 1**). Followed by 4°C for 5 min, 90°C for 5 min, and a hold at 12°C. Annealing temperatures were optimized using a gradient PCR method on a pooled DNA sample. The optimal annealing temperature was selected based upon the separation between positive and negative droplets, and the lowest "rain" i.e., droplets defined as neither positive or negative. The primer concentration was optimized by conducting a test assay on a representative pooled DNA sample, at various primer concentrations ranging from 100 to 250 nM. A final primer concentration of 100 nm was selected for the assays. To test for inhibitor and matrix effects, 10-fold dilutions of pooled DNA samples were quantified.

Droplets were analyzed using the Biorad QX200™ Droplet Reader and the absolute quantification (ABS) experimental setup. Results were visualized using the QuantaSoft™ Software (Bio-Rad, version 1.7.4) to provide an absolute quantification of the ARG per nanogram of DNA. Reactions producing fewer than 10,000 droplets were excluded and the droplet digital PCR reaction was repeated. The threshold was defined using the auto-select function in the QuantaSoft™ software (Bio-Rad, version 1.7.4). In cases where an appropriate threshold was not automatically selected, a threshold was manually chosen. An example of a positive and negative result are provided in **Supplementary Figure 1A**. All samples were analyzed in duplicate in different PCR runs to confirm the technical reproducibility. Copies of each ARG/ng-DNA were normalized to the copies of 16S rRNA gene/ng-DNA to provide a relative ARG copy number/16S rRNA gene. The limit of blank (LOB) was calculated using Eqs 2, 3 (Armbruster and Pry, 2008) was used to determine the limit of detection (LOD) of samples. To confirm the calculated LOD values, assays were performed using six dilutions of a positive sample (**Supplementary Figure 1B**), and the 95% LOD was determined based upon the probability of detection at each concentration.

$$LOB\ =\ Mean_{Blank} + 1.645\ (SD_{Blank}) \tag{2}$$

$$LOD\ =\ LOB + 1.645\ (SD_{Lowest\ sample}) \tag{3}$$

## 2.4. Sequence diversity of ARGs

A multiplexed amplicon sequencing approach was used to analyze sequence variant diversity among the ARGs detected in the reactors. ARGs were amplified using a multiplex PCR kit (Qiagen) with the following reaction conditions; 95°C for 15 min. followed by 25 cycles of 94°C for 30 s, 60°C for 90 s, and 72°C for 60 s, and a final extension step at 60°C for 30 min. Amplicons obtained from individual PCR reactions (using one set of primers per reaction) were pooled and used as a positive control. The products of the multiplex PCR reaction were purified using SPRI Select beads (Beckman Coulter) to remove primer dimers at a sample to bead ratio of 0.8. Samples were barcoded and pooled at equimolar concentration. The pooled samples were sequenced on the Illumina MiSeq PE250 platform at McGill University and Génome Québec Innovation Centre (Montréal, QC, Canada).

ARG Amplicon sequence variants (ARG-ASVs) were defined as sequences which differed by at least one single nucleotide variant (SNP) within the amplified region of the targeted gene (around 275 base pairs). To distinguish between sequencing errors and actual sequence variants, a stringent filtering process was applied as described in Section "2.5. Bioinformatics."

## 2.5. Bioinformatics

Reads from each sample were split according to their forward and reverse primer sequences allowing for one sequencing error per primer sequence using a custom script available upon request. Read pairs where both or one of the reads was missing a primer sequence at the beginning or where the primer sequences found did not correspond to each other were removed. Subsequently, we used Trimmomatic v. 0.39 to trim all reads using the following settings: LEADING: 3 TRAILING: 3, SLIDINGWINDOW:4:15 and MINLEN:36. Then we used vsearch v2.13.3 to merge the trimmed read pairs before converting them to fasta format. The merged reads where then sorted and clustered with an identity of 1 and a minimum length of 100 bases while keeping track of the cluster size using the -size out option.

PCR and sequencing errors created many unique or very low count amplicon sequence variants that we removed using a custom R script. First, we tested if the distribution of read counts for each amplicon sequence variant produced by an individual primer pair followed a Poisson distribution (centered around the mean of all counts) and corrected the resulting *p*-values (subtracted from 1 such that amplicon sequence variants with high read counts had low *p*-values) using the Bonferroni correction. If none of the amplicon sequence variant have a corrected *p*-value below 0.5, we removed the whole dataset, as this indicated that we are not able to distinguish real amplicon sequence variants from those generated

by PCR or sequencing errors (noise sequence variants). If any amplicon sequence variants survived the filtering, we aimed to remove the noise sequence variants from the datasets by finding the minimum of a density function based on the total data for each gene (including noise sequence variants) and removing all amplicon sequence variants with counts less than the minimum found. By comparing with other filtering approaches [e.g., DADA2 (Callahan et al., 2016) or minimum absolute value], it was found that the filtering adopted here was the most stringent, but was still able to recover the diversity of synthetic mixes of sequence variants.

We subsequently combined all reads corresponding to a specific resistance gene (including multiple primers amplifying the same gene). Files were re-replicated using a custom python script available upon request (using the Pandas module), before constructing a table of allelic distribution across samples equivalent to an OTU table for each resistance gene using vsearch v2.13.3's cluster_fast option with the output option. Unique consensus sequence variants were obtained using the centroids option. To ensure that the resulting amplicon sequence variants were the products of amplification of the target ARG, we blasted all consensus sequences to a custom ARG database using the diamond (v0.9.32.133) blastx option with an e-value of 3 and a minimum identity of 80. Consensus sequences that were not similar to any entries in the ARG database were removed from the analysis.

## 2.6. Statistics

The Mann-Whitney U test was used to determine if there was a statistically significant increase in the abundance of each ARG with immigration. Samples taken from the reactors with immigration (receiving Syntho and influent solids) were compared to the control groups at a significance level of $p < 0.05$.

Procrustes analysis was performed using the R Vegan package (Oksanen et al., 2022) to determine whether the microbial community of the reactors correlated with the ARG profile. Procrustes was used to compare the ARG and microbial community ordinations. ARG data was standardized to means of 0 and standard deviation of 1. Using the R Vegan package, Principal Component Analysis (PCA) was conducted for the ARG dataset based on the Euclidean distances. Principle coordinate analysis (PCoA) was performed using Jaccard distance on the microbial community data, as this distance was previously shown to most effectively display the impact of immigration on the community in the current experiment (Gibson et al., 2023a). The function "Protest" was used with 999 permutations to test the significance between the configurations.

## 2.7. Database analysis of amplicon sequence variants

The NCBI database (NCBI Research Coordinators, 2013) was used to search for previously reported hosts of the detected ASVs. To evaluate the mobility of each ASV, PLSDB (Galata et al., 2019) was used to determine whether they had been previously reported within plasmids. In this analysis, only 100% identity and coverage results were considered as ASVs could vary by as little as a single SNP.

# 3. Results

## 3.1. Impact of immigration on the abundance of ARGs in the activated sludge

Reactors were operated under highly controlled conditions to test the impact of immigration on antibiotic resistance in the activated sludge. All 27 reactors in the three Blocks (three different inoculum) received a synthetic wastewater (Syntho) feed, which allowed the influent wastewater composition to be carefully controlled throughout reactor operation. To ensure the reactors were operating at steady state, the chemical oxygen demand and suspended solids concentrations were monitored over time and observed to be relatively constant (steady-state). After operating the reactors for 12 SRTs and ensuring steady state was reached, during Phase 2 in each Block (nine reactors in total; Block A-La Prairie AS, Block B-Cowansville AS, and Block C- Pincourt AS), three reactors received synthetic wastewater with added influent solids to simulate the impact of immigration. Another three of the reactors received autoclaved influent solids and acted as a substrate control. The final three reactors received Syntho only as a continuity control to establish a baseline for the level of AMR without immigration.

The impact of influent immigration on the activated sludge microbial community is discussed at length in Gibson et al. (2023a). Briefly, immigration impacted the microbial community composition of the activated sludge, and reactors with immigration became more similar to the microbial community of the influent solids. Up to 25% of sequencing reads were observed to be contributed through influent immigration, representing a significant proportion of the activated sludge community. Using a mass balance approach, it was observed that the growing immigrant population typically exhibited a lower and often negative net growth rates in the activated sludge, when compared to the core resident genera which typically displayed a positive net growth rate. In Gibson et al. (2023a), focus was placed on the impact of immigration on the microbial community composition of the activated sludge alone, whilst in this publication the impact on AMR is explored.

To determine the impact of immigration on AMR in the AS, digital droplet PCR was used to quantitatively assess the concentration of fifteen ARGs in the reactor samples and influent wastewater. Results showed that immigration caused a significant increase in the relative abundance of eleven of the fifteen ARGs in the activated sludge when compared to the control groups (sterile control and no immigration control together) (**Figure 2**; Mann–Whitney U Test; $p < 0.05$). Genes observed to increase in abundance were distributed in several classes of antimicrobial resistance such as ARGs against fluoroquinolones (*qnr*B and *qnr*S), beta-lactams (*bla*TEM and *bla*MOX), macrolides (*mph*E), diaminopyrimidines (*dfr*A) and tetracyclines (*tet*Q and *tet*O). Three out of four of the efflux pump-associated multi-antimicrobial resistance genes quantified showed a significant increase in concentration with immigration (*mar*R, *msr*D and *rob*A). Genes such as *bla*MOX were present in the reactors with and without immigration, whilst others such as *mar*R and *qnr*B were detected in the activated sludge mixed liquor only with immigration.

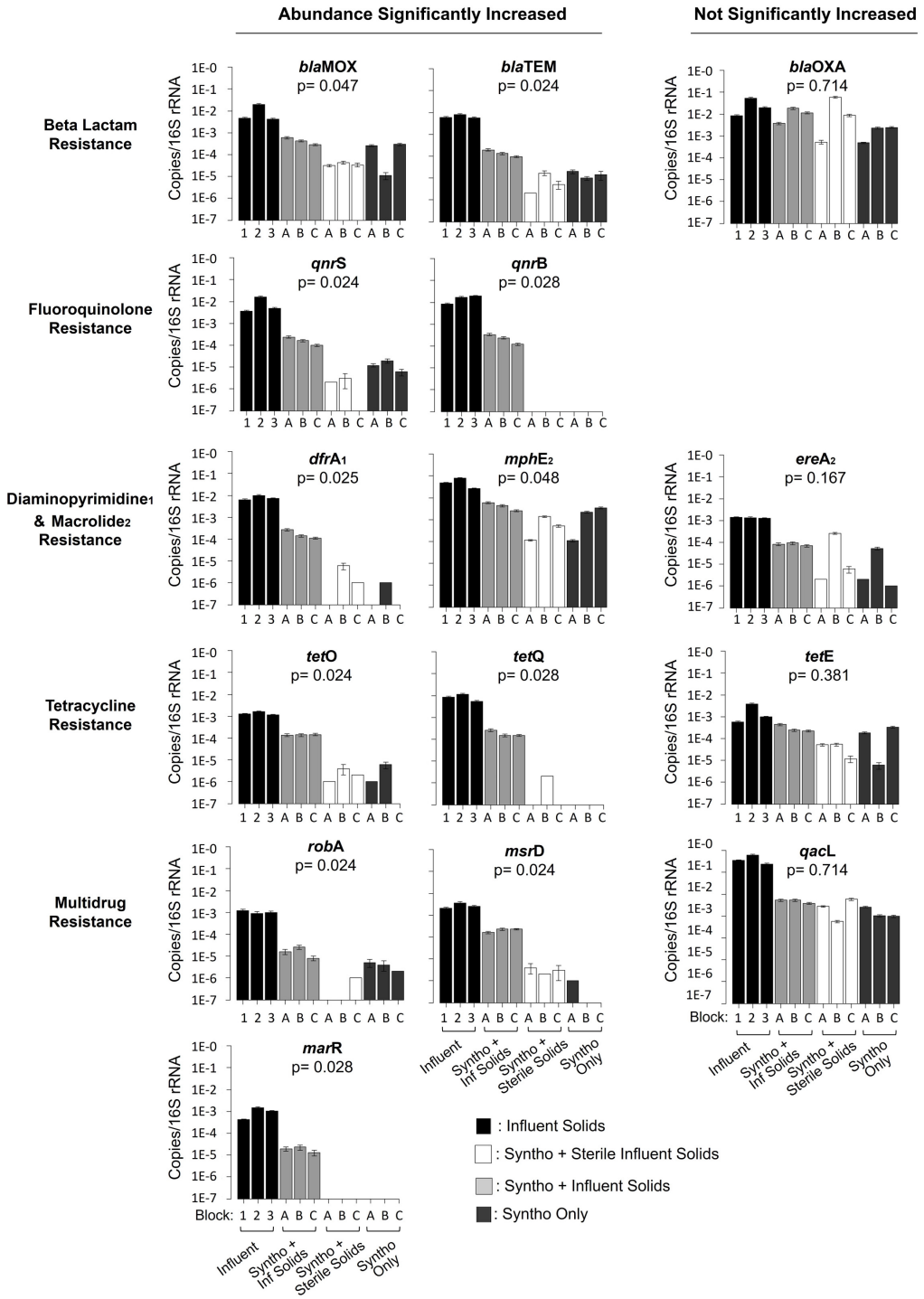


FIGURE 2
Quantification of antibiotic resistance genes using droplet digital PCR. Reactors with immigration received Syntho and influent solids. Reactors receiving Syntho and sterile influent solids acted as a substrate control. Reactors receiving Syntho only acted as a no immigration continuity control. The Block represents the inoculum source of the reactors; A- La Prairie ML, B- Cowansville ML, C- Pincourt ML, Influent samples are numbered based upon the order received by the reactors during Phase 2. Each bar represents a composite sample of three biological replicates. The Error bars represent the standard error between duplicates. The Mann-Whitney U Test was used to assess the statistical significance of the change in abundance of each ARG with immigration when compared to the sterile and no immigration control combined.

The relative abundances of over 70% (11/15) of quantified ARGs increased in the activated sludge with immigration. However, they typically remained lower than those in the influent solids. To determine the impact of immigration on the overall ARG load, the absolute ARG concentrations were calculated (**Supplementary Table 2**) using information on reactor operation including the volatile suspended solid concentration, yield of DNA/g-VSS, 16S rRNA gene/ng-DNA and gene abundance (16S rRNA gene)

(**Supplementary Table 4**; Gibson et al., 2023a). It was observed that the load of genes such as *bla*OXA increased by 0.42 log gene copies/L between the influent and mixed liquor. Whilst others such as *rob*A reduced by 1.14 logs of gene copies/L between the influent and activated sludge. Consequently, despite the reduction in ARG relative abundance (copies/16S rRNA gene) between the influent solids and activated sludge, high absolute ARG concentrations remained.

## 3.2. Correlation between the microbial community composition and ARG profile

In numerous studies, the microbial community composition has increasingly emerged as a key determinant of ARG content (Forsberg et al., 2014; Wu et al., 2017; Zhou et al., 2017). In continuity with these observations, a Procrustes analysis was performed to determine whether the observed changes in the abundance of ARGs in the reactors correlated with changes in the microbial community composition with immigration. Procrustes analysis using the Jaccard distance matrix revealed a significant correlation (Procrustes $M^2 = 0.60$, $p = 0.015$) between the microbial community compositions of the reactor activated sludge and the profiles and concentrations of ARGs they carried (**Figure 3B**). However, this correlation was not significant (Procrustes $M^2 = 0.73$, $p = 0.290$; note that lower $M^2$ means a better correlation between the datasets) when using the Bray-Curtis dissimilarity (**Figure 3D**).

## 3.3. Analysis of ARG amplicon sequence variants

Digital droplet PCR showed that the relative abundance of over 70% (11 out of 15) of the ARGs investigated significantly increased with immigration. However, questions remained about the exact dynamics occurring at the interface between the influent and activated sludge. Chief among them was whether the increase in abundance of an ARG was due to the introduction of genes originating from the influent. In other words, were the observed changes in the activated sludge likely due to direct ARG immigration or other changes induced by the presence of influent solids? To investigate the immigration dynamics at greater depth, a multiplexed amplicon sequencing approach was used to detect ARG-ASVs within the influent and reactor samples. By utilizing short read sequences, sequence diversity within a specific region of each ARG (around 275 base pairs) could be used as a marker to track the movement of genes between the influent and activated sludge. After stringent filtering based on the Poisson distribution, ARG-ASV information was obtained for eleven of the fifteen ARGs analyzed (**Figure 4**). The four remaining targets (*msr*D, *mar*R, *qnr*B, and *qnr*S) were undetected after the filtering process either because they did not survive the stringent filtering process (*msr*D and *qnr*B), or insufficient reads were obtained resulting in no detection (*qnr*S and *mar*R). Amplicon sequencing of the eleven ARGs revealed different ASV distributions or concurrence profiles between the influent and the activated sludge mixed liquors (**Figure 4**). In several cases, the ARG-ASVs were specific to either the influent or reactors, with few examples of concurrence in the reactors and the received influent solids. This demonstrates that PCR based methods over-simplified the ARG dynamics at the interface between the influent and activated sludge.

The concurrence profiles between the influent and the activated sludge reactors could be classified into 6 similarity groups that were typically confined either to the ARGs that significantly increased in abundance with influent immigration (Groups 1–3) or to ARGs with abundances that statistically remained unchanged (Groups 4–6; **Figure 4**). As summarized in **Table 1**, *Group 1* consists of ARGs for which the same and single ASV was observed in all samples (genes *mph*E and *tet*Q). This concurrence profile is consistent with direct immigration causing the significant increases in the abundances of these genes. *Group 2* collates ARGs with an ASV observed only in the control reactor samples, but not in the live immigration reactor or the influent samples (gene *bla*MOX and *bla*TEM). This concurrence profile is also consistent with direct immigration overwhelming the detection of the ARG-ASV observed in the control reactor. *Group 3* concurrence profiles are characterized by ARG-ASVs observed only in the influent, but not in the reactors (genes *dfr*A, *tet*O, *rob*A). This profile appears to follow a counter selection dynamic, whereby one or more of the influent sequence ASVs did not successfully immigrate between the influent and activated sludge. This demonstrated that the presence of a given ARG-ASV in the influent and the significant increase of an ARG with immigration, does not definitively predict the presence of the ASV within the activated sludge as could have been inferred using ddPCR results alone.

The *Group 4* profile which was only observed for *tet*E appeared to be a mixture of Group 2 and 3 profiles, suggesting that these two mechanisms could be at interplay. Group 3 and 4 ARGs exemplify the complexity of interactions at the interface between the influent and activated sludge. Considering the Procrustes results (**Figure 3**), the increase in the abundances of these ARGs could be associated with the increase in relative abundance of the bacterial populations that carry these ARGs instead (Group 3) or simultaneously (Group 4) to direct ARG immigration.

The last two profiles of concurrences were observed for ARGs that did not significantly increase in abundance (**Figure 4**). *Group 5* profile was only observed for *qac*L and showed ASVs that were only observed in some samples from reactors receiving influent solids (both live and autoclaved). These ASVs were in low abundances in these samples. Thus, they may have been below the detection limit in the influent or control reactors, and immigration made them detectable in some circumstances possibly due to small variations in community compositions as in Groups 3 and 4. Finally, the genes of *Group 6* ($bla_{OXA}$ and *ere*A) harbored 5 ASVs each present seemingly at random in samples from the influent or the reactors under different experimental conditions. Consequently, no clear profiles could be identified, and immigration did not appear to affect these genes.

## 3.4. Database information on the genetic context of ASVs

To investigate the genetic context of ARG-ASVs, the NCBI database and PLSDB (Galata et al., 2019) were utilized to gain

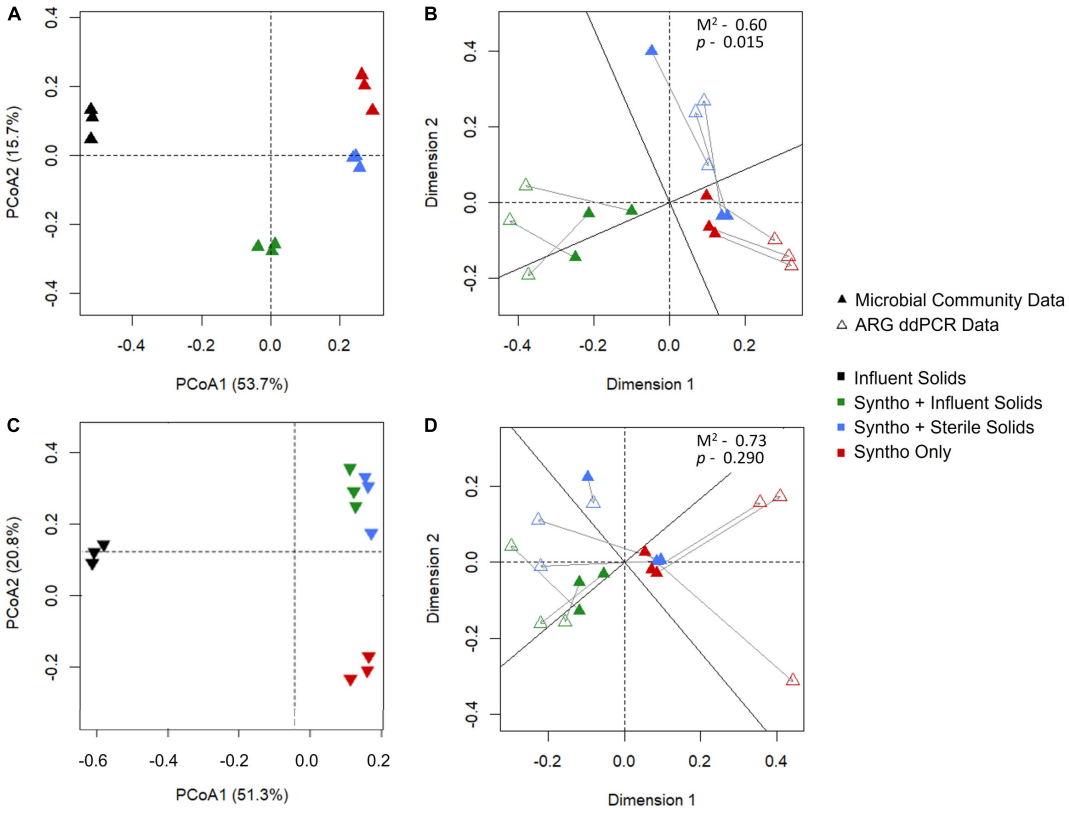


FIGURE 3
Procrustes analysis to investigate the correlation between the microbial community and ARG composition. **(A)** Microbial community of the reactors visualized using Jaccard dissimilarity as determined by 16S rRNA gene sequencing. **(B)** Procrustes analysis of microbial communtiy and ARG profile with Jaccard dissimilarity. **(C)** Microbial community of the reactors visualized using Bray Curtis dissimilarity as determined by 16S rRNA gene sequencing. **(D)** Procrustes analysis of microbial communtiy and ARG profile with Bray Curtis distance.

information about previously reported hosts and gene occurrence on plasmids (**Supplementary Table 3**). To exemplify this approach and establish hypotheses for future work, genes from group 2–5 (**Table 1**) were analyzed, as unique ASVs were detected in either the reactors or influent samples.

In group two, analysis of the *bla*TEM ARG using the NCBI database revealed the ARG-ASVs to have previously been reported in similar bacterial hosts (**Supplementary Table 3**), which included taxa from the genus *Acinetobacter*, *Enterobacter,* and *Klebsiella* to name a few. The *bla*TEM ASV-1 was present in numerous variants of the *bla*TEM gene (over 60) including TEM-29, TEM-169, and TEM-26 whilst ASV-2 was present in only TEM-229, TEM-116, TEM-162, TEM-181, and TEM-157. Analysis of the two ARG-ASVs in PLSDB revealed both to have been previously reported on plasmids. Plasmids containing ARG-ASV 1 have been detected in numerous settings including in humans, animals and the environment (water). Whilst plasmids containing *bla*TEM ASV-2 have been reported in fewer settings, which included soil, feed additives and *Orcytes gigas* (rhinoceros beetle).

In group 3, analysis of the ASVs of the *dfr*A gene found that *dfr*A ASV-1 corresponded to the *dfr*A-5 gene, and ASV-2 the *dfr*A-14 variant of the gene (Alcock et al., 2020). ASV-1 (*dfr*A-5) and ASV-2 (*dfr*A-14) are phylogenetically closely related (Sánchez-Osuna et al., 2020) and are commonly observed within integrons and on plasmids. As with the *bla*TEM ASVs, both *dfr*A ASVs have been previously reported in similar host including taxa from the genus *Aeromomas, Enterobacter*, and *Citrobacter*.

In group 4, similar selection patterns were observed with the *tet*E ARG (**Figure 2**). The influent solids contained two ASVs of the *tet*E ARG. ASV-1 was detected in the reactors even without immigration, whilst ASV-2 did not successfully immigrate. The NCBI database returned no matches with 100% identity for sequence variant 1. The hosts of ASV-2 appeared to somewhat overlap with those of ASV-3 that was detected within the reactors. Interestingly, it was observed that ASV-2 was primarily reported to occur on plasmids in the NCBI database (NCBI Research Coordinators, 2013), whilst ASV-3 was more commonly chromosomal.

# 4. Discussion

## 4.1. Immigration impacted ARG relative abundance in the activated sludge

Droplet digital PCR revealed that the relative abundance of 11 of the 15 ARGs quantified increased with immigration. The previous analysis of the community composition data of the current reactor experiment demonstrated that the impact of immigration was better visualized using the Jaccard dissimilarity

10.3389/fmicb.2023.1155956

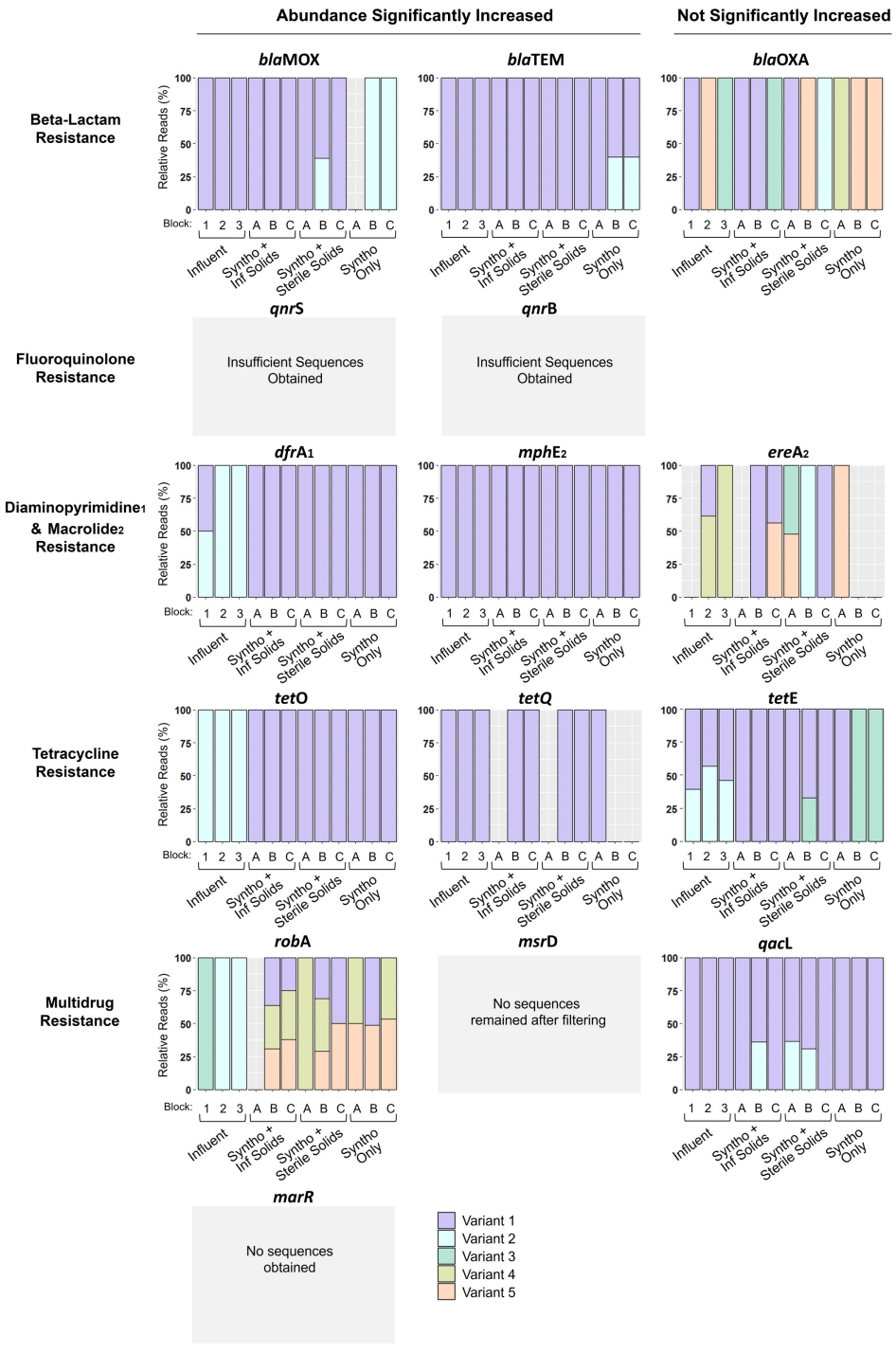


FIGURE 4
ARG ASVs detected using multiplexed amplicon sequencing. Reactors with immigration received Syntho and influent (Inf) solids. Reactors receiving Syntho and sterile influent solids acted as a substrate control. Reactors with Syntho only acted as a no immigration control. Each sample represents a pool of biological triplicates. Block represents the inoculum of the reactor A- La Prairie Mixed Liquor, B- Cowansville Mixed Liquor, C- Pincourt Mixed Liquor. Influent 1, 2, and 3 represent the order in which they were fed to the reactors during Phase 2, with influent 3 received for the final solid retention time (SRT). All reactor samples analyzed were obtained from the final day of Phase 2. The *msr*D, *mar*R, *qnr*B, and *qnr*S gene ASVs were undetected after the sequence filtering process either because they did not survive the stringent filtering process (*msr*D and *qnr*B), or insufficient reads were obtained resulting in no detection (*qnr*S and *mar*R).

than the Bray-Curtis dissimilarity, suggesting that immigration impacts the composition of lower-abundance taxa in the mixed liquor (Gibson et al., 2023a). Consistent with this result, Procrustes analysis revealed a significant correlation between the microbial community composition and ARG profiles only when visualized with Jaccard dissimilarity. Taken together, this suggests that the changes in the ARG profiles observed is due to immigration of taxa mainly occurring at low abundances within the activated sludge.

Whilst the concentrations of the majority of ARGs increased with immigration, others such as *bla*OXA and *qac*L did not significantly change (Figure 2). The presence of these genes in similar abundance under all reactor conditions suggests that they are likely associated with the core resident populations, which were defined as taxa that occurred under all reactor conditions (i.e., independent of immigration).

## 4.2. Dynamics of ARG amplicon sequence variants between influent and activated sludge

Immigration impacted the concentration and diversity of ARGs in the activated sludge. However, it remained to be seen whether the increase in the abundance of ARGs with immigration was due to direct ARG transport or other changes associated with influent immigration. Recent studies have demonstrated ARG-ASVs to occur in samples originating from different sources (Zhang et al., 2021). Therefore, it was hypothesized that the influent wastewater, which is strongly influenced by anthropogenic activities (Guo et al., 2019), could contain different ARG-ASVs compared to the activated sludge. The detection of unique ARG-ASVs would enable a more detailed analysis of the immigration dynamics between the influent and activated sludge.

Based upon the neutral model and the assumption of ecological equivalence (i.e., equal fitness of competitors), ASVs detected in the influent would be expected to immigrate into the activated sludge (Harris et al., 2017). In both group 3 and 4, unique ASVs were observed in the influent, which could have been introduced into the reactors with immigration. However, in only one instance was ARG-ASV immigration unequivocally observed in the current study (Figure 4). Among the *bla*MOX gene, a new ASV was introduced into the reactors with immigration (Figure 4). With the introduction of this sequence ASV, the indigenous *bla*MOX sequence ASV-2, which was present without immigration, was no longer detected, suggesting either competition among the hosts of these ARG-ASVs or simply that the low concentration of the indigenous resident ASV was overwhelmed by the immigrant ASV. The *bla*MOX ASV-1 was also detected in the reactors receiving sterile influent solids, suggesting that the gene persisted in the influent solids and activated sludge reactors after autoclaving. Counter selection of ARG-ASVs between the influent and activated sludge was more frequently observed, suggesting that ARG immigration is likely not dictated solely by neutral processes and is impacted by other factors. This conclusion is supported by recent studies which have demonstrated that in WWTP samples obtained from five different countries, the resistome composition varies between the influent and activated sludge (Dai et al., 2022).

Counter selection of ARG ASVs was frequently observed between the influent and activated sludge, which suggested that direct immigration of ARGs was not occurring between the two environments. Despite this, significant increases in the relative abundances of many of these ARGs were observed in the activated sludge with immigration. Supported by the results from Procrustes analysis which showed a positive correlation between the microbial community and ARGs, this suggests that the relative abundance was instead impacted by the microbial community changes caused by immigration. This is consistent with previous studies that have identified the microbial community composition to be the main driver of AMR content in numerous environments (Munck et al., 2015; Luo et al., 2017).

The results from ARG amplicon sequencing demonstrate the complexity of ARG dynamics at the interface between the influent and activated sludge. Given the frequent observation of counter selection of ARG-ASVs, PCR based approaches alone cannot be used to accurately predict the AMR the activated sludge or infer the origin of ARGs. These data also support the contrasting results reported in the literature, which are likely influenced by the methods used and targets selected. Future studies should consider the use of amplicon sequencing approaches to enable a more accurate assessment of ARG dynamics and source tracking.

TABLE 1 Concurrence profiles of ARGASVs in the influent and reactor samples.

| Group | Genes | Description | Conclusions |
|---|---|---|---|
| 1 | *mph*E, *tet*Q | Same single ASV observed in all samples | Consistent with direct immigration |
| 2 | *bla*MOX, *bla*TEM | Unique ASV present in control reactors that is not detected with immigration or in the influent solids | Direct immigration and suppression dynamics |
| 3 | *dfr*A, *tet*O, *rob*A | Unique ASVs present in the influent solids only | Counter Selection |
| 4 | *tet*E | Both 2 and 3: Unique ASVs present in the control groups and influent solids | Mixture of direct immigration, counter selection and suppression dynamics |
| 5 | *qac*L | Unique ASV only present in reactors receiving influent solids (live and autoclaved) | Possible direct immigration of ASVs occurring below detection limit |
| 6 | *bla*OXA, *ere*A | Numerous ASVs distributed throughout the influent and reactor samples | ASVs randomly distributed |

## 4.3. Genetic context of ARG amplicon sequence variants

Given the differences in the environmental conditions and microbial community between the influent and mixed liquor, counter selection of ARG-ASVs was not surprising. The successful immigration of a given ARG-ASV is likely associated with the ability of the host to adapt and establish itself under different environmental conditions, or the mobility of the gene that may be an indicator of the likelihood of transfer to hosts better adapted to the reactor environment. To further investigate these factors, ARG-ASVs were analyzed using the NCBI database and PLSDB (Galata et al., 2019).

In group 2, analysis of the *bla*TEM sequences revealed the two ARG-ASVs to have been previously reported in similar bacterial hosts and both to occur in plasmids (Supplementary Table 3). Within the influent and reactor samples *bla*TEM ASV-1 was most frequently observed. Plasmids containing this ASV have been previously detected in a diverse range of environments

(Galata et al., 2019). Given that both *bla*TEM ASVs were detected among similar hosts, it could be suggested that the persistence of ASV-1 is linked to the ability of plasmids containing this ASV to move between environments.

In group 3, using multiplexed amplicon sequencing two ASVs of the *dfr*A gene were identified. The *dfr*A ASV-1 corresponded to the *dfr*A-5 gene, and ASV-2 the *dfr*A-14 variant of the gene. A 2011 review of class 1 and 2 integrons in pathogenic gram-negative bacteria identified *dfr*A-5 (ASV-1) in chicken and pig samples, as well as estuarine and carriage water. In the same study, the dfrA-14 gene was reported in pig, cattle and chicken samples, but not in aquatic settings (Stokes and Gillings, 2011). More recently, *dfr*A-14 has been observed in surface waters (Kohler et al., 2020) and WWTP effluent (Che et al., 2022). The widespread detection of both ASV-1 and ASV-2 in clinical, agricultural, and environmental settings does not support the theory of selection due to niche differences between the influent and reactors. However, both ASV-1 and 2 have been observed in similar hosts, suggesting competition may occur resulting in the loss of ASV-2 (**Supplementary Table 3**).

In group 4, *tet*E ASV-2 appeared most frequently in plasmids, ASV-3 was more commonly reported to be chromosomal. Previous studies have demonstrated chromosomal mutations to carry a larger fitness cost than plasmid acquired resistance (Vogwill and Maclean, 2015), however, ASV-3 was found to persist in the reactors and ASV-2 was undetected. ASV-2 has been associated with numerous plasmids found in water environments including PC1579, a conjugative plasmid recently reported to carry a novel Metallo-β-lactamase gene (Cheng et al., 2021), and plasmid pWLK-NDM, which was identified in environmental isolates carrying *bla*NDM-1 and *bla*KPC-2 resistance genes (Dang et al., 2020). Given the previous reports of ASV-2 in aquatic environments, it would be expected that ARB carrying this gene would be capable of growing within the reactor environment. However, ASV-2 remained undetected in the activated sludge suggesting again that competition for resources may be occurring.

### 4.4. Development of multiplexed amplicon sequencing

Multiplexed amplicon sequencing of ARGs is a relatively new technique requiring optimisation to ensure all primer pairs work successfully in tandem (Smith et al., 2022; Gibson et al., 2023b). Overall, eleven of the fifteen ARG targets produced data on ASV. Of the primers not successfully producing ARG-ASV information, this was often due to low levels of amplification. Considering the stringent Poisson distribution-based filters applied to the amplicon sequencing data, low count ASVs may also have been excluded during data processing. Future method developments should optimize primer design to ensure sufficient sequencing reads are obtained for all positive targets to improve resolution.

Future development of the multiplexed amplicon sequencing approach should also carefully consider which region of the ARG sequence to target. Among group 1 of concurrence profiles, low sequence diversity was found in the targeted region of the gene. The multiplexed amplicon sequence targets used herein with Illumina MiSeq protocols include only a small section of the ARG sequence (around 275 bp). Consequently, sequence diversity in other regions may have been missed. By considering regions of high genetic diversity in future design, this technique could be optimized to cover mutations of concern for example those impacting the phenotypic resistance.

### 4.5. Future application of ARG sequence diversity analysis

The monitoring of ARG ASVs at the immigration interface revealed various immigration patterns such as (i) suppression of the indigenous activated sludge ASV by the immigrant, or conversely (ii) counter selection and complete immigration failure of the influent ASV. These immigration profiles are reported for the first time here and highlight the crucial information that can be gained using our multiplex amplicon sequencing techniques.

Unique ASVs were observed among the influent and reactor samples, which highlights the potential for amplicon sequencing approaches to be utilized in the future for ARG source tracking purposes. To enable this, widespread sampling of reservoirs of antimicrobial resistance should be considered to identify ARG ASV markers present in different environments. Compared to techniques such as full metagenome sequencing, the novel amplicon sequencing approach applied here is relatively low cost and produces data that is more easily managed. In the future, such techniques could be applied for source tracking of ARG contamination in the environment and assessment of potential ARG mobility.

## Data availability statement

The datasets presented in this study can be found in online repositories. The names of the repository/repositories and accession number(s) can be found below: The European Nucleotide Archive, ERP146025.

## Author contributions

CG designed the study, conducted the digital droplet PCR, developed the multiplexed amplicon sequencing approach, analyzed the data, and prepared the manuscript. SK developed the multiplexed amplicon sequencing approach, developed the bioinformatics pipeline, processed the sequencing data, and reviewed the manuscript. NK developed the multiplexed amplicon sequencing approach and prepared samples for sequencing. DF obtained funding, supervised the research, and revised the manuscript. All authors contributed to the article and approved the submitted version.

## Funding

This work was funded by NSERC through a Discovery grant (NSERC RGPIN-2016-06498) and a Strategic Program grant (NSERC STPGP 521349-18). NSERC had no role in the design of

this study. CG and BG were partly funded by the McGill University Engineering Doctoral Award.

## Acknowledgments

We thank Sophie Zhang, Julia Qi, Carlos Vasquez Ochoa, Nouha Klai, Zeinab Bakhshijooybari, and Shameem Jauffur for their assistance with reactor operation. We would also like to acknowledge the assistance of the operators and staff at Cowansville, La Prairie, and Pincourt wastewater treatment plants for access to the facilities and help with sampling. Finally, we are indebted to Biorad for the training provided and loan of the digital droplet PCR equipment.

## Conflict of interest

The authors declare that the research was conducted in the absence of any commercial or financial relationships that could be construed as a potential conflict of interest.

## Publisher's note

All claims expressed in this article are solely those of the authors and do not necessarily represent those of their affiliated organizations, or those of the publisher, the editors and the reviewers. Any product that may be evaluated in this article, or claim that may be made by its manufacturer, is not guaranteed or endorsed by the publisher.

## Supplementary material

The Supplementary Material for this article can be found online at: https://www.frontiersin.org/articles/10.3389/fmicb.2023.1155956/full#supplementary-material

## References

Abadii, A. T. B., Rizvanov, A. A., Haertlé, T., and Blatt, N. L. (2019). World Health Organization report: Current crisis of antibiotic resistance. *Bionanoscience* 9, 778–788. doi: 10.1007/s12668-019-00658-4

Alcock, B. P., Raphenya, A. R., Lau, T. T. Y., Tsang, K. K., Bouchard, M., Edalatmand, A., et al. (2020). CARD 2020: Antibiotic resistome surveillance with the comprehensive antibiotic resistance database. *Nucleic Acids Res.* 48, D517–D525. doi: 10.1093/NAR/GKZ935

Armbruster, D. A., and Pry, T. (2008). Limit of blank, limit of detection and limit of quantitation. *Clin. Biochem. Rev.* 29:S49.

Bharti, R., and Grimm, D. G. (2021). Current challenges and best-practice protocols for microbiome analysis. *Brief. Bioinform.* 22, 178–193. doi: 10.1093/BIB/BBZ155

Boeije, G., Corstanje, R., Rottiers, A., and Schowanek, D. (1999). Adaptation of the CAS test system and synthetic sewage for biological nutrient removal. *Chemosphere* 38, 699–709. doi: 10.1016/S0045-6535(98)00311-7

Callahan, B. J., Mcmurdie, P. J., Rosen, M. J., Han, A. W., Johnson, A. J. A., and Holmes, S. P. (2016). DADA2: High-resolution sample inference from illumina amplicon data. *Nat. Methods* 13, 581–587. doi: 10.1038/nMeth.3869

Che, Y., Xia, Y., Liu, L., Li, A. D., Yang, Y., and Zhang, T. (2019). Mobile antibiotic resistome in wastewater treatment plants revealed by nanopore metagenomic sequencing. *Microbiome* 7:44. doi: 10.1186/S40168-019-0663-0/FIGURES/5

Che, Y., Xu, X., Yang, Y., Bøinda, K., Hanage, W., Yang, C., et al. (2022). High-resolution genomic surveillance elucidates a multilayered hierarchical transfer of resistance between WWTP- and human/animal-associated bacteria. *Microbiome* 10:16. doi: 10.1186/S40168-021-01192-W/FIGURES/6

Cheng, Q., Zheng, Z., Ye, L., and Chen, S. (2021). Identification of a novel metallo-β-Lactamase, VAM-1, in a foodborne *Vibrio alginolyticus* isolate from China. *Antimicrob. Agents Chemother.* 65:e0112921. doi: 10.1128/AAC.01129-21

Dai, D., Brown, C., Bürgmann, H., Larsson, D. G. J., Nambi, I., Zhang, T., et al. (2022). Long-read metagenomic sequencing reveals shifts in associations of antibiotic resistance genes with mobile genetic elements from sewage to activated sludge. *Microbiome* 10:20. doi: 10.1186/S40168-021-01216-5/FIGURES/6

Dang, B., Zhang, H., Li, Z., Ma, S., and Xu, Z. (2020). Coexistence of the blaNDM-1-carrying plasmid pWLK-NDM and the blaKPC-2-carrying plasmid pWLK-KPC in a *Raoultella ornithinolytica* isolate. *Sci. Rep.* 10:2360. doi: 10.1038/s41598-020-59341-4

Forsberg, K. J., Patel, S., Gibson, M. K., Lauber, C. L., Knight, R., Fierer, N., et al. (2014). Bacterial phylogeny structures soil resistomes across habitats. *Nat. Lett.* 509, 612–616. doi: 10.1038/nature13377

Galata, V., Fehlmann, T., Backes, C., and Keller, A. (2019). PLSDB: A resource of complete bacterial plasmids. *Nucleic Acids Res.* 47, D195–D202. doi: 10.1093/NAR/GKY1050

Gao, P., Munir, M., and Xagoraraki, I. (2012). Correlation of tetracycline and sulfonamide antibiotics with corresponding resistance genes and resistant bacteria in a conventional municipal wastewater treatment plant. *Sci. Total Environ.* 421–422, 173–183. doi: 10.1016/J.SCITOTENV.2012.01.061

Gibson, C., Kraemer, S. A., Klimova, N., Vanderweyen, L., Klai, N., Guo, B., et al. (2023b). *Multiplexed amplicon sequencing reveals high allelic diversity of antibiotic resistance genes in Québec sewers*. bioRxiv [Preprint]. doi: 10.1101/2023.03.06.531290

Gibson, C., Jauffur, S., Guo, B., and Frigon, D. (2023a). Activated sludge microbial community assembly: The role of influent microbial community immigration. *bioRxiv* [Preprint]. doi: 10.1101/2023.01.25.525574

Guo, B., Liu, C., Gibson, C., and Frigon, D. (2019). Wastewater microbial community structure and functional traits change over short timescales. *Sci. Total Environ.* 662, 779–785. doi: 10.1016/j.scitotenv.2019.01.207

Harris, K., Parsons, T. L., Ijaz, U. Z., Lahti, L., Holmes, I., and Quince, C. (2017). Linking statistical and ecological theory: Hubbell's unified neutral theory of biodiversity as a hierarchical Dirichlet process. *Proc. IEEE* 105, 516–529. doi: 10.1109/JPROC.2015.2428213

Jankowski, P., Gan, J., Le, T., McKennitt, M., Garcia, A., Yanaç, K., et al. (2022). Metagenomic community composition and resistome analysis in a full-scale cold climate wastewater treatment plant. *Environ. Microbiomes* 17, 1–20. doi: 10.1186/S40793-022-00398-1/TABLES/2

Kohler, P., Tijet, N., Kim, H. C., Johnstone, J., Edge, T., Patel, S. N., et al. (2020). Dissemination of verona integron-encoded metallo-β-lactamase among clinical and environmental Enterobacteriaceae isolates in Ontario, Canada. *Sci. Rep.* 10:18580. doi: 10.1038/s41598-020-75247-7

Lapara, T. M., Burch, T. R., McNamara, P. J., Tan, D. T., Yan, M., and Eichmiller, J. J. (2011). Tertiary-treated municipal wastewater is a significant point source of antibiotic resistance genes into Duluth-superior harbor. *Environ. Sci. Technol.* 45, 9543–9549. doi: 10.1021/ES202775R/SUPPL_FILE/ES202775R_SI_001.PDF

Le, T. H., Ng, C., Tran, N. H., Chen, H., and Gin, K. Y. H. (2018). Removal of antibiotic residues, antibiotic resistant bacteria and antibiotic resistance genes in municipal wastewater by membrane bioreactor systems. *Water Res.* 145, 498–508. doi: 10.1016/J.WATRES.2018.08.060

Liu, S. S., Qu, H. M., Yang, D., Hu, H., Liu, W. L., Qiu, Z. G., et al. (2018). Chlorine disinfection increases both intracellular and extracellular antibiotic resistance genes in a full-scale wastewater treatment plant. *Water Res.* 136, 131–136. doi: 10.1016/J.WATRES.2018.02.036

Luo, G., Li, B., Li, L.-G., Zhang, T., and Angelidaki, I. (2017). Antibiotic resistance genes and correlations with microbial community and metal resistance genes in full-scale biogas reactors as revealed by metagenomic analysis. *Environ. Sci. Technol.* 51, 4069–4080. doi: 10.1021/acs.est.6b05100

Munck, C., Albertsen, M., Telke, A., Ellabaan, M., Nielsen, P. H., and Sommer, M. O. A. (2015). Limited dissemination of the wastewater treatment plant core resistome. *Nat. Commun.* 6:8452. doi: 10.1038/ncomms9452

Munir, M., Wong, K., and Xagoraraki, I. (2011). Release of antibiotic resistant bacteria and genes in the effluent and biosolids of five wastewater utilities in Michigan. *Water Res.* 45, 681–693. doi: 10.1016/J.WATRES.2010.08.033

NCBI Research Coordinators (2013). Database resources of the National Center for Biotechnology Information. *Nucleic Acids Res.* 41, D8–D20. doi: 10.1093/NAR/GKS1189

O'Neill, J. (2014). *Review on antimicrobial resistance. Antimicrobial Resistance: Tackling a crisis for the health and wealth of nations*. London: Wellcome Trust.

Oksanen, J., Simpson, G. L., Blanchet, F. G., Kindt, R., Legendre, P., Minchin, P. R., et al. (2022). *Vegan: Community ecology package*.

Pang, Y., Huang, J., Xi, J., Hu, H., and Zhu, Y. (2016). Effect of ultraviolet irradiation and chlorination on ampicillin-resistant *Escherichia coli* and its ampicillin resistance gene. *Front. Environ. Sci. Eng.* 10:522–530. doi: 10.1007/s11783-015-0779-9

Qin, K., Wei, L., Li, J., Lai, B., Zhu, F., Yu, H., et al. (2020). A review of ARGs in WWTPs: Sources, stressors and elimination. *Chin. Chem. Lett.* 31, 2603–2613. doi: 10.1016/J.CCLET.2020.04.057

Quintela-Baluja, M., Abouelnaga, M., Romalde, J., Su, J. Q., Yu, Y., Gomez-Lopez, M., et al. (2019). Spatial ecology of a wastewater network defines the antibiotic resistance genes in downstream receiving waters. *Water Res.* 162, 347–357. doi: 10.1016/J.WATRES.2019.06.075

Reichert, G., Hilgert, S., Alexander, J., Rodrigues de Azevedo, J. C., Morck, T., Fuchs, S., et al. (2021). Determination of antibiotic resistance genes in a WWTP-impacted river in surface water, sediment, and biofilm: Influence of seasonality and water quality. *Sci. Total Environ.* 768:144526. doi: 10.1016/J.SCITOTENV.2020.144526

Rizzo, L., Manaia, C., Merlin, C., Schwartz, T., Dagot, C., Ploy, M. C., et al. (2013). Urban wastewater treatment plants as hotspots for antibiotic resistant bacteria and genes spread into the environment: A review. *Sci. Total Environ.* 447, 345–360. doi: 10.1016/j.scitotenv.2013.01.032

Sánchez-Osuna, M., Cortés, P., Llagostera, M., Barbé, J., and Erill, I. (2020). Exploration into the origins and mobilization of di-hydrofolate reductase genes and the emergence of clinical resistance to trimethoprim. *Microb. Genomics* 6:mgen000440. doi: 10.1099/mgen.0.000440

Smith, S. D., Choi, J., Ricker, N., Yang, F., Hinsa-Leasure, S., Soupir, M. L., et al. (2022). Diversity of antibiotic resistance genes and transfer elements-quantitative monitoring (DARTE-QM): A method for detection of antimicrobial resistance in environmental samples. *Commun. Biol.* 5:216. doi: 10.1038/s42003-022-03155-9

Staley, C., Kaiser, T., Vaughn, B. P., Graiziger, C., Hamilton, M. J., Kabage, A. J., et al. (2019). Durable long-term bacterial engraftment following encapsulated fecal microbiota transplantation to treat *Clostridium difficile* infection. *mBio* 10, e01586-19. doi: 10.1128/mbio.01586-19

Stokes, H. W., and Gillings, M. R. (2011). Gene flow, mobile genetic elements and the recruitment of antibiotic resistance genes into gram-negative pathogens. *FEMS Microbiol. Rev.* 35, 790–819. doi: 10.1111/j.1574-6976.2011.00273.x

Sun, S., Geng, J., Li, B., Ma, L., Sun, X., Meng, F., et al. (2021). Temporal variations of antibiotic resistance genes in influents and effluents of a WWTP in cold regions. *J. Clean. Prod.* 328:129632. doi: 10.1016/J.JCLEPRO.2021.129632

United Nations Environment Programme (2022). *Environmental dimensions of antimicrobial resistance: Summary for policymakers*. Nairobi: United Nations Environment Programme.

Vogwill, T., and Maclean, R. C. (2015). The genetic basis of the fitness costs of antimicrobial resistance: A meta-analysis approach. *Evol. Appl.* 8, 284–295. doi: 10.1111/eva.12202

Von Wintersdorff, C. J. H., Penders, J., Van Niekerk, J. M., Mills, N. D., Majumder, S., Van Alphen, L. B., et al. (2016). Dissemination of antimicrobial resistance in microbial ecosystems through horizontal gene transfer. *Front. Microbiol.* 7:173. doi: 10.3389/FMICB.2016.00173/BIBTEX

Wu, D., Huang, X.-H., Sun, J.-Z., Graham, D. W., and Xie, B. (2017). Antibiotic resistance genes and associated microbial community conditions in aging landfill systems. *Environ. Sci. Technol.* 51, 12859–12867. doi: 10.1021/acs.est.7b03797

Xia, S., Jia, R., Feng, F., Xie, K., Li, H., Jing, D., et al. (2012). Effect of solids retention time on antibiotics removal performance and microbial communities in an A/O-MBR process. *Bioresour. Technol.* 106, 36–43. doi: 10.1016/J.BIORTECH.2011.11.112

Zaheer, R., Noyes, N., Ortega Polo, R., Cook, S. R., Marinier, E., Van Domselaar, G., et al. (2018). Impact of sequencing depth on the characterization of the microbiome and resistome. *Sci. Rep.* 8:5890. doi: 10.1038/s41598-018-24280-8

Zhang, A. N., Gaston, J. M., Dai, C. L., Zhao, S., Poyet, M., Groussin, M., et al. (2021). An omics-based framework for assessing the health risk of antimicrobial resistance genes. *Nat. Commun.* 12:4765. doi: 10.1038/s41467-021-25096-3

Zhang, M., Chen, S., Yu, X., Vikesland, P., and Pruden, A. (2019). Degradation of extracellular genomic, plasmid DNA and specific antibiotic resistance genes by chlorination. *Front. Environ. Sci. Eng.* 13:38. doi: 10.1007/s11783-019-1124-5

Zhou, Z.-C., Zheng, J., Wei, Y.-Y., Chen, T., Dahlgren, R. A., Shang, X., et al. (2017). Antibiotic resistance genes in an urban river as impacted by bacterial community and physicochemical parameters. *Environ. Sci. Pollut. Res.* 24, 23753–23762. doi: 10.1007/s11356-017-0032-0

Zhu, Y., Wang, Y., Zhou, S., Jiang, X., Ma, X., and Liu, C. (2018). Robust performance of a membrane bioreactor for removing antibiotic resistance genes exposed to antibiotics: Role of membrane foulants. *Water Res.* 130, 139–150. doi: 10.1016/J.WATRES.2017.11.067

frontiers | Frontiers in Microbiology

TYPE Original Research
PUBLISHED 26 April 2023
DOI 10.3389/fmicb.2023.1130708



OPEN ACCESS

EDITED BY
Tao Li,
Shanghai Veterinary Research Institute (CAAS), China

REVIEWED BY
Tao He,
Jiangsu Academy of Agricultural Sciences (JAAS), China
Ruichao Li,
Yangzhou University, China

*CORRESPONDENCE
Li-Na Qin
✉ qinlna@mail.sysu.edu.cn
Bin Yan
✉ yanbin222@foxmail.com
Min Dai
✉ daimin1015@cmc.edu.cn

†These authors have contributed equally to this work

‡PRESENT ADDRESS
Li-Na Qin,
Guangdong Province Translational Forensic Medicine Engineering Technology Research Center, Sun Yat-sen University, Guangzhou, China

SPECIALTY SECTION
This article was submitted to Antimicrobials, Resistance and Chemotherapy, a section of the journal Frontiers in Microbiology

RECEIVED 23 December 2022
ACCEPTED 27 March 2023
PUBLISHED 26 April 2023

CITATION
Yang Y, He R, Wu Y, Qin M, Chen J, Feng Y, Zhao R, Xu L, Guo X, Tian G-B, Dai M, Yan B and Qin L-N (2023) Characterization of two multidrug-resistant *Klebsiella pneumoniae* harboring tigecycline-resistant gene *tet*(X4) in China.
*Front. Microbiol.* 14:1130708.
doi: 10.3389/fmicb.2023.1130708



# Characterization of two multidrug-resistant *Klebsiella pneumoniae* harboring tigecycline-resistant gene *tet*(X4) in China

Yanxian Yang[1,2,3†], Ruowen He[1,2,3,4†], Yiping Wu[1,2,3†], Mingyang Qin[5,6†], Jieyun Chen[1,2,3], Yu Feng[1,2,3], Runping Zhao[7], Lei Xu[7], Xilong Guo[1,2,3], Guo-Bao Tian[1,2,3], Min Dai[7]*, Bin Yan[1,2,8]* and Li-Na Qin[9,10]*‡

[1]Program in Pathobiology, the Fifth Affiliated Hospital, Zhongshan School of Medicine, Sun Yat-sen University, Guangdong, China, [2]Advanced Medical Technology Center, The First Affiliated Hospital, Zhongshan School of Medicine, Sun Yat-sen University, Guangzhou, China, [3]Key Laboratory of Tropical Diseases Control, Ministry of Education, Sun Yat-sen University, Guangzhou, China, [4]Microbiome Medicine Center, Department of Laboratory Medicine, Zhujiang Hospital, Southern Medical University, Guangzhou, China, [5]School of Basic Medical Sciences, Xinxiang Medical University, Xinxiang, China, [6]School of Public Health, Shandong University, Jinan, China, [7]School of Laboratory Medicine, Chengdu Medical College, Chengdu, China, [8]Department of Neonatal Surgery, Guangzhou Women and Children's Medical Center, Guangzhou, China, [9]Faculty of Forensic Medicine, Zhongshan School of Medicine, Sun Yat-sen University, Guangzhou, China, [10]Guangdong Province Translational Forensic Medicine Engineering Technology Research Center, Sun Yat-sen University, Guangzhou, China

**Objectives:** Tigecycline is recognized as one of the last-line antibiotics to treat serious bacterial infection caused by carbapenem-resistant *Klebsiella pneumoniae* (CRKP). The plasmid-borne gene *tet*(X4) mediates high resistance to tigecycline. However, the prevalence and genetic context of *tet*(X4) in *K. pneumoniae* from various sources are not fully understood. Here, we investigated the prevalence of *tet*(X4)-positive *K. pneumoniae* and characterized the genetic context of *tet*(X4)-bearing plasmids in *K. pneumoniae* isolates.

**Methods:** Polymerase chain reaction (PCR) was used to detect the *tet*(X4) gene. The transferability of the *tet*(X4)-carrying plasmids was tested by conjugation assays. The *Galleria mellonella* infection model was used to test virulence of *tet*(X4)-positive strains. Whole-genome sequencing and genome-wide analysis were performed to identify the antimicrobial resistance and the virulence genes, and to clarify the genetic characteristics of the *tet*(X4)-positive isolates.

**Results:** Among 921 samples, we identified two *tet*(X4)-positive *K. pneumoniae* strains collected from nasal swabs of two pigs (0.22%, 2/921). The two *tet*(X4)-positive isolates exhibited high minimum inhibitory concentrations to tigecycline (32–256mg/L) and tetracycline (256mg/L). The plasmids carrying the *tet*(X4) gene can transfer from the donor strain *K. pneumoniae* to the recipient strain *Escherichia coli* J53. Genetic analysis of the complete sequence of two *tet*(X4)-carrying plasmids pTKPN_3-186k-tetX4 and pTKPN_8-216k-tetX4 disclosed that the *tet*(X4) gene was flanked by delta IS*CR2* and IS*1R*, which may mediate the transmission of the *tet*(X4) gene.

**Conclusion:** The prevalence of *tet*(X4)-positive *K. pneumoniae* among different sources was low. IS*CR2* and IS*1R* may contribute to the horizontal transfer of *tet*(X4) gene. Effective measures should be taken to prevent the transmission of *tet*(X4)-producing *K. pneumoniae* in humans or animals.

KEYWORDS

*Klebsiella pneumoniae*, tigecycline resistance, *tet*(X4), horizontal transfer, swine

# Introduction

*Klebsiella pneumoniae* is a common cause of antimicrobial-resistant opportunistic infections in hospitalized patients (Wyres et al., 2020). In clinical, *K. pneumoniae* can cause a variety of infection diseases, including bacteremia, urinary tract infections, pneumonia, and liver abscesses (Hansen et al., 1998; Siu et al., 2012). In recent years, carbapenem resistant *K. pneumoniae* (CRKP) infection rates have increased alarmingly (Low et al., 2018). Tigecycline has been regarded as one of the "last resort" antimicrobials to fight against CRKP (Seifert et al., 2018).

Tigecycline is the first generation of glycylcycline, which has been used since 2005. It is one of the last choice of treatment for serious infection, especially those caused by extensively drug-resistant Enterobacteriaceae (Sun et al., 2019). Shortly after the first usage, a multi-drug resistant (MDR) *K. pneumoniae* strain (reduced tigecycline sensitivity, MIC = 4 μg/ml) was isolated in a hospital, significantly compromising the efficacy of tigecycline (Ruzin et al., 2005). To date, there are several known mechanisms associated with tigecycline resistance in *K. pneumoniae*, including the enhanced expression of resistance–nodulation–cell division (RND)-type efflux pumps such as AcrAB-TolC and OqxAB, mutations in the ribosomal S10 protein (encoded by *rpsJ* and *lon* genes; Ruzin et al., 2005; Villa et al., 2014; He et al., 2015; Fang et al., 2016), acquisition of plasmid-mediated *tmexCD1-toprJ1* efflux pump (Lv et al., 2020), mutation of *tet*(A) gene (Du et al., 2018).

In recently, four plasmid-borne *tet*(X) variants mediating tigecycline resistance [*tet*(X3), *tet*(X4), *tet*(X5), and *tet*(X6)] have been detected in various species of bacteria obtained from animals, animal-derived foods, humans and environment samples in China (He et al., 2019; Chen et al., 2020; Dong et al., 2022). Among these *tet*(X) variants, *tet*(X4) gene is widely identified in *E. coli* isolates from food animals (Li Y. et al., 2021; Yu et al., 2021; Wang et al., 2022). To date, only a few studies have reported *tet*(X4)-positive *K. pneumoniae* isolated from pork and clinical sources (Li et al., 2022; Liu et al., 2022). Overall, the epidemiology and characteristics of *tet*(X)s-positive *K. pneumoniae* isolates are not fully understood. Here, we investigated the prevalence of *tet*(X) genes in *K. pneumoniae* isolates and further described the *tet*(X4)-harboring plasmids in *K. pneumoniae* isolates.

# Materials and methods

## Sample collection and identification of *tet*(X)s-positive *Klebsiella pneumoniae* strains

To determine the prevalence of *tet*(X)s-positive *K. pneumoniae* strains in animal-associated and clinical samples, 921 samples from pigs and humans in China were collected (Supplementary Table S1). Specifically, a total of 590 samples from a pig farm (56 swine nasal swabs; Guangdong province, China) and a swine slaughter house (419 swine nasal swabs, 67 swine anal swabs, and 48 skin swabs of workers; Guangdong province, China) were collected from October to November 2020. Besides, 184 human anal swab specimens including 171 hospitalized patients and 13 healthy individuals from hospital A collected in 2019 were also included. All samples were subjected to selection on brain heart infusion (BHI) plates containing tigecycline (2 mg/L). After incubation at 37°C for 16–18 h, the tigecycline-resistant colonies were selected. Then detection of the *tet*(X) genes was carried out by PCR using specific primers in Supplementary Table S2. Species identification was achieved by Matrix-assisted laser desorption/ionization time-of-flight mass spectrometry (MALDI-TOF MS). In addition, 147 clinical nonduplicate *K. pneumoniae* isolates were collected from bloodstream samples in four hospitals (named as B, C, D, and E) located in Guangdong province in China during the period 2008–2018, and all strains were tested for the presence of *tet*(X) genes.

## Antimicrobial susceptibility testing

The susceptibility to tetracycline (TET), chloramphenicol (CHL), ciprofloxacin (CIP), ceftazidime (CAZ), gentamicin (GEN), amikacin (AMK), cefotaxime (CTX), trimethoprim-sulfamethoxazole (SXT), imipenem (IMP), ampicillin (AMP), fosfomycin (FOS), and rifampin (RIF) was determined by the agar dilution method according to the Clinical and Laboratory Standards Institute (CLSI) guidelines (CLSI, 2019). MICs of MICs of tigecycline (TGC) and colistin (CT) were determined by the broth dilution method according to the guidelines of EUCAST (2021). The *E. coil* ATCC25922 served as quality control.

## Plasmid conjugation

Conjugation experiments were performed to test the transferability of the *tet*(X4)-harboring plasmids, using a sodium azide resistant *E. coli* J53 as the recipient. Briefly, a culture of *tet*(X4)-producing isolates and the recipient strain *E. coli* J53 were mixed (ratio of 1:9) in BHI broth and subjected to incubation for 6–8 h. The mixture was then spread on BHI agar plates containing 100 mg/L sodium azide and 1 mg/L tigecycline to select transconjugants that had acquired the *tet*(X4)-harboring plasmid. Colonies that grew on selective plates after incubation for 16–24 h at 37°C were further confirmed by PCR and Sanger sequencing.

## *Galleria mellonella* infection model

The *Galleria mellonella* infection model was used to test virulence and pathogenesis of *tet*(X4)-positive *K. pneumoniae* strains, which was carried out as described previously with slight modifications (Buckner et al., 2018). Overnight cultures of *K. pneumoniae* strains were washed with phosphate-buffered saline (PBS) and further adjusted with PBS

to concentrations of $1 \times 10^6$ CFU/ml. The larvae were injected with 10 uL of bacterial solution and negative control groups were inoculated with 10 uL of PBS, the hvKP4 *K. pneumoniae* strain was used as the hypervirulent control (Gu et al., 2018). Then the larvae were incubated at 37°C in the dark and the survival rates of the larvae were recorded. Kaplan–Meier survival curves were plotted using GraphPad Prism, and the log rank (Mantel-Cox) test was used to analyze the significant difference ($p < 0.05$) of the survival rates in *G. mellonella* infection model.

## Genome sequencing and bioinformatics analysis

Genomic DNA of *tet*(X)s-positive *K. pneumoniae* isolates was extracted using the Qiagen Blood & Tissue kit (Qiagen, Hilden, Germany). DNA libraries were constructed with 350-bp paired-end fragments and sequenced using an Illumina HiSeq 2000 platform. In addition, the PacBio Sequel System was performed to long-read sequencing the TKPN_8 strain. The sequencing reads were assembled into contigs using SPAdes version 3.10 (Bankevich et al., 2012). Genome sequences were annotated using Prokka (version 1.13.3; Seemann, 2014). Multilocus sequence typing (MLST) of isolates was conducted using MLST v2.11 based on assembled contigs (Raisanen et al., 2020). The core genes of bacterial genomes were extracted and aligned using Roary (Page et al., 2015). RAxML v8.2.10 was used to construct a maximum likelihood phylogeny of the strains (Stamatakis, 2006), then the phylogenetic tree was visualized by iTOL (Letunic and Bork, 2016). The SNP (sequence-based) and core-genome-based MLST (cgMLST) strategies on BacWGSTdb 2.0 were used for source tracking bacterial pathogens, and the phylogenetic tree was generated and visualized by Grapetree (Feng et al., 2021). Capsule (K) loci was identified using Kaptive (Wick et al., 2018). To obtain the complete sequence of *tet*(X)s-carrying plasmid, we combined the sequencing data from the genomic DNA and the plasmids, and predicted gaps were closed by PCR and Sanger sequencing using primers listed in Supplementary Table S3. Plasmid replicons, insertion sequences, antimicrobial resistance determinants and virulence factors were determined using online tools.[1] Easyfig was used to visualize the genetic comparisons.

# Results

## Identification of *Klebsiella pneumoniae* isolates harboring *tet*(X4)

In this study, the prevalence of *tet*(X)s-positive *K. pneumoniae* was 0.22% (2/921). The two *tet*(X4)-carrying strains, designated as TKPN_3 and TKPN_8, were collected from different swine nasal swabs (one was isolated from the pig farm; the other was isolated from a swine slaughter house). No other *tet*(X) variants were detected in *K. pneumoniae* strains.

The MLST analysis declared that *K. pneumoniae* TKPN_3 and TKPN_8 belong to ST35 and ST193, respectively (Table 1). To conduct the phylogenetic analysis of TKPN_3 and TKPN_8, the whole-genome sequencing data of 45 *K. pneumoniae* strains were download from NCBI database, including 40 *tet(X4)*-negative strains of ST35 and ST193, and five *tet(X4)*-positive strains belonging to ST727, ST43, ST1418, ST35, and ST327. A phylogenetic tree for 47 *K. pneumoniae* strains based on SNPs of core genomes was constructed. It showed that the *K. pneumoniae* strains were clustered into three distinct clusters, and *tet(X4)*-positive strains were dispersed on different branches, all of which were isolated from China between 2019 and 2021 (Figure 1). For source tracking bacterial pathogens, the genome sequences of TKPN_3 and TKPN_8 were submitted to BacWGSTdb and none close strains were found based on SNP (sequence-based) strategy. The core-genome-based MLST (cgMLST) analysis showed that 86 and 8 strains were, respectively, closed to TKPN_3 and TKPN_8, but had more than 340 different alleles (Supplementary Figure S1). In order to explore the evolution and transmission of the *tet*(X)s-positive *K. pneumoniae*, more sequencing data may be needed for phylogenetic analysis.

## The antimicrobial resistance phenotype and genotype of *tet*(X4)-positive *Klebsiella pneumoniae*

*Klebsiella pneumoniae* TKPN_3 and TKPN_8 were resistant to tigecycline, tetracycline, rifampin, chloramphenicol and ampicillin, but were susceptible to gentamicin, imipenem, amikacin, fosfomycin and colistin. TKPN_3 and TKPN_8 showed resistance to tigecycline with MIC of 256 and 32 mg/L, respectively. In addition, TKPN_3 was also resistant to ciprofloxacin, ceftazidime, cefotaxime and trimethoprim-sulfamethoxazole, while TKPN_8 was susceptible to them (Table 1).

Except for the *tet*(X4) gene, WGS data revealed that TKPN_3 harbored other 18 antibiotic-resistant genes (ARGs), including three quinolone resistance genes (*oqxB*, *oqxA*, *qnrS1*), two β-lactams resistance genes ($bla_{\text{CTX-M-3}}$, $bla_{\text{SHV-33}}$), one sulphonamide resistance gene (*sul2*), one trimethoprim resistance gene (*dfrA27*), one rifampicin resistance gene (*arr-3*), one fosfomycin resistance gene (*fosA6*), one macrolide resistance gene [*mph*(A)], one tetracycline resistance gene [*tet*(A)], five aminoglycoside resistance genes [*aac(6′)-Ib-cr*, *aadA16*, *aph(3″)-Ib*, *aph(6)-Id*, *ant(3″)-Ia*], one chloramphenicol resistance gene (*floR*) and one lincomycin resistance gene [*lnu*(G)]. In the isolate TKPN_8, multiple resistance genes were also identified, including *tet*(X4) along with other 11 ARGs including three quinolone resistance gene (*oqxB*, *oqxA*, *qnrS1*), one β-lactam resistance gene ($bla_{\text{SHV-61}}$), one sulphonamide resistance gene (*sul2*), one fosfomycin resistance gene (*fosA6*), one tetracycline resistance gene [*tet*(A)], two aminoglycoside resistance genes [*aph(3″)-Ib*, *aph(6)-Id*], chloramphenicol resistance gene (*floR*) and one lincomycin resistance gene [*lnu*(G); Table 1]. In general, these two *tet*(X4)-positive *K. pneumoniae* strains have similar antimicrobial resistance phenotype and genotype. Moreover, TKPN_3 showed higher level of tigecycline resistance compared with TKPN_8, and correspondingly, mutations involving regulators of multidrug efflux pump were also found in strain TKPN_3. Amino acid mutations were identified in RamR at T141I and in Lon at A299T.

1 https://cge.cbs.dtu.dk/services/

10.3389/fmicb.2023.1130708

TABLE 1 Characteristics of the two *tet*(X4)-positive *Klebsiella pneumoniae* isolates.

| | | | Transconjugant | | Recipient |
|---|---|---|---|---|---|
| Characteristics | *K. pneumoniae* TKPN_3 | *K. pneumoniae* TKPN_8 | *E. Coli* J53-pTKPN_3-186k-tetX4 | *E. coli* J53-pTKPN_8-216k-tetX4 | *E. coli* J53 |
| Source | Pig farm | Swine slaughter house | / | / | This lab |
| Isolation site | Swine nasal swab | Swine nasal swab | / | / | / |
| Year | 2020 | 2020 | / | / | / |
| MLST | 35 | 193 | / | / | / |
| Capsular serotypes | KL71 | KL63 | / | / | / |
| Plasmid replicon type | ColRNAI, IncFIA(HI1), IncFIB(K), IncFIB(pKPHS1), IncFII, IncHI1A, IncHI1B(R27), IncQ1, IncQ2, IncX4 | ColRNAI, IncFIA(HI1), IncFIB(K), IncFII, IncHI1A, IncHI1B(R27), IncR | IncHI1B(R27), IncHI1A, IncFIA(HI1) | IncHI1B(R27), IncHI1A, IncFIA(HI1) | / |
| MICs (mg/L) | | | | | |
| Tigecycline | 256 | 32 | 32 | 32 | 0.25 |
| Tetracycline | >256 | 256 | 128 | 128 | ≤1 |
| Chloramphenicol | >128 | >128 | 128 | 128 | 8 |
| Ciprofloxacin | 4 | 0.5 | ≤0.03 | ≤0.03 | ≤0.03 |
| Colistin | 0.5 | 0.5 | 0.25 | 0.25 | ≤0.125 |
| Ceftazidime | 32 | ≤1 | ≤1 | ≤1 | ≤1 |
| Gentamicin | 2 | ≤1 | ≤1 | ≤1 | ≤1 |
| Cefotaxime | 64 | ≤1 | ≤1 | ≤1 | ≤1 |
| Trimethoprim-Sulfamethoxazole | >64 | ≤0.25 | ≤0.25 | ≤0.25 | ≤0.25 |
| Fosfomycin | ≤16 | ≤16 | ≤16 | ≤16 | ≤0.125 |
| Amikacin | 2 | ≤1 | 2 | 2 | ≤1 |
| Ampicillin | >256 | 64 | 8 | 8 | ≤0.5 |
| Rifampin | >128 | 16 | 16 | 16 | ≤0.5 |
| Imipenem | 1 | ≤0.25 | 0.5 | 0.5 | 0.5 |
| Resistance genes | | | | | |
| Glycyrylcyclin | *tet*(X4) | *tet*(X4) | *tet*(X4) | *tet*(X4) | / |
| Aminoglycoside | *aac(6′)-Ib-cr*, *aadA16*, *aph(3″)-Ib*, *aph(6)-Id*, *ant(3″)-Ia* | *aph(3″)-Ib*, *aph(6)-Id* | / | / | / |
| Beta-lactam | $bla_{CTX-M-3}$, $bla_{SHV-33}$ | $bla_{SHV-61}$ | / | / | / |
| Fosfomycin | *fosA6* | *fosA6* | / | / | / |
| Macrolide | *mph*(A) | / | / | / | / |
| Phenicol | *floR* | *floR* | / | / | / |
| Quinolone | *oqxB*, *oqxA*, *qnrS1* | *oqxB*, *oqxA*, *qnrS1* | / | / | / |
| Rifampicin | *ARR-3* | / | / | / | / |
| Sulphonamide | *sul2* | *sul2* | / | / | / |
| Tetracycline | *tet*(A) | *tet*(A) | / | / | / |
| Lincosamide | *lnu*(G) | *lnu*(G) | / | / | / |
| Trimethoprim | *dfrA27* | / | / | / | / |

MLST, multilocus sequence typing.

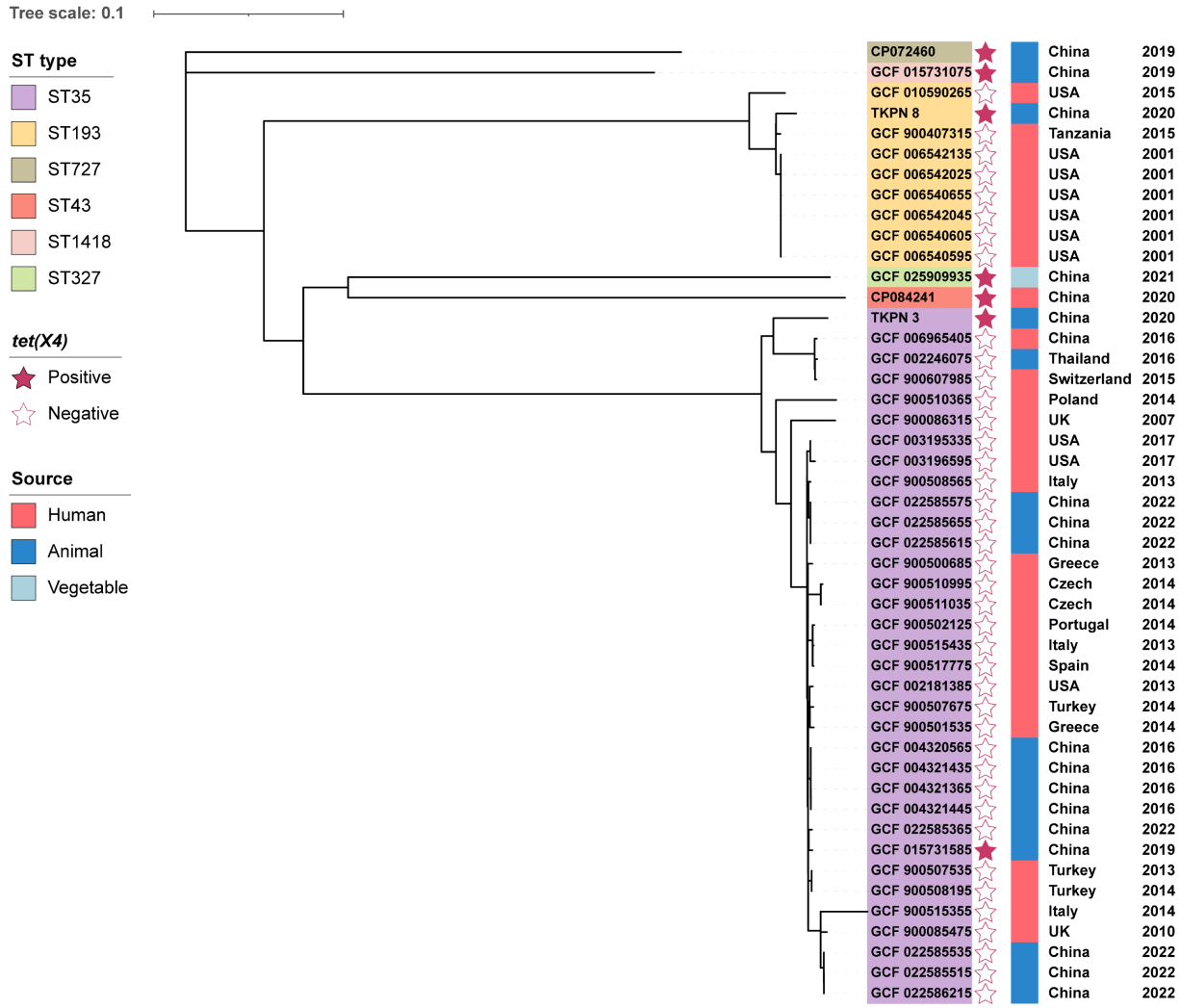


FIGURE 1
Phylogenetic analysis of 47 *K. pneumoniae* from different sources and their basic characterization. The phylogenetic tree was constructed by RAxML based on SNPs of core genomes.

## The virulence phenotype and genotype in *Klebsiella pneumoniae* TKPN_3 and TKPN_8

In addition to resistance genes, a total of 78 different virulence factors were identified among these two *tet*(X4) positive isolates. These genes include various siderophores such as enterobactin (encoded by *entABCEF*, *fepABCDG*, *fes*, and *ybdA* genes), aerobactin (encoded by *iucABCD* and *iutA* genes) and salmochelin (encoded by *iroE* gene). Moreover, the gene clusters *tssABCD* and *tssFGHIJKLM* encoding type VI secretion system, which was proved to be beneficial to bacterial competition, cell invasion, type-1 fimbriae expression and *in vivo* colonization in *K. pneumoniae* (Hsieh et al., 2019), were detected in TKPN_3 and TKPN_8. In addition, the capsular serotypes of the TKPN_3 and TKPN_8 strains were identified as KL71 and KL63, respectively. Then the virulence of two strains was demonstrated by *Galleria mellonella* infection model. After 12 h post-infection, the survival rate of *G. mellonella* larvaes injected with TKPN_3 and TKPN_8 was 50%. Overall, no difference in survival was observed for *G. mellonella* infected by TKPN_3 and TKPN_8 compared with HvKP4 (TKPN_3 vs. HvKP4, $p = 0.606$; TKPN_8 vs. HvKP4, $p = 0.326$; Supplementary Figure S2).

## The transferability of *tet*(X4)-harboring plasmid from *Klebsiella pneumoniae*

To further determine the transferability of *tet*(X4) gene, conjugation assays were conducted. It showed that the *tet*(X4)-carrying plasmids form TKPN_3 and TKPN_8 could be successfully transferred from *K. pneumoniae* to *E. coli* J53. The two *tet*(X4)-harboring plasmids were denoted as pTKPN_3-186k-tetX4 and pTKPN_8-216k-tetX4. The conjugation frequencies of pTKPN_3-186k-tetX4 and pTKPN_8-216k-tetX4 were $(1.0 \pm 0.1) \times 10^{-4}$ and $(5.4 \pm 0.7) \times 10^{-5}$ cells per recipient, respectively. Compared with the recipient strain *E. coli* J53, the MICs of the transconjugants J53/pTKPN_3-186k-tetX4 and J53/pTKPN_8-216k-tetX4 for tigecycline and tetracycline increased by 128-fold, respectively.

## Genetic characteristics of *tet*(X4) in pTKPN_3-186k-tetX4 and pTKPN_8-216k-tetX4

The genetic features of *tet*(X4)-carrying plasmid pTKPN_3-186k-tetX4 of TKPN_3 was analyzed in depth. To obtain the complete sequence of this plasmid, the sequencing data of the genomic DNA and the plasmids DNA were combined, and predicted gaps were closed by PCR and Sanger sequencing. pTKPN_3-186k-tetX4 was a 186,211 bp plasmid and encoded 218 predicted open reading frames (ORFs). The backbone of the *tet*(X4)-carrying plasmid pTKPN_3-186k-tetX4 showed a typical mosaic structure with multiple replicon types including IncHI1B(R27), IncHI1A and IncFIA (HI1). The genes involved in conjugation were identified including *traC*, *traD*, *traG*, *traI*, *traJ*, *traU*, and *mobI*. The *tet*(X4) gene and another five antimicrobial resistance genes $bla_{TEM-1B}$, *ant(3″)-Ia*, *qnrS1*, *floR*, and *lnu*(G) were found in pTKPN_3-186k-tetX4. The mobile element IS*1R* (IS*1* family, 768 bp) was located upstream of *tet*(X4) and delta IS*CR2* (IS*91* family, 977 bp) was found in downstream of *tet*(X4), which may contribute to the transmission of the *tet*(X4) gene (Figure 2). Additionally, two complete insertion sequence IS*26* and two truncated transposons Tn*2* were identified downstream of *tet*(X4) in pTKPN_3-186k-tetX4. The pTKPN_3-186k-tetX4 shared a similar plasmid backbone (99% coverage and 100% identity) against p1919D62-1 (GenBank accession number: CP046007.1), which isolated from a swine *E.coli* strain 1919D62 in China. The other two plasmids with high similarity with our plasmid were pSZ6R-tetX4 (GenBank accession number: MW940627.1) and pAB4-4-tetX4 (GenBank accession number: MW940615.1). The two plasmids pSZ6R-tetX4 and pAB4-4-tetX4 were isolated from *Citrobacter* sp. and *Klebsiella sp*. strains, respectively, (Figure 2).

The complete sequence of another *tet*(X4)-positive plasmid pTKPN_8-216k-tetX4 was obtained by long-read sequencing. pTKPN_8-216k-tetX4 was 216,814 bp in size and also belongs to an IncHI1B(R27)/IncHI1A/IncFIA(HI1) type hybrid plasmid. pTKPN_8-216k-tetX4 exhibited a high similarity (74% coverage, 100% identity) with pTKPN_3-186k-tetX4, in particular, it had an additional ~30 kp fragment. This fragment was similar to pCY814036-iucA (GenBank accession number: CP093152.1; Figure 2). pCY814036-iucA was a multi-drug resistant and hypervirulent hybrid plasmid and isolated from a *K. pneumoniae* strain in China. pTKPN_8-216k-tetX4 also carried the conjugation-related genes *traC*, *traD*, *traG*, *traI*, *traJ*, *traU*, and *mobI*. In addition to *tet(X4)* gene, *aph(3″)-Ib*, *aph(6)-Id*, *floR*, *sul2* and *tet(A)* were identified in pTKPN_8-216k-tetX4. It was worth noting that similar to pTKPN_3-186k-tetX4, *tet(X4)* gene was flanked by mobile elements IS*1R* and IS*CR2* in pTKPN_8-216k-tetX4 (Figure 2).

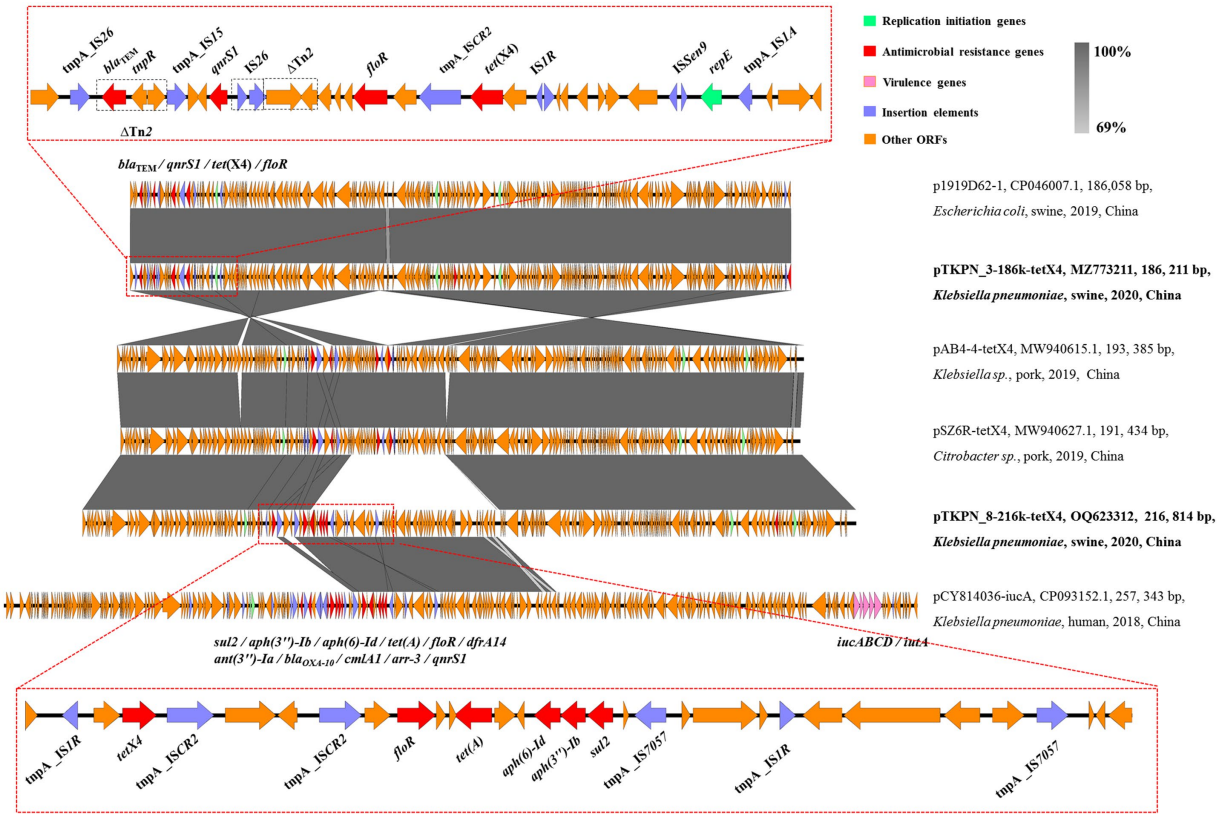


FIGURE 2
Structure analysis of plasmids pTKPN_3-186k-tetX4 and pTKPN_8-216k-tetX4. Major structural features of pTKPN_3-186k-tetX4 and pTKPN_8-216k-tetX4 were compared with those of plasmids p1919D62-1 (GenBank accession no. CP046007.1), pAB4-4-tetX4 (GenBank accession no. MW940615.1), pSZ6R-tetX4 (GenBank accession no. MW940627.1), and pCY814036-iucA (GenBank accession no. CP093152.1). Gray shading indicates shared regions with a high degree of homology (>69%). Red and pink represent the antimicrobial resistance genes and virulence genes, respectively, and purple is the insertion elements.

## Discussion

To date, the plasmid-borne *tet*(X) genes have been identified in >15 different Gram-negative species, with *tet*(X4)-positive *E. coli* isolated from food-producing animals being the most common (He et al., 2019; Sun et al., 2019). The *tet*(X4)-carrying *K. pneumoniae* strains has so far been rarely reported. A recently investigation showed 58 *tet*(X4)-positive strains were isolated from 139 fresh pork samples and the most strains were identified as *E. coli* (55/58), only two were *K. pneumoniae* (Li R. et al., 2021). In this study, two *tet*(X4)-harbouring tigecycline resistant *K. pneumoniae* were detected from swine nasal swabs in China. According to previous study, the prevalence of *tet*(X) genes in *K. pneumoniae* was significantly lower than in *Escherichia coli* (3.84%, 95/2475) and *Acinetobacter* spp. (5.02%, 193/3846; Chen et al., 2020; Sun et al., 2020). Although the *tet*(X4) gene was present in *K. pneumoniae* at a low prevalence, the TKPN_3 and TKPN_8 strains also contained many important virulence factors (Hsieh et al., 2019; Wang et al., 2020), such as enterobactin and aerobactin, and showed high virulence phenotype. Given the harmfulness of *K. pneumoniae* in clinical infections, the emergence of a *tet*(X4)-positive strain should be alarmed.

Until now, *tet*(X4)-bearing plasmids ranged from 9 to 315 kb and were categorized as ColE2-like, IncQ, IncX1, IncX4, IncA/C2, IncFII, IncFIB, IncI1, and hybrid plasmids with different replicons (Li R. et al., 2020), which suggested that *tet*(X4) gene could be captured by a range of mobile genetic elements circulating among bacterial strains. Moreover, the mobile elements, particularly IS*CR2* and IS*1R*, could assist the integration and spread of *tet*(X4) gene between different plasmids. The host range of the *tet*(X4) gene is likely to be further expanded. According to *tet*(X4)-bearing plasmid type distribution, IncFIB(K)/IncFIA(HI1)/IncX1 hybrid plasmids were the most widespread in the sequenced plasmids (Li R. et al., 2020). In this study, both pTKPN_3-186k-tetX4 and pTKPN_8-216k-tetX4 belonged to IncHI1B(R27)/IncHI1A/IncFIA(HI1) hybrid plasmid type, which have been reported in several different species such as *E. coli*, *Salmonella enterica* and *Citrobacter* sp. Correspondingly, pTKPN_3-186k-tetX4 and pTKPN_8-216k-tetX4 was confirmed to be able to transfer from *K. pneumoniae* to *E. coli*. In contrast, IncFII-type plasmid carrying *tet*(X4) in *K. pneumoniae* was found to be non-self-transferable and could be only co-transferred with the help of other conjugative plasmids (Zhai et al., 2022). It is possible that pTKPN_3-186k-tetX4-like plasmids will become more widespread in the near future.

Worrisomely, the *tet*(X)-mediated tigecycline resistance has been detected in carbapenem- and colistin-resistant *Acinetobacter* spp. and *Escherichia* spp. strains (Chen et al., 2020; Li Y. et al., 2020). Future efforts are needed to prevent and monitor the emergence of *tet*(X)-mediated tigecycline- and carbapenem- resistant *K. pneumoniae* from all related sectors. Our data contributes to understanding of the genetic characteristic of *tet*(X4) and their transferabilities in *K. pneumoniae*.

## Data availability statement

The names of the repository/repositories and accession number(s) can be found at: https://www.ncbi.nlm.nih.gov/genbank/, MZ773211 and OQ623312.

## Author contributions

L-NQ, BY, and MD: conceptualization. YY and RH: data curation. YY, RH, YW, and MQ: investigation. YY, RH, YW, MQ, JC, YF, RZ, LX, and XG: methodology. G-BT, L-NQ, BY, and MD: resources. YY and RH: visualization. YY, RH, YW, and MQ: writing original draft. L-NQ, BY, MD, and G-BT: writing, review and editing. All authors contributed to the article and approved the submitted version.

## Funding

This work was supported by the National Natural Science Foundation of China (grant number 82061128001 and 81830103 to G-BT), Guangdong Natural Science Foundation (grant number 2017A030306012 to G-BT), National Key Research and Development Program (grant number 2017ZX10302301 to G-BT), Project of High-level Health Teams of Zhu hai in 2018 (The Innovation Team for Antimicrobial Resistance and Clinical Infection to G-BT), and the Project 111 (grant number B12003 to G-BT).

## Conflict of interest

The authors declare that the research was conducted in the absence of any commercial or financial relationships that could be construed as a potential conflict of interest.

## Publisher's note

All claims expressed in this article are solely those of the authors and do not necessarily represent those of their affiliated organizations, or those of the publisher, the editors and the reviewers. Any product that may be evaluated in this article, or claim that may be made by its manufacturer, is not guaranteed or endorsed by the publisher.

## Supplementary material

The Supplementary material for this article can be found online at: https://www.frontiersin.org/articles/10.3389/fmicb.2023.1130708/full#supplementary-material

## References

Bankevich, A., Nurk, S., Antipov, D., Gurevich, A. A., Dvorkin, M., Kulikov, A. S., et al. (2012). SPAdes: a new genome assembly algorithm and its applications to single-cell sequencing. *J. Comput. Biol.* 19, 455–477. doi: 10.1089/cmb.2012.0021

Buckner, M. M. C., Saw, H. T. H., Osagie, R. N., Mcnally, A., Ricci, V., Wand, M. E., et al. (2018). Clinically relevant plasmid-host interactions indicate that transcriptional and not genomic modifications ameliorate fitness costs of

*Klebsiella pneumoniae* carbapenemase-carrying plasmids. *MBio* 9, e02303–e02317. doi: 10.1128/mBio.02303-17

Chen, C., Cui, C. Y., Yu, J. J., He, Q., Wu, X. T., He, Y. Z., et al. (2020). Genetic diversity and characteristics of high-level tigecycline resistance *Tet(X)* in Acinetobacter species. *Genome Med.* 12:111. doi: 10.1186/s13073-020-00807-5

CLSI (2019). *Performance standards for antimicrobial susceptibility testing, 29th*. Annapolis Junction, MD: Clinical and Laboratory Standards Institute.

Dong, N., Zeng, Y., Cai, C., Sun, C., Lu, J., Liu, C., et al. (2022). Prevalence, transmission, and molecular epidemiology of *tet(X)*-positive bacteria among humans, animals, and environmental niches in China: an epidemiological, and genomic-based study. *Sci. Total Environ.* 818:151767. doi: 10.1016/j.scitotenv.2021.151767

Du, X., He, F., Shi, Q., Zhao, F., Xu, J., Fu, Y., et al. (2018). The rapid emergence of tigecycline resistance in $bla_{KPC-2}$ harboring *Klebsiella pneumoniae*, as mediated in vivo by mutation in *tetA* during tigecycline treatment. *Front. Microbiol.* 9:648. doi: 10.3389/fmicb.2018.00648

EUCAST (2021). *European committee on antimicrobial susceptibility testing breakpoint tables for interpretation of MICs and zone diameters European committee on antimicrobial susceptibility testing breakpoint tables for interpretation of MICs and zone diameters, version 11.0*. Sweden: EUCAST.

Fang, L., Chen, Q., Shi, K., Li, X., Shi, Q., He, F., et al. (2016). Step-wise increase in tigecycline resistance in *Klebsiella pneumoniae* associated with mutations in *ramR*, lon and rpsJ. *PLoS One* 11:e0165019. doi: 10.1371/journal.pone.0165019

Feng, Y., Zou, S., Chen, H., Yu, Y., and Ruan, Z. (2021). BacWGSTdb 2.0: a one-stop repository for bacterial whole-genome sequence typing and source tracking. *Nucleic Acids Res.* 49, D644–D650. doi: 10.1093/nar/gkaa821

Gu, D., Dong, N., Zheng, Z., Lin, D., Huang, M., Wang, L., et al. (2018). A fatal outbreak of ST11 carbapenem-resistant hypervirulent *Klebsiella pneumoniae* in a Chinese hospital: a molecular epidemiological study. *Lancet Infect. Dis.* 18, 37–46. doi: 10.1016/s1473-3099(17)30489-9

Hansen, D. S., Gottschau, A., and Kolmos, H. J. (1998). Epidemiology of *Klebsiella bacteraemia*: a case control study using Escherichia coli bacteraemia as control. *J. Hosp. Infect.* 38, 119–132. doi: 10.1016/s0195-6701(98)90065-2

He, F., Fu, Y., Chen, Q., Ruan, Z., Hua, X., Zhou, H., et al. (2015). Tigecycline susceptibility and the role of efflux pumps in tigecycline resistance in KPC-producing *Klebsiella pneumoniae*. *PLoS One* 10:e0119064. doi: 10.1371/journal.pone.0119064

He, T., Wang, R., Liu, D., Walsh, T. R., Zhang, R., Lv, Y., et al. (2019). Emergence of plasmid-mediated high-level tigecycline resistance genes in animals and humans. *Nat. Microbiol.* 4, 1450–1456. doi: 10.1038/s41564-019-0445-2

Hsieh, P. F., Lu, Y. R., Lin, T. L., Lai, L. Y., and Wang, J. T. (2019). *Klebsiella pneumoniae* type VI secretion system contributes to bacterial competition, cell invasion, type-1 fimbriae expression, and in vivo colonization. *J. Infect. Dis.* 219, 637–647. doi: 10.1093/infdis/jiy534

Letunic, I., and Bork, P. (2016). Interactive tree of life (iTOL) v3: an online tool for the display and annotation of phylogenetic and other trees. *Nucleic Acids Res.* 44, W242–W245. doi: 10.1093/nar/gkw290

Li, Y., Li, Y., Bu, K., Wang, M., Wang, Z., and Li, R. (2022). Antimicrobial resistance and genomic epidemiology of tet(X4)-bearing bacteria of pork origin in Jiangsu, China. *Genes* 14:36. doi: 10.3390/genes14010036

Li, R., Li, Y., Peng, K., Yin, Y., Liu, Y., He, T., et al. (2021). Comprehensive genomic investigation of tigecycline resistance gene *tet(X4)*-bearing strains expanding among different settings. *Microbiol. Spectr.* 9:e0163321. doi: 10.1128/spectrum.01633-21

Li, R., Lu, X., Peng, K., Liu, Z., Li, Y., Liu, Y., et al. (2020). Deciphering the structural diversity and classification of the mobile tigecycline resistance gene *tet(X)*-bearing plasmidome among bacteria. *mSystems* 5, e00134–e00120. doi: 10.1128/mSystems.00134-20

Li, Y., Wang, Q., Peng, K., Liu, Y., Li, R., and Wang, Z. (2020). Emergence of carbapenem- and tigecycline-resistant proteus cibarius of animal origin. *Front. Microbiol.* 11:1940. doi: 10.3389/fmicb.2020.01940

Li, Y., Wang, Q., Peng, K., Liu, Y., Xiao, X., Mohsin, M., et al. (2021). Distribution and genomic characterization of tigecycline-resistant *tet(X4)*-positive *Escherichia coli* of swine farm origin. *Microb. Genom.* 7:000667. doi: 10.1099/mgen.0.000667

Liu, C., Dong, N., Zeng, Y., Lu, J., Chen, J., Wang, Y., et al. (2022). Co-transfer of last-line antibiotic resistance and virulence operons by an IncFIBk-FII-X3-ColKP3 hybrid plasmid in *Klebsiella pneumoniae*. *J. Antimicrob. Chemother.* 77, 1856–1861. doi: 10.1093/jac/dkac121

Low, Y. M., Chong, C. W., Yap, I. K. S., Chai, L. C., Clarke, S. C., Ponnampalavanar, S., et al. (2018). Elucidating the survival and response of carbapenem resistant *Klebsiella pneumoniae* after exposure to imipenem at sub-lethal concentrations. *Pathog. Glob. Health* 112, 378–386. doi: 10.1080/20477724.2018.1538281

Lv, L., Wan, M., Wang, C., Gao, X., Yang, Q., Partridge, S. R., et al. (2020). Emergence of a plasmid-encoded resistance-nodulation-division efflux pump conferring resistance to multiple drugs, including tigecycline, in *Klebsiella pneumoniae*. *MBio* 11, e02930–e02919. doi: 10.1128/mBio.02930-19

Page, A. J., Cummins, C. A., Hunt, M., Wong, V. K., Reuter, S., Holden, M. T., et al. (2015). Roary: rapid large-scale prokaryote pan genome analysis. *Bioinformatics* 31, 3691–3693. doi: 10.1093/bioinformatics/btv421

Raisanen, K., Lyytikainen, O., Kauranen, J., Tarkka, E., Forsblom-Helander, B., Gronroos, J. O., et al. (2020). Molecular epidemiology of carbapenemase-producing *Enterobacterales* in Finland, 2012-2018. *Eur. J. Clin. Microbiol. Infect. Dis.* 39, 1651–1656. doi: 10.1007/s10096-020-03885-w

Ruzin, A., Visalli, M. A., Keeney, D., and Bradford, P. A. (2005). Influence of transcriptional activator RamA on expression of multidrug efflux pump AcrAB and tigecycline susceptibility in *Klebsiella pneumoniae*. *Antimicrob. Agents Chemother.* 49, 1017–1022. doi: 10.1128/AAC.49.3.1017-1022.2005

Seemann, T. (2014). Prokka: rapid prokaryotic genome annotation. *Bioinformatics* 30, 2068–2069. doi: 10.1093/bioinformatics/btu153

Seifert, H., Blondeau, J., and Dowzicky, M. J. (2018). In vitro activity of tigecycline and comparators (2014-2016) among key WHO 'priority pathogens' and longitudinal assessment (2004-2016) of antimicrobial resistance: a report from the T.E.S.T. study. *Int. J. Antimicrob. Agents* 52, 474–484. doi: 10.1016/j.ijantimicag.2018.07.003

Siu, L. K., Yeh, K. M., Lin, J. C., Fung, C. P., and Chang, F. Y. (2012). *Klebsiella pneumoniae* liver abscess: a new invasive syndrome. *Lancet Infect. Dis.* 12, 881–887. doi: 10.1016/S1473-3099(12)70205-0

Stamatakis, A. (2006). RAxML-VI-HPC: maximum likelihood-based phylogenetic analyses with thousands of taxa and mixed models. *Bioinformatics* 22, 2688–2690. doi: 10.1093/bioinformatics/btl446

Sun, J., Chen, C., Cui, C. Y., Zhang, Y., Liu, X., Cui, Z. H., et al. (2019). Plasmid-encoded tet(X) genes that confer high-level tigecycline resistance in *Escherichia coli*. *Nat. Microbiol.* 4, 1457–1464. doi: 10.1038/s41564-019-0496-4

Sun, C., Cui, M., Zhang, S., Liu, D., Fu, B., Li, Z., et al. (2020). Genomic epidemiology of animal-derived tigecycline-resistant *Escherichia coli* across China reveals recent endemic plasmid-encoded *tet(X4)* gene. *Commun. Biol.* 3:412. doi: 10.1038/s42003-020-01148-0

Villa, L., Feudi, C., Fortini, D., Garcia-Fernandez, A., and Carattoli, A. (2014). Genomics of KPC-producing *Klebsiella pneumoniae* sequence type 512 clone highlights the role of RamR and ribosomal S10 protein mutations in conferring tigecycline resistance. *Antimicrob. Agents Chemother.* 58, 1707–1712. doi: 10.1128/AAC.01803-13

Wang, J., Lu, M. J., Wang, Z. Y., Jiang, Y., Wu, H., Pan, Z. M., et al. (2022). Tigecycline-resistant *Escherichia coli* ST761 carrying *tet(X4)* in a pig farm, China. *Front. Microbiol.* 13:967313. doi: 10.3389/fmicb.2022.967313

Wang, G., Zhao, G., Chao, X., Xie, L., and Wang, H. (2020). The characteristic of virulence, biofilm and antibiotic resistance of *Klebsiella pneumoniae*. *Int. J. Environ. Res. Public Health* 17:6278. doi: 10.3390/ijerph17176278

Wick, R. R., Heinz, E., Holt, K. E., and Wyres, K. L. (2018). Kaptive web: user-friendly capsule and lipopolysaccharide serotype prediction for *Klebsiella* genomes. *J. Clin. Microbiol.* 56, e00197–e00118. doi: 10.1128/JCM.00197-18

Wyres, K. L., Lam, M. M. C., and Holt, K. E. (2020). Population genomics of *Klebsiella pneumoniae*. *Nat. Rev. Microbiol.* 18, 344–359. doi: 10.1038/s41579-019-0315-1

Yu, Y., Cui, C. Y., Kuang, X., Chen, C., Wang, M. G., Liao, X. P., et al. (2021). Prevalence of *tet(X4)* in *Escherichia coli* from duck farms in Southeast China. *Front. Microbiol.* 12:716393. doi: 10.3389/fmicb.2021.716393

Zhai, W., Tian, Y., Lu, M., Zhang, M., Song, H., Fu, Y., et al. (2022). Presence of mobile tigecycline resistance gene tet(X4) in clinical *Klebsiella pneumoniae*. *Microbiol. Spectr.* 10:e0108121. doi: 10.1128/spectrum.01081-21

frontiers | Frontiers in Microbiology

TYPE Methods
PUBLISHED 11 May 2023
DOI 10.3389/fmicb.2023.1160224



OPEN ACCESS

EDITED BY
Tao Li,
Chinese Academy of Agricultural Sciences, China

REVIEWED BY
Min Yue,
Zhejiang University, China
Dominic Frigon,
McGill University, Canada

*CORRESPONDENCE
Beatriz Martínez-López
✉ beamartinezlopez@ucdavis.edu

†These authors have contributed equally to this work and share first authorship

RECEIVED 06 February 2023
ACCEPTED 12 April 2023
PUBLISHED 11 May 2023

CITATION
Kim J, Rupasinghe R, Halev A, Huang C, Rezaei S, Clavijo MJ, Robbins RC, Martínez-López B and Liu X (2023) Predicting antimicrobial resistance of bacterial pathogens using time series analysis. *Front. Microbiol.* 14:1160224. doi: 10.3389/fmicb.2023.1160224



# Predicting antimicrobial resistance of bacterial pathogens using time series analysis

Jeonghoon Kim[1†], Ruwini Rupasinghe[2†], Avishai Halev[1], Chao Huang[3], Shahbaz Rezaei[3], Maria J. Clavijo[4], Rebecca C. Robbins[5], Beatriz Martínez-López[2*] and Xin Liu[3]

[1]Department of Mathematics, University of California, Davis, Davis, CA, United States, [2]Department of Medicine and Epidemiology, Center for Animal Disease Modeling and Surveillance (CADMS), School of Veterinary Medicine, University of California, Davis, Davis, CA, United States, [3]Department of Computer Science, University of California, Davis, Davis, CA, United States, [4]Department of Veterinary Diagnostic & Production Animal Medicine (VDPAM), Iowa State University, Ames, IA, United States, [5]R.C. Robbins Swine Consulting Services, PLLC, Amarillo, TX, United States

Antimicrobial resistance (AMR) is arguably one of the major health and economic challenges in our society. A key aspect of tackling AMR is rapid and accurate detection of the emergence and spread of AMR in food animal production, which requires routine AMR surveillance. However, AMR detection can be expensive and time-consuming considering the growth rate of the bacteria and the most commonly used analytical procedures, such as Minimum Inhibitory Concentration (MIC) testing. To mitigate this issue, we utilized machine learning to predict the future AMR burden of bacterial pathogens. We collected pathogen and antimicrobial data from >600 farms in the United States from 2010 to 2021 to generate AMR time series data. Our prediction focused on five bacterial pathogens (*Escherichia coli, Streptococcus suis, Salmonella sp., Pasteurella multocida,* and *Bordetella bronchiseptica*). We found that Seasonal Auto-Regressive Integrated Moving Average (SARIMA) outperformed five baselines, including Auto-Regressive Moving Average (ARMA) and Auto-Regressive Integrated Moving Average (ARIMA). We hope this study provides valuable tools to predict the AMR burden not only of the pathogens assessed in this study but also of other bacterial pathogens.

KEYWORDS

**antimicrobial resistance, antibiotics, bacterial pathogen, time series analysis, SARIMA**

## 1. Introduction

The discovery of antimicrobials is one of the best advances in therapeutic medicine in humans and animals. Over time, microbes have evolved and developed resistance mechanisms against these antimicrobial compounds. Increasing resistance to the available antimicrobials and stagnation of developing novel antimicrobials limit treatment options for patients with infectious diseases. Therefore, the emergence, dissemination, and persistence of microbes that are resistant to existing antimicrobials pose an enormous threat to public and animal health. Antimicrobials are extensively used in the food animal industry to treat bacterial infections and promote health, welfare, and production. According to Food and Drug Administration (FDA), ~80% of all antibiotics in the United States in 2011 were sold for use in animal husbandry, and ~70% of them belonged to the antibiotic classes used in human medicine (medically important antibiotics; FDA Department of Health and Human Services, 2011). Pig farming is one of the leading sectors using antimicrobials. Thus, increased levels of AMR are anticipated in swine farms due to the selective pressure of these

antimicrobials and can spread via pork, direct contact with pigs, or discharge of swine waste into the environment.

A key to preventing AMR emergence and spread is early and accurate detection of potential AMR, which promotes selecting appropriate antimicrobials and facilitating the prompt investigation of drug-resistant disease outbreaks. Routine monitoring and surveillance can enable exemplary stewardship by detecting AMR emergence, tracing AMR patterns, and effectively targeting antimicrobial interventions and mitigation strategies. Currently, antimicrobial susceptibility testing (AST) is the primary method for detecting AMR and selecting effective antimicrobials against bacterial pathogens, which involves culturing the bacteria in the presence of a panel of various antimicrobials. Effective antimicrobials can be determined by detecting Minimum Inhibitory Concentration (MIC), where antimicrobials with lower MIC values are considered more effective (susceptible) because less of the drug is needed to inhibit bacterial growth. However, these procedures can be expensive and time-consuming, depending on the growth rate of the bacteria and MIC testing procedures. Alternative methods, such as DNA sequencing technologies, are increasingly used to detect AMR at the molecular level, but they require robust bioinformatics tools to evaluate the genomic structure of the microbial resistomes. Thus, most clinical laboratories still depend primarily on conventional AST to conduct clinical therapy and observe AMR over time. Nevertheless, most farms may not have the resources (e.g., time and budget) to perform routine testing to detect AMR and quantify the AMR burden in field settings. Therefore, developing a tool to predict AMR burden based on available data, such as prior AMR information (susceptible/resistance) against common antimicrobials, could be very useful to better inform decision-making about antimicrobial use at the farm level, which consequently helps mitigate AMR.

Machine learning has been widely employed for studying AMR, highlighting its importance in predicting resistance levels mainly using features directly from genotypes (Pesesky et al., 2016; Nguyen et al., 2018, 2019; Wang et al., 2022). However, there are situations where we do not obtain genomic data to predict AMR levels but only preserve historical phenotype information. Time series analysis is a great solution to relevant tasks for such situations. Time series has shown great performances in studying AMR (López-Lozano et al., 2000; Hsueh et al., 2005; Aldeyab et al., 2008; Guo et al., 2019; Jeffrey et al., 2021; Strahlberg, 2021), and sometimes their methods are limited to Auto-regressive Integrated Moving Average (ARIMA; Chatfield, 2003) or subcategory methods that cannot properly incorporate seasonal behavior of AMR levels. Among many time series approaches, the Seasonal Auto-regressive Integrated Moving Average (SARIMA; Chatfield, 2003) has received significant attention because of its outstanding performance in time series forecasting. SARIMA shows its usefulness when some degrees of seasonality-periodic fluctuations occur repeatedly in the time series.

In this study, we used the SARIMA algorithm to predict the future burden of AMR (AMR proportions) of five bacterial pathogens (*Escherichia coli, Streptococcus suis, Salmonella sp., Pasteurella multocida,* and *Bordetella bronchiseptica*) prevalent in the studied swine farms using the prior resistance information. The data included the number of tested pathogens with confirmed resistance (based on MIC interpretations) to their corresponding antimicrobials. Instead of direct use of binary (susceptible and resistance) classified data, we generated integrated time series data, i.e., quarterly-based AMR proportions for each of the study pathogens. This approach enabled us to overcome the limitations of missing data over time. We also compared the performance of SARIMA to that of Auto-Regressive Moving Average (ARMA; Wold, 1938), Auto-Regressive Integrated Moving Average (ARIMA; Chatfield, 2003), and three other forecasting baseline methods as follows: Naïve, Seasonal Naïve, and one-lagged prediction (Ryu and Sanchez, 2003; Reza Hoshmand, 2009). These three baselines were selected as benchmarks in our study because they are often used in forecasting tasks and are simple yet effective. We believe that predicting AMR proportions using time series models can provide valuable information to facilitate the selection of appropriate antimicrobials against pathogens and the prompt investigation of drug-resistance disease outbreaks.

## 2. Materials and methods

In this section, we discuss the workflow, time series analysis methods, and experimental design. Workflow after data collection includes data processing (irregular binary data to quarterly time series data) and time series analysis (model parameter selection and model train/test; Figure 1).

### 2.1. Data collection

In this study, we used pathogen and antimicrobial information from >600 farms owned by two swine production systems in the United States. The samples were collected from pigs infected with one of five bacterial pathogens (*Escherichia coli, Streptococcus suis, Salmonella sp., Pasteurella multocida,* and *Bordetella bronchiseptica*) from 2010 to 2021 and tested for AMR against a panel of antimicrobials (Table 1). The resistance level of each pathogen against antimicrobials was detected by determining MIC and classified into two groups as follows: susceptible (*S*) and resistant (*R*), based on an interpretation report received from the American Association of Veterinary Laboratory Diagnosticians (AAVLD) accredited laboratory in the United States.

### 2.2. Data processing for time series analysis

For each pathogen, different groups of antimicrobials were employed for experiments (see Table 1). One challenge is that there were missing data points between certain time periods. To tackle this, we constructed a quarterly time series dataset by integrating the data points every quarter. We converted our data points to a quarterly basis dataset and define $Res(Pathogen, Antimicrobial)$ the resistance time series for each pathogen and antimicrobial as below.

$$Res(Pathogen, Antimicrobial) = (r_1, r_2, \cdots, r_n), \quad (1)$$

where $r_i = Proportion(R) = \frac{\#\text{ of } R}{\#\text{ of } (R+S)}$ over the $i$th quarter ($R$ and $S$ stand for resistant and susceptible, respectively). Figure 1 shows how we processed our dataset. Figure 2 shows examples

of quarterly based time series constructed for pathogens and antimicrobials, and all of the time series examples are presented as solid lines in Supplementary Figures 1–5. With the constructed data, we focused on predicting AMR proportions in times series for each *Res*(*Pathogen*, *Antimicrobial*) in our data.

We also output the mean and the standard deviations of *Res*(*Pathogen*, *Antimicrobial*) which can be an indicator for the averaged AMR proportions and dynamics of each time series (Table 1). We also observed different degrees of fluctuation in the processed dataset. For example, *Res*(*Escherichia coli*, *Ampicillin*) changes more dynamically than *Res*(*Escherichia coli*, *Tiamulin*) (Figure 2 and Table 1).

## 2.3. AR(I)MA, SARIMA, and three baselines

### 2.3.1. ARMA and ARIMA

Auto-Regressive Moving Average (ARMA) model consists of two parts, such as autoregressive (AR) and moving average (MA) parts (Wold, 1938). The model is usually referred to as $ARMA(p, q)$, where $p$ and $q$ are the order of the AR and MA parts, respectively (Valipour et al., 2012). AR part takes previous observations as inputs to predict future values. MA part uses previous errors between predicted and observed as predictors for future values. *ARIMA* model consists of three parts, such as AR, MA, and the integrated (I) parts (Chatfield, 2003). The model is usually referred to as $ARIMA(p, d, q)$, where $p$ and $q$ are the same as for the ARMA model, and $d$ is the degree of differencing. The integrated part refers to the differencing of observations to allow time series to become stationary.

### 2.3.2. SARIMA

Seasonal Auto-regressive Integrated Moving Average (SARIMA) model (Chatfield, 2003), as an advanced method of ARIMA with a seasonal component, overcomes the limitation that ARIMA cannot tackle data with periodic behavior properly. In this study, we employed SARIMA to predict AMR proportions for bacterial pathogens considering AMR proportions vary over time with a potential seasonality.

A typical SARIMA model has seven parameters, referred to as $SARIMA(p, d, q)(P, D, Q)_S$, where $(p, q)$ and $(P, Q)$ are the order of the non-seasonal and seasonal (autoregressive, moving) models, respectively, $d$ and $D$ are the numbers of non-seasonal and seasonal differences, respectively, and $S$ is the periodic seasonality term. Choosing appropriate parameters is a key process for the optimal SARIMA performance. To this end, autocorrelation and partial autocorrelation functions are utilized. To be precise, we first determine non-seasonality components $(p, d, q)$, and then, we find proper seasonal parameters $(P, D, Q)_S$ using autocorrelation function and partial autocorrelation function. Time series datasets often have trends in time series and changes in the statistical structure of the series, which means non-stationarity. To find non-seasonality parameters, trend and seasonality in time series should be removed using differencing techniques. After the removal of trend and seasonality, the autocorrelation function and partial autocorrelation function help determine non-seasonal parameters. Additionally, we also check the $p$-value between time series data and its lagged time series, and the number of lags with the lowest $p$-value determines seasonality parameter S for the SARIMA model. However, these steps do not always guarantee finding a specific set of parameters for the optimal SARIMA model. In many cases, parameter exploration using grid search is required, which means that we set some possible candidates for parameters and check the SARIMA model performance to find sets of parameters with the best performance.

### 2.3.3. Three baselines

*Naïve* method is the simplest time series forecasting method where all remaining forecast is set equal to the observation made in the last timestamp as below.

$$F_{T+t} = Y_T \text{ for } t > 0, \tag{2}$$

where $F$ and $Y$ are forecasting and observed times series, respectively. $T$ and $T + t$ are the timestamps of the last observation and the forecast time, respectively.

*Seasonal Naïve* method is an extension of the Naïve method with a seasonality. It predicts the forecasts based on the same timestamp in the previous cycle as below.

$$F_{T+t} = Y_{T+t-s(k-1)} \text{ for } t > 0, \tag{3}$$

where $s$ is seasonality and $k$ is completed cycles.

*One-lagged prediction* methods rely on the most recently acquired data (Ryu and Sanchez, 2003). One-lagged prediction utilizes the data from the previous timestamp to forecast the current timestamp as shown below.

$$F_{T+1} = Y_T \text{ for } t > 0. \tag{4}$$

## 2.4. Experiments

### 2.4.1. Parameter selection for SARIMA

For accurate AMR time series prediction, it is crucial to find appropriate SARIMA parameters (Ma et al., 2021). We selected *Escherichia coli* and *Neomycin* because *Res*(*Escherichia coli*, *Neomycin*) provides the largest number of data points to work with, and it shows visible seasonality. We have seven parameters to determine as follows: $(p, d, q)$, $(P, D, Q)$, and $S$. After using the differencing method to find parameter $d$ and to remove the trend component in *Res*(*Pathogen*, *Antimicrobial*), autocorrelation function, partial autocorrelation function, $p$-value analysis, and parameter exploration were attempted to assessing SARIMA parameters. We choose optimal SARIMA parameters that predict *Res*(*Escherichia coli*, *Neomycin*) with the lowest error.

### 2.4.2. ARMA and ARIMA parameter selection

Similar to SARIMA, we also employed parameter exploration to find the optimal parameters for ARMA and ARIMA. *Res*(*Escherichia coli*, *Neomycin*) was utilized for this process. We

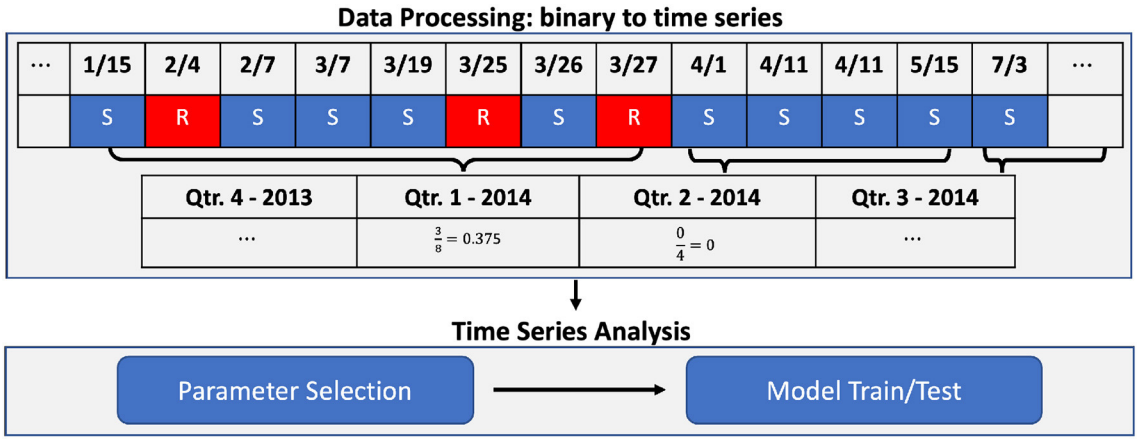


FIGURE 1
Workflow chart. Data processing example [from irregular binary data to quarterly based time series: *Res*(*Pathogen*, *Antimicrobial*)] and time series analysis.

**TABLE 1** Full data of antimicrobial and pathogens used for study.

| | *Escherichia coli* | *Streptococcus suis* | *Salmonella sp.* | *Pasteurella multocida* | *Bordetella bronchiseptica* |
|---|---|---|---|---|---|
| Clindamycin | 1.0/0.0 | 0.8/0.18 | 1.0/0.0 | 1.0/0.01 | 1.0/0.0 |
| Tiamulin | 0.99/0.03 | 0.16/0.1 | 1.0/0.01 | 0.58/0.29 | 1.0/0.01 |
| Tylosin | – | – | – | 0.98/0.06 | – |
| Ampicillin | 0.71/0.22 | 0.03/0.06 | 0.58/0.27 | 0.03/0.07 | 1.0/0.02 |
| Gentamicin | 0.32/0.16 | – | 0.51/0.39 | – | 0.04/0.1 |
| Oxytetracycline | 0.88/0.13 | 0.93/0.1 | – | 0.23/0.26 | 0.03/0.1 |
| Penicillin | 1.0/0.0 | 0.18/0.13 | 1.0/0.0 | 0.19/0.28 | 1.0/0.0 |
| Spectinomycin | 0.9/0.22 | – | – | – | – |
| Tilmicosin | 0.99/0.03 | 0.73/0.21 | 1.0/0.0 | 0.21/0.31 | – |
| Chlortetracycline | 0.88/0.13 | 0.93/0.1 | – | 0.03/0.07 | 0.04/0.11 |
| Sulphadimethoxine | – | 0.61/0.22 | – | – | 0.97/0.08 |
| Ceftiofur | – | 0.04/0.06 | – | 0.0/0.02 | – |
| Enrofloxacin | 0.34/0.25 | 0.07/0.07 | 0.29/0.38 | 0.0/0.02 | – |
| Florfenicol | 0.84/0.09 | 0.03/0.07 | 0.9/0.14 | 0.02/0.07 | 0.83/0.17 |
| Neomycin | 0.34/0.25 | 0.73/0.17 | 0.57/0.39 | 0.07/0.14 | – |
| Sulfa./trimethoprim | 0.26/0.27 | – | 0.32/0.32 | – | 0.89/0.14 |
| Tulathromycin | – | – | – | 0.0/0.01 | 0.04/0.1 |

Note that – indicates that corresponding data are not used in the experiments.
Two numbers provided indicate mean and standard deviation of data, i.e., an indicator for averaged AMR proportions and how dynamically (uncertain) the time series is changing, respectively.

conducted two experiments for ARMA and ARIMA independently because ARMA does not take parameter $d$ into account while ARIMA considers it.

### 2.4.3. Time series-based AMR proportions prediction

We selected seven combinations of parameters from previous analysis on *Res*(*Escherichia coli*, *Neomycin*) and applied the chosen seven combinations of parameters to other *Res*(*Pathogen*, *Antimicrobial*) to predict the AMR proportions. Specifically, for each *Res*(*Pathogen*, *Antimicrobial*), seven experiments with different parameter sets were conducted. Each experiment returned a rooted mean squared error as a performance measurement. We also used three baselines as follows: Naïve, Seasonal Naïve (we set four as the seasonality period), and one-lagged prediction. All baselines also outputted root mean squared error values for each

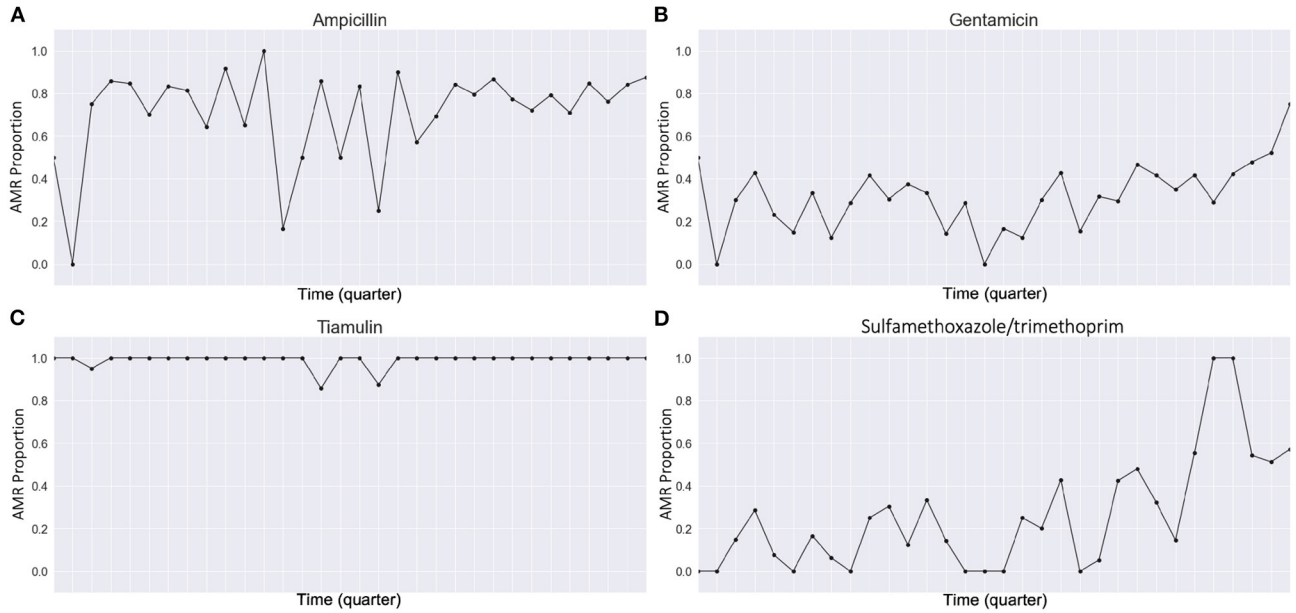


FIGURE 2
Examples of our processed quarterly based AMR proportions time series. **(A)** *Res(Escherichia coli, Ampicillin)*, **(B)** *Res(Escherichia coli, Gentamicin)*, **(C)** *Res(Escherichia coli, Tiamulin)*, and **(D)** *Res(Escherichia coli, Sulfamethoxazole/trimethoprim)*.

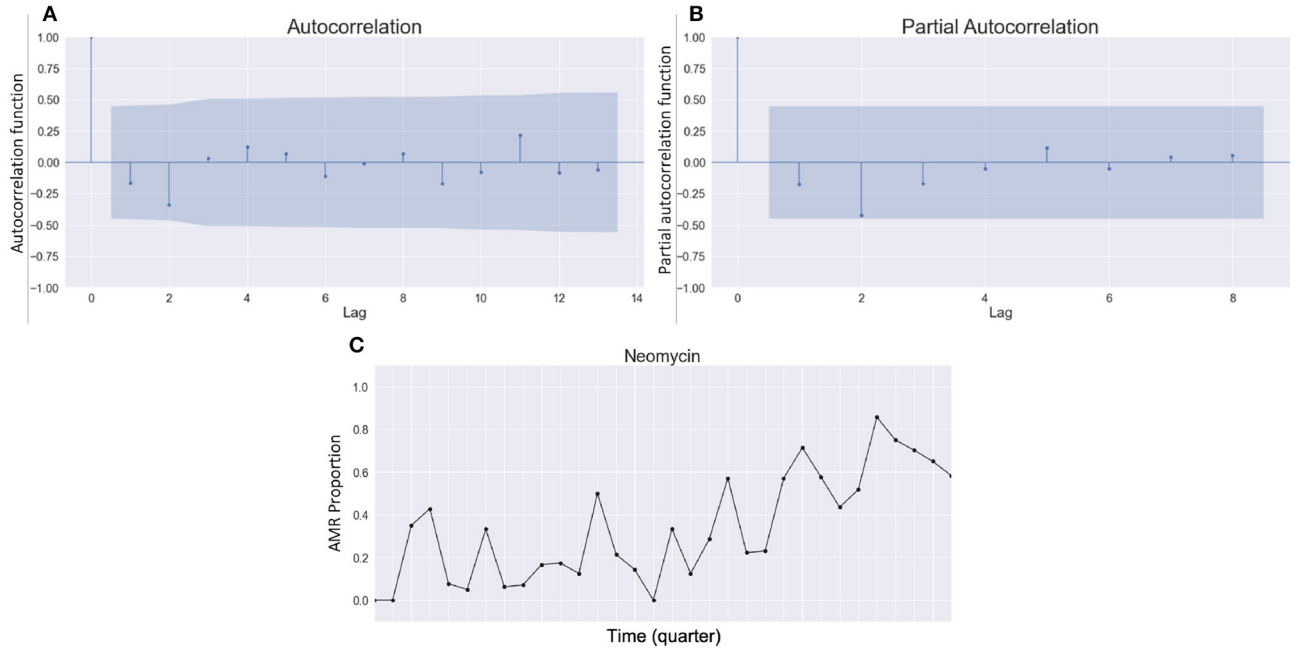


FIGURE 3
Autocorrelation function and partial autocorrelation function analysis for parameter selection. **(A)** Autocorrelation function plot, **(B)** partial autocorrelation function plot, and **(C)** AMR time series for *Escherichia coli* and Neomycin, i.e., *Res(Escherichia coli, Neomycin)*.

*Res*(*Pathogen*, *Antimicrobial*). All experiments were conducted in Python (version 3.7.6).

# 3. Results

## 3.1. Seven selected sets of SARIMA parameters

As shown in Figure 3, the autocorrelation function and partial autocorrelation function provided information on choosing the right parameters for SARIMA. *P*-value analysis for the *Res*(*Escherichia coli*, *Neomycin*) and its lagged time series with a different number of lags were also used to find the seasonal parameter S. From these, we can determine our parameter S = 12, but other parameters were not found properly from autocorrelation function and partial autocorrelation function analysis. There were no significant patterns of gradual decay or recurring cycles observed in either the autocorrelation or partial autocorrelation plots (Figure 3). Specifically, there is no data point with a lag value greater than zero that fell outside the confidence interval (blue shade area) in either plot (Figure 3), resulting in making it unable to estimate the appropriate parameters for a moving average (MA) or autoregressive (AR) models. From these analyses, the parameters of the time series model could not be satisfactorily determined without a parameter search.

In this regard, we explore the set of parameters that output the lowest error estimation measured by rooted mean squared error. In other words, we conducted trial and error for finding appropriate undetermined parameters remained. Our parameter exploration includes integers from 0 to 5 for three parameters $p$, $d$, $q$, and from 0 to 6 for the other three parameters $P$, $D$, $Q$, for which we end up having $6^3 7^3$ combinations to attempt. For each attempt with a combination of parameters, SARIMA predicted *Res*(*Escherichia coli*, *Neomycin*), i.e., tried to predict the 10% of the last values in *Res*(*Escherichiacoli*, *Neomycin*) after being trained with the first 90% of the *Res*(*Escherichia coli*, *Neomycin*), and a prediction error was reported. With outputted errors, we selected seven parameter combinations that return the lowest rooted mean squared error values because the next best one after these seven has a relatively big gap in the errors from the first seven parameters, and interestingly, our three parameters $(P, D, Q)_S$ are fixed as $(1, 0, 1)_{12}$ while seven different $(p, d, q)$ are acquired from Table 2.

## 3.2. Seven parameter sets for ARMA and ARIMA

To find the parameter sets that predicted *Res*(*Escherichia coli*, *Neomycin*) with the lowest errors, we explored integers from 0 to 5 for all parameters $(p, q)$ and $(p, d, q)$ for ARMA and ARIMA, respectively. Each experiment requires $6^3$ and $6^2$ iterations to search independently. In the end, seven sets of $(p, d, q)$ and $(p, q)$ that outputted the lowest rooted mean squared error were selected (Table 2).

## 3.3. Error estimation for AMR proportions prediction

For each *Res(Pathogen, Antimicrobial)* time series prediction using SARIMA, the seven previously selected SARIMA parameter sets were applied. Each experiment outputted a rooted mean squared error value which represents how good the prediction is, i.e., the lower the rooted mean squared error value, the more accurate the method (Figure 4). The lowest error value was provided among seven errors from seven experiments of SARIMA for each *Res(Pathogen, Antimicrobial)*. For each ARMA and ARIMA, seven parameters were conducted, and the lowest rooted mean squared error values were outputted among seven different experiments. We observed that our SARIMA method showed lower rooted mean squared error values compared to ARMA, ARIMA, and the other three baselines in general. The rooted mean squared error gap between SARIMA and three baselines became bigger when the AMR proportion time series [*Res*(*Pathogen*, *Antimicrobial*)] have greater deviation values (equivalently, more dynamical). This is because higher deviation implies more fluctuation in AMR proportion time series that are harder to predict. For example, rooted mean squared error values were similar between SARIMA and three baselines for *Res*(*Escherichia coli*, *Tilmicosin*) (standard deviation: 0.03), while root mean squared error gap became bigger for *Res*(*Escherichia coli*, *Enrofloxacin*) (standard deviation: 0.03; Figure 4 and Table 1).

# 4. Discussion

This study investigated the plausibility of executing data-driven forecasting of the future AMR burden using the available resistance data in >600 swine farms in the United States from 2010 to 2021. AMR burden was quantified quarterly by calculating the proportions of resistant strains of five crucial bacterial pathogens (*Escherichia coli, Streptococcus suis, Salmonella sp., Pasteurella multocida,* and *Bordetella bronchiseptica*) against their corresponding antimicrobials. The bacterial species assessed in this study were the most prevalent swine bacterial pathogens dispersed within the studied farms, significantly affecting their health, welfare, and productivity. These pathogens can cause various infections in pigs, including respiratory, gastrointestinal, and/or systemic infections, and antimicrobials are the primary mode of therapy and prevention of these infectious diseases (Robbins et al., 2014). Therefore, early and accurate detection of potential AMR of these pathogens is essential to determine the appropriate antimicrobials to use against and monitor for drug-resistant disease outbreaks. In this study, we used three machine learning-based time series analyses to predict the future AMR proportions in the studied farms and compared their performances to select the most efficient and accurate approach for future use. According to our findings, SARIMA predicted AMR proportions accurately and outperformed ARMA, ARIMA, and three baselines according to the rooted mean squared error value. However, parameter exploration remains a light limitation due to the potential computational burden because the key to prediction using SARIMA was to find appropriate

10.3389/fmicb.2023.1160224

TABLE 2 Seven selected parameters of SARIMA, ARMA, and ARIMA used for overall AMR proportions prediction acquired from *Res(Escherichia coli, Neomycin)* analysis.

| | SARIMA | | | | | | | ARMA | | | ARIMA | | | |
|---|---|---|---|---|---|---|---|---|---|---|---|---|---|---|
| No. | p | d | q | P | D | Q | S | No. | p | q | No. | p | d | q |
| #1 | 1 | 1 | 4 | 1 | 0 | 1 | 12 | #1 | 3 | 2 | #1 | 3 | 2 | 1 |
| #2 | 2 | 2 | 3 | 1 | 0 | 1 | 12 | #2 | 3 | 0 | #2 | 2 | 2 | 3 |
| #3 | 3 | 0 | 4 | 1 | 0 | 1 | 12 | #3 | 3 | 1 | #3 | 2 | 2 | 1 |
| #4 | 3 | 1 | 4 | 1 | 0 | 1 | 12 | #4 | 1 | 0 | #4 | 3 | 2 | 2 |
| #5 | 4 | 0 | 0 | 1 | 0 | 1 | 12 | #5 | 1 | 1 | #5 | 3 | 1 | 0 |
| #6 | 4 | 3 | 4 | 1 | 0 | 1 | 12 | #6 | 1 | 2 | #6 | 2 | 1 | 0 |
| #7 | 4 | 2 | 4 | 1 | 0 | 1 | 12 | #7 | 1 | 3 | #7 | 2 | 2 | 2 |

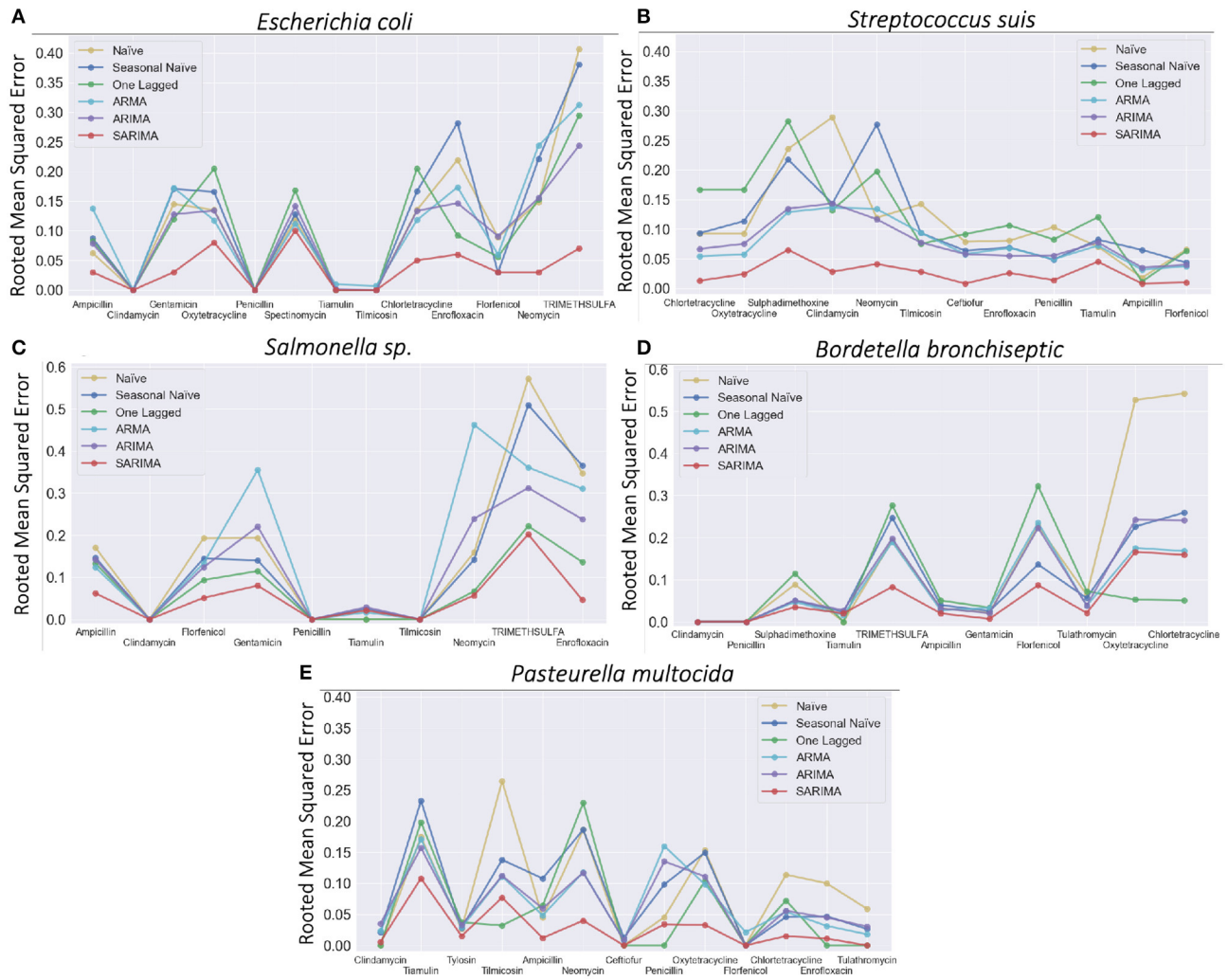


FIGURE 4
Rooted mean squared errors for five pathogens with corresponding antimicrobials. **(A)** *Escherichia coli*, **(B)** *Streptococcus suis*, **(C)** *Salmonella sp.*, **(D)** *Bordetella bronchiseptica*, and **(E)** *Pasteurella multocida*.

parameters which cannot always be acquired from the general process using partial autocorrelation function.

According to this study, we observed distinct temporal trends in AMR proportions for the five pathogens against their corresponding antimicrobials during the study period (Supplementary Figures 1–5). For example, pathogens, such as *Escherichia coli* and *Salmonella sp.*, showed very high or increasing trends of AMR proportions against Enrofloxacin, Neomycin,

Sulfamethoxazole/trimethoprim, and Clindamycin, etc., while *Streptococcus suis* exhibited low resistance to ampicillin, ceftiofur, enrofloxacin, florfenicol, and tiamulin. Most of the studied antimicrobials are effective against *Pasteurella multocida*, whereas *Bordetella bronchiseptica* displayed higher resistance levels against most antimicrobials assessed in our study. Nevertheless, these quarterly based-AMR proportions showed frequent fluctuations in most pathogens against their corresponding antimicrobials throughout the study period (Supplementary Figures 1–5). However, our SARIMA models were able to correctly capture all these individual trends and predict the future AMR proportions with high accuracy. Specifically, our study demonstrated that SARIMA works well for dynamic time series, such as AMR proportion time series for the studied five pathogens even if it is difficult to fairly compare our results to those from other relevant studies, as each system has its unique data samples and methods. In addition, this method could be applied to predict other unexplored pathogens unless the available data are limited. In other words, this work can be generalized to AMR proportion time series for any pairs of pathogens and antimicrobials. Furthermore, our SARIMA model can also be applied to other time series analyses in the domain, such as swine mortality rate.

Early detection of emerging AMR and future prediction of AMR burden and trends are vital to comprehend the extent of the threat and implement appropriate antimicrobial interventions and mitigation strategies. Numerous studies have explored various ML algorithms to study AMR using available phenotypic data (López-Lozano et al., 2000; Hsueh et al., 2005; Aldeyab et al., 2008; Guo et al., 2019; Jeffrey et al., 2021; Strahlberg, 2021) and genotypes (Pesesky et al., 2016; Nguyen et al., 2018, 2019; Wang et al., 2022). Specifically, the recent advancements in affordable and rapid DNA sequencing technologies (e.g., whole genome sequencing) combined with ML approaches have drastically transformed AMR surveillance and prediction prospects. Predicting pathogens that might express AMR by using their genomics data has shown great promise in the real-time detection of AMR determinants. However, this process requires robust bioinformatics tools and advanced analytical skillsets to assess the microbial genomic structure and the resistomes, and these limitations still preclude cost-effective, user-friendly, and rapid antimicrobial resistance surveillance. In addition, phenotyping approaches provide direct visual evidence of interaction between a bacterial strain and an antimicrobial. Thus, most clinical laboratories, to date, rely mainly on traditional AST to guide clinical therapy and monitor AMR over time. Therefore, the SARIMA model we proposed in our study will be an efficient and practical alternative to predict AMR burden, especially for situations where we do not have genomic data but only have historical phenotype information.

There are a few limitations to our study. The AMR data used for prediction were comprised of data from multiple swine farms within the United States. Although these farms were managed under two major swine production systems, individual farms can have different management practices, biosecurity measures, treatment protocols, etc. Previous studies disclosed various factors, such as transportation, farm management, housing conditions, metals consumption, feeding strategies, antimicrobial usage, and co-infections that can affect the spread of antimicrobial-resistant bacteria and the AMR levels in a farm (Mathew et al., 2003; Dewulf et al., 2007; Medardus et al., 2014; Luiken et al., 2022; Odland et al., 2022). However, we did not incorporate these factors in our study. Thus, the future AMR burden (proportions) can vary from the predicted levels due to the variations in these farm factors. Since the AMR predictions were made using a limited number of swine farms in the United States, we cannot generalize our findings to the entire swine population in the United States. Therefore, we cannot generalize our findings to the entire swine population in the United States. However, our results depict the potential of using time series analysis to predict AMR levels within a farm or geographical region. In this study, we transformed the AMR data into a binary variable (susceptible/resistance) using breakpoints acquired from the interpretation report from AAVLD-accredited laboratories in the United States. Some of these breakpoints were extrapolated from other species (e.g., human and canine) if swine-specific breakpoints were not available for a pathogen–antimicrobial combination (Watts et al., 2018; Lubbers et al., 2020). Breakpoint MICs depend on the clinical pharmacology of antimicrobials and are generally specific for bacterial-antimicrobial-host-disease-tissue-dosing regimen combinations (Watts et al., 2018; CLSI, 2019; Lubbers et al., 2020); thus, different testing laboratories may use different standards for resistance classifications, which may cause misclassifications of pathogens. Nevertheless, predicting AMR burden directly from MIC values will minimize these misclassifications or classification errors. Hence, future studies are suggested to perform time series analysis based on the raw MIC data.

## 5. Conclusion

This study proposed to use time series methods for the prediction of future AMR burden by constructing the quarterly based AMR proportion times series. The SARIMA approach showed low errors in terms of rooted mean squared error compared with ARMA, ARIMA, and three other forecasting baselines, and it worked even for highly dynamic time series. We believe that our time series prediction can help to advise using appropriate antimicrobials and reduce the risk related to AMR events by predicting anticipation of AMR occurrences in farms or geographical regions. Furthermore, our study may also contribute to the analysis of similar problems and scenarios.

## Data availability statement

The data analyzed in this study is subject to the following licenses/restrictions: The dataset used in this study cannot be publicly available. Requests to access these datasets should be directed to BM-L, beamartinezlopez@ucdavis.edu.

## Author contributions

JK designed the study, developed the Python codes for experiments, carried out the analysis of experimental results, and wrote the draft of the manuscript. BM-L and RR collected, cleaned, and verified the data. RR contributed to writing the introduction and discussion parts, especially from biological perspectives. AH, CH, SR, and XL helped to justify methodologies in this study

and to edit the method explanation part. MC and RCR helped to develop ideas and analyze the results. All authors participated in the discussion and interpretation of the results and read, edited, and approved the final manuscript.

## Funding

This study was partially supported by NSF through grants OIA-2134901, IIS-1838207, CNS 1901218, USDA-020-67021-32855, and USDA 2021-68014-34143.

## Acknowledgments

The authors would like to thank swine industry collaborators and producers for the provision of data.

## Conflict of interest

RCR is sole proprietor of R.C. Robbins Swine Consulting Services, PLLC, United States.

The remaining authors declare that the research was conducted in the absence of any commercial or financial relationships that could be construed as a potential conflict of interest.

## Publisher's note

All claims expressed in this article are solely those of the authors and do not necessarily represent those of their affiliated organizations, or those of the publisher, the editors and the reviewers. Any product that may be evaluated in this article, or claim that may be made by its manufacturer, is not guaranteed or endorsed by the publisher.

## Supplementary material

The Supplementary Material for this article can be found online at: https://www.frontiersin.org/articles/10.3389/fmicb.2023.1160224/full#supplementary-material

## References

Aldeyab, M. A., Monnet, D. L., López-Lozano, J. M., Hughes, C. M., Scott, M. G., Kearney, M. P., et al. (2008). Modelling the impact of antibiotic use and infection control practices on the incidence of hospital-acquired methicillin-resistant *Staphylococcus aureus*: a time-series analysis. *J. Antimicrob. Chemother*. 62, 593–600. doi: 10.1093/jac/dkn198

Chatfield, C. (2003). *The Analysis of Time Series: An Introduction, 6th Edn*. Chapman and Hall/CRC. doi: 10.4324/9780203491683

CLSI. (2019). *Understanding Susceptibility Test Data as a Component of Antimicrobial Stewardship in Veterinary Settings, 1st Edn*. CLSI report VET09. Wayne, PA: Clinical and Laboratory Standards Institute.

Dewulf, J., Catry, B., Timmerman, T., Opsomer, G., de Kruif, A., and Maes, D. (2007). Tetracycline-resistance in lactose-positive enteric coliforms originating from Belgian fattening pigs: degree of resistance, multiple resistance and risk factors. *Prevent. Vet. Med*. 78, 339–351. doi: 10.1016/j.prevetmed.2006.11.001

FDA Department of Health and Human Services (2011). *Summary Report on Antimicrobials Sold or Distributed for Use in Food-Producing Animals*. FDA Department of Health and Human Services.

Guo, W., Sun, F., Liu, F., Cao, L., Yang, J., and Chen, Y. (2019). Antimicrobial resistance surveillance and prediction of Gram-negative bacteria based on antimicrobial consumption in a hospital setting: a 15-year retrospective study. *Medicine* 98:e17157. doi: 10.1097/MD.0000000000017157

Hsueh, P.-R., Chen, W.-H., and Luh, K.-T. (2005). Relationships between antimicrobial use and antimicrobial resistance in Gram-negative bacteria causing nosocomial infections from 1991–2003 at a university hospital in Taiwan. *Int. J. Antimicrob. Agents* 26, 463–472. doi: 10.1016/j.ijantimicag.2005.08.016

Jeffrey, B., Aanensen, D. M., Croucher, N. J., and Bhatt, S. (2021). Predicting the future distribution of antibiotic resistance using time series forecasting and geospatial modelling. *Wellcome Open Res*. 5, 1–26. doi: 10.12688/wellcomeopenres.16153.1

López-Lozano, J.-M., Monnet, D. L., Yagüe, A., Burgos, A., Gonzalo, N., Campillos, P., et al. (2000). Modelling and forecasting antimicrobial resistance and its dynamic relationship to antimicrobial use: a time series analysis. *Int. J. Antimicrob. Agents* 14, 21–31. doi: 10.1016/S0924-8579(99)00135-1

Lubbers, B. V., Diaz-Campos, D., Schwarz, S., and Clinical and Laboratory Standards Institute. (2020). *Performance Standards for Antimicrobial Disk and Dilution Susceptibility Tests for Bacteria Isolated From Animals. 5th Edn. CLSI supplement VET01S*. Clinical and Laboratory Standards Institute.

Luiken, R. E. C., Heederik, D. J. J., Scherpenisse, P., Van Gompel, L., van Heijnsbergen, E., Greve, G. D., et al. (2022). Determinants for antimicrobial resistance genes in farm dust on 333 poultry and pig farms in nine European countries. *Environ. Res*. 208:112715. doi: 10.1016/j.envres.2022.112715

Ma, S., Liu, Q., and Zhang, Y. (2021). A prediction method of fire frequency: based on the optimization of SARIMA model. *PLoS ONE* 16:255857. doi: 10.1371/journal.pone.0255857

Mathew, A. G., Arnett, D. B., Cullen, P., and Ebner, P. D. (2003). Characterization of resistance patterns and detection of apramycin resistance genes in Escherichia coli isolated from swine exposed to various environmental conditions. *Int. J. Food Microbiol*. 89, 11–20. doi: 10.1016/S0168-1605(03)00124-7

Medardus, J. J., Molla, B. Z., Nicol, M., Morrow, W. M., Rajala-Schultz, P. J., Kazwala, R., et al. (2014). In-feed use of heavy metal micronutrients in U.S. swine production systems and its role in persistence of multidrug-resistant salmonellae. *Appl. Environ. Microbiol*. 80, 2317–2325. doi: 10.1128/AEM.04283-13

Nguyen, M., Brettin, T., Long, S. W., Musser, J. M., Olsen, R. J., Olson, R., et al. (2018). Developing an *in silico* minimum inhibitory concentration panel test for *Klebsiella pneumoniae*. *Sci. Rep*. 8:421. doi: 10.1038/s41598-017-18972-w

Nguyen, M., Long, S. W., McDermott, P. F., Olsen, R. J., Olson, R., Stevens, R. L., et al. (2019). Using machine learning to predict antimicrobial MICs and associated genomic features for nontyphoidal salmonella. *J. Clin. Microbiol*. 57:e01260-18. doi: 10.1128/JCM.01260-18

Odland, C. A., Edler, R., Noyes, N. R., Dee, S. A., Nerem, J., and Davies, P. R. (2022). Evaluation of the impact of antimicrobial use protocols in porcine reproductive and respiratory syndrome virus-infected swine on phenotypic antimicrobial resistance patterns. *Appl. Environ. Microbiol*. 88, e0097021. doi: 10.1128/AEM.00970-21

Pesesky, M. W., Hussain, T., Wallace, M., Patel, S., Andleeb, S., Burnham, C.-A. D., et al. (2016). Evaluation of machine learning and rules-based approaches for predicting antimicrobial resistance profiles in gram-negative bacilli from whole genome sequence data. *Front. Microbiol*. 7:1887. doi: 10.3389/fmicb.2016.01887

Reza Hoshmand, A. (2009). *Business Forecasting: A Practical Approach*. Routledge. doi: 10.4324/9780203874011

Robbins, R. C., Almond, G., and Byers, E. (2014). *Swine Diseases and Disorders*. Oxford: Academic Press, 261–276. doi: 10.1016/B978-0-444-52512-3.00134-0

Ryu, K., and Sanchez, A. (2003). The evaluation of forecasting methods at an institutional foodservice dining facility. *J. Hosp. Financ. Manage*. 11, 27–45. doi: 10.1080/10913211.2003.10653769

Strahlberg, D. (2021). Antibiotics resistance forecasting: a comparison of two time series forecast models. *SIAM Undergrad. Res. Online* 14, 383–399. doi: 10.1137/20S1365284

Valipour, M., Banihabib, M. E., and Behbahani, S. M. R. (2012). Parameters estimate of autoregressive moving average and autoregressive integrated moving average

models and compare their ability for inflow forecasting. *J. Math. Stat.* 8, 330–338. doi: 10.3844/jmssp.2012.330.338

Wang, H., Jia, C., Li, H., Yin, R., Chen, J., Li, Y., et al. (2022). Paving the way for precise diagnostics of antimicrobial resistant bacteria. *Front. Mol. Biosci.* 9:976705. doi: 10.3389/fmolb.2022.976705

Watts, J. L., Sweeney, M. T., and Lubbers, B. V. (2018). Antimicrobial susceptibility testing of bacteria of veterinary origin. *Microbiol. Spectr.* 6. doi: 10.1128/microbiolspec.ARBA-0001-2017

Wold, H. (1938). *A Study in the Analysis of Stationary Time Series*. Stockholm: Almgrist and Wiksell.

# Frontiers in Microbiology

**Explores the habitable world and the potential of microbial life**

The largest and most cited microbiology journal which advances our understanding of the role microbes play in addressing global challenges such as healthcare, food security, and climate change.

---

## Discover the latest Research Topics

See more →


**Frontiers**

Avenue du Tribunal-Fédéral 34
1005 Lausanne, Switzerland
frontiersin.org

**Contact us**

+41 (0)21 510 17 00
frontiersin.org/about/contact